National Library of Canada
Canadian Theses Service
Ottawa, Canada
K1A 0N4

Bibliothèque nationale du Canada
Service des thèses canadiennes

NOTICE

The quality of this microform is heavily dependent upon the quality of the original thesis submitted for microfilming. Every effort has been made to ensure the highest quality of reproduction possible.

If pages are missing, contact the university which granted the degree.

Some pages may have indistinct print especially if the original pages were typed with a poor typewriter ribbon or if the university sent us an inferior photocopy.

Reproduction in full or in part of this microform is governed by the Canadian Copyright Act, R.S.C. 1970, c. C-30, and subsequent amendments.

AVIS

La qualité de cette microforme dépend grandement de la qualité de la thèse soumise au microfilmage. Nous avons tout fait pour assurer une qualité supérieure de reproduction.

S'il manque des pages, veuillez communiquer avec l'université qui a conféré le grade.

La qualité d'impression de certaines pages peut laisser à désirer, surtout si les pages originales ont été dactylographiées à l'aide d'un ruban usé ou si l'université nous a fait parvenir une photocopie de qualité inférieure.

La reproduction, même partielle, de cette microforme est soumise à la Loi canadienne sur le droit d'auteur, SRC 1970, c. C-30, et ses amendements subséquents.

NL-339 (r. 88/04) c

Canada

THE UNIVERSITY OF ALBERTA

THIXOTROPIC BEHAVIOUR OF OIL SANDS TAILINGS SLUDGE

by

LESLAW CZESLAW BANAS

A THESIS

SUBMITTED TO THE FACULTY OF GRADUATE STUDIES AND RESEARCH

IN PARTIAL FULFILLMENT OF THE REQUIREMENTS FOR THE DEGREE

OF MASTER OF SCIENCE

DEPARTMENT OF CIVIL ENGINEERING

EDMONTON, ALBERTA

SPRING 1991

National Library of Canada
Bibliothèque nationale du Canada

Canadian Theses Service
Service des thèses canadiennes

Ottawa, Canada
K1A 0N4

The author has granted an irrevocable non-exclusive licence allowing the National Library of Canada to reproduce, loan, distribute or sell copies of his/her thesis by any means and in any form or format, making this thesis available to interested persons.

The author retains ownership of the copyright in his/her thesis. Neither the thesis nor substantial extracts from it may be printed or otherwise reproduced without his/her permission.

L'auteur a accordé une licence irrévocable et non exclusive permettant à la Bibliothèque nationale du Canada de reproduire, prêter, distribuer ou vendre des copies de sa thèse de quelque manière et sous quelque forme que ce soit pour mettre des exemplaires de cette thèse à la disposition des personnes intéressées.

L'auteur conserve la propriété du droit d'auteur qui protège sa thèse. Ni la thèse ni des extraits substantiels de celle-ci ne doivent être imprimés ou autrement reproduits sans son autorisation.

ISBN 0-315-66712-5

Canada

THE UNIVERSITY OF ALBERTA

RELEASE FORM

NAME OF AUTHOR: LESLAW CZESLAW BANAS

TITLE OF THESIS: THIXOTROPIC BEHAVIOUR OF OIL SANDS TAILINGS SLUDGE

DEGREE: MASTER OF SCIENCE

YEAR THIS DEGREE GRANTED: SPRING 1991

Permission is hereby granted to THE UNIVERSITY OF ALBERTA LIBRARY to reproduce single copies of this thesis and to lend or sell such copies for private, scholarly or scientific research purposes only.

The author reserves other publication rights, and neither the thesis nor extensive extracts from it may be printed or otherwise reproduced without the author's written permission.

L. Banas

L. C. Banas

Permanent Address:
10495 - 24 Avenue
Edmonton, Alberta
T6J 4S2

Date: April 12, 1991

THE UNIVERSITY OF ALBERTA

FACULTY OF GRADUATE STUDIES AND RESEARCH

The undersigned certify they have read, and recommend to the Faculty of Graduate Studies and Research, for acceptance, a thesis entitled THIXOTROPIC BEHAVIOUR OF OIL SANDS TAILINGS SLUDGE submitted by LESLAW CZESLAW BANAS in partial fulfillment of the requirements for the degree of MASTER OF SCIENCE.

.....

Dr. J. D. Scott, Supervisor

.....

Dr. D. C. Sego, Commitee Chairman

.....

Dr. N. Rajaratnam

.....

Dr. M. J. Dudas

Dated April 12, 1991

ABSTRACT

Oil sands tailings sludge is a waste by-product of synthetic crude production from the oil sands mining operations located in northern Alberta. The sludge is a high water content slurry material consisting of water, silt, clay, and bitumen which consolidates slowly.

One of the factors affecting self-weight consolidation of the sludge is thixotropic gain in strength of the soil. To arrive at a comprehensive, long-term consolidation model of the sludge, the time dependent strength properties of the material need to be thoroughly understood. To address this problem, sludges of six different water contents were tested for their peak and residual undrained shear strength parameters at time intervals after mixing ranging from zero to 700 days. Two methods of measuring shear strength were used: viscosity measurements and vane shear testing. The analyses investigated the absolute and relative gain of both peak and residual thixotropic strengths at constant water contents. The influence of water content on relative thixotropy was also analyzed. The thixotropic properties of the sludge were compared with those of other soils.

The tests revealed that the sludge is a highly thixotropic soil with the highest rate of strength gain taking place in the first several hours after mixing. The highest absolute gain in strength was [illegible] kPa in 300 days for the liquid limit sludge. The highest relative thixotropic effect was found in the 233% water content (30% solids content) sludge which reached a thixotropic ratio of 21 in 470 days. Self-weight consolidation of the sludge appeared to have a reducing effect on thixotropic strength. When compared to other soils, the sludge

exhibited highest relative thixotropy. The liquidity index-residual undrained shear strength relationship for the sludge was similar to those for other soils.

Acknowledgements

This research was conducted at the University of Alberta under the supervision of Dr. J. Don Scott. His invaluable guidance, expertise, patience, and encouragement throughout the course of this study are greatly appreciated.

Thanks are also extended to Dr. D. C. Sego for his assistance in my first steps at this university as an undergraduate student.

I would like to express my gratitude to the technical staff of the Department of Civil Engineering. Special thanks to Steve Gamble who spent countless hours providing assistance throughout this project. Appreciation is also extended to Christine Hereygers and Jay Khajuria for their help.

I am grateful to Syncrude Canada Ltd. for supplying me with the samples of the oil sands tailings sludge. Mike MacKinnon is to be thanked for his interest in my work.

Financial support for this project was provided by the Natural Sciences and Engineering Research Council of Canada from Dr. Scott's NSERC Operating Grant OGP 0872 and is gratefully acknowledged.

I wish to thank my parents for their continuing love and support. I feel very fortunate to be their son.

I wish to express my greatest appreciation to my wife, Urszula. Without her love, patience, support, and encouragement I could not have achieved this goal.

Finally, I would like to dedicate this thesis to my daughter, Kaja, who changed my life and has been an inspiration throughout the last two years.

Table of Contents

Chapter Page

1. INTRODUCTION 1

1.1 Definition of Problem 1

1.2 Objective of Research Program 2

1.3 Scope of Thesis 2

1.4 Organization of Thesis 3

2. LITERATURE REVIEW 5

2.1 Oil Sands Tailings 5

2.1.1 Origin 5

2.1.2 Oil Sand Operations 6

2.1.3 Oil Sands Tailings Sludge 8

2.2 Thixotropy 11

2.3 Soft Soil Behaviour 15

2.3.1 Uniqueness of Soft Soils 15

2.3.2 Strength Testing in Very Soft Soils 18

2.4 Strength Testing of Oil Sands Tailings Sludge 21

2.5 Summary of Important Findings 24

3. EXPERIMENTAL PROGRAM 28

3.1. Slurry Description and Preparation 28

3.1.1. Origin of Specimens 28

3.1.2. Index Properties 29

3.1.3. Slurry Containers 32

3.1.4. Drying and Centrifuging of Sludge 33

3.1.5. Diluting with Pond versus Distilled Water 34

3.1.6. Mixing 34

3.2. Testing Equipment and Techniques 35
3.2.1. Viscosity Measurements 35
3.2.1.1. Theoretical Background 35
3.2.1.2 Brookfield Synchro-Lectric Viscometer 38
3.2.1.3 Testing Procedure 40
3.2.2 Shear Vane Testing 42
3.2.2.1 Theoretical Analysis 42
3.2.2.2 Standard Vane Shear Apparatus 47
3.2.2.3 Modified Apparatus 48
3.2.2.4 Data Acquisition System 50
3.2.2.5 Testing Procedure 51
3.2.3 Cavity Expansion Testing 53
3.2.3.1 Theoretical Analysis 54
3.2.3.2 Testing Apparatus 57
3.2.3.3 Testing Procedure 58
3.3 Test Selection 59
3.3.1 Index Tests 59
3.3.1.1 Origin of Samples 59
3.3.2 Viscosity Tests 59
3.3.2.1 Water/Solids Content of Sludge 59
3.3.2.2 Age of Sludge 60
3.3.3 Shear Vane Tests 61
3.3.3.1 Water/Solids Content of Sludge 61
3.3.3.2 Age of Sludge 61
3.3.4 Experiment Designation 62
4. LABORATORY TEST RESULTS 72

4.1 Index Tests 72
4.1.1 Water Content 72
4.1.2 Atterberg Limits 73
4.1.3 Grain Size Distribution 74
4.1.4 Specific Gravity 77
4.1.5 Bitumen Content 77
4.1.6 pH 78
4.2 Viscosity Test Results 78
4.2.1 Sludge 400 79
4.2.2 Sludge 300 80
4.2.3 Sludge 233 81
4.2.4 Sludge 150 82
4.2.5 Sludge 100 85
4.2.6 Influence of Temperature on Viscosity 87
4.2.7 Summary of Viscosity Tests Results 87
4.3 Shear Vane Test Results 89
4.3.1 Sludge 400 90
4.3.3 Sludge 233 92
4.3.4 Sludge 150 92
4.3.5 Sludge 100 94
4.3.6 Effect of Vane Diameter and Number of Vane Blades on Shear Stress 95
4.3.7 Sludge 47 96
4.3.8 Summary of Shear Vane Testing 98
5. ANALYSIS OF TIME DEPENDENT STRENGTH BEHAVIOUR 126
5.1 Method of Analysis 126
5.2 Viscosity Measurements 128

5.2.1 Viscosity Readings at a Constant Water Content....128
5.2.2 Thixotropic Viscosity Ratios....133
5.2.3 Residual/Remoulded Viscosity Ratios....135
5.2.4 Liquidity Index-Residual Viscous Resistance Relationship....136
5.3 Undrained Vane Shear Strength....137
5.3.1 Shear Strength at a Constant Water Content....137
5.3.2 Thixotropic Strength Ratios from Vane Shear Tests....142
5.3.3 Residual/Remoulded Shear Strength Ratios....143
5.4 Effect of Water Content on Thixotropic Ratio....144
5.5 Liquidity Index-Residual Shear Strength Relationship....146
5.6 Comparison of Shear Strength Tests to Viscosity Tests....149
5.7 Comparison to Other Thixotropic Tests on Sludge....152
5.8 Effect of Self-Weight Consolidation on Thixotropic Strength....152
5.9 Comparison to Other Thixotropic Soils....154
6. CONCLUSIONS AND RECOMMENDATIONS....203
6.1 Conclusions....203
6.1.1 Test Results....203
6.1.2 Testing Equipment and Procedures....204
6.2 Recommendations for Further Research....205
REFERENCES....207
APPENDIX A. Viscosity Test Plots....213

APPENDIX B. Apparent Viscosity Plots 256
APPENDIX C. Shear Vane Test Plots 300

List of Tables

Table Page

Table 4.1 Atterberg Limits for Sludge 100

Table 4.2 Viscosity Test Results for Sludge 400 101

Table 4.3 Viscosity Test Results for Sludge 300 102

Table 4.4 Viscosity Test Results for Sludge 233 103

Table 4.5 Comparison of Sensitivities for Different Spindles 104

Table 4.6 Viscosity Test Results for Sludge 150 105

Table 4.7 Viscosity Test Results for Sludge 100 106

Table 4.8 Shear Vane Test Results for Sludge 400 107

Table 4.9 Shear Vane Test Results for Sludge 300 108

Table 4.10 Shear Vane Test Results for Sludge 233 109

Table 4.11 Shear Vane Test Results for Sludge 150 110

Table 4.12 Shear Vane Test Results for Sludge 100 111

Table 4.13 Shear Vane Test Results for Sludge 47 112

List of Figures

Figure — Page

2.1 Stylized cross section of Syncrude's tailings pond 26

2.2 Typical grain size distribution for sludge 27

3.1 Flow curves for model materials 64

3.2 Variation of viscosity with strain rate for model materials 64

3.3 Torque cell for the vane shear apparatus 68

3.4 Theoretical curves for expansion of spherical cavity for initial radius 1 mm, with E/c=6, c=0.2 kPa 69

3.5 Cavity expansion test 01 - stress history 70

3.6 Cavity expansion test 01 - pressure vs. volume 70

4.1 Grain size distribution for tailings sludge 113

4.2 Grain size distribution for tailings sludge (Microtrac method) 113

4.3 Viscosity test V40010M 114

4.4 Viscosity test V40040D 114

4.5 Viscosity test V40680D 115

4.6 Viscosity test V30006D 115

4.7 Viscosity test V30660D 116

4.8 Viscosity test V23001H 116

4.9 Viscosity test V23494D 117

4.10 Viscosity test V23005D at different temperatures 117

4.11 Viscosity test V15680D 118

4.12 Viscosity test V15470D 118

4.13 Viscosity test V1000M 119

4.14 Viscosity test V10005D at different temperatures 119

4.15 Vane shear test S40000M 120

4.16 Vane shear test S40050DP 120

Figure Page

4.17 Vane shear test S30050DP....121

4.18 Vane shear test S23000M 121

4.19 Vane shear test S15020DP....122

4.20 Vane shear test S15680DR....122

4.20 Vane shear test S10000M 123

4.22 S10: Residual strength at 470, 680 & 701 days 123

4.23 S10: Peak strength at 470, 680 & 701 days....124

4.24 Vane shear test S47000M 125

4.25 Vane shear test S147001DP....125

5.1 Viscometer readings vs. time for sludge 400 - 16,320 hrs 158

5.2 Viscometer readings vs. time for sludge 400 - 240 hrs 158

5.3 Viscometer readings vs. time for sludge 400 - 16,320 hrs 158

5.4 Viscosity readings for w=400% (I_L=15.2) 159

5.5 Viscosity readings for w=400% (I_L=15.2) 159

5.6 Viscometer readings vs. time for sludge 300 - 15,840 hrs 160

5.7 Viscometer readings vs. time for sludge 300 - 240 hrs 160

5.8 Viscometer readings vs. time for sludge 300 - 15,840 hrs 160

5.9 Viscosity readings for w=300% (I_L=11.2) 161

5.10 Viscosity readings for w=300% (I_L=11.2) 161

5.11 Viscometer readings vs. time for sludge 233 - 16,368 hrs 162

5.12 Viscometer readings vs. time for sludge 233 - 240 hrs 162

5.13 Viscometer readings vs. time for sludge 233 - 16,368 hrs 162

5.14 Viscosity readings for w=233% (I_L=8.5)....163

5.15 Viscosity readings for w=233% (I_L=8.5)....163

5.16 Viscometer readings vs. time for sludge 150 - 16,320 hrs 164

5.17 Viscometer readings vs. time for sludge 150 - 240 hrs 164

Figure

Page

5.18 Viscometer readings vs. time for sludge 150 - 16,320 hrs 164

5.19 Viscosity readings for w=150% (I_L=5.2).....165

5.20 Viscosity readings for w=150% (I_L=5.2).....165

5.21 Viscometer readings vs. time for sludge 100 - 16,320 hrs 166

5.22 Viscometer readings vs. time for sludge 100 - 240 hrs 166

5.23 Viscometer readings vs. time for sludge 100 - 16,320 hrs 166

5.24 Viscosity readings for w=100% (I_L=3.2).....167

5.25 Viscosity readings for w=100% (I_L=3.2).....167

5.26 Thixotropic viscosity ratios to 680 days.....168

5.27 Thixotropic viscosity ratios to 500 hours.....169

5.28 Thixotropic viscosity ratios to 240 hours.....169

5.29 Residual/remoulded viscosity ratios.....170

5.30 Residual/remoulded viscosity ratios to 600 hours 171

5.31 Residual/remoulded viscosity ratios to 240 hours 171

5.32 Liquidity index-residual viscosity relationship for sludge.....172

5.33 Shear strength vs. time for sludge 400 - 16,320 hrs 173

5.34 Shear strength vs. time for sludge 400 - 240 hrs 173

5.35 Shear strength vs. time for sludge 400 - 16,320 hrs 173

5.36 Shear strength for w=400% (I_L=15.2) 174

5.37 Shear strength for w=400% (I_L=15.2) 174

5.38 Shear strength vs. time for sludge 300 - 16,320 hrs 175

5.39 Shear strength vs. time for sludge 300 - 240 hrs 175

5.40 Shear strength vs. time for sludge 300 - 16,320 hrs 175

5.41 Shear strength for w=300% (I_L=11.2) 176

5.42 Shear strength for w=300% (I_L=11.2) 176

5.43 Shear strength vs. time for sludge 233 - 16,320 hrs 177

Figure Page

5.44 Shear strength vs. time for sludge 233 - 240 hrs 177
5.45 Shear strength vs. time for sludge 233 - 16,320 hrs 177
5.46 Shear strength for w=233% (I_L=8.5) 178
5.47 Shear strength for w=233% (I_L=8.5) 178
5.48 Shear strength vs. time for sludge 150 - 16,320 hrs 179
5.49 Shear strength vs. time for sludge 150 - 240 hrs 179
5.50 Shear strength vs. time for sludge 150 - 16,320 hrs 179
5.51 Shear strength for w=150% (I_L=5.2) 180
5.52 Shear strength for w=150% (I_L=5.2) 180
5.53 Shear strength vs. time for sludge 100 - 16,320 hrs 181
5.54 Shear strength vs. time for sludge 100 - 240 hrs 181
5.55 Shear strength vs. time for sludge 100 - 16,320 hrs 181
5.56 Shear strength for w=150% (I_L=3.2) 182
5.57 Shear strength for w=150% (I_L=3.2) 182
5.58 Shear strength vs. time for sludge 47 - 16,320 hrs.....183
5.59 Shear strength vs. time for sludge 47 - 240 hrs.....183
5.60 Shear strength vs. time for sludge 47 - 16,320 hrs.....183
5.61 Shear strength for w=47% (I_L=1.0) 184
5.62 Shear strength for w=47% (I_L=1.0) 184
5.63 Thixotropic strength ratios to 700 days.....185
5.64 Thixotropic strength ratios to 600 hrs.....186
5.65 Thixotropic strength ratios to 240 hrs.....186
5.66 Residual/remoulded shear strength ratios to 680 days 187
5.67 Residual/remoulded shear strength ratios to 600 hours 188
5.68 Residual/remoulded shear strength ratios to 240 hours 188
5.69 Influence of water content on thixotropic ratio 189

Figure Page

5.70 Influence of water content on residual/remoulded strength ratio.....190

5.71 Liquidity index-residual shear strength relationship.....191

5.72 Liquidity index-residual shear strength relationship at low range of I_L 192

5.73 Shear strength and viscosity ratios for w=400% 193

5.74 Shear strength and viscosity ratios for w=400% 193

5.75 Shear strength and viscosity ratios for w=300% 194

5.76 Shear strength and viscosity ratios for w=300% 194

5.77 Shear strength and viscosity ratios for w=233% 195

5.78 Shear strength and viscosity ratios for w=233% 195

5.79 Shear strength and viscosity ratios for w=150% 196

5.80 Shear strength and viscosity ratios for w=150% 196

5.81 Shear strength and viscosity ratios for w=100% 197

5.82 Shear strength and viscosity ratios for w=100% 197

5.83 Comparison to other sludge testing.....198

5.84 Self-weight consolidation of sludge 199

5.85 Thixotropic ratio in some typical clays and sludge 200

5.86 Thixotropic ratio in three clay minerals and sludge.....201

5.87 Effect of liquidity index on thixotropic ratio at 100 days 202

A.1 Viscosity test V40000M.....214

A.2 Viscosity test V40005M.....214

A.3 Viscosity test V40010M.....214

A.4 Viscosity test V40020M.....215

A.5 Viscosity test V40030M.....215

A.6 Viscosity test V40001H.....215

A.7 Viscosity test V40002H.....216

Figure Page

A.8 Viscosity test V40003H....216
A.9 Viscosity test V40004H....216
A.10 Viscosity test V40008H....217
A.11 Viscosity test V40012H....217
A.12 Viscosity test V40018H....217
A.13 Viscosity test V40024H....218
A.14 Viscosity test V40002D....218
A.15 Viscosity test V40003D....218
A.16 Viscosity test V40004D....219
A.17 Viscosity test V40005D....219
A.18 Viscosity test V40010D....219
A.19 Viscosity test V40020D....220
A.20 Viscosity test V40033D....220
A.21 Viscosity test V40040D....220
A.22 Viscosity test V40064D....221
A.23 Viscosity test V40070D....221
A.24 Viscosity test V40160D....221
A.25 Viscosity test V40470D....222
A.26 Viscosity test V40680D....222
A.27 Viscosity test V30000M....222
A.28 Viscosity test V30005M....223
A.29 Viscosity test V30010M....223
A.30 Viscosity test V30020M....223
A.31 Viscosity test V30030M....224
A.32 Viscosity test V30001H....224
A.33 Viscosity test V30002H....224

Figure Page

A.34 Viscosity test V30003H....225
A.35 Viscosity test V30004H....225
A.36 Viscosity test V30008H....225
A.37 Viscosity test V30012H....226
A.38 Viscosity test V30018H....226
A.39 Viscosity test V30024H....226
A.40 Viscosity test V30002D....227
A.41 Viscosity test V30003D....227
A.42 Viscosity test V30004D....227
A.43 Viscosity test V30005D....228
A.44 Viscosity test V30006D....228
A.45 Viscosity test V30010D....228
A.46 Viscosity test V30020D....229
A.47 Viscosity test V30040D....229
A.48 Viscosity test V30050D....229
A.49 Viscosity test V30160D....230
A.50 Viscosity test V30470D....230
A.51 Viscosity test V30660D....230
A.52 Viscosity test V23000M....231
A.53 Viscosity test V23005M....231
A.54 Viscosity test V23010M....231
A.55 Viscosity test V23020M....232
A.56 Viscosity test V23030M....232
A.57 Viscosity test V23001H....232
A.58 Viscosity test V23002H....233
A.59 Viscosity test V23003H....233

Figure Page

A.60 Viscosity test V23004H....233
A.61 Viscosity test V23008H....234
A.62 Viscosity test V23012H....234
A.63 Viscosity test V23018H....234
A.64 Viscosity test V23001D....235
A.65 Viscosity test V23002D....235
A.66 Viscosity test V23003D....235
A.67 Viscosity test V23004D....236
A.68 Viscosity test V23005D....236
A.69 Viscosity test V23010D....236
A.70 Viscosity test V23020D....237
A.71 Viscosity test V23040D....237
A.72 Viscosity test V23075D....237
A.73 Viscosity test V23090D....238
A.74 Viscosity test V23494D....238
A.75 Viscosity test V23682D....238
A.76 Viscosity test V15000M....239
A.77 Viscosity test V15005M....239
A.78 Viscosity test V15010M....239
A.79 Viscosity test V15020M....240
A.80 Viscosity test V15030M....240
A.81 Viscosity test V15001H....240
A.82 Viscosity test V15002H....241
A.83 Viscosity test V15003H....241
A.84 Viscosity test V15004H....241
A.85 Viscosity test V15008H....242

Figure Page

A.86 Viscosity test V15012H....242
A.87 Viscosity test V15018H....242
A.88 Viscosity test V15001D....243
A.89 Viscosity test V15002D....243
A.90 Viscosity test V15003D....243
A.91 Viscosity test V15004D....244
A.92 Viscosity test V15005D....244
A.93 Viscosity test V15010D....244
A.94 Viscosity test V15020D....245
A.94 Viscosity test V15030D....245
A.95 Viscosity test V15040D....245
A.96 Viscosity test V15051D....246
A.97 Viscosity test V15092D....246
A.98 Viscosity test V15470D....246
A.100 Viscosity test V15680D....247
A.101 Viscosity test V10000M....247
A.102 Viscosity test V1005M....247
A.103 Viscosity test V10010M....248
A.104 Viscosity test V10020M....248
A.105 Viscosity test V10030M....248
A.106 Viscosity test V10001H....249
A.107 Viscosity test V10002H....249
A.108 Viscosity test V10003H....249
A.109 Viscosity test V10004H....250
A.110 Viscosity test V10008H....250
A.111 Viscosity test V10012H....250

Figure Page

A.112 Viscosity test V10018H....251
A.113 Viscosity test V10001D....251
A.114 Viscosity test V10002D....251
A.115 Viscosity test V10003D....252
A.116 Viscosity test V10004D....252
A.117 Viscosity test V10005D....252
A.118 Viscosity test V10006D....253
A.119 Viscosity test V10010D....253
A.120 Viscosity test V10020D....253
A.121 Viscosity test V10021D....254
A.122 Viscosity test V10040D....254
A.123 Viscosity test V10095D....254
A.124 Viscosity test V10473D....255
A.125 Viscosity test V10680D....255
B.1 Apparent viscosity V40000M....257
B.2 Apparent viscosity V4000....257
B.3 Apparent viscosity V40010M....257
B.4 Apparent viscosity V40020M....258
B.5 Apparent viscosity V40030M....258
B.6 Apparent viscosity V40001H....258
B.7 Apparent viscosity V40002H....259
B.8 Apparent viscosity V40003H....259
B.9 Apparent viscosity V40004H....259
B.10 Apparent viscosity V40008H....260
B.11 Apparent viscosity V40012H....260
B.12 Apparent viscosity V40018H....260

Figure Page

B.13 Apparent viscosity V40001D....261
B.14 Apparent viscosity V40002D....261
B.15 Apparent viscosity V40003D....261
B.16 Apparent viscosity V40004D....262
B.17 Apparent viscosity V40005D....262
B.18 Apparent viscosity V40010D....262
B.19 Apparent viscosity V40020D....263
B.20 Apparent viscosity V40033D....263
B.21 Apparent viscosity V40040D....263
B.22 Apparent viscosity V40064D....264
B.23 Apparent viscosity V40070D....264
B.24 Apparent viscosity V40160D....264
B.25 Apparent viscosity V40470D....265
B.26 Apparent viscosity V40680D....265
B.27 Apparent viscosity V30000M....265
B.28 Apparent viscosity V30005M....266
B.29 Apparent viscosity V30010M....266
B.30 Apparent viscosity V30020M....266
B.31 Apparent viscosity V30030M....267
B.32 Apparent viscosity V30001H....267
B.33 Apparent viscosity V30002H....267
B.34 Apparent viscosity V30003H....268
B.35 Apparent viscosity V30004H....268
B.36 Apparent viscosity V30008H....268
B.37 Apparent viscosity V30012H....269
B.38 Apparent viscosity V30018H....269

Figure Page

B.39 Apparent viscosity V30001D....269
B.40 Apparent viscosity V30002D....270
B.41 Apparent viscosity V30003D....270
B.42 Apparent viscosity V30004D....270
B.43 Apparent viscosity V30005D....271
B.44 Apparent viscosity V30006D....271
B.45 Apparent viscosity V30010D....271
B.46 Apparent viscosity V30020D....272
B.47 Apparent viscosity V30040D....272
B.48 Apparent viscosity V30050D....272
B.49 Apparent viscosity V30160D....273
B.50 Apparent viscosity V30470D....273
B.51 Apparent viscosity V30660D....273
B.52 Apparent viscosity V23000M....274
B.53 Apparent viscosity V23005M....274
B.54 Apparent viscosity V23010M....274
B.55 Apparent viscosity V23020M....275
B.56 Apparent viscosity V23030M....275
B.57 Apparent viscosity V23001H....275
B.58 Apparent viscosity V23002H....276
B.59 Apparent viscosity V23003H....276
B.60 Apparent viscosity V23004H....276
B.61 Apparent viscosity V23008H....277
B.62 Apparent viscosity V23012H....277
B.63 Apparent viscosity V23018H....277
B.64 Apparent viscosity V23001D....278

Figure Page

B.65 Apparent viscosity V23002D....278
B.66 Apparent viscosity V23003D....278
B.67 Apparent viscosity V23004D....279
B.68 Apparent viscosity V23005D....279
B.69 Apparent viscosity V23010D....280
B.70 Apparent viscosity V23020D....280
B.71 Apparent viscosity V23040D....281
B.72 Apparent viscosity V23075D....281
B.73 Apparent viscosity V23090D....281
B.74 Apparent viscosity V23494D....282
B.75 Apparent viscosity V23682D....282
B.76 Apparent viscosity V15000M....282
B.77 Apparent viscosity V15005M....283
B.78 Apparent viscosity V15010M....283
B.79 Apparent viscosity V15020M....283
B.80 Apparent viscosity V15030M....284
B.81 Apparent viscosity V15001H....284
B.82 Apparent viscosity V15002H....284
B.83 Apparent viscosity V15003H....285
B.84 Apparent viscosity V15004H....285
B.85 Apparent viscosity V15008H....285
B.86 Apparent viscosity V15012H....286
B.87 Apparent viscosity V15018H....286
B.88 Apparent viscosity V15001D....286
B.89 Apparent viscosity V15002D....287
B.90 Apparent viscosity V15003D....287

Figure Page

B.91 Apparent viscosity V15004D....287
B.92 Apparent viscosity V15005D....288
B.93 Apparent viscosity V15010D....288
B.94 Apparent viscosity V15020D....288
B.95 Apparent viscosity V15030D....289
B.96 Apparent viscosity V15040D....289
B.97 Apparent viscosity V15051D....289
B.98 Apparent viscosity V15092D....290
B.99 Apparent viscosity V15470D....290
B.100 Apparent viscosity V15680D....290
B.101 Apparent viscosity V10000M....291
B.102 Apparent viscosity V10005M....291
B.103 Apparent viscosity V10010M....291
B.104 Apparent viscosity V10020M....292
B.105 Apparent viscosity V10030M....292
B.106 Apparent viscosity V10001H....292
B.107 Apparent viscosity V10002H....293
B.108 Apparent viscosity V10003H....293
B.109 Apparent viscosity V10004H....293
B.110 Apparent viscosity V10008H....294
B.111 Apparent viscosity V10012H....294
B.112 Apparent viscosity V10018H....294
B.113 Apparent viscosity V10001D....295
B.114 Apparent viscosity V10002D....295
B.115 Apparent viscosity V10003D....295
B.116 Apparent viscosity V10004D....296

Figure Page

B.117 Apparent viscosity V10005D....296
B.118 Apparent viscosity V10010D....296
B.119 Apparent viscosity V10001D....297
B.120 Apparent viscosity V10020D....297
B.121 Apparent viscosity V10021D....297
B.122 Apparent viscosity V10040D....298
B.123 Apparent viscosity V10095D....298
B.124 Apparent viscosity V10473D....298
B.125 Apparent viscosity V10680D....299
C.1 Vane shear test S40000M....301
C.2 Vane shear test S40002HR....302
C.3 Vane shear test S40002HP....302
C.4 Vane shear test S40008HR....303
C.5 Vane shear test S40008HP....303
C.6 Vane shear test S40001DR....304
C.7 Vane shear test S40001DP....304
C.8 Vane shear test S40002DR....305
C.9 Vane shear test S40002DP....305
C.10 Vane shear test S40005DR....306
C.11 Vane shear test S40005DP....306
C.12 Vane shear test S40010DR....307
C.13 Vane shear test S40010DP....307
C.14 Vane shear test S40020DR....308
C.15 Vane shear test S40020DP....308
C.16 Vane shear test S40033DR....309
C.17 Vane shear test S40033DP....309

Figure Page

C.18 Vane shear test S40040DR....310
C19 Vane shear test S40040DP....310
C.20 Vane shear test S40050DR....311
C.21 Vane shear test S40050DP....311
C.22 Vane shear test S40060DR....312
C.23 Vane shear test S40060DP....312
C.24 Vane shear test S40070DR....313
C.25 Vane shear test S40070DP....313
C.26 Vane shear test S40160DR....314
C.27 Vane shear test S40160DP....314
C.28 Vane shear test S40470DR....315
C.29 Vane shear test S40470DP....315
C.30 Vane shear test S40680DR....316
C.31 Vane shear test S40680DP....316
C.32 Vane shear test S30000M....317
C.33 Vane shear test S30002HR....318
C.34 Vane shear test S30002HP....318
C.35 Vane shear test S30008HR....319
C.36 Vane shear test S30008HP....319
C.37 Vane shear test S30001DR....320
C.38 Vane shear test S30001DP....320
C.39 Vane shear test S30002DR....321
C.40 Vane shear test S30002DP....321
C.41 Vane shear test S30006DR....322
C.42 Vane shear test S30006DP....322
C.43 Vane shear test S30010DR....323

Figure Page

C.44 Vane shear test S30010DP....323
C.45 Vane shear test S30020DR....324
C.46 Vane shear test S30020DP....324
C.47 Vane shear test S30030DR....325
C.48 Vane shear test S30030DP....325
C.49 Vane shear test S30041DR....326
C.50 Vane shear test S30041DP....326
C.51 Vane shear test S30050DR....327
C.52 Vane shear test S30050DP....327
C.53 Vane shear test S30160DR....328
C.54 Vane shear test S30160DP....328
C.55 Vane shear test S30470DR....329
C.56 Vane shear test S30470DP....329
C.57 Vane shear test S30680DR....330
C.58 Vane shear test S30680DP....330
C.59 Vane shear test S23000M....331
C.60 Vane shear test S23002HR....332
C.61 Vane shear test S23002HP....332
C.62 Vane shear test S23008HR....333
C.63 Vane shear test S23008HP....333
C.64 Vane shear test S23001DR....334
C.65 Vane shear test S23001DP....334
C.66 Vane shear test S23002DR....335
C.67 Vane shear test S23002DP....335
C.68 Vane shear test S23005DR....336
C.69 Vane shear test S23005DP....336

Figure Page

C.70 Vane shear test S23010DR....337
C.71 Vane shear test S23010DP....337
C.72 Vane shear test S23020DR....338
C.73 Vane shear test S23020DP....338
C.74 Vane shear test S23030DR....339
C.75 Vane shear test S23030DP....339
C.76 Vane shear test S23041DR....340
C.77 Vane shear test S23041DP....340
C.78 Vane shear test S23050DR....341
C.79 Vane shear test S23050DP....341
C.80 Vane shear test S23072DR....342
C.81 Vane shear test S23072DP....342
C.82 Vane shear test S23090DR....343
C.83 Vane shear test S23090DP....343
C.84 Vane shear test S23490DR....344
C.85 Vane shear test S23490DP....344
C.86 Vane shear test S23680DR....345
C.87 Vane shear test S23680DP....345
C.88 Vane shear test S15000M....346
C.89 Vane shear test S15002HR....347
C.90 Vane shear test S15002HP....347
C.91 Vane shear test S15008HR....348
C.92 Vane shear test S15008HP....348
C.93 Vane shear test S15020HR....349
C.94 Vane shear test S15020HP....349
C.95 Vane shear test S15001DR....350

Figure Page

C.96 Vane shear test S15001DP....350
C.97 Vane shear test S15002DR....351
C.98 Vane shear test S15002DP....351
C.99 Vane shear test S15003DR....352
C.100 Vane shear test S15003DP....352
C.101 Vane shear test S15005DR....353
C.102 Vane shear test S15005DP....353
C.103 Vane shear test S15010DR....354
C.104 Vane shear test S15010DP....354
C.105 Vane shear test S15020DR....355
C.106 Vane shear test S15020DP....355
C.107 Vane shear test S15040DR....356
C.108 Vane shear test S15040DP....356
C.109 Vane shear test S15045DR....357
C.110 Vane shear test S15045DP....357
C.111 Vane shear test S15090DR....358
C.112 Vane shear test S15090DP....358
C.113 Vane shear test S15470DR....359
C.114 Vane shear test S15470DP....359
C.115 Vane shear test S15680DR....360
C.116 Vane shear test S15680DP....360
C.117 Vane shear test S15684DR....361
C.118 Vane shear test S15684DP....361
C.119 Vane shear test S10000M....362
C.120 Vane shear test S10002HR....363
C.121 Vane shear test S10002HP....363

Figure Page

C.122 Vane shear test S10008HR 364
C.123 Vane shear test S10008HP 364
C.124 Vane shear test S10001DR....365
C.125 Vane shear test S10001DR....365
C.126 Vane shear test S10002DR....366
C.127 Vane shear test S10002DP....366
C.128 Vane shear test S10005DR....367
C.129 Vane shear test S10005DP....367
C.130 Vane shear test S10006DR....368
C.131 Vane shear test S10006DP....368
C.132 Vane shear test S10010DR....369
C.133 Vane shear test S10010DR....369
C.134 Vane shear test S10015DP....370
C.135 Vane shear test S10020DR....371
C.136 Vane shear test S10020DP....371
C.137 Vane shear test S10040DR....372
C.138 Vane shear test S10040DP....372
C.139 Vane shear test S10090DR....373
C.140 Vane shear test S10090DP....373
C.141 Vane shear test S10470DR....374
C.142 Vane shear test S10470DP....374
C.143 Vane shear test S10680DR....375
C.144 Vane shear test S10680DP....375
C.145 Vane shear test S10701DR....376
C.146 Vane shear test S10701DP....376
C.147 Vane shear test S47000M 377

Figure Page

C.148 Vane shear test S47002HR 378
C.149 Vane shear test S47002HP 378
C.150 Vane shear test S47008HR 379
C.151 Vane shear test S47008HP 379
C.152 Vane shear test S47001DR....380
C.153 Vane shear test S47001DP....380
C.154 Vane shear test S47002DR....381
C.155 Vane shear test S47002DP....381
C.156 Vane shear test S47005DR....382
C.157 Vane shear test S47005DP....382
C.158 Vane shear test S47007DR....383
C.159 Vane shear test S47007DP....383
C.160 Vane shear test S47010DR....384
C.161 Vane shear test S47010DP....384
C.162 Vane shear test S47021DR....385
C.163 Vane shear test S47021DP....385
C.164 Vane shear test S47060DR....386
C.165 Vane shear test S47060DP....386
C.166 Vane shear test S47087DR....387
C.167 Vane shear test S47087DP....387
C.168 Vane shear test S47160DR....388
C.169 Vane shear test S47160DP....388
C.170 Vane shear test S47181DP....389
C.171 Vane shear test S47194DR....390
C.172 Vane shear test S47194DP....390
C.173 Vane shear test S47410DR....391

Figure Page

C.174 Vane shear test S47410DP.....391

C.175 Vane shear test S47460DR.....392

C.176 Vane shear test S47460DP.....392

C.177 Vane shear test S47510DP.....393

C.178 Vane shear test S47523DR.....394

C.179 Vane shear test S47523DP.....394

List of Plates

Plate		Page
3.1	Sludge Containers	63
3.2	Brookfield Viscometer with a T-bar Spindle	65
3.3	Torque Cell Calibration System	66
3.4	Torque Cell and Moment Cylinder	67

1. INTRODUCTION

1.1 Definition of Problem

Society's increasing awareness of environmental issues has brought stricter pollution regulations to industrial operations. The mining industry has traditionally produced vast amounts of waste which cause disposal problems. In surface mining operations, the resulting waste, tailings, are generally in the form of a slurry. The common method of disposal of a slurry is to transport and contain then in a pond that can cover a large area; tens of square kilometers in the case of oil sands plants.

In northern Alberta, production of synthetic bitumen from oil sand deposits has resulted in open pit mining operations on a large scale. Syncrude Canada Ltd. removes in excess of 22 million cubic metres of overburden on an annual basis in order to secure access to the oil sands (Lord and Isaac, 1989). The annual oil sands feed for the extraction process reached more than 100 million tonnes in 1987 (MacKinnon, 1989) which resulted in 85 million tonnes of tailings solids. In the first ten years of operation, Syncrude's tailings pond has accumulated 215 million cubic metres of sludge and waste water. The tailings pond and dykes occupy an area of 22 km^2.

The continuous growth of the pond is caused by extremely slow rates of consolidation of the oil sands tailings sludge contained in the pond. It has been recognized that one of the main factors negatively affecting consolidation of the sludge is the thixotropic gain in strength of the material.

In order to improve existing disposal methods and assess the feasibility of new schemes, a thorough understanding of the long term consolidation and strength behaviour of the sludge is necessary. Consolidation of the sludge has

been investigated both in the field and the laboratory, however studies have not arrived at a comprehensive long term model of its behaviour.

At present, little is known about the factors influencing the consolidation of the oil sands tailings sludge. Very limited laboratory and field data exist concerning the time dependent strength properties of the material.

1.2 Objective of Research Program

The purpose of the research program in this thesis is to determine the time dependent strength behaviour of the oil sands tailings sludge. Thixotropic properties of the sludge will be described in both qualitative and quantitative terms. The influence of such factors as: time, water content and self-weight consolidation on thixotropy of the sludge will be investigated and determined. Comparisons to other very soft soils will be made.

To gather the necessary information to analyze the problem, the development of laboratory equipment and procedures were required. The equipment had to be capable of determining the strength parameters of the soil in both the undisturbed and remoulded state. Different methods of testing were employed; new methods were tried and assessed and existing methods were modified to suit the needs of the test program.

1.3 Scope of Thesis

The laboratory tests to determine the time dependent strength properties of the oil sands tailings sludge were performed by two methods; viscosity measurements and undrained shear vane testing. In addition, initial work was performed with a novel testing method; the cavity expansion test. Self-weight consolidation measurements were carried out throughout the test program. The viscosity measurements yielded peak and residual index strength

properties. The shear vane testing determined real values of peak and residual undrained shear strength.

Sludges of six different water contents were prepared and tested for their strength. Water contents ranged from 47% (the liquid limit of the material) to 400%. The tests were performed at different elapsed time intervals after complete remoulding; the times varied from 0 to 700 days.

The test results allowed for the rheological classification of the sludge and for the development of relationships between time and both peak and residual shear strength. The results are also used to determine a correlation between water content and thixotropy. The consolidation measurements are used to describe the role of self-weight consolidation in thixotropic hardening.

The relationship between liquidity index and residual shear strength of the sludge is derived and compared to empirical correlations found for other soils. A comparison of thixotropy in the oil sands tailings sludge to other soils is made.

The determination of such rheological parameters of the slurry as viscosity and yield strength is beyond the scope of this thesis. As well, the investigation and analysis of microstructural physico-chemical processes responsible for thixotropic phenomenon is left for further research.

1.4 Organization of Thesis

Throughout the body of this thesis, all corresponding figures and tables are presented at the end of each individual chapter.

Chapter 2 contains a survey of literature relevant to this work. Background information on the oil sands tailings sludge is presented. The phenomenon of thixotropy is then described in detail. Soft soil behaviour and testing are also reviewed.

Chapter 3 describes the laboratory equipment developed and fabricated for this testing program and presents the test procedures that were followed. The description of the material that was tested is also included in this Chapter.

The results of the laboratory tests are given in Chapter 4. The viscosity measurements are presented first, and the vane shear strength results follow. Only selected figures from the tests are presented. The complete sets of the laboratory data is presented in the figures contained in Appendices A, B and C.

The analysis and discussion of the experimental results are presented in Chapter 5. The findings are compared with other research.

Chapter 6 summarizes the important conclusions and observations that were developed throughout the thesis and makes recommendations for further research.

2. LITERATURE REVIEW

2.1 Oil Sands Tailings

2.1.1 Origin

Oil sands in Alberta, located in deposits in the northern part of the province, contain about 900 billion barrels of crude bitumen. Of the three large main deposits, underlying an estimated area of 48,000 square kilometers, the McMurray Formation in the Athabasca deposit is the largest having oil reserves exceeding 146 billion cubic meters over an area of 32,000 square kilometers (Berkowitz and Speight, 1975; Outtrim and Evans, 1978). About 10% of the Athabasca deposit is economically recoverable by surface mining (less than 45 m of overburden) and it is the only one on which commercial oil sand mining operations currently exist.

Athabasca oil sand is a Lower Cretaceous, fine to medium grained uniform sand of 30% average porosity, containing two pore fluids, bitumen and water, and occasionally some free gas. The sand structure is dense and interpenetrative owing to diagenesis which resulted in dissolution and recrystallization of quartz at grain boundaries during the time of burial. The sand grains are water wet with the majority of the water occurring as pendular rings surrounding the grain-to- grain contact points. The water forms a continuous phase throughout the oil sand matrix. Bitumen occupies the remaining pore space and also forms a continuous phase throughout the oil sand structure. Gases are dissolved within the liquid phases and depending on in situ temperatures and pressures are occasionally present as free gas (Scott and Kosar, 1984; Takamura, 1982). The bitumen content (as a percentage of the bulk mass) ranges from 0 to 20% and averages around 11%. The amount of water relative to the bulk mass varies from 3 to 6% (average 5%). The sand

accounts for approximately 70% of the oil sand mass and the fines, clay and silt particles, average 14% (Pollock, 1988). Clay minerals are present in this formation in fine-grained basal deposits, in uppermost strata as dense clayey silts and clay beds up to a meter thick, in oil-free silt seams in the oil-rich zone, in sand pores as authigenic clays, and in rip-up clasts. The uppermost and lowermost McMurray Formation beds are of low oil content, and are not used for bitumen extraction (Dusseault et al., 1989).

2.1.2 Oil Sand Operations

There are two oil sand surface mining operations in the Athabasca deposit. They are Syncrude Canada Ltd. and Suncor Ltd. Both use similar processes in heavy oil recovery. Oil sands open pit mines are developed by removing glacial deposits, clayey Clearwater Formation strata, and upper McMurray Formation overburden and depositing them in the mined-out area or in overburden dumps. The bituminous sands are mined using bucketwheels or draglines. Ore is conveyed to a stockpile or blending facility from which a feedstock goes to an extraction process (Dusseault et al., 1989). The bitumen is extracted by the Clark Hot Water Process which is a hot water froth-flotation process. The bitumen is upgraded to a conventional refinery feedstock by coking to remove carbon and hydrotreating to add hydrogen (Dusseault and Scott, 1982). Details of the extraction process can be found elsewhere (Adam, 1985). Between 1978 and 1987 Syncrude Canada Ltd. extracted about 65 x 10^6 m^3 of bitumen from oil sands and produced over 50 x 10^6 m^3 of synthetic crude oil (MacKinnon, 1989). The extraction process requires large quantities of water: 1 m^3 of oil sand feed uses 1.8 m^3 of water (or about 15 m^3 of water per 1 m^3 of synthetic crude oil). The resulting waste stream is a mixture of the so' mineral matter initially present in the ore, the hot water and the caustic so

(NaOH) added to achieve efficient separation, and the unrecovered portion of the bitumen. The unrecovered bitumen is usually about 5-10% of the original bitumen content. Other waste materials are the solid mine overburden, which is transported and dumped, and the high carbon content product of the coking system which is either burned as fuel or stockpiled for possible later use (Dusseault and Scott, 1982). The fluid wastes are contained in a tailings pond in the northern part of Syncrude's Lease 17. The pond is built around the former Beaver Creek valley and is enclosed by dykes and beaches composed of compacted tailings sand. The tailings stream solids content is dominated by sand-sized quartz grains and is coarse-grained with a small proportion of fine-grained material. The tailings slurry, pumped at a solids content of 50 to 55%, is transported by a pipeline system to the dykes where the sand containing some fines is used to build the pond dykes and beaches. The tailings stream amounts to 130 x 10^6 metric tonnes every year (Scott and Cymerman, 1984) and the projected tailings pond surface water area is 17 square kilometers (MacKinnon, 1989). The total area disturbed by the pond and the dikes amounts to 22 km^2. Approximately 44 x 10^6 m^3 of sand is deposited per year (300 x 10^6 m^3 total up to 1987). The remaining solids form a thin slurry (7 - 10% solids by mass) which flows into the pond. The fines stream settles out and consolidates fairly rapidly to a solids content of 20%. However, the large volume of mining results in approximately 14 x 10^6 m^3 of liquid sludge forming every year. Water released during sedimentation and consolidation is returned to the plant for reuse. About 70% of the plant water requirements are reclaimed from the pond (MacKinnon, 1989). The volume of water and sludge in the pond is growing at a rate of about 0.25 m^3 per tonne of oil sand feed.

The major components of the tailings pond include: water (clarified water in the surface zone and water in the sludge), mineral solids (sands, silts, clays),

dissolved solids (inorganic and organic components, process chemicals, and leachates), and bitumen (unrecovered during extraction). The pond exhibits stratification with several distinctive zones as recognized by MacKinnon (1989) (Figure 2.1):

- "Free" Water Zone (0 -10 m depth),
- Sludge Interface (10-11 m depth),
- "Immature" Sludge Zone (11-17 m depth) - upper 7 m of the sludge zone where the initial settling and consolidation of the sludge occurs during first 2-3 years,
- "Mature" Sludge Zone (>17 m depth) - lower sludge zone where the later stages of consolidation occur. Solids content increases with depth. Sludge in this zone is greater than three years in age.

Sedimentation of the sludge is a fairly rapid process and the pond is, as concluded by Scott and Dusseault (1982), MacKinnon (1989) and others, an effective settling area for the oil sands tailings. The fines settle rapidly to a density at which the principle of effective stress governs further consolidation behaviour. Further consolidation after this initial consolidation is very slow and causes concern.

2.1.3 Oil Sands Tailings Sludge

The grain size analysis of the sludge shows that it is about 5% fine-grained sand, 30% silt size and 65% clay size (Scott and Dusseault, 1980). Typical grain size distribution curves of tailings sands and tailings sludge are shown in Figure 2.2 (after Scott and Cymerman, 1984). The clay mineralogy of the sludge is dominated by kaolinite and illite clays. Smectite is present in very small amounts and comes almost exclusively from the upper portion of the McMurray Formation. Vermiculite is present as a minor ingredient and comes

from the lower part of the formation. Chlorite is uncommon. Mixed layered clays are common, but seldom exceed 10% of the total clay minerals present (Scott et al., 1985). Roberts et al. (1980) reports approximately 80% kaolinite, 15% illite, about 1.5% each of montmorillonite and chlorite, and 2% mixed layer clay minerals. Kessick (1980) states 65% kaolinite and 35% illite for the clay mineral fraction of sludge, whereas Dusseault et al. (1989) summarize that the sludge is dominantly kaolinite (55-65%) and illite (30-40%), with minute traces of mixed-layer clay minerals. Sludge mineral composition is consistent over time and from place to place in the pond because the ore-body mineralogy is consistent, ore is blended before extraction, and mixing occurs during extraction, transportation and deposition (Dusseault et al., 1989). The bitumen content in the sludge based on the total mass of the sludge averaged around 2.1% by 1986 (MacKinnon, 1989) for 31% solids. If the bitumen is calculated as a percent of the mass of the mineral solids, its content is 6.8%.

From the predominance of silt and low plastic clay in the sludge solids it would be expected to classify the material on the plasticity chart as a low plastic clay. However, the presence of bitumen and the fact that the clay minerals are well dispersed during the extraction process influence the plasticity of the material. Scott et al. (1985) report the range of Atterberg limit data from the sludge. The liquid limit varies from 40 to 80% and the plasticity index ranges from less than 20 to slightly higher than 50%. In addition to variations in clay mineralogy, the range reflects such factors as ionic concentration and bitumen content. The same authors conclude that the higher values of Atterberg limits in general indicate greater bitumen content and finer-grained sludge.

The oil sands tailings sludge exhibits a characteristic called thixotropy. Thixotropy, or gel strength, of the sludge was first reported by Kessick (1979).

It is interesting that the clay minerals present in the sludge do not show significant thixotropic effects as is discussed in Section 2.3. It is the additives, intense agitation and elevated temperature (85° C) during the extraction process that make the clay particles well dispersed. Kessick (1979) postulates three conditions necessary for the sludge to form a gel structure at its normal pH:

- the presence of residual bitumen,
- the presence of a clay bound organic component to confer surface activity on the clay particles,
- the clay particles must have been initially well dispersed.

There is evidence that some of the organic material in the sludge is intimately bound to the clays and even in situ the clays have vestigal tannic or lignic material adsorbed on surfaces (Scott et al, 1985; Kessick, 1979). Humic material and asphaltenes are suggested to be the dominant organic molecules. An increase in organic content as grain size decreases was also reported (Scott et al., 1985). The same authors also investigated thixotropic behaviour of the sludge and found that gel strength development is meaningful for any sludge of solids content 20% (400% water content) by weight or greater. They attribute the high gel strength to the high residual bitumen content, as ordinary kaolinite/illite slurries do not show such increases. On the other hand, Danielson and MacKinnon (1990) conclude in their research that the presence of bitumen does not appear to be the controlling factor in the gel strength of the sludge.

The significance of the development of thixotropic strength in the sludge is reflected in hindrance of the consolidation of sludge at low stresses. The development of an effective stress without loss of water seriously retards the process of water efflux under self-weight at low stresses (Scott and Dusseault,

1980; Scott et al., 1985). In effect, the upper metres of the sludge in the pond do not achieve the solids content expected, when compared to other materials, in as short a time. An apparent shear strength as a result of thixotropic hardening can also be beneficial if it is required to suspend coarse material such as sand in the sludge by mixing. At greater depths in the pond, according to Scott et al., 1985, thixotropy loses some of its significance as other stresses build up and gel strength contributes only a small percentage to effective stress.

2.2 Thixotropy

The term thixotropy was originally coined to describe an isothermal, reversible gel-sol (solid-liquid) transition due to mechanical agitation (Mewis, 1979). This phenomenon takes place in many classes of materials such as crude oil and oil products, liquid crystals, rubber, greases and waxes, soils, foods and many others. Thixotropy is classified as a rheological process and from this perspective it is described as a continuous decrease in apparent viscosity with time under shear and a subsequent recovery of viscosity when the flow is discontinued (Mewis, 1979).

Thixotropy is of interest to the geotechnical engineer as studies suggest that the phenomenon is of general occurrence in the majority of clay-water systems. From the geotechnical point of view, thixotropy can be defined as a process of softening caused by remoulding, followed by a time-dependent return to the original harder state at a constant water content and constant porosity (Mitchell, 1960).

An analysis of the literature on thixotropy shows that there are two main approaches to the subject: microscopic and macroscopic. Osipov et al. (1984) give an in-depth view of microstructural changes of clay soils during

thixotropic strength loss and restoration. The scanning electron microscope is used as the main tool in this type of research. Although important in understanding the phenomenon, this approach is of greater interest to colloidal physicists. For this reason, any detailed discussion of the microstructure of clays associated with thixotropy would be beyond the scope of this thesis. The macroscopic approach to the subject was considered more relevant and was studied in detail. Factors affecting thixotropic behaviour of clays and properties affected by it along with laboratory findings are presented below.

Thixotropic effects in remoulded natural clays have been studied by Moretto (1948) and Skempton and Northey (1952). These investigations attempted to determine the extent to which thixotropic hardening could contribute to sensitivity of clays. Seed and Chan (1957) focused their attention on compacted clays and found that these soils may also exhibit appreciable thixotropic strength gain with time. Mitchell (1960) summarizes all aspects of thixotropy in a paper that is considered a classic on the subject. Many other authors (Locat et al., 1985, Bentley, 1979) discuss thixotropy usually in conjunction with sensitivity of clays.

Thixotropic strength gain is measured as a ratio of strength at time t to strength at time 0, immediately after remoulding (or compaction). For saturated clays, this ratio is called the acquired sensitivity and for compacted clays, the thixotropic strength ratio (Seed and Chan, 1957). It has been shown that this ratio can reach values as high as 6 (Moretto, 1948). Several factors have been pointed as directly affecting thixotropy. These are: the mineralogy of the clay, water content, rate of loading, axial strain and, of course, time. A brief discussion of each follows.

1. Clay mineralogy.

Skempton and Northey (1952) tested three clay minerals: kaolin, illite and bentonite. In their findings, kaolin exhibits almost no thixotropy and illite shows a moderate regain of its strength. In contrast, bentonite shows a remarkable regain at very short time intervals and continued regaining strength at a high rate even after a year. This suggests that clays with a high content of bentonite should exhibit high thixotropy while clays with a high kaolinite content will generally lack a strength regain. However, tests at the University of California have shown that even kaolinite may be made very thixotropic by the addition of a dispersing agent in order to reduce the degree of flocculation present in the natural material (Mitchell, 1960).

2. Water Content.

Water content appears to be of primary importance in thixotropic behaviour. Generally, thixotropic effects have been found to increase with increasing water content. Seed and Chan (1957) draw the lower boundary at the plastic limit and found that soils with water contents approaching the plastic limit showed no or very little thixotropy. On the other hand, Mitchell (1960) proves in his tests on samples with water contents near the plastic limit that thixotropy can be significant even at low water contents. The evidence is conflicting at water contents greater than the liquid limit. Skempton and Northey (1952) found that some of the soil samples were slightly less thixotropic at such water contents while others showed a significant increase in thixotropy. No explanation of this phenomenon has been found in the literature. Seed and Chan (1957) provide evidence that the magnitude of thixotropic effect is not related directly to the Atterberg limits. The liquidity

index was the only parameter that could be related to the thixotropic behaviour of the soil.

3. Rate of Loading.

In general, it has been found that for saturated clays the strength is reduced with a decrease in rate of loading. However, Seed and Chan (1957) argue that for a specimen whose strength is strongly influenced by thixotropy, the longer the duration of the test, the greater will be the thixotropic strength acquired by the specimen. Therefore, the total effect of an increase in time of loading will be a combination of the following two factors:

a) a tendency for the strength to decrease because of the increased time available for creep deformation,

b) a tendency for the strength to increase because of the increased time available for thixotropic effects to develop.

4. Axial Strain.

Seed and Chan (1957) investigated thixotropic strength ratios for different values of axial strain and concluded that thixotropic effects became increasingly significant at smaller strains. For example, the thixotropic strength ratio after one week for saturated samples was close to 1.9 for 1% axial strain and only 1.3 for 10% strain.

5. Time

Thixotropy is a time-dependent phenomenon, therefore time plays a key role in the process of strength regain. Tests on marine clays indicate two stages of strength recovery: a rapid one with a duration of about 15 minutes followed by a slower one of longer duration (Locat et al, 1985). Mitchell (1960) states that there appears to be no unique relationship between thixotropic strength ratio

and time. However, in all tests, strength of the specimens was increasing with time (the longest test duration was 610 days).

6. Thixotropy and Consolidation

Thixotropy can also affect such processes as consolidation by altering the compressibility of the soil. Mitchell (1960) argues that it would seem reasonable that thixotropic effects during consolidation lead to a smaller compression index, hence retarding the process, than would be obtained if there were no thixotropy. However, he recommends more detailed investigations on this subject.

7. Thixotropy and Sensitivity

Thixotropy is usually associated with sensitivity of clays. Skempton and Northey (1952) conclude from their work that whereas in clays with medium sensitivity it is possible that sensitivity may be due entirely to thixotropy, this could not be the case in sensitive and extra-sensitive clays where other factors such as leaching are mainly responsible for high sensitivity.

2.3 Soft Soil Behaviour

2.3.1 Uniqueness of Soft Soils

Soil mechanics is based on several principal concepts which are employed to describe soil behaviour. Perhaps, the most important principle is that of effective stress. It states that changes in effective stress rather than changes in total stress are responsible for the deformation of soil. Effective stress σ' is defined as the difference between total stress σ and pore fluid pressure u:

$$\sigma' = \sigma - u \qquad (2.1)$$

This equation states nothing about forces contributing to σ'. Chatterji and Morgenstern (1989) state that the "classical definition of effective stress has

been found to be inadequate in explaining the volume change and shear strength characteristics of swelling or active clay-water systems because it excludes the net physico-chemical forces of interaction present in such systems". If all microscopic interparticle forces are considered, the effective stress can be expressed as follows (Chatterji and Morgenstern, 1989):

$$\sigma' = \sigma'_i + (R - A) \qquad (2.2)$$

where σ' can be defined as the "apparent effective stress", σ'_i the "true effective stress", (R-A) the net interparticle stress due to the physico-chemical environment, and Equation (2.2) the "modified effective stress law" for active clay-water systems. R is a measure of repulsive (double layer) forces and A is the sum of attractive (Van der Waal's and electrostatic) forces.

Chatterji and Morgenstern (1989) carried out residual strength comparisons for large strain direct shear tests on sodium montmorillonite before and after leaching with distilled water under constant volume conditions. The researchers showed that the residual strength relationship for the clay must incorporate the physico-chemical stress, (R-A). Their measurements of the (R-A) stress appeared to agree well with theoretical estimates of net physico-chemical stresses. Their conclusions are:

- residual strength is a function of the true effective stress, σ'_i, and, by inference, peak strength is also a function of σ'_i,
- volume change (consolidation) is a function of the true effective stress,
- pore water salinity does not affect the true effective stress, σ'_i.

Elder (1985) states that some evidence exists that shear strength is controlled by σ'_i alone but that volume changes may be governed additionally by R and A. Only in cases where either R and A are both negligible or R=A, will deformations be governed by σ'_i and the conventional effective stress principle will be valid. Some researchers (e.g. Sridharan and Rao, 1973)

labeled σ'_i the "modified effective stress" and (R-A) the "intrinsic effective stress". Chatterji and Morgenstern (1989), as well as many others (Kenney et al., 1967; Kulkarni, 1973; Sridharan and Rao, 1973), have shown that intrinsic effective stress can play a significant role in influencing the apparent effective stress in soft soils. Einsele et al. (1974) studied physical properties and behaviour of illite, kaolinite and montmorillonite during settling and self-weight consolidation and found that at low effective stresses the ratio of undrained peak shear strength to effective overburden pressure was disproportionately high. They attributed this to the intrinsic shear strength component acting in addition to the true effective stress. Similar high ratios have been found in the sludge in the Syncrude tailings pond (Scott, 1987).

Crawford (1963) studied shear strength of an undisturbed clay. The author observed that at zero effective stress, shear strength was present in the soil and attributed it to the soil's structure, that is, electrochemical (intrinsic) stresses. In the conclusion, the author expresses his opinion that at low effective stresses the accepted effective stress concepts are inadequate and cannot be used with confidence.

Some of the factors influencing the intrinsic effective stress are particle concentration and arrangement, fluid salt concentration, pH, Eh, conductivity and dielectric constant (Elder, 1985). Been (1980) and Elder (1985) concluded in their research that the compression behaviour of soft soils cannot be described adequately only in terms of the macroscopic quantity; apparent effective stress.

Despite increasing research efforts in recent years, behaviour of very soft soils and properties of fine-grained slurries are still poorly understood. There is a need for a broader multi-disciplinary approach to the problem. Theoretical and experimental studies in colloid chemistry, sedimentology and soil

mechanics will contribute to the development of a comprehensive understanding of soft soils (Bowden, 1988).

2.3.2 Strength Testing in Very Soft Soils

Strength testing in very soft soils under low effective stresses is not well documented and there is in general a lack of such studies in the literature. Both, the complexity of the measurement problem and the uncertainties of the findings might have contributed to this deficiency. Variability of the results and often conflicting conclusions suggest that strength behaviour under low stresses is understood rather poorly. To fill the apparent research void, the University of Oxford initiated its soft soil research program in 1977 and has been quite active in this area. Work done by Been (1980), Elder (1985) and Bowden (1988) proved very helpful in pursuing the experimental objectives of this thesis.

Because of the very low shear strength of soft sediments and slurries, samples will not stand unsupported and conventional triaxial testing cannot be carried out. Instead, strength testing on such soils has to be done either in situ or using field-type inserted instruments. In these cases, effective stress paths followed during shearing are impossible to distinguish. Crawford (1963) lists some of the factors influencing the results of such tests:

- method of testing and its effect on mode of failure (predetermined or free),
- orientation of failure zone,
- boundary conditions,
- size of failure zone, strain to failure,
- rate of testing,
- soil disturbance due to insertion of testing equipment,
- time between insertion and testing.

Results of these tests are often presented in the form of an undrained shear strength (c_u) which is defined as half the difference between the major (σ_1) and minor (σ_3) principal stresses at failure:

$$c_u = \frac{1}{2} (\sigma_1' - \sigma_3')_f = \frac{1}{2} (\sigma_1 - \sigma_3)_f \qquad (2.3)$$

Elder (1985) compiled data from many sources in a plot of liquidity index (I_L) against remoulded shear strength (c_{ur}). The shear strength results were obtained by different methods including vane, fall cone, erosion flume, viscometer and UU triaxial test. For liquidity indices greater than 0.4, Elder describes the best fit curve by:

$$c_{ur} = c_{ur} (@ \text{ liquid limit}) / I_L^3 \qquad (2.4)$$

However, the shear strength at the liquid limit varies widely: from 0.5 to 4 kPa for different soils although theoretically it should be constant. Evidence suggests (Karlsson, 1977; Sherwood and Ryley, 1970) that the method using the Cassagrande apparatus for determining the liquid limit is prone to unnecessary errors linked to operator variability. The fall cone method should be used instead as more reliable. Based on a constant value of c_{ur} = 1.6 kPa at the liquid limit obtained by the cone method, Leroueil et al., (1983) found that for many soils in the range $0.5<I_L<2.5$ shear strengths can be expressed by:

$$c_{ur} \text{ (kPa)} = (I_L - 0.21)^{-2} \qquad (2.5)$$

Carrier and Beckman (1984) in their studies of highly plastic phosphatic slurries and natural soft clays observed that activity affects residual shear strength of clays. The authors expressed the relationship for soils with liquidity indices of at least 5.0 by the following equation:

$$c_{ur} = p_{atm} \left\{ \frac{0.166}{0.163 + \dfrac{37.1e-(wp)}{(Ip)[4.14+(A)^{-1}]}} \right\}^{6.33} \qquad (2.6)$$

where A is the activity , p_{atm} - atmospheric pressure, e - void ratio, w_P - plastic limit, and I_P - plasticity index of the soil.

In stronger soils, it is often assumed that the ratio of undrained shear strength to vertical effective stress is constant. This is not true for soils with water contents above the liquid limit as shown by Elder (1985). The author suggests a relationship between remoulded undrained shear strength and vertical effective stress in a normally consolidated soil based on a combination of other models:

$$c_{ur} = c\ \sigma_v'^{0.43} \qquad (2.7)$$

where c is a constant dependent on plasticity index and activity for a particular soil. The relationship might apply at very low strengths or high liquidity indices.

Locat and Demers (1988) investigated rheological behaviour of some remoulded sensitive clays. The researchers found a good correlation of viscosity and remoulded shear strength with liquidity index for remoulded sensitive clays at high water contents. For liquidity indices between 1.5 and 6, they found the following relationships for the plastic viscosity (η) and undrained shear strength of a soil with liquidity index:

$$\eta = (9.27 / I_L)^{3.33} \qquad (2.8)$$

and

$$c_{ur} = (19.8 / I_L)^{2.44} \qquad (2.9)$$

In conclusion, they recommended viscometric testing on a routine basis for soft soils as a good tool to relate viscosity to remoulded shear strength and liquidity index.

Some researchers have studied the influence of aging on the strength of saturated soils and while it appears that with a constant void ratio the remoulded undrained shear strength is not time dependent, the peak unremoulded shear strength shows a significant though variable influence with time. There is no unique relationship between the peak unremoulded

shear strength and time with other soil parameters, such as the Atterberg limits,

Bjerrum and Lo (1963) investigated the influence of time on the strength properties of a normally consolidated clay. The authors noted that older samples showed greater strength and smaller failure strains. This was attributed to the forming of cohesive bonds between particles with time.

Elder (1985) found a significant increase in the peak shear strength with time for a constant liquidity index and only a small increase in the residual strength. He did not observe a unique relationship between peak shear strength and vertical effective stress although he found a good correlation between remoulded (residual) shear strength and effective stress.

Bowden (1988) observed a peak shear strength increase with the passage of time at all effective stress levels, though the rate of increase was slower at higher stress levels. On the other hand, the author states that at any given water content, peak shear strength increased with the passage of time, and time-related effects were more significant at higher effective stress/shear strength levels. For residual shear strength, conflicting trends were observed with respect to the influence of time which was probably caused by a lower accuracy of measurements due to the low range of strengths observed. In effect, the sensitivity (c_{up}/c_{ur}; the ratio of the peak unremoulded to the residual shear strength) varied substantially although it showed influence of both the passage of time and the level of effective stress.

2.4 Strength Testing of Oil Sands Tailings Sludge

Several researchers have studied some aspects of the undrained strength behaviour of oil sands tailings sludge. The reported cases, however, represent only a narrow perspective on the subject and do not arrive at a comprehensive

model of the soil's strength behaviour. Most of the authors recognize thixotropy as a unique property of the sludge and limit themselves to investigating factors responsible for the phenomenon or to conducting experiments over a relatively short passage of time.

The state of understanding of the consolidation behaviour of the oil sands tailings sludge is at a significantly higher level due to the volume of research studies carried out, mainly at the University of Alberta. Scott and Dusseault (1980), Scott and Cymerman (1984), Scott and Chichak (1985 a, b, c), Lund (1985), Scott, Dusseault and Carrier III (1986), Isaac (1987), and others investigated consolidation and permeability characteristics of the sludge and various sludge/sand, sludge/overburden mixes. Perhaps the most complete work is that by Pollock (1988). In all the aforementioned experimental work it was concluded that consolidation of the sludge was affected by thixotropic hardening and further studies of this linkage were recommended.

Kessick (1979) compared rheological and stability characteristics of the sludge with those of a 5% montmorillonite gel. The author determined gel strength of the slurries by directly measuring the torque of a Fann Model Viscometer rotated at low rates. The tests were carried up to 100 minutes of rest time after stirring. Both slurries showed similar behaviour in which the strength continued to increase with time.

Yong et al. (1982) studied dynamic processes which take place during aging of sludge. A gel strength profile of a sludge pond is presented where gel strengths were determined from Bingham curves (see Section 3.2.1.1) by using the Rheomat 15 viscometer. The author shows there is some correlation between gel strength and clay:water ratio. He also points out that thixotropic regain occurs in samples aged overnight.

Scott, Dusseault and Carrier III (1985) measured apparent viscosity and apparent yield strength of sludge samples and various sludge/sand mixes. For "mature" sludge, the apparent viscosity was about 10 Pa•s and the apparent yield strength 70 Pa. The authors plot gel-strength development with time for different mixes showing that the most rapid gain in strength occurs in less than twenty hours with little or no increase after twenty days. The gel strength is presented as "apparent rheidity" (viscosity) which is related in some linear fashion to the former.

Isaac (1987) devised an experiment to "find some relationship between strength, time and apparent viscosity of sand and sludge mixes". Ten samples with a sand to fines ratio of 4:1 and a moisture content of 22 to 23% were tested after a rest period varying from one to thirty-three days. Undisturbed and remoulded undrained shear strengths were measured using the Swedish fall cone and laboratory vane. It was found that the undisturbed strengths rose rapidly from 0.60 kPa to 1.70 kPa, where they seemed to remain fairly constant. The remoulded strengths rose from 0.45 to 0.80 kPa. The author also reports an experiment where a 30% solids sludge air-dried to and tested at its liquid limit yielded an undrained shear strength of 1.66 kPa and when allowed to rest for twenty-four hours the strength rose to 4.25 kPa.

Danielson and MacKinnon (1990) investigated rheological properties of sludge samples. Using the Haake Rotovisco Viscometer, the upper yield strength, fluid viscosity, lower yield strength, and plastic viscosity were determined as a function of time. It was concluded that the upper yield strength is dependent on the aging and shear history of the tested sludge whereas fluid viscosity (apparent viscosity at a shear rate of 2770 sec^{-1}; as defined by the authors), lower yield strength and plastic viscosity did not appear time or shear history dependent. The authors also postulated that the thixotropic gain in strength

was active for a period of 10-15 hours after remoulding beyond which no further increase in strength was observed. For one particular sample (26.6% solids content or 276% water content) a peak upper yield strength of about 10 Pa was measured which was approximately 1.8 times greater than the initial upper yield strength.

From the above, it can be seen that the oil sands tailings sludge and its thixotropic behaviour has been approached from the rheological perspective and experiments have been conducted by means of various viscometers. On the other hand, geotechnical strength tests have concentrated on sludge/sand and sludge/overburden mixes. The lack of geotechnical strength tests on pure sludge can perhaps be explained by the inability of standard equipment to measure the very low shear strengths encountered in high water content slurries.

2.5 Summary of Important Findings

1. Oil sands tailings sludge is a very soft soil of high water content characterized by its industrial origin and with properties affected by three unique features: high content of chemical additives, presence of bitumen and chemical and mechanical dispersion of particles.
2. The sludge causes a disposal problem not only because of the very large volumes being generated but also because it consolidates at extremely slow rates. This delayed consolidation has been linked to thixotropic hardening.
3. Thixotropy is of common occurrence in clay-water systems and is a function of clay mineralogy, water content and chemistry, time and shear strains, among others. Other researchers have postulated that it decreases the rate of consolidation of a soil.

4. Very soft soils are unique in the fact that the principle of effective stress should be modified when applied to them to include the intrinsic effective stress (physico-chemical forces).
5. Behaviour of very soft soils is still not well understood. Strength testing of such soils is not well documented and lacks in uniformity of methods and equipment.
6. There have been empirical relationships developed for very soft soils correlating the undrained residual shear strength with liquidity index. No relationships between peak shear strengths and index properties have been found.
7. There have been few studies investigating strength characteristics of the sludge. Lack of appropriate testing equipment appears to be a main obstacle. Thixotropic studies of the sludge have been of short duration.

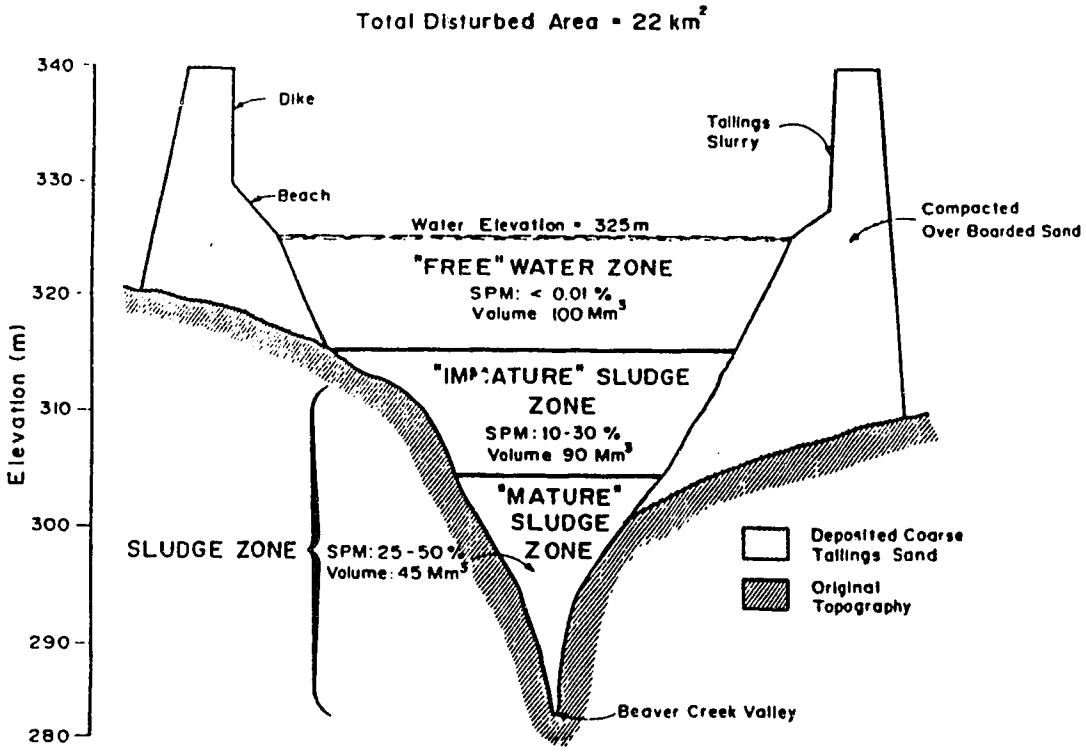

Figure 2.1 Stylized cross section of Syncrude's tailings pond (after MacKinnon, 1989)

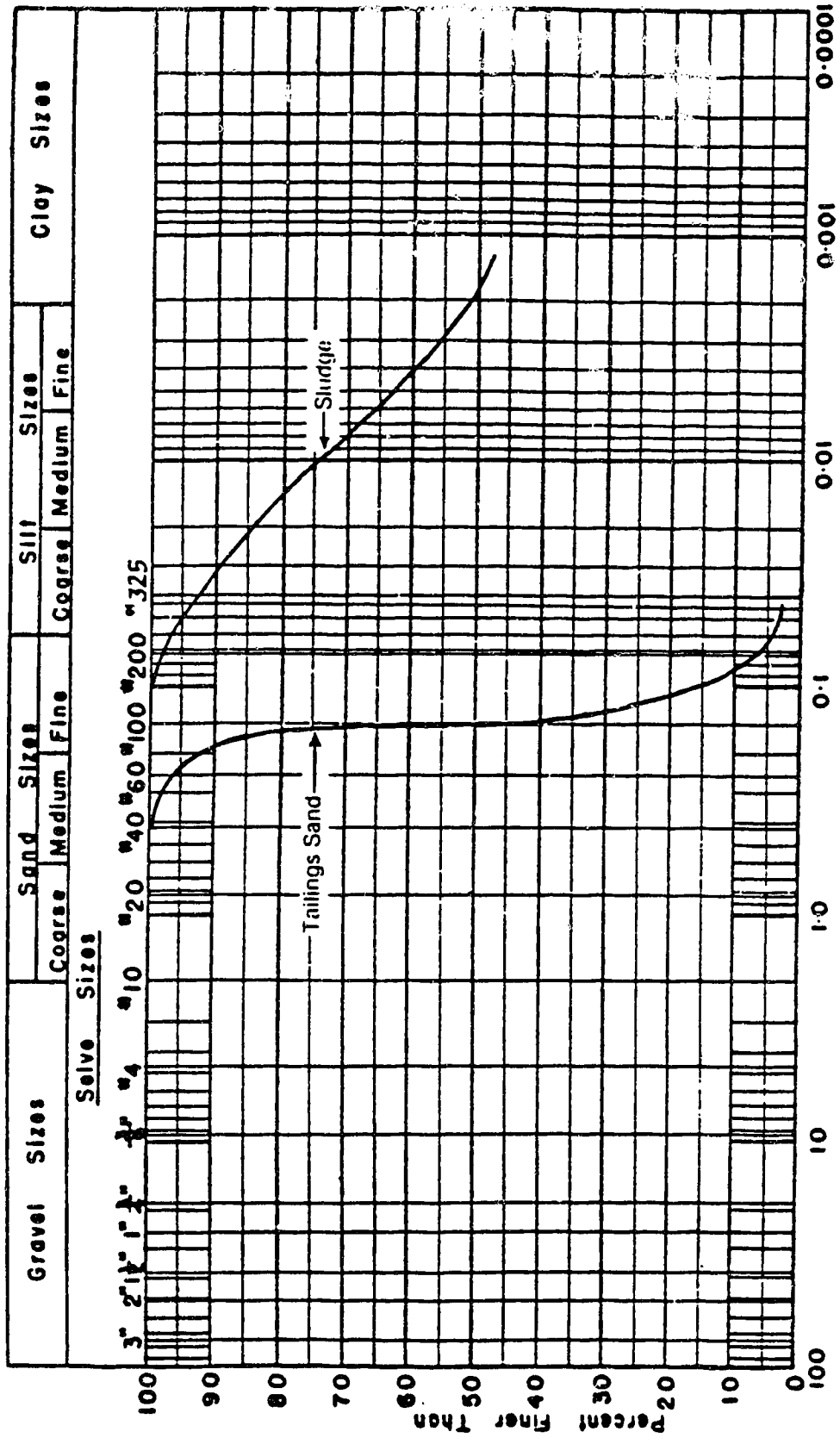

Figure 2.2 Typical grain size distribution for sludge (after Scott and Cymerman, 1984)

3. EXPERIMENTAL PROGRAM

3.1. Slurry Description and Preparation

3.1.1. Origin of Specimens

The oil sands tailings sludge used in the experimental program can be divided into two origins. Both samples of sludge were collected from the Mildred Lake tailings pond in Syncrude's Oil Sand Lease property located in northern Alberta. What sets them apart is the time when they were pumped out of the pond and their subsequent storage. The first batch of sludge was, in fact, a mixture of several shipments of the slurry collected from the pond between 1983 and 1986, transported to Edmonton and stored in a tank located at the Syncrude Research centre. The first component of the mixture was pumped from the pond in the summer of 1983 from a depth of 15 - 16 m below the water surface at a central location of the pond. It was the same sludge that was used in the 10 meter high standpipe experiment program at the University of Alberta. The other major component of the mixture represented sludge collected in the summer of 1986 from the northern part of the pond at a depth of 15 - 16 m below water surface. In the tank, the sludge went through the process of consolidation and biochemical changes associated with time and elevated temperature. The sludge used for this research was obtained from Syncrude on July 8, 1988. A 45 gallon drum was filled to 3/4 of its height with thick, mature sludge coming through a valve from the bottom of the tank. There was no prior mixing of the content of the tank therefore the sample represented only the most dense material. This sludge was used for all long term tests (680 days). The second batch, consisting of two 45 gallon drums was received from Syncrude Research on January 2, 1989, after a larger shipment of sludge had been sent to Edmonton for research purposes. The sludge was

pumped from the pond during the summer of 1988. The intake was located in the northern part of the pond at a depth of 13 - 15 m below water surface in the "immature" sludge zone. The water content of both batches of sludge was measured upon receiving. It was determined that the water content in the first batch of sludge was 168% (37% solids content) and in the second batch 270% (27% solids content).

3.1.2. Index Properties

- Water Content

The water content of the sludge is defined as the weight of the water divided by the weight of the dry solids including bitumen:

$$w = \frac{M_w}{M_b + M_s} \times 100\% \qquad (3.1)$$

It should be noted that other definitions of water content of sludge exist in the literature (Lord and Cameron, 1985), where bitumen is considered a liquid rather than a solid:

$$w_s = \frac{M_w}{M_s} \times 100\%, \qquad (3.2)$$

or:

$$w_m = \frac{M_w}{M_t} \times 100\% \qquad (3.3)$$

where: M_w = mass of water

M_b = mass of bitumen

M_s = mass of solids

M_t = mass of total soil volume = $M_w + M_b + M_s$

The definition used here is consistent with the point of view that during consolidation of sludge bitumen remains with the solid particles permanently and behaves like a semi-solid rather than a liquid. This view is supported by experimental evidence (Scott and Dusseault, 1982). The procedure of measuring water content was in accordance with ASTM D2216 - 80 "Laboratory

Determination of Water (Moisture) Content of Soil, Rock, and Soil-Aggregate Mixtures".

- Atterberg Limits

Test procedures to determine the liquid and plastic limit of the sludge followed the standard ASTM D4318 - 84 practises. The samples of the sludge were air-dried to the water contents close to the liquid and plastic limits and only distilled water was used for mixing purposes.

- Grain Size Distribution

The grain size distribution of the sludge was determined using the hydrometer method in accordance to ASTM D422 - 63 "Particle-Size Analysis of Soils" with the following modifications. Due to the nature of the slurry, two methods were followed in this test. In the first, a sample was tested "as received" with all the bitumen left in the slurry and without drying. A 4 to 6% solution of dispersing agent (Calgon) was used. In some cases, foam (froth) appeared on the surface creating difficulties in conducting the test. In such cases, the sample was left for about twenty minutes during which the foam subsided, then it was remixed and, when no foam was present, the actual testing commenced. The specific gravity of sludge solids (Equation 3.4) was used in calculations. The other method required a bitumen extraction process to be carried out prior to the hydrometer test. In this method, a sample consisted of mineral grains only with traces of organic residue. However, the specimen was completely dried during the extraction test. Visual examination of the soil determined that, at least macroscopically, it did not require pulverizing. As in the first practice, a dispersing agent of 4 to 6% solution of Calgon was used. The specific gravity of the mineral grains was used in the calculations.

Both ways of preparing the samples have their potential flaws. In the first, the lighter bitumen may be adhered to the mineral particles and may slow their

rate of settlement. As a result, the grain distribution curve would be shifted towards the finer grain size. In the other method, the elevated temperature during the extraction and drying procedure may cause cementation and bonding of particles thus giving a lower fines content. The results will be presented and discussed in Chapter 4.

- Bitumen Content

The bitumen content is defined as mass of bitumen over the mass of mineral grains only. A Modified Method 2.7 (AOSTRA, 1979) "Determination of Bitumen, Water and Solids Content of Oil Sands" was used to determine the bitumen content. The sludge sample was separated into bitumen, water and solids by refluxing with toluene in a solids extraction apparatus. Condensed solvent and co-distilled water were continuously separated in a trap, the water being retained in the graduated section. The solvent was recycled through the extraction timble of the extraction apparatus to dissolve the bitumen. The solids were determined gravimetrically by combining the contributions for solids retained by the extraction thimble and for the non-filtered solids. The bitumen content was determined by difference.

- Specific Gravity

The specific gravity of the sludge solids is a weighted average of the bitumen and mineral particles and is defined as follows:

$$G_{ss} = \frac{b + 1}{b/G_b + 1/G_s} \qquad (3.4)$$

where b is the bitumen content as defined above, G_b is the specific gravity of the bitumen (1.03) and G_s is the specific gravity of the mineral grains. The specific gravity of the mineral grains was determined in accordance to the

procedure outlined in ASTM D854 - 83 "Standard Test Method for Specific Gravity of Soils".

3.1.3. Slurry Containers

A number of containers were needed to store samples of sludge up to 680 days. The containers had to fulfill several criteria:

- impermeable,
- rigid and strong to minimize disturbance during storage, moving and testing of the samples,
- chemically inert,
- diameter large enough to allow at least four viscosity measurements, one vane shear, one fall cone, and one cavity test in different locations of the planar cross-section,
- height permitting insertion of oversized vane even after long term self-weight consolidation.

A 297 mm (11 11/16") outside diameter PVC sewer pipe was selected as the material closest suited to the objectives of the research. A total of eighteen 191 mm (7 1/2") high pieces were cut and machined. A 6.4 mm (1/4") PVC bottom was attached to each piece by means of Weld On plastic pipe cement and see-through clear acrylic lids were fabricated to prevent moisture escape from the sludge in containers. The purpose of using see-through lids was to monitor any changes on the surface of samples. In some cases, a plastic wrap was used as a container's seal. Plate 3.1 shows several filled and sealed containers stored on laboratory benches which were constructed for purposes of this research.

3.1.4. Drying and Centrifuging of Sludge

An efficient and relatively quick method of bringing the water content of sludge from the initial to that required had to be devised as volumes of sludge were substantial. In most cases the water content was to be lowered. The method that best modeled the processes of settling and consolidation of the sludge, both occurring in the pond, was centrifuging. Implementation of this method, however, proved to be highly impractical due to the low volumes the available centrifuge was able to handle thus making it time consuming work. Moreover, it was found that after about eight hours of centrifuging at 1600 r.p.m. the water content of the sludge was only lowered to 120% (45% solids content) and further efforts were bringing very little change in water content. The other method which was eventually adopted consisted of evaporating of water from the sludge. It should be noted that this method increases the salt content of the pore water which may affect the strength properties of the sludge. This dilemma had to be addressed and it was decided to determine the Atterberg limits on both, centrifuged and air-dried sludge. The results will be presented and discussed in Chapter 4 of this thesis. The steps in sample preparation were as follows. The sludge was thoroughly mixed in the drum in which it was received. This ensured a uniform material throughout the drum. A container was then filled with the sludge extracted from the drum. Subsequently, the container was set aside to air-dry at room temperature or it was put in a fume hood to accelerate water evaporation. During the process of drying, the slurry was frequently mixed to maintain uniformity of the sludge and more material was added to the container to make up for the evaporated volume of water. When, judging by the consistency of the sludge, the target water content was being approached, the actual water content was determined.

If the water content was equal to that required, the sample was mixed again, sealed by the means of a lid or a plastic wrap and set aside for its period of aging. If the water content was still too high the drying and mixing was continued. If the water content was too low (too much water evaporated from the sample) distilled water was added until the desired water content was achieved.

3.1.5. Diluting with Pond versus Distilled Water

The question whether to use pond or distilled water for diluting the sludge was answered by following a simple rule: if the sludge was considered to achieve its current water content through sedimentation and consolidation, pond water was added. If, however, the sludge was dried down to the current water content, distilled water was added. The purpose of this distinction was to maintain the original salt content of the sludge or, to be more precise, to not increase the salt concentration. For instance, pond water was added to the sludge taken from the drums to create samples with water contents of 300% and 400% because the water content of the sludge in the drums was lowered through consolidation, either in the pond or the storage tank.

3.1.6. Mixing

Mixing was a very important aspect of sample preparation and it was carried out frequently throughout the project. The main purpose of mixing was to provide a material of uniform consistency. Furthermore, mixing was performed when a sample had to be remoulded. Two mixing tools were used: one, a power drill with a mixing blade extension, for most of the sludge, and the other, a Hobart heavy duty mixer with a paddle mixing blade, for the high solids content sludge.

3.2. Testing Equipment and Techniques

3.2.1. Viscosity Measurements

3.2.1.1. Theoretical Background

Rheological properties of very soft soils and slurries are becoming increasingly more used among geotechnical engineers in describing the soils' behaviour. Rheology is concerned with the flow of any substance whether a gas, a liquid, or even deformation of metals. It embraces flow in all its aspects, whether of momentary or continued duration and all the effects that influence flow. Viscosity, on the other hand, is merely one aspect of the flow process. Defined, it is a measure of the internal friction resisting the movement of each layer of material as it moves past an adjacent layer (Brookfield, 1961).

Locat and Demers (1988) state that for some sensitive clays there are positive relationships between plastic viscosity, yield stress, remoulded shear strength, and liquidity index. It has been observed that soft clays and slurries display non-Newtonian flow behavior. The flow properties of Newtonian fluids are easily characterized by one parameter known as viscosity. This value can be obtained by means of Newton's law which states that a plot of shear stress (τ) versus shear rate ($\dot{\gamma}$) is linear and the slope of the line is the viscosity:

$$\eta = \frac{\tau}{\dot{\gamma}} \qquad (3.5)$$

The assumption in this type of flow is that, at a given temperature, viscosity is independent of the rate of shear. This is illustrated in Figure 3.1; curve A, a straight line of slope η through the origin, represents Newtonian flow. It is convenient to represent the behaviour of flowing materials by means of flow curves, that is, graphs of shear stress against strain rate, as in Figure 3.1. An

equivalent representation is by means of a graph of viscosity against strain rate (Figure 3.2). Unlike Newtonian fluids, non-Newtonian systems may be both shear and time dependent. There are several models proposed for non-Newtonian fluids. One of them is the Bingham model illustrated by curve B in Figures 3.1 and 3.2. This behavior can easily be represented by two parameters: a yield stress (the extrapolated intercept at zero shear rate) and the plastic viscosity (the slope of the line using the yield stress as the origin) (Rosen and Foster, 1978). The model represents a solid but is used only when flow occurs. It is postulated that the material behaves as an elastic solid for stresses less than a yield stress and that, for greater stresses (Whorlow, 1980),

$$\tau - \tau_Y = \eta_{PL}\,\dot{\gamma} \tag{3.6}$$

The behavior of many clay slurries may be represented reasonably adequately, over a limited range of strain rates, by the Bingham model. Whorlow (1980) states that from his experience the behavior of all materials departs significantly from the model in at least one respect. The flow curve is not linear, except over a very limited range of strain rates; the strain rate for a particular stress is likely to be different, probably higher, if the stress has decreased to this value rather than increasing to it; and the yield stress is not well defined.

The Power Law fluid model may be expressed by the following equation:

$$\tau = k\,\dot{\gamma}^{\,n} \tag{3.7}$$

where n is the power law index, and k is the fluid consistency parameter. The flow curve, Fig. 3.1(C), becomes linear if logarithmic scales are used on the axes; the slope of the curve will be n and the intercept log (k). For a power law fluid with $n<1$, the viscosity decreases as the shear rate increases, Fig. 3.1(C) and 3.2(C), and the fluid is said to show shear thinning (Whorlow, 1980). Shear thinning should not be confused with thixotropy which is a time-dependent

effect. A more precise way of describing this kind of behaviour is to say that the fluid is pseudoplastic, implying that it shows a time-independent decrease of viscosity with an increase in shear rate but, unlike the Bingham model, does not have a yield stress (Whorlow, 1980). For n>1, shear thickening materials are encountered, that is, materials which increase in viscosity as the the rate of shear increases, Fig. 3.1(D) and 3.2(D).

The Herschel-Bulkley model represents a large number of materials for which the flow curve is no longer straight above the yield stress, Fig. 3.1(E) and 3.2(E)

$$\tau = \tau_Y + k\dot{\gamma}^n . \qquad (3.8)$$

The Bingham and power law models can be regarded as special cases of this model.

Another special case of the Herschel-Bulkley model is a group of fluids described by means of the Casson equation (Rosen and Foster, 1978):

$$\tau^{1/2} = \tau_Y + k\dot{\gamma}^{1/2}. \qquad (3.9)$$

There appears to be some confusion in the literature as to the term 'viscosity'. Whorlow (1980) explains: "Some workers restrict the use of the term 'viscosity' to materials for which η is constant and in other cases they call η the 'apparent viscosity'. Unfortunately, the term 'apparent viscosity' is also used in a different sense, as the name for the quantity calculated from measurements in a particular instrument using a calibration formula which is appropriate only to fluids of constant viscosity." Therefore, to obtain a value of apparent viscosity the corresponding shear stress and shear rate must be directly defined. It is incorrect to refer to the viscometer's rotational speed as shear rate, as sometimes is encountered in the literature. By itself, the apparent viscosity measured under only one set of conditions is of relatively

little value with non-Newtonian fluids, and measurements at two or more speeds must be reported (Back, 1959).

3.2.1.2 Brookfield Synchro-Lectric Viscometer

From a large variety of viscometers available on the market, the Brookfield Synchro-Lectric Viscometer, model RVT was selected for this research. There were several reasons for choosing this particular apparatus. The viscometer had been purchased prior to commencing of this project and an experimental procedure and results were available. Of more importance, for the planned large number of tests, simplicity and ease of operation was a key factor. An important feature of the Brookfield viscometer was the Helipath Stand which, combined with the T-bar spindles, offered the least disturbance of the material during experiments (see Plate 3.2).

Brookfield viscometers are perhaps the most popular instruments in rheological measurements world-wide. They employ the well-known principle of rotational viscometry: they measure viscosity by sensing the torque required to rotate a spindle at constant speed while immersed in the sample fluid. The torque is proportional to the viscous drag on the immersed spindle, and thus to the viscosity of the fluid. The basic model, the dial reading Synchro-Lectric Viscometer drives a cylinder or disc, which is called a "spindle", in a fluid and measures the torque, necessary to overcome the viscous resistance to the induced movement, through a beryllium copper spring which indicates on the viscometer's dial the degree to which the spring is rotated. The instrument is able to measure over a number of rpm ranges since, for a given drag, or spring deflection, the actual viscosity is proportional to the spindle speed, and is also related to the spindle's size and shape. For a material of given viscosity, the drag will be greater as the spindle

size and/or rotational speed increase. The minimum range of the viscometer is obtained by using the largest spindle at the highest speed and the maximum range by using the smallest spindle at the lowest speed. The viscometer is powered by a precision synchronous inductor type motor. Speed changes are effected by a gear train having eight speeds. Speeds are changed from the lowest, 0.5 rpm, to the highest, 100 rpm, by means of turning a speed control knob. The viscometer is provided with a clutch lever. Depressing the lever raises the dial against the pointer and "holds" the instrument's reading. When the clutch is released the dial will lower and the pointer will be free to seek its own position. The torque beryllium copper spring is extremely resistant to fatigue and does not change its characteristics even after hundreds of thousands of flexings. Its calibration as listed by the manufacturer is 7187.0 dyne-centimeters (7.187×10^{-4} N•m) which corresponds to the full dial scale. The viscometer comes equipped with a set of 7 spindles. The spindles are of disc shape and provide apparent viscosity determinations in a variety of liquids. An optional, cylindrically shaped spindle had been purchased in addition to the standard spindles for rheological measurements in oil sands tailings sludge. This spindle provides a scientifically defined spindle geometry for calculating shear stress and shear rate values as well as viscosity. In spite of the fact that a similar material was used in this research the disc and cylindrical spindles could not be used. That was due to the nature of the experiments. Inserting a spindle into a specimen would cause so much disturbance in the delicate gel structure that obtaining a true peak value of viscosity would be impossible. Theoretically, a spindle could be immersed in a specimen immediately after remoulding and left there for the period of aging until the actual test would take place. However, with the number of tests going into hundreds and aging periods up to 680 days, this solution was not practical.

To resolve this problem, it was decided to use the so called T-bar spindles. Six T-bars, with crossbar lengths ranging from 10.9 to 48.1 mm, come as standard equipment with another Brookfield accessory, the helipath stand. The uniqueness of the helipath stand lies in its ability to slowly lower or raise the viscometer so that its rotating shearing element will describe a helical path into the test sample. The vertical speed of the movement is 22.2 mm per minute. By always cutting into fresh material meaningful measurements of peak shear resistance can be made. Unfortunately, this feature comes with a trade-off: T-bar spindles do not have directly definable shear rate and shear stress values. While T-bar spindles can be successfully used for determining viscosity of Newtonian fluids, no mathematical models are available for calculating viscosity functions for non-Newtonian fluids. Therefore, measurements conducted with these spindles cannot be regarded as apparent viscosity values but can only be treated as index values. The test results in this research are therefore treated as index values and only "viscometer readings" are used in the analysis of the thixotropic behaviour of the sludge. An exception is the plotting of the "apparent viscosity" (as described in 3.2.1.1) versus the rotational speed of the instrument for the purpose of comparing the effect of the shear rate with the model curves available in the literature.

3.2.1.3 Testing Procedure

Each viscosity test consisted of four sets of measurements. Each set was performed at a different rotational speed: 1.0, 2.5, 5.0, and 10.0 rpm. Within each set, there were two groups of readings: peak and residual. The viscometer was located in a designated place in the laboratory for all viscosity tests. Before each test, the helipath stand and the viscometer were both checked for horizontal position and adjusted, if necessary, with the help of three levelling

screws. A container with a sludge specimen was then placed directly under the viscometer. Special care were taken to assure no disturbance to samples during handling. Containers with sludge for short term tests (zero to five days after remoulding) were aging either directly underneath the viscometer, so they would not have to be moved, or on the bench next to it, so their travel would be minimal. The next step involved selecting an appropriate T-bar spindle and fastening it to the viscometer by the means of a chuck, weight, and closer assembly. The lid or plastic wrap was then removed from the container, the rotational speed was set, the drive unit of the helipath stand was engaged, the viscometer lowered and readings were taken. After a remoulded value was established the spindle was brought back above the sludge surface, removed, and cleaned. The cylindrical container was then turned, so the next immersion point would be at least three spindle diameters away from the previous one, a different rotational speed was set, and the whole procedure was repeated. After a complete test (four rotational speeds), the temperature of the sludge was measured and recorded.

i) Peak Values

Recording peak values was much more difficult compared to residual readings. Accuracy and effectiveness were required from the operator as this part of the test took only slightly more than a minute (about 70 seconds). Depending on the rotational speed of the viscometer, two to ten readings had to be taken and recorded in the span of that time. The dial could be monitored only during one third of a full revolution because the other two thirds were not visible. Peak readings were recorded from the surface of the sludge to a depth of 25.4 mm (1 inch). For the speeds of 1.0 and 2.5 rpm the spindle was rotating continuously but for 5.0 and 10.0 rpm the rotation of the spindle was stopped after each reading for several seconds. It was discovered that with the two higher speeds

the rate of rotation was so high compared to the vertical travel that the sludge was being constantly disturbed and in order to obtain "true" undisturbed readings the spindle had to be stopped until it reached a new layer of the material. If suspicious values were recorded, the test was repeated at a different location within the same specimen. The highest value was taken as the peak reading.

ii) Residual Values

All residual readings were taken at an arbitrarily chosen depth of 25.4 mm, measured from the surface of the sludge or the water-sludge interface in case of detectable self-weight consolidation. When the spindle reached that depth and peak readings were completed the helipath stand was stopped. Subsequently, readings were taken at every revolution until they displayed no further decrease or if they started to increase. The duration of this part of the test varied from two minutes for the shortest tests to over eight hours for the longest (680 days) tests. The lowest value was taken as the residual reading.

iii) Data Recording and Processing

All readings were taken and recorded manually on a specially formatted sheet. Data from test report sheets was then entered into a Macintosh SE computer and processed using Cricket Graph application software. Each viscosity test was presented in form of two plots: viscometer reading versus viscometer rotational speed, and "apparent viscosity" versus viscometer rotational speed. The results will be discussed in depth in Chapter 4.

3.2.2 Shear Vane Testing

3.2.2.1 Theoretical Analysis

The shear vane test is one of the most widely used methods for determination of the undrained shear strength of soft clays. Both, in situ and in the

laboratory, it gives a rapid and reliable estimate of the undrained strength. The vane shear device was developed independently in Sweden and Germany during 1928 and 1929 (Arman, et al., 1975). Although some historical records date the development of the vane test back to the Olsson vane borer in 1910s, it was not until the late 1940s that the field vane was developed in its modern form by such people as Carlson (1948) and Skempton (1948) (Mahmoud, 1988). Cadling and Odenstad (1950) carried out an extensive investigation of the the vane shear test in which they examined various possible factors expected to influence the measurements of the vane shear strength. Since then, the test has been the subject of interest for numerous authors who have attempted to analyze the test experimentally and theoretically to gain better understanding of this apparently simple device, and to establish why the measurements of the vane shear strength is often different from the undrained soil shear strength measured with other methods. For this reason, the vane test has been subjected to considerable criticism expressed by many authors, among them Schmertmann (1975). Flaate (1966) suggested the following assumptions for calculating the undrained shear strength of soils from the vane device:

1. The soil is completely undrained; i.e., no consolidation takes place either during the installation or the actual test.
2. No disturbance is caused by the installation of the vane.
3. The remoulded zone around the vane is very small. (This necessitates a very small area ratio.)
4. There is no progressive failure. The maximum applied torque overcomes the fully-mobilized shear strength along a cylindrical surface.
5. Isotropic strength conditions exist in the soil mass.

Cadling and Odenstad (1950) developed the relationship between shear strength and torque described by:

$$\tau_{max} = \frac{2T}{\pi D^2 (H + \frac{D}{3})} \qquad (3.10)$$

where $\tau_{max} = c_u$ = undrained shear strength, T = torque, D = vane diameter, and H = vane height. Skempton (1948) observed that the failure surface had a larger diameter than that of the vane and modified Equation (3.10) including an effective diameter taken as 1.05 of the vane diameter. Flaate (1966) further modified the relationship by assuming the shear strength at the ends of the sheared cylinder to be mobilized proportionally to the radial distance from the centre of the vane:

$$\tau_{max} = \frac{8}{9} \frac{T}{\pi D^3}, \qquad D = H/2 \qquad (3.11)$$

The effects of the vane shape and size were investigated by Flaate (1966), Osterberg (1956), Eden and Hamilton (1956), Andresen and Sallie (1966), Arman et al. (1975), and many others. Cadling and Odenstad (1950) indicated the vane size had no influence on vane strength for the remoulded clay tested. Arman et al. (1975) concluded that vane shear strengths were generally independent of vane size. In the same study, however, field vane measurements were observed to yield significantly greater strengths than laboratory shear vane tests.

The area ratio of a vane is defined as the ratio of the cross-sectional area of the vane to cross-sectional area of the sheared cylinder, which is directly proportional to the vane size. An optimum area ratio recommended by various authors ranges between 10% and 25%.

A height to diameter ratio of 2 has been accepted by most manufacturers of vane shear devices as universal. Cadling and Odenstad (1950) showed that, when an H/D ratio of 2 is maintained, the vane diameter has no effect on the results. Bazett et al. (1953) and Osterberg (1956) reached similar conclusion.

The criticism of the shear vane test concentrates around several main factors which affect interpretation of results. As listed by Elder (1985), these factors are:

1. A predetermined failure surface, nominally a vertical cylinder. Wilson (1963) observed that the initial surface was almost square at low rotation angles. Rush (1974) confirmed that prefailure strains were consistent with Wilson's observation.

2. The shear stress distributions on the horizontal and vertical failure surface are not known accurately even for isotropic soil states. It is generally agreed that the shear stress on the vertical surface is approximately constant away from the ends but that the shear stress on the horizontal surfaces is highly non linear and very small near the axis (Menzies and Merrifield, 1980; Donald et al., 1977). Jackson (1969) modified the conventional analysis (3.10) to give:

$$\tau_{max} = \frac{2T}{\pi D^2 (H + \frac{D}{N})} \qquad (3.12)$$

N = 3.0 - uniform shear on horizontal surfaces,

N = 3.5 - parabolic shear on horizontal surfaces,

N = 4.0 - triangular shear on horizontal surfaces,

N = 3.7 - empirical correlation (Yarra Clay).

Wroth (1984) suggested a power law relationship to describe this variation:

$$\tau = \tau_{max} (\frac{r}{D/2})^n \, , \, n \approx 5 \qquad (3.13)$$

at radius r from the axis of a vane of diameter D and height H. Assuming τ_{max} is fully mobilized on the vertical surface, the shear strength ($c_u = \tau_{max}$) may be obtained in terms of the total torque exerted, T as:

$$\tau_{max} = \frac{2T}{\pi D^2 (H + \frac{D}{n+3})} \qquad (3.14)$$

As shown by Wroth (1984), for a H : D ratio of 2 and for n = 5 the resistance measured is almost entirely due to the shear stress on the vertical plane which contributes 94% of the total torque. For n = 1 (triangular distribution), the vertical surface shear contributes only 89% of the total torque.

3. Anisotropy of strength. Many authors studied this problem using vanes with different H : D ratios or using diamond shaped blades (e. g. Aas, 1965; Richards et al., 1975; Menzies and Mailey, 1976). Donald et al. (1977) concluded that the strength on [illegible] surfaces could not be estimated by any current method, unless the soil is isotropic and non work-softening. Additional doubts arise with progressive failure where peak strengths are mobilized at different rotations on different planes (Wiesel, 1973).

4. Rotation rate. Cadling and Odenstad (1950) showed that a strength measured at a rotation rate of 60°/min was 20% higher than strengths determined at a rotation rate of 6°/min. Monney (1974) found that laboratory strengths obtained at a rotation rate of 90°/min were nearly 30% higher than strengths measured at 1°/min. Migliore and Lee (1971) observed that laboratory strength differences resulting from different rotation rates were greater on samples of higher quality. This observation was also corroborated by Smith and Richards (1976). Perlow and Richards (1977) proposed an angular shear velocity of 0.15 mm/s as the standard for both laboratory and in-situ measurements. Thus, laboratory measurements made using the standard 0.5-in. (12.7-mm) diameter vane should be made at a rotation rate of about 80°/min (23 mrad/s). Larger vane sizes should be rotated at reduced rates in accordance with:

$$v = r\,\omega \tag{3.15}$$

in which v = angular shear velocity, r = vane blade radius, and ω = vane rotation rate.

The advantage of comparing shear strengths at a standard angular shear velocity is that many of the uncertainties associated with rotation rate and vane size would be eliminated.

5. Consolidation of soil around the vane. Rush (1974) reported increase in strength with a delay between insertion and testing amounting to a 20% rise after about one day. After which the strength then remained constant. Aas (1965) showed that, if the vane is left one day after penetration, the average ratio between failure torques observed in consolidated-undrained and undrained tests varies between 1.28 and 1.52. There was no significant difference between the shear strength observed in the tests where the vane was left for one day and in the tests where it was left for two or three days.

In spite of all the uncertainties and variabilities described above, vane shear testing remains the most widely used in soils which are too soft to sample for triaxial testing. It is the source of most data relating undrained strength to liquidity index (e.g. Skempton and Northey, 1953; Bjerrum, 1954; Mitchell, 1956; Shannon and Wilson, 1964; and others). Due to the physical properties of the oil sands tailings sludge triaxial testing was impossible to conduct and vane shear testing was the only widely used geotechnical method of determining the undrained shear strength of the material. In this research the accuracy of strength measurements was less important than their consistency because the objective was to study the relative change in strength with time.

3.2.2.2 Standard Vane Shear Apparatus

One of the most popular laboratory shear vane testing instruments is the Wykeham-Farrance miniature vane shear test apparatus. The machine's main components are a frame and stand, a vane mounting assembly, a miniature vane, a torque sensor and a means of displaying torque as a function of

angular rotation. A typical four-blade vane is 12.7 mm wide and 12.7 mm long (0.5 in x 0.5 in). The torque sensor may be either a strain gage mounted electronic torque cell or a calibrated spring, the latter usually being used in this particular apparatus. Four torsional springs of different stiffnesses are available as torque measuring devices. The rotation rate of the vane itself is far from constant and may differ by an order of magnitude or more from the applied constant rate at the top of the spring (Lee, 1985). The vane rate is far below the spring top rate until a peak torque is reached. After failure, if the soil displays a strength reduction with further strain, the vane rate becomes higher than the spring top rate.

Despite its limitations, the minivane has been, as Lee (1985) puts it, "the workhorse of the marine geotechnical community for over 20 years and is still probably the most commonly used procedure for estimating shearing strength".

3.2.2.3 Modified Apparatus

Modifications made to the standard vane apparatus were inspired by the work of Elder (1985) and Bowden (1988). The hand operated drive mechanism was replaced with a Pittmann 12 volt DC motor which was controlled by an Atex variable DC power supply. The motor was connected with the drive mechanism through two belt-driven gears. The smaller gear had 20 teeth, the larger - 60 teeth. This arrangement allowed a constant vane rotational speed of anywhere between 0° and 120° per minute. The torque measuring spring was replaced with a rigid transducer consisting of a hollow brass shaft machined over a necked middle region to 3.00 ± 0.01 mm OD (Figure 3.3). Two types were fabricated: one, with a wall thickness of 0.15 ± 0.01 mm, for low strength measurements, and the other, with a wall thickness of 0.35 ± 0.01 mm - twice

the capacity of the first, for slurries of higher strengths/lower water contents. The first type of torque cell had a yield torque of approximately 180 Nmm, the second - 360 Nmm. Each transducer was equipped with a Kyowa (KFC-2-D2-23) four arm balanced strain gauge bridge which measured the electric signal, in volts, directly proportional to the applied torque and independent of axial stress. The torque cells were calibrated using the system shown in Plate 3.3 and 3.4. The system consisted of a calibration moment cylinder with a "V" groove connected through the vane mounting assembly with the torque cell, two contort holders with rotating disks attached to them, and a set of weights. Weights of known mass were suspended by a thin fishing line from a free-rotating disk and connected to the moment cylinder. The two lines representing moment arms were parallel to each other and both were in a horizontal position. The signal response for each pair of weights was recorded and plotted giving the calibration curve. The curves were linear over the range of torques encountered in this research and a single calibration constant was used for each torque cell to convert transducers signals to applied torques. Assuming validity of Equation (3.14) for the undrained strength

$$c_u = \tau_{max} = \frac{2T}{\pi D^2 (H + \frac{D}{n+3})}$$

values of c_u accurate to 1 Pa or smaller could be obtained with this system.

Three custom-made shear vanes were used for the strength testing. Two of them, with the H : D ratio of 2.0, had four blades, the third, one with a ratio 1.0, had six blades. The smallest vane, still larger however than the standard one, was 40 mm high by 20 mm wide and was constructed of sheet stainless steel with a thickness of 0.35 mm, and fixed at the top to a rod of diameter 4.7 mm. This vane was designated with the description 20 mm vane. The next vane was

very similar to the 20 mm vane, with the exception that it was larger; its dimensions were 30 mm by 60 mm and it was labeled 30 mm vane. The largest vane, the 80 mm vane, had six blades as opposed to the standard four, H : D ratio of 1.0, and diameter of 80 mm. It was fabricated from stainless steel 1 mm thick and sharpened at the lower edge to assure entry with minimum disturbance. The 80 mm vane was used in most of the tests, 20 mm vane - in all liquid limit samples, and 30 mm vane - only occasionally as a check between the other two vanes. The ASTM D 4648 - 87 Standard Method for Laboratory Miniature Vane Shear Test for Saturated Fine-Grained Clayey Soils recommends that the vane displace no more than 15% of the soil being tested as defined by the vane area ratio:

$$V_A = \frac{\text{Cross-section area of the vane}}{\text{Cross-section area of failure cylinder}} \qquad (3.16)$$

All three vanes had the vane area ratios well below the recommended maximum: 20 mm vane had 4.5%, 30 mm vane 3.0%, and 80 mm vane 4.8%.

The reasoning behind using a six-blade vane instead of the standard four-blade one was the assumption that with the large diameter of the vane and extremely low strength/stiffness of the slurry, six blades would mobilize much greater volume of the material than four blades. This method would closer approach the ideal circular failure surface and minimize the problem of progressive failure.

3.2.2.4 Data Acquisition System

The electric signal coming from the torque transducer was amplified by a Measurements Group Instrument Division Model P3500 strain gauge indicator and sent to a Fluke 2240B data logger which had an Option 17 board mounted on it. The data logger was interfaced with an IBM-clone personal computer

equipped with two disk drives. The data acquisition was controlled by the Techtran software, a computer program written by the electronic personnel in the Department of Civil Engineering at the University of Alberta. This particular system was capable of recording two readings per second which was especially important in the initial stage of the shearing tests where the peak strength was reached within first ten degrees of vane rotation. The readings were stored on 5 1/4 inch magnetic diskettes.

3.2.2.5 Testing Procedure

The testing procedure was in accordance with the ASTM D 4648 - 87 unless otherwise specified. The modifications of the vanes were discussed in details earlier. It should be added that the standard recommends blades with the height diameter ratio of 2:1 although it permits using a ratio of 1:1, with a vane blade diameter varying from 12.7 to 25.4 mm. Vane rotational rates were determined according the angular shear velocity approach as recommended by Perlow and Richards (1977) and advocated by the ASTM standard. Based on the proposed velocity of 0.15 mm/s and equation 3.15, the following rates were chosen:

20 mm vane - 60°/min vs. 51.6°/min recommended

30 mm vane - 40°/min vs. 34.4°/min recommended

80 mm vane - 15°/min vs. 12.9°/min recommended.

All chosen rotation rates corresponded to the angular shear velocity of 0.17 mm/s. The achieved accuracy of the rotation with the modified apparatus was within ± 2°/min. The ASTM standard recommends a constant rate of 60 to 90°/min for typical vanes but makes a reference to the earlier described approach.

According to the standard, the vane should be inserted in the sample to a minimum depth equal to twice the height of the blade to ensure that the top of the vane blade is embedded at least one vane blade height below the sample surface. This procedure was followed for the 20 and 30 mm vanes. However, for the 80 mm vane the recommended insertion depth was impossible to achieve due to low sample height to vane blade height ratios. Instead, a constant depth of 25 millimeters below the sample surface to the top of the blade was adopted for the 80 mm vane.

The peak strength was reached usually within the first ten degrees of vane rotation and the accuracy of determining the value of it depended on the rotation rate. As mentioned earlier, the system was capable of taking two readings per second, therefore the number of readings recorded during the first ten degrees varied from 20 for the 20 mm vane to 80 for the 80 mm vane. Thus, it was more possible to miss the true peak value with the 20 mm vane than with the 80 mm vane.

To obtain the residual strength, rotation of the vane was continued until readings were constant and did not decrease any further for at least 40 degrees of rotation or if they started to increase again continually. The ASTM standard recommends a minimum of five to ten revolutions of the vane in order to obtain the remoulded strength. However, in this case, that recommendation was not followed for several reasons. Firstly, due to the consistency of the slurry the full remoulding was achieved much sooner; depending on the age and the water content it varied from 180° (half revolution) to a maximum of 1440° (4 revolutions). Secondly, the time factor played a significant role: tests performed with the 80 mm vane required 24 minutes to complete one revolution and it was decided to limit these tests to 2 revolutions and, in cases of low water content/old age samples, to 3 revolutions. This procedure gave

satisfactory results. When the 20 mm vane was used with the liquid limit samples, the shearing continued for four full revolutions when it was deemed necessary.

Data processing and reduction required several steps. As mentioned earlier, raw data, in form of time and voltage readings, was stored in files on 5 1/4" floppy disks. Each file was then transformed to a Lotus-readable format. The next step required using another computer as files were imported to Lotus format and stored on smaller, 3 1/2" disks. The size of the files was reduced by deleting all redundant channels. The files were then ready to be transferred to the Apple computer system. The transfer was made possible by an Apple File Exchange program installed on an Apple Mac II computer. The transferred files were then read by the Excel program. The final step involved taking the disks to a Macintosh SE computer, transferring the files to a Cricket Graph format and reducing the data. The results of each test were then plotted in form of a stress-strain diagram.

3.2.3 Cavity Expansion Testing

Cavity expansion testing was originally to be included as an integral part in this research program and a considerable amount of work had been done in literature search, equipment design, and preliminary testing. However, it was later realized that with the number of other tests and a far-from-perfect state of development of this test, cavity expansion testing would be a separate research topic in itself and it was beyond the scope of this thesis. Therefore, further efforts were halted. Presented here, are the results of the preliminary work done on cavity expansion testing in this research program.

The concept of cavity expansion testing in slurries followed Elder (1985). Most of what is presented in this section is based on Elder's work. Although the

problem of cavity expansion had been considered theoretically long before Elder, there had been no practical developments in actual testing. Elder was first to build an apparatus employing the theory of expansion of a spherical cavity in soil. Spherical (or hemispherical) cavity analysis is used to model aspects of pile and cone penetration, where expansion occurs from a zero initial radius, and cylindrical analysis is used to interpret the pressuremeter test with expansion from a finite radius, determined by borehole size.

3.2.3.1 Theoretical Analysis

Spherical expansion analyses are formulated in spherical co-ordinates (r, θ) where symmetry applies. The self-weight of soil is assumed negligible. The equation of equilibrium of a soil element at a distance r from the centre of the cavity reduces to

$$\frac{\partial \sigma_r}{\partial r} + \frac{2}{r}(\sigma_r - \sigma_\theta) = 0 \qquad (3.17)$$

where σ_r is the radial stress and σ_θ the circumferential stress. A homogeneous and isotropic soil mass is assumed. The cavity is surrounded by a plastic region extending from the current cavity radius R_c (initial value R_{c0}) to a radial distance R_p, beyond which linear elastic behaviour occurs. Solution of the problem requires use of a relationship describing the yield behaviour and for soils the Mohr-Coulomb criterion is suitable

$$\sigma_r - \sigma_\theta = (\sigma_r + \sigma_\theta)\sin\phi + 2c\cos\phi \qquad (3.18)$$

Bishop, Hill and Mott (1945) solved the case of a frictionless ($\phi = 0$) incompressible medium where equation (3.18) reduces to the Tresca criterion and Gibson (1950) analyzed the cohesionless case ($c = 0$) for a purely frictionless material, also assuming incompressible conditions. Vesic (1972) provided the most general analysis in which he considers the conditions at an

ultimate cavity pressure, p_u, only and uses the Mohr Coulomb criterion. The total volume changes of the elastic and plastic zones are assumed equal to the change in volume of the cavity and the result is written as

$$p_u = (p_o + c\cot\phi)\frac{3(1+\sin\phi)}{3-\sin\phi}\frac{G/c_u}{1+\varepsilon_v G/c_u}^{\frac{4\sin\phi}{3(1+\sin\phi)}} \qquad (3.19)$$

where the expression is a close approximation for $\varepsilon_v < 0.15$ and $0 < \phi < 45^o$ and p_o is the initial uniform stress in the soil, c_u the undrained strength and G the elastic shear modulus. The average volumetric strain ε_v has to be determined in some way as a function for some volume change-stress relationship. This analysis is not valid for $\phi = 0$, where the Bishop et al solution applies. Elder (1985) in his study assumed undrained (incompressible) conditions. The undrained soil moduli are related by $G = E/3$ and the cohesion, c, is equivalent to the undrained strength c_u. His analysis follows that by Bishop, Hill and Mott but retains several terms assumed negligible in the original analysis, in order to assess their importance in very soft soils. The assumptions of isotropy and homogeneity apply and the initial total stress state is assumed to be p_o everywhere in the soil ($r > R_{Co}$). The effect is considered of an increase in cavity pressure from p_o by an amount Δp, causing a radial displacement u(r) and stress changes $\Delta\sigma_r, \Delta\sigma_\theta$ at a radial distance r. Yield will occur (initially at $r=R_C$) when

$$\Delta\sigma_r - \Delta\sigma_\theta = 2c \qquad (c = c_u) \qquad (3.20)$$

and that occurs when

$$\Delta p = 4c/3\,, \quad R_C = R_{Co}/(1 - \frac{c}{E}) \qquad (3.21)$$

and following this a plastic region will surround the cavity to a radius R_p, with an elastic region outside. Eventually, Elder arrives at the equation which gives the relationship between the cavity pressure, p, and the cavity radius, R_C

$$p = p_o + \frac{4}{3}c\,\{1 + \ln[\frac{E}{3c}\,\frac{(1-R_{Co}^3/R_C^3)}{1-c/E + c^2/3E^2}]\} \qquad (3.22)$$

which is valid only after yield has occurred at the cavity wall. At $R_C \rightarrow \infty$, a limiting value of p will be reached, which effectively will be observed (within 1% of Δp_L) when $R_C \geq 4R_{Co}$. This value will be

$$p_L = p_o + \frac{4}{3} c \{1 + \ln[\frac{E}{3c} /(1\text{-}c/E + c^2/3E^2)]\} \qquad (3.23)$$

To obtain maximum information from a particular expansion test, Elder suggests plotting Δp vs. $\ln(1- R_{Co}^3/R_C^3)$. The slope will then be 4c/3 giving the undrained strength ($c = c_u$), and the intercept (as $R_C >> R_{Co}$) will be $4c/3\{1 + \ln[\frac{E}{3c} /(1\text{-}c/E + c^2/3E^2)]\}$. The tangent to the curve at the intercept will then give the undrained strength.

In summary of Elder's analysis, if a spherical cavity of radius R_{Co} exists in an isotropic soil mass with initial stress p_o everywhere, the cavity will begin to expand when the cavity pressure p exceeds p_o. Soil behaviour will initially be elastic everywhere until the yield criterion (3.20) is satisfied at the cavity surface. This will occur when

$$R_C = R_{Co}/(1\text{-}c/E) \quad = 1.5\ R_{Co} \text{ if } E/c = 3$$
$$< 1.1\ R_{Co} \text{ if } E/c > 11 \qquad (3.24)$$

and the cavity pressure when the first yield occurs will be

$$p = p_o + \frac{4}{3}c \qquad (3.25)$$

As the cavity is expanded further it will be surrounded by a plastic soil region to a radius R_P, in which the radial total stress, σ_r, will be

$$p_o + \frac{4}{3}c \leq \sigma_r \leq p \qquad (3.26)$$

and an elastic region beyond this where $\sigma_r < p_o + \frac{4}{3}c$. At large cavity radii the cavity pressure will tend to the limiting value given by equation 3.19. For E/c > 10 the total increase in cavity pressure will be approximately

$$\Delta p = p_L - p_o \approx \frac{4}{3}c \{1 + \ln\frac{E}{c}\} \qquad (3.27)$$

and will be attained within 1% when $R_C \geq R_{Co}$.

Two theoretical curves (Figure 3.4) reprinted after Elder show pressure vs. volume and pressure vs. radius plots for a typical example where the initial cavity radius is 1 mm, the undrained strength c is 0.2 kPa and E/c = 6. It can be seen that yield is not defined well on either curve and that the limiting pressure is attained with relatively small volume increase.

3.2.3.2 Testing Apparatus

A controlled pumping system was required which could create a fluid filled cavity volume at a controlled and preset rate, from which volume changes with time could be calculated. The cavity pressure had to be measured remotely with high reliability. Pressures would be very low, therefore a very sensitive and accurate measuring device was required. The cavity fluid should not mix with water nor diffuse into the soil pores.

The system which was developed used Elder's concept, however numerous practical changes were introduced into the design. Elder contained the cavity fluid in an acrylic cylinder with an inside moving piston which was connected to a stepping motor, giving a flow rate control of 0 to 10 ml/min. In this program, a high precision syringe pump was used as the volume control device. The pump - an ISCO LC-5000 Syringe Pump, was capable of delivering flow at a continuously variable rate of 1.5 to 400 ml/hr (0.025 to 6.7 ml/min). Thick walled "zero volume change" nylon tubing connected the pump with a stainless steel 1.6 mm (1/16") tubing mounted on an adjustable holding frame. One end of the "C" shaped steel tubing played the role of the hypodermic injection needle used in Elder's design and was inserted directly into the slurry while the other end was fastened to a pressure transducer. The holding frame, in turn, was mounted on the shear vane apparatus stand. Correction factors were required to be established in order to account for pressure losses

between the cavity and the transducer. The cavity fluid which was eventually selected was silicon oil of high viscosity and of a density slightly lower than that of water. In order to check if cavities were in fact spherical, an injection of silicon oil was made into a small sludge filled beaker, then the sample was frozen and, subsequently, cut and examined. Good results were obtained using this method confirming the assumption that buoyancy effects were not significant.

3.2.3.3 Testing Procedure

An initial testing procedure was established and although only slightly different from that of Elder's it required further refining. The injecting part of the steel tubing was positioned vertically and silicon oil was expelled from the tip to form a drop preventing air from entering the tubing. The tip was then lowered slowly to a depth of 25 mm (1") from the sludge surface and left there to allow excess pressure to dissipate; this was indicated by steady transducer readings. The cavity was then expanded at an appropriate constant rate of volume increase with continuous recording of time (i.e. cavity volume) and cavity pressure. As opposed to Elder's method, there was no provision for measuring pore pressures at different locations in the specimen. As mentioned earlier, only few preliminary tests were conducted and no results as such will be presented. However, Figures 3.5, 3.6 and 3.7 show plots of stress history, cavity pressure vs. cavity volume and cavity pressure vs. cavity radius, respectively, for one of the tests. The shapes of the curves are similar to these presented by Elder thus confirming the validity of cavity expansion testing for oil sands tailings sludge.

3.3 Test Selection

This Section describes classification of the tests and explains their selection.

3.3.1 Index Tests

3.3.1.1 Origin of Samples

A set of index tests: water content, Atterberg limits, grain size distribution, specific gravity, and bitumen content was run on representative specimens of sludge obtained from two different sources: the storage tank and directly from the pond. The purpose was to assess if there were any differences in index properties between these two types of sludge and, if so, whether the differences were insignificant enough as to treat them as the same soil from a geotechnical point of view.

3.3.2 Viscosity Tests

3.3.2.1 Water/Solids Content of Sludge

Initially six different water/solids contents were selected to be investigated. These were: 400% (20%), 300% (25%), 233% (30%), 150% (40%), 100% (50%), and 47% (68%) water content (solids content), the last one representing the liquid limit of the slurry. These particular water contents were chosen to represent layers of sludge of different age as they exist in the pond. 400% water content (20% solids content) sludge represents thin slurry after completion of sedimentation process. After reaching this solids content, any increase in sludge density arrives from the process of self weight consolidation (Scott and Dusseault, 1982). It takes about two years for the sludge in the pond to consolidate to a solids content of 30%. The sludge at this point is termed "mature" - anything less then 30% solids (233% water) is called "immature" sludge. Therefore, in this research there are two "immature" water content

sludges (400 and 300%) and four "mature" ones (233, 150, 100, and 47%). It should be added, however, that 100% water content (50% solids) sludge could be treated as the limit which has not yet been reached in the pond: Dusseault, Scafe and Scott (1989) state that at the base of the sludge column in the pond, where high stresses have acted for years, there is a zone of higher solids content sludge, 40 - 45% by weight, and MacKinnon (1989) found in his annual pond surveys highest solids concentrations of 44.7% at depths greater than 28 meters. Sludge at its liquid limit could not possibly exist in the pond and the purpose of testing sludge of such high solids content was to compare with other researchers' findings, which usually concentrate on water contents at or below the liquid limit. It was later determined that viscosity measurements in such a relatively dense (liquid limit) material were beyond the capability of the viscometer and testing of these specimens was limited to the shear vane.

3.3.2.2 Age of Sludge

Time was perhaps the most important variable in this research. Age of the sample, or time, was measured from the moment when the process of remoulding, or physical agitation of the material, was ceased. Originally, specimens were to be tested from age zero up to 320 days. In effect, the longest "aging" lasted over 680 days. Because it was believed that the greatest increase in thixotropy occurred in the initial few days following remoulding, tests were scheduled at ever increasing time intervals. For each water content, the nominal test schedule was as follows (time after remoulding): 0, 5 minutes, 10 minutes, 20 minutes, 30 minutes, 1 hour, 2 hours, 3 hours, 4 hours, 8 hours, 12 hours, 18 hours, 24 hours, 2 days, 3 days, 4 days, 5 days, 10 days, 20 days, 40 days, 80 days, 160 days, 470 days, and 680 days. There were some deviations, which were small and not significant, from the schedule and they were dictated by

the need to increase the number of experiments in order to gain a better understanding of the material's behaviour.

3.3.3 Shear Vane Tests

3.3.3.1 Water/Solids Content of Sludge

The selection of specimens based on water/solids content of the sludge for the vane shear testing was identical to that for the viscosity measurements. Therefore, the specimens of sludge were divided into six groups: 400% (20%), 300% (25%), 233% (30%), 150% (40%), 100% (50%), and 47% (68%) water (solids) content. The only difference between the viscosity measurement part of the program and the shear vane testing part in this respect was that the testing of the liquid limit specimens ($w \approx 47\%$) was only carried out by the shear vane.

3.3.3.2 Age of Sludge

Because of the duration of a single vane shear test and time required for its preparation, it was impossible to schedule experiments with short time intervals as was done with the viscosity measurements. Therefore, the number of tests in the initial period after remoulding was greatly reduced in relation to the viscosity tests. For every one of the six water content, the test schedule was as follows: 0 (immediately after remoulding), 2 hours, 8 hours, 24 hours, 2 days, 5 days, 10 days, 20 days, 40 days, 80 days, 160 days, and 470 days. Again, there were some deviations from this plan; many tests were added, many were repeated - for higher reliability and better understanding.

3.3.4 Experiment Designation

The total number of experiments exceeded two hundred. It was necessary then to describe each experiment in a short, symbolic manner. There were three important variables every description had to contain: type of the test (viscosity versus vane shear), water content, and age of the sample. To maintain consistency, each description contained seven symbols: two letters and five digits. The first letter described the type of the test: "V" for viscosity, "S" for vane shear. Next, there were two digits and they uniquely described the initial water content of the sample: "40" for 400%, "30" for 300%, "23" for 233%, "15" for 150%, "10" for 100%, and "47" for 47% water content. Following, there were three digits and a letter describing the age of the sample; last letter indicating time units: "M" for minutes, "H" for hours, and "D" for days. For example, "S10680D" indicates the shear vane test for 100% water content sludge at 680 days after remoulding, and "V40000M": viscosity measurement for 400% water content sludge at zero minutes after remoulding. For test results, there was another letter added at the end of a symbol: "P" for the peak value and "R" for the residual value.

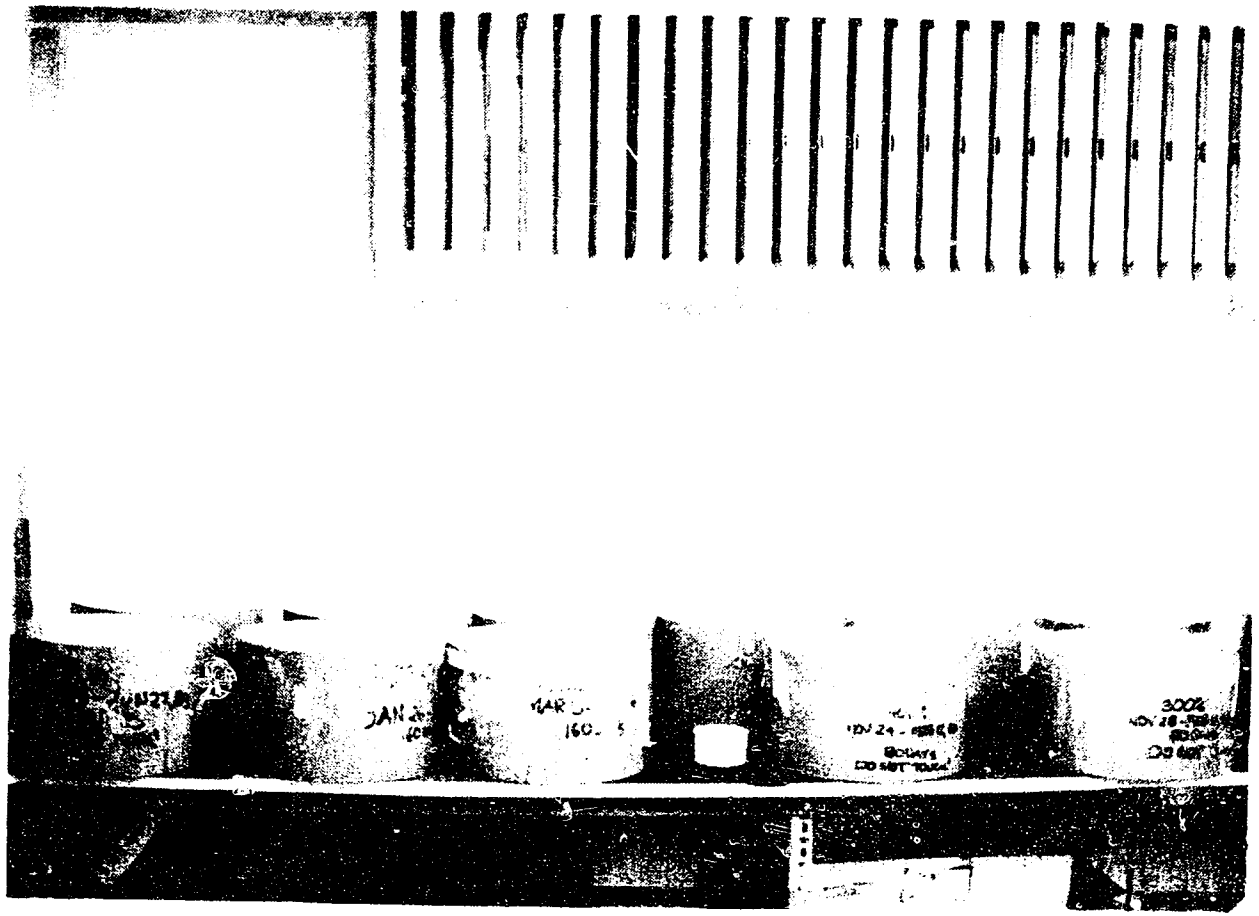

Plate 3.1 Sludge Containers

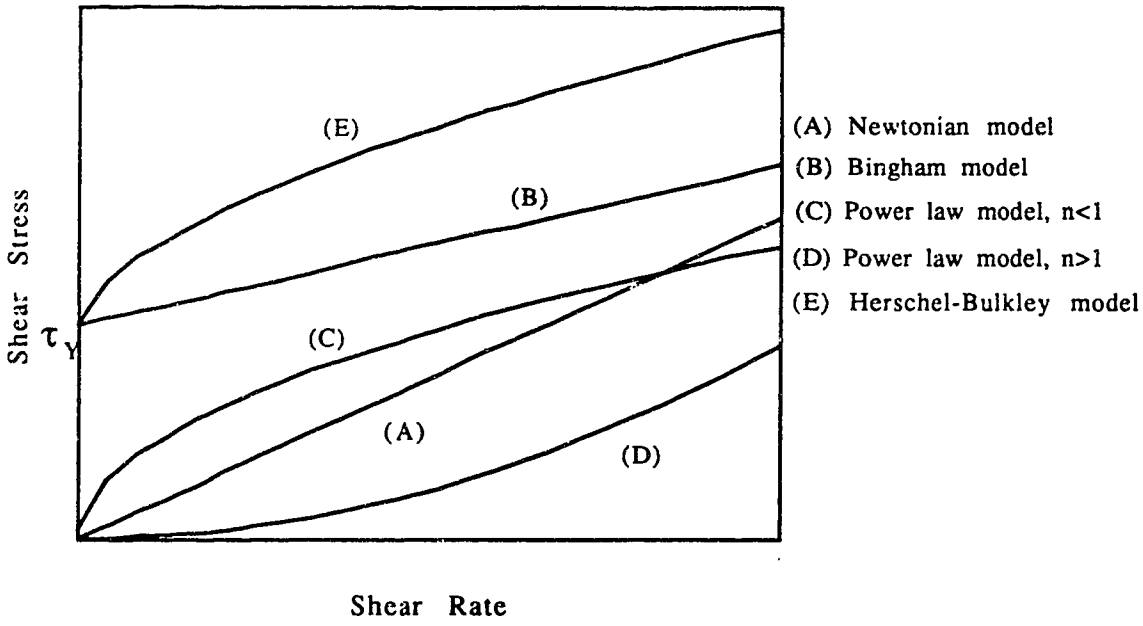

Figure 3.1 Flow Curves for Model Materials

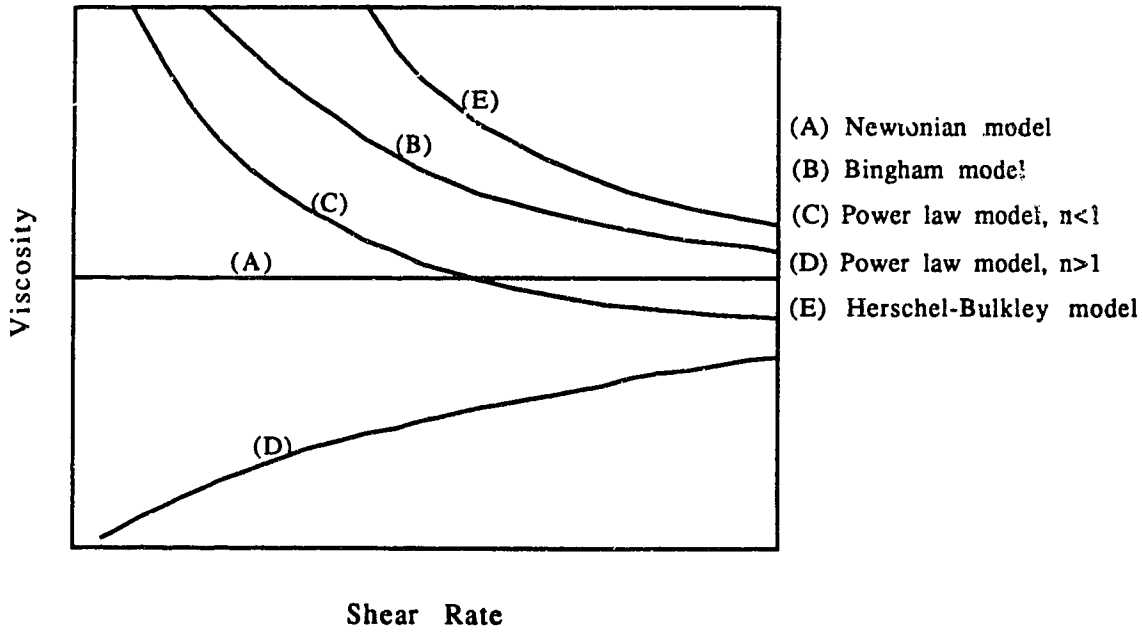

Figure 3.2 Variation of Viscosity with Strain Rate for Model Materials

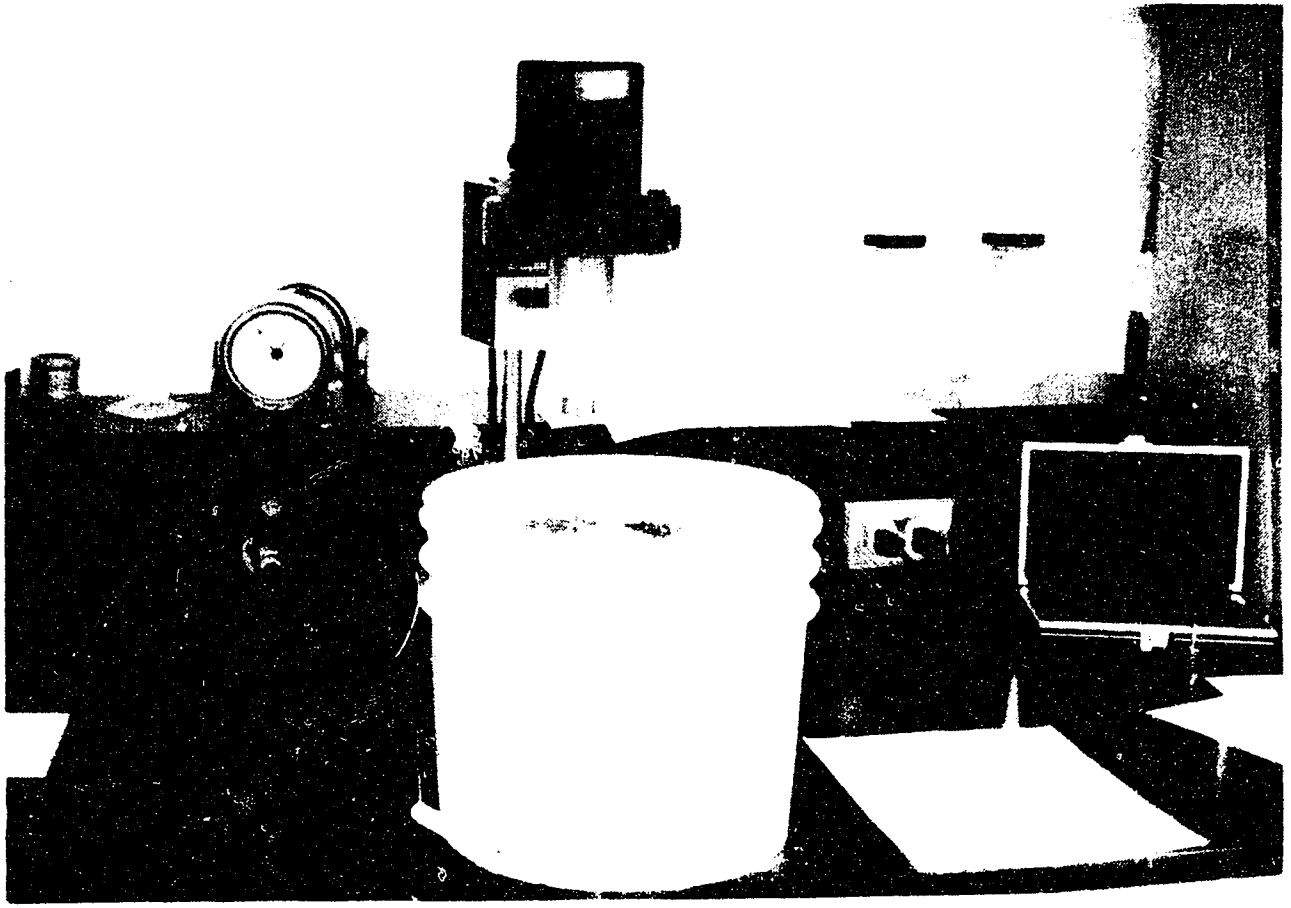

Plate 3.2 Brookfield Viscometer with a T-bar Spindle

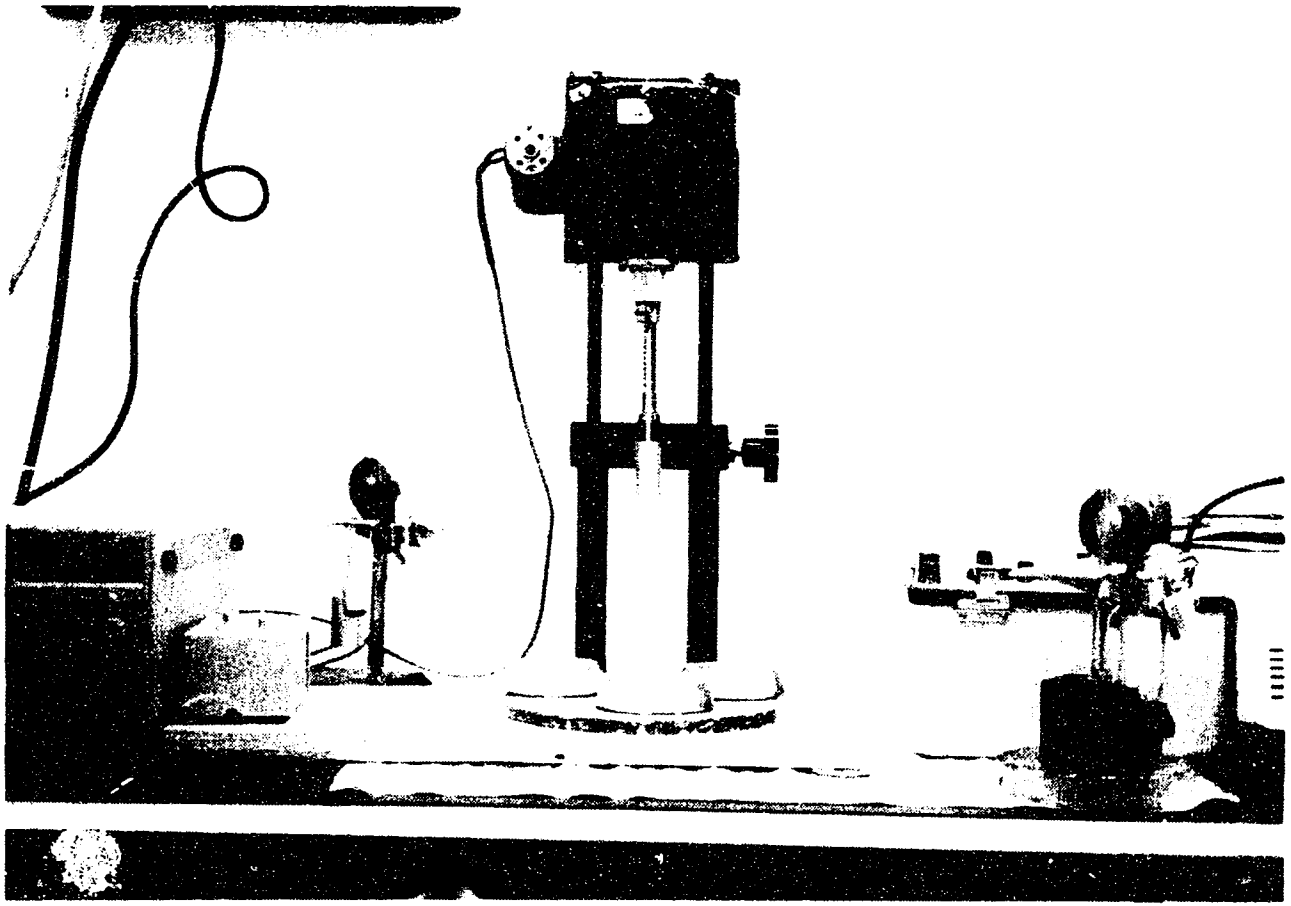

Plate 3.3 Torque Cell Calibration System

Plate 3.4 Torque Cell and Moment Cylinder

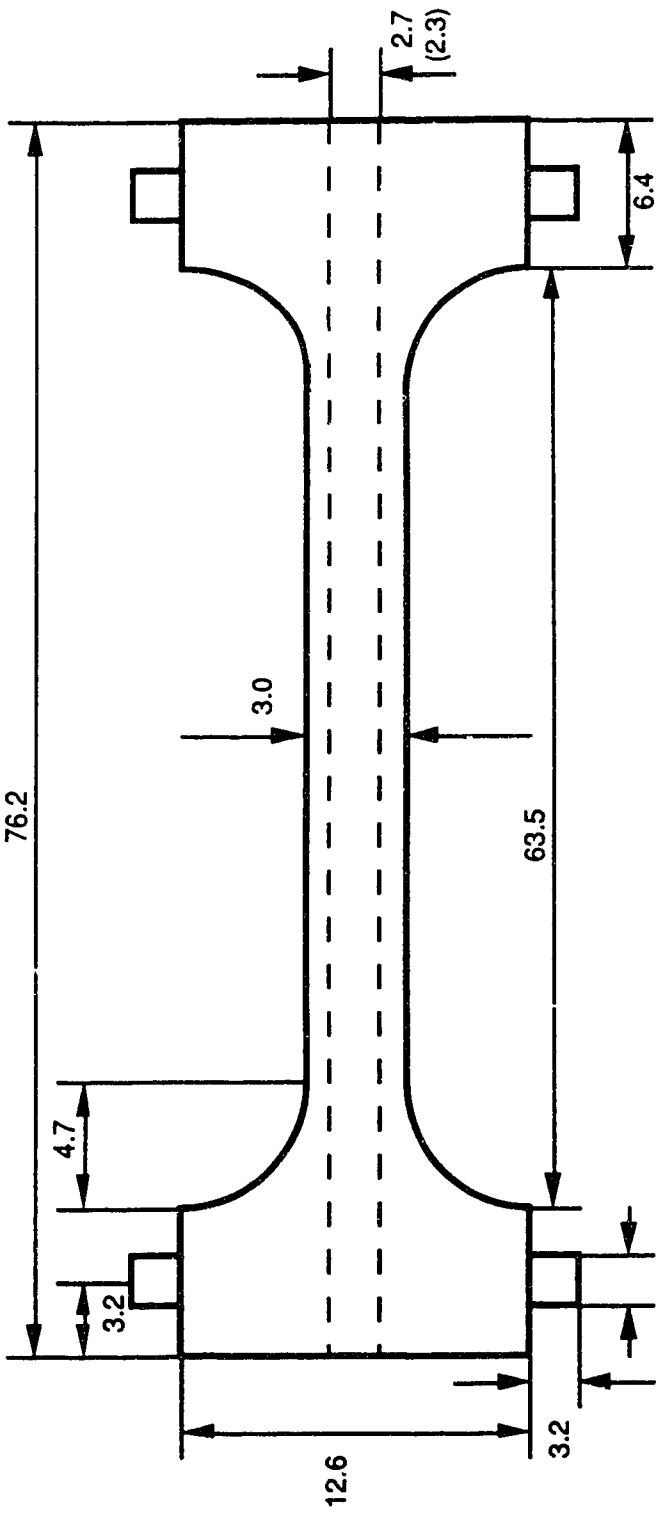

Note: - All dimensions in mm
- Wall thickness 0.15mm (0.35mm)
- Tolerance of the shaft 0.01mm

Figure 3.3 Torque Cell for Vane Shear Apparatus

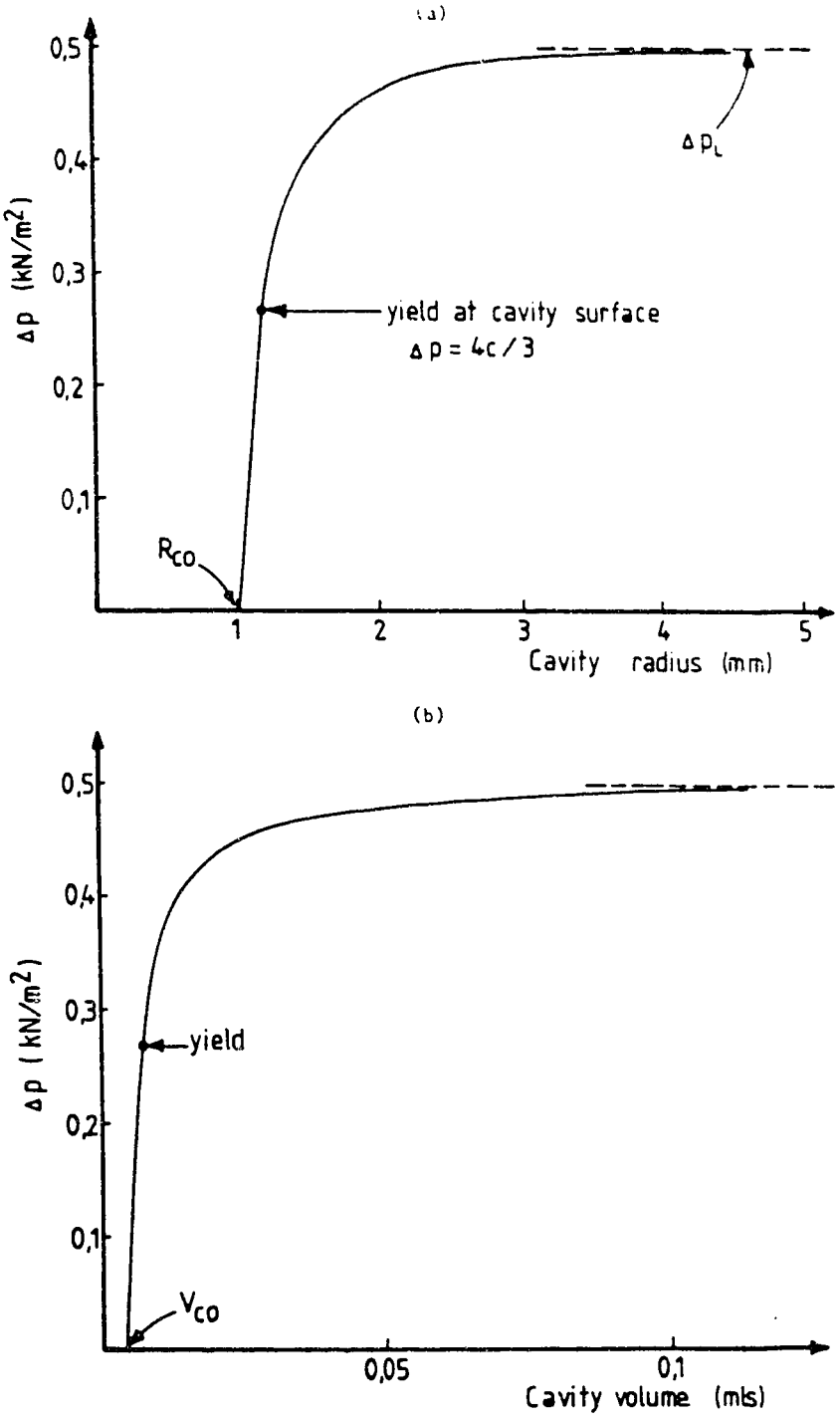

Figure 3.4 Theoretical curves for expansion of spherical cavity for initial radius 1 mm, with E/c=6, c=0.2kPa. After Elder (1985)

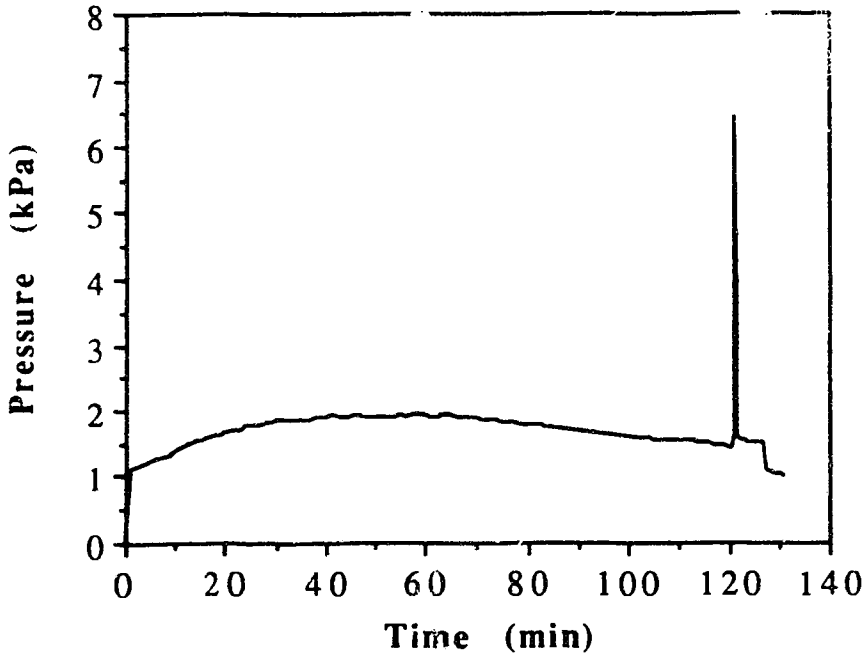

Figure 3.5 Cavity Expansion Test 01- Stress History

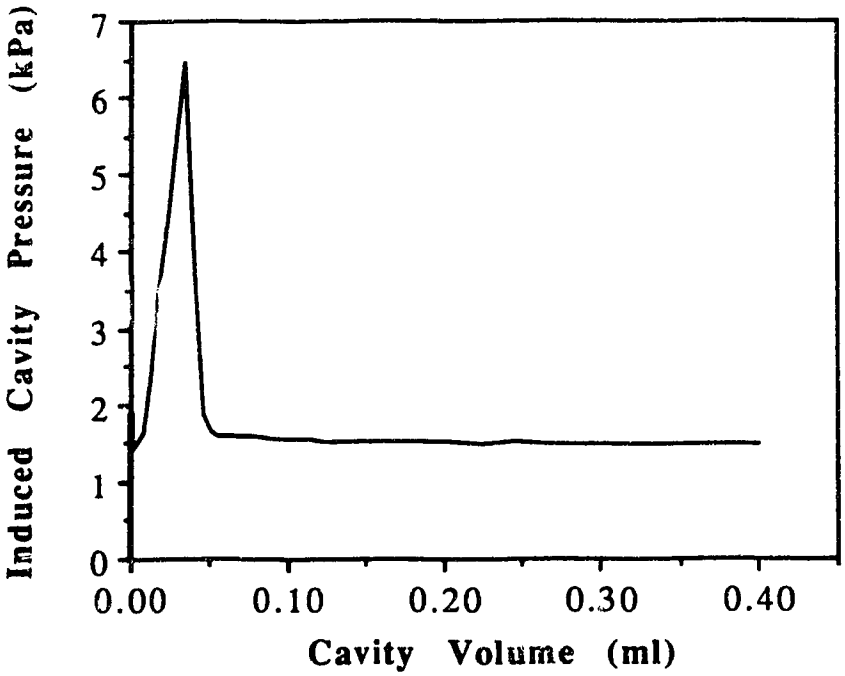

Figure 3.6 Cavity Expansion Test 01, Pressure vs. Volume

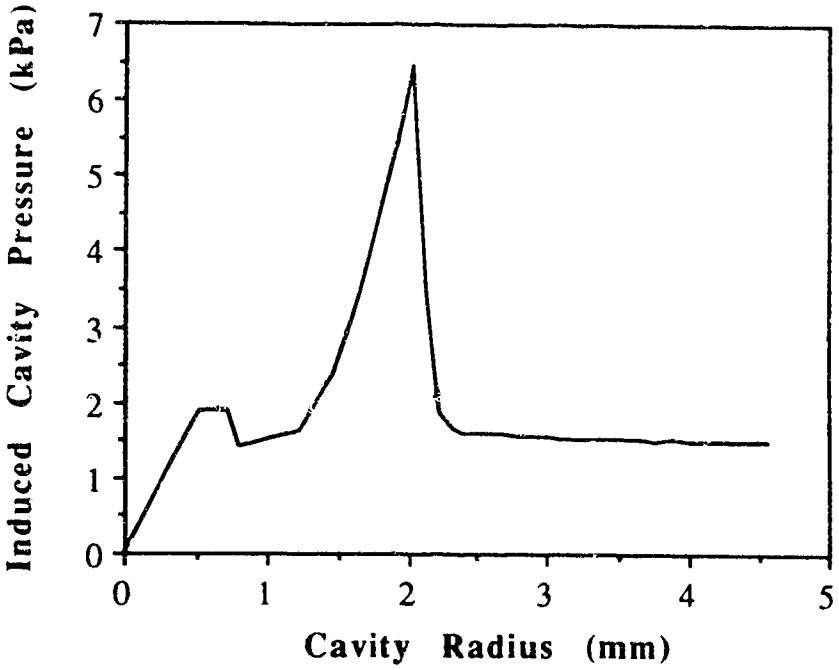

Figure 3.7 Cavity Expansion Test 01, Pressure vs. Radius

4. LABORATORY TEST RESULTS

This Chapter presents the results of the experiments conducted during this research program. Index tests are discussed first, along with their significance and impact on the two major groups of experiments: viscosity measurements and vane shear testing. This data is followed by viscosity test results presented in a form of shear stress versus shear rate and "apparent" viscosity versus shear rate plots, and vane shear test results in a form of shear stress versus shear strain plots.

4.1 Index Tests

Oil sands tailings sludge as a geotechnical material was described in detail in Chapter 2. Here, the results of index tests will be presented and discussed from the perspective based on the fact that two batches of the sludge were used. Differences, if any, between the two batches will be exposed and their possible influence on the test results will be considered.

4.1.1 Water Content

The initial water content of the two sludges (batch 1 and batch 2) showed a large difference. Batch 1 sludge had a water content of 168% (37% solids content) whereas the sludge from batch 2 showed a 270% water content (27% solids content). This difference is explained by the history of storage of the two sludges. Batch 1 sludge had been stored in a tank for several years prior to sampling and the sample came from the bottom of the tank without mixing of the contents. Thus, it had such a low water content. Batch 2 had been collected directly from the tailings pond relatively shortly (4 months) before it was received in the laboratory.

Results obtained from Syncrude Research (MacKinnon, 1991) showed a solids content of 36% for batch 1 and 28% for batch 2 sludge which translates to a water content 178% and 257%, respectively.

4.1.2 Atterberg Limits

Six Atterberg limit tests on representative sludge samples were performed on several occasions. The purpose of these tests was to position the material on the plasticity chart as well as to determine differences between the two batches of the sludge and the two methods of dewatering. The slurry was thus divided into batch 1 and batch 2 samples and, furthermore, batch 2 sludge was tested in two categories: evaporated and centrifuged. The term "centrifuged" should not in this case be taken literally as the specimens were dewatered partially by centrifuging and partially by evaporating - centrifuging did not bring any visible effects for water contents lower than about 100%. Table 4.1 summarizes the results of Atterberg limits tests. Scott et al. (1985) report the full available range of liquid limit data from sludge to be between 40 and 80%. According to the authors, variations in the data reflect several factors other than clay mineralogy including ionic concentration, bitumen content and total percent clays in the mineral solids. In general, higher values reflect greater bitumen content and finer-grained sludge. The results of this research fall within these boundaries. The range of the liquid limit is between 44 and 57%. One detail, however, should be pointed out to better understand the complexity of the sludge's behaviour. The tests were performed by two different methods. In the first method, the sample was thoroughly mixed (remoulded) just prior to each blow count trial. In the second method, the regular liquid limit test procedure was followed and complete remoulding was not done. This latter procedure does not take into account the critical role that time plays in the

soil's strength testing. Method one was used in four Atterberg limit tests, and method 2 in two tests. Results obtained by method 2 were in the range 53 to 58% for the liquid limit and 21 to 23% for the plastic limit, and those obtained by method 1 varied from 44 to 47% for the liquid limit and 20 to 26% for the plastic limit. These tests results confirm the thixotropic phenomenon occurring in the oil sands tailings sludge. The difference in the liquid limit between batch 1 and batch 2 sludge appears to be small in both cases; 3 and 5 percentage points, respectively. The difference, therefore, between the two sludge batches should not have any important bearing on viscosity and strength test results. Similarly, the difference in the liquid limit between evaporated and centrifuged specimens, 3 percentage points, can be considered small.

As shown in Table 4.1, based on the above, the typical results were: w_l = 46%, w_p = 21%, and I_p = 25%.

4.1.3 Grain Size Distribution

Samples representing sludge from batch 1 and batch 2 were analyzed for grain size distribution using the standard ASTM hydrometer test method with two different ways of preparing the soil for the test, as described in Chapter 3 (Section 3.1.2). Seven tests altogether were conducted, three on batch 1 sludge and four on batch 2 sludge, and the resulting grain size curves are shown in Figure 4.1. Circle shaped symbols represent batch 1, square symbols indicate batch 2; furthermore, shaded symbols denote extracted (bitumen-free) sludge. In the legend, the abbreviation "Ex" stands for an extracted sample, a "C" means a centrifuged sludge, and the rest - either a second digit or a letter "E" implies evaporated sludge. Appropriate specific gravities (see Section 4.1.4) were used for calculations. Since, as described later in Section 4.1.4, the determined specific gravities of the mineral grains did not appeared to be

correct, values closer to 2.70 were also used. The differences in grain size distribution using the different specific gravities were considered small. A distinctive feature of the graph is a rather large difference between curves obtained from extracted material tests and those from as-received sludge tests. The extracted sludge curves imply a minus 2 micron content of only 6 to 11%. Typical grain size curves for tailings sludge as presented by Scott and Chichak (1985) and Scott and Cymerman (1984) also show a much higher minus 2 micron content: 40 to 50%. The sand content in the two test procedures is from 10 to 15%; within the boundaries in the above references. A possible explanation of this unusually low clay content is that the high temperature associated with the extraction process of the sludge caused flocculation or bonding of the finer particles thus dramatically altering the grain size distribution of the material. It is thought that, in this case, cementing is limited to clay and silt size particles and is not detectable through visual inspection. Furthermore, mechanical pulverizing by means of a pestle does not guarantee a return to the original grain size distribution.

The five curves representing hydrometer tests on wet, bitumen-included sludge correspond well with the above referenced typical grain size distribution curves for oil sands tailings sludge. This result applies to both batch 1 and batch 2 sludge. Batch 1 is consistently coarser than batch 2 sludge. The former has a minus 2 micron content of 40 to 45% and a sand content of 10 to 16%, whereas the latter displays a minus 2 micron content of 57 to 59% and indicates no presence of sand size particles. The coarser nature of batch 1 sludge was to be expected in view of the origins of the two batches (see Section 3.1.1).

As discussed in Section 3.1.2, hydrometer testing of sludge without extracting bitumen, called here "as-received sludge", may result in a grain size distribution curve distorted toward finer sizes.

From the above, it can be seen that there is a need for an improved method of performing hydrometer tests on oil sands tailings sludge as neither method presented here probably results in a true grain size distribution.

Syncrude Research employs the Microtrac apparatus for determining particle size distribution of the sludge. A typical sample preparation includes extraction of bitumen and hand pulverizing the dry soil with a pestle. Results of Microtrac analyses of batch 1 and batch 2 sludge were obtained from Syncrude Research (MacKinnon, 1991) and are shown in Figure 4.2. Both curves do not extend to the minus 2 micron size range. By extrapolation, the minus 2 micron content is fairly low: 12 to 15% for batch 1 sludge and 17 to 20% for batch 2 sludge; only slightly higher than that for corresponding extracted samples in the hydrometer analysis and still much lower than that reported from other hydrometer testing on the sludge. In spite of pulverizing, a possible explanation would again be flocculation of the fine particles. The sand content is 7 and 2%, respectively, lower than batch 1 and higher than batch 2 for the "as-received" hydrometer tests. The results, however, are consistent in that batch 1 sludge is coarser than batch 2 sludge. In general, the Microtrac method is subject to criticism for testing fine silts and clays and the hydrometer method is preferred owing to its wide usage in geotechnical engineering.

It is concluded that, for engineering purposes, the hydrometer test on as-received sludge be used for determining grain size distribution. This test procedure models the sedimentation process in the tailings pond and therefore represents field behaviour.

4.1.4 Specific Gravity

The specific gravity of the sludge solids was calculated using Equation 3.4 which states that this property is a weighted average of the bitumen and mineral portions of the sludge. The three variables in this equation, bitumen content, specific gravity of the bitumen and specific gravity of the mineral grains had to be determined in order to use the equation. The bitumen content is described in the next section, the specific gravity of the bitumen was taken as 1.03, and the specific gravity of the mineral grains was determined on extracted samples of sludge 1 and sludge 2. These were 2.56 and 2.52, respectively. The results seem too low for a clay soil which should have a specific gravity of approximately 2.70. An explanation of this is that the extraction process did not remove all of the bitumen from the sludge which consequently decreased the specific gravity of the mineral grains. Another possibility is that air bubbles adhered to the surface of the mineral grains because of precipitated chemicals.

The resulting specific gravity of the sludge solids was 2.36 for batch 1 sludge and 2.37 for batch 2 sludge. Centrifuged sludge solids had a specific gravity of 2.40.

4.1.5 Bitumen Content

The bitumen content of four separate sludge samples was determined through an extraction process as described in Section 3.1.2. In order to make the bitumen content independent of the water content of the sludge, the results are given as a percent of the mass of the mineral grains. Batch 1 sludge displayed a slightly higher bitumen content: 6.1% as compared with batch 2 sludge: 4.6%. Centrifuged sludge (batch 2) had the lowest bitumen content: 3.7%.

Syncrude Research reports a bitumen content (defined as the percent of the total sludge mass) of 2.75% for batch 1 sludge and 1.40% for batch 2 sludge (MacKinnon, 1991). In terms of percent of the mass of the mineral grains, the bitumen contents are 7.7 and 5.0%, respectively, similar to those determined in this research.

4.1.6 pH

pH measurements were conducted twice over the course of the experimental program. The first measurement was conducted directly in the barrel of batch 2 sludge within the first several days after receiving the slurry. The pH was 8.5. The second measurement was conducted after about 700 days on the same material and with prior mixing. This time, the pH was 8.0.

4.2 Viscosity Test Results

As discussed earlier in Chapter 3, the results of each viscosity test are presented in the form of two graphs, one showing a plot of the rotational rate of viscometer (strain rate) versus viscometer reading (shear stress), the other, shear rate versus "apparent viscosity". Because of the limitations of the viscometer such rheological properties as yield strength, viscosity or apparent viscosity could not be determined. Two values from each test, arbitrarily chosen index parameters representing viscometer peak and residual readings at 1 rpm, were used in the analysis of the results. The graphs themselves had a dual role: firstly, the best-fit curves were compared to the model rheological curves presented in Chapter 3 (Figure 3.1 and 3.2) for material classification purposes. Secondly, they could indicate potential invalidity of the 1 rpm index value. Therefore, the graphs should be looked at

more from a qualitative rather than a quantitative perspective. Appendices A and B contain complete sets of graphs resulting from the viscosity tests.

4.2.1 Sludge 400

For specimens labelled "Sludge 400" the initial water content of 400% stayed at that level for about three days after mixing before consolidation could be visually noticed and the water content had to be measured accordingly. The difficulty with such thin sludge was that even with the most sensitive spindle, viscometer readings were very low, adversely affecting the accuracy and increasing the degree of scatter of the results. The manufacturer of the viscometer suggests operating in the upper end of the scale (close to 100) for best results. With readings as low as 0.4 on a scale of 100 it is obvious that in such cases all factors influencing viscosity could play an important role. As all readings were taken manually, the operator's error was proportionally greater with lower values. It is a well documented fact that viscosity is very sensitive to temperature. Although the temperature was always recorded during tests, maintaining it at the same level was impossible; the difference was as high as 4^0 C. In addition, no temperature correction factor could be found in the literature for viscosity of the sludge and results could not be normalized to the same temperature. The scatter of readings, both peak and residual, is clearly illustrated in Figure 4.3. This 10 minute test plot is typical for "young" samples and is characterized by very low readings and their high scatter, a small difference between peak and residual values, and power law best-fit curves in the form of Equation 3.8 for both sets of readings. Both, strain rate - stress and strain rate - viscosity plots indicate a Herschel-Bulkley model material. With higher elapsed times readings become more consistent, better fitting the curves and the difference between peak and residual values

becomes more pronounced. An emerging pattern is that of a power law flow line for peak values and a straight line (Equation 3.6) for residual readings. In fact, starting at 18 hours, all but three tests display this trend. A typical example is shown in Figure 4.4, a plot for the 40 day test. This behaviour indicates that the material in its undisturbed state complies with the Herschel-Bulkley model fluid, once remoulded, however, it is similar to the Bingham model fluid. The three earlier mentioned exceptions, the 33, 64 and 470 day tests, can be best described by two straight lines, thus indicating the Bingham model for both sets of readings. It should be added, however, that the difference between the power law and the straight line curve best fit is often so small that the two fits could be considered interchangeable. Of interest is the remoulded behaviour of the 680 day sample. It appears that with increasing shear strain rate the shear resistance is decreasing, as seen in Figure 4.5. This is clearly inconsistent with all the other results and probably indicates better remoulding at higher rpm.

Table 4.2 summarizes the result of viscosity test for sludge 400. A complete set of plots can be seen in Figures A.1 through A.26 and B.1 through B.26.

4.2.2 Sludge 300

Sludge 300 was characterized by the samples' initial 300% water content (25% solids content). Consolidation of the sludge was first noticed in containers after about four days of rest. Studying the appearance of the graphs one must notice a few characteristics: most of the curves have similar shapes, scatter of the points is very small in most cases, and there is a highly pronounced pattern in rheological behaviour. Out of 24 flow curves for the undisturbed state, 22 are best fitted by the power law shape, 2 by a straight line. Out of 25 flow curves for the residual values, 24 are best fitted by a straight line. Figure 4.6 showing

the 6 day test is a good example of this pattern. The best fit by either a straight line or a power law curve improves with longer test times and it is generally better than that for sludge 400 which is probably due to higher readings, that is, better accuracy of the instrument. The results strongly suggest that the sludge behaves like a Herschel-Bulkley material in its undisturbed state and it is a typical Bingham material when remoulded. Again, as was the case with sludge 400, the longest (660 days) test exhibited a shear stress decrease as the shear rate increased (Figure 4.7).

Table 4.3 summarizes the results of sludge 300 viscosity tests and Figures A.27 through A.51 and B.27 through B.51 contain plots of the results.

4.2.3 Sludge 233

A total of 24 viscosity tests were conducted on specimens with an initial water content of 233% (30% solids content). First sign of consolidation of the specimens were noticed after about 15 days of rest. Increasing values of viscometer readings as compared to sludge 400 and 300 were encountered in this series of tests. The lowest reading at 1 rpm was just below 2 for remoulded sludge, the highest was 84 for the 682 day test. The water content decreased to 158% during 682 days of self-weight consolidation. The peak viscometer behaviour of the 233 sludge samples once again showed predominantly the Herschel-Bulkley model behaviour: 19 test plots were best fitted by a power law curve while 4 (1 hour, 2 hour, 3 hour, and 4 hour tests) were best described by a straight line indicating a Bingham fluid. These four tests happen to display the Bingham model for both, peak and residual flow lines (see Figure 4.8). The residual curves were best fitted by a straight line in 21 cases and by a power law equation in 3 cases (5 minute, 8 hour and 12 hour test). Of those 21 residual tests best fitted by a straight line not all can be said to display the Bingham

model behaviour. The 494 day test residual flow line shows the phenomenon encountered in the longest test for sludge 400 and 300: after reaching the yield strength, τ_Y, the shear stress decreases with a shear rate increase (Figure 4.9). For all practical purposes the residual flow lines for tests at 90 and 682 days can be considered horizontal thus not fitting into the Bingham model. The scatter of the results does not appear to be of great concern although the difference in temperature might have influenced the results as it can be seen in Figure 4.10 where two sets of readings were taken at temperatures differing by 3.8 degrees Celsius (18.7 and 22.5° C).

The summary of the results of viscosity tests of sludge 233 is shown in Table 4.4 and complete sets of plots are included in Figures A.52 through A.75 and B.52 through B.75.

4.2.4 Sludge 150

Twenty-five viscosity tests were conducted on sludge specimens with an initial water content of 150% (40% solids content). The self-weight consolidation process caused a reduction of the water content over a period of 680 days from 150% to 129% (44% solids content). No evidence of consolidation was noticed for at least 92 days. The sample tested at 470 days showed a water content of 141%, therefore consolidation started some time between 92 and 470 days. A complicating aspect in this series of tests was the fact that three different spindles were used with the Brookfield viscometer. The largest, most sensitive spindle T-A could handle readings up to the fifty-one day test. Starting at the 92 day test, peak readings, especially at high rpms, exceeded the upper limit of the viscometer scale and a smaller spindle had to be used. The longest, 680 day test could only be handled by spindle T-C. Whereas the rheological classification of the material was done on a qualitative rather than

quantitative basis and the size of the spindle did not affect it, the results used for further analysis had to be normalized to represent common-spindle readings. For a linear shear stress - shear strain rate relationship, in other words for Newtonian fluids, readings of all spindles are interrelated through unique factors. For example, readings obtained by using spindle T-B will give the same readings as spindle T-A at an identical rotational rate if multiplied by 2.0. This, however, does not hold true for non-Newtonian fluids one of which is the oil sands tailings sludge. In order to normalize all 1 rpm results, the following method was used. A series of measurements was conducted on sludge 150 and 100 samples at 1 rpm using different spindles. It was shown that independently of the size of the spindle, the ratios of the peak to residual readings at 1 rpm were constant for a given sample. Table 4.5 gives the results of the measurements. The relative difference between corresponding ratios is within accepted experimental error (10%). The ratio of peak to residual reading in general was called "sensitivity" of a given sludge sample and is included in the last column of the results tables (Table 4.2, 4.3, 4.4, 4.6, and 4.7). Furthermore, in all tests it was possible to obtain a residual reading at 1 rpm with spindle T-A. To calculate a peak 1 rpm reading for spindle T-A, the residual reading of spindle T-A had to be multiplied by the sensitivity of the sludge specimen determined by using any other spindle, as shown in the following equation:

$$P_{T\text{-}A} = R_{T\text{-}A} \frac{P_{T\text{-}B}}{R_{T\text{-}B}} \qquad (4.1)$$

where $P_{T\text{-}A}$ - peak 1 rpm spindle T-A normalized reading,

$R_{T\text{-}A}$ - residual 1 rpm spindle T-A reading,

$P_{T\text{-}B}$ - peak 1 rpm spindle T-B (or other) reading,

$R_{T\text{-}B}$ - residual 1 rpm spindle T-B (or other) reading.

It should be noted that all figures from viscosity testing show the results obtained with a spindle that was actually used and these readings are not normalized for the T-A spindle. In fact, it is indicated in figures what spindle was used, if different from T-A. On the other hand, the results listed in the tables are all normalized to T-A readings. A normalized result can be easily recognized by a value greater than 100 which is the upper limit of the viscometer scale.

As far as the rheological classification is concerned, sludge 150 exhibited all characteristics observed in sludges with higher water contents. In the undisturbed state (peak strength behaviour), there is a strong evidence that the material is best represented by Herschel-Bulkley model: twenty-one flow lines are best fitted by power law curves, three by straight lines. The three are: thirty minute, eight hour and forty day tests. In the remoulded state, whether partially or completely, there is little doubt that sludge 150 is a Bingham fluid: twenty-four residual flow lines are straight lines and only one (twelve hour test) could be represented better (judged by the r^2 correlation factor) by a power law curve. The 680 day test, however, showed again a decrease in shear resistance (Figure 4.11) only confirming the long term behaviour pattern observed in previously discussed sludges. The 470 day test residual flow line cannot be strictly classified as Bingham, either. The line is perfectly horizontal thus not showing any shear stress increase with a decreasing shear strain rate, as seen in Figure 4.12. Another interesting observation is the fact that the shear resistance of the 680 day sludge sample is less than that of the 470 day one in both, peak and residual terms, despite the lower water content and a longer time effect of the former. The peak resistance at 1 rpm decreased from 112 (normalized) at 470 days (141% water content) to 111 units at 680 days (129% water content); the difference is small

in absolute terms but is considered important in determining the thixotropic effect. The residual resistance decreased even more: from 40 units at 470 days to 30 units at 680 days. An in-depth explanation of this apparent inconsistency in the sludge behaviour is given in Chapter 5.

All flow lines in diagrams appear to be well fitted to the data points and, with the exception of nearly-horizontal straight lines, correlation factors are generally greater than 0.95.

The summary of viscosity test results for sludge 150 is shown in Table 4.6. Shear stress-shear strain rate and apparent viscosity-shear strain rate plots are included in Figures A.76 through A.100 and B.76 through B.100.

4.2.5 Sludge 100

Twenty-five viscosity tests were completed on sludge samples with an initial water content of 100% (50% solids content). This was the only designated water content in viscosity measurement program where there was no self-weight consolidation observed over the period of 680 days, that is, the water content remained constant throughout all tests. Four different spindles had to be used during measurements in order to handle the wide range of shear resistance of sludge 100: spindle T-A was in use for tests from 0 to 24 hours, spindle T-B handled tests from 2 to 5 days and the 20 day test, spindle T-C was used for tests starting on day six to 680 days, with the exception of the above mentioned 20 day test and 470 day test for which spindle T-D was utilized. As was the case with sludge 150, peak 1 rpm results obtained with spindle T-B, T-C or T-D were normalized to T-A readings using Equation 4.1. Figure 4.13 illustrates three flow lines for remoulded sludge 100 constructed from readings of three spindles: T-A, T-B and T-C. All three flow lines show a very good fit with the corresponding data points, some similarity among the slopes of the lines can

be noticed, especially between line T-C and T-B. However, as mentioned in Section 4.2.4, there are no unique factors interrelating the readings of different spindles.

Rheological classification of sludge 100 is generally consistent with the previously discussed sludges. Out of twenty four tests, twenty peak flow lines are best described by power law curves (Herschel-Bulkley model) and four by straight lines (Bingham model). There is no logical pattern in which the sludge would change its peak behaviour from the Herschel-Bulkley to Bingham model; the straight lines are representing the 6, 21, 95, and 680 day test. As the Bingham model is a special case of the Herschel-Bulkley model, the above can be regarded as coincidental. On the other hand, all of the twenty-five residual flow lines are straight lines which, by no means, could be deemed coincidental. This classifies the remoulded (completely and partially) sludge as a Bingham model material. That is with the exception of the two "oldest" samples, 473 and 680 days, where the remoulded flow lines exhibit a negative slope.

Other irregularities include an unexpected drop in the peak resistance for the 21 day sludge and a substantial reduction in both, peak and residual shear resistance for the 680 day sludge: the peak resistance at 1 rpm decreased from 272 at 473 days to 186 units at 680 days whereas the residual resistance at 1 rpm decreased from 93 to 47 units in the same time interval - a reduction of almost 50%! A similar tendency was observed for sludge 150 (see Section 4.2.4).

The majority of the data points displayed good correlation with the best fit flow line curves which is confirmed by the correlation factors approaching 1.0. As was pointed out before, temperature differences could play a significant role in influencing the results. For example, it can be seen in Figure 4.14 that for

two sets of readings taken at temperatures differing by 4.1 degrees C the results can vary by as much as 30%.

For a complete set of sludge 100 viscosity tests results, see Table 4.7, for a complete set of graphs, see Figures A.101 through A.125 and B.101 through B.125.

4.2.6 Influence of Temperature on Viscosity

Temperature seems to have a strong influence on viscosity of the sludge as was shown in several examples in the preceding sections of this chapter. It is believed that this influence is caused by the presence of the bitumen in the sludge. The main fluid component of sludge, water, in the temperature range of 15 to 25°C, changes its viscosity from 1.140 Pa•s to 0.894 Pa•s, respectively; a decrease of 22% (Streeter and Wylie, 1981). Peacock (1988) shows viscosity variation of Athabasca bitumen in the 20 to 200°C temperature range and below 20°C. From the plots, it was estimated that an increase in temperature from 15 to 25°C causes a decrease in viscosity from approximately 2300 Pa•s to just over 400 Pa•s; a change of 83%. Furthermore, the change of water viscosity in the considered temperature range is less than 0.02% of the change in the bitumen's viscosity! It is possible that viscosity of the sludge is a function of both temperature and bitumen content. The higher the bitumen content the greater may be the influence of temperature on the viscosity of the sludge.

4.2.7 Summary of Viscosity Tests Results

From the preceding presentation of the results of viscosity tests on sludge with varying water content, it can be concluded that the material is a non-Newtonian fluid characterized by its yield viscosity (or yield shear resistance)

and distinctive flow lines for undisturbed and remoulded states. There is enough evidence to classify the sludge as a Herschel-Bulkley model material in its undisturbed state and as a Bingham model fluid when remoulded. Although the Bingham model is a special case of the broader Herschel-Bulkley model, the sludge undergoes an apparent change in rheological behaviour during transition from the remoulded to undisturbed state (or vice versa). It is believed that this change is closely associated with thixotropy of the slurry or, if rephrased, such a change in general is a sign of the thixotropic nature of a fluid. Furthermore, it seems that with a higher water content the soil behaves more like a Herschel-Bulkley material, with a decreasing water content the behaviour shifts toward the Bingham model, especially in the remoulded state. Locat and Demers (1988) investigated rheological properties of some sensitive natural clay soils. The authors observed that the soils could be described by two models: Bingham and Casson (somewhat similar to Herschel-Bulkley model). Furthermore, they noticed that the Bingham-type soils exhibited a pronounced thixotropic behaviour while the Casson-type soils were only slightly thixotropic. Considering the fact that the authors worked only with remoulded soils, their findings are consistent with the results of this research.

A break in the otherwise consistent trend of the soil gaining shear resistance with time was observed for the lower water content sludges after 470 days. This could be explained by an experimental error or it could indicate a significant change in the soil's behaviour. A possible explanation is that after reaching a certain time (age) and at a certain water content the thixotropic gain in strength ceases or even reverses itself. However, more evidence is required to support this theory. Chapter 5 will address the time dependent behaviour in more detail.

Due to the limited capacity of the available equipment such important rheological properties as viscosity, apparent viscosity or yield viscosity could not be determined; instead, an arbitrarily selected index property was used for further analysis. A definite disadvantage to the testing was imposed by the lack of resources to control the test room temperature. It was shown earlier that changes in the temperature during testing could account for errors as high as 30%. It is recommended that detailed studies of the effect of temperature on viscosity of the sludge be undertaken and appropriate correction factors obtained.

4.3 Shear Vane Test Results

The undrained shear strength of the oil sands tailings sludge studied in this research was the most extensive to-date experimental program of its kind. To reach the objective, the shear vane apparatus described in Section 3.2.2 was developed and a total of 106 vane strength tests were performed on sludge samples ranging in water content and age. Results of each test were presented in a form of a typical stress-strain diagram where strain was expressed as the rotation angle of the vane. The peak and the residual shear strength were then determined from the plot and recorded for further analysis. The strain (angle) at which the peak strength was reached was also determined from the plot. Each test was represented by two plots, one showing the full test for residual strength, and the other showing the initial part of the test for the peak strength determination. Soil sensitivity for each test was reported. The strict definition of soil sensitivity is the ratio of peak to remoulded shear strength, but it is common to substitute residual strength for remoulded strength when the remoulded strengths are not readily available. This practice was followed here.

Appendix C contains a complete set of figures of the shear vane tests.

4.3.1 Sludge 400

Sixteen undrained shear tests were performed on sludge samples with the initial water content of 400% (20% solids content). Because of extremely low shear stresses measured in this series of tests, the likelihood of experimental error was proportionally greater than in the lower water contents samples. With the shear stress accuracy of the testing system estimated at 1 Pascal, the initial short term tests were prone to discrepancies. For instance, tests up to 20 days after remoulding displayed a peak strength of less than 10 Pa (Figure 4.15) whereas all tests denoted S40 (sludge 400) showed residual strengths only in few cases marginally higher than 10 Pa. In all cases, the peak strength was clearly indicated on the plot by the distinctive shape of the stress-strain curve. It varied from a low of 4.2 Pa for the two-hour test to a high of 144 Pa for the 680 day test. The residual strength increased in a far less dramatic fashion; from 2.0 Pa to 10.5 Pa during the same passage of time. A good indication of the validity of each test was the vane rotation angle at which the slurry reached its peak strength. This angle was fairly consistent for most of the tests and varied from 5 to 8 degrees. However, the 50 day sludge (Figure 4.16) exhibited lower than expected peak and residual strengths but it also showed a higher strain to peak than other samples; 12 degrees, which makes the results of this test doubtful.

It should be perhaps added that determining the residual, as opposed to the peak, strength of each test was a task requiring more than finding the lowest recorded reading. The stress-strain curve had to be closely examined, possible trends observed and the effect of so called "electronic noises" eliminated. A good example of "electronic noise" can be seen in Figure 4.15.

The peak and residual strength of each sludge 400 sample along with their sensitivity and final water content are presented in a tabular form in Table 4.8. A corresponding set of stress-strain diagrams is included in Appendix C, Figures C.1 through C.31.

4.3.2 Sludge 300

This part of the testing program consisted of fifteen vane shear tests on sludge samples with an initial water content of 300%. Undrained shear strength varied from a low of 3 Pascals for the remoulded sludge to a high of 170 Pa (peak strength) for the 680 day sample (168% water content). The test results show consistency and in most cases their validity is supported by similar strain-to-peak angles which are between 6 to 8 degrees. As was the case with sludge 400, the initial test stress-strain curve showed a relatively high degree of scatter caused by a combination of extremely low shearing resistance, "electronic noise" and thixotropic effects which, in the initial phase, may exceed remoulding exerted by the vane blades. Two tests on separate samples were conducted at 50 days. The resulting curves are shown in Figure 4.17. Although the residual strengths are similar (5.6 vs. 5.2 Pa), the peak strengths differ by as much as 25% (27.9 vs. 21.0 Pa). However, the same difference expressed in absolute terms: 7 Pa, is not very significant taking into account all above listed factors as well as possible temperature difference (temperature was not recorded during shearing tests), rotation rate variations and imperfections in slurry homogeneity.

The test results are shown in Table 4.9 and all S30 stress-strain curves are included in Figures C.32 to C.58.

4.3.3 Sludge 233

Fifteen vane shear tests were carried out for samples labelled sludge 233. Generally, the tests showed all the characteristics discussed for the previous two sets of tests: S40 and S30. The measured shear resistance varied from 4.4 Pa (shortly after mixing) to 210 Pa (peak at 680 days). An excellent example of a very strong thixotropic effect during the first minutes following mixing is illustrated in Figure 4.18. Despite the fact that the time elapsed between the mixing of the slurry and the start of the vane shear test was in the range of about 2 minutes, a distinctive peak can be observed in the stress-strain curve proving that a high gain in strength takes place immediately following mixing. Initially, the gel structure is destroyed (a drop in strength as seen in Fig. 4.18) by the rotating vane blades but gradually the curve climbs upwards as the rate of thixotropy exceeds the constant rate of remoulding. The same phenomenon could not be observed in later tests which could indicate that the most rapid gain in strength occurs within a short time after mixing.

The strain-to-peak angles vary from 5 to 10 degrees and shapes of the curves do not imply major irregularities.

The graphs representing S23 tests are shown in Figures C.57 through C.85 and the test results are summarized in Table 4.10.

4.3.4 Sludge 150

The S15 series of experiments consisted of 18 vane shear tests on sludge 150 specimens varying in age from zero to 684 days after remoulding. In general, the results followed the established trends from the previous series of tests of an increasing shearing resistance with the passage of time with some exceptions such as the 5-day test in which both, the peak and residual values of strength were lower than indicated by the trend, albeit not significantly.

Tests performed on two separate samples at 20 days (Figure 4.19) showed one peak strength 23% (or 28 Pa) lower than the other and the residual strength of the respective sample 26% (or 10.7) lower than the other. Both sets of values were however used for further analysis for the reasons explained in Section 4.3.2. The 50 day test, although originally completed, could not be included in a graphical form among others as the whole data file was destroyed by a computer virus. The peak shear strength of the sample was salvaged due to the fact that in each test the highest voltage was recorded manually in addition to the electronic data acquisition system as a double check.

Very interestingly, a phenomenon which was first observed during viscosity measurements of sludge 150 and 100 repeated itself in shear testing. The phenomenon lends itself to a large decrease in peak and residual shearing resistance over the time period between 470 and 680 days. In this particular case, the peak strength decreased from 314 Pa at 470 days to 260 Pa at 680 days and the residual strength decreased from 67 to 20 Pa, respectively. Since there was enough room left to run another vane test in the 680 day sample, the test was repeated four days later (at 684 days). The resulting peak strength was almost identical to the previous one: 256 Pa. The residual strength after two full revolutions was higher this time: 38 Pa, but still much lower than that at 470 days. It should be added that the residual strength at 680 days is at the level of that at zero time which, combined with the lower water content at 680 days (129%), sounds questionable. The shape of the stress-strain curve appears to be correct with no fluctuations (Figure 4.20) and the strain-to-peak angle (11 degrees) is within the accepted range. No reasonable explanation can be offered for this anomaly.

Table 4.11 summarizes the results of the shear tests for sludge 150 and Appendix C contains all respective stress-strain curves in Figures C.86 to C.116.

4.3.5 Sludge 100

A total of 17 vane shear tests were carried out on specimens of sludge 100 (50% solids content): three of these tests were run on freshly remoulded material. As it was mentioned in Section 4.2.5, sludge 100 did not show any self-weight consolidation or water content change over the course of testing. The sludge, although still a slurry, had a thick consistency and in order to obtain a homogeneous sample, considerably more mixing effort was required when compared to sludges with higher water contents. Notwithstanding this effort, occasional small concentrations of denser material were detected during examination of samples, which might help explain some of the scatter of the results.

Figure 4.21 shows six stress-strain curves for freshly remoulded sludge 100. Three of the tests were performed with the most sensitive, 80 mm vane, in two others the 30 mm vane was used, and the 20 mm vane was used in one test. The reason of using different vanes was to check if their resulting shear stresses were compatible. As seen in the figure, the three vanes, with the exception of one 80 mm vane test, give similar results, especially in the initial stages of the test. It is clear that the 80 mm vane gives the most consistent appearing curves due to its high sensitivity. Two 80 mm vane tests give almost identical results (remoulded strength of 89 and 86 Pa), with the third one showing shear strength well below the other two (62 Pa). As it turned out, the time elapsed between mixing of the sludge and actual testing was much shorter for the latter test than for most other tests (approximately 2 minutes versus the average of 6 minutes). The value of 62 Pa, therefore, was taken as the true remoulded shear strength in the light of the results of longer tests and the fact that the total angles of vane rotation for the two higher value tests were only

120 and 150°, respectively, which might have been insufficient for proper remoulding even at zero time.

The results of later tests suggest that sludge 100 behaves somewhat less consistently than the previously discussed mixes. The scatter of the residual strength results is significantly higher which might be caused by a different degree of soil remoulding during the tests and/or non-homogeneity as discussed earlier in this Section. The test at 680 days gave reduced strengths both, peak and residual in comparison with the 470 day test and it was repeated 21 days later at 701 days. The results were unchanged, as can be seen in Figure 4.22. These tests confirmed the trend observed before, as with the viscosity tests for sludge 100, and the viscosity and shear tests for sludge 150. This time, however, the residual strength was even lower than the zero remoulded strength (up to 40% reduction). The reduction in peak shearing resistance was even higher (Figure 4.23) than in sludge 150: 33% vs. 19%, despite the fact that in sludge 100 no consolidation took place in the corresponding time interval.

The strain to peak angle varied between 5 and 10 degrees and the peaks were well defined in all curves. The data of the 15 day test was partially destroyed by a computer virus.

The summary of the results of S10 testing is presented in Table 4.12 and the corresponding set of graphs is included in Appendix C, Figures C.117 through C.144.

4.3.6 Effect of Vane Diameter and Number of Vane Blades on Shear Stress

All vane shear strength tests for sludges with water contents of 100% and higher were conducted using the 80 mm diameter vane. Two smaller, less sensitive vanes were fabricated to handle the higher strengths of sludge 47.

Their diameters were 20 and 30 mm, respectively. As it turned out, the 30 mm vane had its shaft made to small and, in effect, was laterally unstable. Therefore, it could not be relied upon and was not used on regular basis. The 20 mm vane was used for all tests with the sludge 47.

As discussed in Chapter 3 (Section 3.2.2.1), it has been found that the diameter of the vane has no effect of the shear strength of a soil if the rate of rotation is adjusted accordingly. The rotation rates for the vanes used in this research program were determined on the basis of a constant angular shear velocity of 0.15 mm/s and Equation (3.15) (Section 3.2.2.1).

The reasoning behind using a six-blade vane instead of the standard four-blade one was the assumption that with the large diameter of the vane and extremely low strength/stiffness of the slurry, six blades would mobilize much greater volume of the material than four blades. This method would closer approach the ideal circular failure surface and minimize the problem of progressive failure. Whereas the number of blades should not affect residual values of shear strength, it is believed that values of peak strength obtained with a large six-blade vane would be closer to the the true peak strength of the soil than those obtained with a four-blade vane of the same diameter.

4.3.7 Sludge 47

Vane shear testing of sludge 47, i.e. sludge at the liquid limit, was different from testing of the other sludges for two reasons. Firstly, as explained in Section 3.2.1 no viscosity measurements were conducted on this sludge, therefore any potential patterns in sludge's behaviour in shear could not be supported by similar findings in rheological tests. Secondly, due to the significantly higher shearing resistance of the material, now measured in kPa, the 20 mm vane was used in these experiments. The handling of the

sludge proved more difficult in several aspects. Mixing was very time and energy consuming, non-uniform water distribution throughout the sample was more likely to occur than in the other sludges and there was a possibility of air pockets trapped in the soil during mixing with the blade. A total of 26 vane shear tests were conducted on liquid limit sludge samples. Figure 4.24 illustrates four vane tests performed on freshly mixed material. A distinctive feature of the graph is sharply defined peaks for all four curves suggesting a high rate of thixotropic gain in strength immediately after mixing. The appearance of Test 2 curve indicates the presence of an air pocket around the vane and that was subsequently confirmed by inspection. The other three tests yielded values of the undrained remoulded shear strength close to 1.5 kPa. As discussed in Chapter 2 (Section 2.3.2), Elder (1985) reported that the range of shear strength at the liquid limit for many soils vary between 0.5 and 4 kPa. Karlsson (1961) found that by using the fall cone method for different soils, the wide range of strength at the liquid limit was reduced to between 1.5 to 2.1 kPa. Leroueil et al. (1983) based on fall cone tests, use a strength of 1.6 for deriving their liquidity index-remoulded shear strength relationship (Equation 2.5). It can be seen that the cited values from the above references correspond very well to the sludge's shear strength at the liquid limit.

Despite higher fluctuations in results than in the other sludges, trends in the soil's behaviour are well defined and show a steady increase in peak strength with time and a relatively constant residual strength over time. Strain-to-peak angles are significantly higher in sludge 47 compared to the other sludges: they are in the range between 15 and 20 degrees as seen in Figure 4.25. The results of four tests (181 days: test 1 & 2, and 510 days: test 1 & 2) were adversely affected by a computer virus: parts of the data were destroyed. There was no definite decrease in peak strength noticed after 470 (460 in two cases) days. In

fact, the trend is not clear after 194 days. A more detailed discussion of the time dependent strength behaviour will be featured in Chapter 5.

Table 4.13 contains the results of the shear vane testing for sludge 47 and Figures C.145 through C.175 in Appendix C show the corresponding stress-strain curves.

4.3.8 Summary of Shear Vane Testing

The modified vane shear testing apparatus proved to be a reliable method of determining the shearing resistance of slurries and low strength soils. Whether the apparatus measures the actual undrained peak shear strength poses another question. In order to determine the true peak strength, a simultaneous mobilization of strength in soil around the circumference of a cylinder sheared by the vane is required. A visual check of this requirement would involve inserting the vane in soil in such a position that the tops of the vane blades are visible at the soil surface, rotating the vane and observing the resulting failure surface. If a full circle is established within a corresponding strain-to-peak angle, the peak undrained strength of soil is believed to be mobilized. If the circle progresses slower, at a rate marginally higher than or equal to the advancement of the blades, progressive failure is taking place.

A series of trial tests was performed on different water content samples to assess whether progressive failure did indeed occur. No evidence was seen to indicate that progressive failure occurred during testing. Also, in practically all stress-strain curves from the shear vane tests there is a well defined peak followed by a dramatic drop in strength. The shape of the curves then indicates that there is no continuous progressive failure and a peak strength is in fact mobilized. The validity of the results for the remoulded sludge is confirmed by the agreement between values of the residual strength obtained

for the liquid limit sludge and other researchers' findings as discussed in the previous Section. Additional agreement with other research for the remoulded vane shear strengths is shown in Chapter 5.

Therefore, it is concluded that the modified vane shear testing apparatus appears to give realistic values for both peak and residual undrained shear strength over the full range of sludge water contents.

Sample	Liquid Limit	Plastic Limit	Plasticity Index
Batch 1.1[2]	53%	21%	32%
Batch 1.2[1]	47%	21%	26%
Batch 1.3[1]	44%	20%	24%
Batch 2.1[2]	58%	23%	35%
Batch 2.2[1]	44%	21%	23%
Batch 2.3c[1]	47%	26%	21%
Method 1 Mode	46%	21%	25%

[1] - Denotes test performed by method 1
[2] - Denotes test performed by method 2
c - Denotes centrifuging

Table 4.1 Atterberg Limits for Sludge

Elapsed Time	Viscometer Reading (at 1 rpm) Peak	Residual	Sensitivity	Actual Water Content
0	0.50	0.50	1.00	400
5 min.	1.25	1.05	1.19	400
10 min.	1.45	1.20	1.21	400
20 min.	1.60	1.45	1.10	400
30 min.	1.95	1.75	1.11	400
60 min.	2.00	1.75	1.14	400
2 hrs	1.90	1.60	1.19	400
3 hrs	2.20	1.80	1.22	400
4 hrs	2.55	1.90	1.34	400
8 hrs	2.60	2.00	1.30	400
12 hrs	2.70	2.15	1.26	400
18 hrs	2.65	2.20	1.20	400
24 hrs*	3.13	2.40	1.30	400
2 days	3.00	2.30	1.30	400
3 days	2.95	2.25	1.31	400
4 days	3.35	2.30	1.46	398
5 days	3.15	2.45	1.29	397.5
10 days*	4.23	2.73	1.55	396
20 days	4.65	2.82	1.65	393
33 days	5.80	2.70	2.15	380
40 days	6.05	3.05	1.98	378
64 days	6.25	2.45	2.55	358
70 days	7.45	3.05	2.44	362
160 days	8.00	3.50	2.29	306
470 days	39.10	10.45	3.74	235
680 days	72.30	16.05	4.50	178

* - Denotes the average of more than one test

Table 4.2 Viscosity Test Results for Sludge 400

Elapsed Time	Viscometer Reading (at 1 rpm) Peak	Residual	Sensitivity	Actual Water Content
0	1.45	1.45	1.00	300
5 min.	2.10	2.00	1.05	300
10 min.	2.55	2.45	1.04	300
20 min.	2.90	2.55	1.14	300
30 min.	3.15	2.85	1.11	300
60 min.	3.05	2.85	1.07	300
2 hrs*	3.33	3.10	1.07	300
3 hrs	3.55	3.50	1.01	300
4 hrs	4.20	3.55	1.18	300
8 hrs	4.40	3.60	1.22	300
12 hrs	4.95	3.40	1.46	300
18 hrs	5.00	3.75	1.33	300
24 hrs*	5.28	3.95	1.34	300
2 days	5.55	3.85	1.44	300
3 days*	6.18	4.35	1.42	300
4 days*	6.63	4.33	1.53	300
5 days*	6.87	4.53	1.52	298
10 days	7.55	4.55	1.66	296
20 days	8.95	5.05	1.77	293
40 days	10.00	5.35	1.87	288
50 days*	11.00	4.90	2.24	286.5
160 days	13.45	5.45	2.47	260
470 days	33.20	10.60	3.13	217
660 days	74.30	16.95	4.38	168

* Indicates the average of more than one test

Table 4.3 Viscosity Test Results for Sludge 300

Elapsed Time	Viscometer Reading (at 1 rpm) Peak	Residual	Sensitivity	Actual Water Content
0	1.80	1.80	1.00	233
5 min.	5.15	4.95	1.04	233
10 min.	5.40	5.00	1.08	233
20 min.	5.80	5.05	1.15	233
30 min.	6.40	5.40	1.19	233
60 min.	6.60	5.45	1.21	233
2 hrs	6.70	5.60	1.20	233
3 hrs	7.10	5.95	1.19	233
4 hrs*	7.50	6.45	1.16	233
8 hrs	7.80	6.35	1.23	233
12 hrs	8.55	6.30	1.36	233
18 hrs	9.25	6.40	1.45	233
24 hrs	9.15	6.50	1.41	233
2 days*	10.90	7.00	1.56	233
3 days	11.45	6.85	1.67	233
4 days	12.50	7.55	1.66	233
5 days*	12.68	6.85	1.85	233
10 days	15.45	7.90	1.96	233
20 days	19.25	8.60	2.24	230
40 days	22.40	9.10	2.46	228
75 days	24.10	9.00	2.68	226
90 days	25.00	9.25	2.70	219
494 days	49.25	14.90	3.31	189
682 days	83.15	15.60	5.33	158

* Indicates the average of more than one test

Table 4.4 Viscosity Test Results for Sludge 233

Test	Spindle	Viscometer Reading (at 1 rpm) Peak	Residual	Sensitivity
V15002D				
	T-A	40.40	26.85	1.505
	T-B	20.90	13.95	1.498
V15010D				
	T-A	51.50	27.35	1.883
	T-B	26.95	15.55	1.733
V15030D				
	T-A	64.65	27.40	2.359
	T-B	35.40	15.75	2.248
V10002H				
	T-A	55.50	41.80	1.328
	T-B	29.25	22.35	1.309
	T-C	15.50	11.90	1.303
V10001D				
	T-A	82.00	47.00	1.745
	T-B	42.90	28.70	1.495
	T-C	22.35	14.40	1.552
V10002D				
	T-A	91.55	49.95	1.833
	T-B	52.05	28.80	1.807
	T-C	27.70	15.50	1.787

Table 4.5 Comparison of Sensitivities for Different Spindles

Elapsed Time	Viscometer Reading (at 1 rpm) Peak	Residual	Sensitivity	Actual Water Content
0	15.45	15.45	1.00	150
5 min.	17.25	15.95	1.08	150
10 min.	17.55	16.25	1.08	150
20 min.	18.15	16.5	1.10	150
30 min.	20.60	17.45	1.18	150
60 min.*	22.23	18.93	1.17	150
2 hrs	25.80	19.95	1.29	150
3 hrs	27.95	21.70	1.29	150
4 hrs	28.90	24.85	1.16	150
8 hrs	28.65	19.90	1.44	150
12 hrs	33.05	25.20	1.31	150
18 hrs*	36.30	25.13	1.44	150
24 hrs	37.30	26.25	1.42	150
2 days	40.40	26.80	1.51	150
3 days	41.60	27.65	1.50	150
4 days*	42.85	25.55	1.68	150
5 days*	42.58	22.45	1.85	150
10 days	51.50	27.35	1.90	150
20 days	63.40	27.90	2.27	150
40 days	61.40	28.30	2.17	150
51 days	67.20	26.00	2.58	150
92 days	75.45	27.40	2.75	150
470 days	112.40	39.70	2.83	141
680 days	111.10	29.80	3.73	129

* Indicates the average of more than one test

Table 4.6 Viscosity Test Results for Sludge 150

Elapsed Time	Viscometer Reading (at 1 rpm) Peak	Residual	Sensitivity	Actual Water Content
0	37.30	37.30	1.00	100
5 min.	40.50	36.00	1.13	100
10 min.	45.20	37.00	1.22	100
20 min.	47.90	38.45	1.25	100
30 min.	49.05	39.65	1.24	100
60 min.	53.20	41.40	1.29	100
2 hrs	55.55	41.80	1.33	100
3 hrs	57.35	41.60	1.38	100
4 hrs	60.00	43.00	1.40	100
8 hrs	62.30	43.05	1.45	100
12 hrs	69.90	44.15	1.58	100
18 hrs	73.60	45.10	1.63	100
24 hrs	82.00	47.00	1.74	100
2 days	91.55	49.95	1.83	100
3 days	87.55	47.90	1.83	100
4 days	93.90	48.50	1.94	100
5 days*	108.35	60.50	1.79	100
6 days	124.90	69.80	1.79	100
10 days*	131.50	56.05	2.35	100
20 days	112.00	56.30	1.99	100
21 days	172.00	63.15	2.72	100
40 days*	155.50	59.10	2.63	100
95 days	205.00	68.70	2.98	100
473 days	272.70	93.25	2.92	100
680 days	185.90	47.00	3.96	100

* Indicates the average of more than one test

Table 4.7 Viscosity Test Results for Sludge 100

Elapsed Time	Undrained Shear Strength (Pa) Peak	Residual	Sensitivity	Actual Water Content
0	2.0	2.0	1.00	400
2 hrs	4.18	2.0	2.09	400
8 hrs	4.64	2.4	1.93	400
24 hrs	5.98	2.5	2.39	400
2 days	6.48	2.6	2.49	400
5 days	6.93	2.0	3.46	398
10 days	8.20	2.8	2.93	396
20 days	9.50	2.2	4.32	393
33 days	12.66	2.6	4.87	380
40 days	15.30	4.2	3.64	378
50 days	7.48	2.0	3.74	370
60 days	12.29	2.5	4.92	362
70 days	15.14	3.6	4.21	362
160 days	24.47	4.5	5.44	306
470 days	96.46	10.5	9.19	235
680 days	144.32	10.0	14.43	178

Table 4.8 Shear Vane Test Results for Sludge 400

Elapsed Time	Undrained Shear Strength (Pa) Peak	Residual	Sensitivity	Actual Water Content
0	3.2	3.2	1.00	300
2 hrs	6.37	3.0	2.13	300
8 hrs	7.60	3.4	2.23	300
24 hrs	10.12	4.0	2.53	300
2 days	9.82	3.8	2.58	300
6 days	13.69	4.2	3.26	298
10 days	13.79	4.6	3.00	296
20 days	17.95	5.2	3.45	293
30 days	23.19	5.5	4.22	291
41 days	24.16	6.0	4.03	288
50 days	27.90	5.6	4.98	286
50 days	20.94	5.2	4.03	287
160 days	40.51	8.1	5.00	260
470 days	76.99	10.5	7.33	217
680 days	169.58	13.4	12.66	168

Table 4.9 Shear Vane Test Results for Sludge 300

Elapsed Time	Undrained Shear Strength (Pa)			Actual Water Content
	Peak	Residual	Sensitivity	
0	4.4	4.4	1.00	233
2 hrs	10.09	6.0	1.68	233
8 hrs	14.97	6.3	2.38	233
24 hrs	16.99	7.5	2.27	233
2 days	19.12	7.0	2.73	233
5 days	23.05	8.4	2.74	233
10 days	29.25	9.3	3.15	233
20 days	30.50	8.2	3.72	230
30 days	34.23	9.2	3.72	230
41 days	35.99	9.3	3.87	228
50 days	37.44	8.6	4.35	227
72 days	48.37	11.5	4.21	226
90 days	50.93	10.1	5.04	219
490 days	126.48	18.6	6.80	189
680 days	210.54	17.3	12.17	158

Table 4.10 Shear Vane Test Results for Sludge 233

Elapsed Time	Undrained Shear Strength (Pa) Peak	Residual	Sensitivity	Actual Water Content
0	19.2	19.2	1.00	150
2 hrs	43.36	26.4	1.64	150
8 hrs	57.70	32.8	1.76	150
20 hrs	64.05	32.0	2.00	150
24 hrs	60.28	27.6	2.18	150
2 days	60.09	27.5	2.19	150
3 days	67.18	27.0	2.49	150
5 days	56.02	23.6	2.37	150
10 days	95.23	31.9	2.99	150
20 days	95.52	29.1	3.28	150
20 days	123.29	39.8	3.10	150
40 days	119.03	32.0	3.72	150
45 days	128.38	34.5	3.72	150
50 days	124.11	-	-	150
90 days	166.24	37.0	4.49	150
470 days	314.27	67.0	4.69	141
680 days	259.95	19.6	13.26	129
684 days	255.97	38.3	6.68	129

Table 4.11 Shear Vane Test Results for Sludge 150

Elapsed Time	Undrained Shear Strength (Pa) Peak	Residual	Sensitivity	Actual Water Content
0	89.0	89.0	1.00	100
0	86.0	86.0	1.00	100
0	62.0	62.0	1.00	100
2 hrs	131.26	107.4	1.22	100
8 hrs	146.73	82.5	1.78	100
24 hrs	156.86	74.0	2.12	100
2 days	163.12	75.5	2.16	100
5 days	208.59	90.6	2.30	100
6 days	225.98	122.2	1.85	100
10 days	287.52	91.2	3.15	100
15 days	271.36	-	-	100
20 days	391.76	48.5	8.08	100
40 days	314.09	80.0	3.93	100
90 days	436.67	112.0	3.90	100
470 days	566.71	108.0	5.25	100
680 days	381.47	54.0	7.06	100
701 days	390.98	53.0	7.38	100

Table 4.12 Shear Vane Test Results for Sludge 100

Elapsed Time	Undrained Shear Strength (kPa) Peak	Residual	Sensitivity	Actual Water Content
0	1.50	1.50	1.00	47
2 hrs	2.59	1.46	1.78	47
8 hrs	2.94	1.51	1.95	47
24 hrs	3.69	1.25	2.95	47
24 hrs	3.55	-	-	47
24 hrs	3.40	-	-	47
2 days	3.53	1.26	2.80	47
5 days	3.58	1.60	2.24	47
7 days	3.60	1.30	2.77	47
10 days	3.78	1.28	2.96	47
10 days	3.80	1.34	2.84	47
10 days	3.99	-	-	47
10 days	4.04	-	-	47
21 days	3.31	1.70	1.94	47
60 days	4.83	1.56	3.10	47
87 days	5.58	1.65	3.38	47
160 days	6.29	2.0	3.15	47
181 days	6.20	-	-	47
181 days	5.73	-	-	47
194 days	6.95	1.90	3.66	47
410 days	6.30	0.63	10.00	47
410 days	6.08	1.65	3.68	47
460 days	6.77	1.87	3.62	47
510 days	5.70	-	-	47
510 days	6.93	-	-	47
523 days	6.21	1.36	4.56	47

Table 4.13 Shear Vane Test Results for Sludge 47

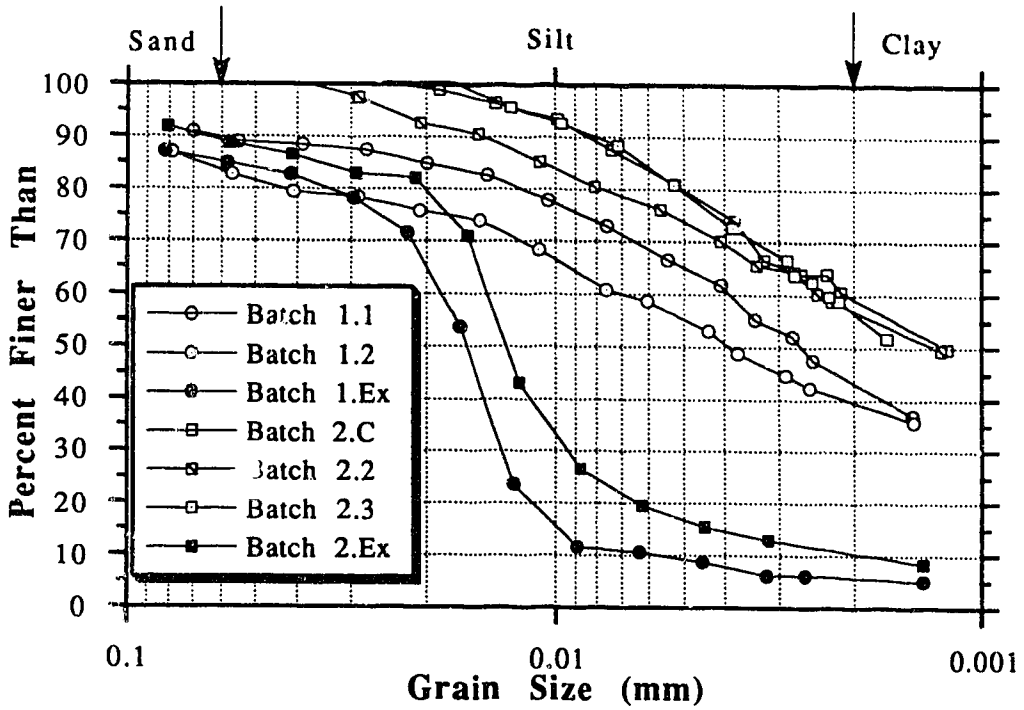

Figure 4.1 Grain Size Distribution for Tailings Sludge

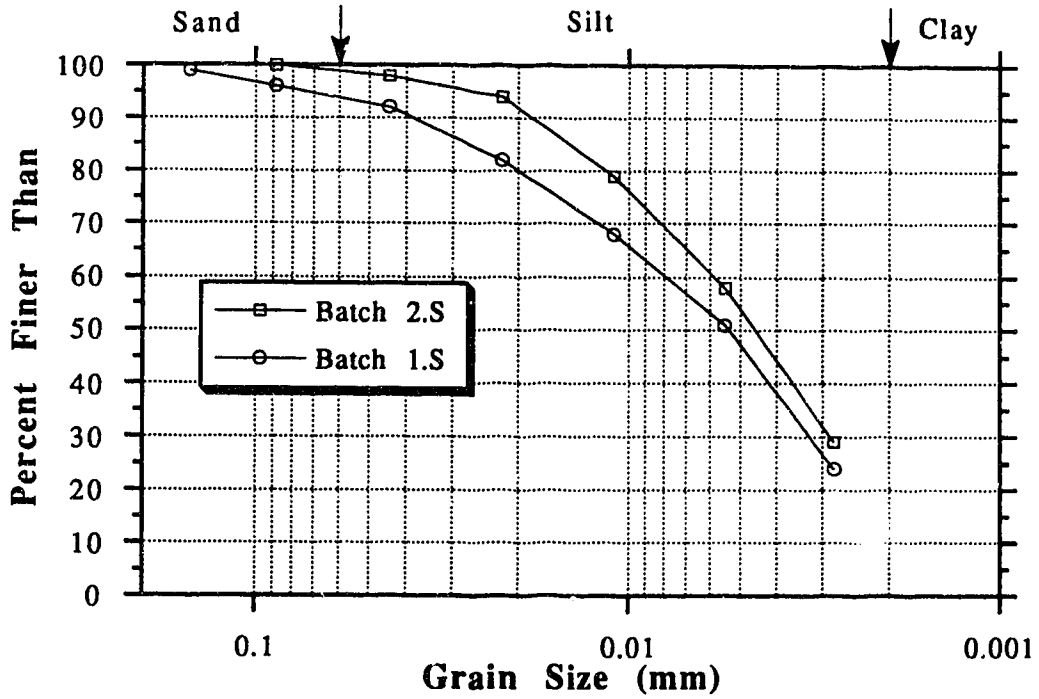

Figure 4.2 Grain Size Distribution for Tailings Sludge (Microtrac Method)

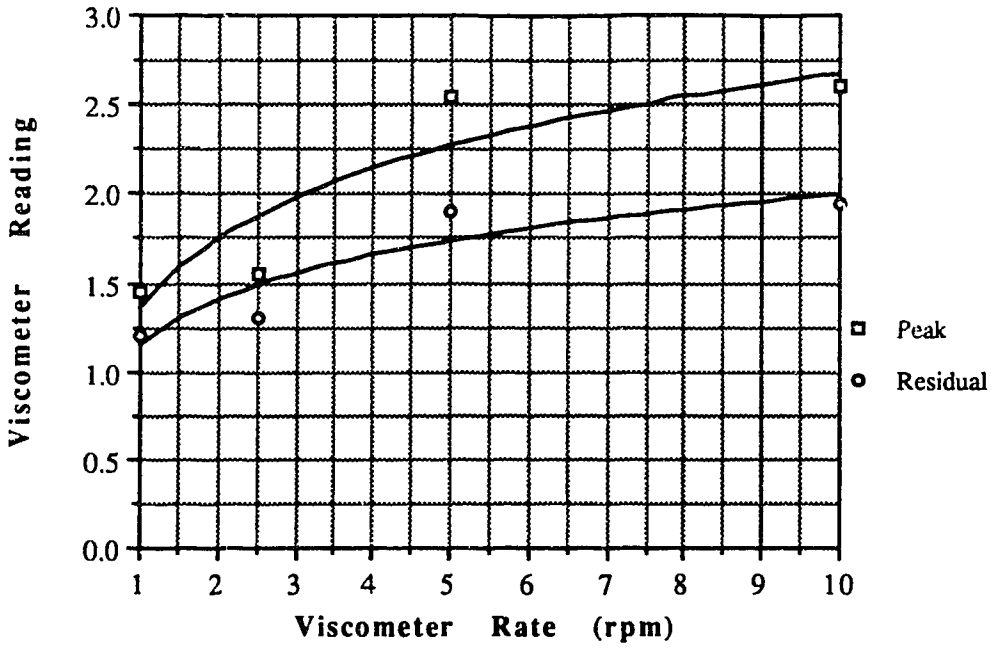

Figure 4.3 Viscosity Test V40010M

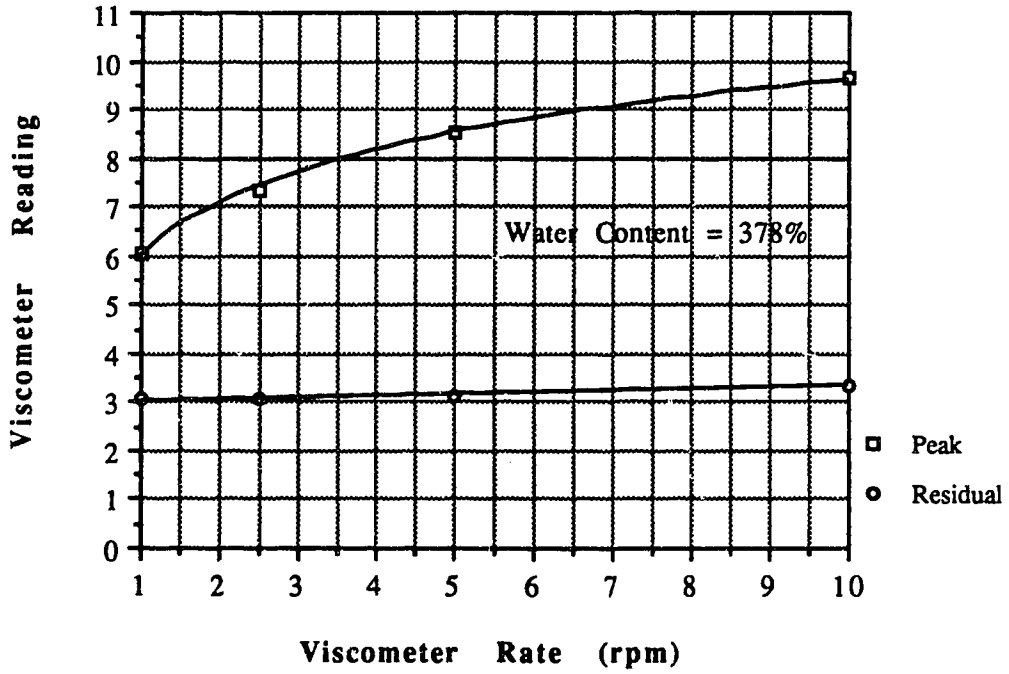

Figure 4.4 Viscosity Test V40040D

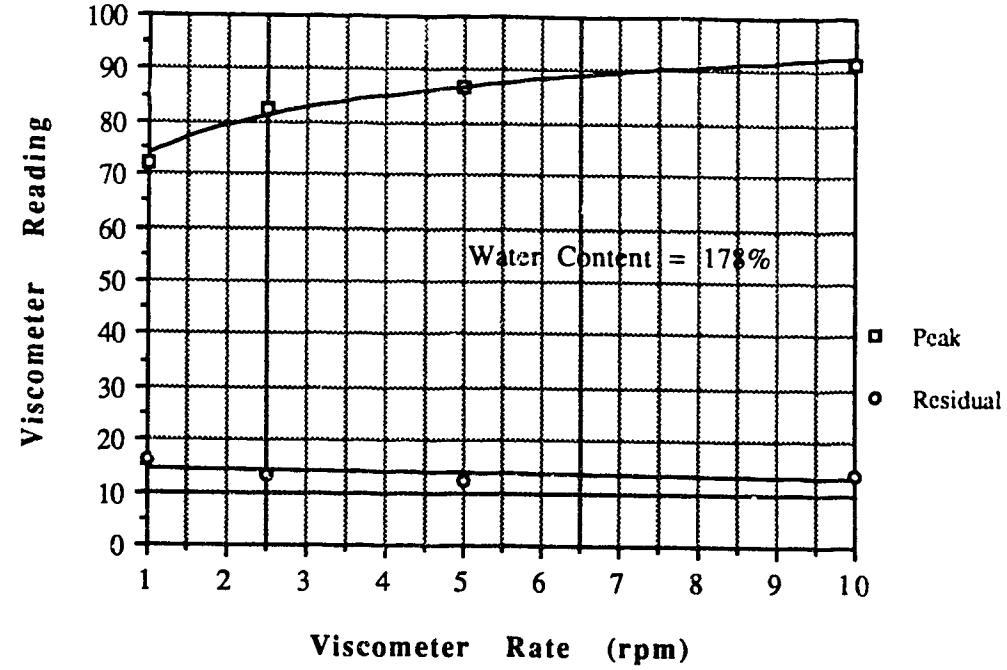

Figure 4.5 Viscosity Test V40680D

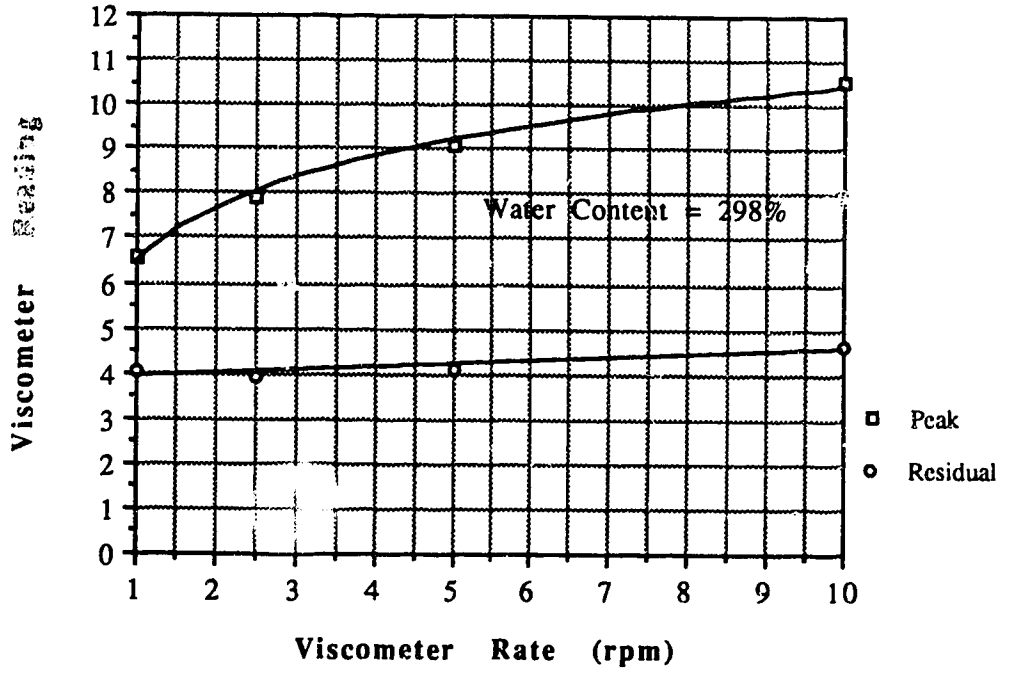

Figure 4.6 Viscosity Test V30006D

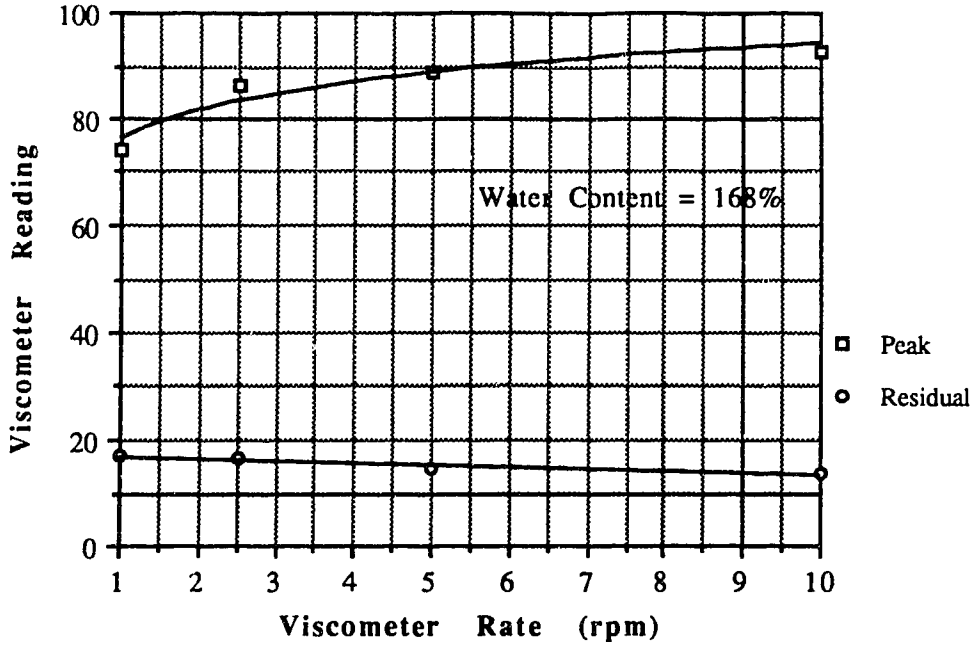

Figure 4.7 Viscosity Test V30660D

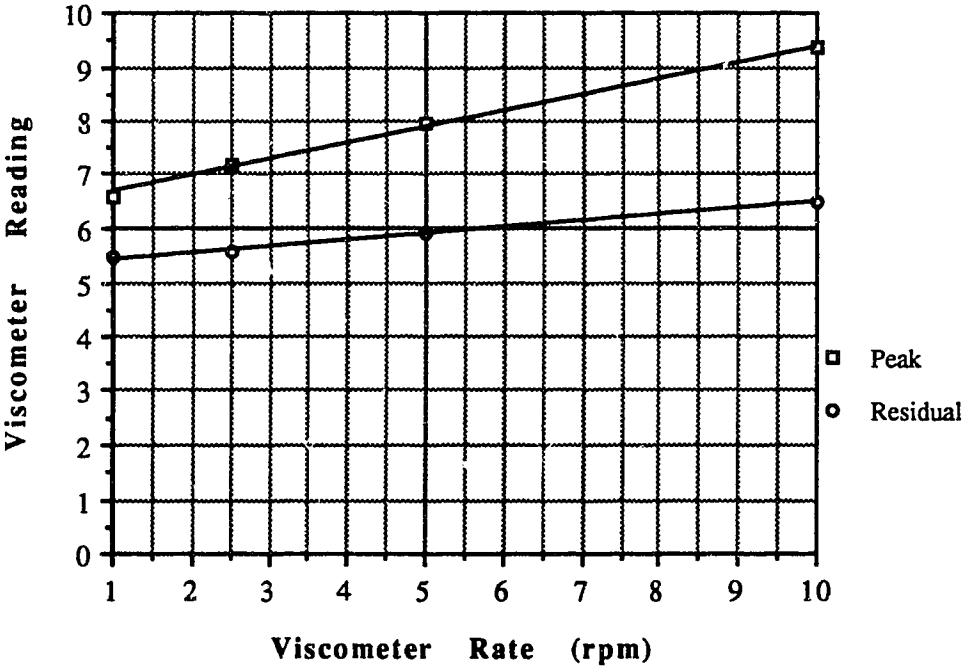

Figure 4.8 Viscosity Test V23001H

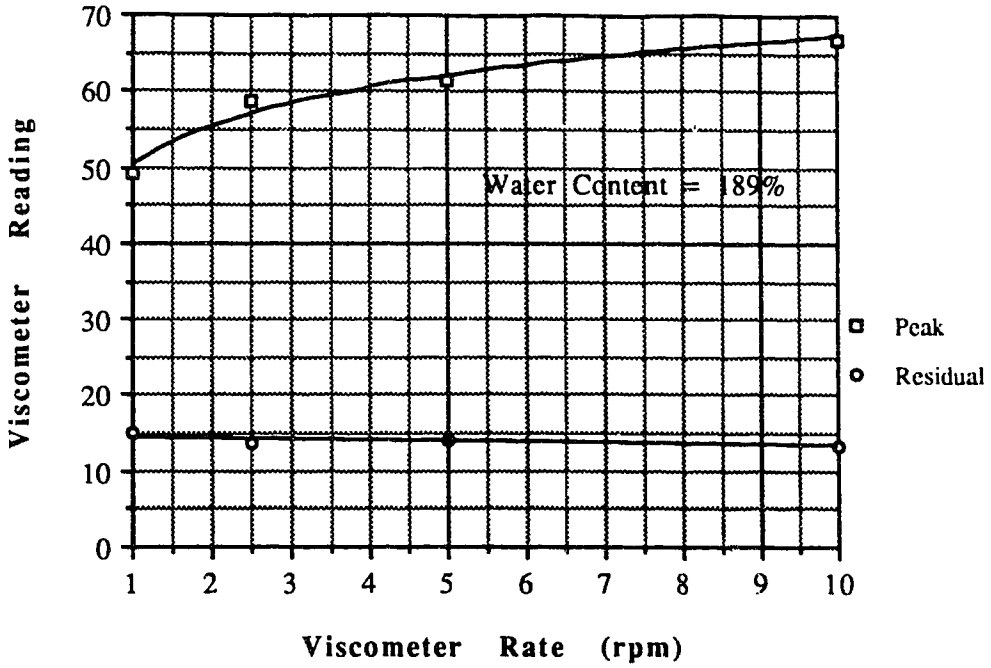

Figure 4.9 Viscosity Test V23494D

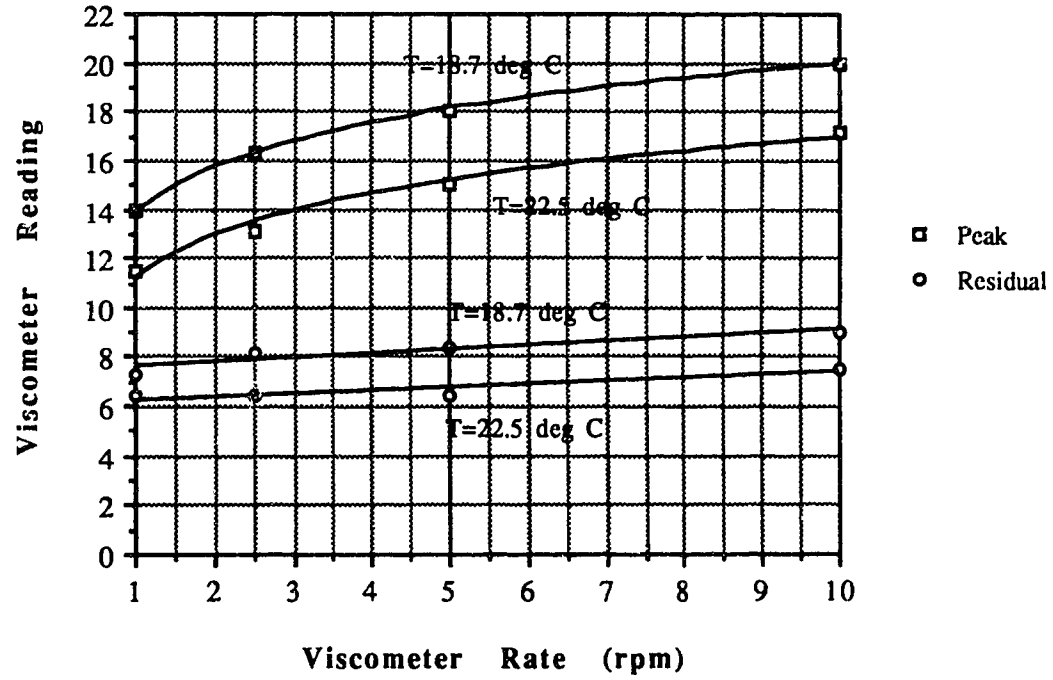

Figure 4.10 Viscosity Test V23005D at Different Temperatures

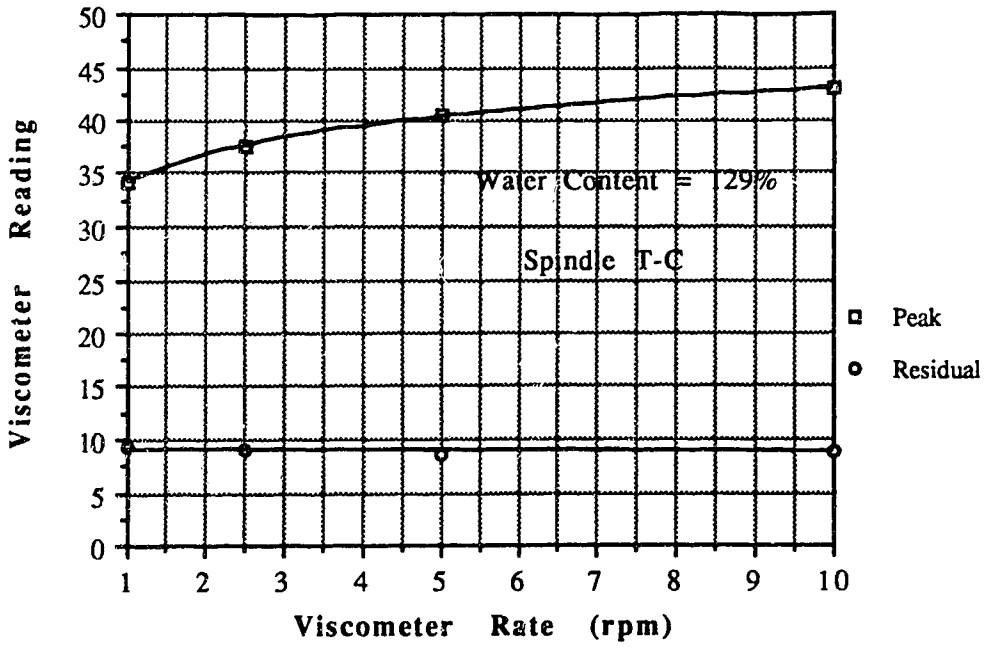

Figure 4.11 Viscosity Test V15680D

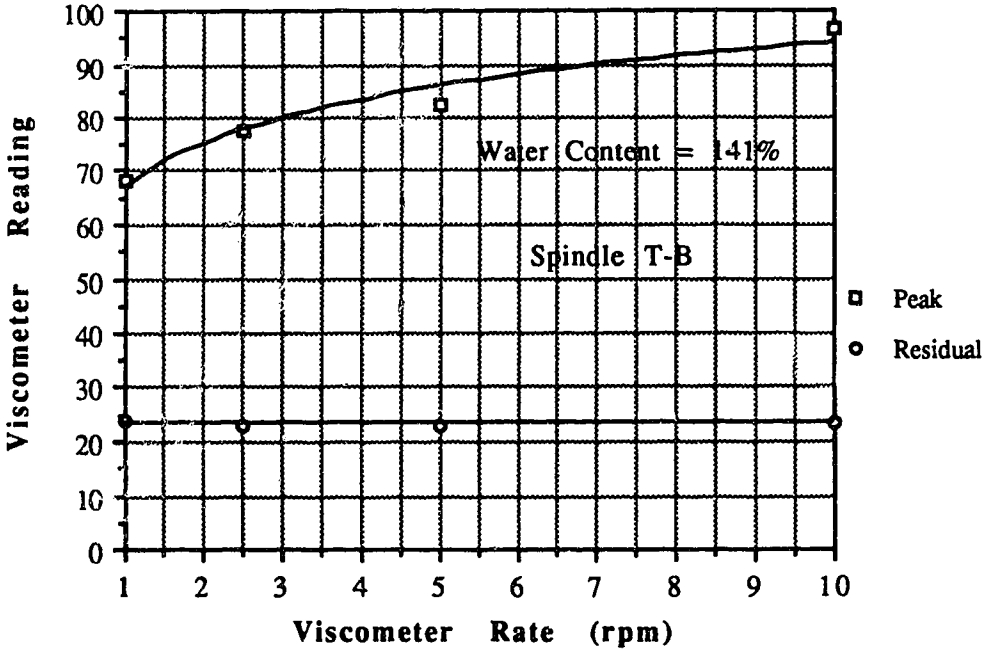

Figure 4.12 Viscosity Test V15470D

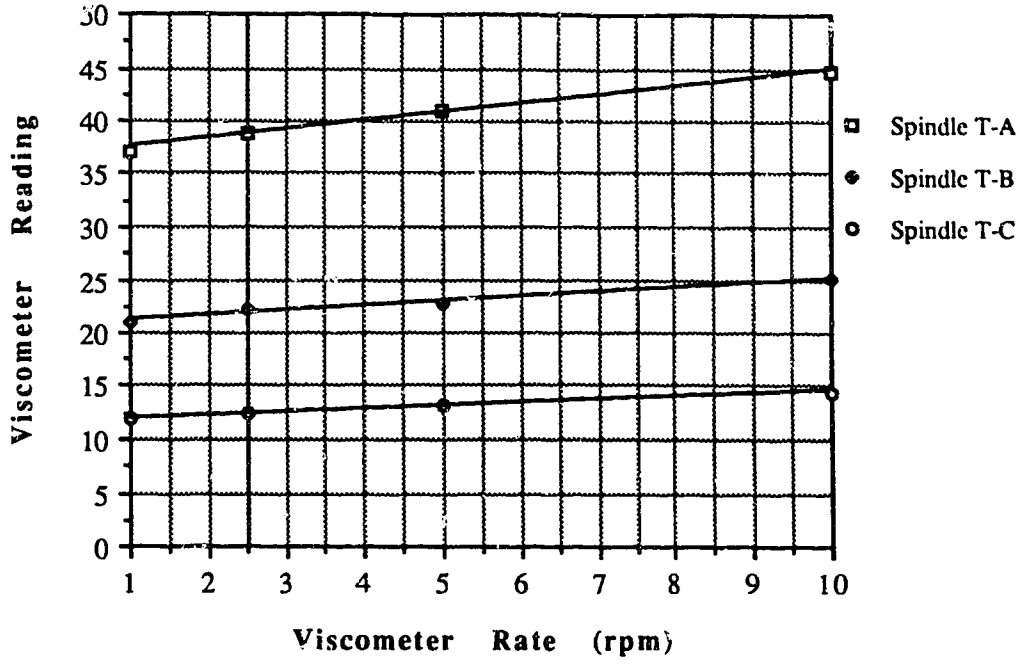

Figure 4.13 Viscosity Test V10000M

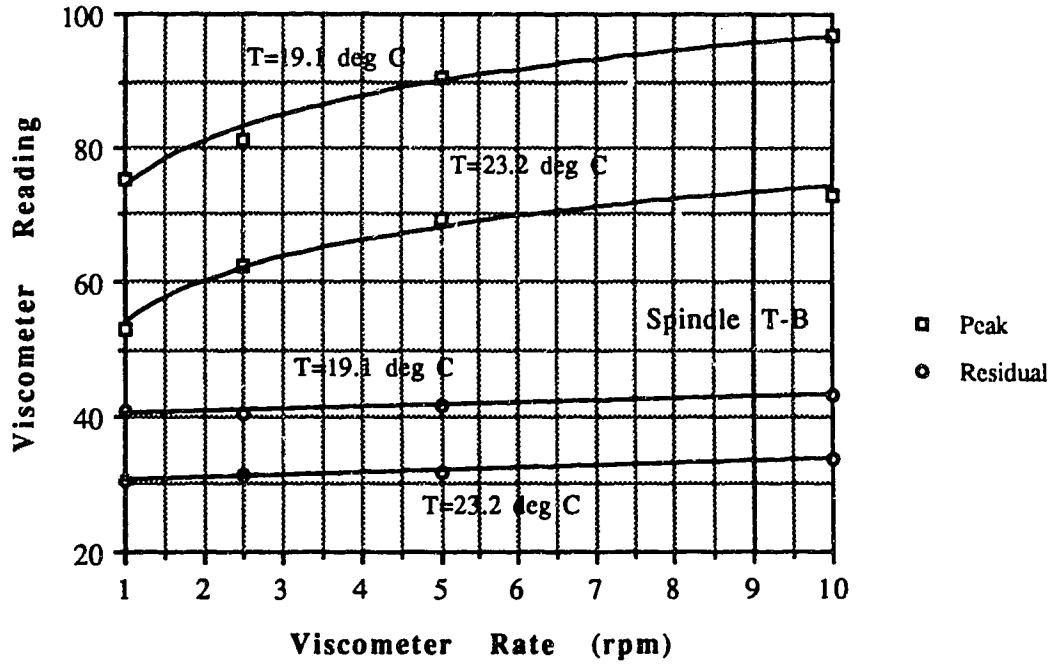

Figure 4.14 Viscosity Test V10005D at Different Temperatures

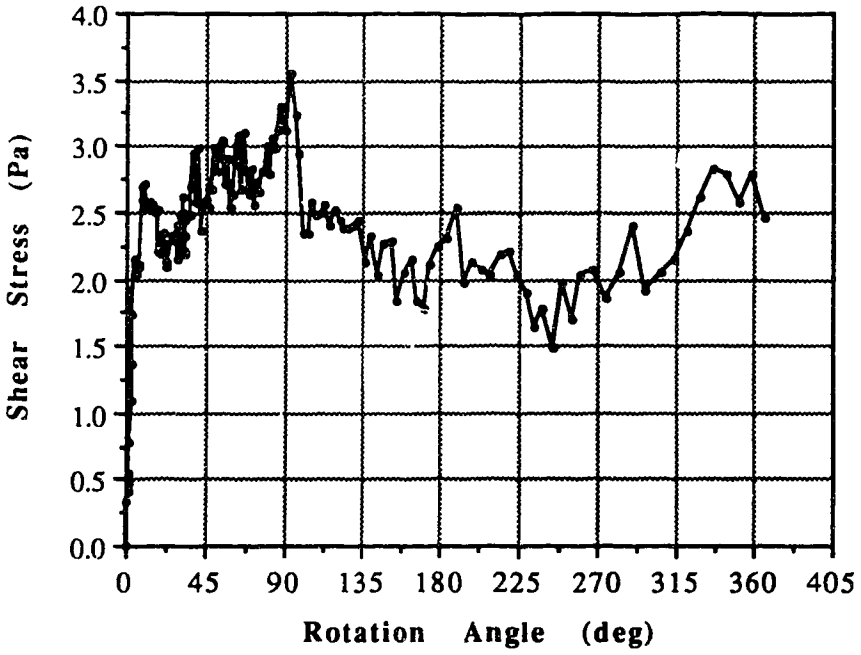

Figure 4.15 Vane Shear Test S40000M

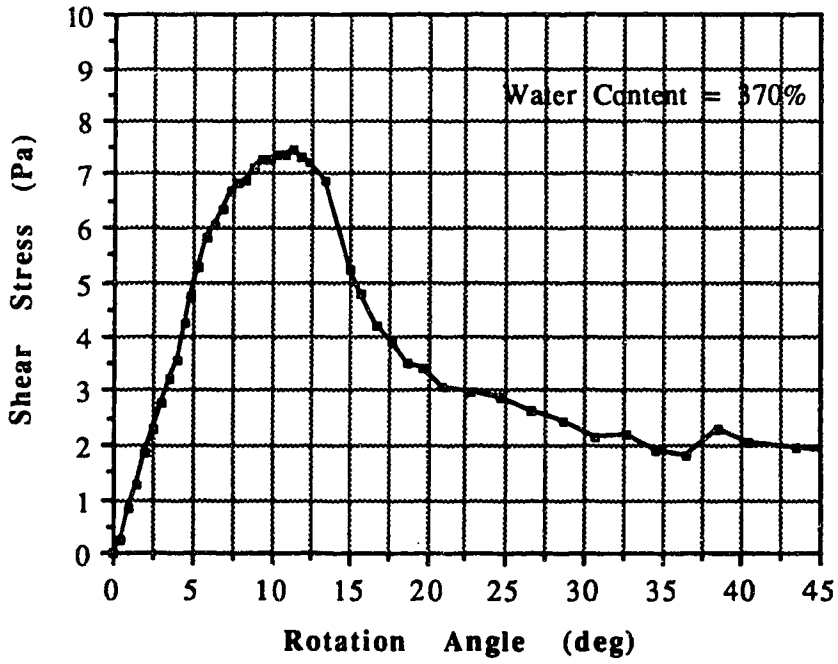

Figure 4.16 Vane Shear Test S40050DP

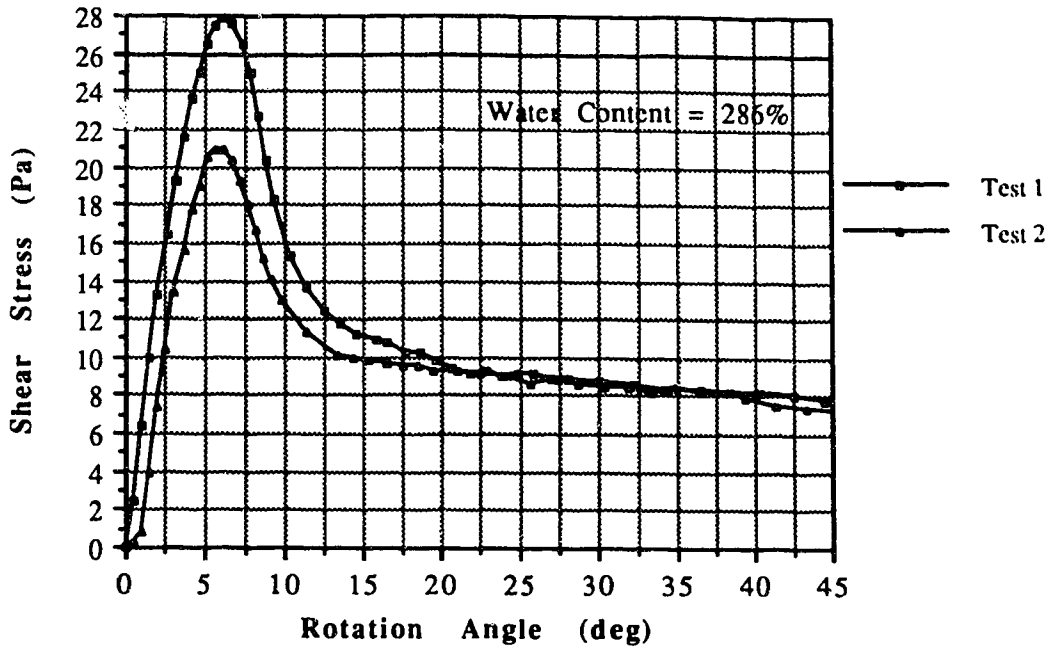

Figure 4.17 Vane Shear Test S30050DP

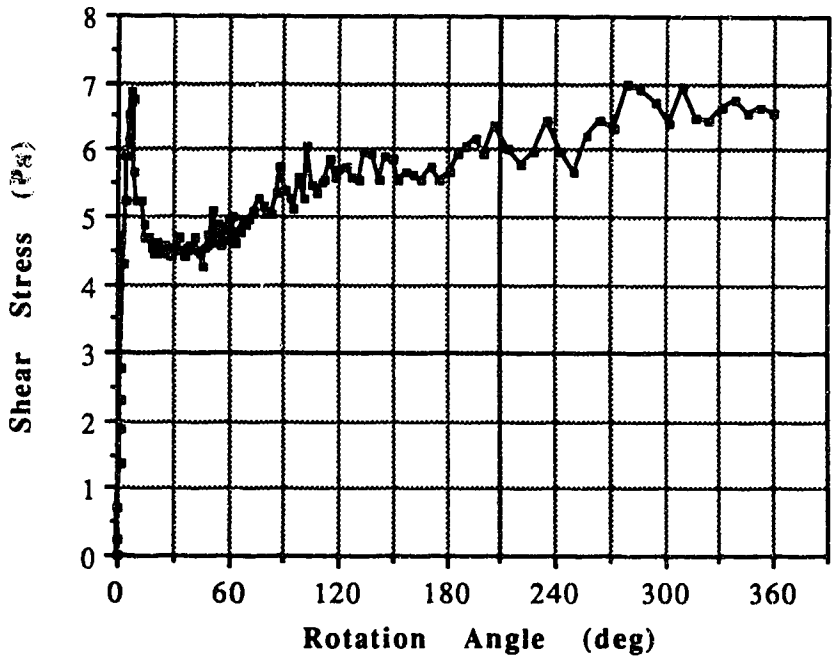

Figure 4.18 Vane Shear Test S23000M

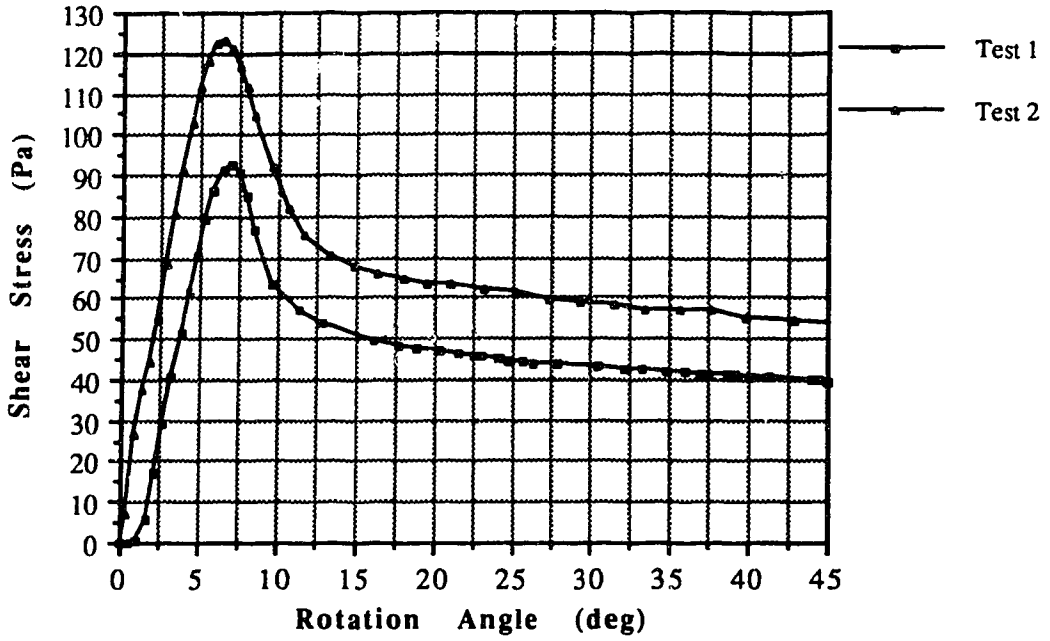

Figure 4.19 Vane Shear Test S15020DP

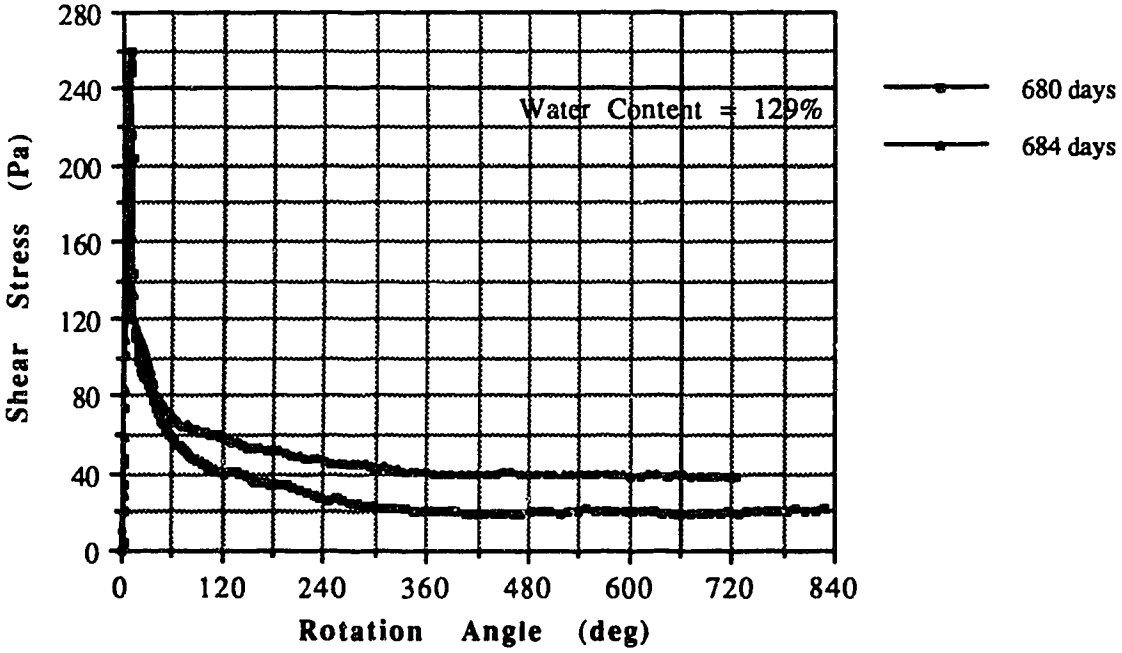

Figure 4.20 Vane Shear Test S15680DR

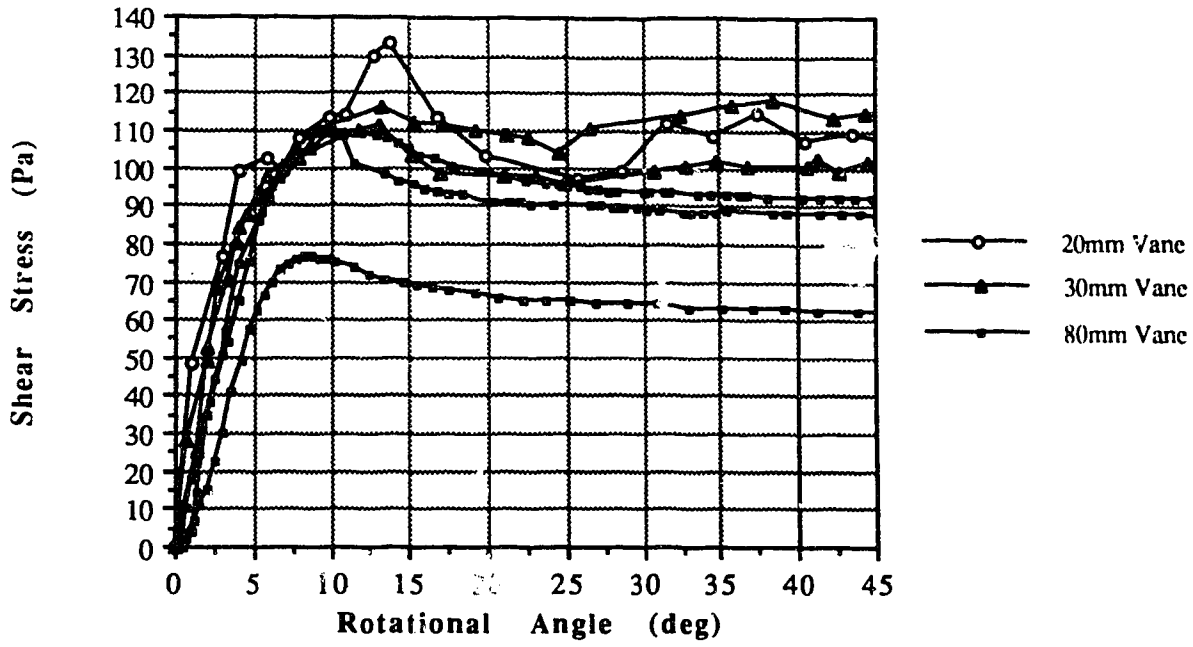

Figure 4.21 Vane Shear Test S10000M

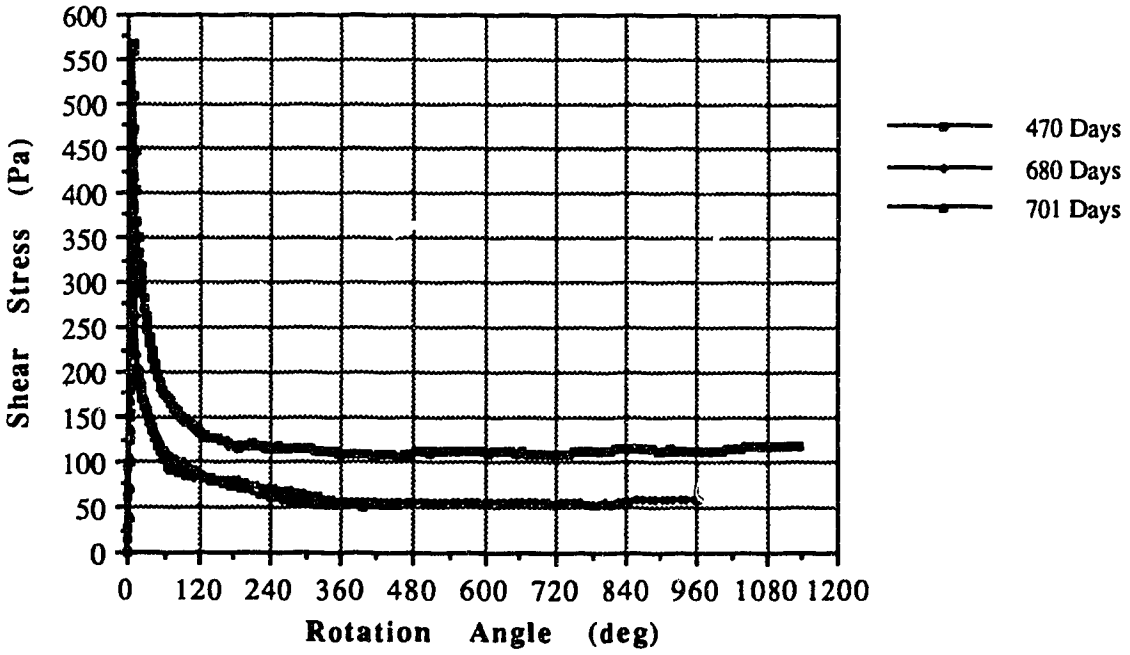

Figure 4.22 S10: Residual Strength at 470, 680 &701 Days

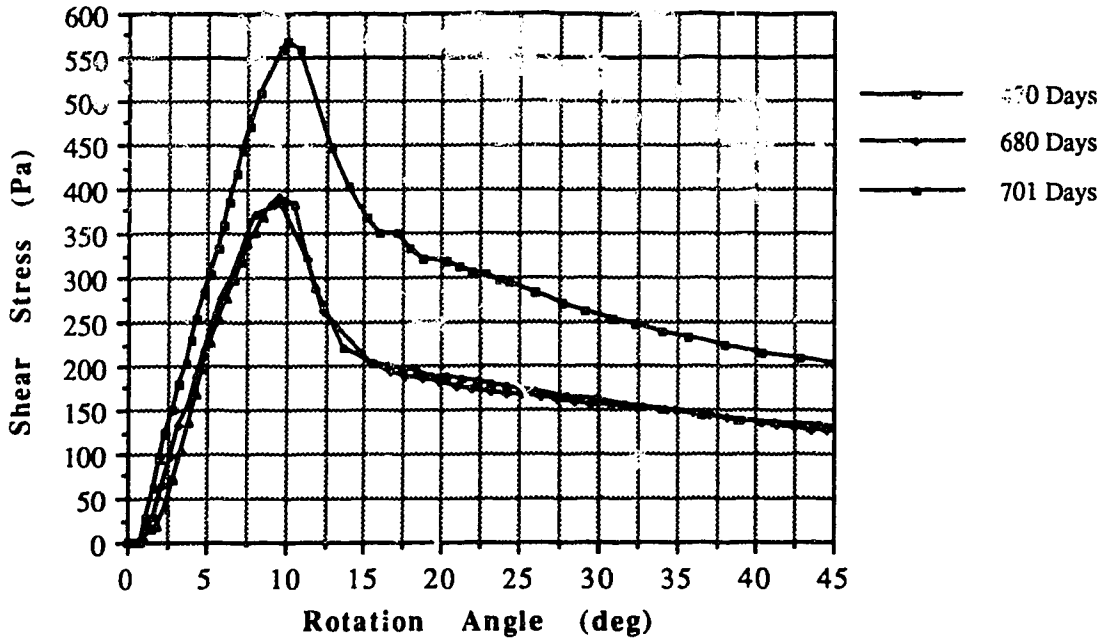

Figure 4.23 S10: Peak Strength at 470, 680 & 701 Days

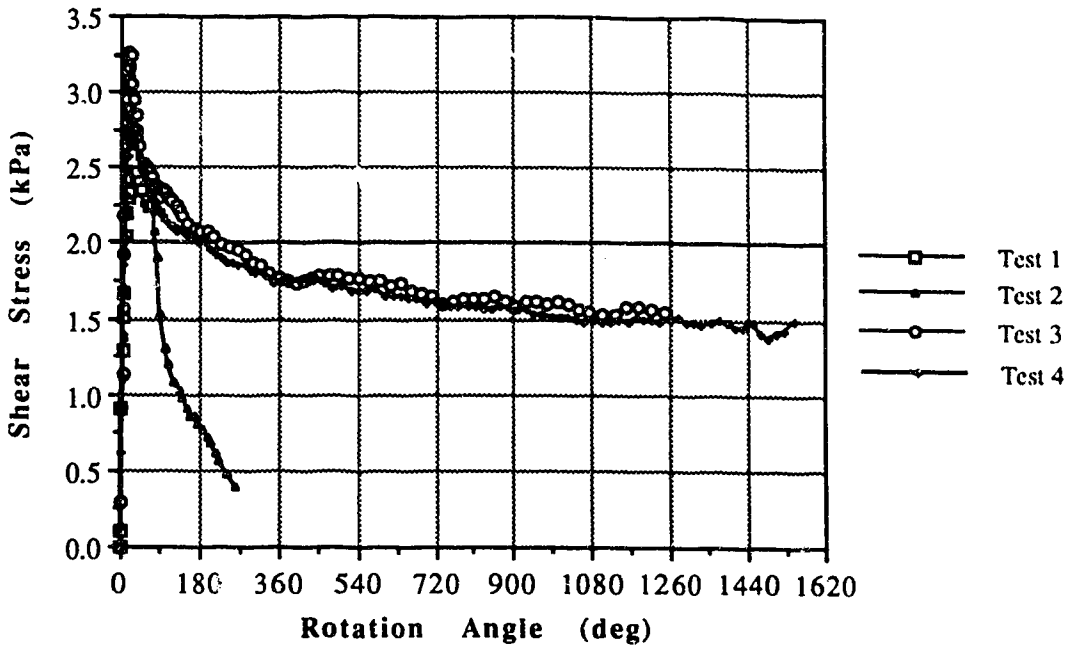

Figure 4.24 Vane Shear Test S47000M

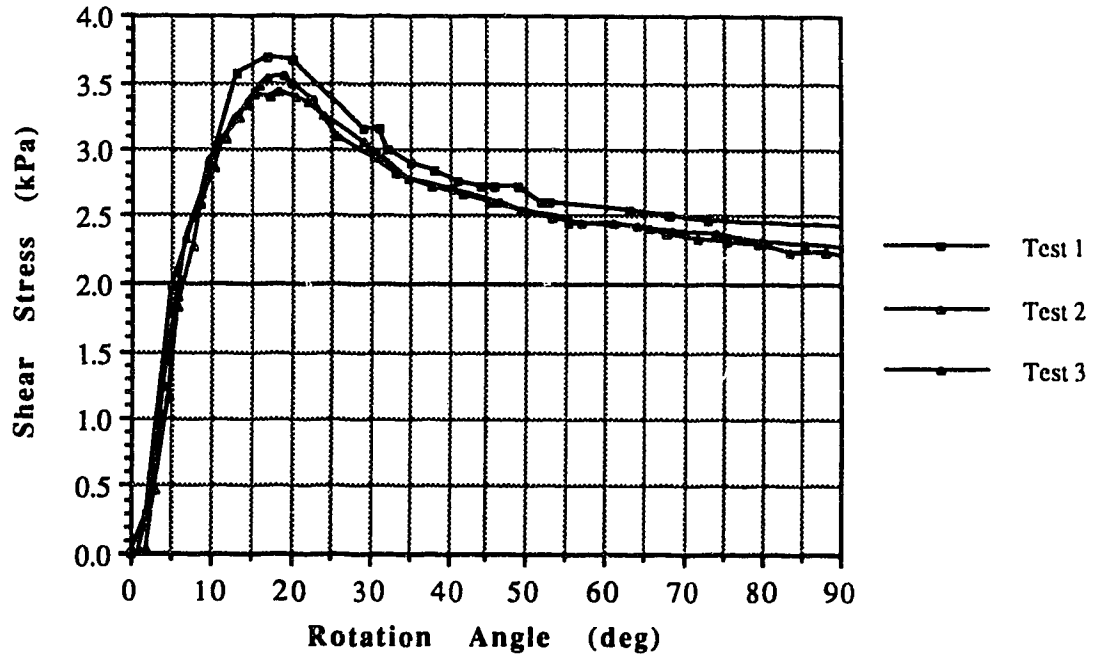

Figure 4.25 Vane Shear Test S47001DP

5. ANALYSIS OF TIME DEPENDENT STRENGTH BEHAVIOUR

5.1 Method of Analysis

As discussed in Chapter 2, in order to determine the extent of thixotropic effects in a saturated soil it is required that the water content of the soil specimen remains constant. In this experimental program however, the original water content could not be sustained, in the high water content specimens, for an extended period of time because of self-weight consolidation. To assess the increase in strength caused by thixotropy alone, the effect of consolidation was taken into account by the following procedure.

The analysis of the results was composed of several steps. In step one, the peak and residual values of shearing resistance obtained from both, viscosity and vane shear tests were plotted against time for each initial water content sludge. Because of the large time span of tests the logarithmic scale was used for the time axis whereas the resistance (viscosity or shear strength) axis remained in the arithmetic scale. For uniformity, the time was expressed in hours. Furthermore, the time axis was subdivided into shorter periods resulting in more graphs. And so, a typical set of graphs for a particular sludge includes the entire testing span; 16320 hours (680 days), a period ending at 3840 hours (160 days) and an initial period of 240 hours (10 days). An arithmetic time scale was used for the latter plot. The viscosity and vane shear strength results are presented separately.

The next step involved a process of fitting a smooth curve through the peak data points. This required a judgement of the results and deciding which of them were to be weighted less than the others. Working simultaneously with the three graphs a best fit curve for each initial water content sludge was constructed.

Having constructed best fit curves, their coordinates (shearing resistance and time) were plotted on a graph along with the corresponding actual water contents. Using interpolation techniques, contour lines for constant water contents were then drawn. For consistency, the constant water contents were chosen the same as the initial water contents, that is 400, 300, 233, 150, 100, and 47%.

It should be noted that every contour line follows a path which is defined as the strength gain path. In the strength gain path, in turn, two separate paths can be distinguished: the time-only strength gain path and the time-consolidation strength gain path. In the time-only path there is no influence of consolidation; the water content of the original slurry remains constant and this part of the contour line is identical to the corresponding best fit curve for the initial water content. The time-consolidation path indicates an increasing influence of the consolidation process and the contour line is corrected for the changing water content. Some contour lines consist exclusively of the time-only strength gain path, whereas others consist of both time-only and time-consolidation strength gain paths. This feature is discussed for each constant water content later in this chapter.

To compare a relative increase in shearing resistance, in both viscosity and undrained shear strength terms, for each water content, the data were also presented in another form: thixotropic ratio versus time, where thixotropic ratio is defined as the ratio of the peak shearing resistance at time t to the shearing resistance at time 0. In this manner, different water contents could be directly compared to each other to assess which water content showed the most influence of thixotropy. Furthermore, thixotropic ratios for viscosity could be compared to those for shear strength to determine what degree of compatibility exists between these two methods of testing.

In the case of residual values, the vane shear and viscosity results were analyzed by plotting the ratio of the residual to remoulded (initial) values versus time. For the time dependency of residual shearing resistance (vane shear and viscosity) any resulting relationship can be deemed as purely thixotropic. In addition, the liquidity index-residual shearing resistance relationship was investigated in order to compare it with information available in the literature for other soils.

5.2 Viscosity Measurements

5.2.1 Viscosity Readings at a Constant Water Content - Sludge 400

Figures 5.1 through 5.3 show plots of viscometer readings at 1 rpm versus time for specimens with the initial water content of 400%. All three figures show the same results but use different scales and ranges for the time axis. In Figure 5.1, the age of sludge is plotted using a logarithmic scale; with this scale, every test result can be identified which is important for the tests performed in the first several hours. The time axis spans from the initial test at 0.01 hours (36 seconds) to the final test at 16,320 hours (680 days). Because the logarithmic scale results in a distorted view of the change in viscosity, Figures 5.2 and 5.3 show an arithmetic scale to supplement Figure 5.1. Figure 5.3 includes the whole span of the tests while Figure 5.2 illustrates the first 10 days of testing. In addition, the best fit curve for the measurements is shown in each of the three graphs for both the peak and residual values.

The same format of graph presentation applies to each sludge and the above description will not be repeated. Furthermore, these three graphs serve an illustrative purpose and represent transition plots between the test results and their analysis. Therefore, the discussion will focus on the contour lines

representing sludges of constant water content rather than on best fit curves for the measurements on which the water content may decrease with time. Figures 5.4 and 5.5 show the viscometer readings for the 400% water content sludge. It should be emphasized that in the case of contour lines the number 400% (or 300, 233, 150, 100 and 47%, respectively) represents a constant water content; not the results on the sludge with an initial water content of 400%. In addition to the water content number, there is another description of the sludge used in analyzing the test results. This is the liquidity index, I_L, a parameter correlating the water content of the material with its Atterberg limits:

$$I_L = \frac{w - w_P}{w_L - w_P} \qquad (5.1)$$

where w is the water content of the soil, w_L is its liquid limit and w_P is its plastic limit. The liquidity index is widely used in geotechnical engineering to compare soils of different water contents, mineralogy, and water chemistry. The two graphs show the same viscometer readings using different scales for the time axis; Figure 5.4 uses the logarithmic scale while Figure 5.5 uses the arithmetic scale. It can be seen on the plots that the test results for the 400% water content sludge are limited to 500 hours (approximately 21 days). This relatively short period of time was determined by self-weight consolidation. By this elapsed time the water content of the sludge (392% at 21 days and 387% at 25 days) had decreased too much by consolidation from the initial value. Carrying extrapolation to long times would increase the error associated with this analytical technique. Besides, sludge at such a high water content does not last much longer (if any) in the tailings pond environment.

For the reasons stated above, the 400% water content (I_L=15.2) viscosity readings are time-only values. The trends in the behaviour of the sludge can

clearly be recognized in Figures 5.4 and 5.5. The measurements start at the "zero" (36 seconds) time with a low viscometer reading of 0.5 and stop at 500 hours (21 days) with a high of approximately 4.4. The highest rate of viscosity gain occurs immediately after mixing with a gradual decrease in the rate of increase observed throughout the duration of the test. Approximately 50% of the measured increase in viscosity takes place within the first 10 hours. At 21 days, the curve, although considerably flatter, is still showing an increase in viscosity which means that thixotropy is acting well beyond the 500 hour mark for such a high water content sludge.

- **Sludge 300**

Figures 5.6, 5.7 and 5.8 show the results of viscosity measurements versus the time after mixing for the sludge with an initial water content of 300%. The results vary from a low of 1.5 at zero time and water content of 300% to a high of 74 at 660 days and 168% water content. Best fit smooth curves were constructed through the data points for peak and residual values.

Figures 5.9 and 5.10 present the viscosity readings versus time for a sludge with a constant water content of 300% or liquidity index of 11.2. The strength gain has two separate components: the time-only strength gain path accounts for the first part of the curve, from zero to approximately 800 hours (33 days) and the time-consolidation path, from 800 to 5000 hours (33 to 208 days). The time-only path is the same as the best fit curve for sludge 300. The time-consolidation path ends at 5000 hours (208 days). There was not sufficient data available to carry the interpolation past 208 days.

The viscosity readings display a high rate of increase in viscosity in the first several hours after mixing with a gradual decrease in the rate seen throughout the whole length of the test. The slope of the curve is very steep for measurements up to 240 hours (10 days) indicating a high rate of viscosity

gain. Then, the viscosity readings are linear on the arithmetic scale plot (Figure 5.10) from 240 to 1000 hours (10 to 42 days) which indicates an almost constant rate of viscosity increase. The gain in viscosity slows considerably after 1000 hours (42 days) reaching a plateau somewhere between 2000 and 3000 hours (83 and 125 days). The values reach a maximum of slightly more than 11 units at that time and then decrease after 3000 hours (125 days) until the end of the test at 208 days dropping to a value of under 9 units. There is no documented case in the literature for a soil in which the thixotropic values decreased after reaching a certain point in time. This trend is discussed later.

- **Sludge 233**

The viscosity test results for the sludge with an initial water content of 233% are shown in Figures 5.11, 5.12 and 5.13. The reported range of readings spans from a low of 1.8 initially to a high of 83 units at 16,320 hours (680 days) and 158% water content. For the two sets of results, peak and residual, two respective best fit curves were constructed through the data points and are shown in the three figures.

The viscosity readings for the 233% constant water content (8.5 liquidity index) sludge, shown in Figures 5.14 and 5.15, follow a strength gain path that consists of the time-only strength gain path from 0 to 1000 hours (0 to 42 days) and the time-consolidation strength path from 1000 to 11,300 hours (42 to 470 days). The viscosity readings stop at 470 days as there was not enough data for the interpolation to continue beyond this time.

As was noticed with the previous two water contents, these viscosity readings show the highest rate of viscosity increase in the initial period of time. This slowly decreasing high rate continues until approximately 1000 hours (42 days) after mixing after which the increase is still observed but at a considerably reduced rate. At 4000 hours (167 days) the viscosity readings

become constant at about 24 units and stays at that level until 7000 hours (292 days). Up to this point the trend is similar to that of the 300% water content. However, there is a dramatic change in behaviour of the material after 292 days: the sludge begins gaining viscosity again and at an increasing rate. This increase in rate is apparent in both figures until the data stops at 11,300 hours (470 days). Because of the variable behaviour pattern of this sludge it can not be predicted for how long this gain in viscosity would continue.

- **Sludge 150**

Figures 5.16, 5.17 and 5.18 contain plots of the viscosity readings versus time for sludge 150, that is the sludge with the initial water content equal 150%. In addition, two best fit curves, one for the peak, one for the residual values, were drawn through the plotted results. The lowest viscometer reading reported in this part of the testing program was 15.5 ("zero" time and 150% water content) and the highest was more than 112 units (11,280 hours or 470 days) at a water content of 141%.

The viscometer readings of the 150% constant water content sludge (liquidity index = 5.2) is presented in Figures 5.19 and 5.20. The curve follows mainly the time-only strength gain path; it continues up to 11,280 hours (470 days) which corresponds to the actual water content of 141%, for the remaining 210 day period (11,280 to 16,320 hours or 470 to 680 days) the measurements follow the time consolidation path.

Three main phases in the strength behaviour can be observed when examining the graphs. Phase one is the initial rapid gain in viscosity followed by a somewhat slower but still high increase until 1000 hours (42 days). Phase two shows a gradual decrease in viscosity gain until the viscometer readings reach a constant value just over 100 units at 11,280 hours (470 days). Finally,

phase three consists of the part of the curve that shows a decrease in viscosity. The overall pattern is very similar to that of the 300% water content sludge.

- **Sludge 100**

The plot of viscosity test results versus time for the sludge with the initial water content of 100% is shown in Figures 5.21 through 5.23. The viscosity results vary from a low of 37 measured immediately after mixing to a high of 278 units at 11,350 hours (473 days). The water content remained constant throughout the duration of this series of experiments (680 days). The best fit curves are included on the same graphs.

Because of the fact that there was no consolidation observed in sludge 100, the strength gain path of the 100% water content (I_L=3.2) has only one component; the time-only strength gain path. That is, the values on Figures 5.24 and 5.25 are identical to the best fit peak viscosity curve on Figures 5.21, 5.22 and 5.23.

There are similarities between this viscosity plot and that for 150% water content; there are also three phases distinguished in the shape of the curve as described earlier. However, in phase two the viscometer readings are still climbing at 11,350 hours (473 days), the peak is reached some time between 11,350 and 16,320 hours (470 and 680 days) and the drop in phase three is more pronounced than in the 150% water content sludge.

5.2.2 Thixotropic Viscosity Ratios

Thixotropic viscosity ratios for all five previously discussed water contents are presented in Figures 5.26, 5.27 and 5.28. From the data, it can be concluded that there appears to be no simple relationship between the water content and the degree of thixotropy (expressed as the thixotropic ratio). The dominant feature of the graphs is that the viscosity ratios can be divided into three distinctive

classes. Class one consists of water contents which display low relative ratios. These are the 100% and 150% water contents which correspond to liquidity indices of 3.2 and 5.2, respectively. It is remarkable that these two viscosity ratio curves are so close to each other that for all practical purposes they can be considered identical, both magnitude- and shape-wise.

It should be noted however that the term "low" thixotropic ratios is used in relation to the others shown. The above given values of the thixotropic ratio are high by other soils' standard as will be discussed later in this chapter.

The second class has only one water content; 300% (I_L=11.2). In all three graphs (Figure 5.26, 5.27, 5.28), this curve places consistently between the other water contents. Its shape is similar to the 100 and 150% ratios, however it reaches its peak sooner than the other two (3000 hours or 125 days).

Class three consists of the two remaining water contents: 400 and 233% (I_L=15.2 and 8.5, respectively). They display the highest thixotropic ratios. Initially, the curves remain very close to each other; after about 120 hours (5 days) the 233% ratios start to climb at a slightly higher rate and when they reach the end of the 400% water content curve at 21 days, the thixotropic ratios are 10.2 for 233% versus 9.0 for 400%. The 233% water content ratio continues its climb alone until it reaches a value of 13.3 at about 4800 hours (200 days). The shape of the last part of the 233% curve is rather inconsistent with what was observed with the other water contents. After 290 days, it begins its dramatic climb, achieving a thixotropic ratio of over 21 at the end of the experimental program (11,280 hours or 470 days).

On the basis of the above measurements, without analyzing the vane shear strength results, it can be concluded that the oil sands tailings sludge displays high and long lasting thixotropic effects. The water (solids) content of the sludge affects the magnitude of thixotropy; generally, thixotropic ratio

increases with increasing water content, however there is no direct relationship. As the 233% water content (30% solids content) shows, there appears to be a certain water content at which the microscopic structure (interparticle distance and orientation) of the soil is optimal for thixotropic gain in strength. Considering Figure 5.28, it can be seen why some researchers (Danielson and MacKinnon, 1990; Isaac, 1987) conclude that the strength gain in sludge appears to stop after a relatively short time; a rapid gain occurs within hours after mixing and the strength gain curve appears to become almost horizontal. Short term testing leads to such conclusions.

5.2.3 Residual/Remoulded Viscosity Ratios

Figures 5.29 to 5.31 present the residual to remoulded viscosity ratio for the five different water contents. The terms "residual" and "remoulded" viscosity (or vane shear strength) should perhaps be defined, as they are often used interchangeably. Here, the remoulded value indicates the measurement obtained from a test conducted immediately after mixing of the specimen (time = 0) whereas the residual value is the lowest reading at time t after considerable shearing has taken place.

In all cases, it can be clearly seen that the residual viscosity increases with passage of time. Furthermore, there is a general trend of higher relative increase in residual strength with increasing water content. However, the 233% water content which shows the highest ratios is an exception, similarly as was the case with peak viscosities. High values of residual viscosity ratios displayed by all the water contents might be in part explained by the construction of the T-bar spindles. A small diameter T-bar coupled with a very low rotation rate (1 rpm) may not offer a high degree of remoulding of the

slurry. Therefore, this discussion will be elaborated on in conjunction with the discussion of the residual vane shear strength (Section 5.3.3).

5.2.4 Liquidity Index-Residual Viscous Resistance Relationship

As discussed in Section 5.5, many researchers have found a relationship between liquidity index and remoulded shear strength for a wide range of soils. Some authors also define the relationship between liquid limit and plastic viscosity for different soils (e.g. Locat and Demers, 1988). However, the index character of viscosity measurements in this research program inhibits any comparison of a potential relationship established here with those found in the literature.

Figure 5.32 shows a plot of liquidity indices versus residual viscometer readings for all tests conducted in this experimental program. Three power law curves were fitted through the data points. Curve one describes the liquidity index-residual viscometer reading relationship at time equal zero and this could be considered as the true remoulded slurry equation. Curve two describes the relationship at 40 days. This particular time was chosen arbitrarily because at 40 days a wide range of liquidity indices was still encountered. These two curves and the two corresponding equations show how the age of sludge affected residual viscosity measurements. Finally, curve three shows the relationship for all data points if the time effect is not included.

All three curves show a good correlation implying that if appropriate calibration factors existed for the T-bar spindles a positive relationship between liquidity index and viscosity could be established.

5.3 Undrained Vane Shear Strength

5.3.1 Shear Strength at a Constant Water Content

- **Sludge 400**

Figures 5.33, 5.34 and 5.35 depict the results of undrained shear vane testing on the sludge with the initial water content of 400% versus time. Different scales are used in the graphs in order to focus on long- and short-time behaviour of the sludge as well as on the slope of the best fit curves. The undrained shear strengths in this series of tests vary from a low of 2 Pascals immediately after mixing to a high of 144 Pascals after 16,320 hours (680 days) at 178% water (36% solids) content. Two curves were fitted through data points, one for the peak values, one for the residual values.

The peak shear strengths for the 400% constant water content sludge are shown in Figures 5.36 and 5.37. The 500 hour limit indicates the span of existence of the 400% water content sludge in these tests. A 400% water content is equivalent to a liquidity index of 15.2 based on the Atterberg limits for the sludge (see Chapter 4, Section 4.1.2). Figure 5.36 uses the logarithmic scale for the time axis to better see the gain in strength in the first several hours whereas in Figure 5.37, the arithmetic scale is used in order to see the overall undistorted change in strength with time. As was mentioned with viscosity measurements, the 400% water content sludge follows the time-only strength gain path. The most dramatic increase in strength occurs in the first two hours following mixing. The curve exhibits a gradual decrease in slope although it still shows continuing gain in strength at an age of 500 hours (21 days). The thixotropic effect accounts for about 7.5 Pa strength gain during this period of time.

- **Sludge 300**

The undrained shear strength versus time resulting from vane testing of the sludge with the initial water content of 300% (25% solids content) is shown in Figures 5.38 through 5.40. The best fit curve for the peak and residual strengths are also shown. The lowest strength measured in this phase of testing was 3.2 Pa for the fully remoulded specimen while the highest was 170 Pa after 680 days of self-weight consolidation resulting in a water content of 168%.

The analysis of the results (Figures 5.41 and 5.42) reveal that the strength gain path for the 300% constant water content (I_L=11.2) can be divided into two distinctive paths: the time-only path up to 800 hours (33 days) and the time-consolidation path from 800 to 5000 hours (33 to 208 days). Again, the most rapid gain in strength occurs in the first two hours after mixing. The constantly diminishing rate of strength increase is apparent in Figure 5.42. At 3,000 hours (125 days), it appears that the strength plateaus and there is only a slow increase in strength until the end of the test at 5000 hours (208 days). The thixotropic gain in strength of the 300% constant water content sludge after 208 days is approximately 25 Pascals. The shape of the plot suggests that thixotropic change for this particular water content is slow after 3000 hours (125 days).

- **Sludge 233**

Figures 5.43, 5.44 and 5.45 present the results of the undrained shear vane testing against time for the 233% initial water content (30% solids content) sludge. The samples varied in age from 0 to 16,320 hours (680 days), in water content from 233 to 158%, and in shear strength from 4.4 to 210 Pascals. Smooth curves were constructed through both peak and residual strength values and are shown in the graphs.

The water content of 233% corresponds to a liquidity index of 8.5 and its shear strength versus time is shown in Figures 5.46 and 5.47. The time-only strength gain path is from zero to about 1000 hours (42 days), and the time-consolidation strength gain path is followed for the rest of the time, that is from 1000 to 11,280 hours (42 to 470 days). The thixotropic gain in strength in 470 days was close to 87 Pa. The unique shape of the 233% water content was also shown in the viscosity analysis (Section 5.2.1). The shear strength increase at this water content appears to be controlled by the time-consolidation path followed. In late stages, the 233% constant water content shear strength is mainly influenced by the strength of slurries with initial water contents of 300% and 400%. The strength of a particular water content sludge then depends on how the sludge arrived at that water content, that is, what initial water content it had and how long it took to consolidate to its present water content.

It should be noted that in the oil sands tailings pond all sludge has the same or a very similar initial water content and follows a similar time-consolidation path. Long term laboratory tests to measure thixotropic strength changes should therefore start with the pond sludge initial water content and follow, if possible, the pond time-consolidation path.

- **Sludge 150**

Figures 5.48, 5.49 and 5.50 show a plot of undrained shear strength versus time for the sludge with an initial water content of 150% (I_L=5.2). The duration of the test was 16,420 hours (684 days) during which the sludge consolidated from 150 to 129% water content (40 and 44% solids content, respectively) and had an undrained shear strength from an initial low of 19 to a high of 314 Pascals. The graphs also include the best fit curves for peak and residual strength.

The time-only strength gain path followed by the 150% constant water content sludge, shown in Figures 5.51 and 5.52, is responsible for almost 70% of the total time of the test, 0 to 11,280 hours (0 to 470 days); the remaining 5,140 hours or 214 days account for the time-consolidation strength gain path. As expected, there was a rapid gain in strength in the first several hours after mixing. The rate of increase slows gradually although it is still rather high after 1,000 hours (42 days). The increase in strength continues until 11,280 hours (470 days). After 470 days, as was first noticed with the viscosity measurements, the sludge shows a decrease in shear strength. The thixotropic gain in strength in the first 470 days is more than 260 Pascals after which the strength drops by about 55 Pa in the next 214 days.

- **Sludge 100**

Figures 5.53, 5.54 and 5.55 show the undrained shear strength versus time for the 100% water content sludge (I_L=5.2). As mentioned earlier, this sludge did not exhibit any self-weight consolidation during the test and, consequently, the water content remained constant. The measured peak shear strength varied from an initial of 62 Pa to a high of 567 Pa at 11,280 hours (470 days). A scatter of results can be noticed in the figures; the explanation of possible causes of it is offered in Section 4.3.5. The overall trends, however, are still readily distinguished. It was decided that the residual shear strength best fit line was horizontal suggesting that the residual strength was time independent. Due to the lack of consolidation in the sludge, the strength gain path consists of the time-only strength gain path (Figures 5.56 and 5.57) and the shear strength is a direct effect of thixotropy. There is a remarkable resemblance between the 100% water content strength curve and that for the 150% water content strength curve (except for strength magnitude) which indicate that secondary factors have little, if any, influence on the time

dependent shear strength of sludge for initial water contents below 233%. The thixotropic effect in the first 11,280 hours (470 days) amounted to about a 500 Pa gain in shear strength; the decrease in strength in the following 5,520 hours (230 days) was in the 180 Pa range.

- **Sludge 47**

Sludge 47 represented the oil sands tailings sludge at its liquid limit of 46% (I_L=1.0). Sludge of such a low water content (68% solids content) is not present in the pond at this stage of the pond development; the highest measured solids content was approximately 52% (Danielson and MacKinnon, 1990) which is equal to 92% water content. As was discussed in Chapter 3, testing the sludge at the liquid limit provides a convenient basis to compare the sludge to other soils. Figures 5.58 through 5.60 are plots of the results of undrained shear strength tests versus time for the liquid limit sludge. Again, a scatter of data points can be noticed in all three graphs. The trend shown by the residual shear strength confirms the one observed for sludge 100: no tendency to increase with time. Therefore, the best fit curve for residual strength is a horizontal line. Similarly, the long term test peak shear strengths are best represented by a horizontal line. The tests continued to 12,550 hours (523 days) with the shear strength increasing from an initial value of 1.5 kPa to a high of 6.6 kPa. Figures 5.61 and 5.62 show some of the tendencies observed earlier for the other water contents: rapid gain in strength in the first several hours, followed by a period of a gradually slower but still high rate of increase in strength until 1000 hours (42 days), followed by a lower rate of increase to approximately 6000 hours (250 days) and constant strength with time to the end of the test (523 days). A distinctive peak and a subsequent drop of the strength with time, as was noticed for the 100% and 150% water contents, was

not observed. The thixotropic gain in strength was approximately 5 kPa which, in absolute terms, is the highest among all considered water contents.

5.3.2 Thixotropic Strength Ratios from Vane Shear Tests

The thixotropic gain in strength has been given in terms of absolute values for every constant water content. To compare the relative increase in strength, thixotropic strength ratios have been calculated for each water content and are illustrated in Figures 5.63 through 5.65. The six water contents can be divided into three distinctive classes as can be seen in all three graphs. Class one, exhibiting the lowest thixotropic ratios, consists of one water content; that of the liquid limit sludge. Despite its lowest position on the graphs, this water content still shows a well defined effect of thixotropy: the thixotropic ratios reach values in excess of 4 after about 125 days and remain constant afterwards. Class three also consists of one water content; that of 233%. As was the case with thixotropic viscosity ratios, this water content displays the highest relative gain in strength. This is evident even in the initial hours after mixing (Figure 5.65). The dominance of the 233% water content increase in strength ratio continues until the end of the test period where it reaches a thixotropic strength ratio of close to 21. Class three which could be described as that of intermediate to high thixotropic ratios has four water contents: 400, 300, 150, and 100% water content. Of the four, the 150% water content shows the highest relative gain in strength; it reaches a thixotropic ratio of 14.5 at 11,300 hours (470 days). Furthermore, the 150% and 100% water contents display a decrease in strength in the final stage of the test duration. The 400% and 300% water contents, on the other hand, still exhibit a moderate increase in strength at the end of their respective tests.

Most of the observations made for the thixotropic viscosity ratio contour lines (Section 5.2.2) are confirmed here. There appears to be no simple relationship between water content (or liquidity index) and degree of thixotropy. Section 5.4 features an in-depth discussion addressing a possibility of such relationship.

5.3.3 Residual/Remoulded Shear Strength Ratios

Figures 5.66, 5.67 and 5.68 show residual to remoulded undrained shear strength ratios versus time for different constant water contents. The remoulded strength measured immediately after mixing of the slurry, whereas the residual strengths are from tests conducted at elapsed times after mixing. As was mentioned earlier, the residual strengths of the 100% water content and liquid limit sludge did not exhibit any increasing trend with time. These measurements indicate that the action of the revolving vane in these sludges caused complete remoulding of the material. The remaining four higher water contents show significant changes in residual strength with time. Figure 5.66 reveals that the 150% water content sludge shows the highest relative increase in residual strength reaching its highest point of about 3.0 after 11,300 hours (470 days). After this, it drops to a ratio of 1.4 at 16,320 hours (680 days). The 233% water content also climbs to a relatively high ratio of 2.4 after 4000 hours (167 days) and then slowly descends over the next 7270 hours (303 days) to a ratio of 1.4. However, the 233% water content has clearly the highest ratios in the first 3000 hours (125 days) which can be seen in Figures 5.67 and 5.68. A behaviour somewhat similar to that of the 233% water content is shown by the 300% water content. The values reach a peak of 1.8 at 2000 hours (83 days) only to dip to a ratio of 1.3 by 5000 hours (208 days). The increase in residual strength of the 400% water content sludge is moderate: the

highest ratio is less than 1.3 after 500 hours (21 days), the end of the test. Section 5.4 discusses the relationship between water content and residual/remoulded strength ratio.

5.4 Effect of Water Content on Thixotropic Ratio

- Peak Strength

It was suggested in Section 5.2.2 that there may be an optimum water content at which thixotropy is a maximum. To investigate the validity of this concept, thixotropic shear strength ratios for the different water contents are shown in Figure 5.69 for time intervals of 2 days, 20 days, 200 days, 450 days, and 700 days. It is apparent that, starting at the liquid limit, thixotropic ratio increases with increasing water content reaching its maximum at 233% water content (I_L=8.5) after which increasing water content causes a decrease in thixotropic ratio. This trend is well defined at three time intervals; 2 days, 20 days and 200 days and more pronounced with higher elapsed times. At 450 days, the relationship could not be extended past 233% water content because of the shorter duration of the higher water content tests. The thixotropic ratios at 700 days show the decrease in shear strength in the long term tests.

The "modified effective stress law" postulated by Chatterji and Morgenstern (1989) as discussed in Chapter 2 offers an explanation for the observed water content-thixotropic ratio relationship. The intrinsic effective stress or net physico-chemical stress (R-A), can have a strong influence on shear strength and compressibility of clay-water systems. At high void ratios, its influence would be small and at low void ratios, it would be a small percentage of the apparent effective stress. At some intermediate void ratio, the physico-chemical stress (R-A) would have the largest relative influence on the apparent effective stress. As thixotropic ratio is the relative increase in shear

strength not the absolute, it shows that the 233% water content sludge has the optimum void ratio for relative thixotropic increase.

The concept of optimum void ratio could help answer some questions associated with the behaviour of the sludge in the pond. Field measurements show (Danielson and MacKinnon, 1990) that sludge with solids contents close to 30%, which corresponds to the water content of 233%, occupies disproportionally large depths in the pond. These field measurements also show that self-weight consolidation of the sludge takes a relatively short time to reach 30% solids content. However, the rate of consolidation after 30% solids content is reached is significantly reduced which results in a thick layer of sludge at or close to this particular solids content. Coupling the concept of an optimum void ratio for maximum relative thixotropic effect with the development of effective stresses in the pond offers a logical explanation for this phenomenon. High relative thixotropy combined with low effective stresses reduces the rate of consolidation.

- **Residual Strength**

To determine any trend between time and residual strength or between water content and residual/remoulded strength ratio, one must first consider whether the residual values are really the lowest that can be obtained or would further rotating of the vane bring even lower results. Elder (1985) found in his experiments that residual strengths after long times were higher than remoulded strengths. He concluded that the vane residual rotation angles used (210°) were insufficient to reattain the fully remoulded state. Bowden (1988) increased the residual rotation angle of the vane to 720° to ensure that full remoulding of the shear surface took place. Bowden concluded that residual strengths did change with the passage of time but trends were conflicting. The vane rotation of 720° (or rotation sufficient for readings to stabilize at a

minimum value) was adopted as a standard for residual strength in this research program. As it appears that complete remoulding was achieved for the 100% water content sludge, the same vane and a similar rotation angle also should be sufficient for higher water contents. In fact, remoulding a soil of high water content should require less effort than remoulding the same soil with a lower water content. If the above is true, then the oil sands tailings sludge does exhibit a time dependency of its undrained residual shear strength at water contents above 100% (I_L=3.2). Figure 5.70 presents plots of the residual to remoulded shear strength ratio versus water content for different time intervals. Five time intervals were selected to illustrate the relationship; 2 days, 20 days, 80 days, 160 days, and 700 days. Although the trend between the relative increase in residual strength and water content is not as clear as was the case for peak strength, the four first time intervals show defined peaks. These measurements agree with the postulation that irreversible changes take place in the sludge with time. It would appear, however, that the magnitude of these irreversible physico-chemical changes is small when compared to the total decrease in strength from peak to residual.

5.5 Liquidity Index-Residual Shear Strength Relationship

Several authors have proposed empirical relationships between remoulded shear strength and water content. The liquidity index is generally used as an appropriate normalization of water content for different soil mineralogies and different water chemistries. A plot of liquidity indices versus residual shear strength from all vane tests conducted during this research program is shown in Figure 5.71. As shown earlier, there is an influence of time on residual strength therefore three different relationships are derived for the sludge.

Relationship one is for truly remoulded sludge (the results are obtained from "zero" time tests) and can be written as:

$$c_{ur} = (17.6/I_L)^{2.52} \qquad (5.2)$$

The undrained shear strength, c_{ur}, in the above and all following relationships is expressed in Pascals.

Relationship two is for residual shear strengths obtained from tests conducted at 40 days of aging. This particular time was chosen because at 40 days there was still a wide range of liquidity indices available without the need of interpolating the data and yet there were enough changes in residual [illegible]n to illustrate the time effect. The resulting equation can be written as:

$$c_{ur} = (23.8/I_L)^{2.28} \qquad (5.3)$$

Finally, the third relationship includes all measurements:

$$c_{ur} = (20.5/I_L)^{2.40} \qquad (5.4)$$

The curves for the first two relationships are included in Figure 5.71, the curve for the third equation is not shown but its position would be between the former two. General relationships for soils proposed by other researchers are also illustrated in Figure 5.71.

Elder (1985) analyzed his and other researchers' data and proposed a relationship for remoulded shear strength at liquidity indices between 0.4 and 20:

$$c_{ur} = c_{uw_L}/I_L^3 = (14.4/I_L)^3 \qquad (5.5)$$

where c_{uw_L} is the undrained shear strength at the liquid limit. To be consistent with Elder, c_{uw_L} = 3 kPa (3,000 Pa in the equation) was used. Elder states that a value closer to 2 kPa might be more appropriate but argues that it would underpredict strengths at liquidity indices higher than 3. When compared to the zero time results for the oil sands tailings sludge, Elder's relationship underestimates the strength at high liquidity indices; by 0.6 Pa or 40% at I_L =

15. If $c_{u w_L}$ = 2 kPa is used in his relationship, the strength is even more underestimated.

Locat and Demers (1988) combining data from the Swedish fall cone and viscosity tests for some remoulded sensitive clays, in the range of liquidity indices between 1.5 and 6, proposed a relationship that can be written as:

$$c_{ur} = (19.8/I_L)^{2.44} \qquad (5.6)$$

The curve representing this equation was plotted to higher values of liquidity indices so it could be compared to the relationships derived in this research. From Figure 5.71, it can be seen that Locat and Demers' relationship offers a remarkably good fit to the remoulded shear strengths of the oil sands tailings sludge.

Two other correlations between remoulded shear strength and liquidity index were considered. Because of their lower range of liquidity indices, these two relationships were plotted on a separate graph and are shown in Figure 5.72. The residual shear strengths of two oil sands sludges are also included: 100% water content and the liquid limit.

Mitchell (1976) determined remoulded shear strength as a function of liquidity index for several clays and constructed approximate limits for the data over a liquidity index range from 0 to 3.5. He attributed the range of values to the different methods of testing used to obtain the data. From Figure 5.72, it is seen that all residual shear strengths of the sludge at the liquid limit are close to the centre of the limits proposed by Mitchell. The agreement for the 100% water content sludge (I_L = 3.2) is not as close as for the liquid limit sludge although the remoulded shear strength (t=0) falls in between the limits. As discussed earlier, the 100% water content residual strength did not show a time dependency, therefore the range of strength seen in the plot is the variation of the measurements.

Leroueil et al. (1983) found that for many soils in the $0.5 < I_L < 2.5$ range, the relationship between remoulded shear strength and liquidity index can be written as:

$$c_{ur} = (25.9/I_L)^{2.27} \qquad (5.6)$$

The curve resulting from this equation was plotted in Figure 5.72. At the liquid limit, the residual strength of the sludge is in close agreement with Leroueil's prediction. At $I_L = 3.2$, where the curve was extrapolated beyond the relationship's upper limit, Equation (5.6) gives a higher value; 118 Pa versus 62 Pa for the sludge.

From the above discussion, it can be concluded that the residual strength of the oil sands tailings sludge in the range of liquidity indices between 1 and 15 is accurately predicted by the relationships derived for many other clays. Therefore, The sludge, despite its unique origin, shows remoulded strength characteristics similar to those in natural sensitive clays. From the geotechnical engineering point of view, the remoulded oil sands tailings sludge is similar to other remoulded sensitive clay soils. Its mineralogy and water chemistry do not give it unique remoulded properties even several years after formation.

5.6 Comparison of Shear Strength Tests to Viscosity Tests

For the two major groups of experiments, viscosity measurements and shear vane strength testing, higher importance was placed on the vane testing. This decision was dictated by several factors. Viscosity measurements, as mentioned earlier, represented an index type of testing because of the limited nature of the equipment. Calibration of the T-bar spindles for non-Newtonian fluids may be possible but that was deemed beyond the scope of this thesis. The vane tests, however, measure a universally used geotechnical engineering parameter;

undrained shear strength. It has been shown earlier that the vane remoulded strengths agree with published data and the validity of these test results appear acceptable. Furthermore, the data base for vane testing is well documented and comparisons with other soils can be readily drawn. Viscosity testing is becoming a new tool in soft soil investigation but it cannot be used for geotechnical design. The objective of the viscosity testing then was to aid and enhance the vane shear testing. A minor objective was to show the usefulness of viscosity testing in soft soil research. The degree of compatibility between the two methods is discussed below.

Thixotropic ratios from viscosity measurements and shear strength measurements for different water contents are compared in Figures 5.73 through 5.82. As usually employed throughout this presentation, both arithmetic and logarithmic scales are used for time in these graphs to better show the data.

The 400% water content thixotropic ratios are presented in Figures 5.73 and 5.74. The viscosity ratios are significantly greater than the shear strength ratios. Apart from numerical values, however, both curves exhibit almost identical trends with time as indicated by their similar shapes.

A good similarity between both methods of testing for the 300% water content sludge can be seen in Figures 5.75 and 5.76. Initially, the viscosity ratios are slightly higher but after 1000 hours (42 days) the shear strength ratios become greater.

As shown previously, the 233% water content sludge developed the highest thixotropic ratio with both the viscosity and shear strength tests reaching a maximum ratio of 21. Figures 5.77 and 5.78 show that both thixotropic ratios are very similar to each other in terms of magnitude as well as increase with time. Especially significant is the agreement displayed for advanced times, 4000 to

11,280 hours (167 to 470 days), where both test methods had the same increase in strength.

The 150% water content sludge shows a good agreement between shear strength and viscosity thixotropic ratio up to about 240 hours (10 days) as illustrated in Figures 5.79 and 5.80. After this period, the shear strength ratio is increasingly larger and after 470 days the difference in the ratios reaches a high value. In spite of this difference, the trends in time-dependent behaviour are similar. Even the final drop in thixotropic ratio is well mirrored in both tests.

The comparison between viscosity and shear strength testing is given in Figures 5.81 and 5.82 for the 100% water content sludge. An overall good agreement is shown with the shear strength ratio displaying higher values throughout the test duration. Again, the shapes of both sets of measurements are similar, including the final drops in the ratios.

Data from the liquid limit tests could not be compared as viscosity measurements were not conducted for this water content for the reasons explained in Section 3.2.1. Furthermore, the residual viscosity and shear strength ratios were not compared to each other because it was concluded that the viscosity apparatus T-bar spindles did not offer a sufficient degree of remoulding.

Viscosity ratios were higher than shear strength ratios at higher water contents. The opposite was true for lower water contents (150 and 100%). In conclusion, the two methods of testing displayed an overall good agreement, especially in reflecting time-dependent trends in strength behaviour of different water content slurries. The agreement in terms of magnitude of the ratios was not nearly as good as the pattern of change with time.

5.7 Comparison to Other Thixotropic Tests on Sludge

Danielson and MacKinnon (1990) conducted tests to determine how the rheological properties of sludge with a solids content of 26.6% (276% water content) changed with time. They used a concentric cylinder viscometer to measure the upper yield strength, fluid viscosity, lower yield strength, and plastic viscosity as a function of time. The test duration was 97.5 hours. The upper yield strength results of their tests (the upper yield strength in viscosity measurements would be an equivalent of the peak shear strength in vane testing) were plotted as thixotropic ratio and are shown in Figure 5.83. The vane shear strength thixotropic ratio of the 300% water content (25% solids content) sludge from this research was plotted on the same graph for comparison. A power law curve was fitted through Danielson and MacKinnon's data. The sludge tested by the shear vane shows significantly higher thixotropic ratios. The difference may be attributed to different testing methods; the viscometer operated at a continuously changing rate of shear whereas the vane was rotated at a constant, very low rate. Both plots confirm however that the most rapid gain in strength occurs in the first 10-15 hours after which the gain continues at a much reduced rate.

5.8 Effect of Self-Weight Consolidation on Thixotropic Strength

Consolidation of a soil results in the soil particles shearing past one another and a subsequent reduction in the physico-chemical bonding or thixotropic strength between the particles. The magnitude of thixotropic strength decrease depends on the rate and amount of consolidation. The slower the rate, the less the effect on thixotropy.

The higher water content sludges in this study underwent self-weight consolidation (Figure 5.84) and it is postulated that it was this process that was

responsible for the decreases shown in thixotropic strength in the long term tests.

As discussed earlier, the strength gain path followed by each water content sludge can be divided into the time-only strength gain path and the time-consolidation strength gain path. Three water contents, 400%, 100% and 46%, followed the time-only strength gain path. The other three, 300%, 233% and 150%, displayed both phases of strength gain. The effect of consolidation on each sludge is discussed below:

- The 400% water content sludge showed a continuous increase in strength over the duration of the test and no consolidation took place during that period.
- The 300% water content sludge gained most of its strength during the time-only path. Consolidation either caused a reduction in strength (Figure 5.10) or resulted in a slow rate of strength increase (Figure 5.42).
- The 233% water content sludge did not show a decrease in strength which would indicate that the rate of increase in particle bonding is higher than the rate of decrease by shearing.
- The 150% water content sludge had a relatively small amount of consolidation. The time-only strength gain path brought a continuous increase in strength (Figures 5.20 and 5.52) and the time-consolidation path was responsible for the drop in strength.
- The 100% water content sludge did not consolidate, yet a strength reduction is apparent in both test procedures (Figures 5.25 and 5.57). Although no firm explanation of this phenomenon can be offered, it is possible that at this water content there is another time dependent physico-chemical factor which is greater than the effect of thixotropy. Because the decrease in strength could not be explained, the index properties of the sludge

specimen used for the 100% water content long term tests were measured at the end of the test. The Atterberg limits of the specimen (Table 4.1, Batch 1.3) and its grain size distribution (Figure 4.1, Batch 1.2) indicate that it is representative of the sludge used in this experimental program.

- The liquid limit sludge is another case of the time-only strength gain path. From Figure 5.84, it can be seen that in the laboratory conditions, the sludge with an initial water content of 400% consolidated to a water content of 235% (30% solids content) after 470 days (1.3 years). In the pond environment because of the longer drainage path, the sludge reaches a solids content of 30% after about 3 years of consolidating (MacKinnon, 1989). The rate of consolidation in the pond is therefore less than half that in this research program. It is possible then that the thixotropic strength loss due to consolidation is less in the pond than in these laboratory tests. Considering the interrelationship between gain in thixotropic strength with time and loss in strength with consolidation with time, research into the physico-chemical processes occurring in the sludge must take both these processes into account. In fact, such research must ensure that the sludge in the laboratory follows the same time-consolidation strength gain path that it follows in the tailings pond.

5.9 Comparison to Other Thixotropic Soils

Thixotropy in general and its various aspects were discussed in Chapter 2. Preceding sections of this chapter were devoted to analyzing thixotropic behaviour of the oil sands tailings sludge. In this section, the sludge will be compared to other soils which display various degrees of thixotropy and whose documented cases have been found in the literature. It appears that thixotropy is mentioned frequently in publications regarding strength behaviour of

sensitive clays. However, there are very few cases in which long term thixotropic behaviour has been investigated in a fashion similar to the one followed in this experimental program. One such case was presented by Moretto (1948). The author tested four different natural clays at water contents at or close to the liquid limit. Unconfined compression tests were conducted on the clay samples with constant water content at different time intervals ranging from 0 to 610 days after remoulding. Acquired sensitivities of the clays as a measure of thixotropy were presented as a function of the period of rest. Skempton and Northey (1952) in their classic paper on the sensitivity of clays, dedicated a part of their study to thixotropy. They used the results obtained by Moretto and added their own tests on three different sensitive clays and three clay minerals. Their findings are presented in a comprehensive graphical form showing percentage thixotropic regain with the passage of time. The work on thixotropy by Skempton and Northey is often cited by other authors (e.g. Seed and Chan, 1957; Mitchell, 1976) but they do not extend Skempton and Northey's time dependent analysis to other soils, higher water contents or prolonged times. In fact, most investigations are limited to elapsed times anywhere from several minutes to several days. Therefore, the observed lack of available data.

To compare the oil sands tailings sludge to other soils exhibiting thixotropy, the results of Moretto (1948) and Skempton and Northey (1952) were plotted with the shear strength test results for the liquid limit sludge. The comparison can be seen in Figure 5.85, for five typical clays and the sludge, and Figure 5.86, for three clay minerals and the sludge. It should be noted that all soils shown in the two figures were tested at (or close to) their respective liquid limits. The plots present gain in strength with time for different soils in form of thixotropic ratio versus time in an arithmetic scale. From Figure 5.85, it can

be seen that the highest degree of thixotropy among the five natural clays is shown by the Beauharnois clay (Laurentian clay) which after 610 days reaches a thixotropic ratio of 4 and may reach a higher ratio with further time. The other four natural clays are well below the Beauharnois clay in terms of thixotropic ratio and it appears that they would never show a thixotropic ratio of more than 2. In the same figure, the thixotropic ratio of the liquid limit sludge is also presented. The sludge has the highest thixotropic ratio and only the Beauharnois clay shows a relatively close increase. It appears that the biggest difference in the relative strength gain between the two clay soils takes place in the first several days after remoulding; the sludge reaches a thixotropic ratio of about 2.4 versus 1.5 for the Beauharnois clay. After this initial rapid increase, the ratios of thixotropic increase are very similar to the end of the tests at approximately 600 days.

In Figure 5.86, the thixotropic ratios for three clay minerals, kaolin, illite clay, and bentonite, are given in comparison to the liquid limit sludge. Kaolin shows almost no thixotropy and illite shows only a small effect. In contrast, the bentonite shows a high gain in strength at very short time intervals. However, the rate of increase reduces significantly after about 50 days where it reaches a ratio of 2.2 and after 200 days, the clay shows a total ratio of approximately 2.4. When comparing the sludge to the clay minerals, it is obvious again that the former exhibits a significantly higher thixotropic effect. Immediately after remoulding, the sludge increases in relative strength at a higher rate than the bentonite. After 50 days, the sludge has a thixotropic ratio of 3.4 and reaches its highest ratio of 4.4 at about 300 days. Although the bentonite appears to be still gaining strength at the end of the testing period, it seems unlikely that it would ever reach the ratio attained by the sludge.

Skempton and Northey (1952) also investigated the influence of water content on thixotropic regain for different clays. The authors show that thixotropic regain decreases with decreasing water content below the liquid limit and suggest that thixotropy may be zero at water contents at or close to the plastic limit. Figure 5.87 contains Skempton and Northey's data and the comparable results of this research. The vertical axis in the plot is defined as the ratio of two ratios; the thixotropic ratio at a particular water content divided by the thixotropic ratio at the liquid limit. In this manner, thixotropic ratios at different water contents were normalized to that at the liquid limit. The ratios were compared at 100 days of aging of the soils. At water contents greater than the liquid limit, the evidence provided by Skempton and Northey is conflicting; two of the clays are slightly less thixotropic and two show increased thixotropy. In this experimental program, only water contents at or above the liquid limit were considered. Thus only two values for the sludge are shown on the plot; water contents of 46% and 100%. The sludge shows increasing thixotropic effects with higher water content, however the increase is not nearly as dramatic as for the Beauharnois clay as seen in Figure 5.87. The bentonite appears to exhibit a similar increase as the sludge however the data is too limited.

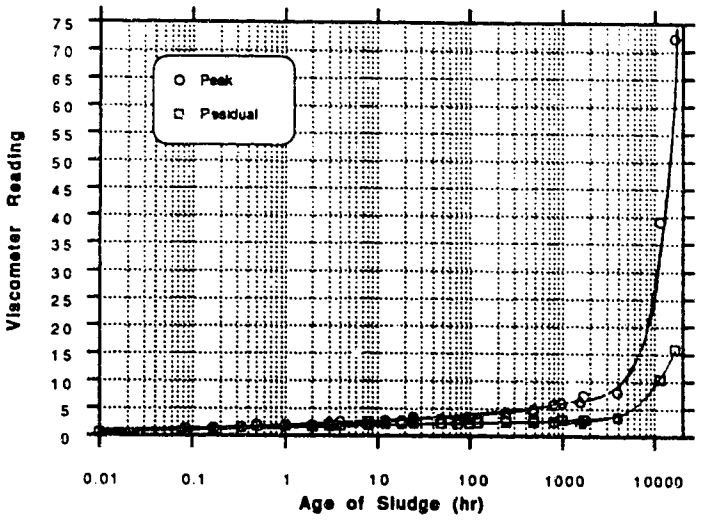

Figure 5.1 Viscometer Readings vs. Time for Sludge 400 - 16,320 hrs

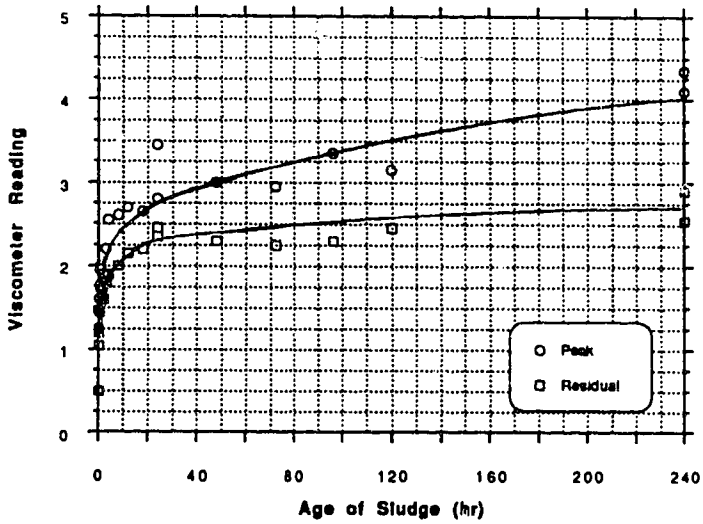

Figure 5.2 Viscometer Readings vs. Time for Sludge 400 - 240 hrs

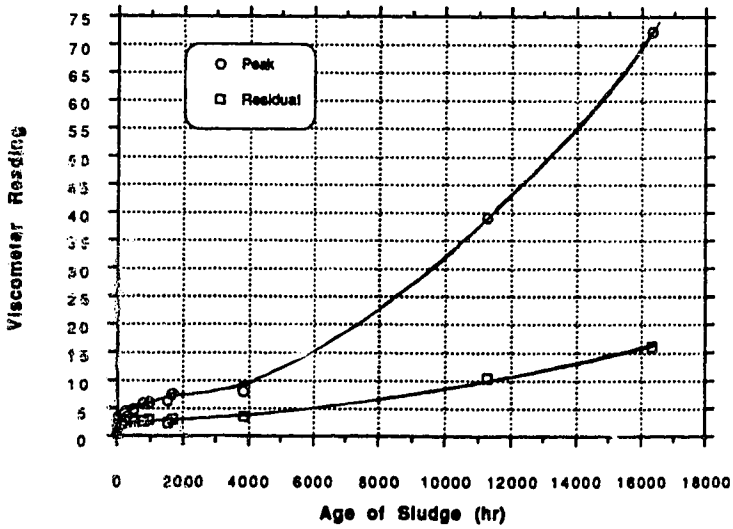

Figure 5.3 Viscometer Readings vs. Time for Sludge 400 - 16,320 hrs

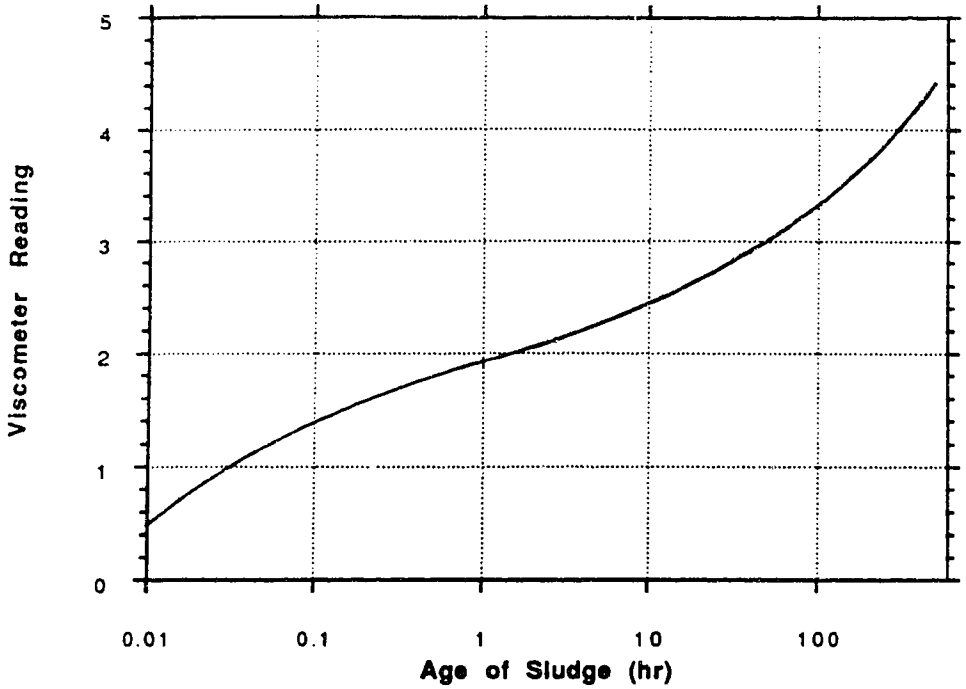

Figure 5.4 Viscosity Readings for w=400% (I_L=15.2)

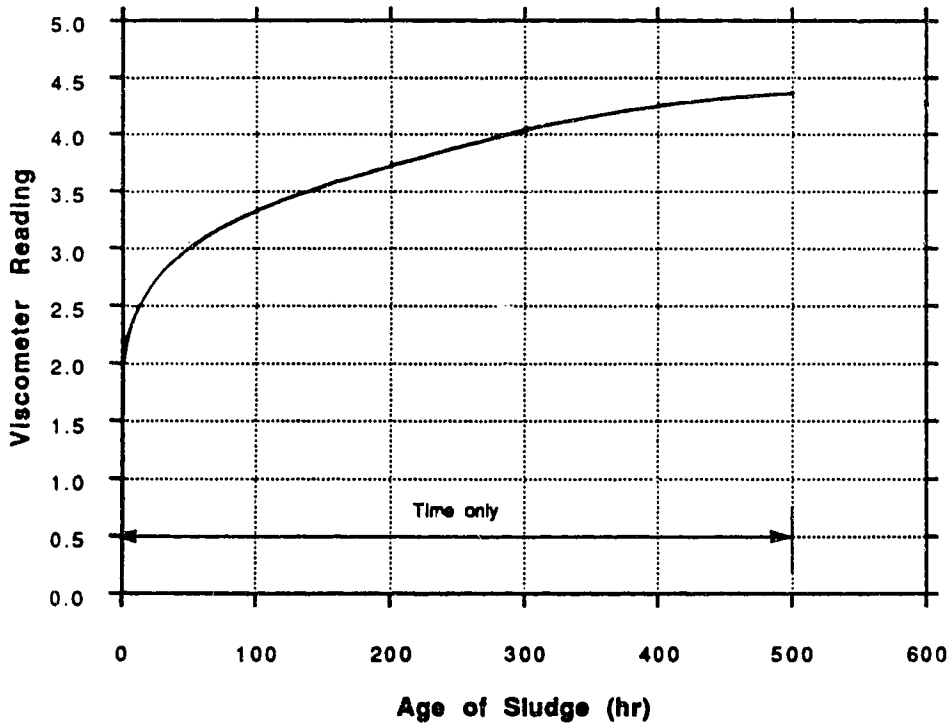

Figure 5.5 Viscosity Readings for w=400% (I_L=15.2)

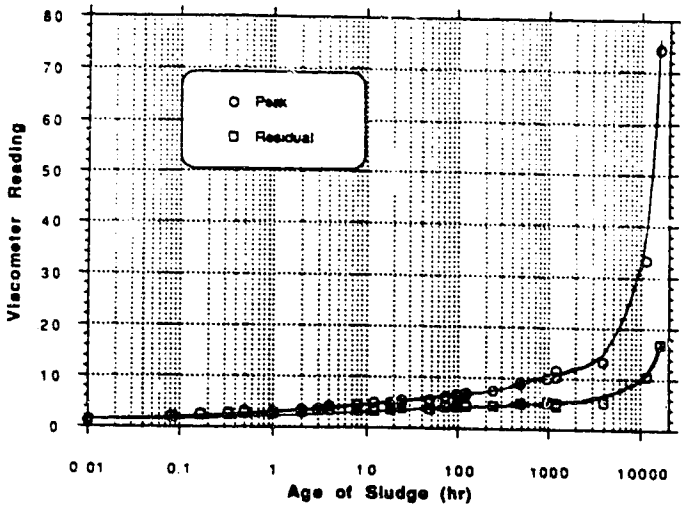

Figure 5.6 Viscometer Readings vs. Time for Sludge 300 - 15,840 hrs

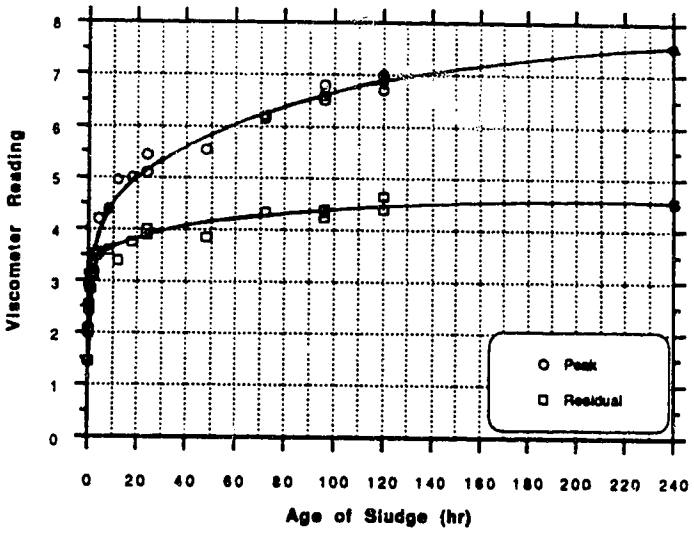

Figure 5.7 Viscometer Readings vs. Time for Sludge 300 - 240 hrs

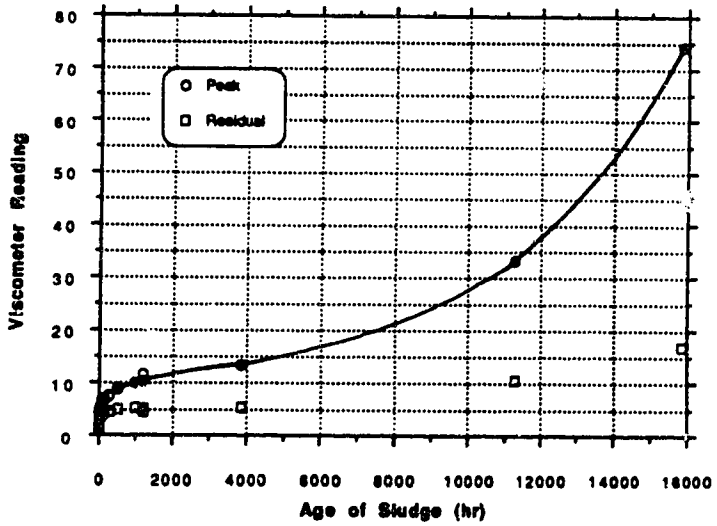

Figure 5.8 Viscometer Readings vs. Time for Sludge 300 - 15,840 hrs

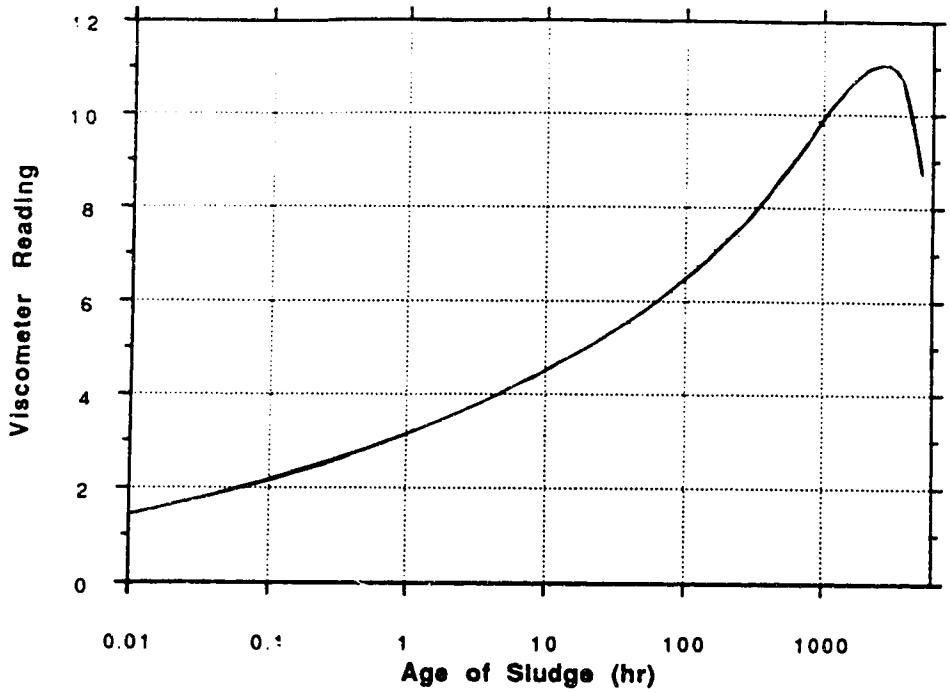

Figure 5.9 Viscosity Readings for w=300% (I_L=11.2)

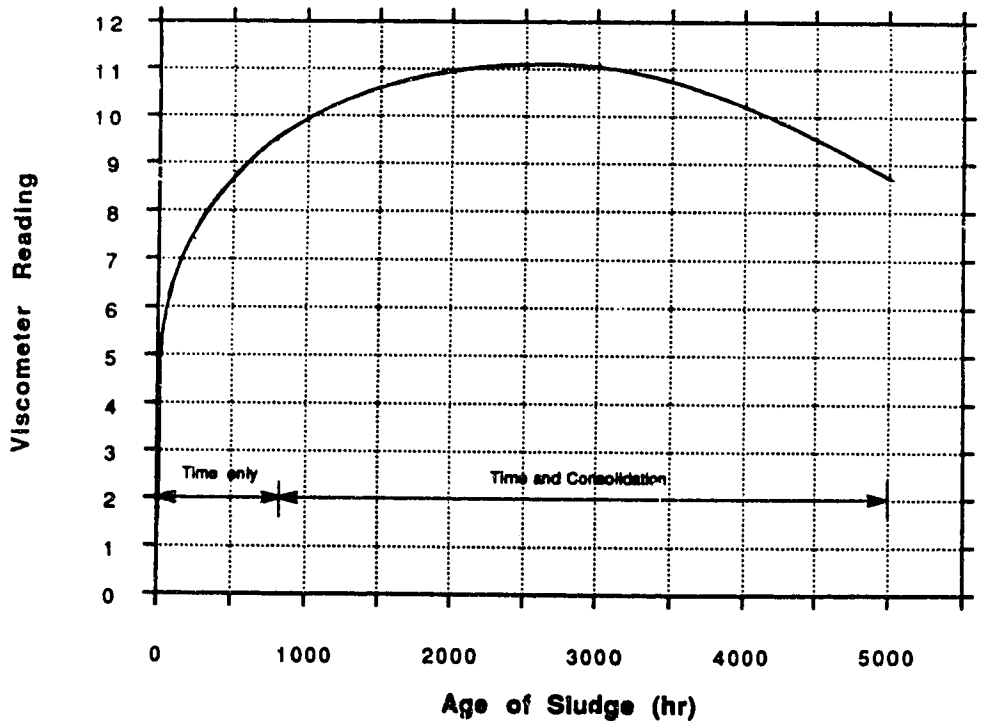

Figure 5.10 Viscosity Readings for w=300% (I_L=11.2)

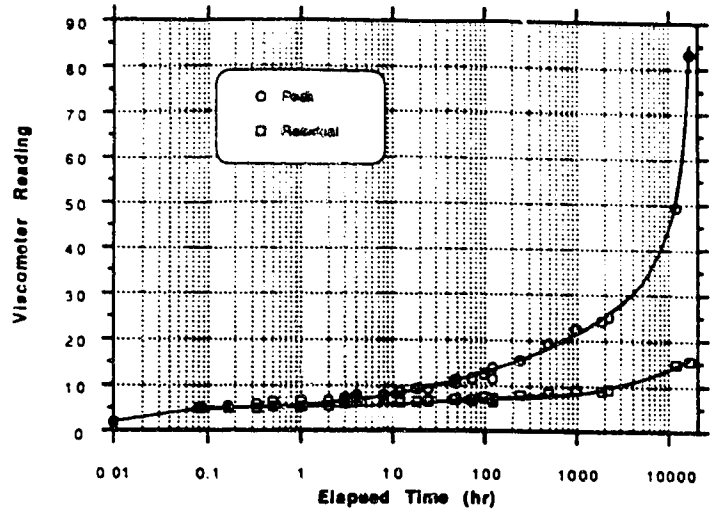

Figure 5.11 Viscosity Readings vs. Time for Sludge 233 - 16,368 hrs

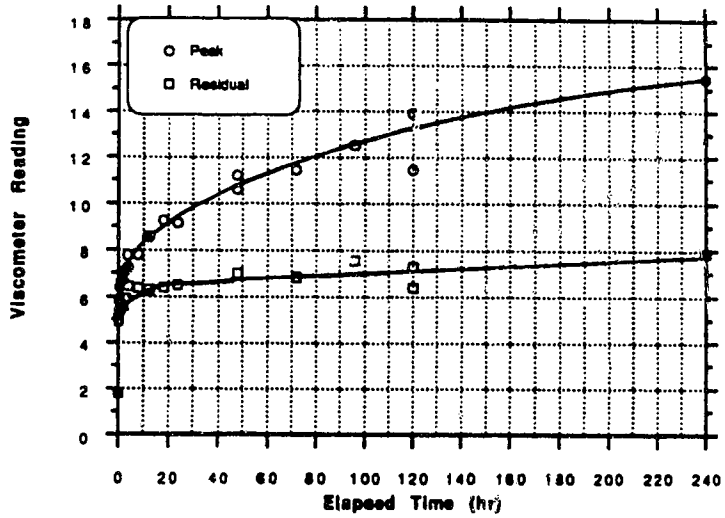

Figure 5.12 Viscometer Readings vs. T[illegible] Sludge 233 - 240 hrs

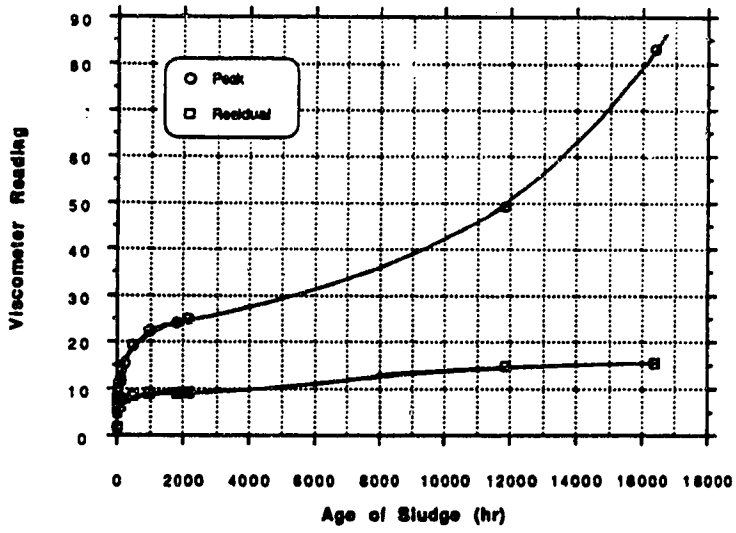

Figure 5.13 Viscometer Readings vs. Time for Sludge 233 - 16,368 hrs

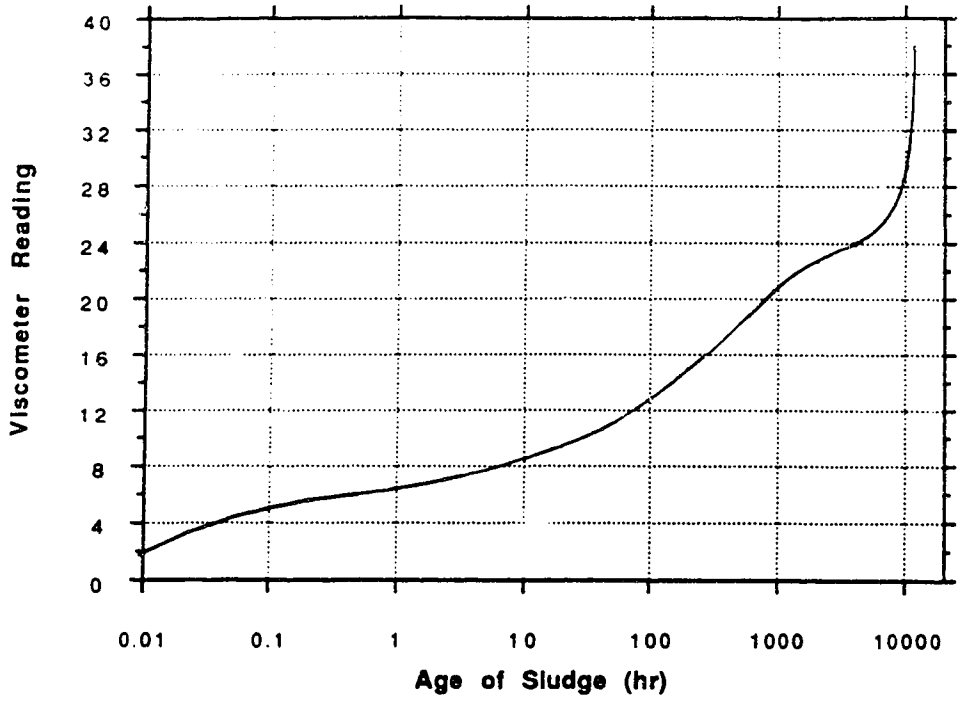

Figure 5.14 Viscosity Readings for w=233% (I_L=8.5)

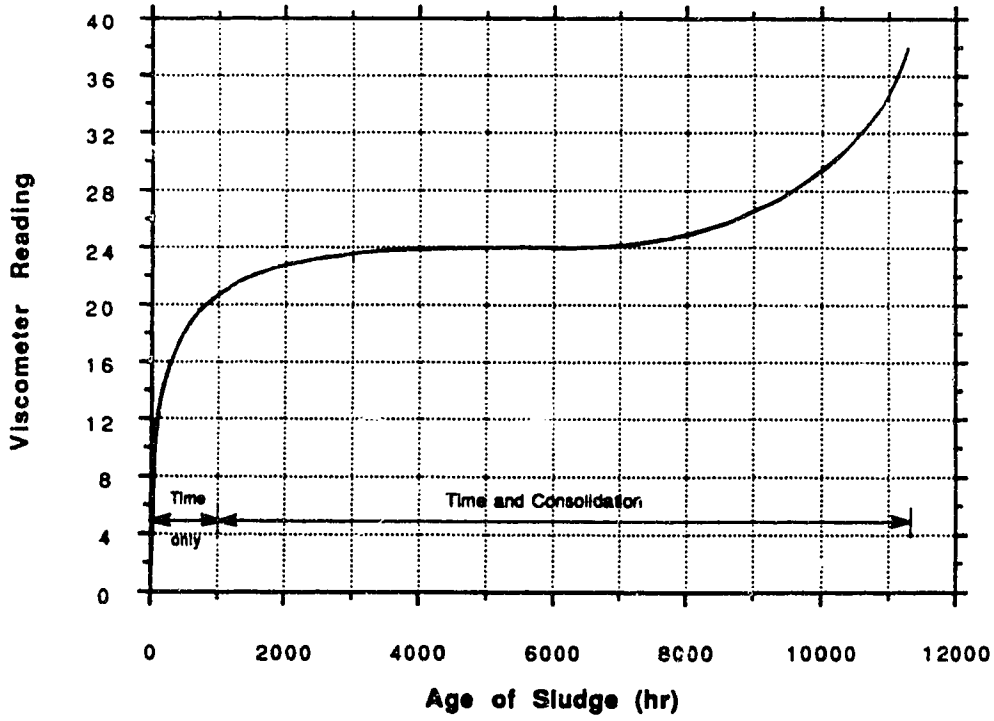

Figure 5.15 Viscosity Readings for w=233% (I_L=8.5)

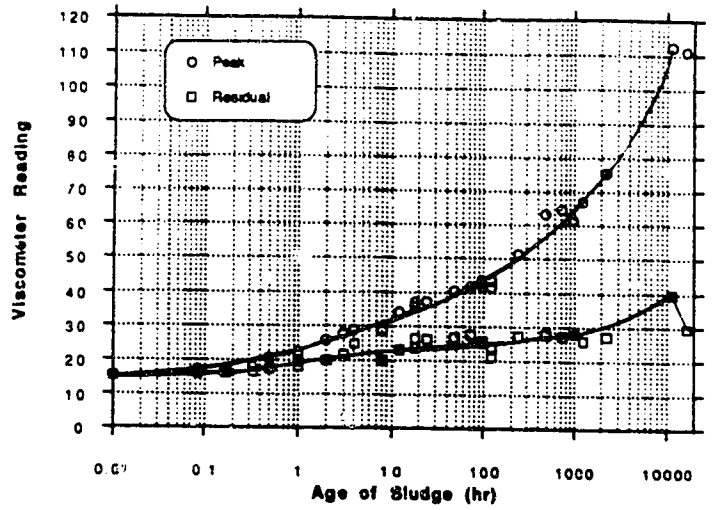

Figure 5.16 Viscometer Readings vs. Time for Sludge 150 - 16,320 hrs

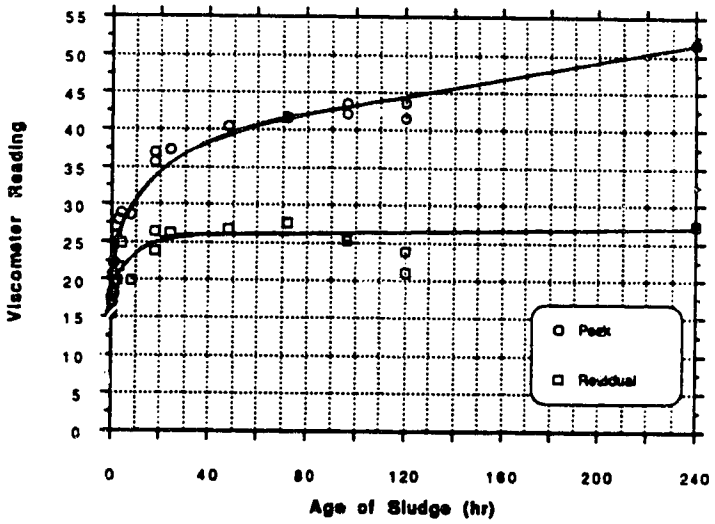

Figure 5.17 Viscometer Readings vs. Time for Sludge 150 - 240 hrs

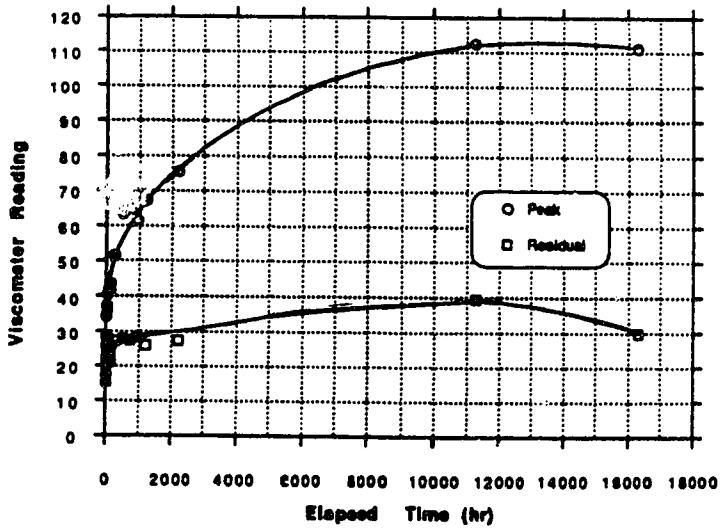

Figure 5.18 Viscometer Readings vs. Time for Sludge 150 - 16,320 hrs

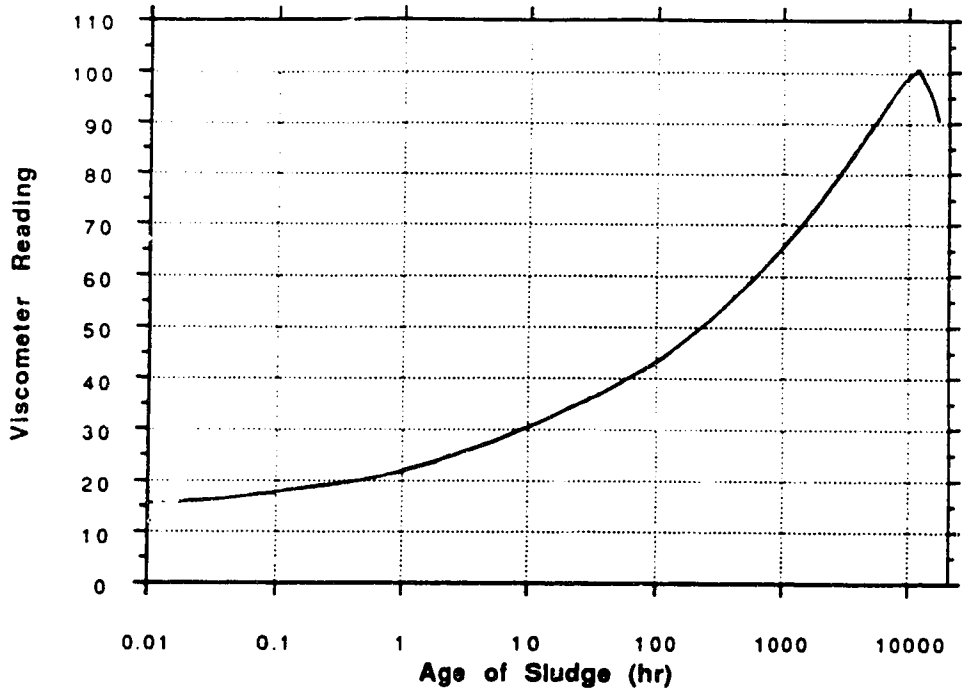

Figure 5.19 Viscosity Readings for w=150% (I_L=5.2)

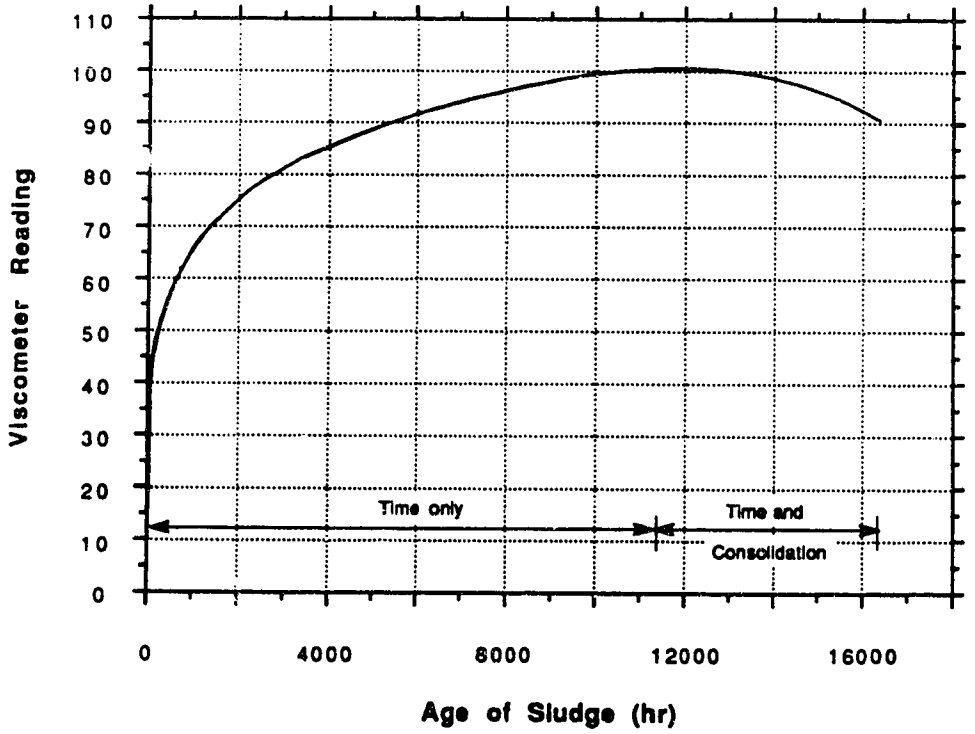

Figure 5.20 Viscosity Readings for w=150% (I_L=5.2)

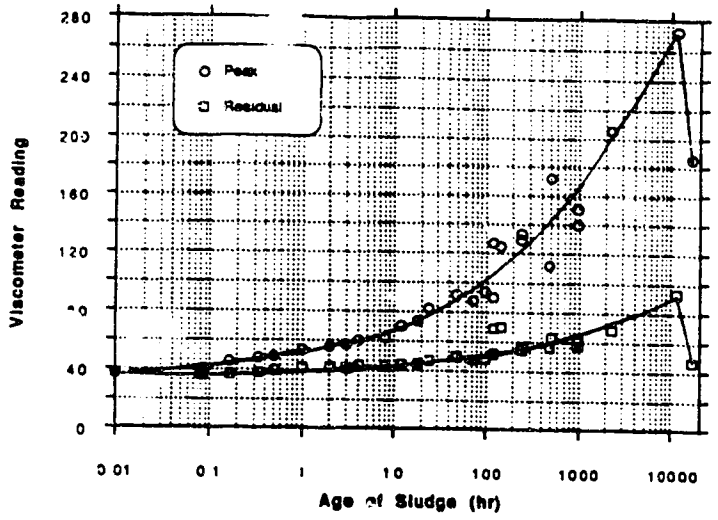

Figure 5.21 Viscometer Readings vs. Time for Sludge 100 - 16,320 hrs

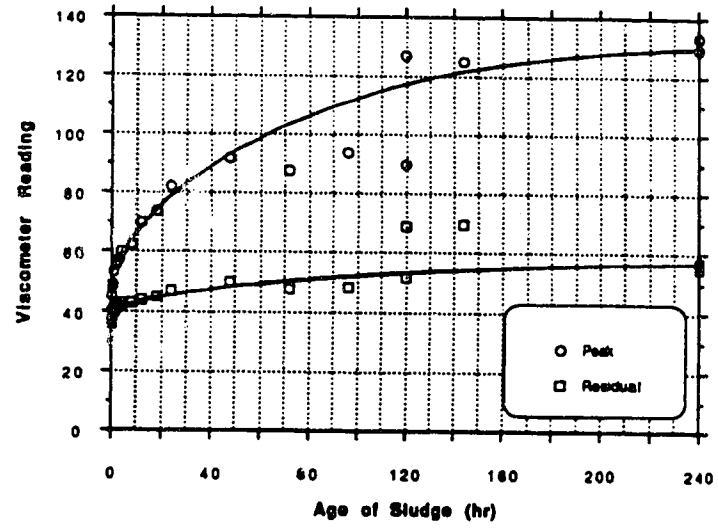

Figure 5.22 Viscometer Readings vs. Time for Sludge 100 - 240 hrs

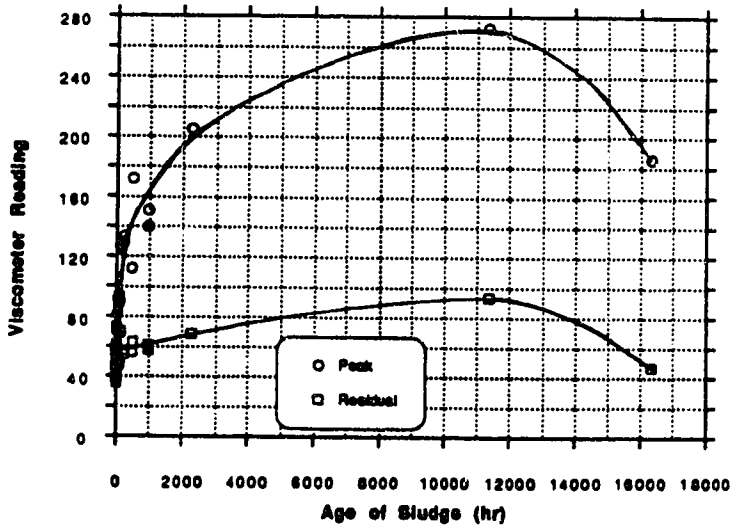

Figure 5.23 Viscometer Readings vs. Time for Sludge 100 - 16,320 hrs

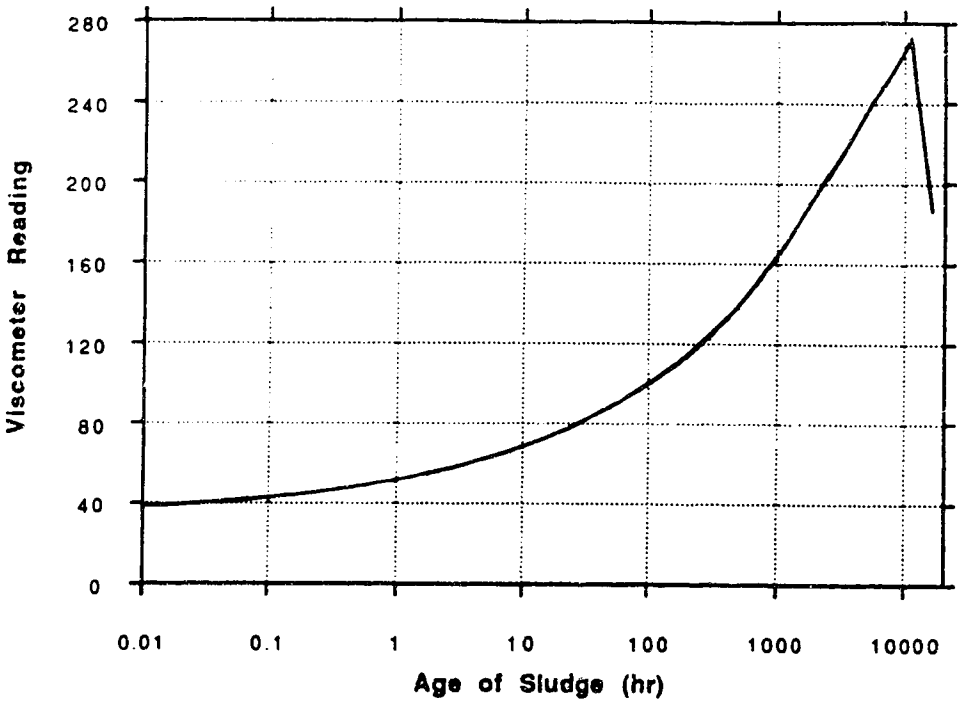

Figure 5.24 Viscosity Readings for w=100% (I_L=3.2)

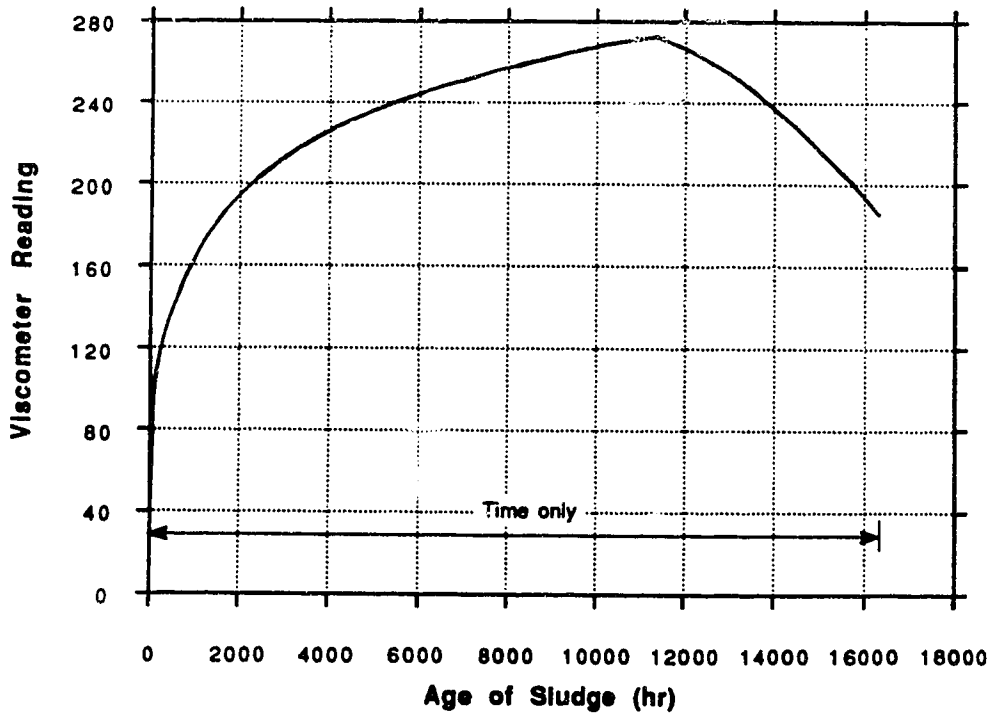

Figure 5.25 Viscosity Contour Line for w=100% (I_L=3.2)

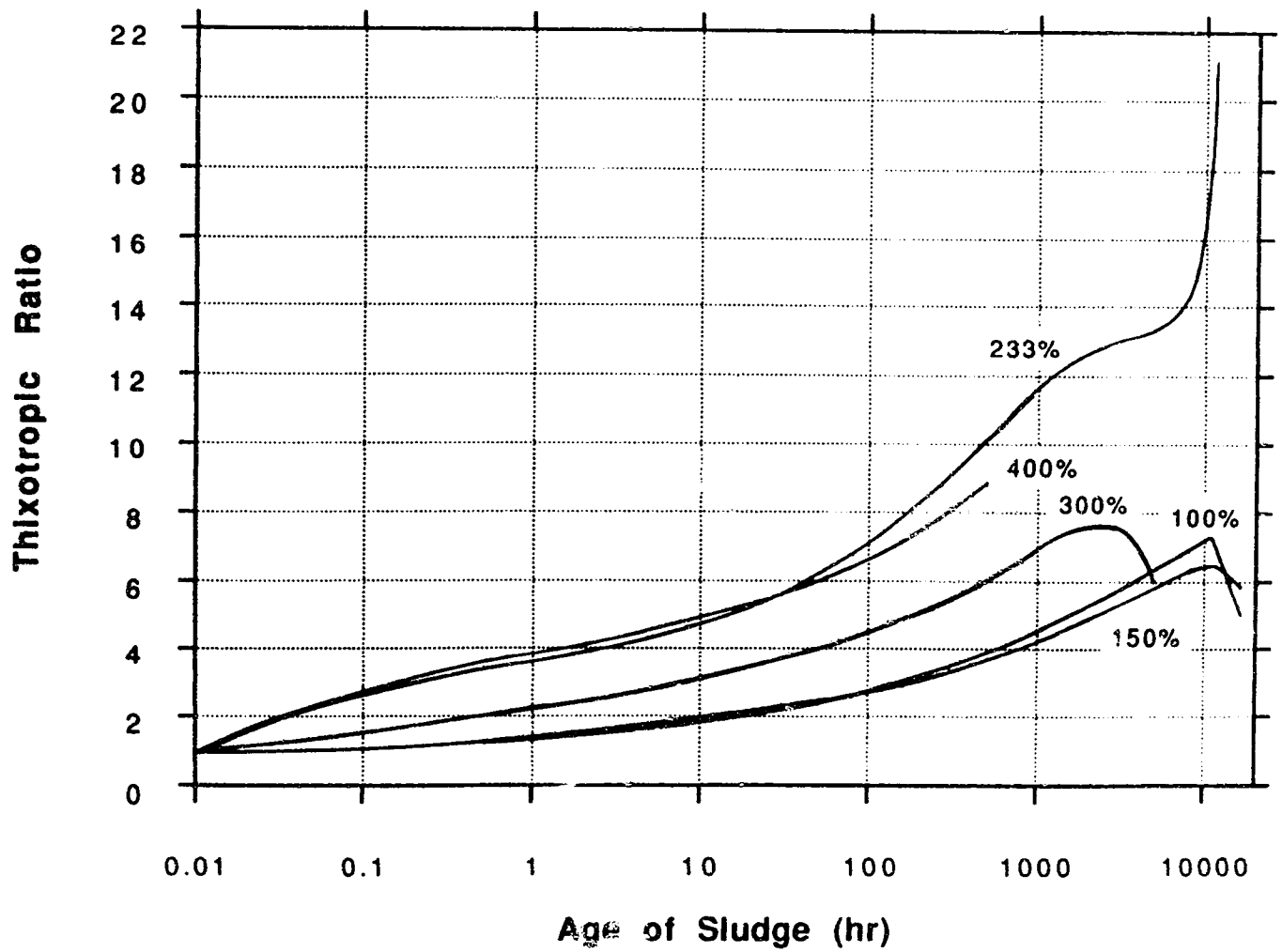

Figure 5.26 Thixotropic Viscosity Ratios to 680 days

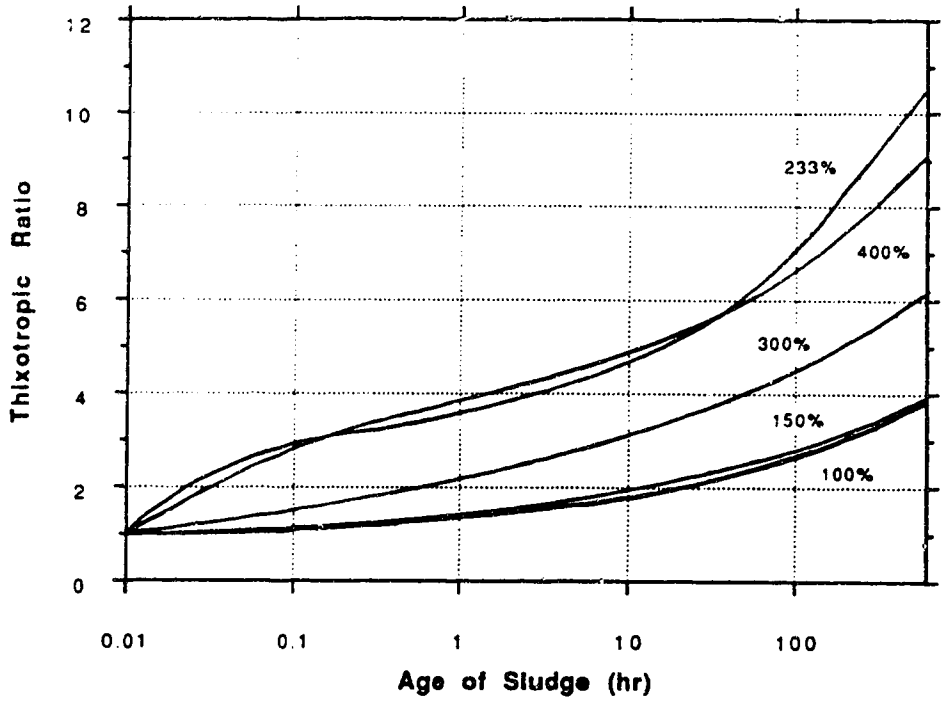

Figure 5.27 Thixotropic Viscosity Ratios to 500 hrs

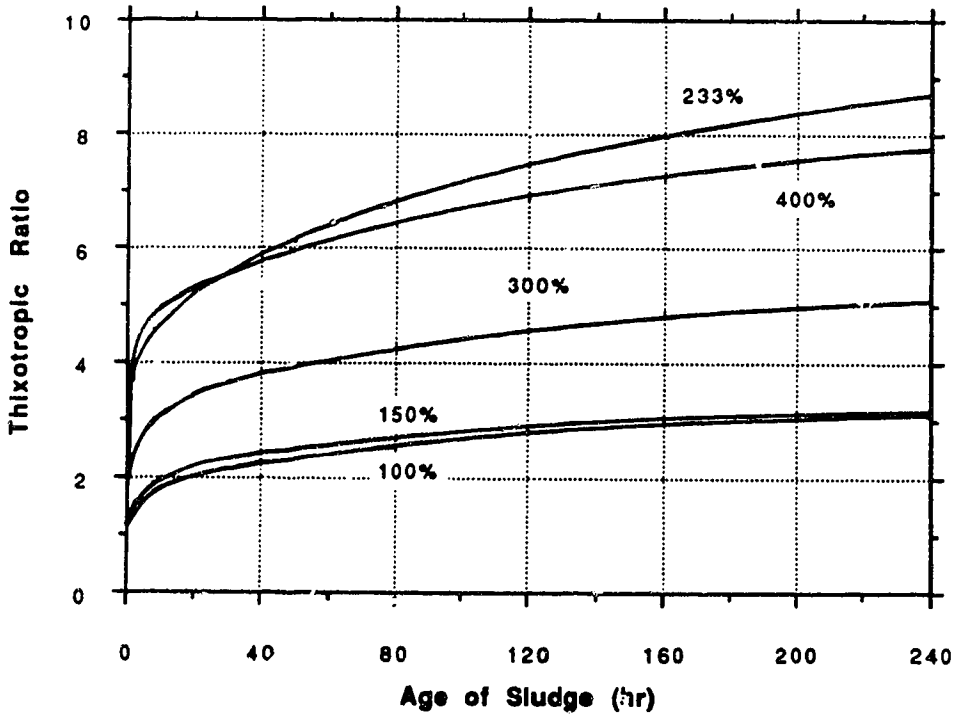

Figure 5.28 Thixotropic Viscosity Ratios to 240 hrs

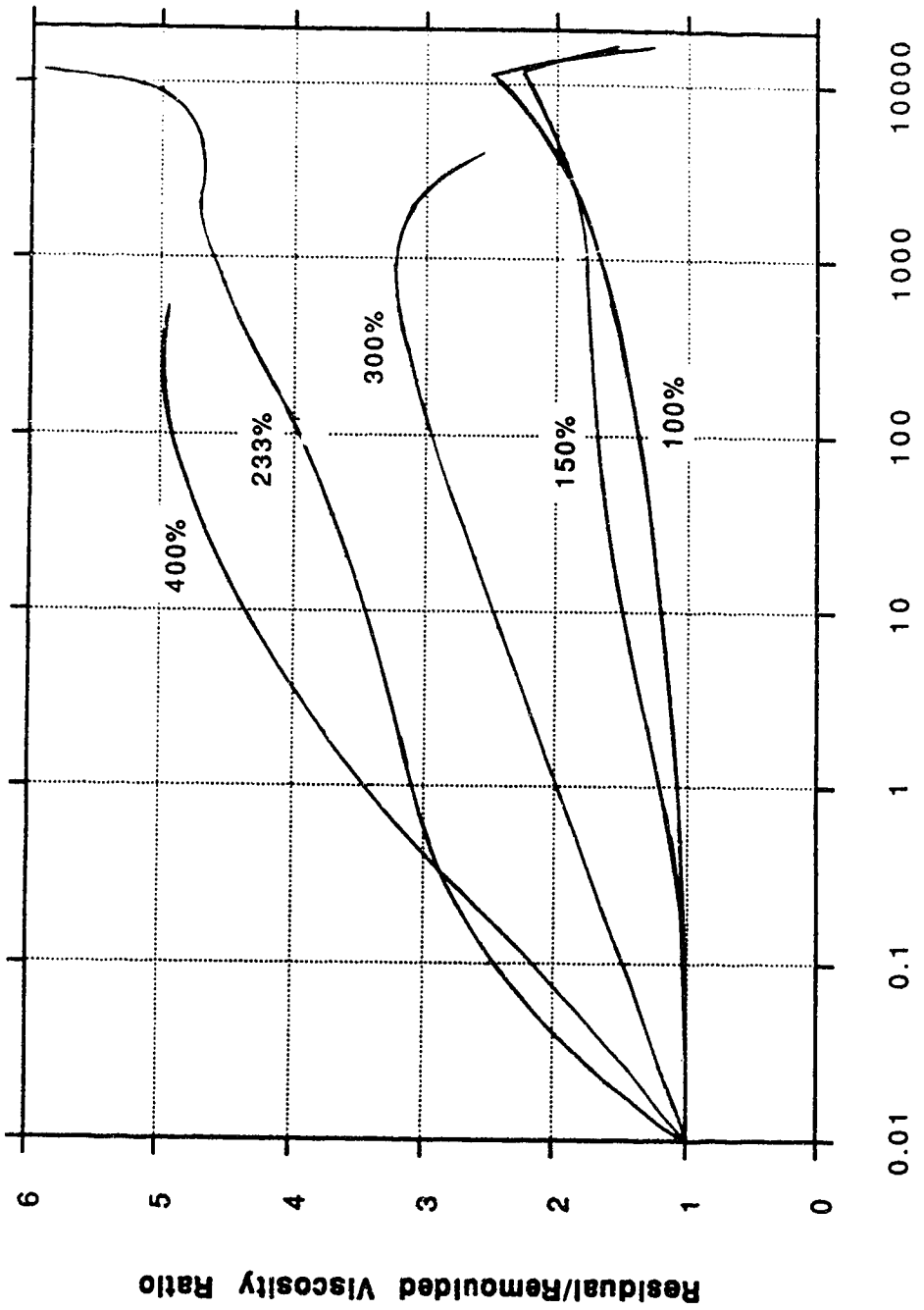

Figure 5.29 Residual/Remoulded Viscosity Ratios

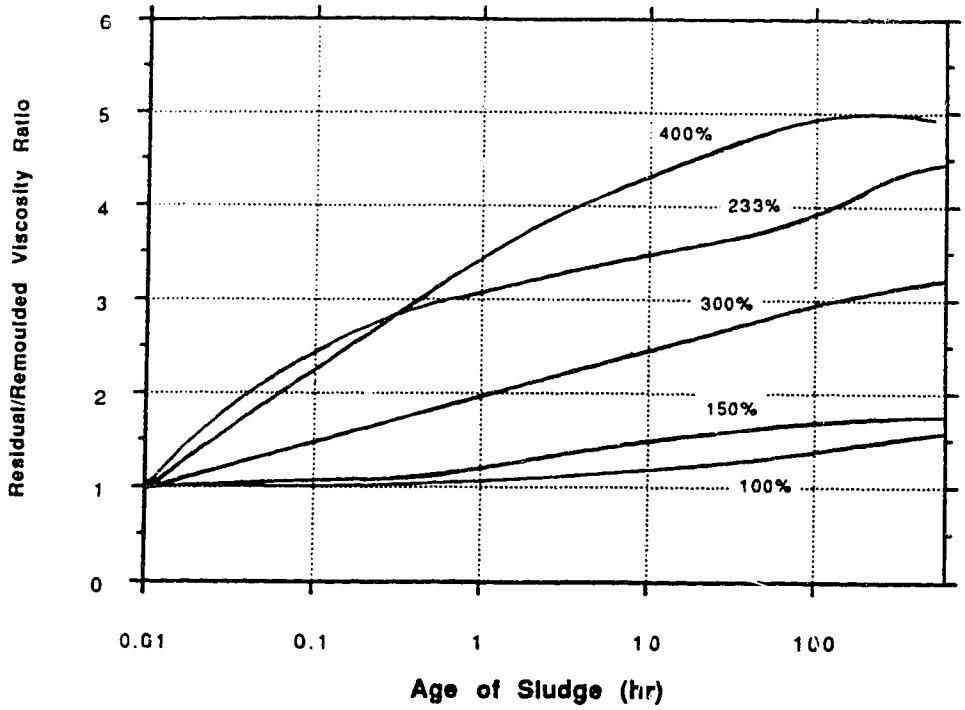

Figure 5.30 Residual/Remoulded Viscosity Ratios to 600 hrs

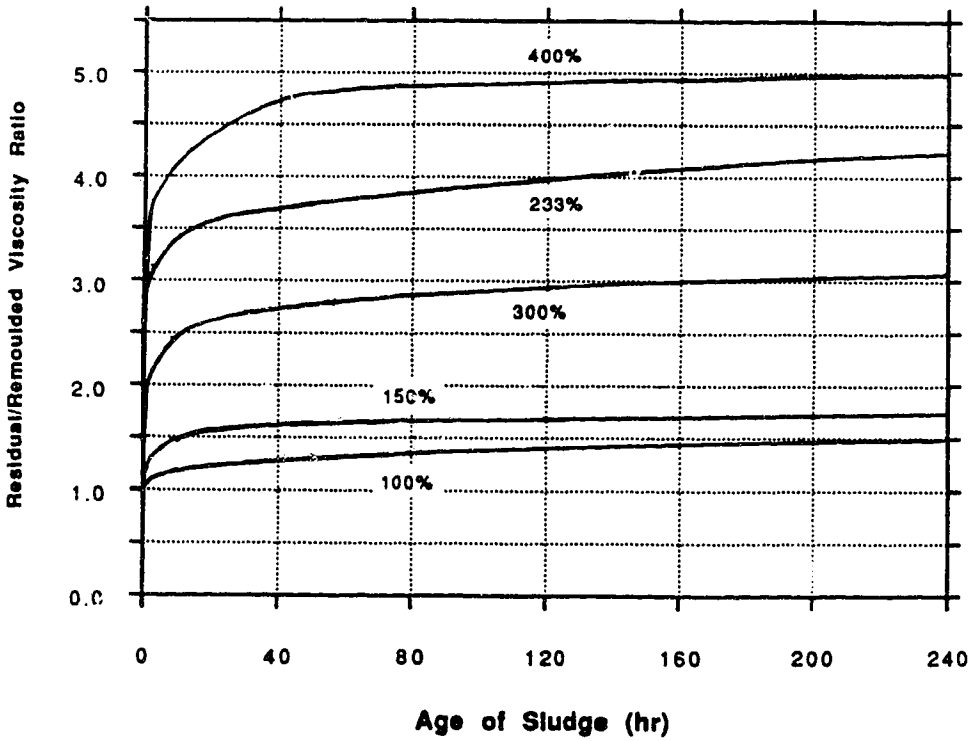

Figure 5.31 Residual/Remoulded Viscosity Ratios to 240 hrs

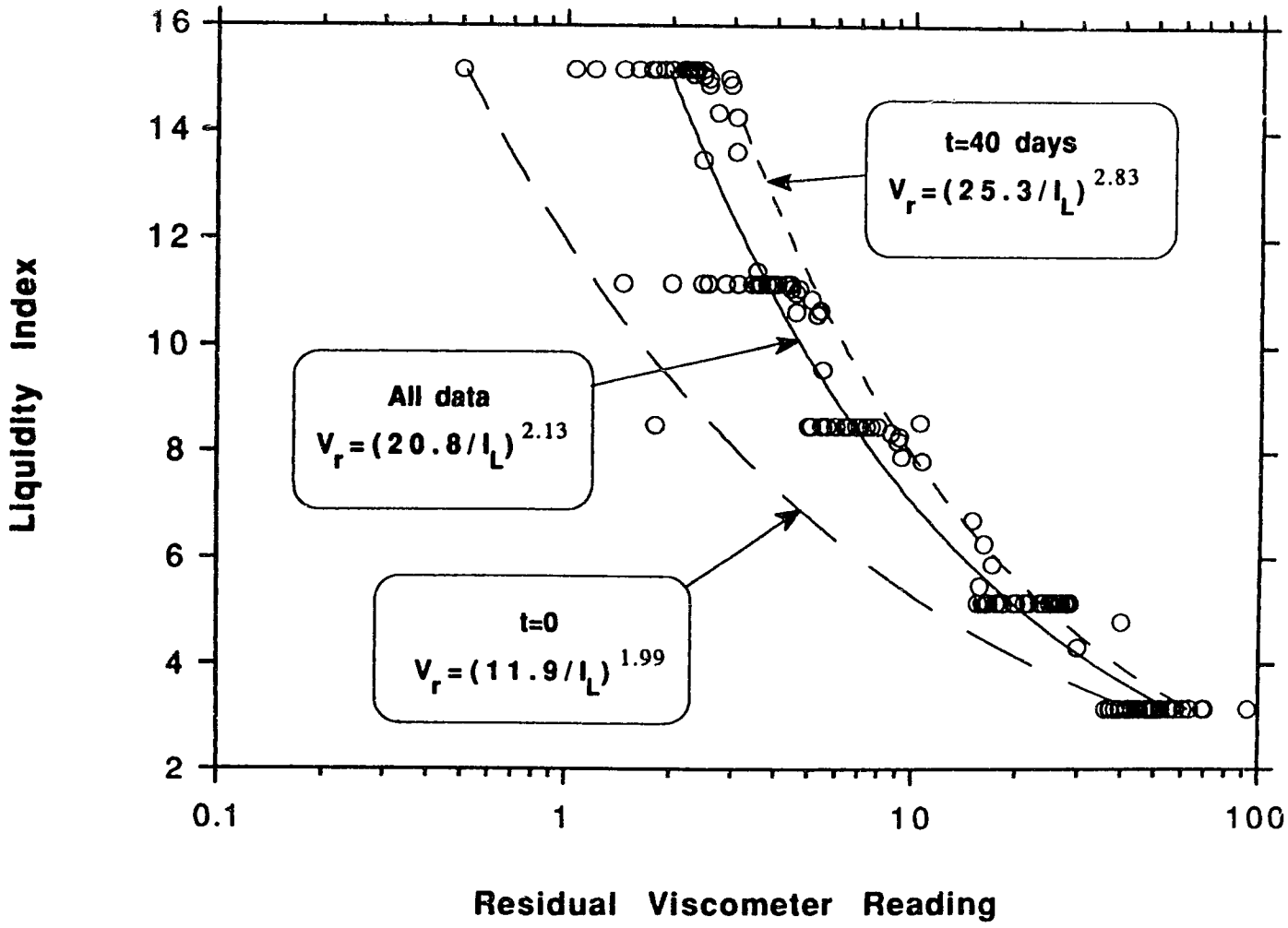

Figure 5.32 Liquidity Index-Residual Viscosity Relationship for Sludge

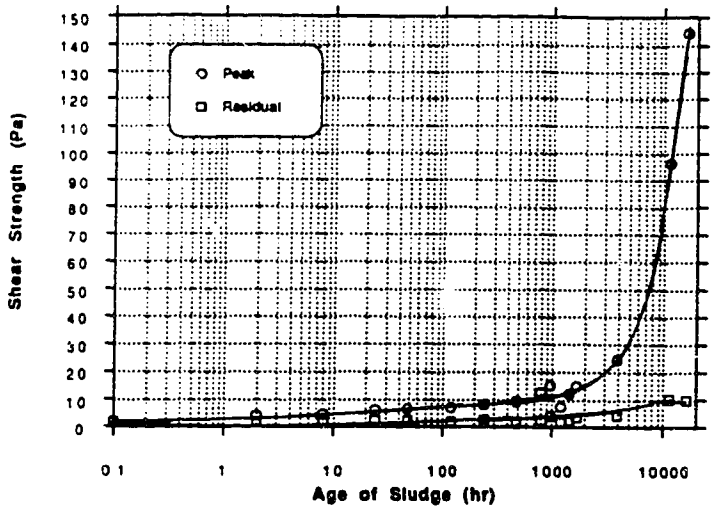

Figure 5.33 Shear Strength vs.Time for Sludge 400 - 16,320 hrs

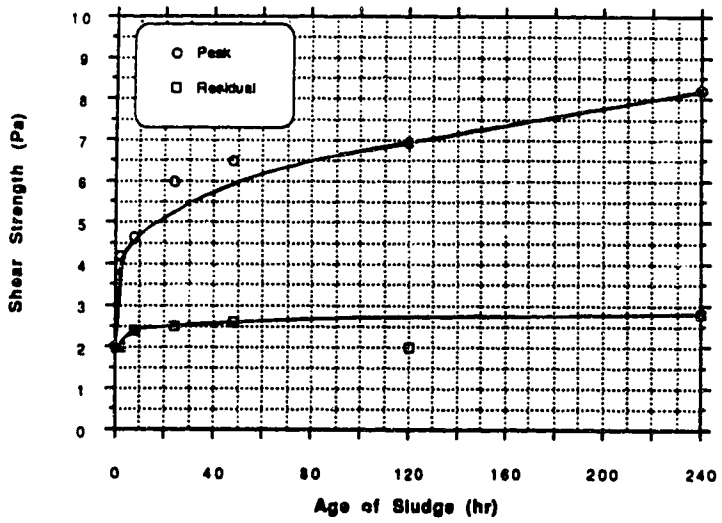

Figure 5.34 Shear Strength vs. Time for Sludge 400 - 240 hrs

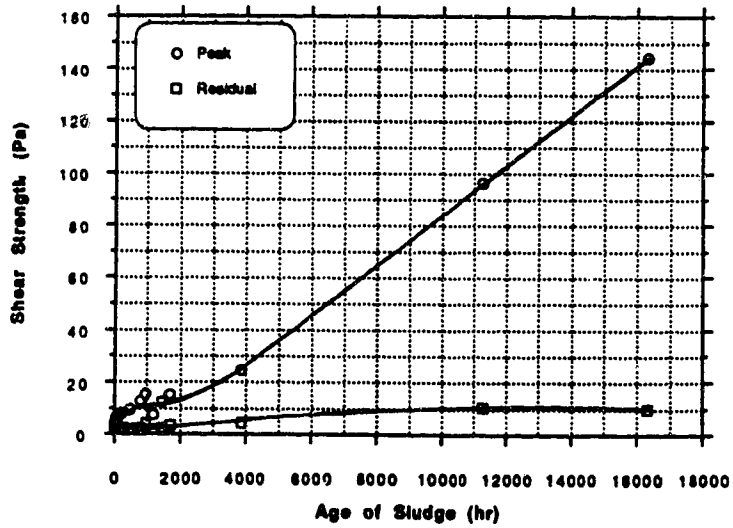

Figure 5.35 Shear Strength vs. Time for Sludge 400 - 16,320 hrs

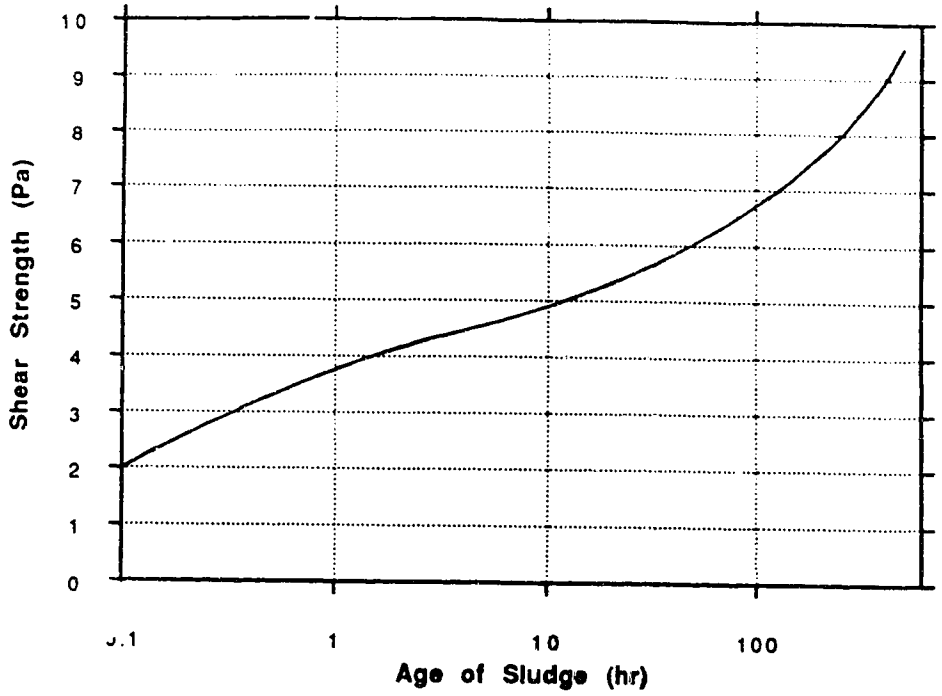

Figure 5.36 Shear Strength for w=400% (I_L=15.2)

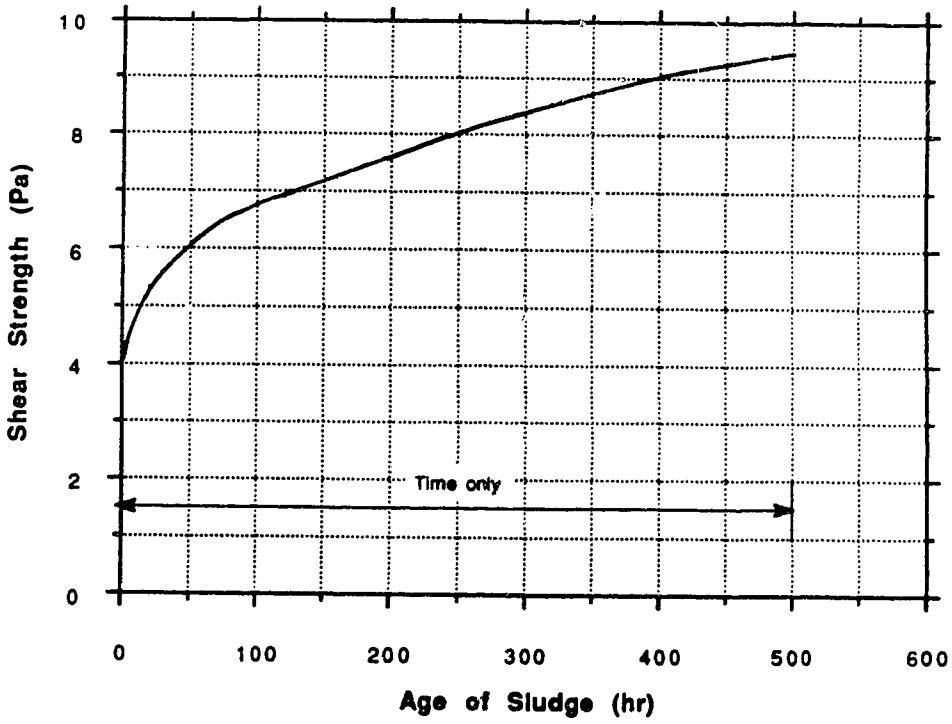

Figure 5.37 Shear Strength for w=400% (I_L=15.2)

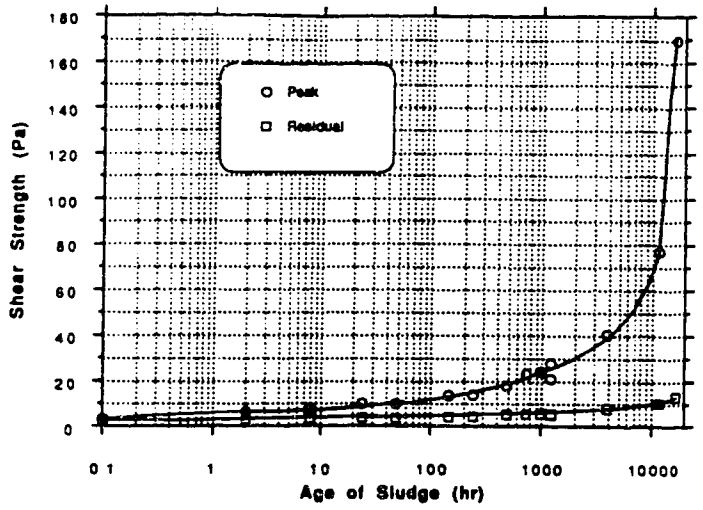

Figure 5.38 Shear Strength vs. Time for Sludge 300 - 16,320 hrs

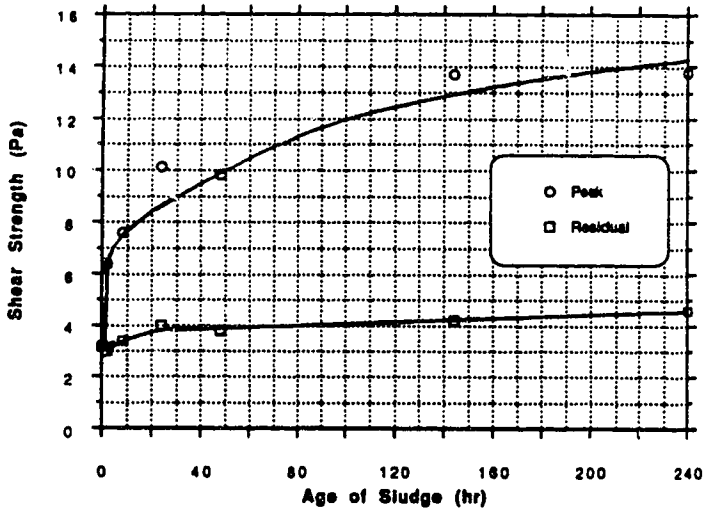

Figure 5.39 Shear Strength vs. Time for Sludge 300 - 240 hrs

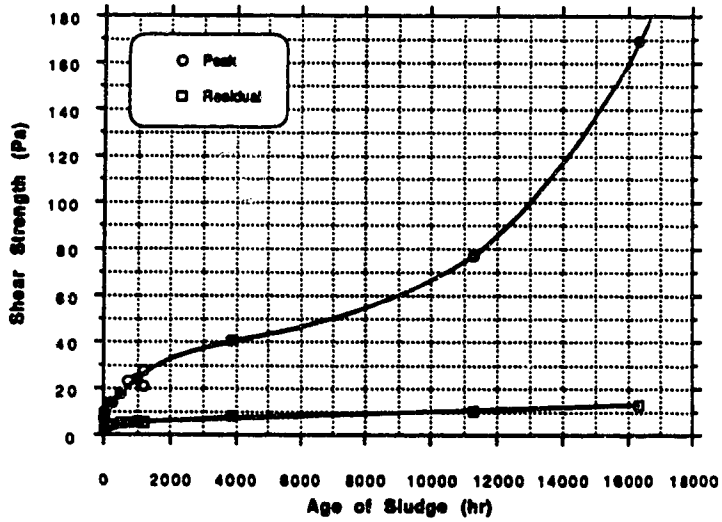

Figure 5.40 Shear Strength vs. Time for Sludge 300, 16,320 hrs

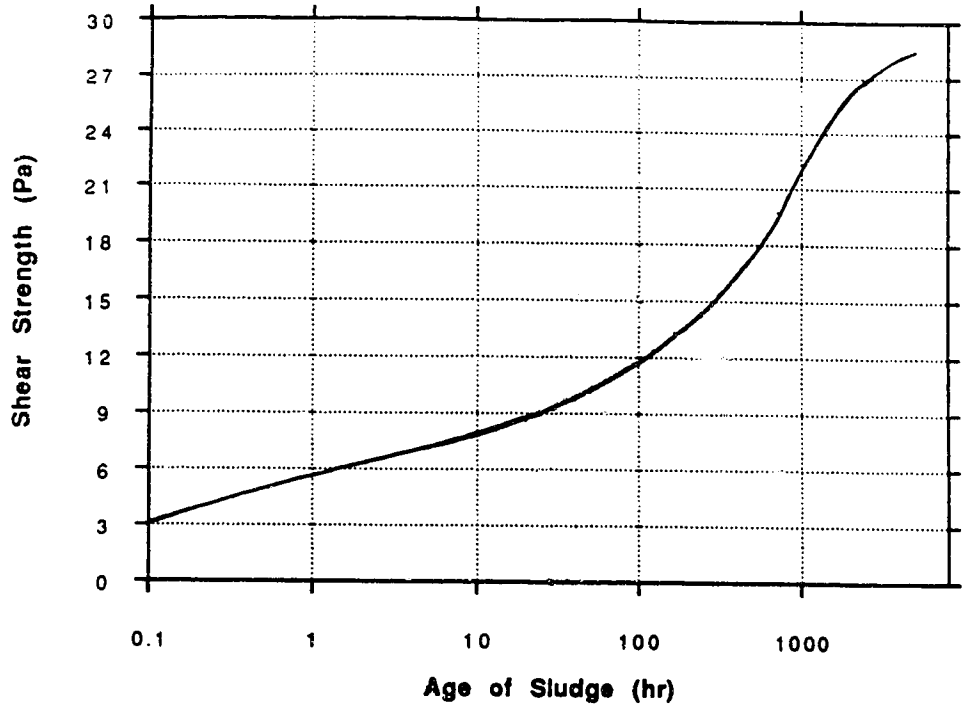

Figure 5.41 Shear Strength for w=300% (I_L=11.2)

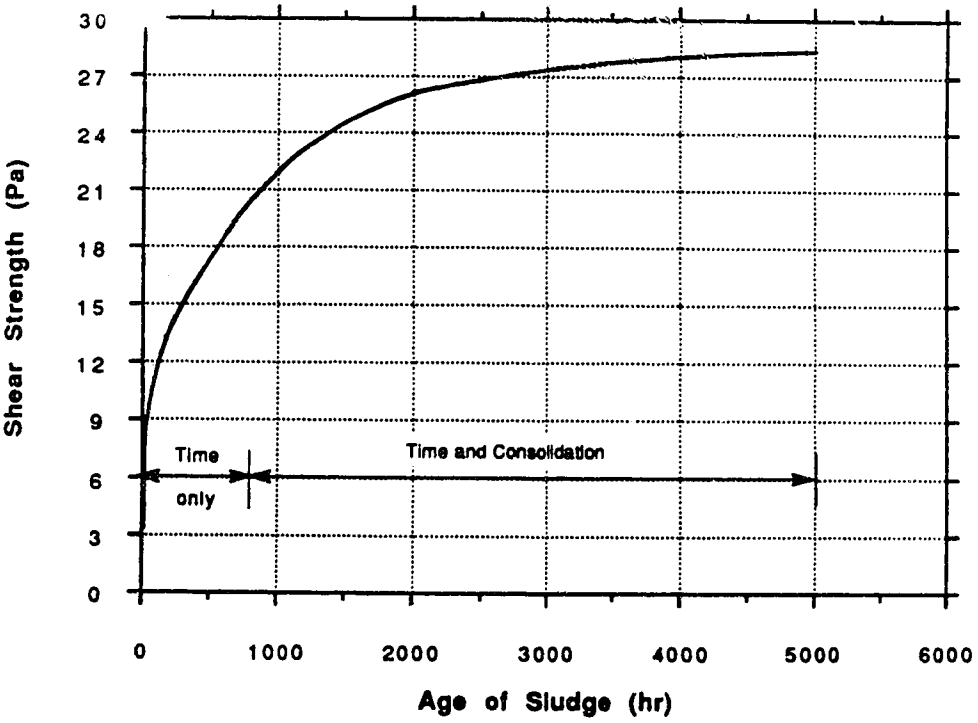

Figure 5.42 Shear Strength for w=300% (I_L=11.2)

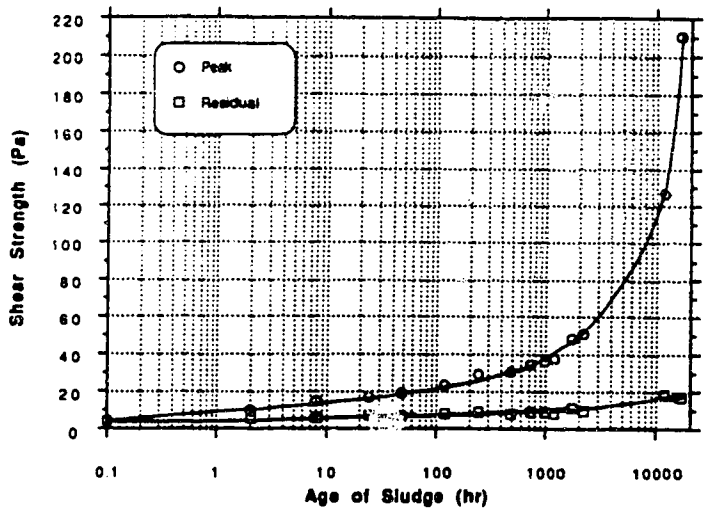

Figure 5.43 Shear Strength vs. Time for Sludge 233 - 16,320 hrs

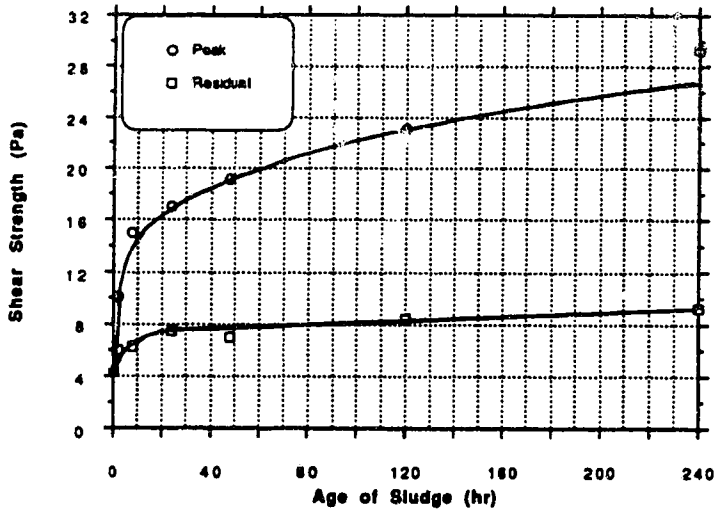

Figure 5.43 Shear Strength vs. Time for Sludge 233 - 240 hrs

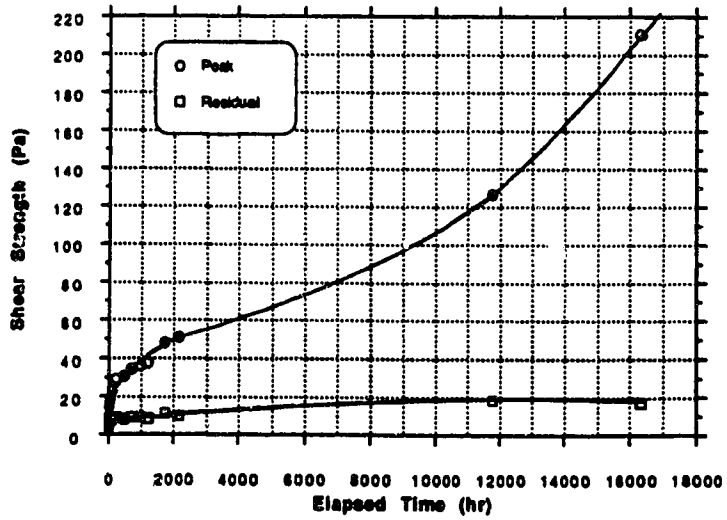

Figure 5.45 Shear Strength vs. Time for Sludge 233 - 16,320 hrs

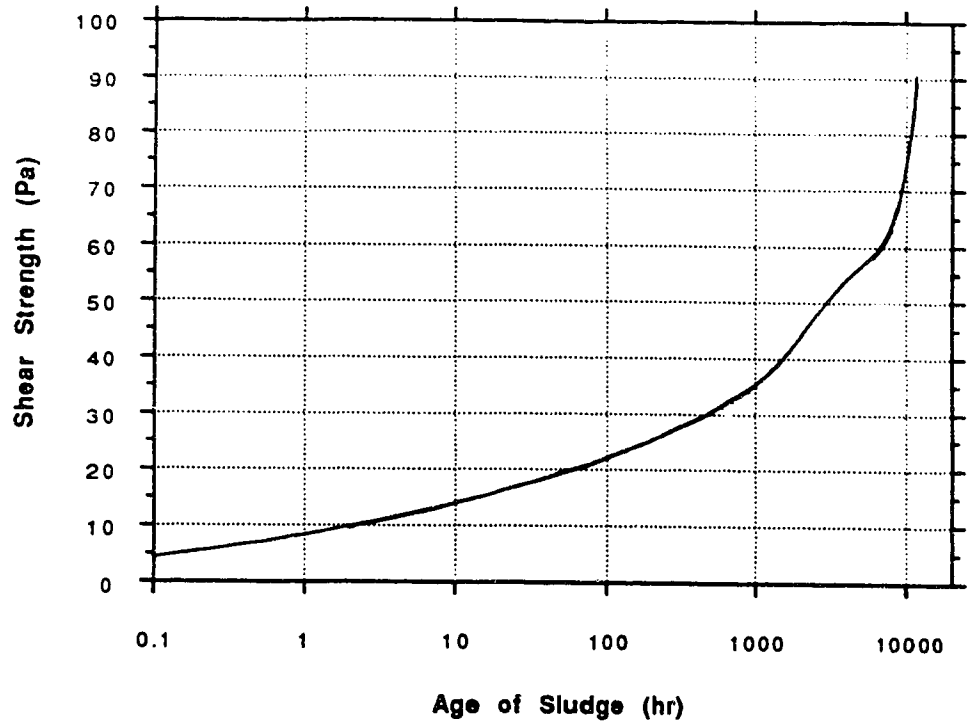

Figure 5.46 Shear Strength for w=233% (I_L=8.5)

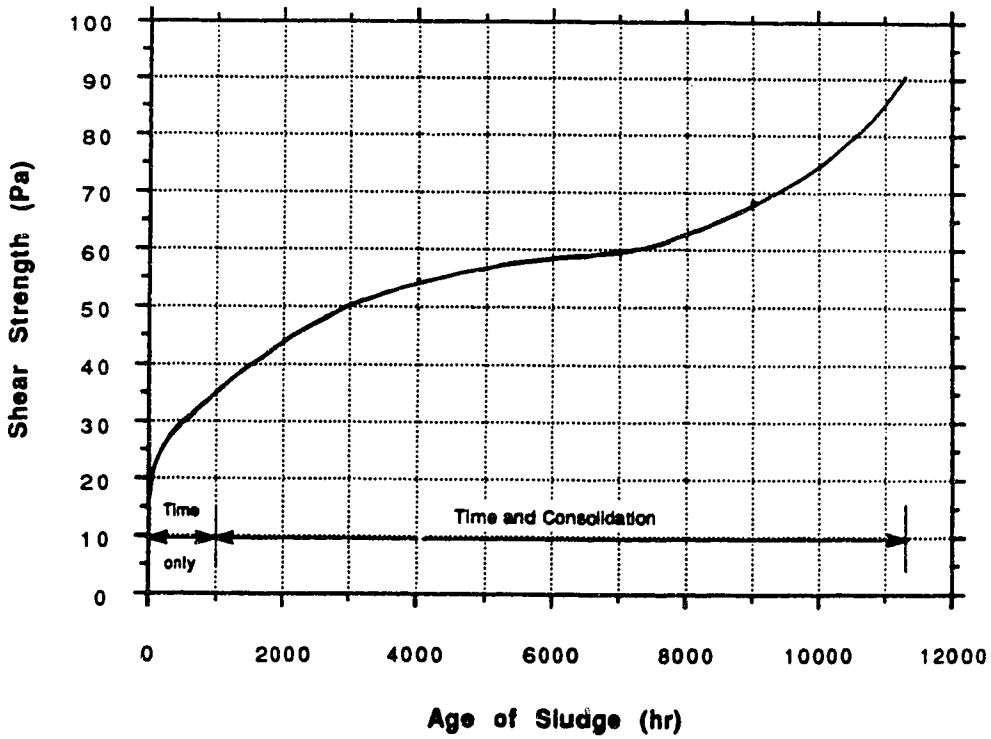

Figure 5.47 Shear Strength for w=233% (I_L=8.5)

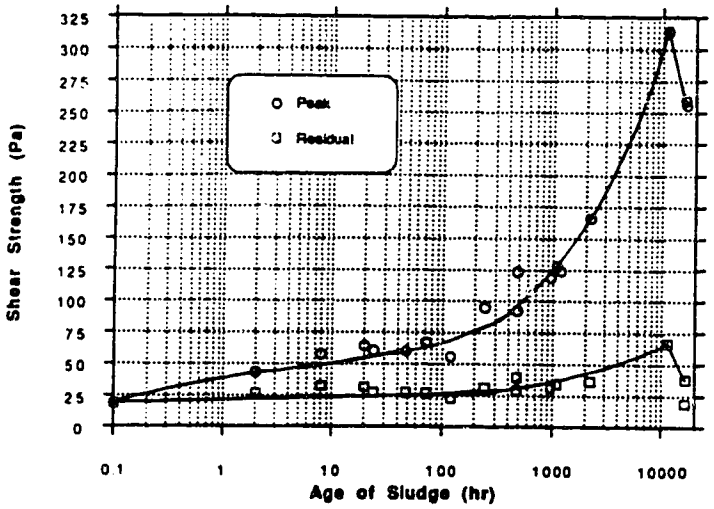

Figure 5.48 Shear Strength vs. Time for Sludge 150 - 16,416 hrs

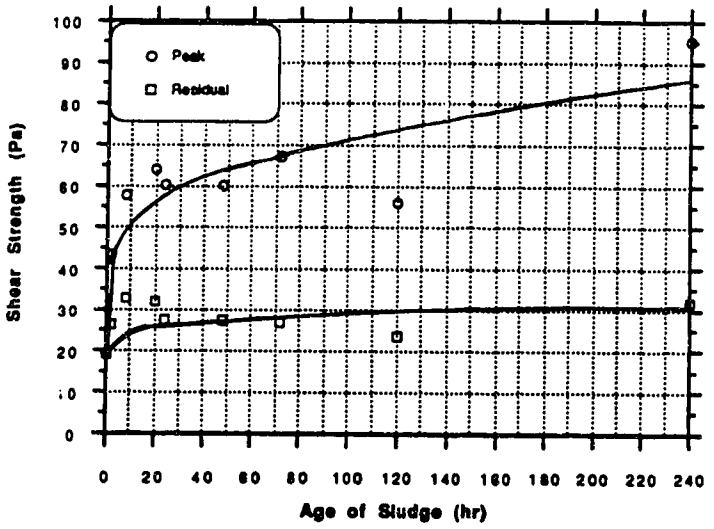

Figure 5.49 Shear Strength vs. Time for Sludge 150 - 240 hrs

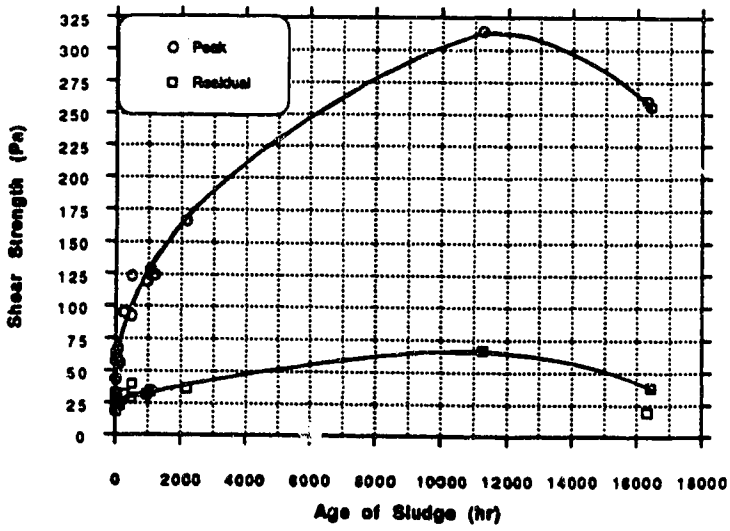

Figure 5.50 Shear Strength vs. Time for Sludge 150 - 16,416 hrs

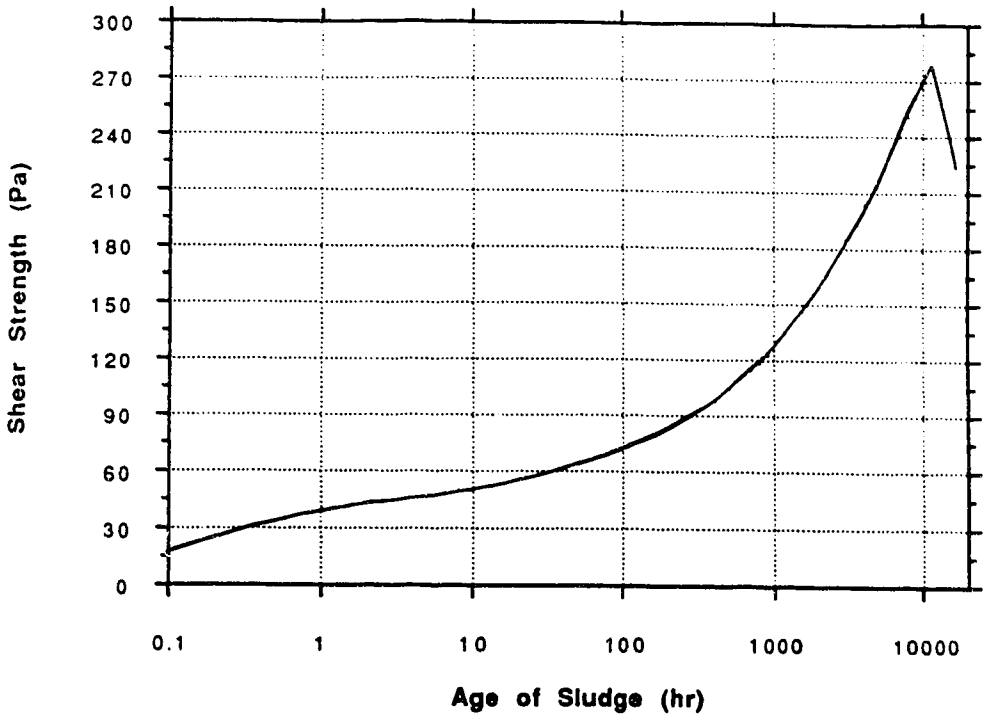

Figure 5.51 Shear Strength for w=150% (I_L=5.2)

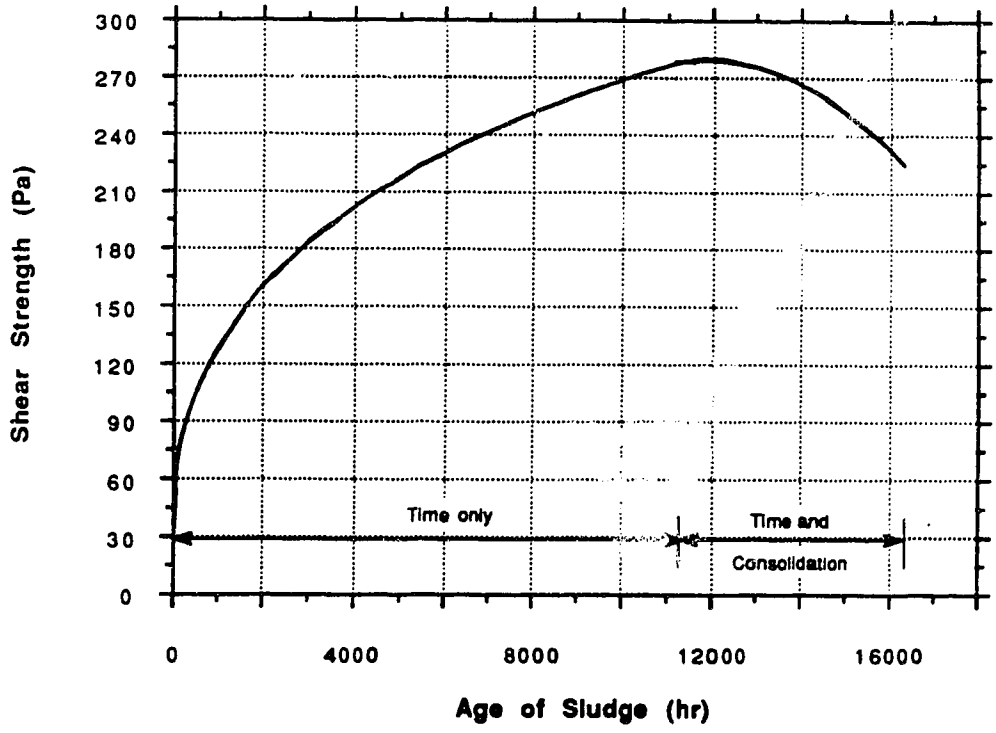

Figure 5.52 Shear Strength for w=150% (I_L=5.2)

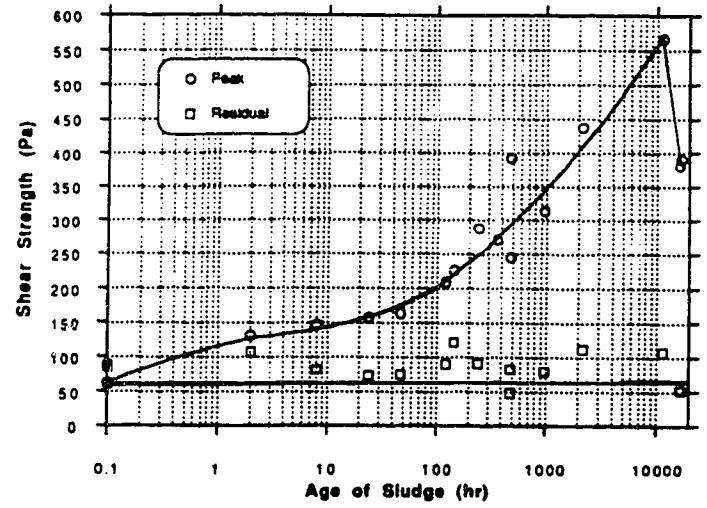

Figure 5.53 Shear Strength vs. Time for Sludge 100 - 16,824 hrs

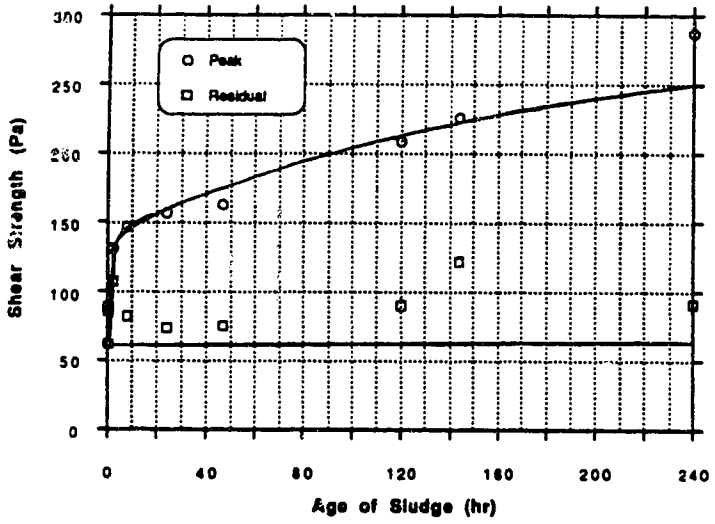

Figure 5.54 Shear Strength vs. Time for Sludge 100 - 240 hrs

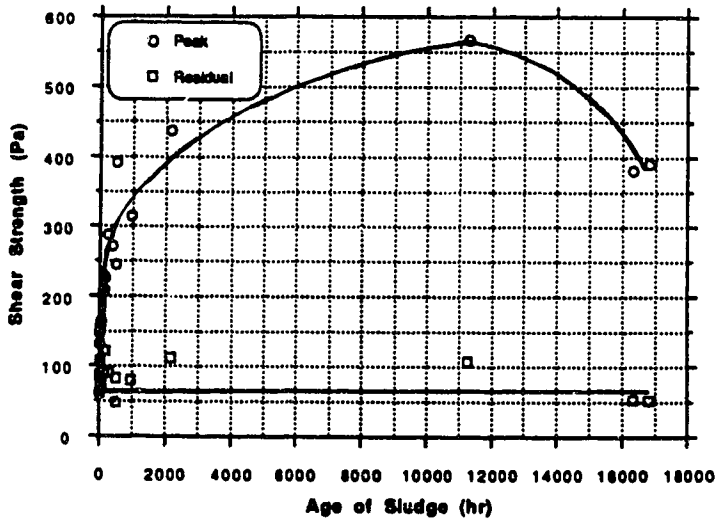

Figure 5.55 Shear Strength vs. Time for Sludge 100 - 16,824 hrs

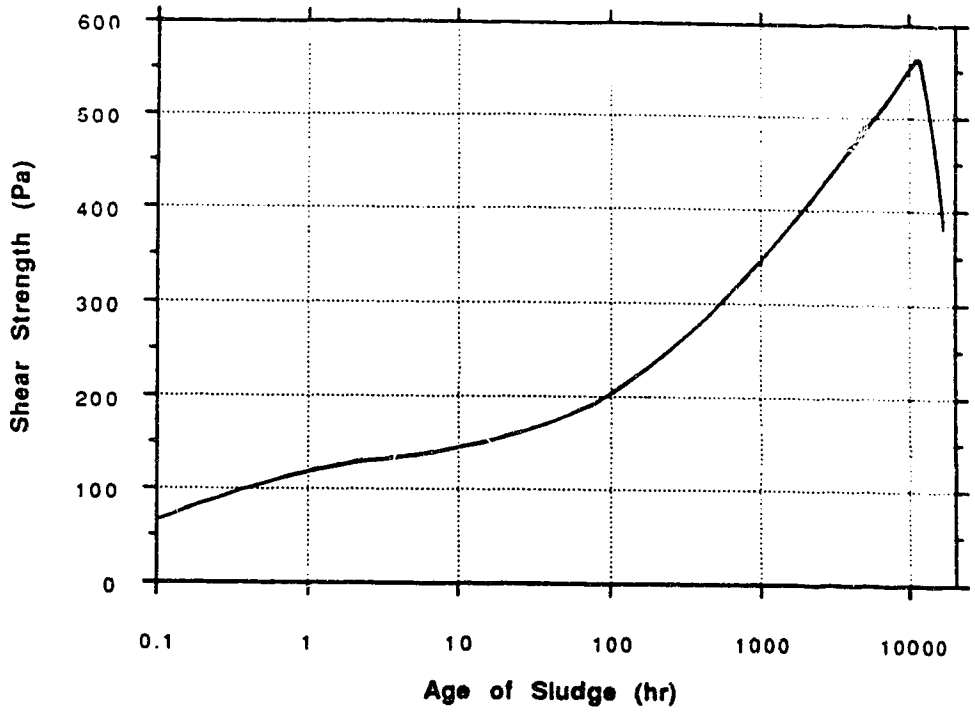

Figure 5.56 Shear Strengthfor w=100% (I_L=3.2)

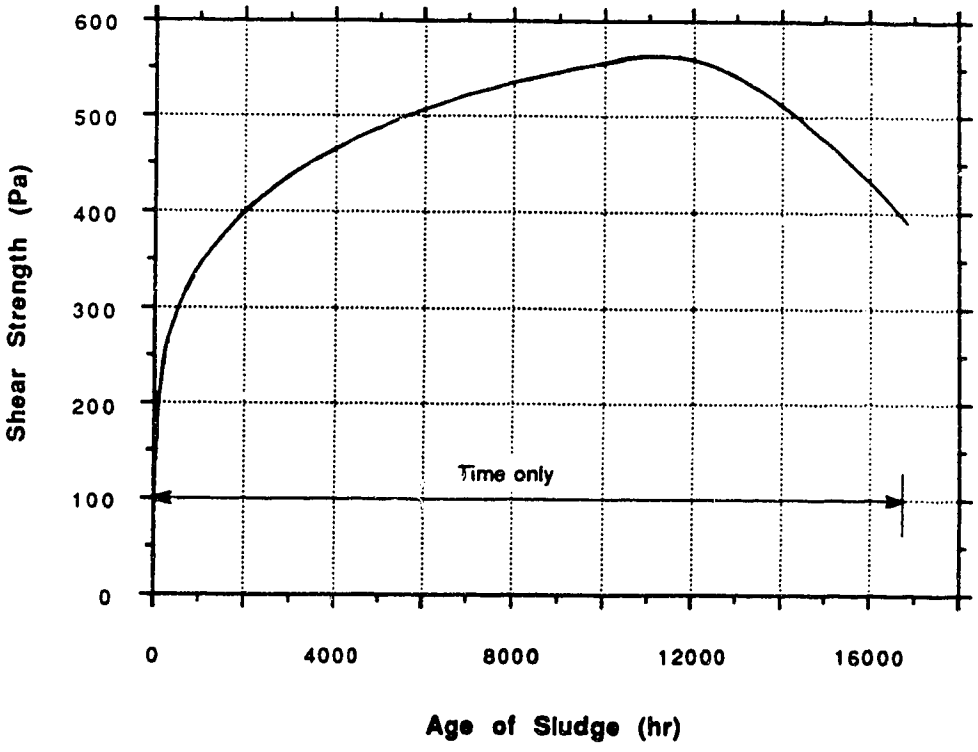

Figure 5.57 Shear Strength for w=100% (I_L=3.2)

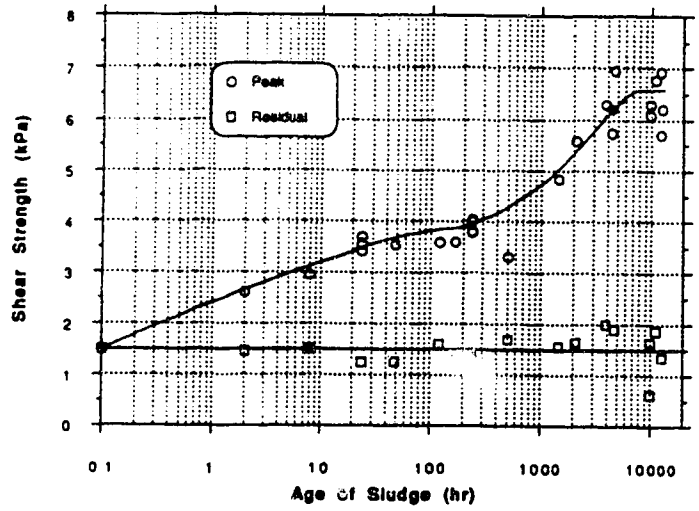

Figure 5.58 Shear Strength vs. Time for Sludge 47 - 12,552 hrs

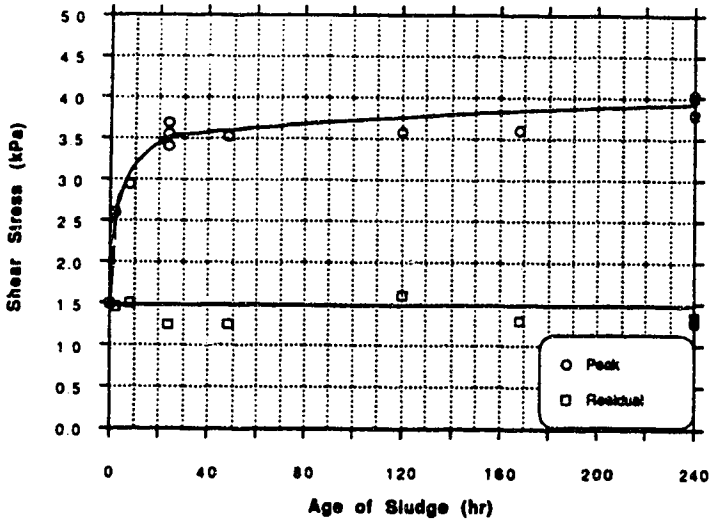

Figure 5.59 Shear Strength vs. Time for Sludge 47 - 240 hrs

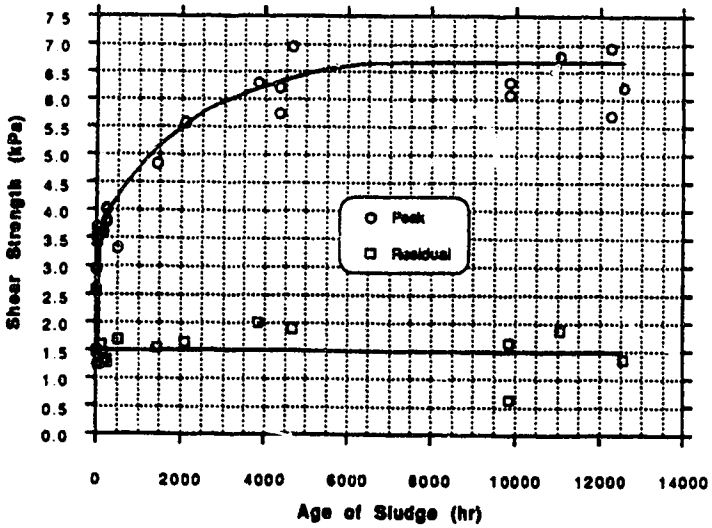

Figure 5.60 Shear Strength vs. Time for Sludge 47 - 12,552 hrs

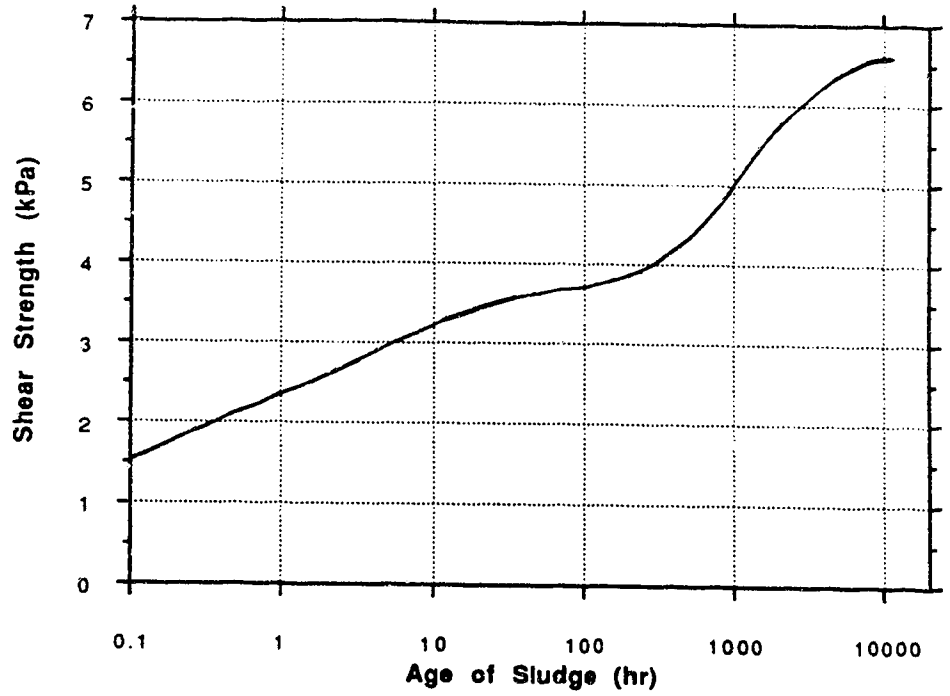

Figure 5.61 Shear Strength for w=46% (I_L=1.0)

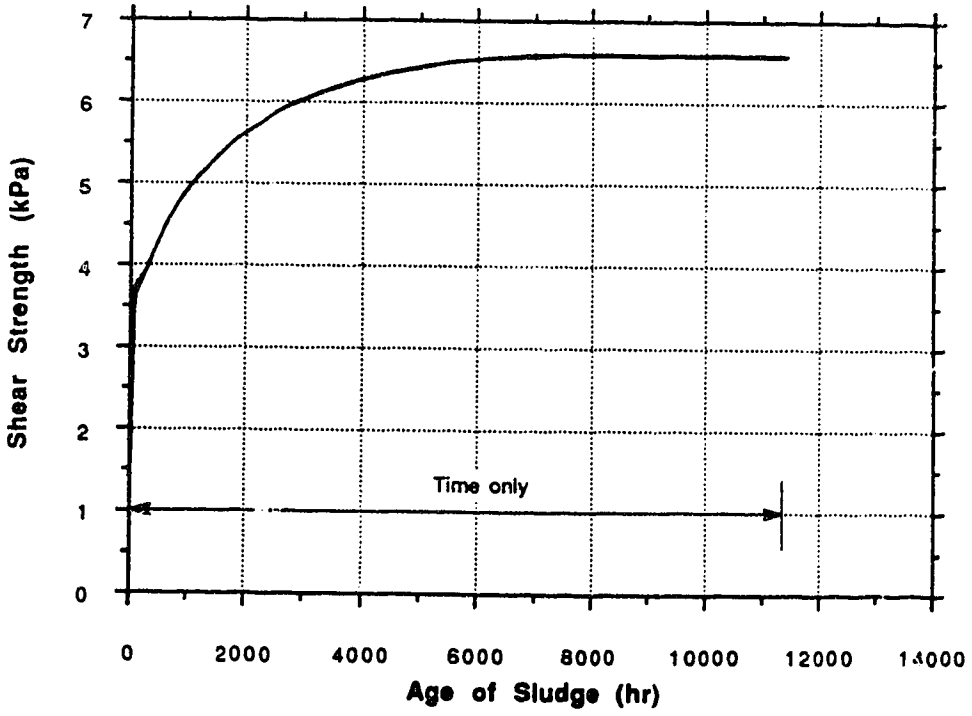

Figure 5.62 Shear Strength for w=46% (I_L=1.0)

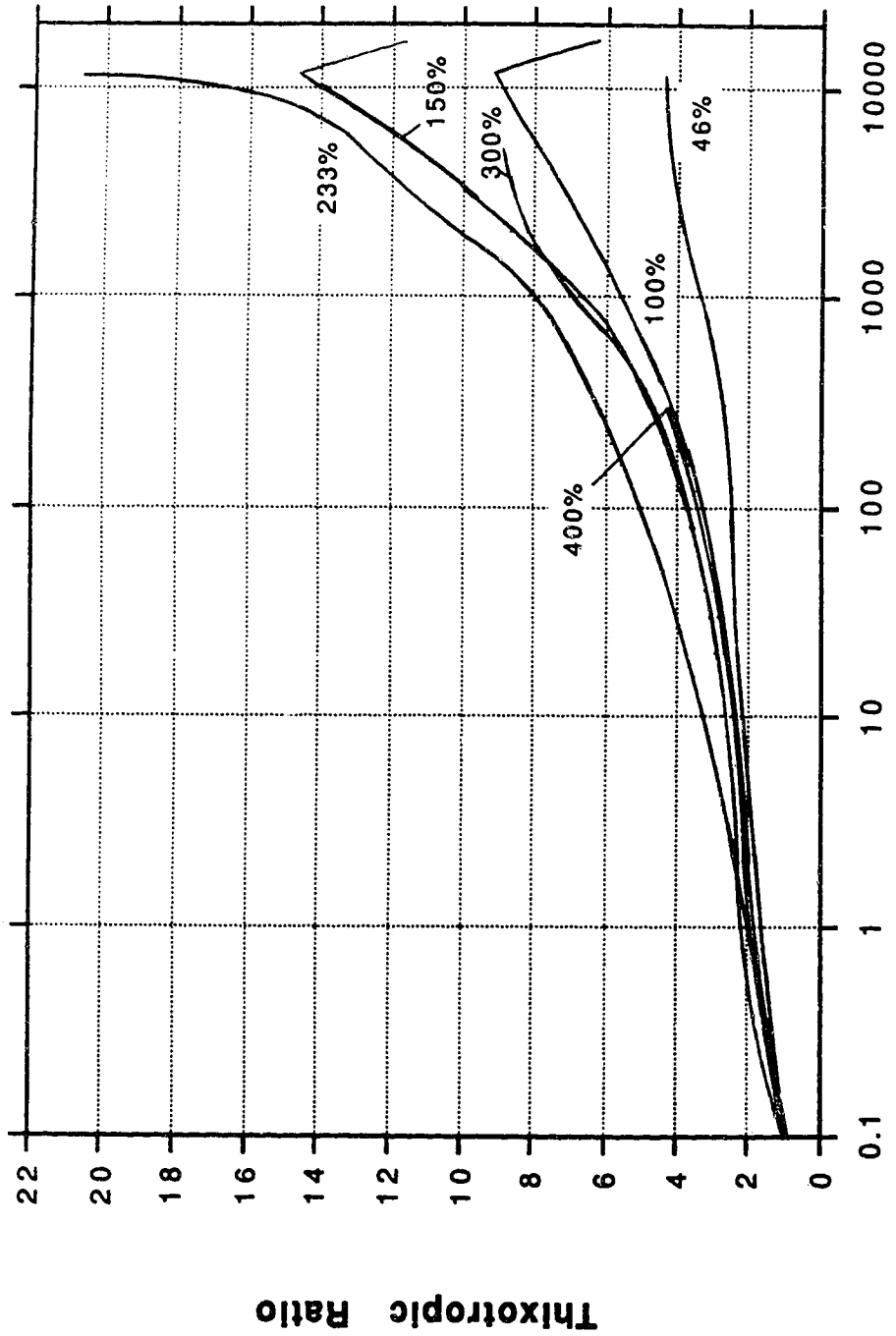

Figure 5.63 Thixotropic Strength Ratios to 700 days

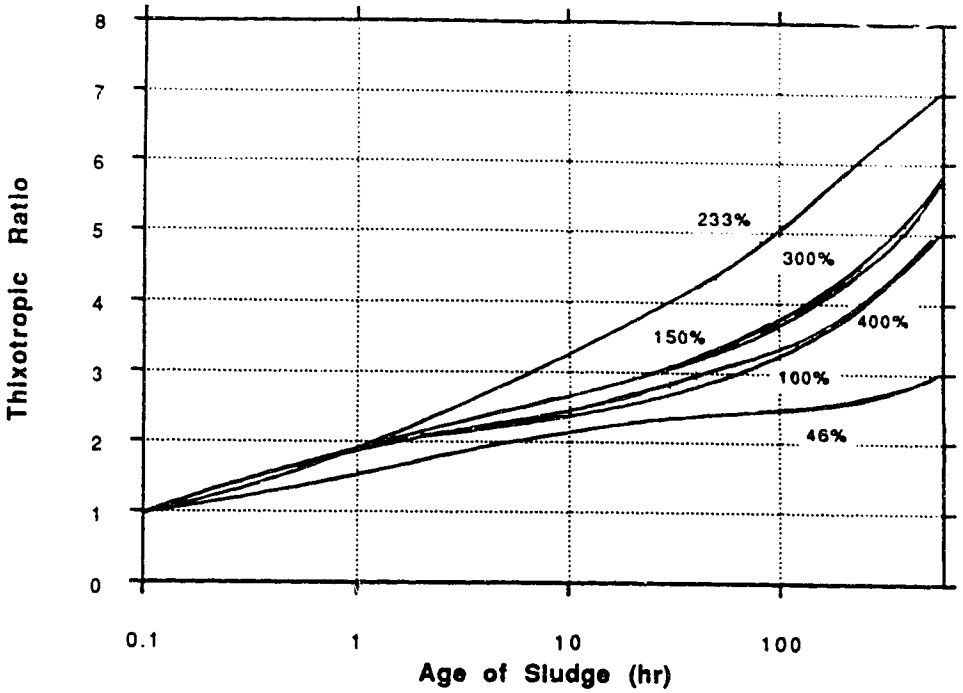

Figure 5.64 Thixotropic Strength Ratios to 600 hrs

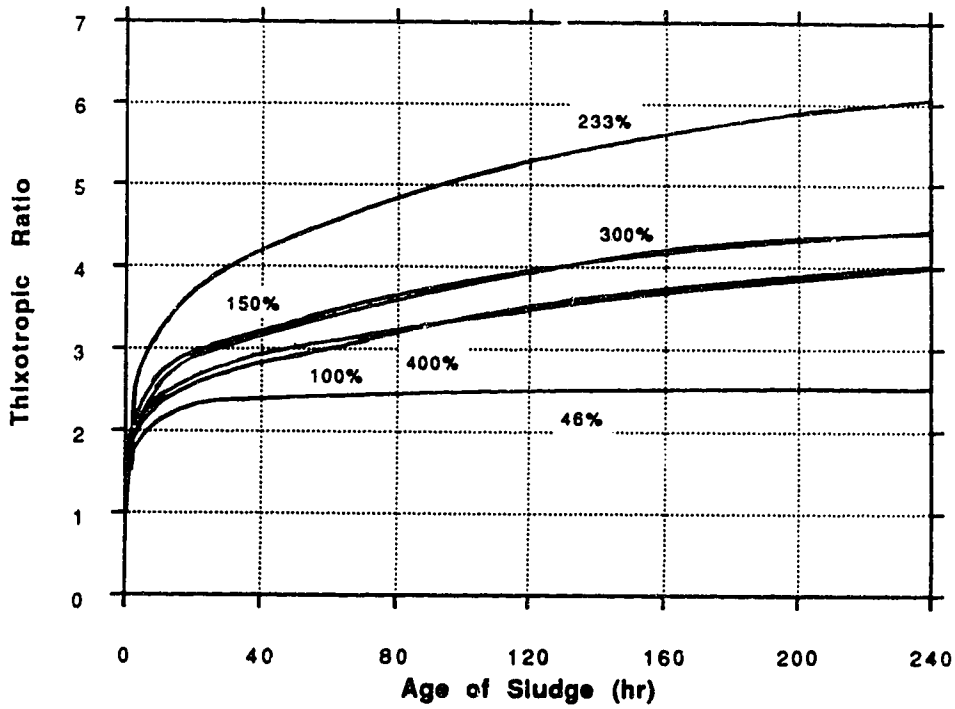

Figure 5.65 Thixotropic Strength Ratios to 240 hrs

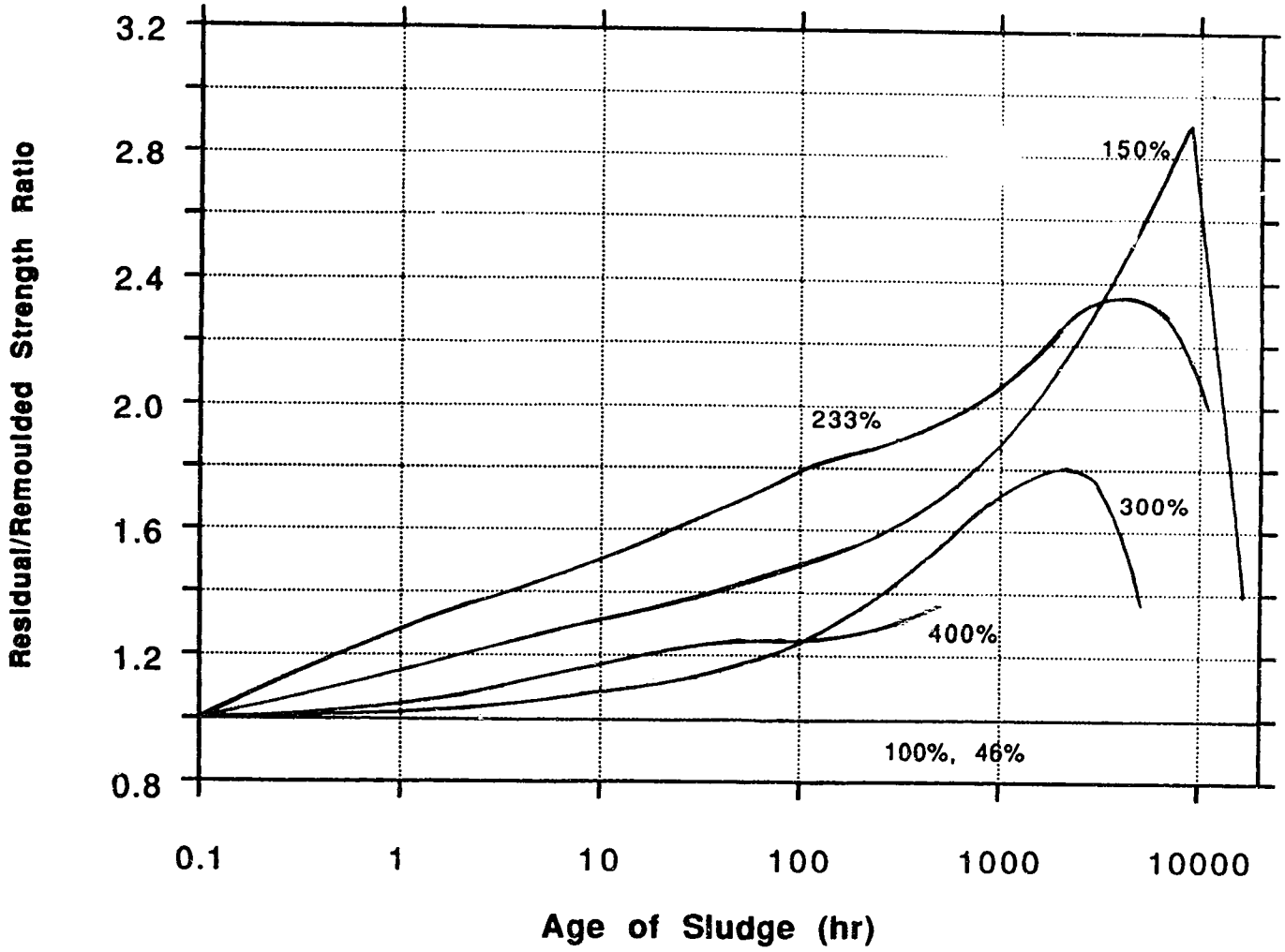

Figure 5.66 Residual/Remoulded Shear Strength Ratios to 680 days

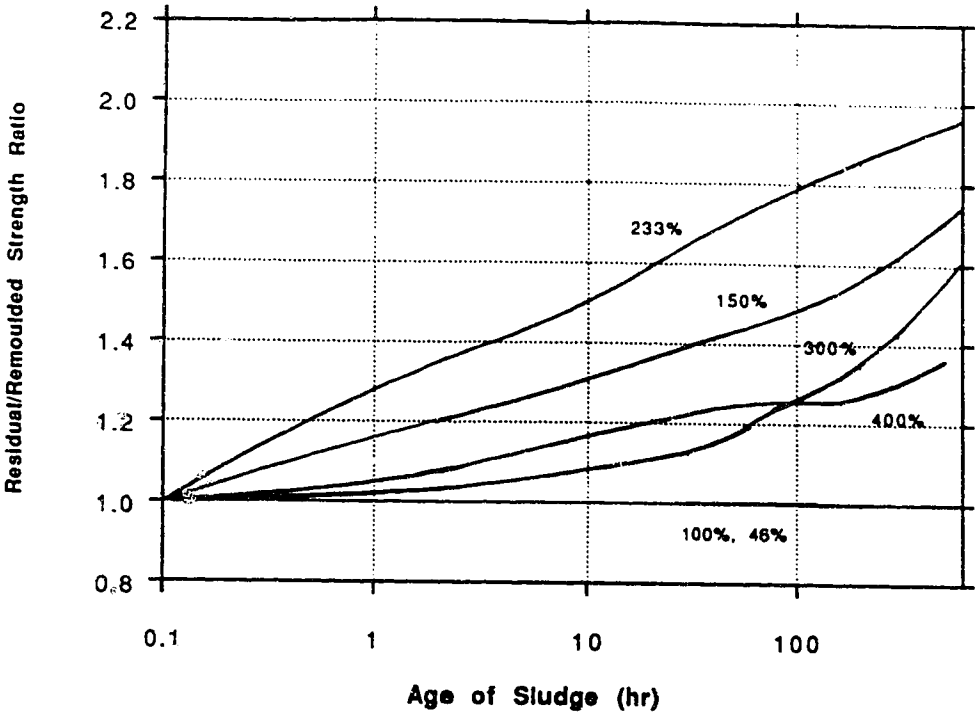

Figure 5.67 Residual/Remoulded Shear Strength Ratios to 600 hrs

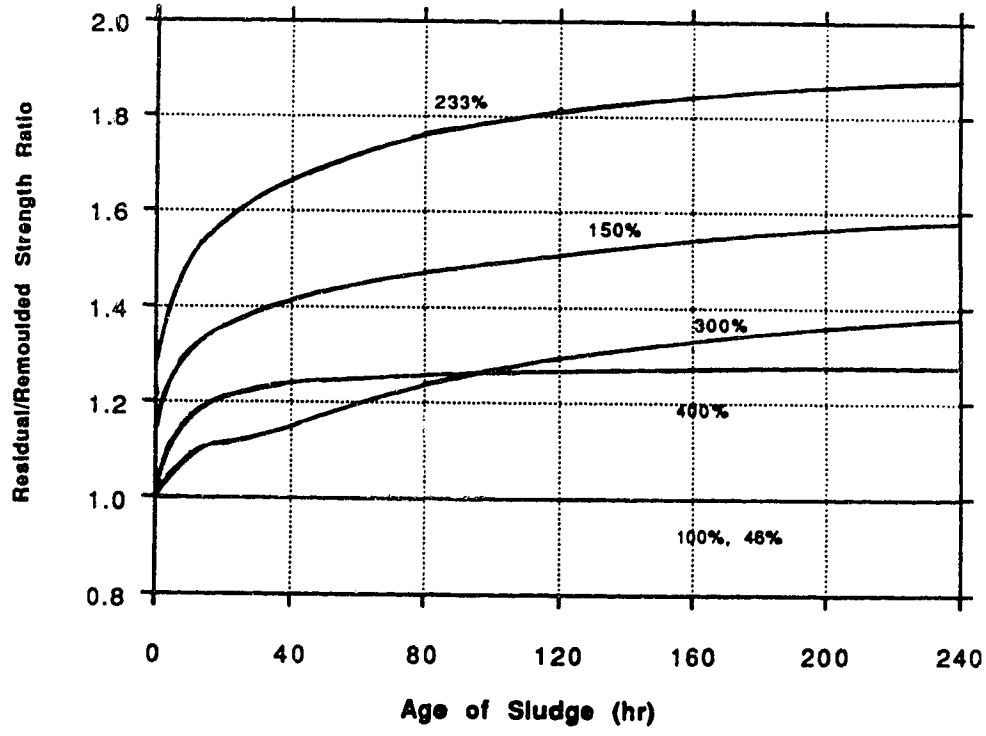

Figure 5.68 Residual/Remoulded Shear Strength Ratios to 240 hrs

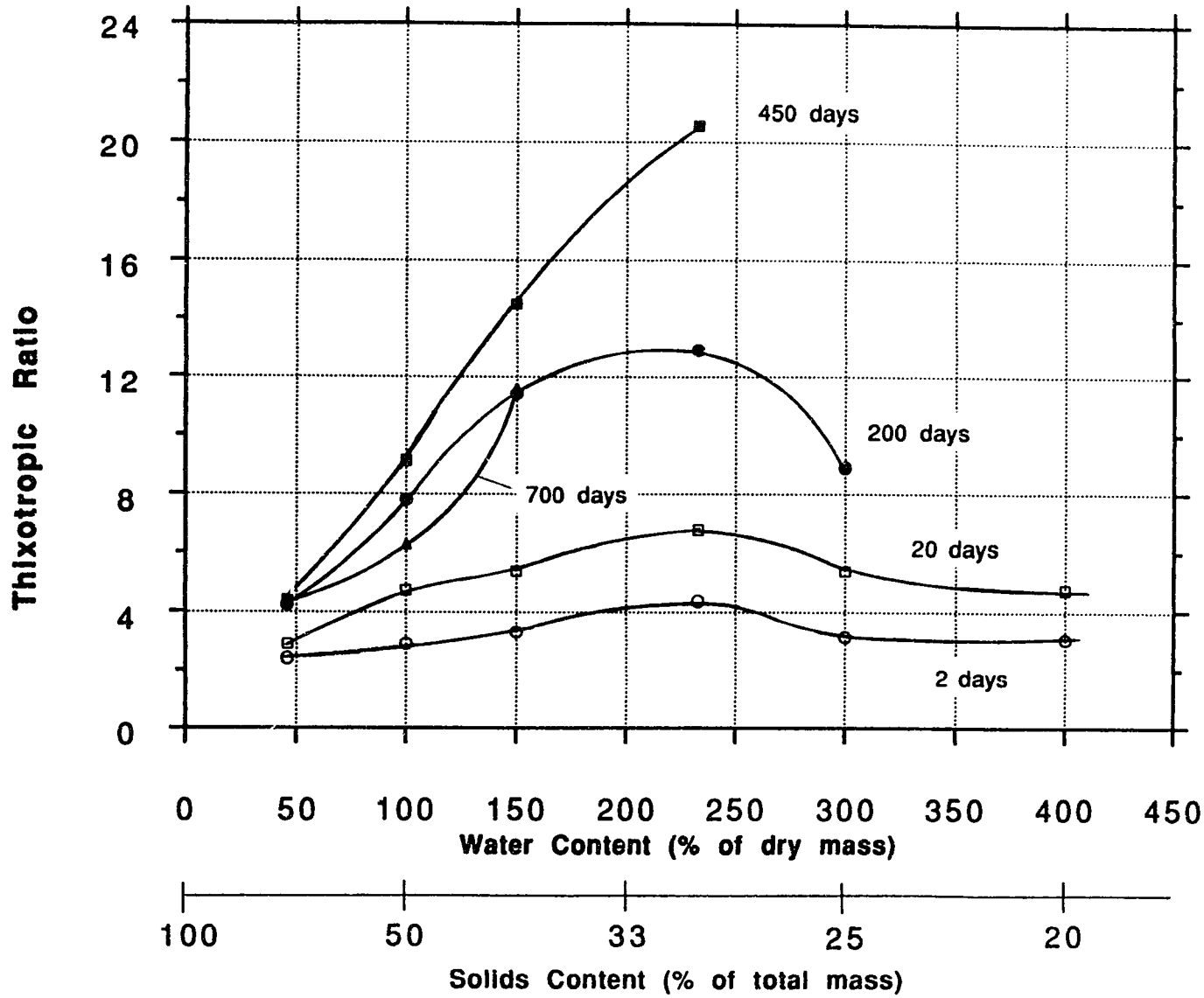

Figure 5.69 Influence of Water Content on Thixotropic Ratio

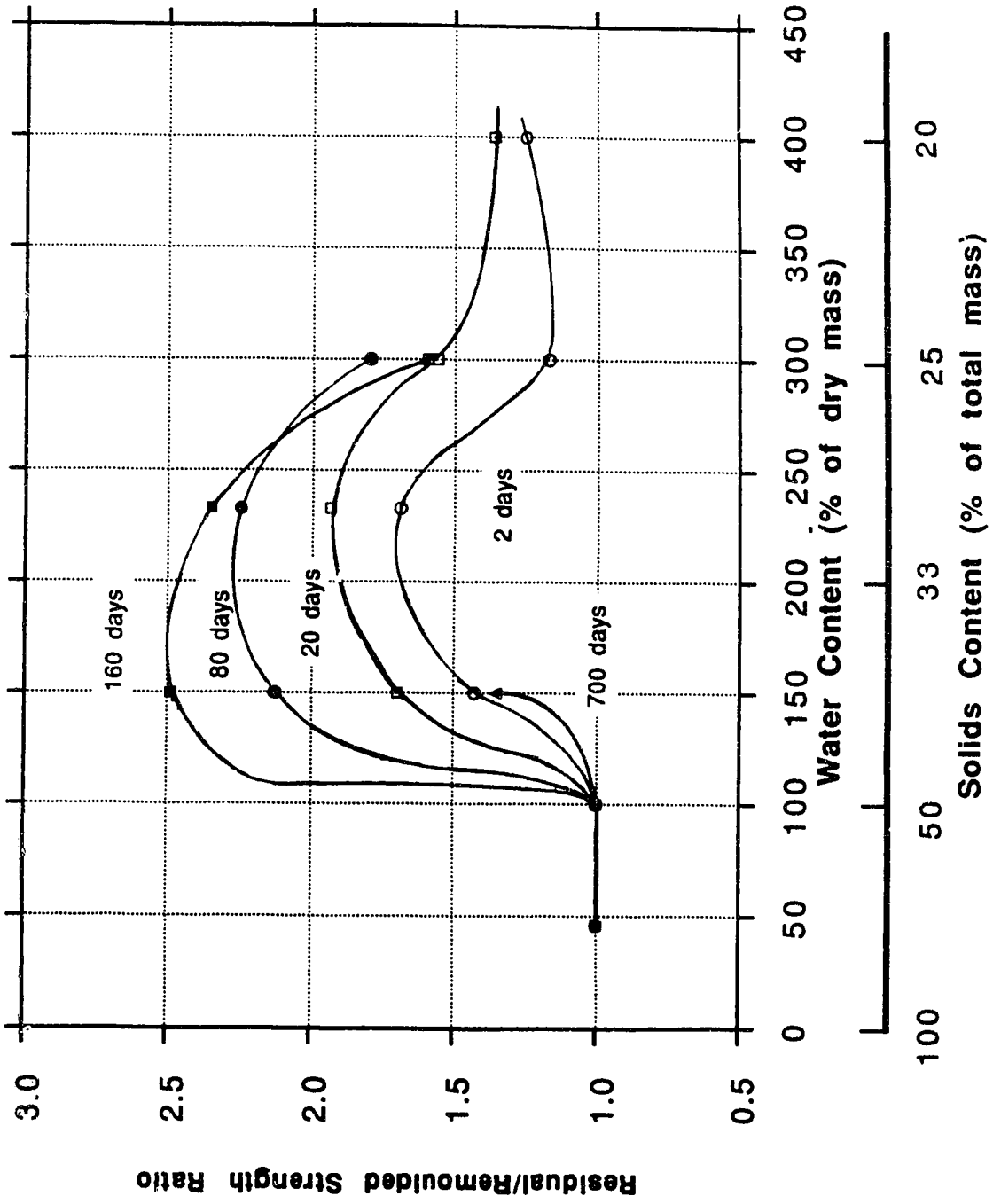

Figure 5.70 Influence of Water Content on Residual/Remoulded Strength Ratio

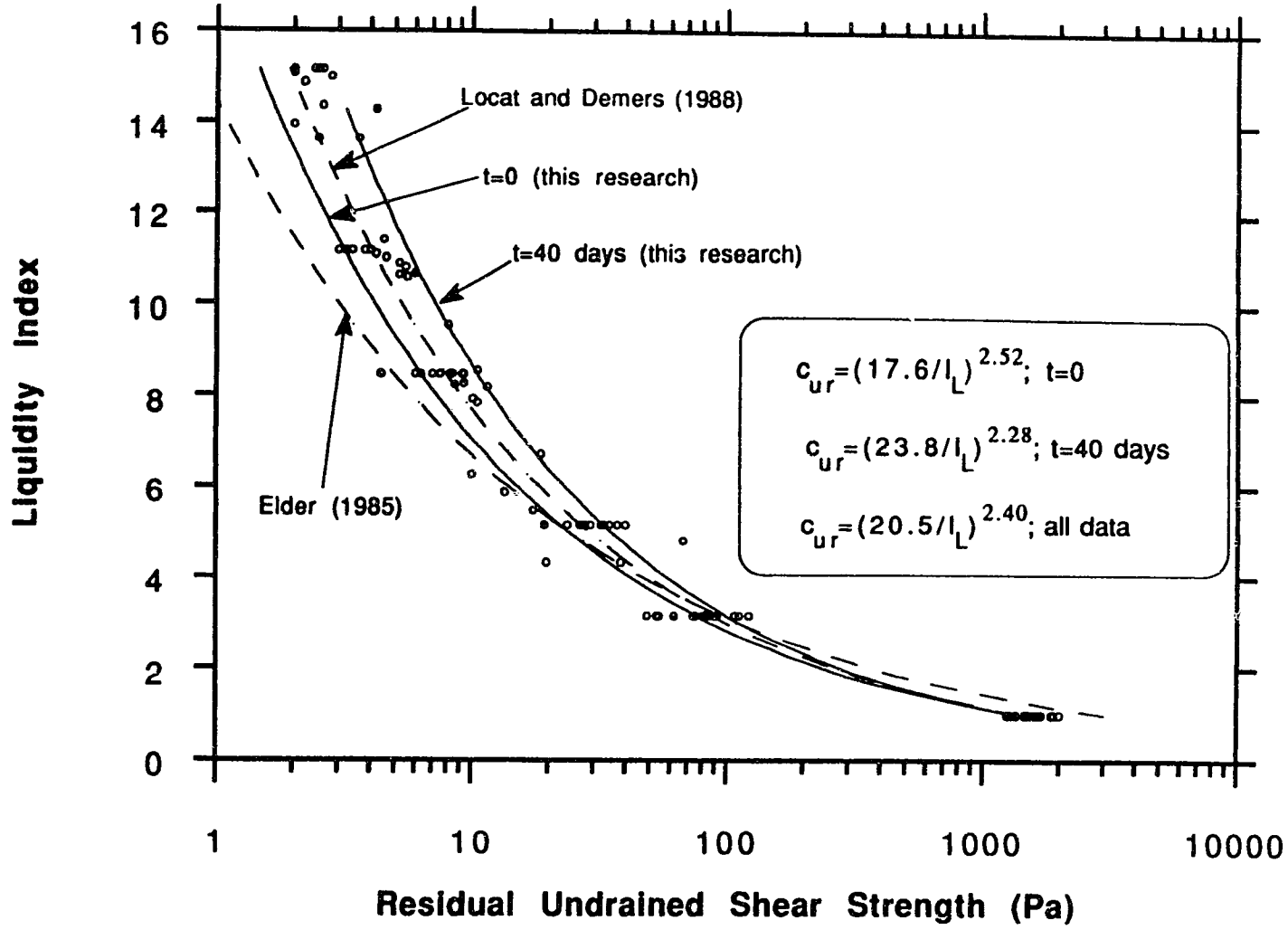

Figure 5.71 Liquidity Index-Residual Shear Strength Relationship

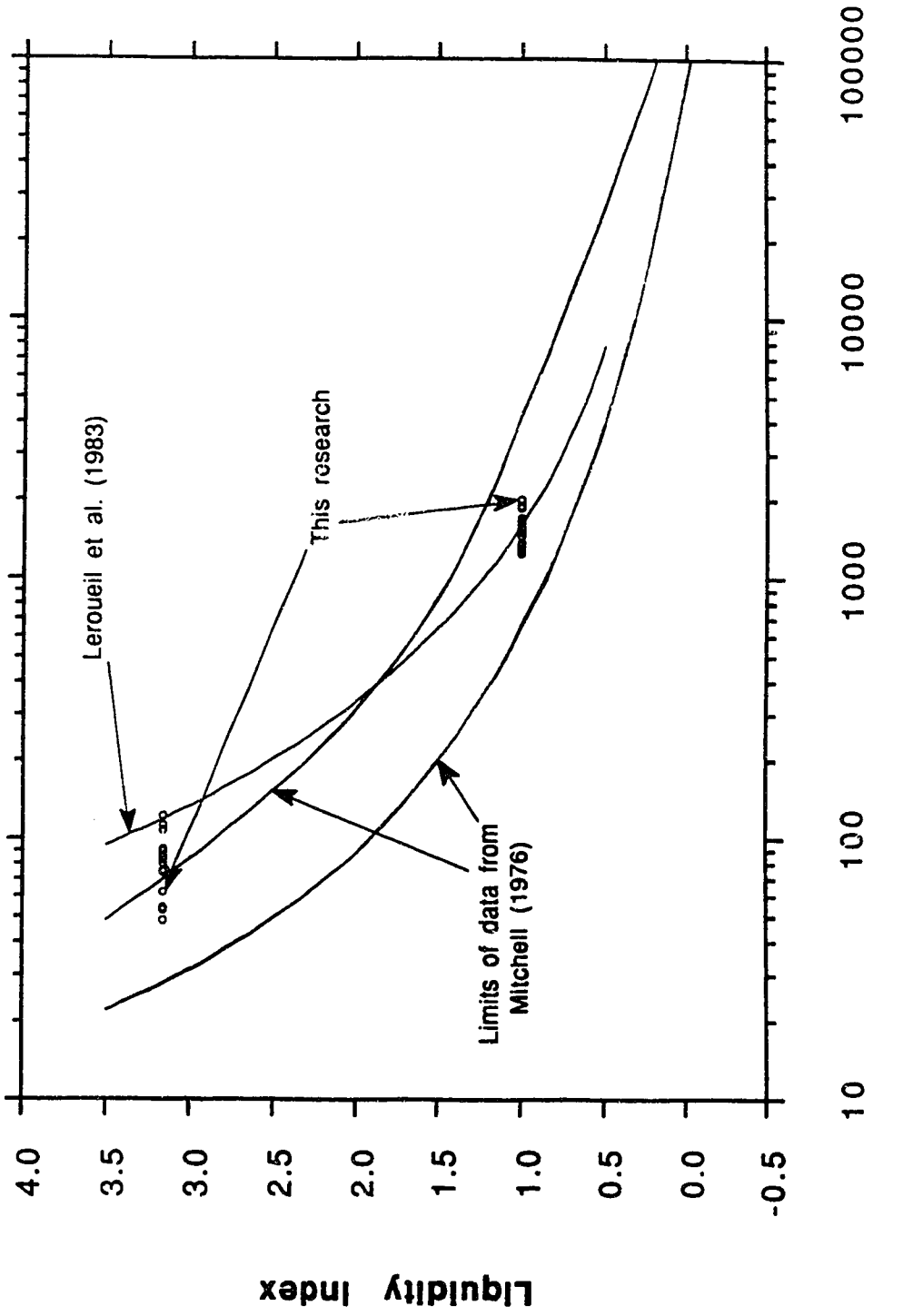

Figure 5.72 Liquidity Index-Residual Shear Strength Relationship at Low Range of I_L

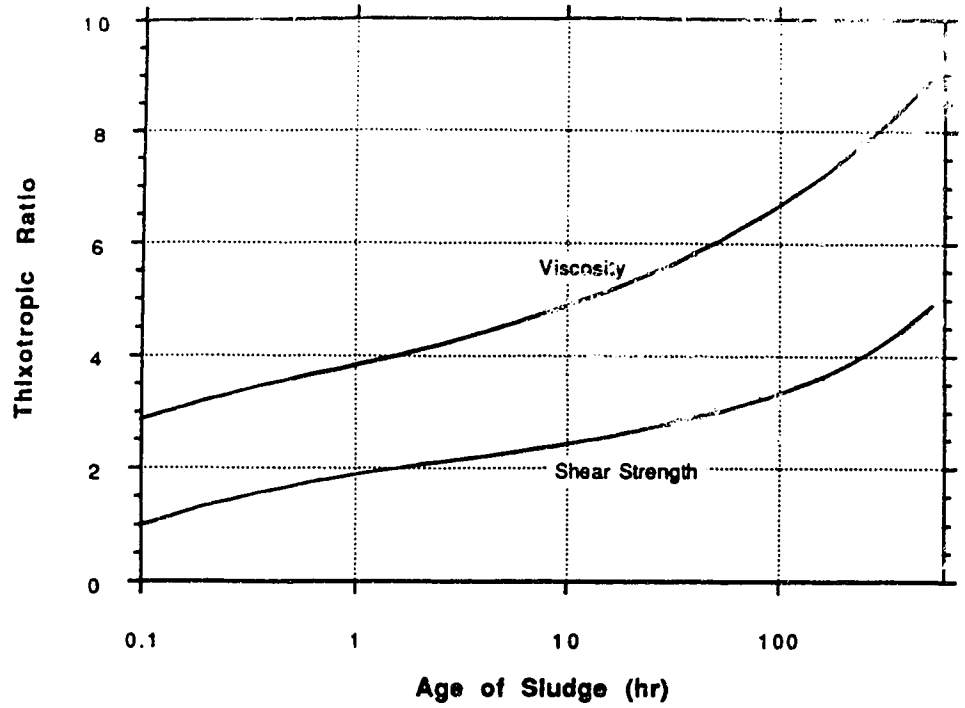

Figure 5.73 Shear Strength and Viscosity Ratios for w=400%

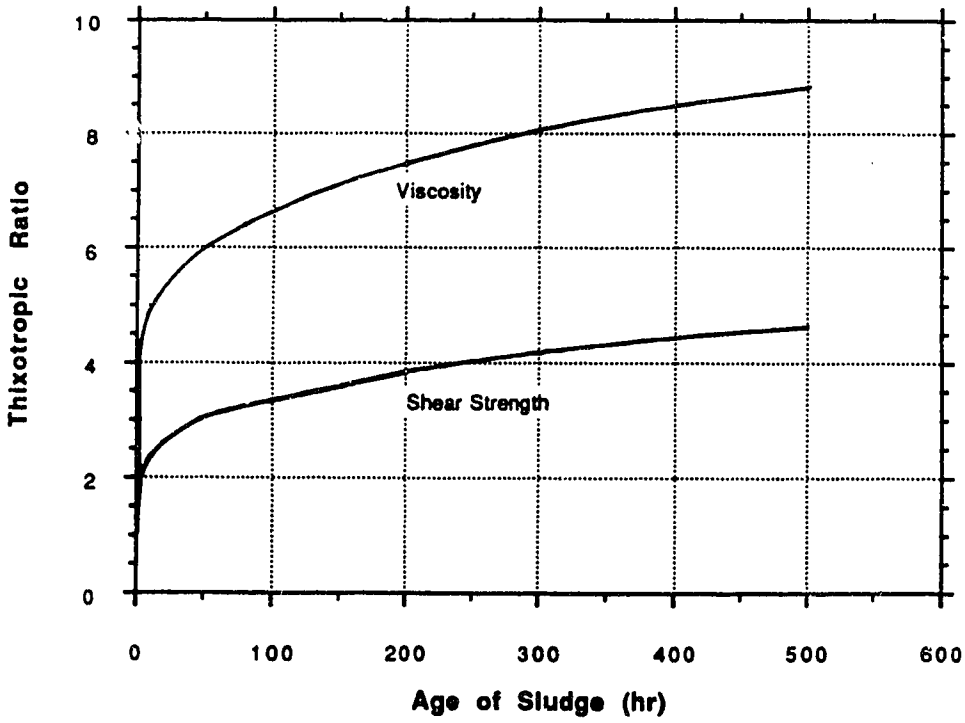

Figure 5.74 Shear Strength and Viscosity Ratios for w=400%

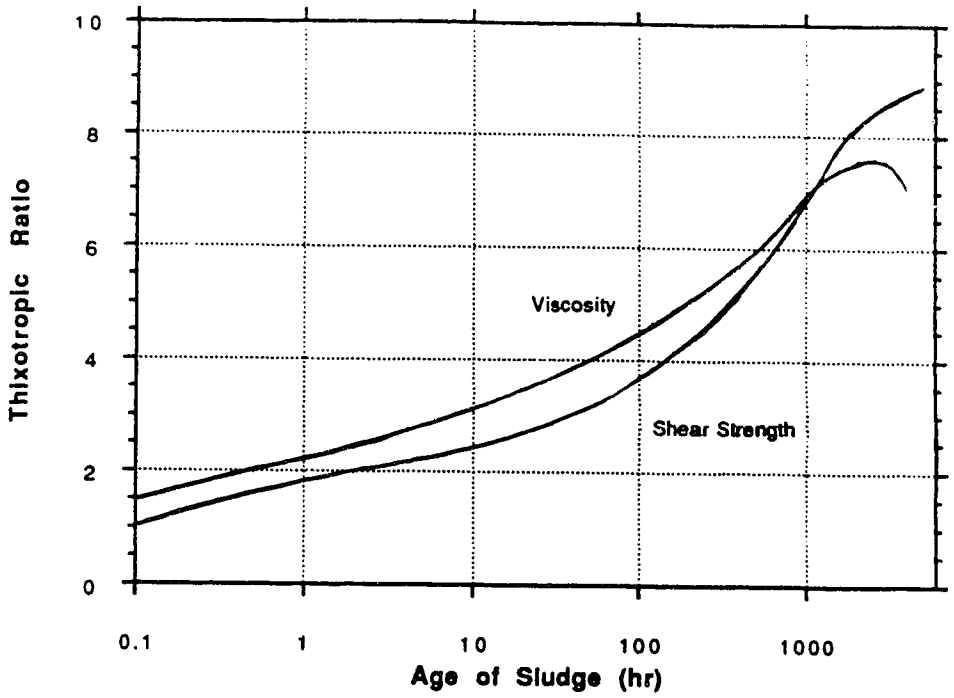

Figure 5.75 Shear Strength and Viscosity Ratios for w=300%

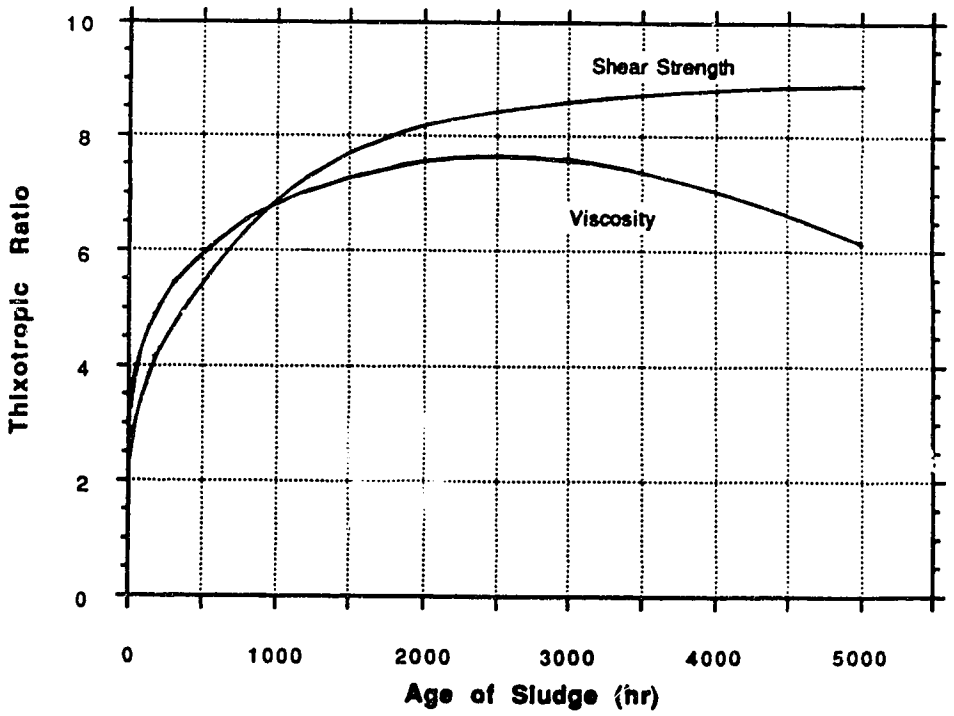

Figure 5.76 Shear Strength and Viscosity Ratios for w=300%

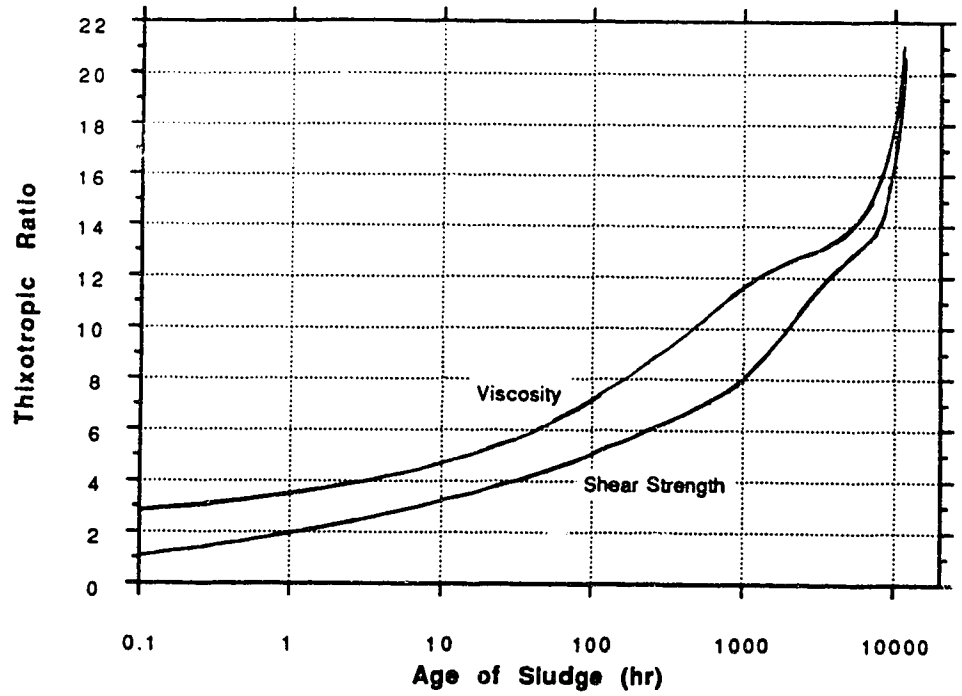

Figure 5.77 Shear Strength and Viscosity Ratios for w=233%

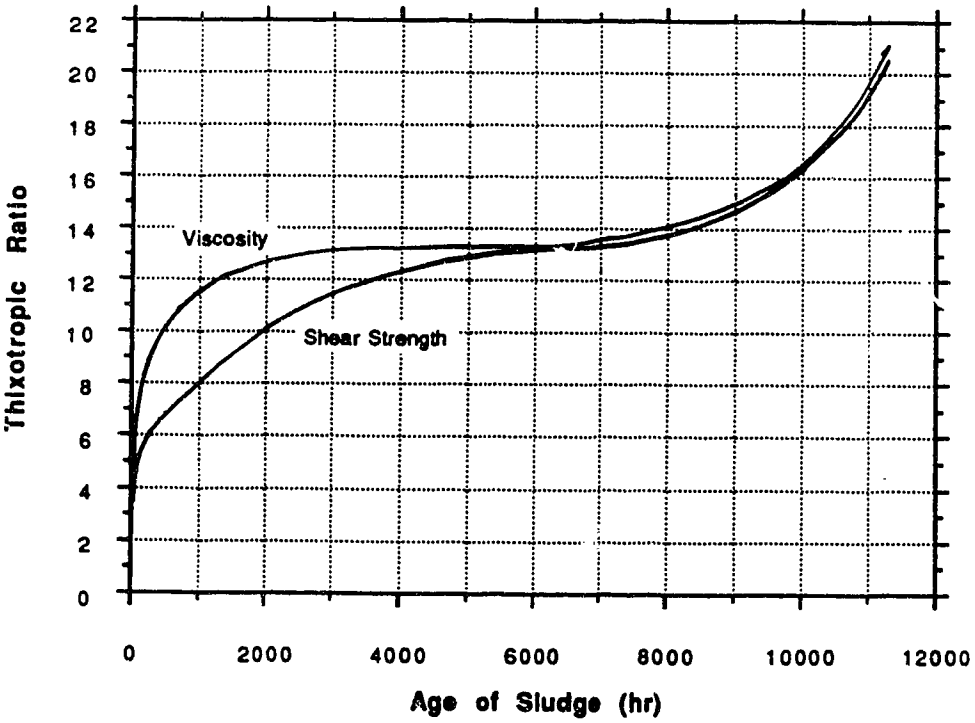

Figure 5.78 Shear Strength and Viscosity Ratios for w=233%

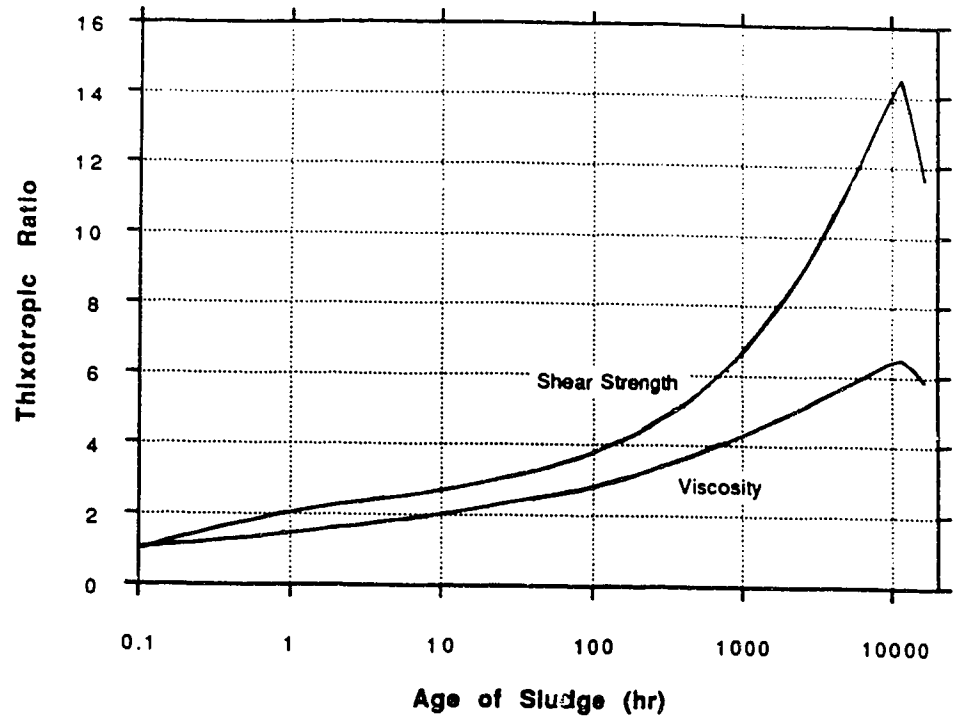

Figure 5.79 Shear Strength and Viscosity Ratios for w=150%

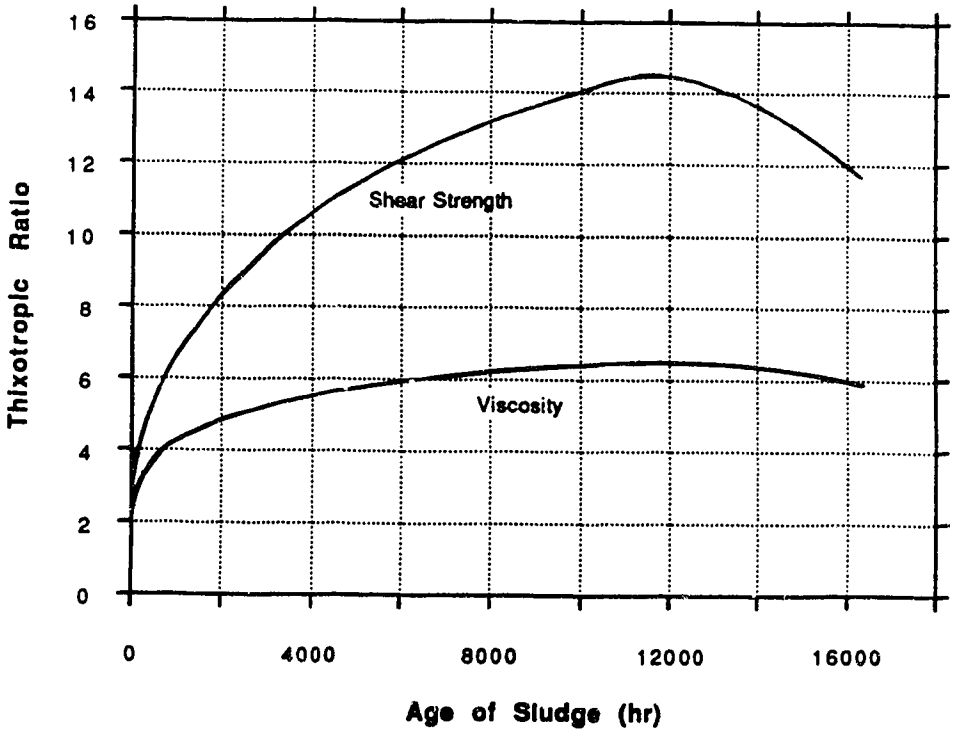

Figure 5.80 Shear Strength and Viscosity Ratios for w=150%

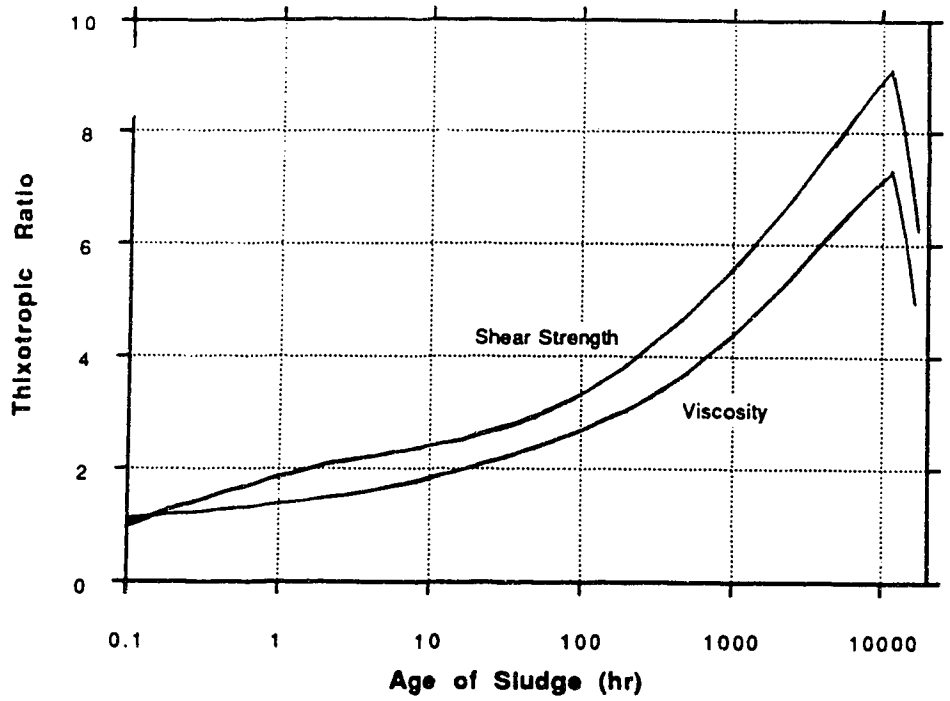

Figure 5.81 Shear Strength and Viscosity Ratios for w=100%

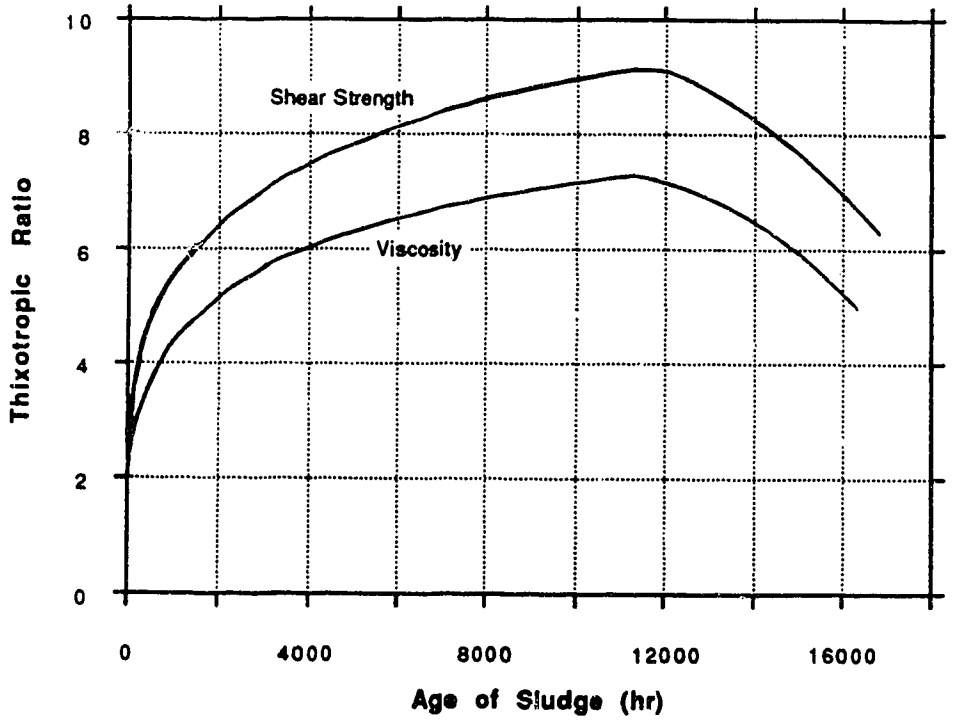

Figure 5.82 Shear Strength and Viscosity Ratios for w=100%

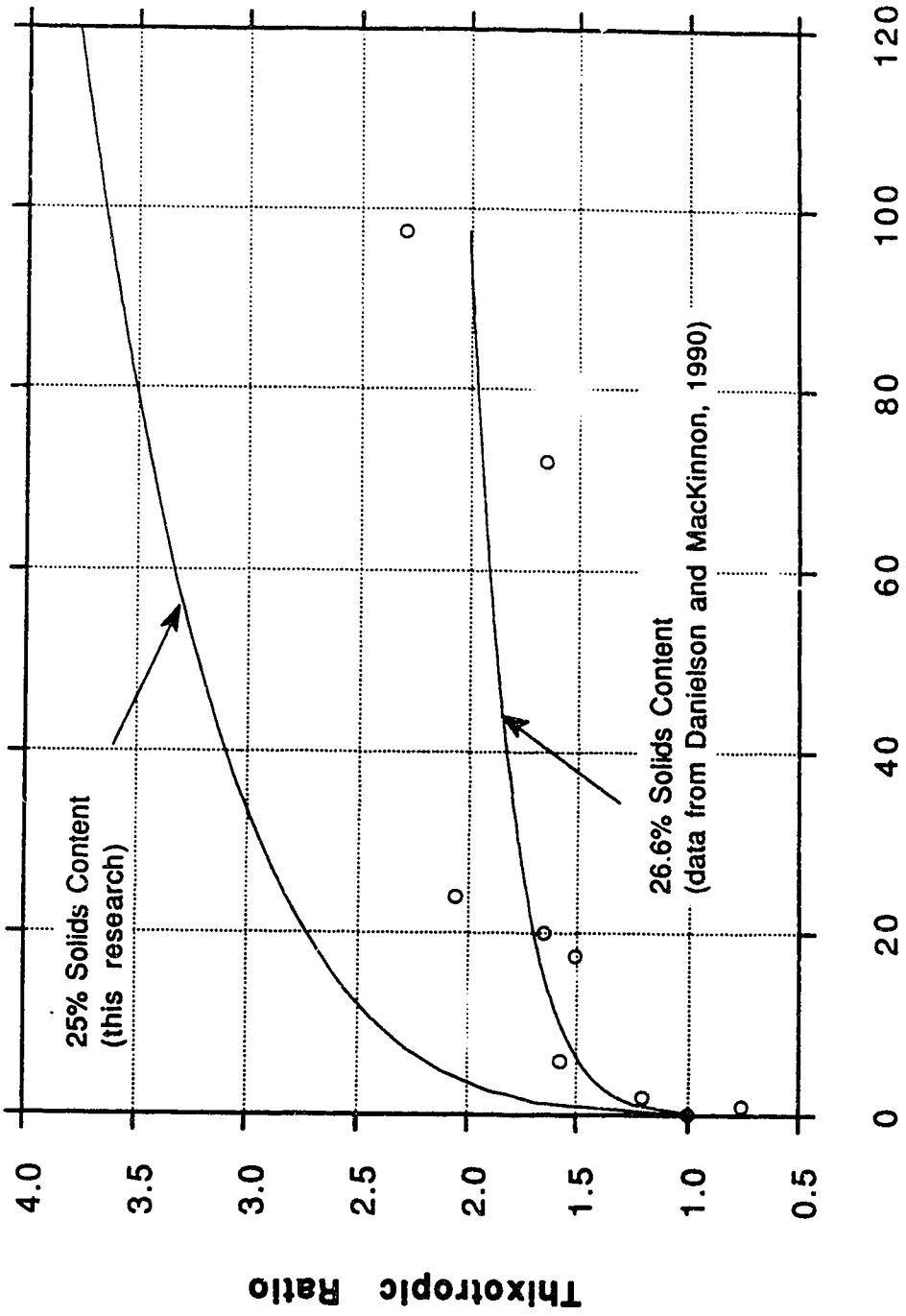

Figure 5.83 Comparison to Other Sludge Testing

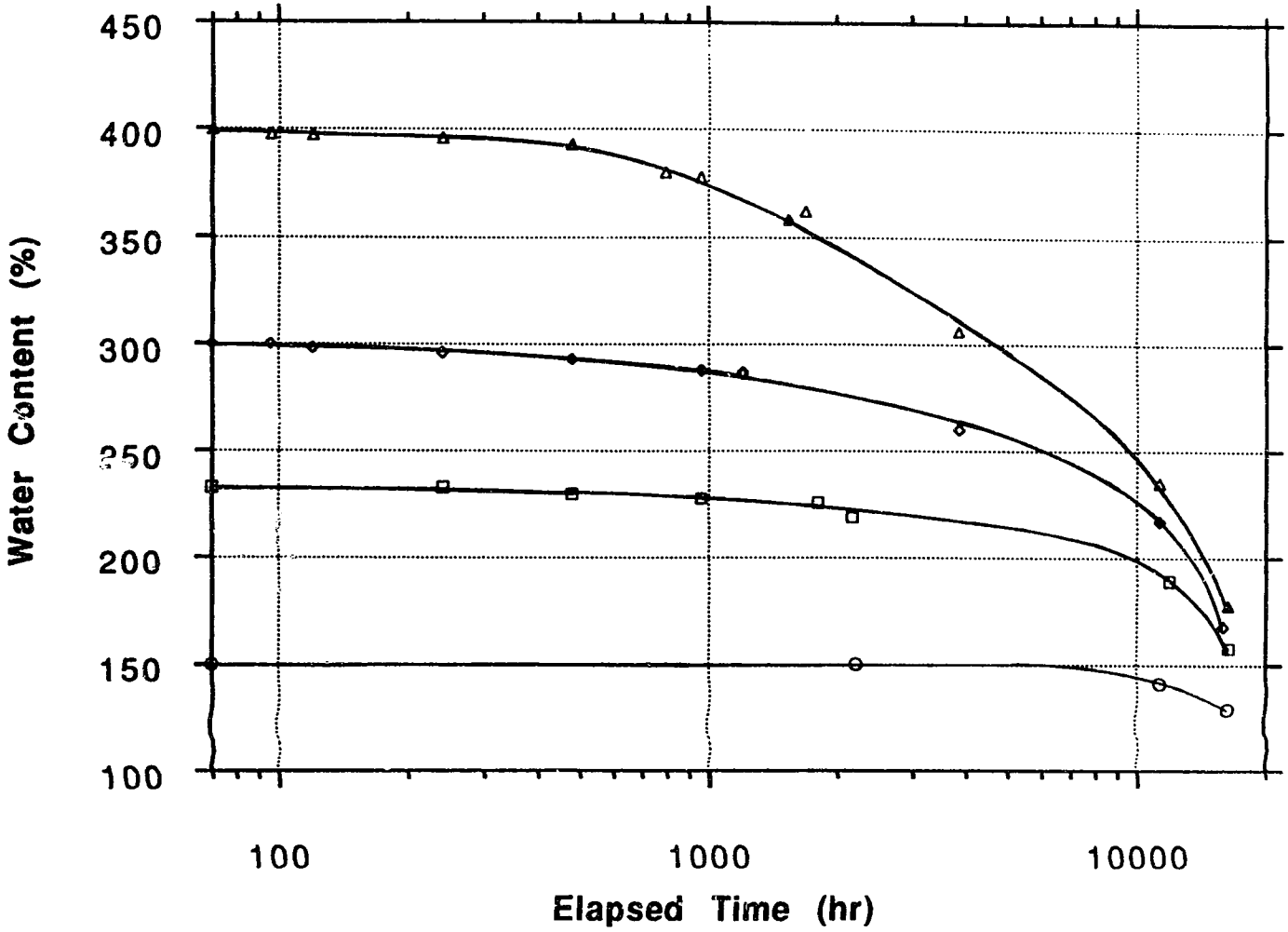

Figure 5.84 Self-Weight Consolidation of Sludge

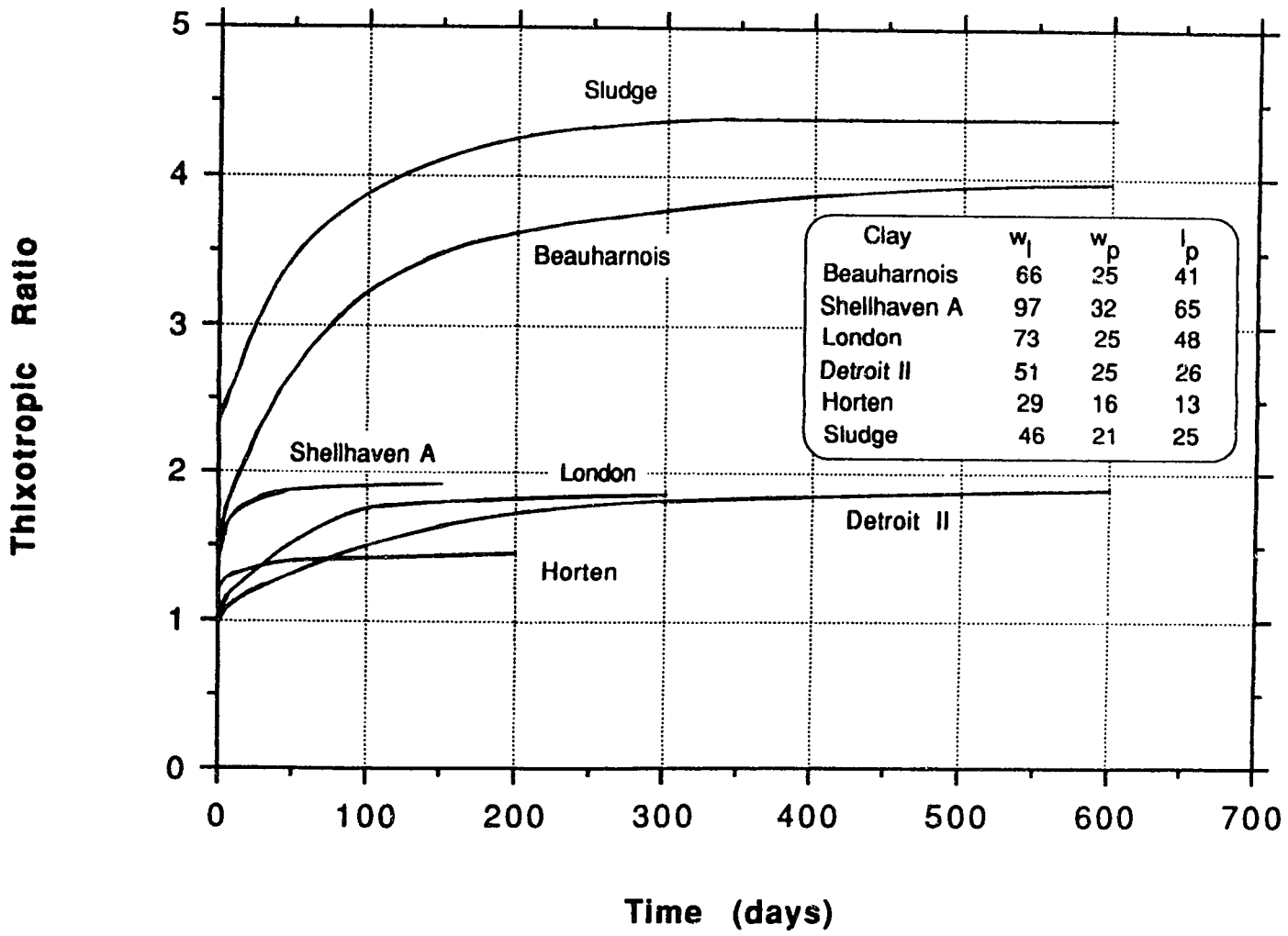

Figure 5.85 Thixotropic Ratio in Some Typical Clays and Sludge

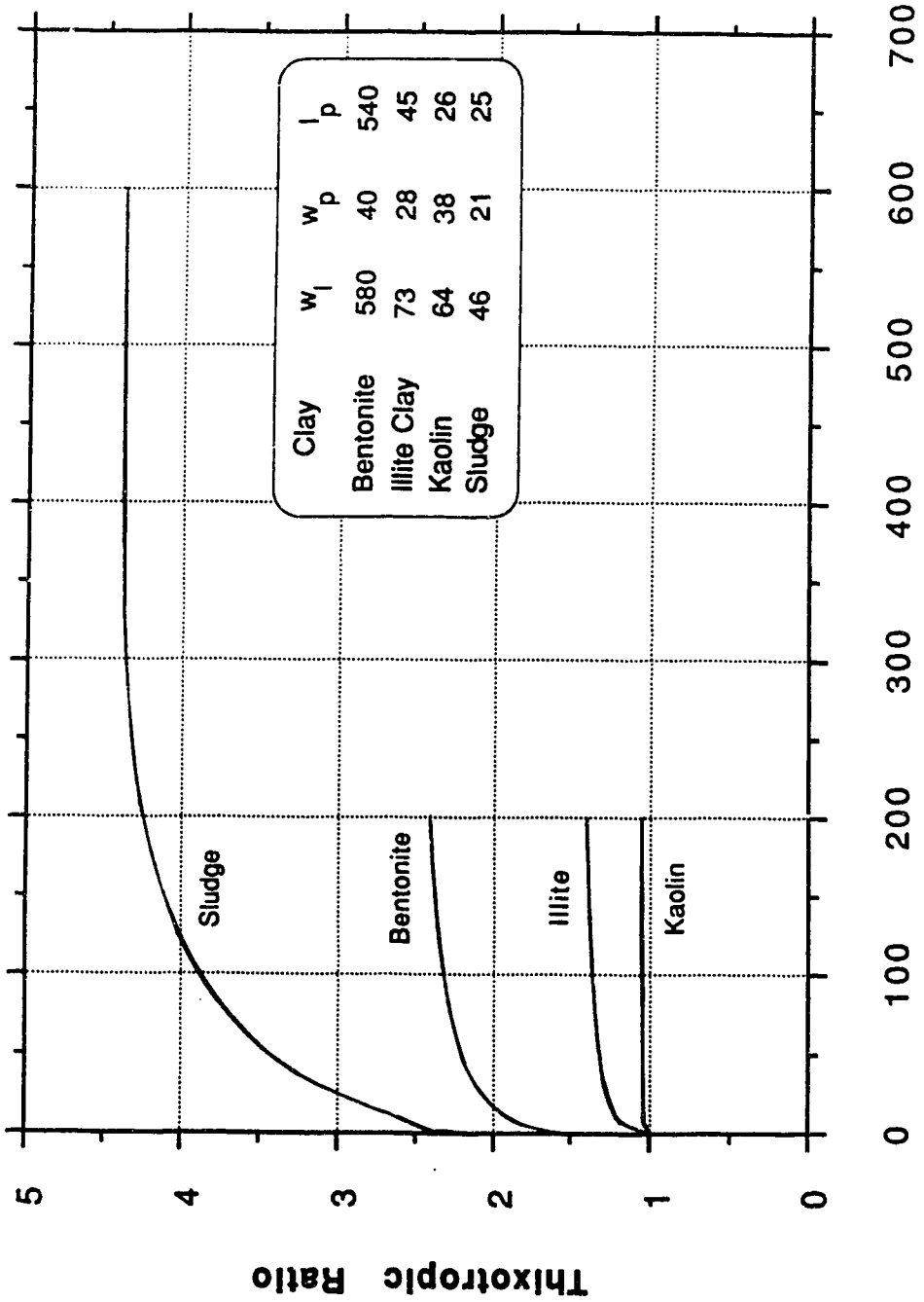

Figure 5.86 Thixotropic Ratio in Three Clay Minerals and Sludge

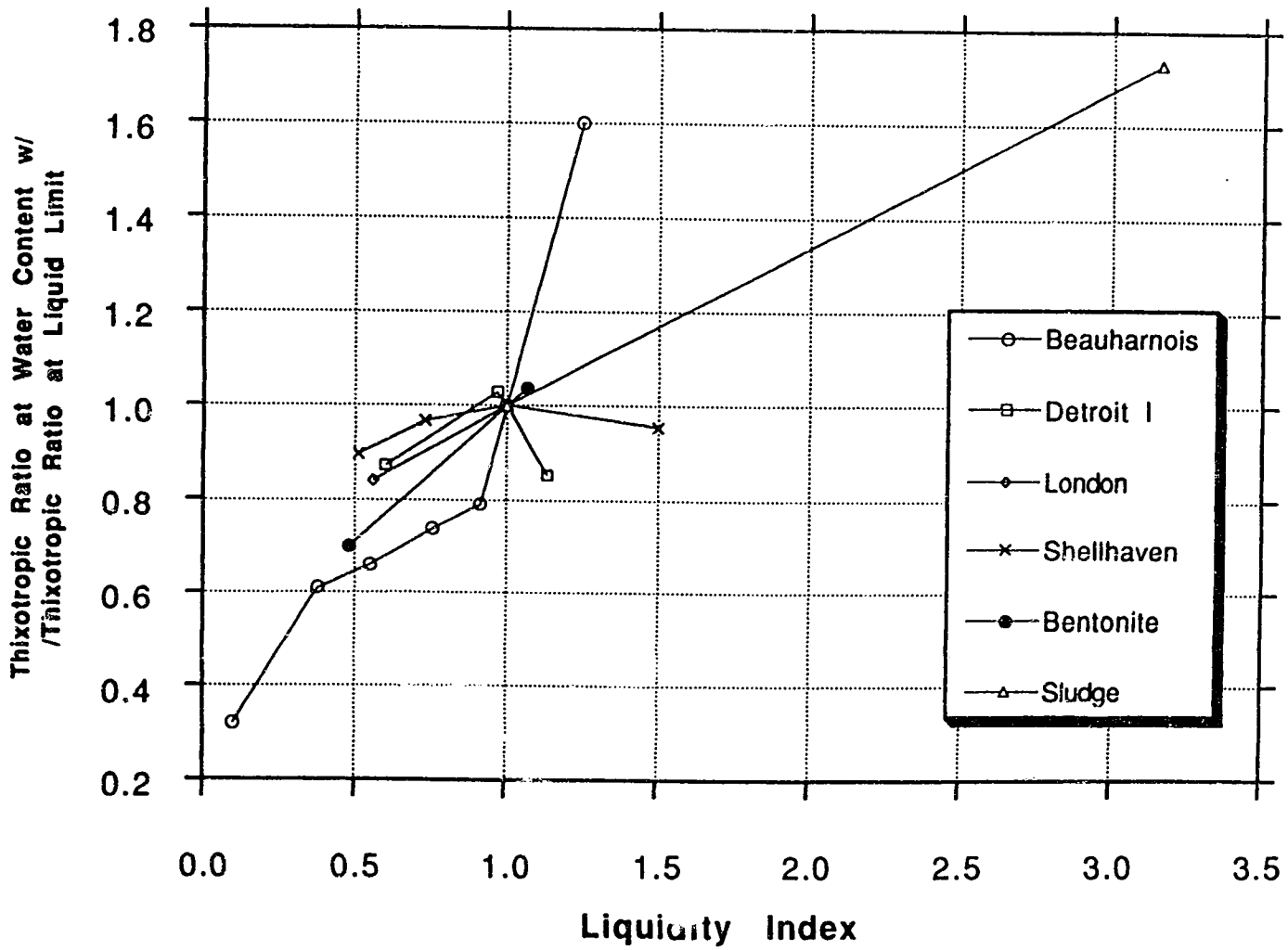

Figure 5.87 Effect of Liquidity Index on Thixotropic Ratio at 100 Days

6. CONCLUSIONS AND RECOMMENDATIONS

6.1 Conclusions

The conclusions of this research program will be presented in a form of two different categories; test results and testing equipment and procedures.

6.1.1 Test Results

1. The main objective of this research program was achieved. The time dependent strength behaviour of oil sands tailings sludge was successfully investigated and described with the aid of two independent testing methods: viscosity measurements and undrained shear vane tests.
2. The oil sands tailings sludge is a highly thixotropic soil. It exhibits higher relative thixotropic gain in strength than typical clays and clay minerals.
3. The effect of thixotropy in sludge is highly dependent on water content. The absolute gain in thixotropic undrained strength increases with decreasing water content. The highest absolute gain in strength, 5.1 kPa in 300 days, was shown by the liquid limit (47% water content) sludge.
4. The relative increase in thixotropy, the thixotropic ratio, indicates that there is an optimum void ratio or solids content for relative thixotropy. At 233% water content (30% solids content) the sludge shows the highest relative gain in strength; a thixotropic ratio of 21 after 470 days. Higher and lower water content sludges show smaller relative values.
5. The rate of thixotropic hardening was highest in the first several hours after mixing for all water content sludges with the undrained shear strength doubling within 6 hours. The rate decreases with time.
6. Self-weight consolidation may be a major factor affecting thixotropy. Particle shearing resulting from consolidation reduces physico-chemical

bonding produced by thixotropy. The higher the rate of consolidation, the smaller the thixotropic gain in strength. Because the rate of consolidation in the pond is slower, the thixotropic effect in the tailings pond may not be affected as much by self-weight consolidation as it was in this experimental program.

7. A laboratory study of physico-chemical properties of the sludge should follow the same time-consolidation strength gain history as that of the sludge in the tailings pond.
8. Residual shear strength of sludge is time dependent at water contents greater than 100%. Physico-chemical bonding is not completely destroyed by large shearing strains.
9. The relationship between residual shear strength and liquidity index for sludge is similar to the empirical correlations developed for other very soft soils.
10. From the rheological perspective, the sludge is classified as a non-Newtonian fluid. In its undisturbed state, the sludge behaves like a Herschel-Bulkley model material; when remoulded, the sludge is a Bingham model fluid. The transition between the two types of rheological behaviour in the sludge is the effect of thixotropy.

6.1.2 Testing Equipment and Procedures

1. Viscosity testing on high water content sludge proved to be a simple and reliable method of describing the change in rheological behaviour and strength properties of the sludge. The viscosity apparatus used in the tests provided index properties not absolute values of viscosity.

2. The modified vane shear apparatus is a highly sensitive and accurate method of determining peak and residual undrained shear strengths of the sludge.
3. The novel cavity expansion method of undrained strength testing of the sludge gave some initial promising results.
4. Both testing methods, viscometer and vane shear, gave similar results in monitoring the long time strength behaviour of the sludge.
5. Special care should be exercised when determining the liquid limit of the sludge. It is required that, due to thixotropy, the blow count be conducted immediately after thorough mixing of the material.
6. For geotechnical engineering purposes, it is recommended that the grain size analysis on the sludge be performed with the standard hydrometer test on the as-received material without oven drying or extracting the bitumen.

6.2 Recommendations for Further Research

1. Long term strength behaviour of the oil sands tailings sludge should be investigated in more detail to develop a quantitative relationship between thixotropy, consolidation and time.
2. The novel method of testing, the cavity expansion test, should be further developed and used for undrained shear strength testing of the sludge as an alternative to vane and viscosity testing.
3. It is necessary to study variation of shear strength and viscosity of the sludge with temperature in order to develop temperature correction factors.
4. The effect of thixotropy determined in this research should be incorporated into the consolidation theory of the sludge in order to understand the long term consolidation behaviour in tailings ponds.

5. Development of equipment capable of determining shear strength of sludge in field conditions is required.
6. An in-situ testing program should be performed to confirm the laboratory results obtained in this thesis.
7. An appropriate method of grain size distribution testing should be developed for the sludge that would take into account the material's unique properties.
8. The effect of pore water chemistry on the strength of the sludge is not adequately understood. A study should be undertaken to investigate this effect.

REFERENCES

Aas G. (1965) "A Study of the Effect of Vane Shape & Rate of Strain on the Measured Values of in Situ Shear Strength of Clays", Proc. 6th ICSMFE, Montreal, Vol.1, pp. 141-145.

Adam D. (1985) "Syncrude's Technology Evolution Since Start-up", Proceedings of 6th Annual Advances in Petroleum Recovery and Upgrading Technology, AOSTRA, Edmonton, Alberta, June 6-7, 20p.

Andresen A. and Sallie S. (1966) "An Inspection Vane", Symposium, Vane Shear and Cone Penetration Resistance, Testing of In Situ Soils, ASTM STP 399.

Arman A., Poplin J.K., Ahmad N. (1975) "Study of the Vane Shear", Proc. Conf. In Situ Measurements of Soil Properties, Raleigh NC, Vol.1, 93.

Back A.L. (1959) "How to Get More Information from Readings of Rotational Viscometers", Rubber Age, January, 5p.

Bazett D.J. et al. (1953) "An Investigation of Test Slides in a Test Trench Excavated in Fissured Sensitive Marine Clays", Proceedings, Highway Research Board No.32, pp. 486-496.

Been K. (1980) "Stress-Strain Behaviour of a Cohesive Soil Deposited under Water", Ph.D. Thesis, University of Oxford.

Bentley S.P. (1979) "A Viscosity Assessment of a Remoulded Sensitive Clay", Can. Geot. Journal 212, pp. 414-419.

Berkowitz N. and Speight J.G. (1975) "The Oil Sands of Alberta", Fuel, Vol.54, pp. 138-149.

Bishop A.W., Hill R. and Mott N.F. (1945) "The Theory of Indentation and Hardness Tests", Proceedings Phys. Society, London, Vol.57, No.3, pp. 147-159.

Bishop A.W. (1960) "The Principle of Effeective Stress", NGI Publication 32, pp. 1-5.

Bjerrum L. (1954) "Geotechnical Properties of Norwegian Marine Clays", Geotechnique 4, No.2, pp. 49-69.

Bjerrum L. and Lo K.Y. (1963) "Effect of Ageing on the Strength Properties of a Normally Consolidated Clay", Geotechnique 13, No.2, p. 147.

Bowden R.K. (1988) "Compression Behaviour and Shear Strength Characteristics of a Natural Silty Clay Sedimented in the Laboratory", Ph.D. Thesis, University of Oxford.

Brookfield D.W. (1961) "Measurement of Rheological Properties", Official Digest of the Federation of Societies for Paint Technology, January, 8p.

Cadling L. and Odenstad S. (1950) "The Vane Borer", Proceedings No.2, Royal Swedish Geotechnical Institute, Stockholm, Sweden.

Carlson L. (1948) "Determination in situ of the Shear Strength of Undisturbed Clay by Means of a Rotating Auger", Proceedings 2nd ICSMFE, Vol.1, pp.265-270.

Carrier III, W.D. and Beckman (1984) "Correlations Between Index Tests and the Properties of Remoulded Clays", Geotechnique 34, No.2, pp. 211-228.

Chatterji P.K. and Morgenstern N.R. (1989) "A Modified Shear Strength Formulation for Swelling Clays", Paper submitted to Symp. on Physico-Chemical Aspects of Soil, Rock and Related Materials, St. Louis, Missouri, June 29, 37p.

Crawford C.B. (1963) "Cohesion of an Undisturbed Sensitive Clay", Geotechnique 13, No.2, pp. 132-146.

Danielson L.J. and MacKinnon M.D. (1990) "Rheological Properties of Syncrude's Tailings Pond Sludge", AOSTRA Journal of Research, Vol.6, No.2, pp. 99-121.

Donald et al. (1977) "The Vane Test - a Critical Appraisal", Proc. 9th ICSMFE, Tokyo, Vol.1, pp. 81-89.

Dusseault M.B. and Scott J.D. (1983) "Tailings Pond Behavior and Characterization of Oil Sand Tailings Sludge", J. Particulate Sc. and Technology, No.1, pp. 295-309.

Dusseault M.B., Scafe D.W. and Scott J.D. (1989) "Oil Sand Mine Waste Management: Clay Mineralogy, Moisture Transfer and Disposal Technology", AOSTRA Journal of Research, Vol.5, No.4, pp. 303-320.

Eden W.J. and Hamilton J.J. (1956) "The Use of Field Vane Apparatus in Sensitive Clays", Symposium, Vane Shear Testing of Soil, ASTM STP 193.

Einsele G., Overbeck R., Schwartz H.U., and Unsold G. (1974) "Mass Physical Properties, Sliding and Erodibility of Experimentally Deposited and Differently Consolidated Clayey Muds", Sedimentology, Vol.21, pp. 339-372.

Elder D.Mc.G. (1985) "Stress Strain and Strength Behaviour of Very Soft Soil Sediment", Ph.D. Thesis, University of Oxford.

Flaate K. (1966) "Factors Influencing the Results of Vane Shear Tests", Can. Geotech. Journal 3, No.1, pp. 18-31.

Gibson R.E. (1950) "Discussion on Paper by Wilson G.", J. of the ICE, Vol.34, p. 382.

Isaac B.A.A. (1987) "Slurry Consolidation Testing for Oil Sands Overburden and Sludge Wastes", M.Eng. Report, University of Alberta, Edmonton, 96p.

Karlsson R. (1961) "Suggested Improvements in the Liquid Limit Test, with Reference to the Flow Properties of Remoulded Clays", 5th ICSMFE, Paris, p. 171.

Karlsson R. (1977) "Consistency Limits: a Manual for the Performance and Interpretation of Laboratory Investigations, part 6.", Swedish Council for Building Research, Stockholm.

Kenney T.C., Moum J. and Berre T. (1967) "An Experimental Study of Bonds in a Natural Clay", Proc. Geotech. Conf. Oslo, Vol.1.

Kessick M.A. (1979) "Structure and Properties of Oil Sands Clay Tailings", J. of Canadian Petroleum Technology, Vol.18, No.1, pp. 49-52.

Kessick M.A. (1980) "Ion Exchange and Dewaterability of Clay Sludges", Int. J. of Miner. Processing, No.6, pp. 277-283.

Kulkarni R.P. (1973) "Effect of Structure on Properties of Marine Clay", Proc. 8th ICSMFE Moscow, Vol.1, pp.217-220.

Law K.T. (1979) "Triaxial-Vane Tests on a Soft Marine Clay", Can. Geot. Journal 16, pp. 11-18.

Lee H. J. (1985) "State of the Art: Laboratory Determination of the Strength of Marine Soils", Strength testing in marine sediments and in-situ measurements, ASTM STP 883, Philadelphia, pp. 181-250.

Leroueil S., Tavenas F. and Le Bihan J.P. (1983) "Proprietes Caracteristiques des Argiles de l'Est du Canada", Can. Geot. Journal 20, pp. 681-705.

Locat J. and Demers D. (1988) "Viscosity, Yield Strength, Remolded Strength, and Liquidity Index Relationships for Sensitive Clays", Can. Geot. Journal 25, pp. 799-806.

Locat J., Berube M.A. and Chagnon J.Y. (1985) "The Mineralogy of Sensitive Clays in Relation to Some Engineering Geology Problems - An Overview", Applied Clay Science, Vol.1, No.1/2, pp. 193-205.

Lord E.R.F. and Cameron R. (1985) " Compaction Characteristics of Athabasca Tar Sand", 38th Can. Geot. Conf., Theory and Practice in Foundation Engineering, Edmonton, Alberta, September, pp. 359-366.

Lund S.T. (1985) "Consolidation Behavior of Oil Sand Tailings Mixtures", B.Sc. Thesis, University of Waterloo, Ontario, 56p.

MacKinnon M.D. (1989) "Development of the Tailings Pond at Syncrude's Oil Sand Plant: 1978-1987", AOSTRA Journal of Research, Vol.5, No.2, pp. 109-132.

MacKinnon M.D. (1991) Personal Communication.

Mahmoud M. (1988) "Vane Testing in Soft Clays", Ground Engineering, October, pp. 36-40.

Menzies B.K., Mailey L.K. (1976) "Some Measurements of Strength Anisotropy in Soft Clays Using Diamond Shaped Shear Vanes", Geotechnique 26, No.3, pp. 535-538.

Menzies B.K., Merrifield C.M. (1980) "Measurements of Shear Stress Distribution on the Edges of a Shear Vane Blade", Technical Note, Geotechnique 30, No.3, pp. 314-318.

Mewis J. (1979) "Thixotropy - A General Review", J. of Non-Newtonian Fluid Mechanics, Vol.6, No.1, pp. 1-20.

Migliore H.J. and Lee H.J. (1971) "Seafloor Penetration Test: Presentation and Analysis of Results", Naval Civ. Eng. Laboratory Technical Note N-1178,Port Hueneme, CA, 60p.

Mitchell J.K. (1960) "Fundamental Aspects of Thixotropy in Soils", J. Soil Mechanics Foundations Div., ASCE, Vol.86, SM 3, pp. 19-52.

Monney N.T. (1974) "Deep-Sea Sediments, Physical and Mechanical Properties", A. L. Inderbitzen, Ed., Plenum Press, New York, 1974, pp. 151-168.

Moretto O. (1948) "Effect of Natural Hardening on the Unconfined Compressive Strength of Remolded Clays", Proc. 2nd ICSMFE, Rotterdam, Vol.1, pp.137-144.

Osipov V.I., Nikolaeva S.K. and Sokolov V.N. (1984) "Microstructural Changes Associated with Thixotropic Phenomena in Clay Soils", Geotechnique 34, No.3, pp. 293-303.

Osterberg J.O. (1956) Introduction, Symposium on Vane Shear Testing of Soils, ASTM STP 193.

Outtrim C.P. and Evans R.G. (1978) "Alberta's Oil Sands Reserves and Their Evaluation", In Redford D.A. and Winestosck A.G. (eds), The Oil Sands of Canada-Venezuela, The Canadian Institute of Mining and Metallurgy , Special Vol.17, pp. 36-66.

Peacock D.H.L. (1988) "Gas Evolution in Athabasca Oil Sands", M.Sc. Thesis, University of Alberta, Edmonton.

Perlow M. and Richards A.F. (1977) "Influence of Shear Velocity on Vane Shear Strength", J. Geotech. Eng. Div., ASCE 103, GT1, pp. 19-32.

Pollock G.W. (1988) "Large Strain Consolidation of Oil Sand Tailings Sludge", M.Sc. Thesis, University of Alberta, Edmonton.

Richards A.F., Palmer H.D. and Perlow M. (1975) "Review of Continental Shelf Marine Geotechnics: Distribution of Soils, Measurements of Properties and Environmental Hazards", Marine Geotechnology 1, No.1, pp. 33-68.

Roberts J.O.L., Yong R.N. and Erskine H.L. (1980) "Surveys of Some Tar Sand Sludge Ponds: Results and Interpretations", Proc. of Applied Oilsands Geoscience Conf., Editor: M.B. Dusseault, University of Alberta, 44p.

Rosen M.R. and Foster W.W. (1978) "Approximate Rheological Characterization of Casson Fluids", Journal of Coatings Technology, Vol.50, No. 643, August, 10p.

Schmertmann J.H. (1975) "Measurement of In Situ Shear Strength", Proc. of ASCE Conf. In Situ Measurements of Soil Properties, Raleigh, Vol.2, p. 57.

Scott J.D. (1987) "Pore Water Pressures and Solids in the Pond", Letter to J. Coward, Syncrude Research, Nov. 3.

Scott J.D. and Chichak M.F. (1985a) "Large Sludge Stand Pipe Consolidation Test 1", Progress Report to February, 1985. Sludge Stand Pipe Testing Contract Agreement C2919-55 for Syncrude Canada Ltd., June, 60p.

Scott J.D. and Chichak M.F. (1985b) "Large Sludge Stand Pipe Consolidation Test 2", Final Report. Sludge Stand Pipe Testing Contract Agreement C4884-55 for Syncrude Canada Ltd., June, 62p.

Scott J.D. and Chichak M.F. (1985c) "Large Sludge Stand Pipe Consolidation Test 3", Progress Report to september, 1985. Sludge Stand Pipe Testing Contract Agreement C4884-55 for Syncrude Canada Ltd., June, 46p.

Scott J.D. and Cymerman G.J. (1984) "Prediction of Viable Tailings Disposal Methods", Proc. Symp.: Sedimentation Consolidation Models, ASCE, San Francisco, California, Oct. 1, 1984, pp. 522-544.

Scott J.D. and Dusseault M.B. (1980) "Behaviour of Oil Sands Tailings", Proc. of the 33rd Can. Geot. Conf., Calgary, Alberta, 33p.

Scott J.D. and Dusseault M.B. (1981) "Disposal of Oil Sands Tailings Sludge", Proc. of the 34th Can. Geot. Conf., Fredericton, N. B., 17p.

Scott J.D. and Dusseault M.B. (1982) "Behaviour of Oil Sands Tailings Sludge", 33rd Ann. Tech. Meeting of the Can. Inst. of Mining and Metallurgy, Calgary, Alberta, June, Paper No. 82-33-85, 20p.

Scott J.D. and Kosar K.M. (1984) "Geotechnical Properties of Athabasca Oil Sands", Paper Presented at WRI-DOE Tar Symp, Vail, Colorado, June 26-29, 1984, 32 p.

Scott J.D., Dusseault M.B. and Carrier III W.D. (1985) "Behavior of the Clay/Bitumen/Water Sludge System from Oil Sands Extraction Plants", Journal of Applied Clay Science, Vol.1, No.2, July, pp. 207-218.

Scott J.D., Dusseault M.B. and Carrier III W.D. (1986) "Large Scale Self-Weight Consolidation Testing", Consolidation of Soils: Testing and Evaluation. ASTM STP 892, Philadelphia, pp. 500-515.

Seed H.B. and Chan C.K. (1957) "Thixotropic Characteristics of Compacted Clays", J. Soil Mechanics Foundations Div., ASCE, Vol.83, SM 4, pp. 1-35.

Sherwood P.T. and Ryley M.D. (1970) "An Investigation of a Cone-Penetrometer Method for the Determination of the Liquid Limit", Geotechnique 20, No.2, pp. 203-208.

Skempton A.W. and Northey R.D. (1952) "The Sensitivity of Clays", Geotechnique 3, No.1, pp. 30-53.

Smith A.D. and Richards A.F. (1976) "Vane Shear Strength at Two High Rotation Rates", Civil Engineering in the Oceans/III, ASCE, pp. 421-423.

Sridharan A. and Venkatappa Rao G. (1973) "Mechanisms Controlling Volume Change of Saturated Clays and the Role of the Effective Stress Concept", Geotechnique 23, 3, p. 359.

Streeter V.L. and Wylie E.J. (1981) "Fluid Mechanics", McGraw-Hill Ryerson Limited.

Takamura K. (1982) "Microscopic Structure of Athabasca Oil Sands", Can. Journal of Chem. Eng., Vol.60, pp. 538-545.

Vesic A.S. (1972) "Expansion of Cavities in Infinite Soil Mass", ASCE 98, SM3, p.265.

Wiesel C.E.R. (1973) "Some Factors Influencing In Situ Vane Tests Results", Proc. of 8th ICSMFE Moscow, vol.1, pp. 475-479.

Wilson N.E. (1963) "Laboratory Vane Shear Tests and the Influence of Pore Water Stresses", ASTM STP 361.

Whorlow R.W. (1980) "Rheological Techniques", Ellis Horwood Limited, Market Cross House, England.

Yong R.N., Sheeran D.E., Sethi A.J. and Erskine H.L. (1982) "The Dynamics of Tar-Sand Tailings", Paper Presented at 33rd Ann. Tech. Meeting of Can. Inst. of Mining and Metallurgy, Calgary, June 1982, Paper No. 82-33-42, 6p.

APPENDIX A. Viscosity Test Plots

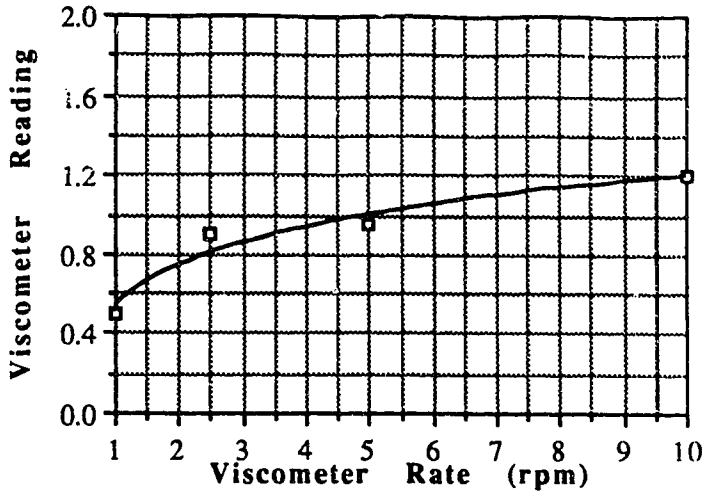

Figure A.1 Viscosity Test V40000M

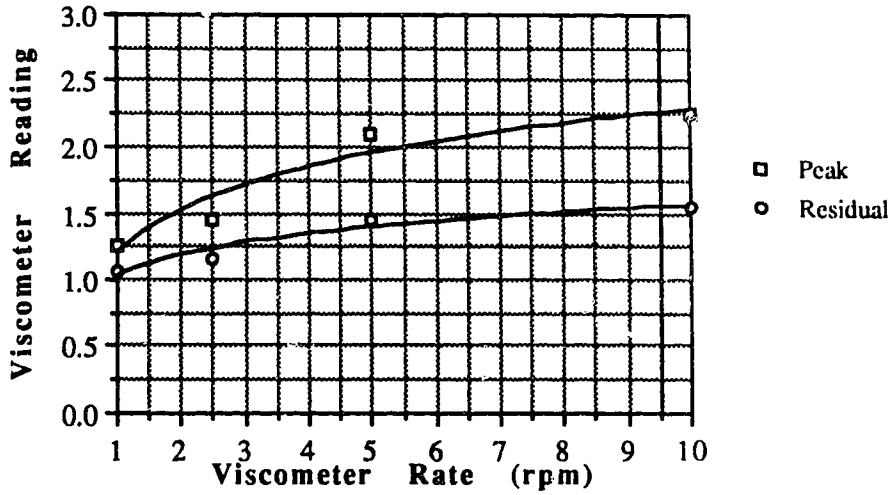

Figure A.2 Viscosity Test V40005M

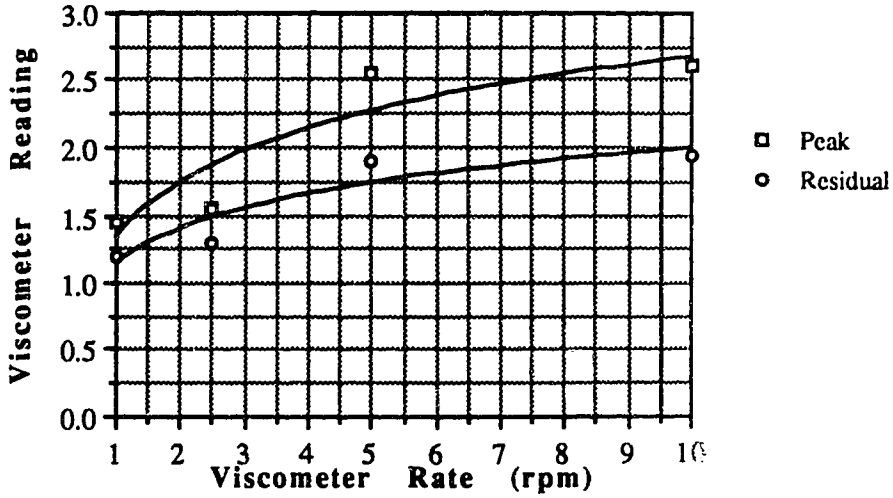

Figure A.3 Viscosity Test V40010M

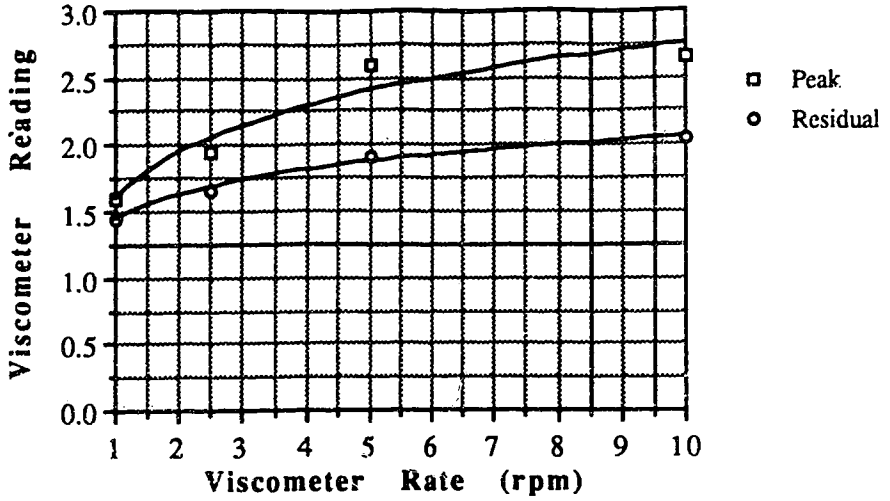

Figure A.4 Viscosity Test V40020M

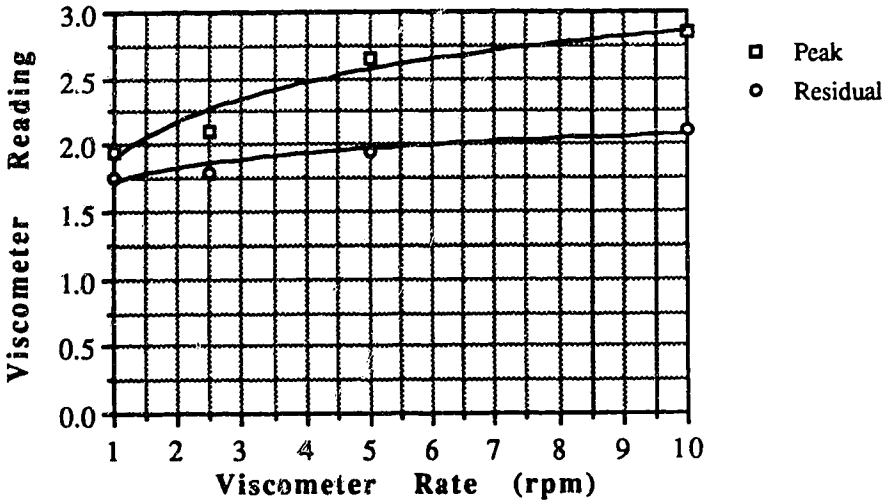

Figure A.5 Viscosity Test V40030M

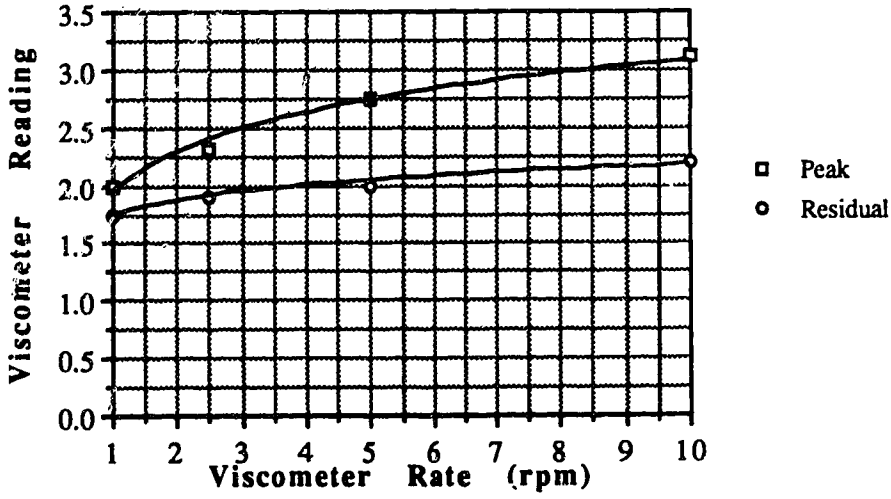

Figure A.6 Viscosity Test V40001H

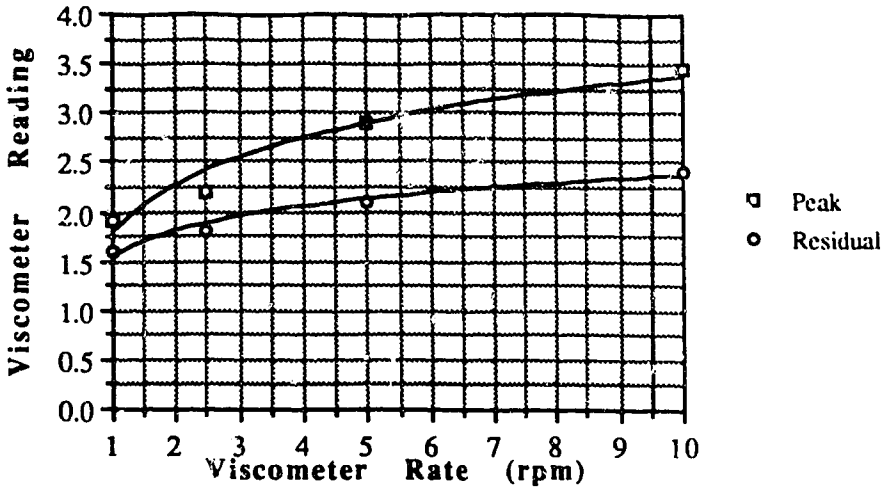

Figure A.7 Viscosity Test V40002H

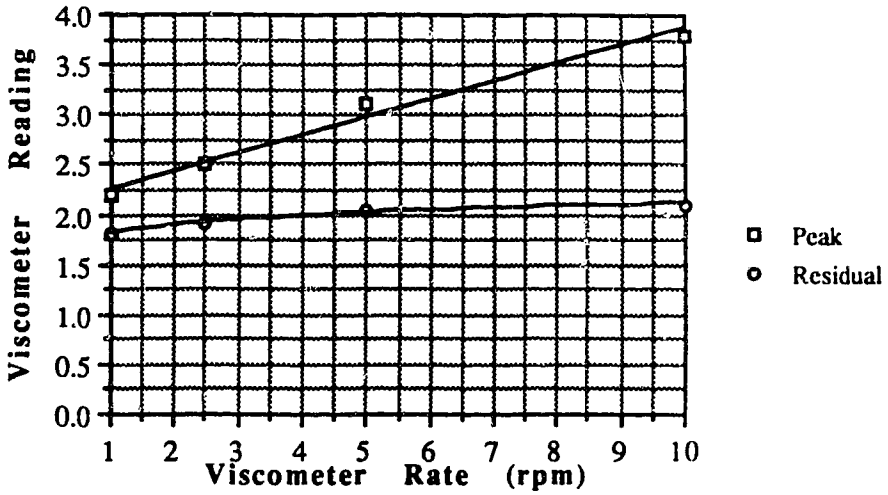

Figure A.8 Viscosity Test V40003H

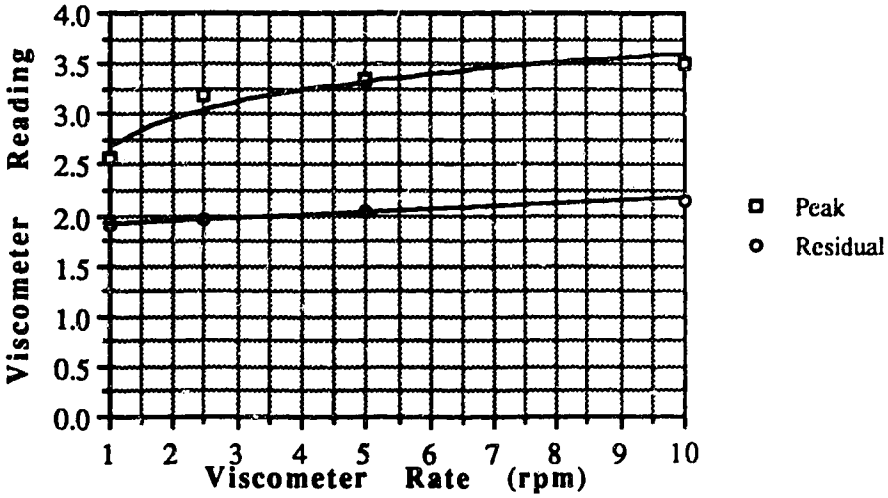

Figure A.9 Viscosity Test V40004H

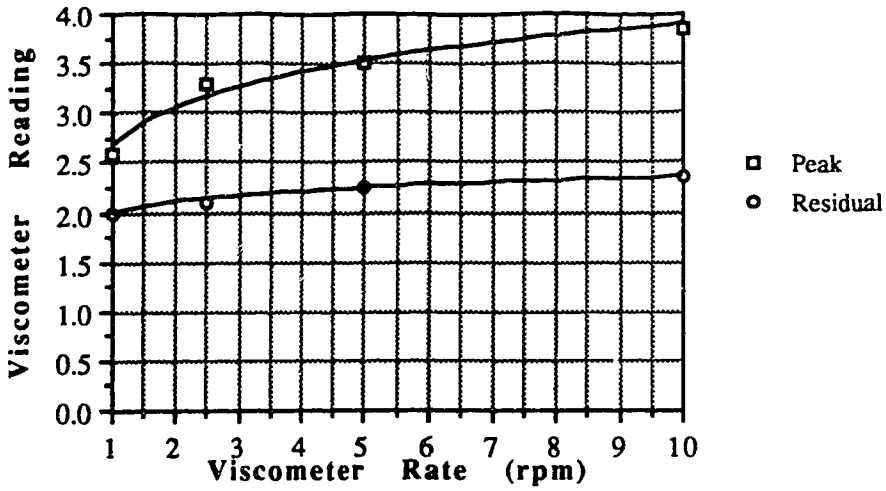

Figure A.10 Viscosity Test V40008H

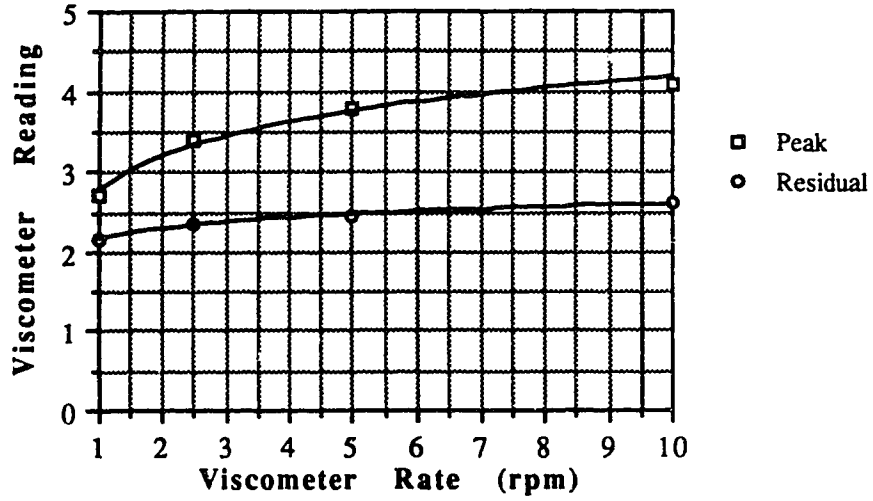

Figure A.11 Viscosity Test V40012H

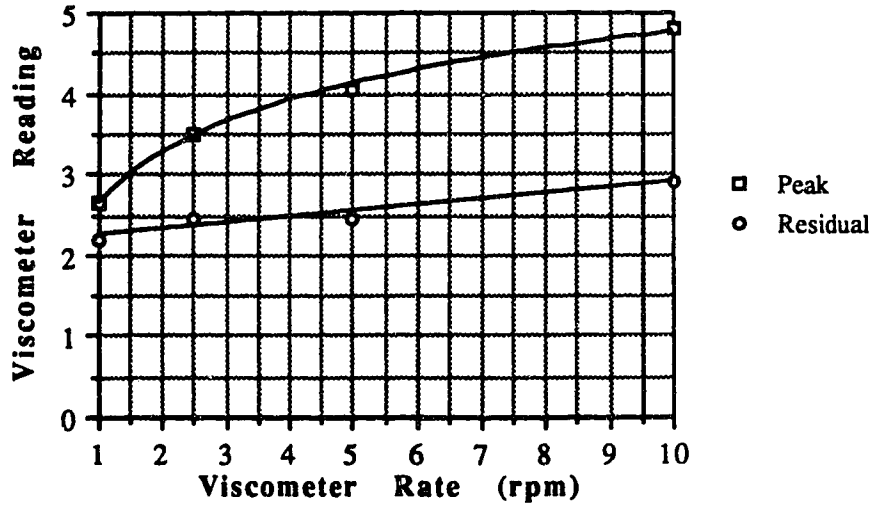

Figure A.12 Viscosity Test V40018H

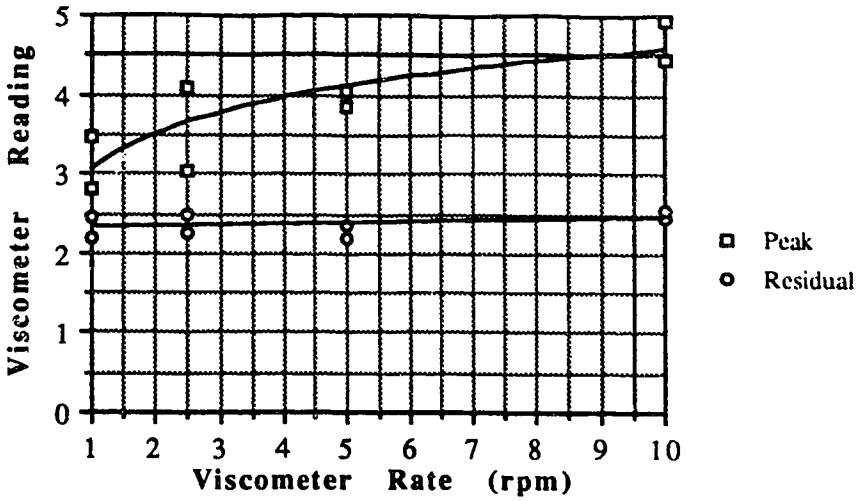

Figure A.13 Viscosity Test V40024H

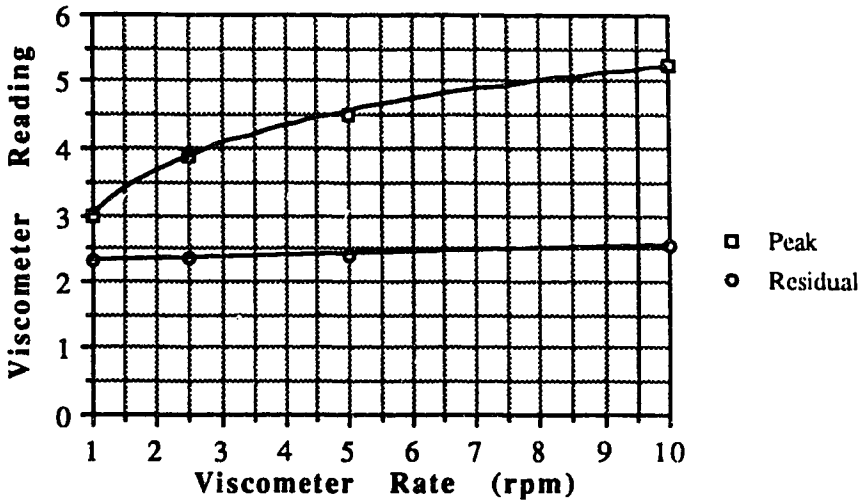

Figure A.14 Viscosity Test V40002D

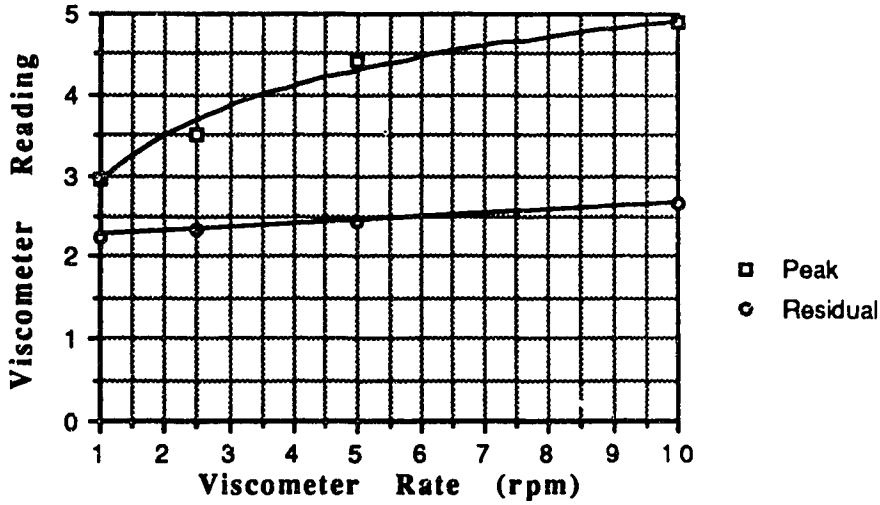

Figure A.15 Viscosity Test V40003D

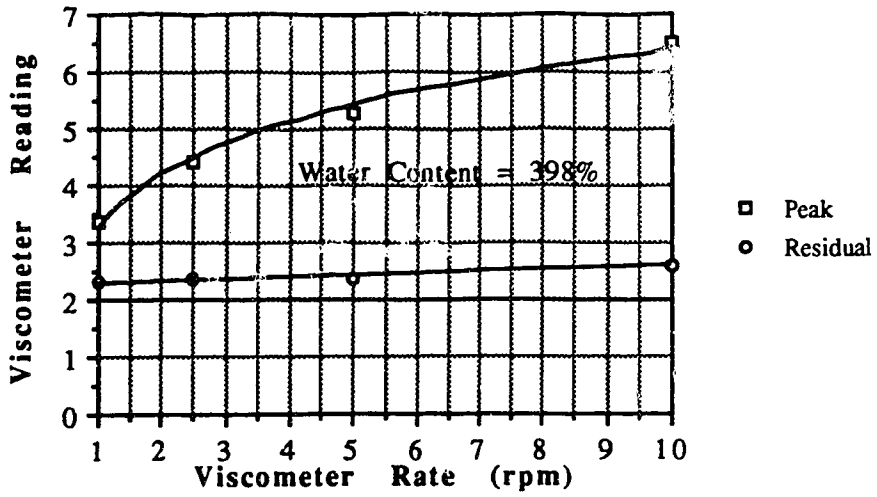

Figure A.16 Viscosity Test V40004D

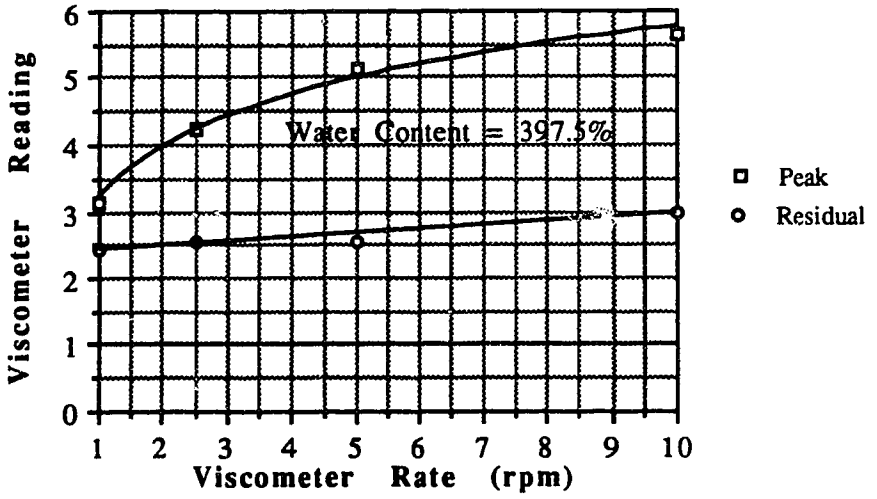

Figure A.17 Viscosity Test V40005D

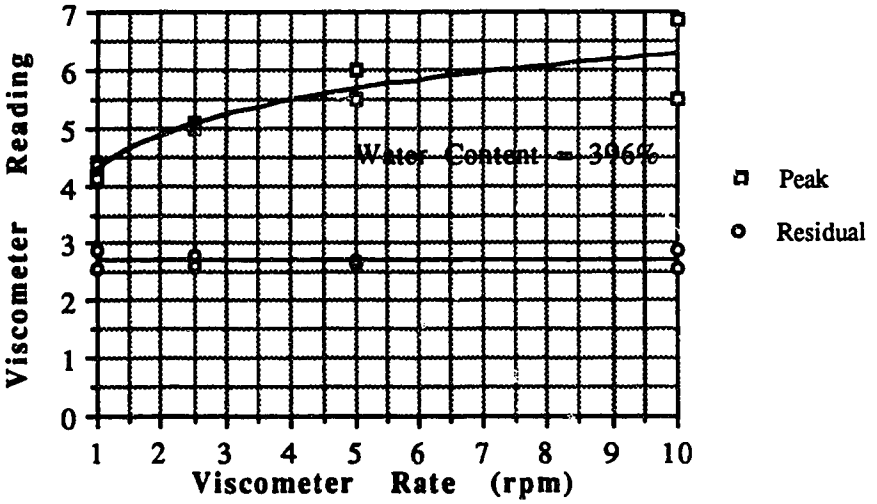

Figure A.18 Viscosity Test V40010D

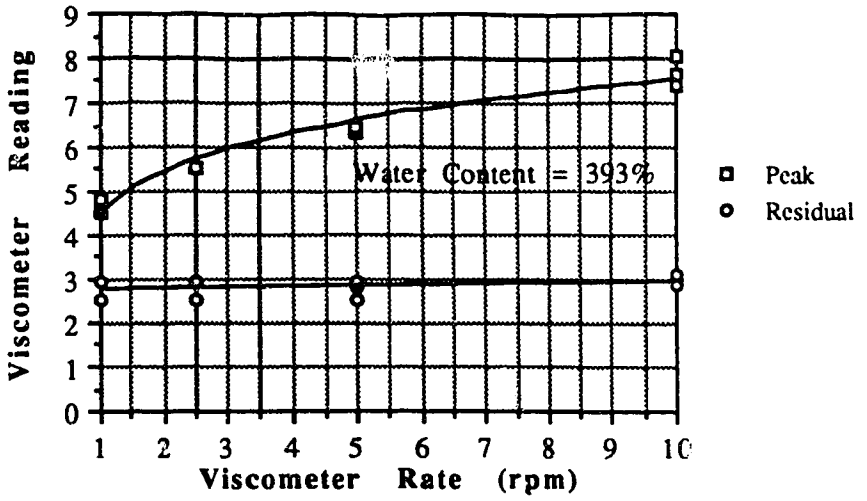

Figure A.19 Viscosity Test V40020D

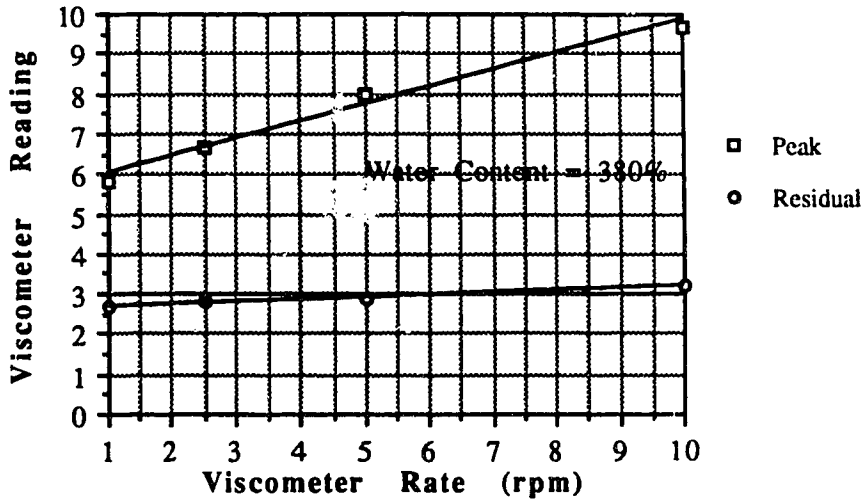

Figure A.20 Viscosity Test V40033D

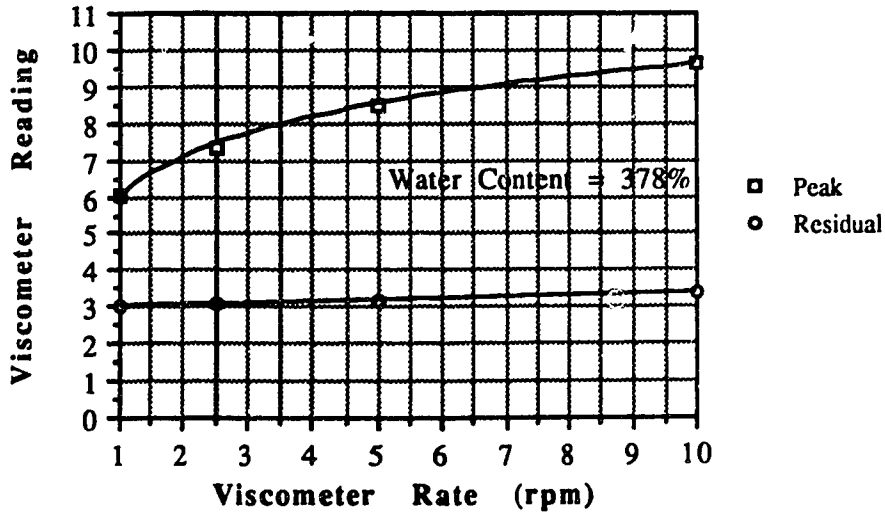

Figure A.21 Viscosity Test V40040D

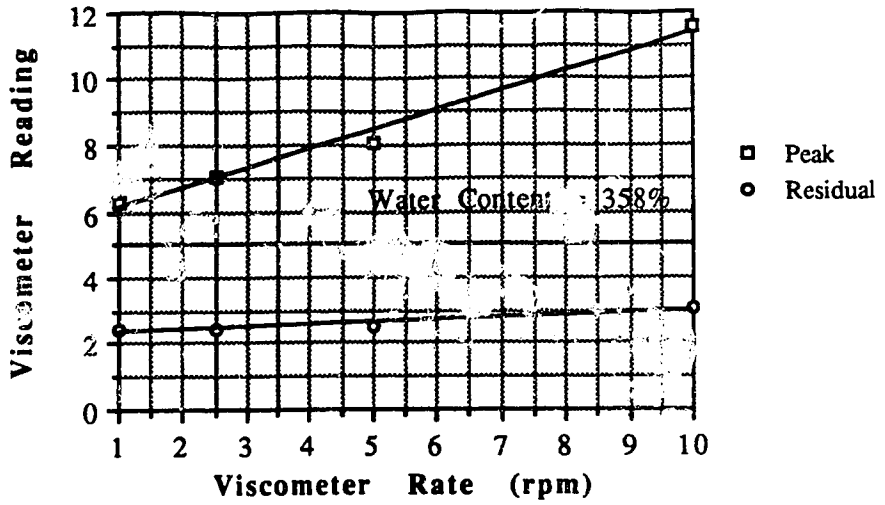

Figure A.22 Viscosity Test V40064D

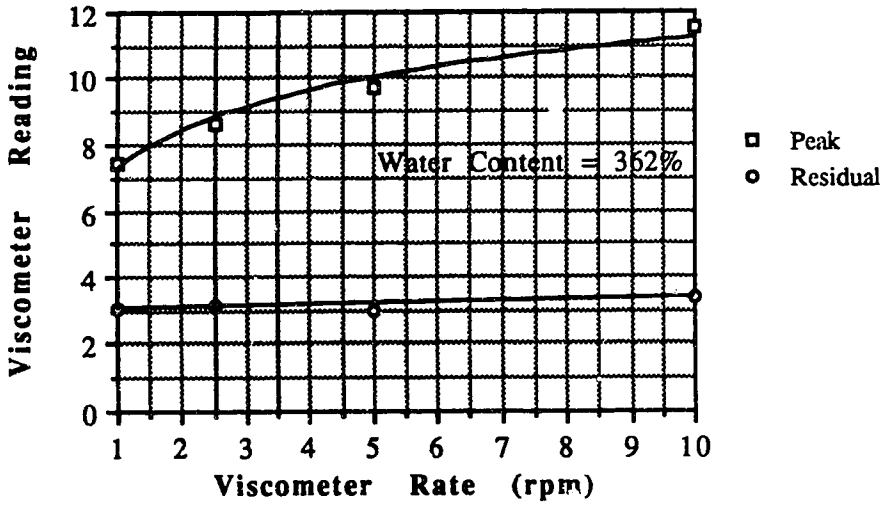

Figure A.23 Viscosity Test V40070D

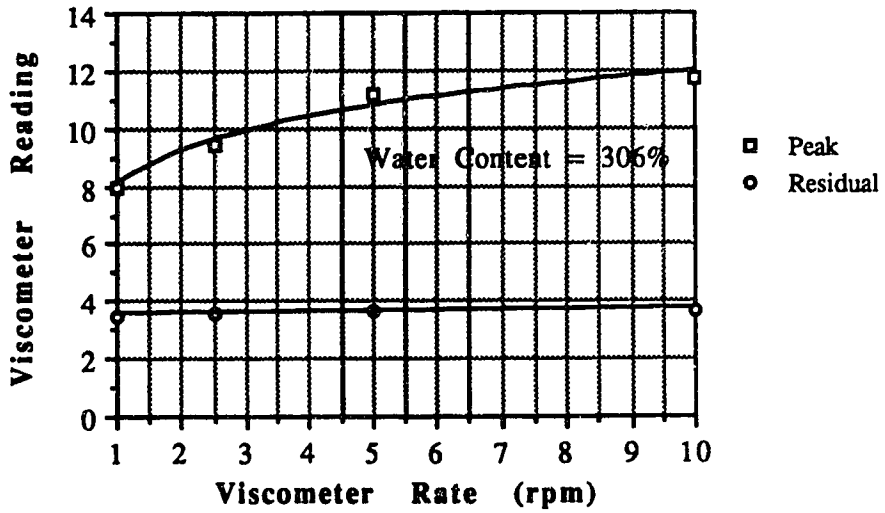

Figure A.24 Viscosity Test V40160D

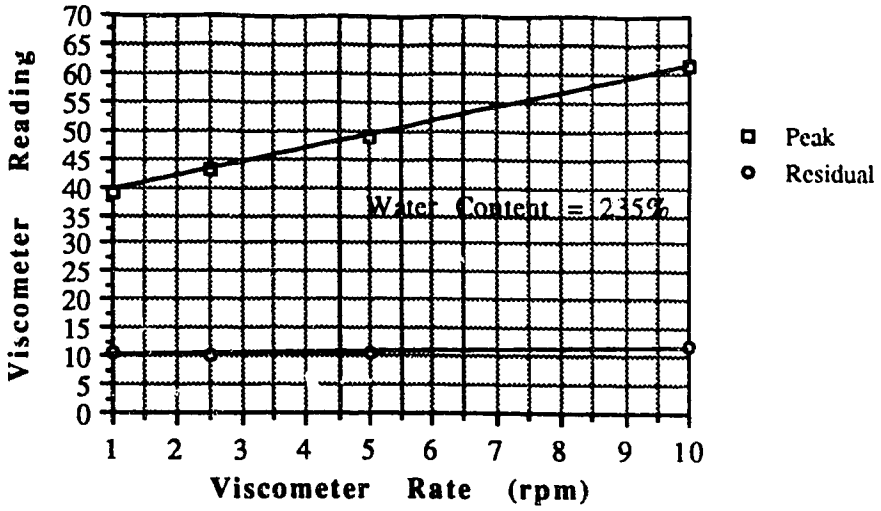

Figure A.25 Viscosity Test V40470D

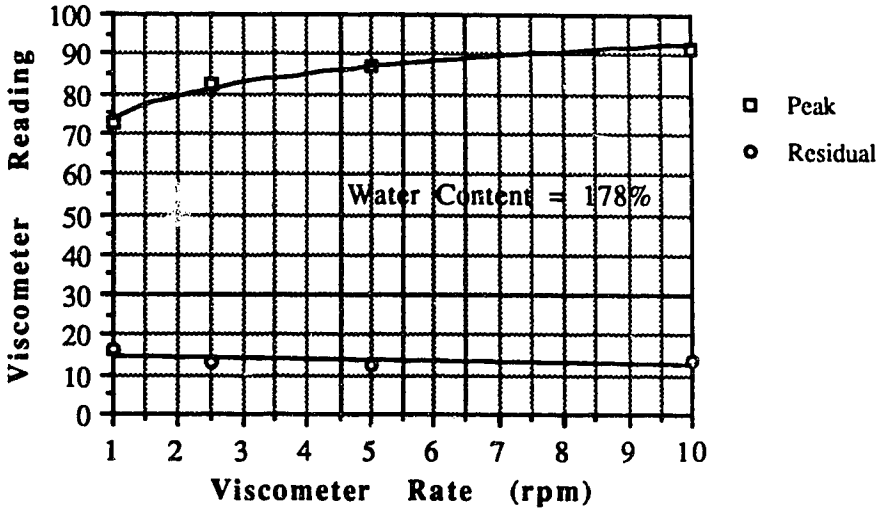

Figure A.26 Viscosity Test V40680D

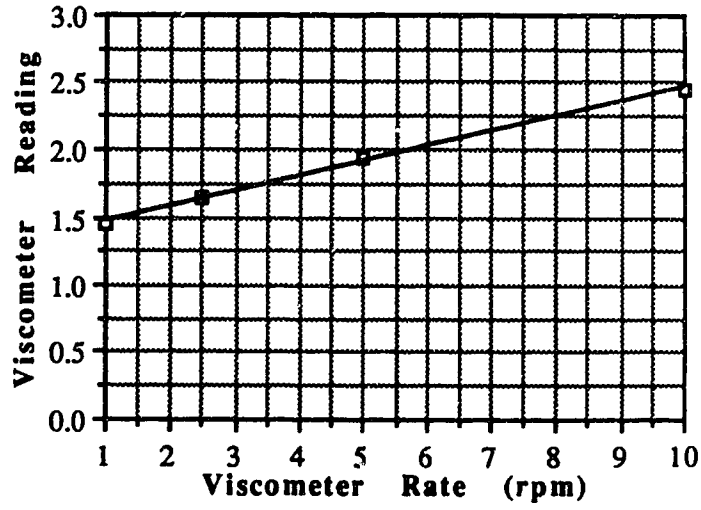

Figure A.27 Viscosity Test V30000M

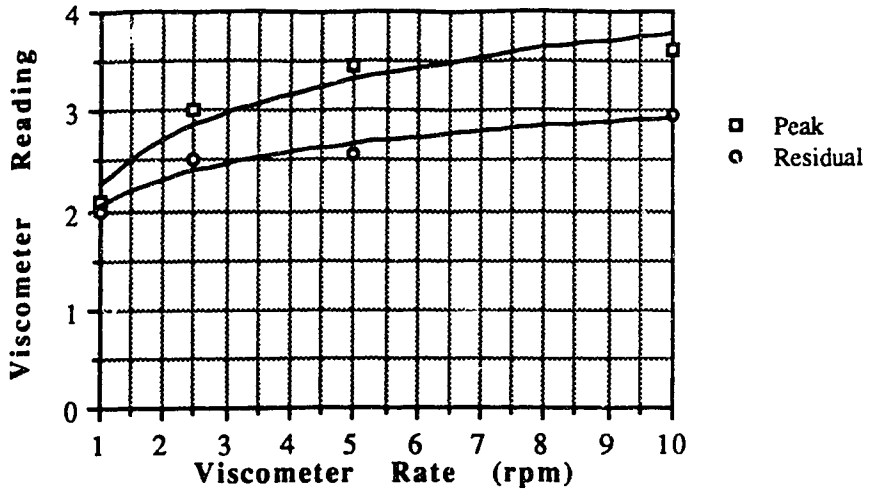

Figure A.28 Viscosity Test V30005M

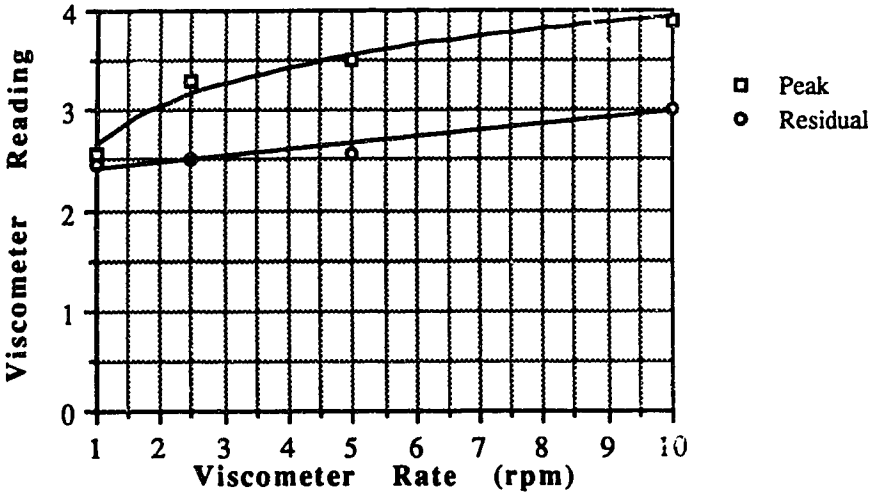

Figure A.29 Viscosity Test V30010M

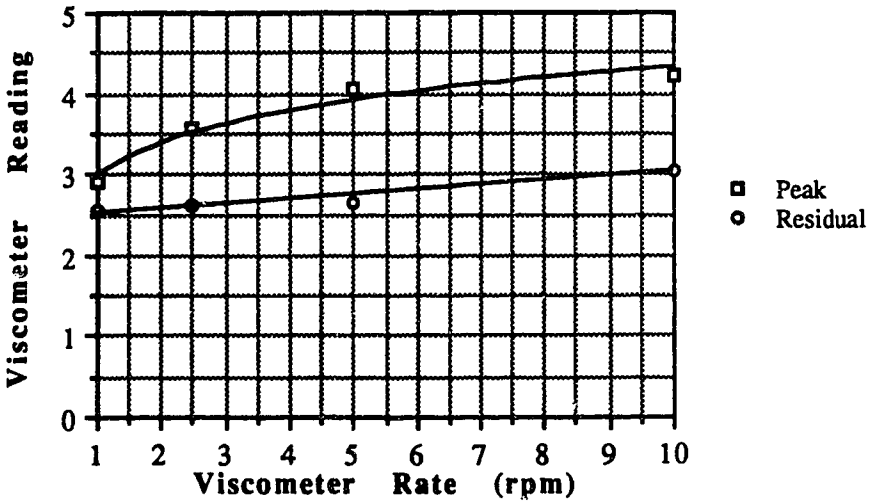

Figure A.30 Viscosity Test V30020M

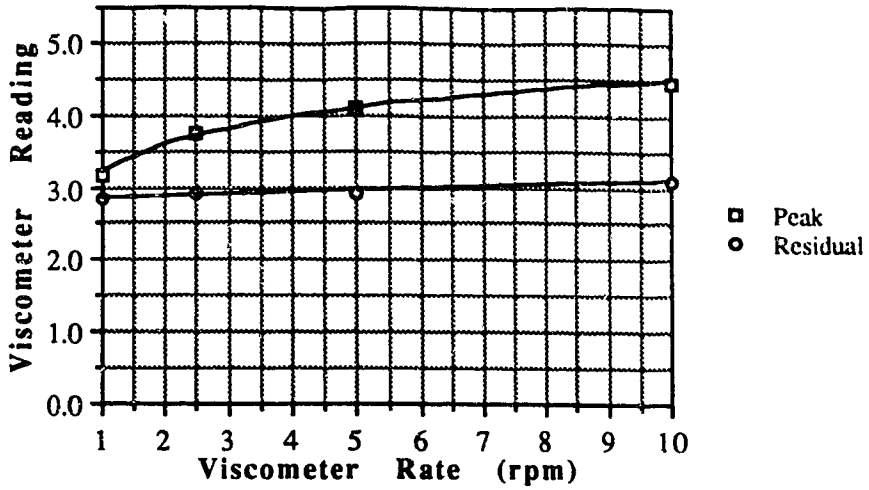

Figure A.31 Viscosity Test V30030M

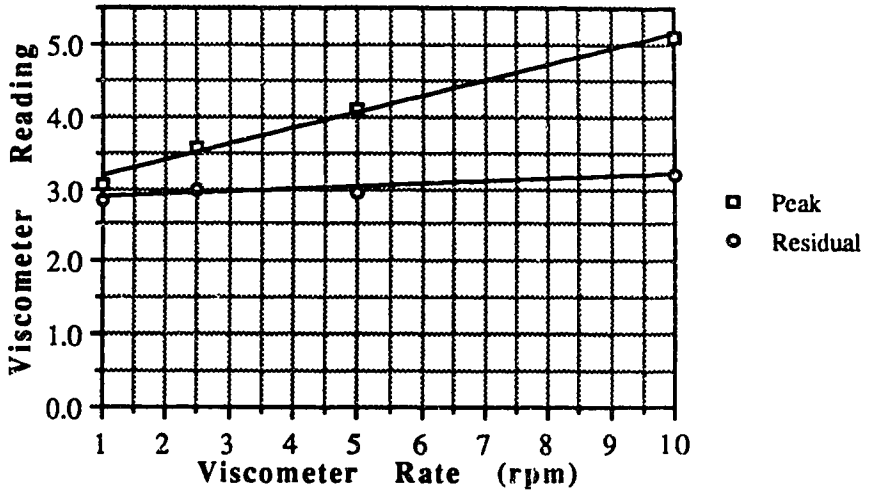

Figure A.32 Viscosity Test V30001H

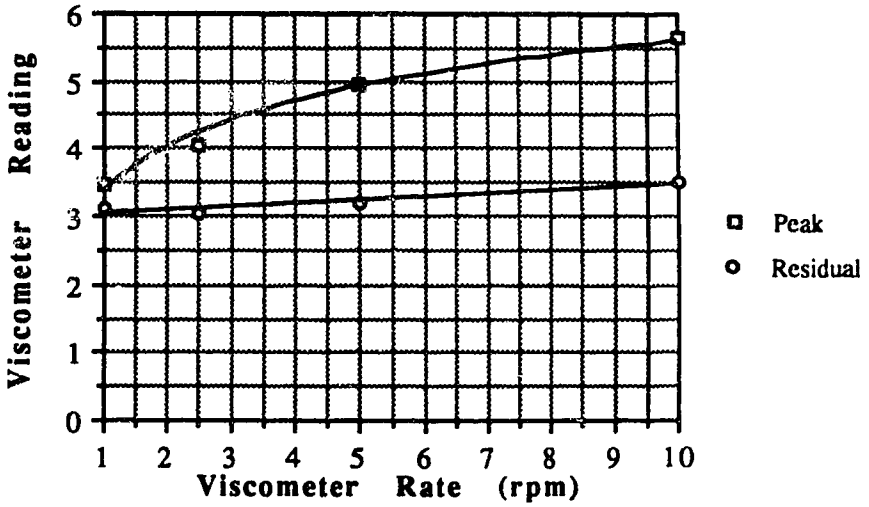

Figure A.33 Viscosity Test V30002H

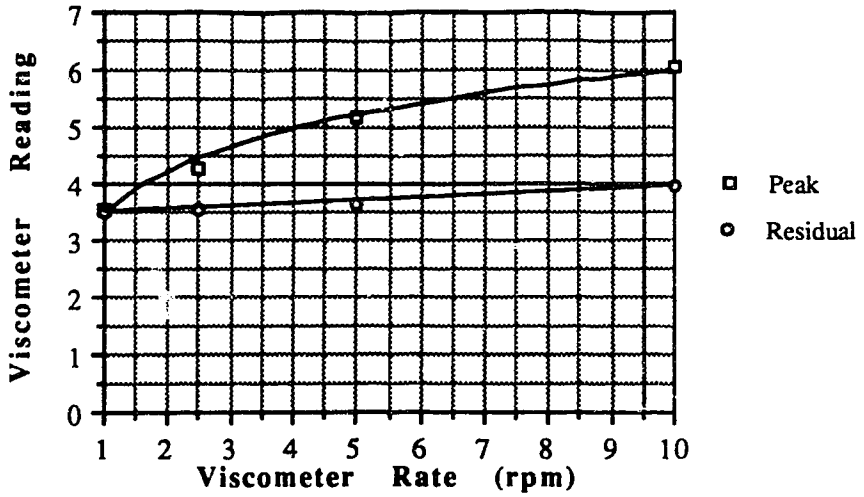

Figure A.34 Viscosity Test V30003H

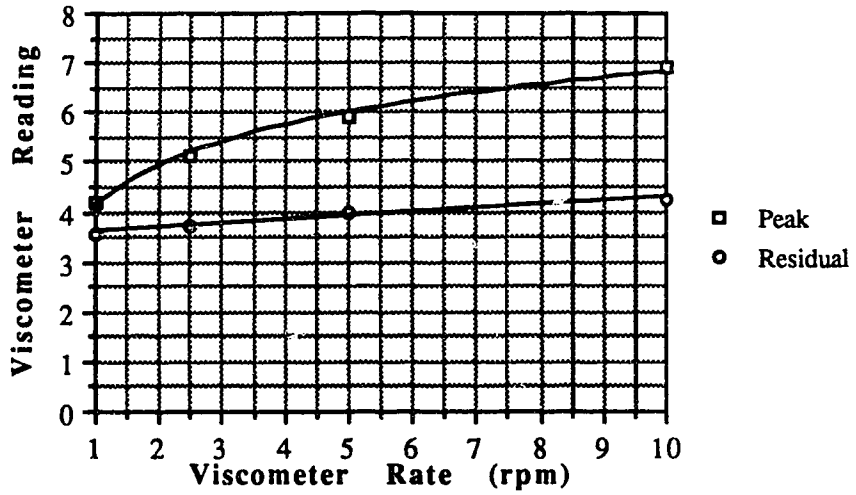

Figure A.35 Viscosity Test V30004H

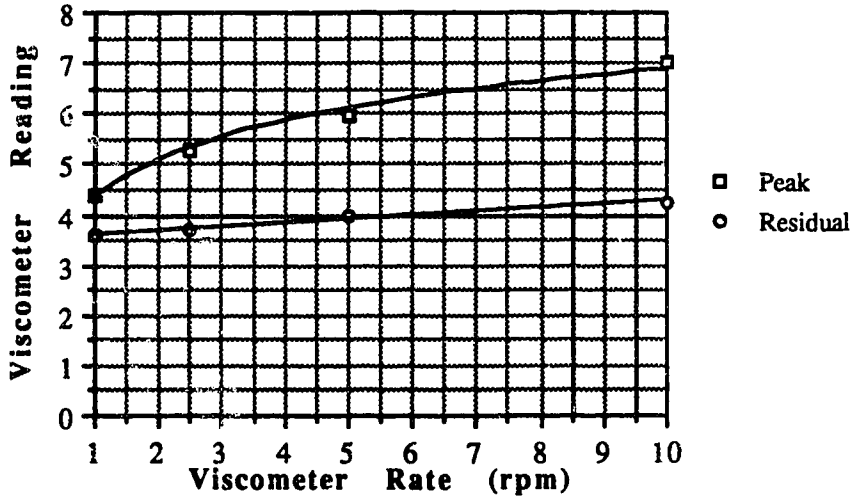

Figure A.36 Viscosity Test V30008H

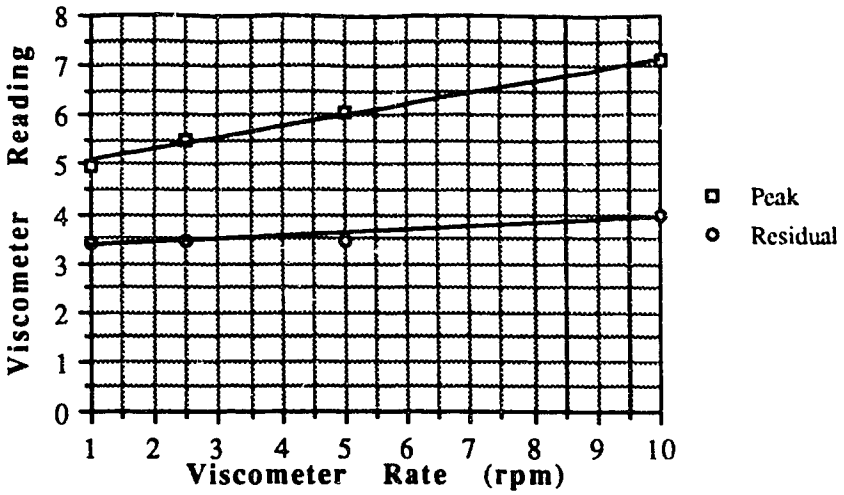

Figure A.37 Viscosity Test V30012H

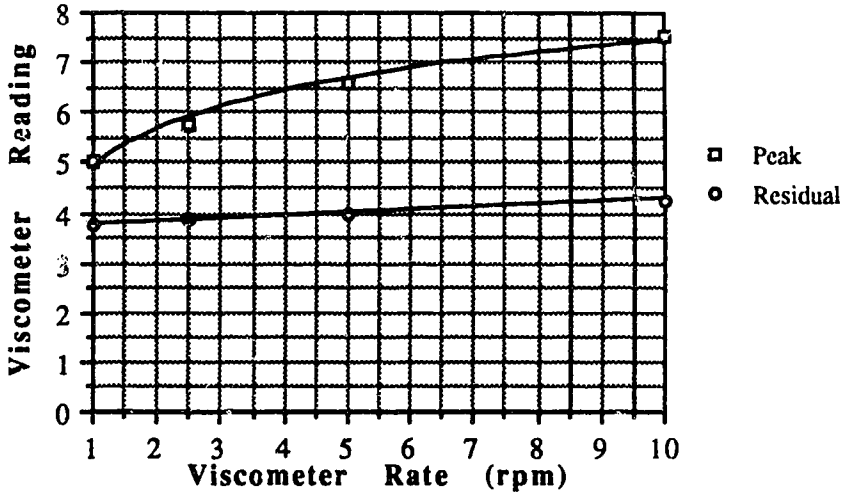

Figure A.38 Viscosity Test V30018H

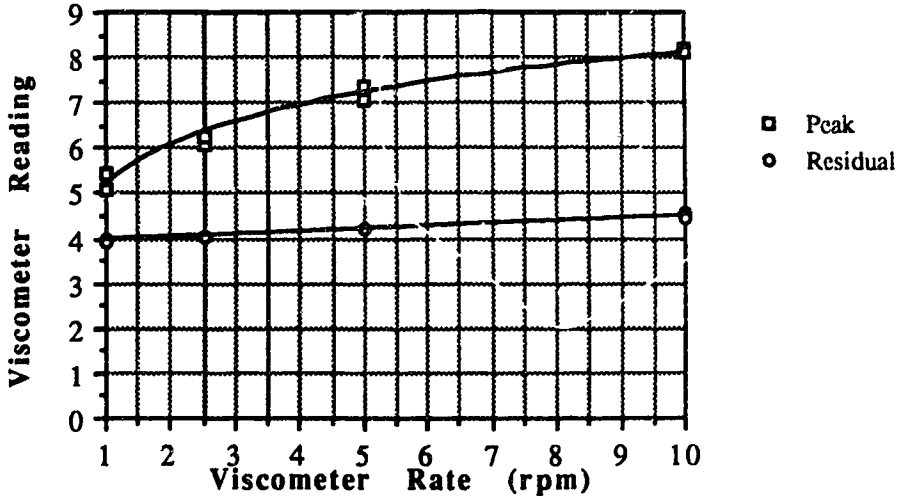

Figure A.39 Viscosity Test V30024H

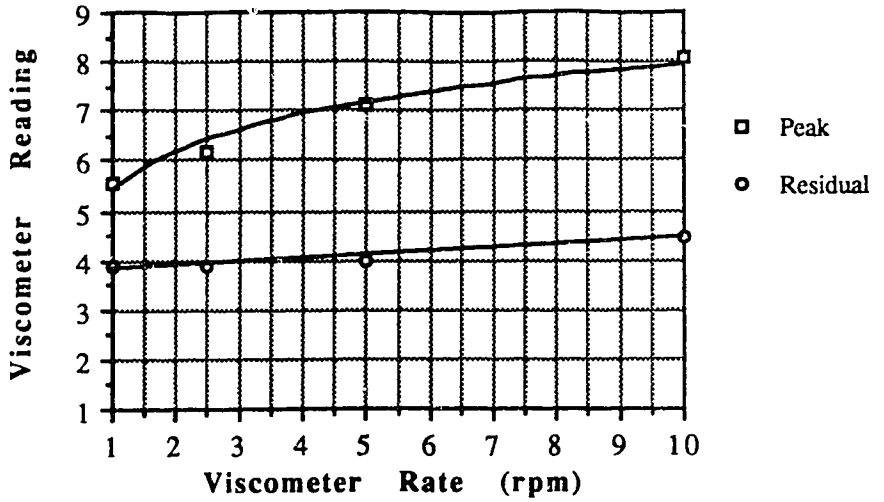

Figure A.40 Viscosity Test V30002D

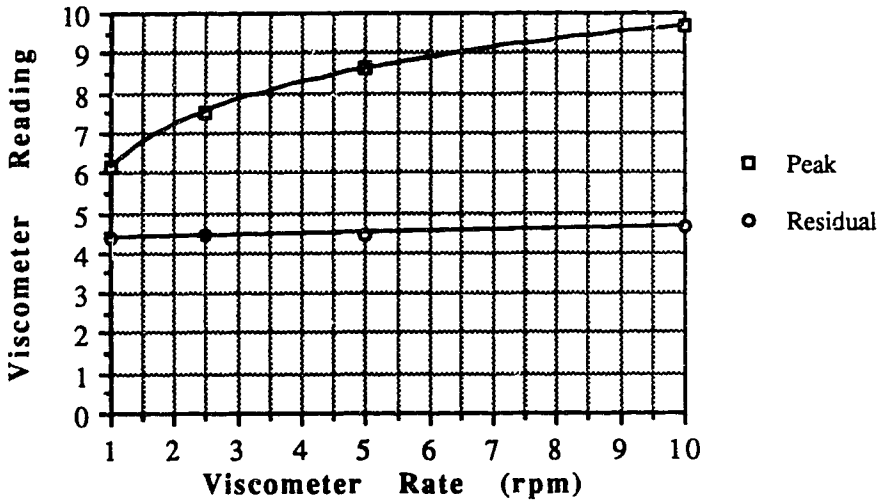

Figure A.41 Viscosity Test V30003D

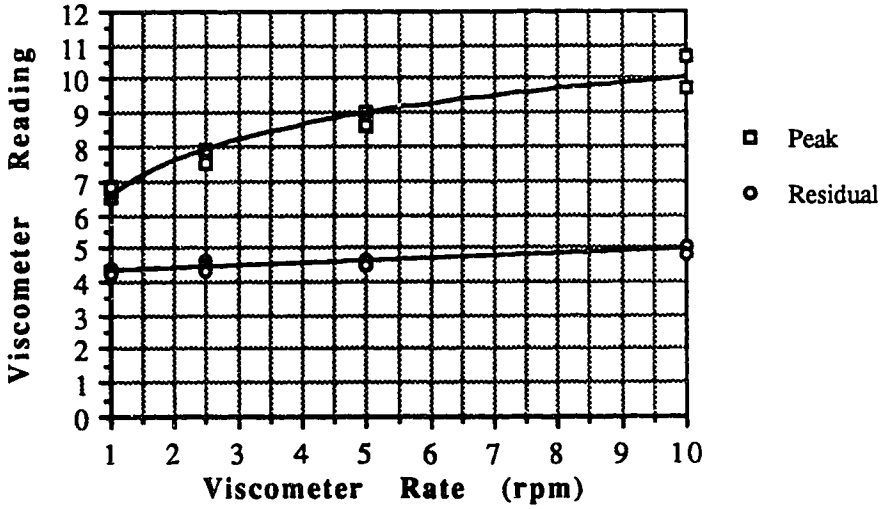

Figure A.42 Viscosity Test V30004D

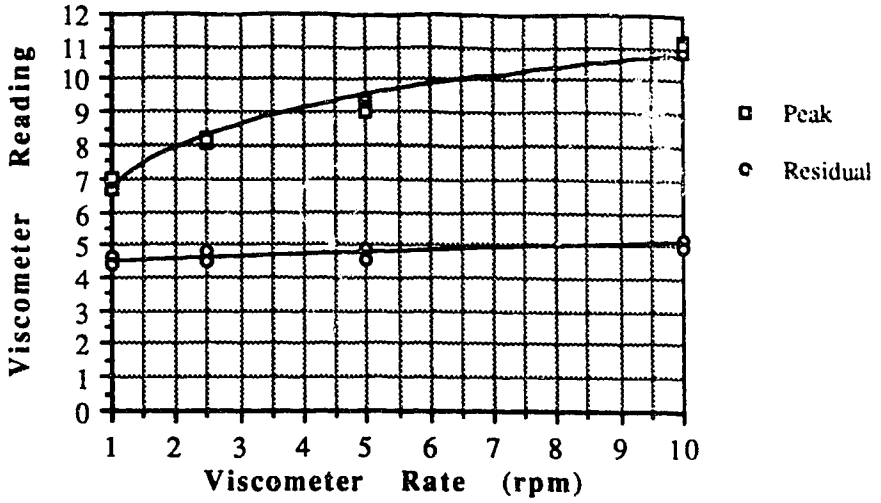

Figure A.43 Viscosity Test V30005D

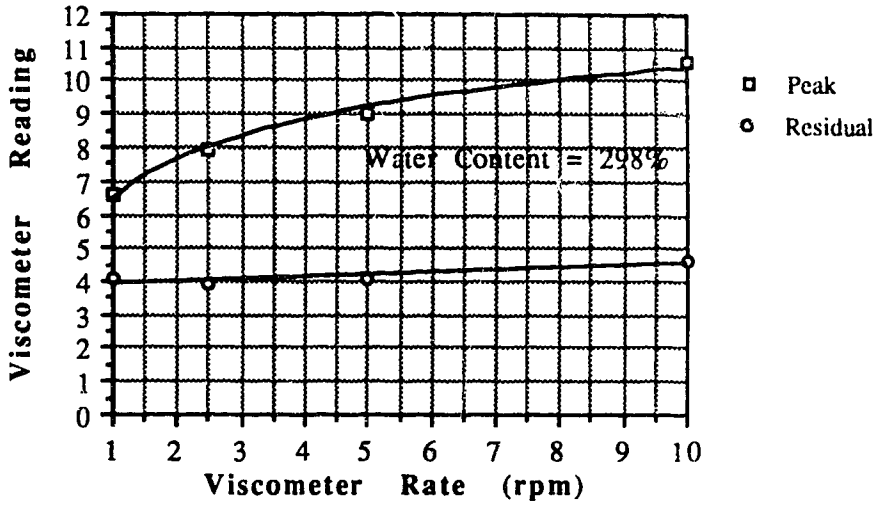

Figure A.44 Viscosity Test V30006D

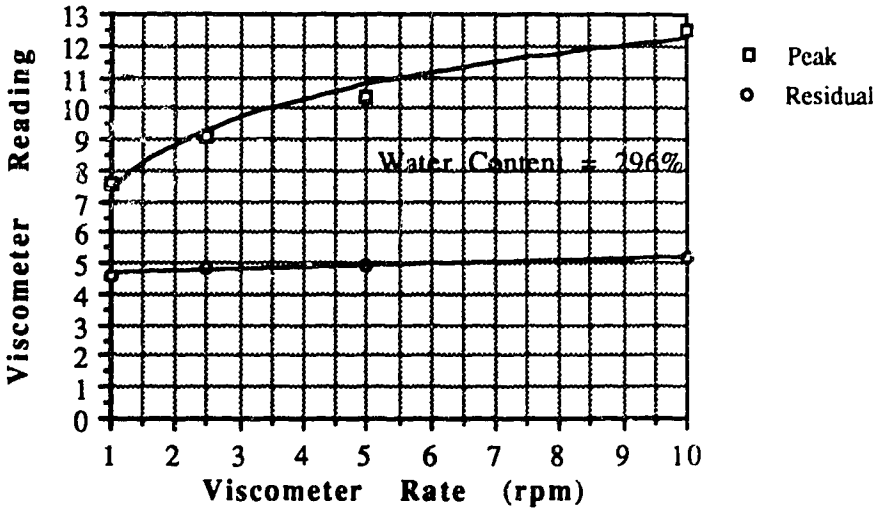

Figure A.45 Viscosity Test V30010D

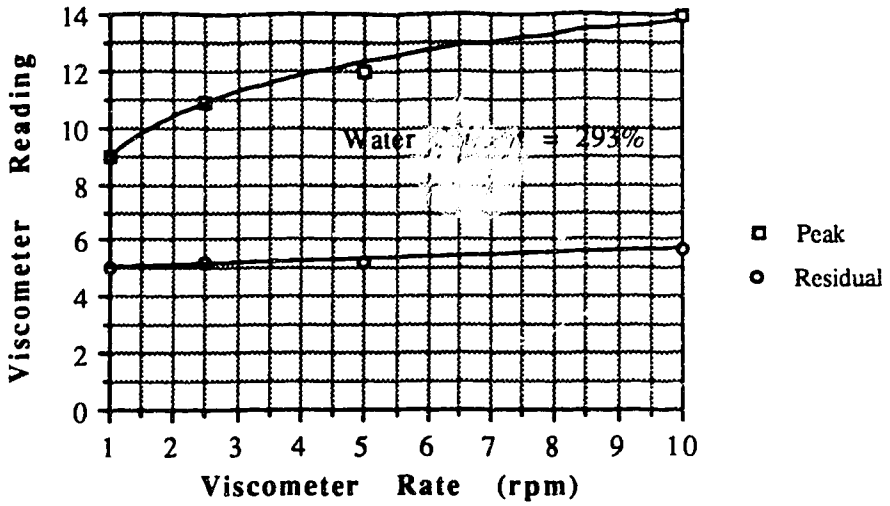

Figure A.46 Viscosity Test V30020D

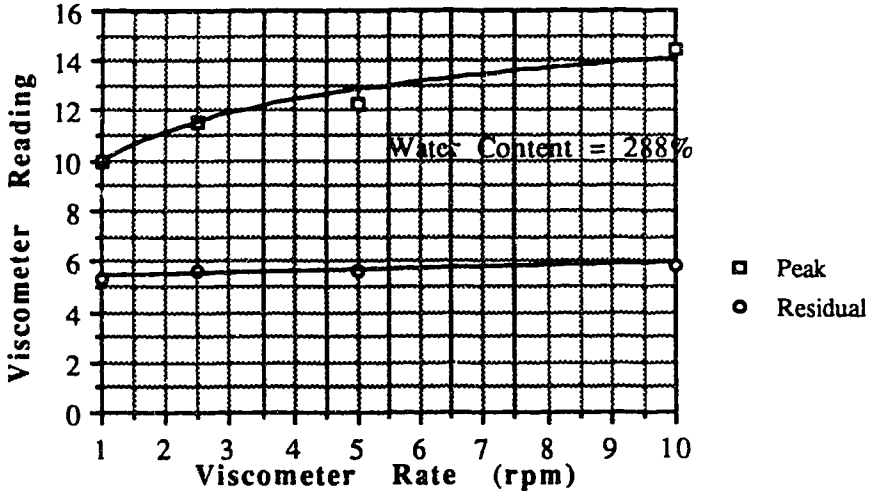

Figure A.47 Viscosity Test V30040D

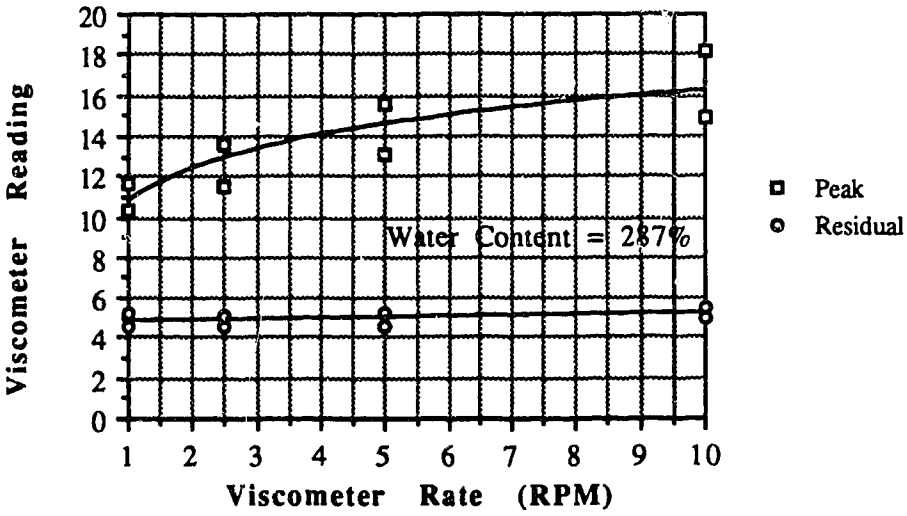

Figure A.48 Viscosity Test V30050D

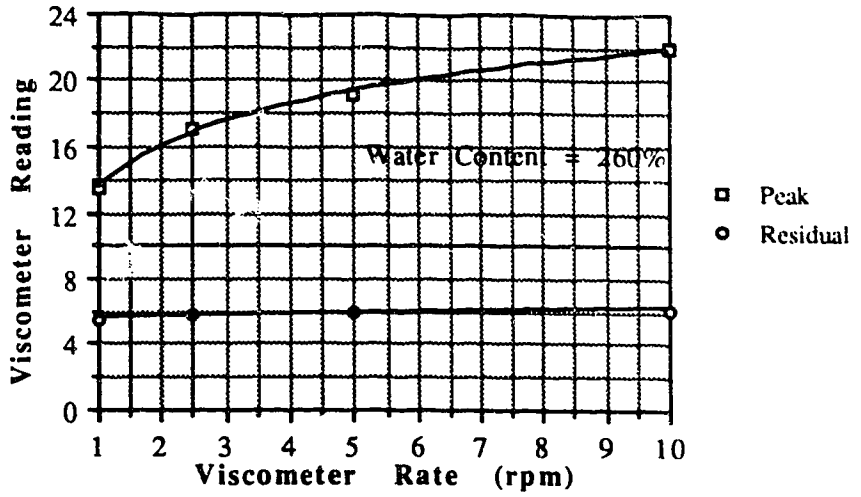

Figure A.49 Viscosity Test V30160D

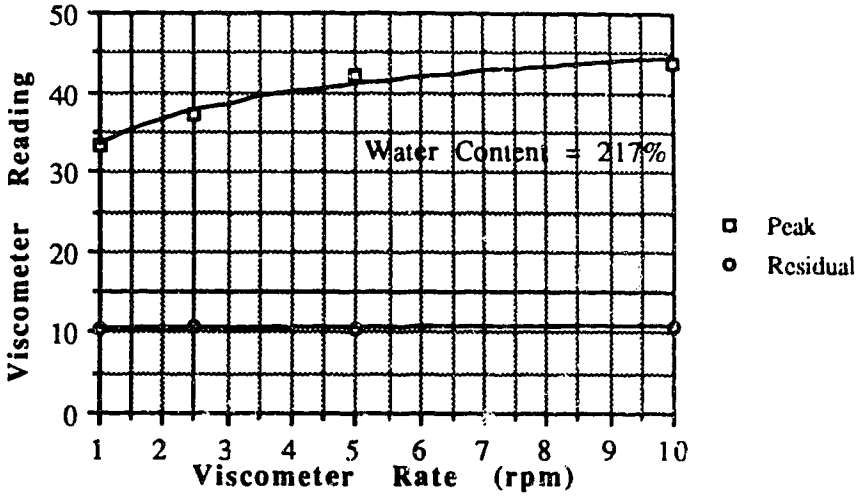

Figure A.50 Viscosity Test V30470D

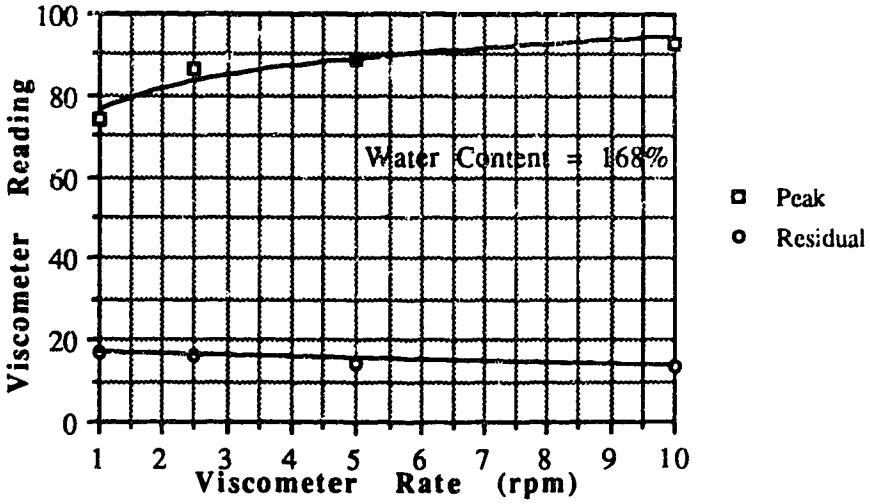

Figure A.51 Viscosity Test V30660D

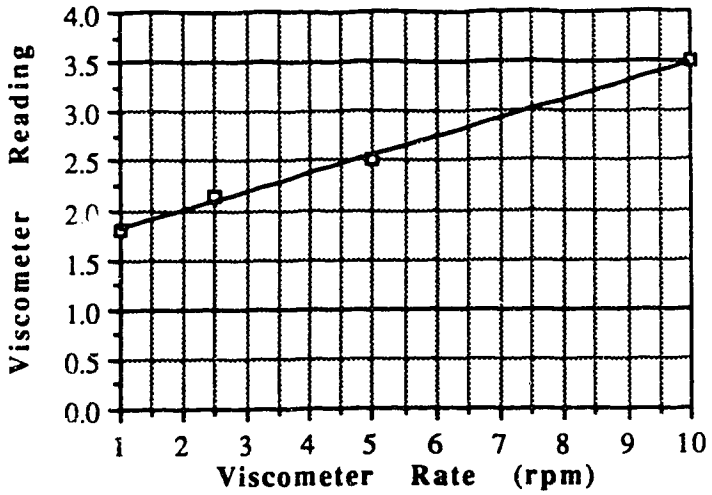

Figure A.52 Viscosity Test V23000M

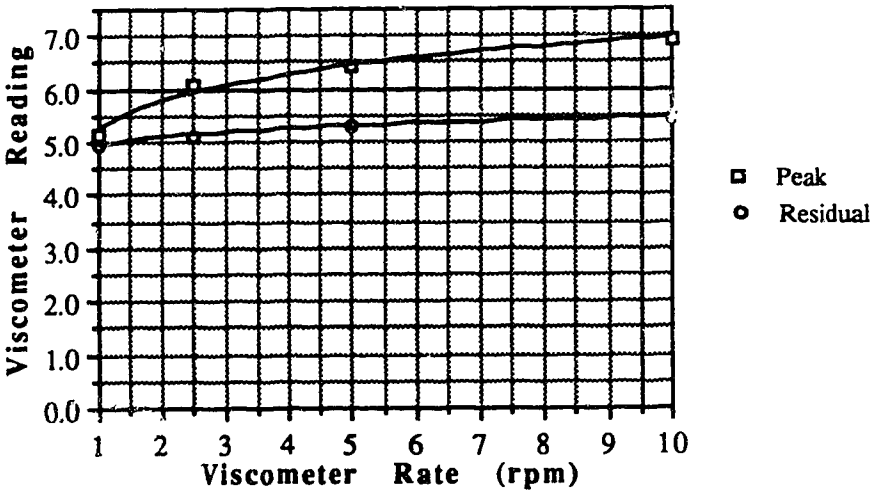

Figure A.53 Viscosity Test V23005M

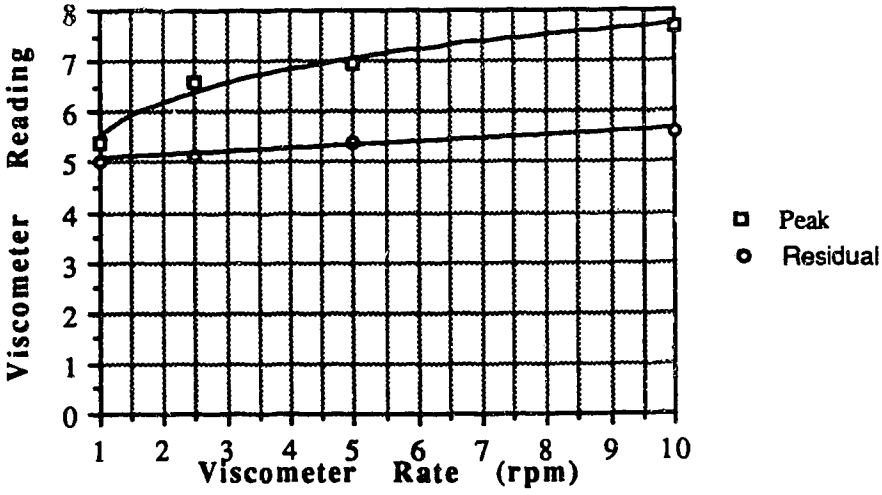

Figure A.54 Viscosity Test V23010M

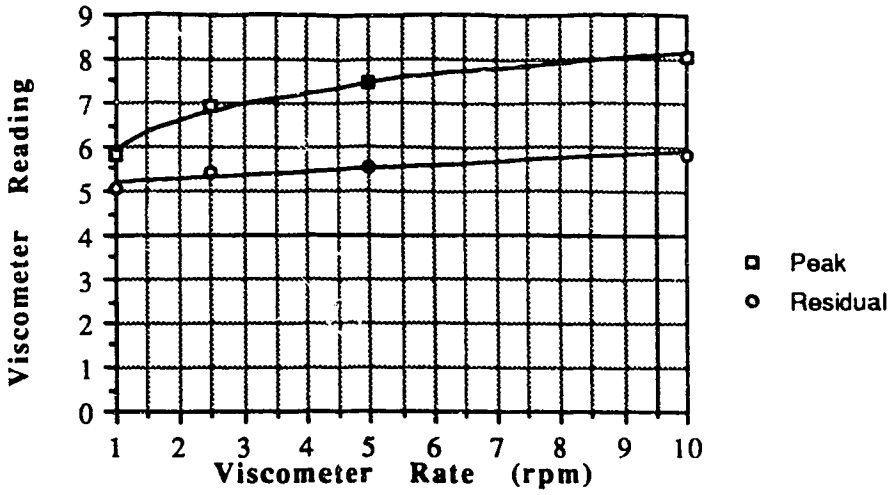

Figure A.55 Viscosity Test V23020M

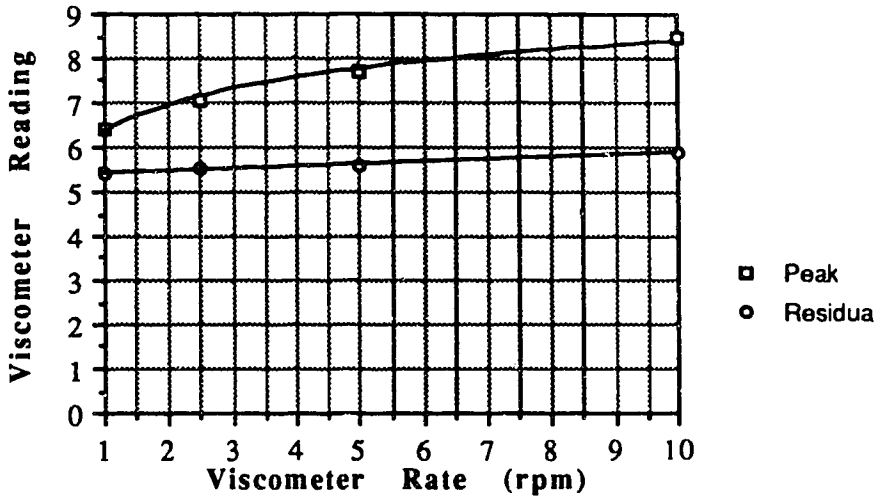

Figure A.56 Viscosity Test V23030M

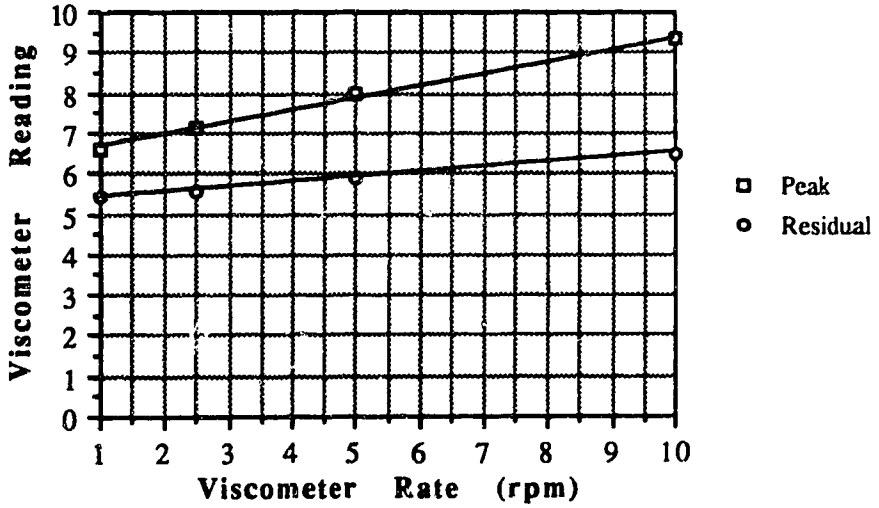

Figure A.57 Viscosity Test V23001H

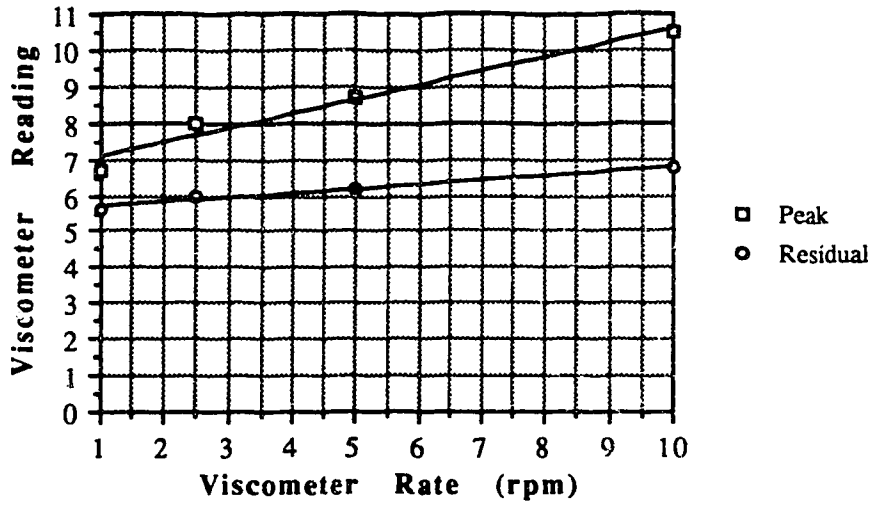

Figure A.58 Viscosity Test V23002H

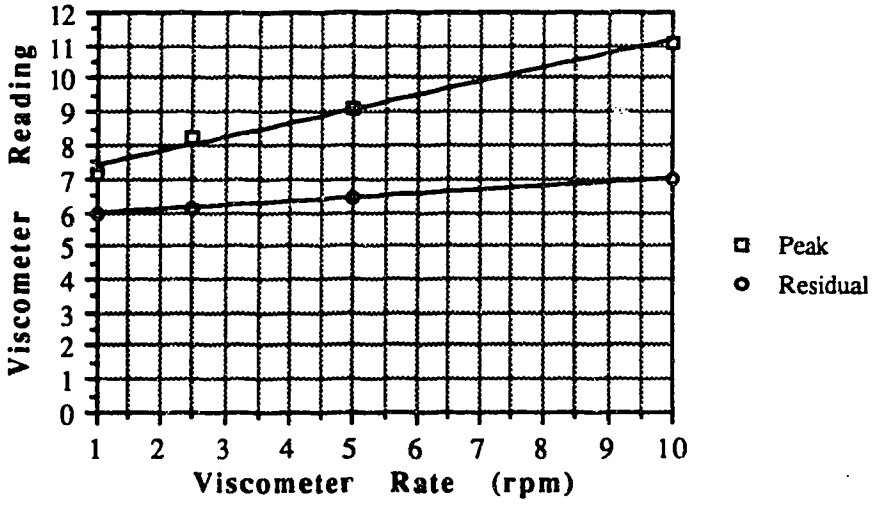

Figure A.59 Viscosity Test V23003H

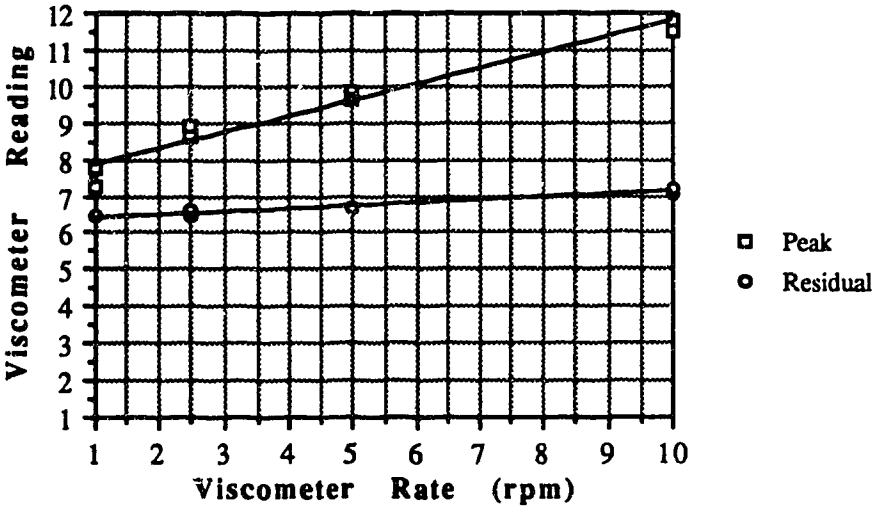

Figure A.60 Viscosity Test V23004H

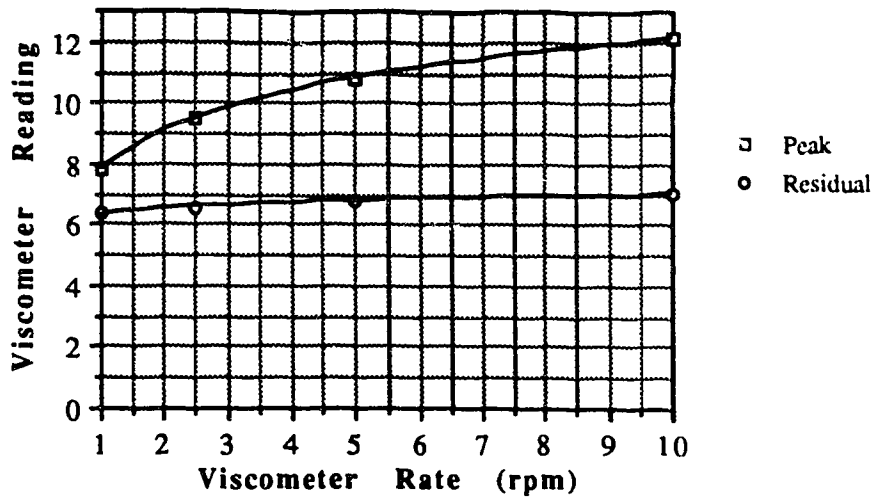

Figure A.61 Viscosity Test V23008H

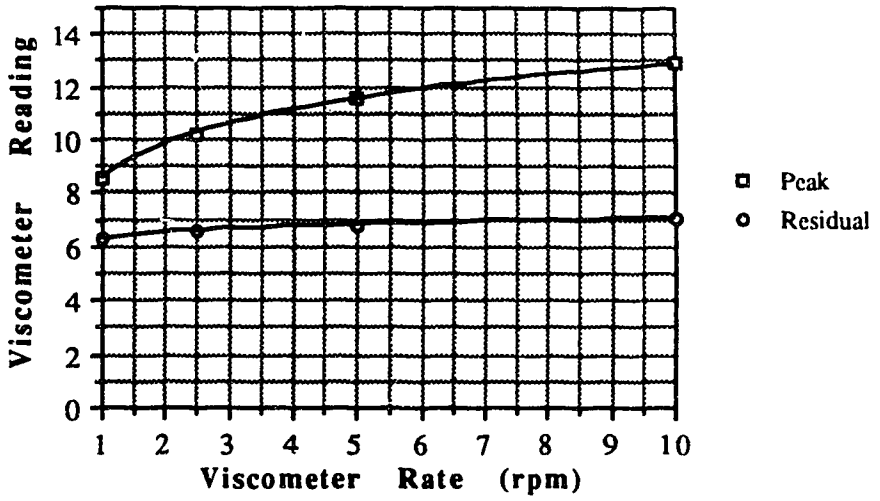

Figure A.62 Viscosity Test V23012H

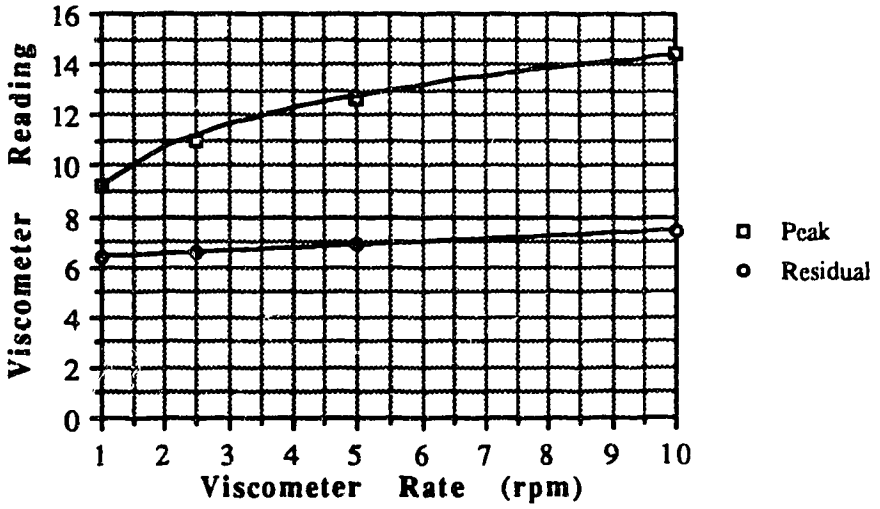

Figure A.63 Viscosity Test V23018H

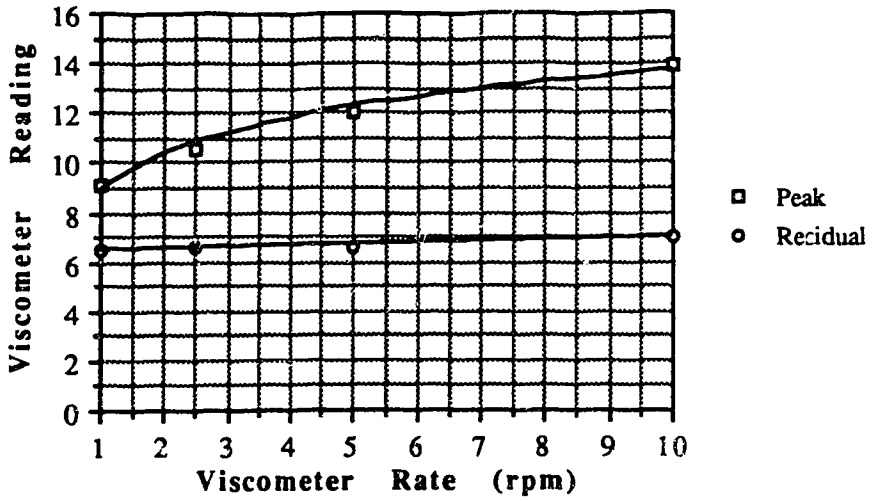

Figure A.64 Viscosity Test V23001D

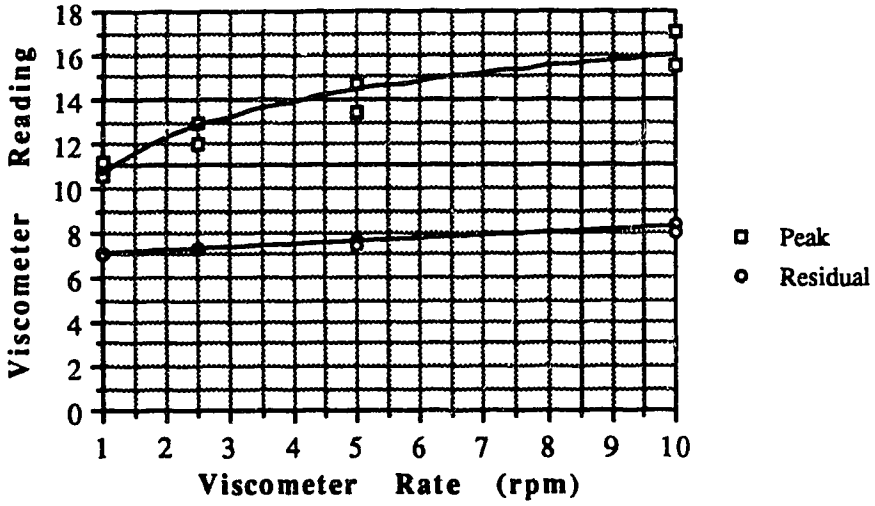

Figure A.65 Viscosity Test V23002D

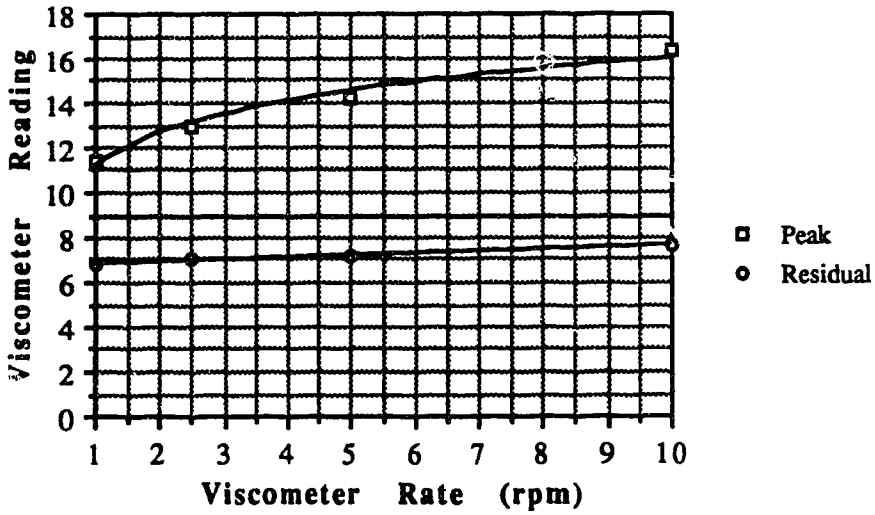

Figure A.66 Viscosity Test V23003D

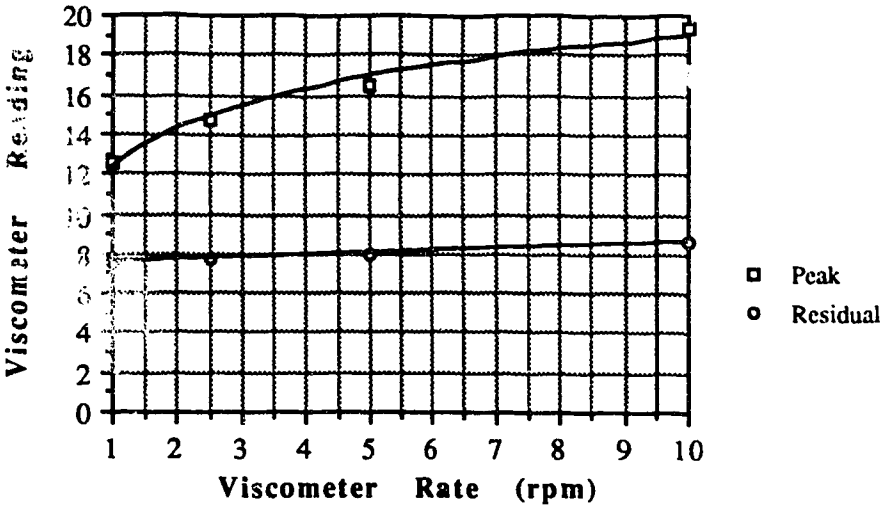

Figure A.67 Viscosity Test V23004D

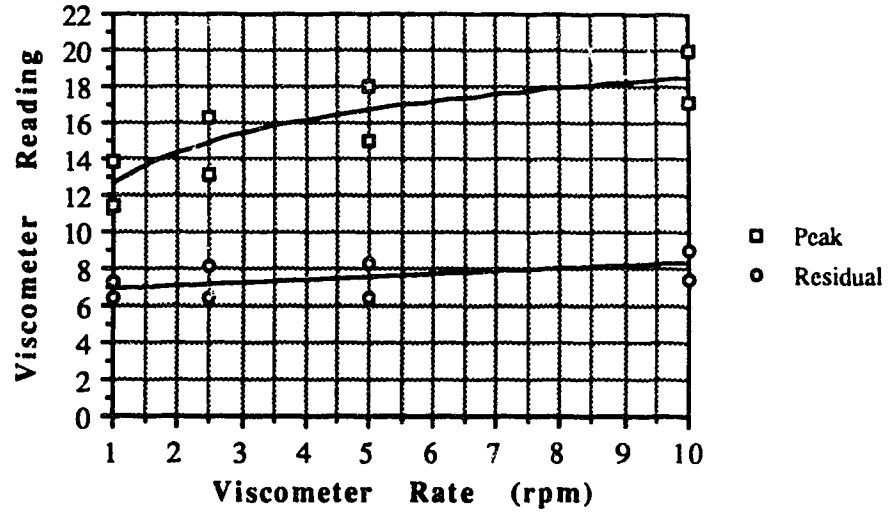

Figure A.68 Viscosity Test V23005D

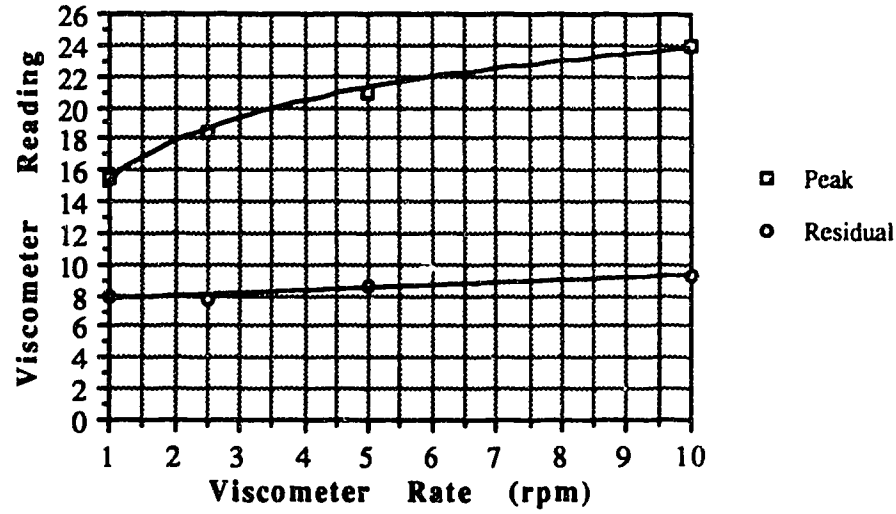

Figure A.69 Viscosity Test V23010D

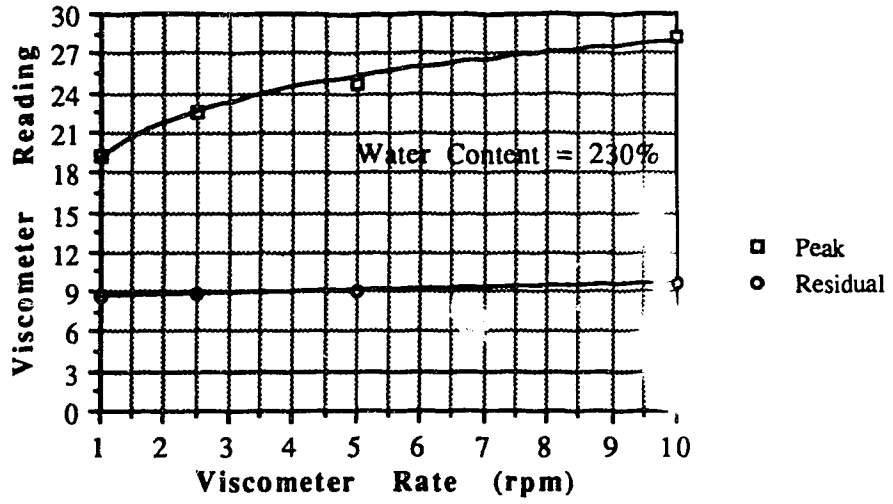

Figure A.70 Viscosity Test V23020D

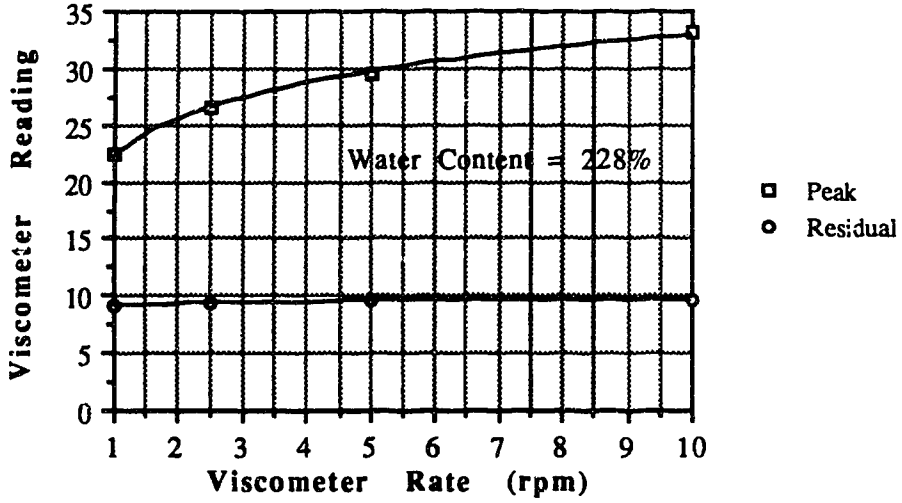

Figure A.71 Viscosity Test V23040D

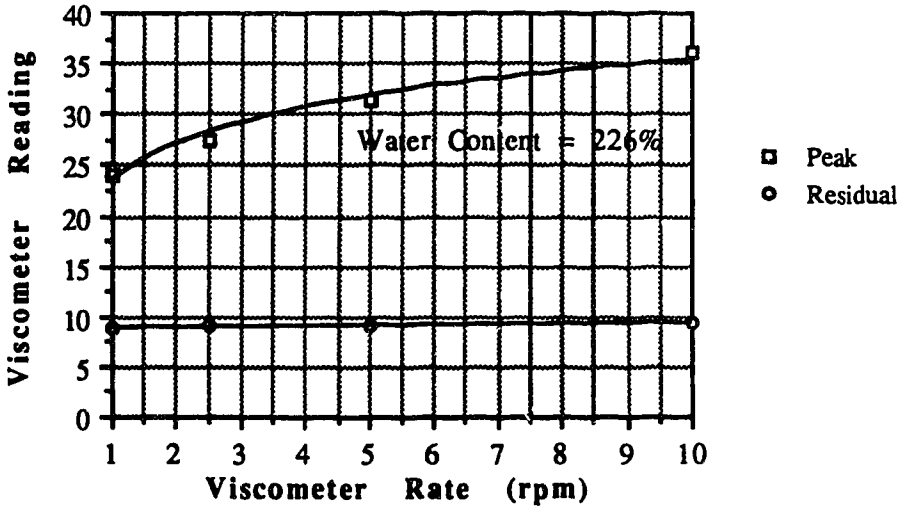

Figure A.72 Viscosity Test V23075D

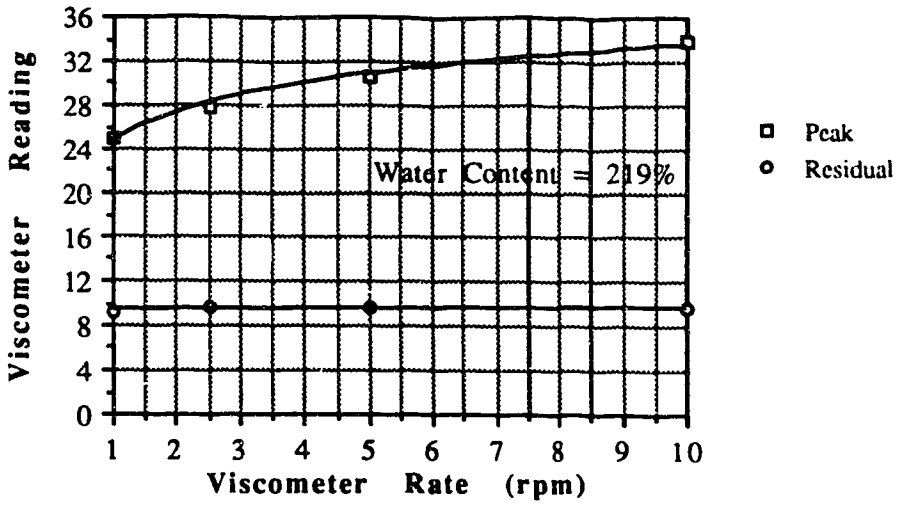

Figure A.73 Viscosity Test V23090D

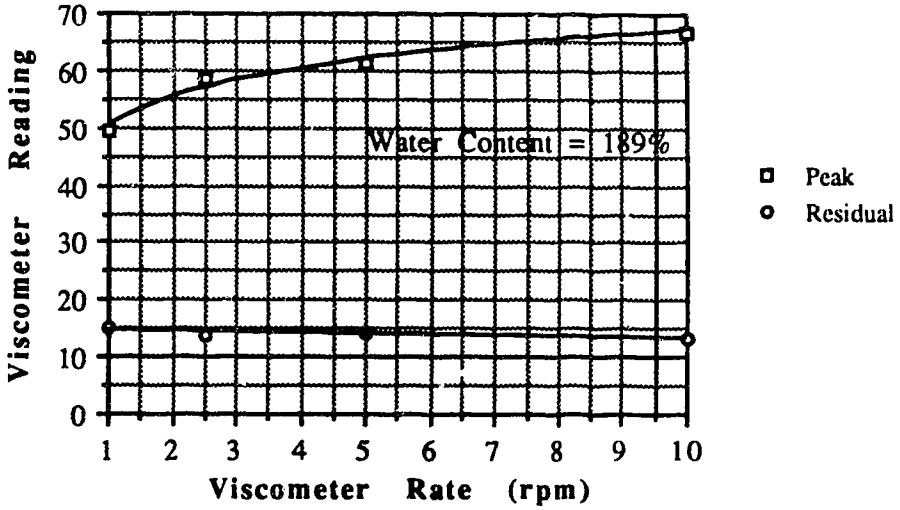

Figure B.74 Viscosity Test V23494D

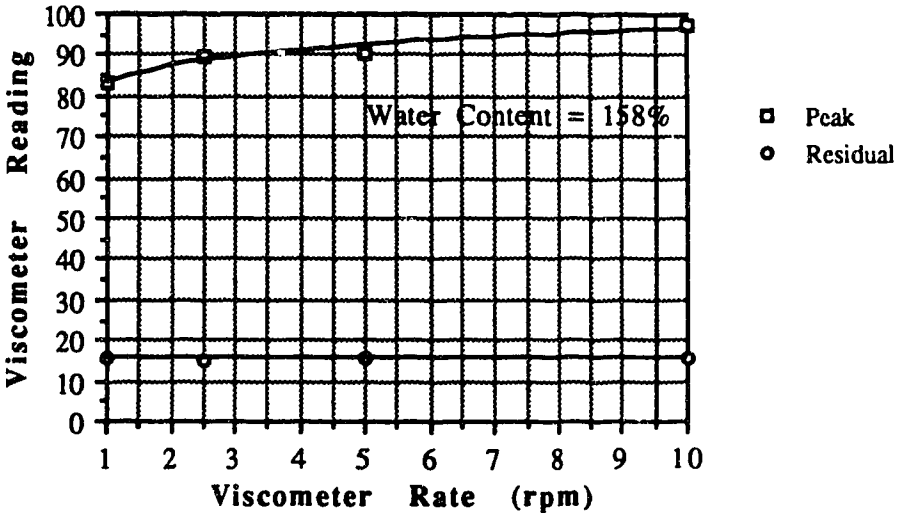

Figure A.75 Viscosity Test V23682D

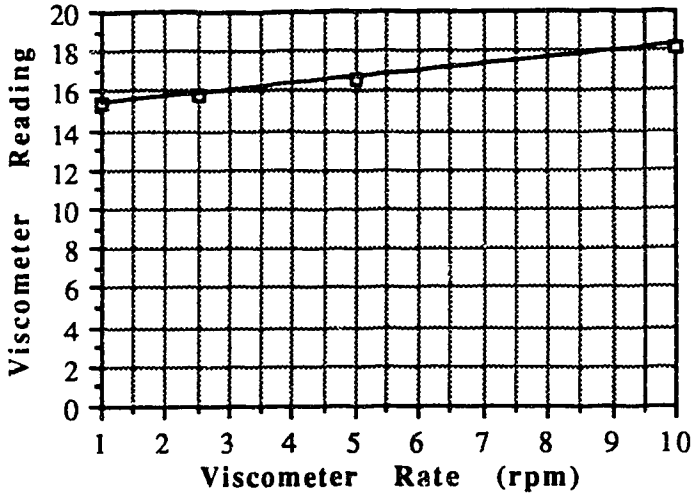

Figure A.76 Viscosity Test V15000M

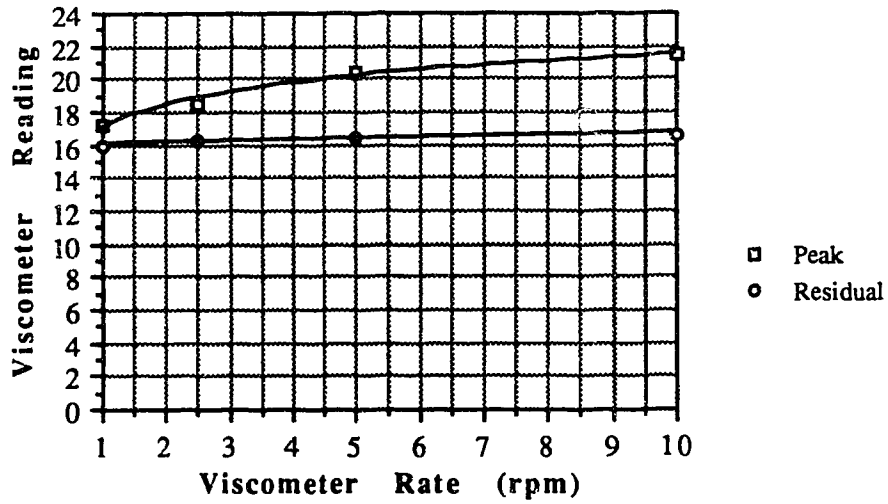

Figure A.77 Viscosity Test V15005M

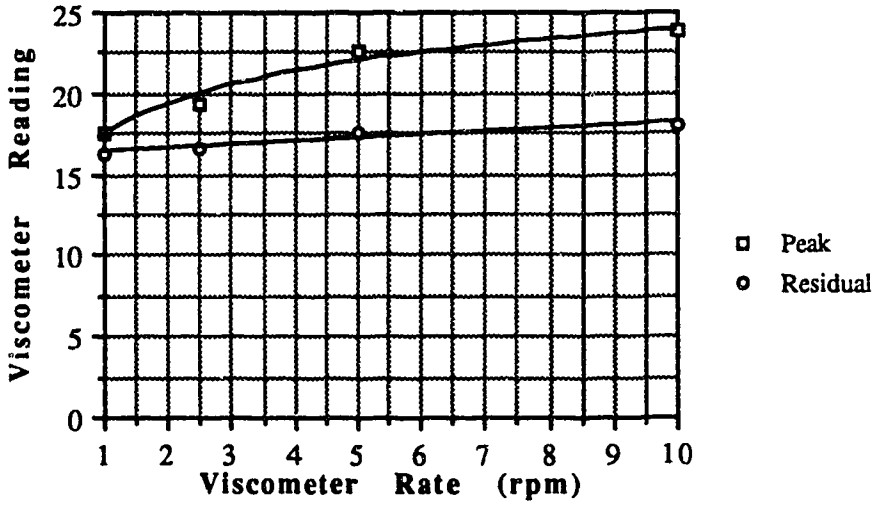

Figure A.78 Viscosity Test V15010M

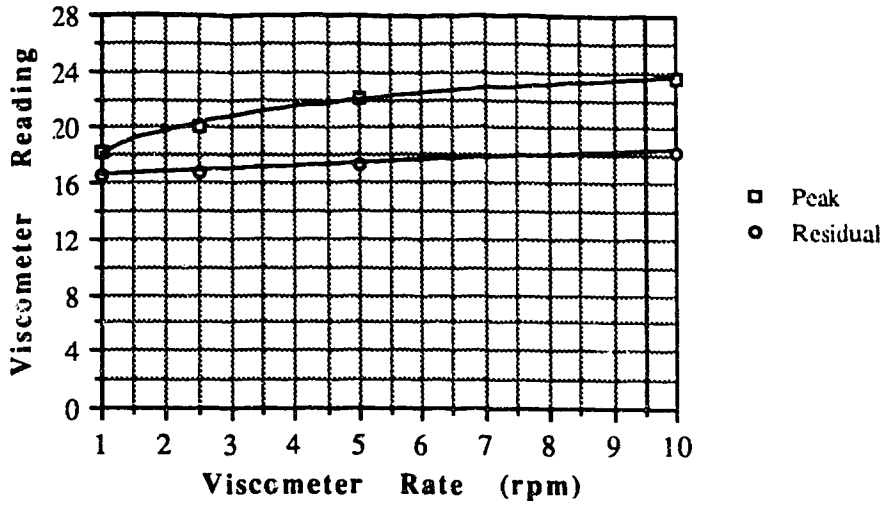

Figure A.79 Viscosity Test V15020M

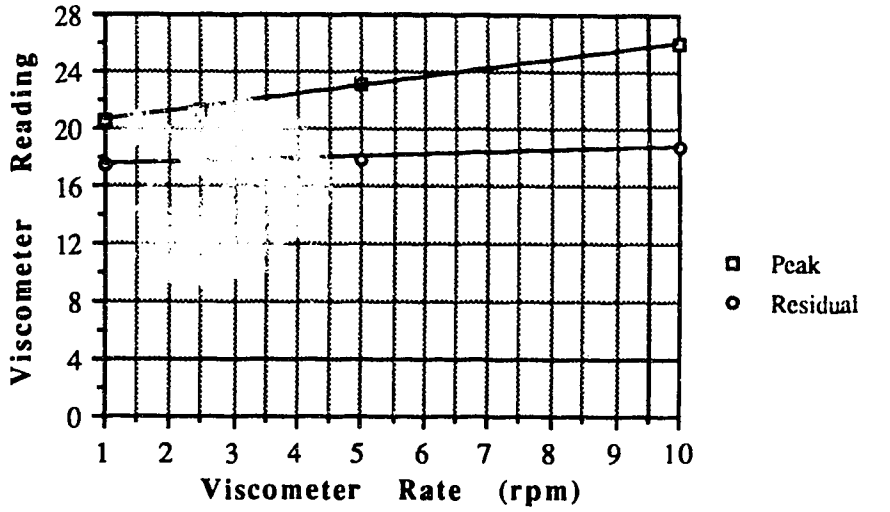

Figure A.80 Viscosity Test V15030M

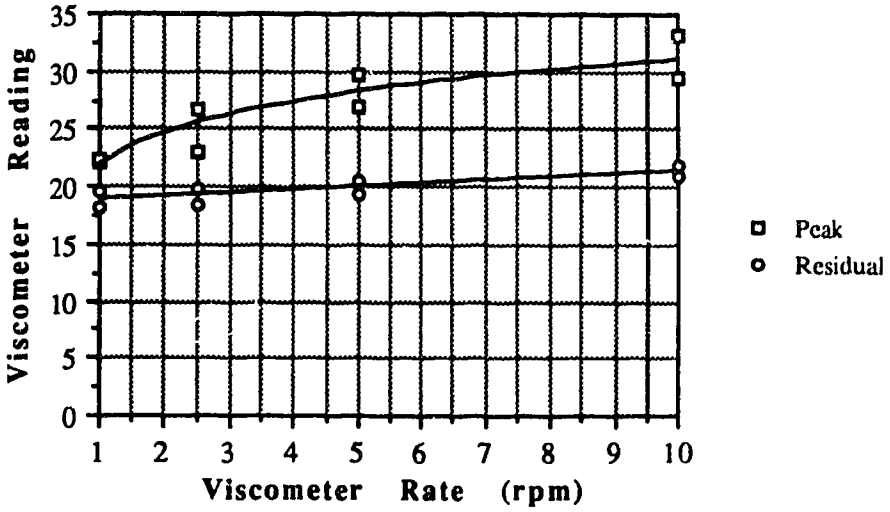

Figure A.81 Viscosity Test V15001H

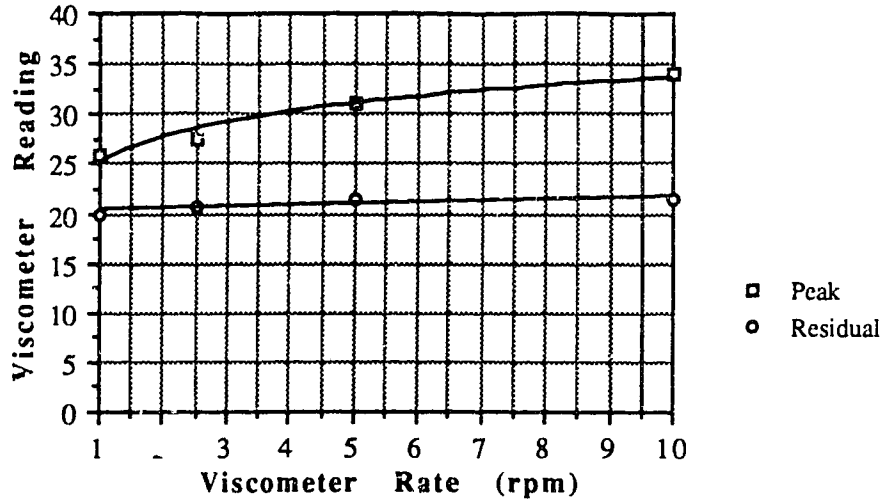

Figure A.82 Viscosity Test V15002H

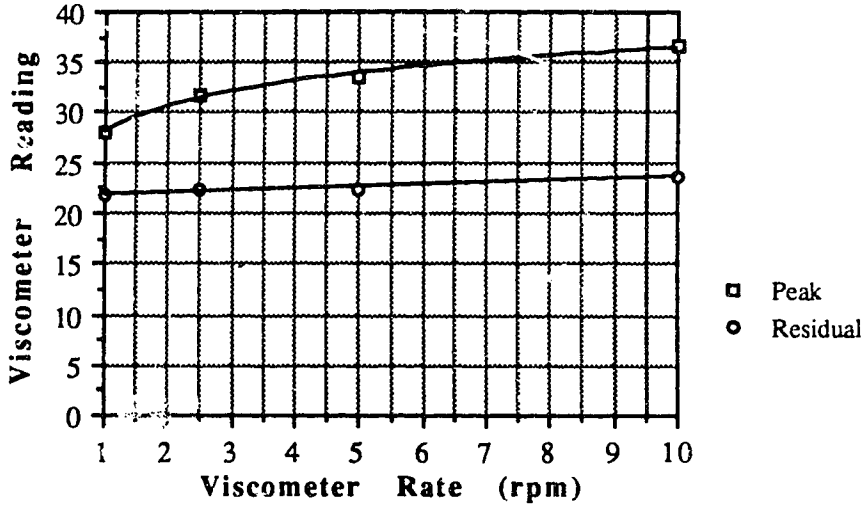

Figure A.83 Viscosity Test V15003H

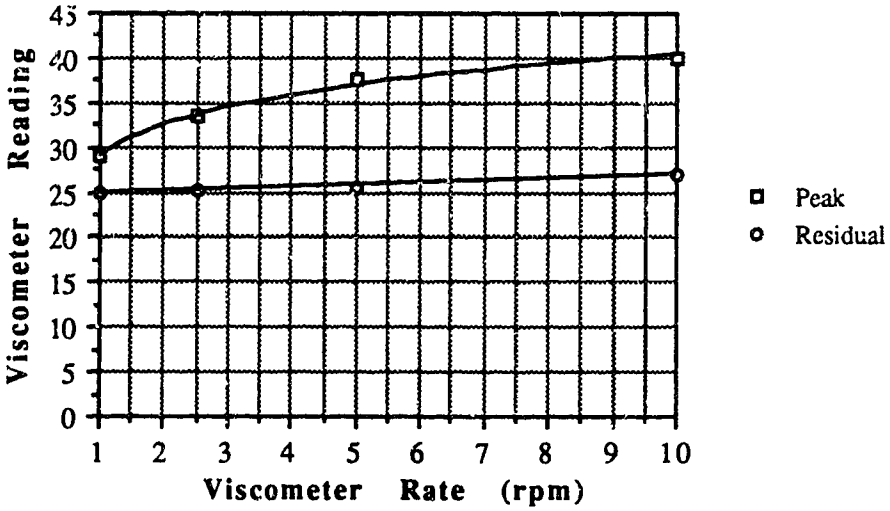

Figure A.84 Viscosity Test V15004H

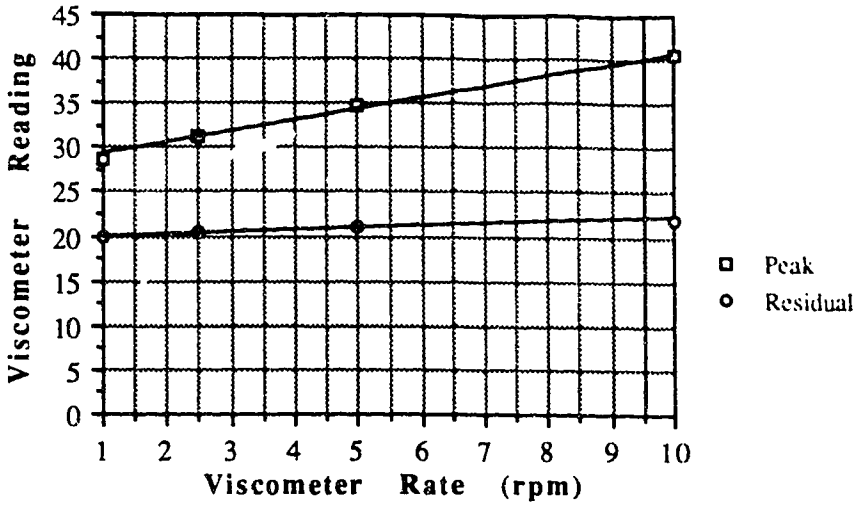

Figure A.85 Viscosity Test V15008H

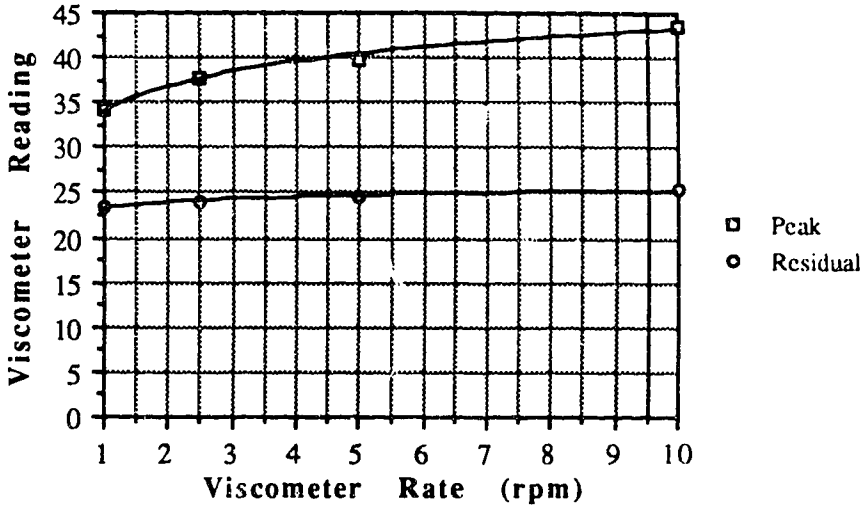

Figure A.86 Viscosity Test V15012H

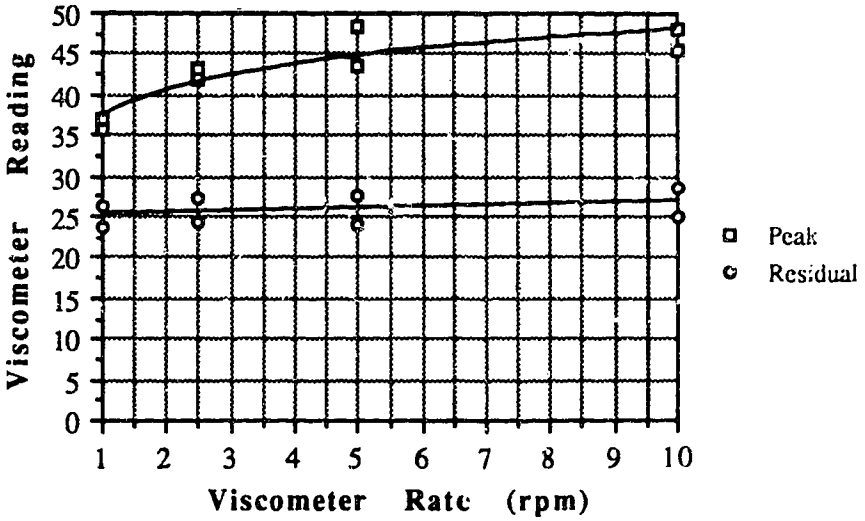

Figure A.87 Viscosity Test V15018H

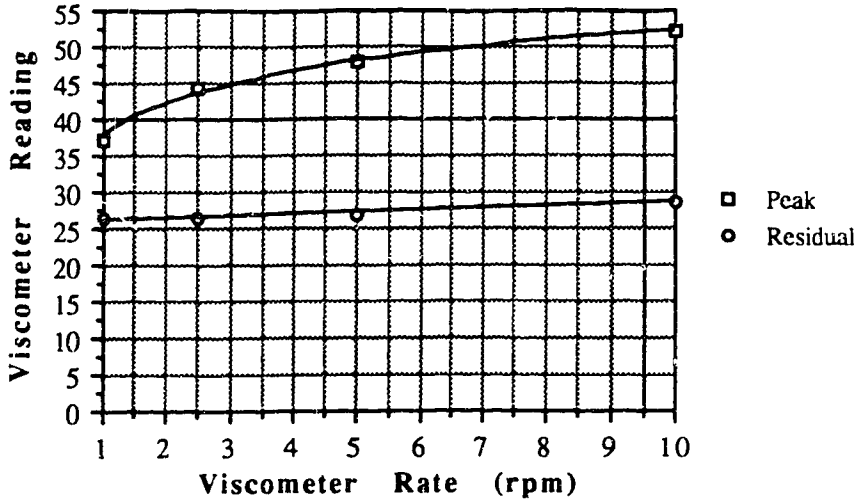

Figure A.88 Viscosity Test V15001D

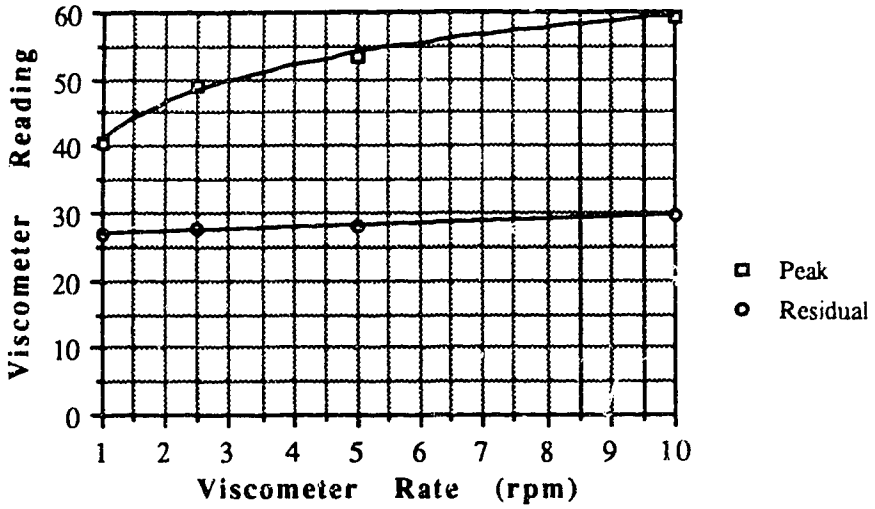

Figure A.89 Viscosity Test V15002D

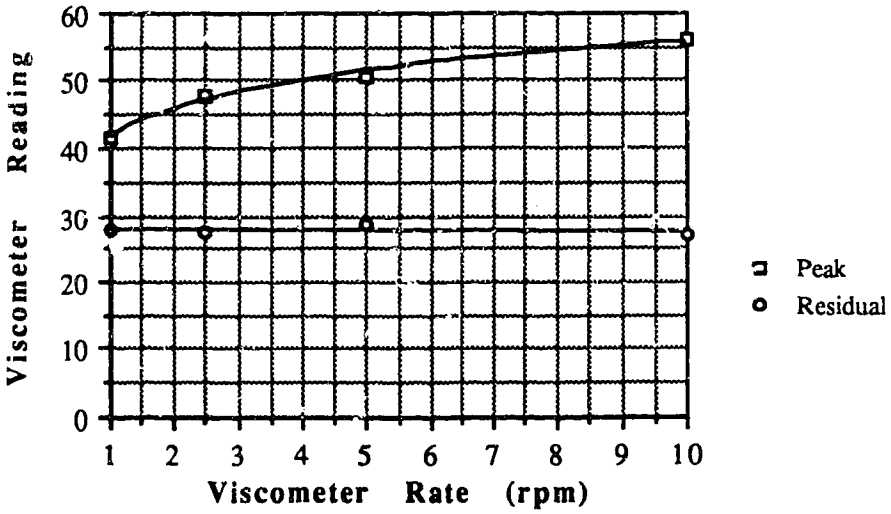

Figure A.90 Viscosity Test V15003D

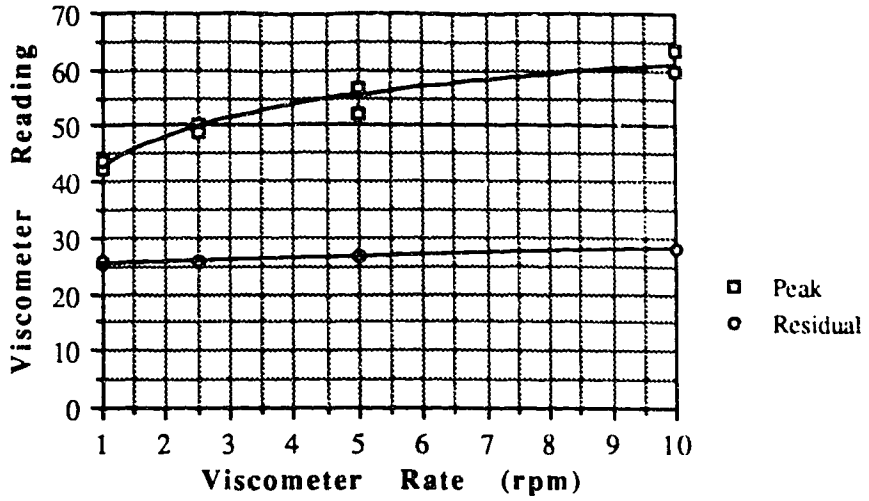

Figure A.91 Viscosity Test V15004D

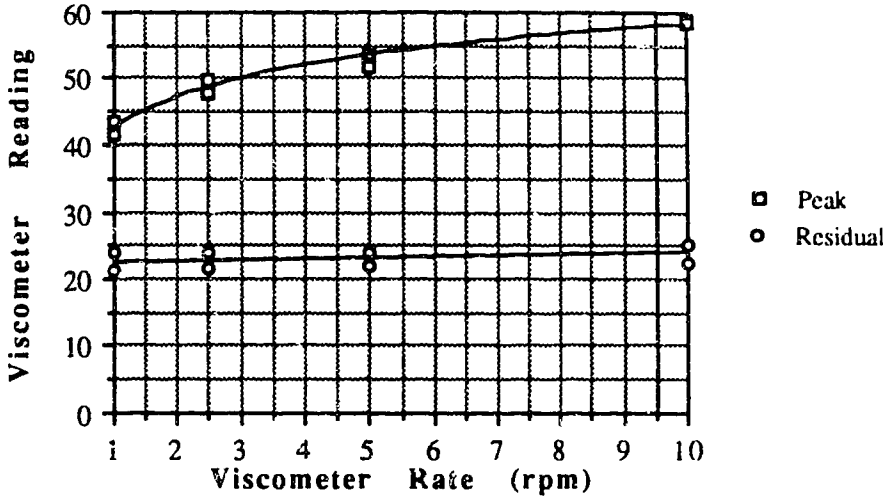

Figure A.92 Viscosity Test V15005D

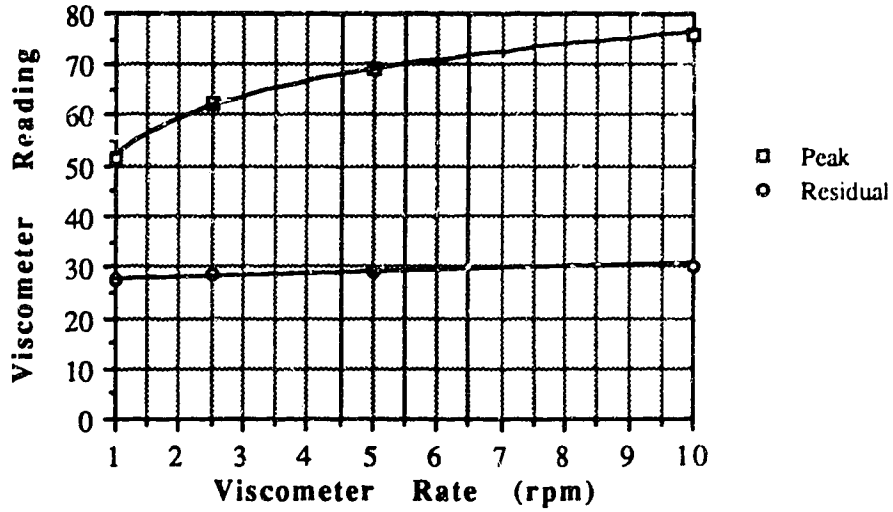

Figure A.93 Viscosity Test 1V15010D

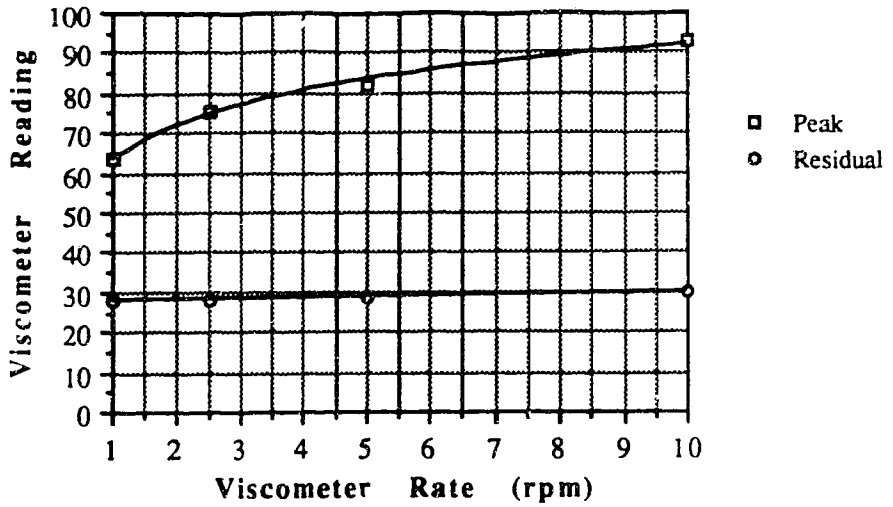

Figure A.94 Viscosity Test V15020D

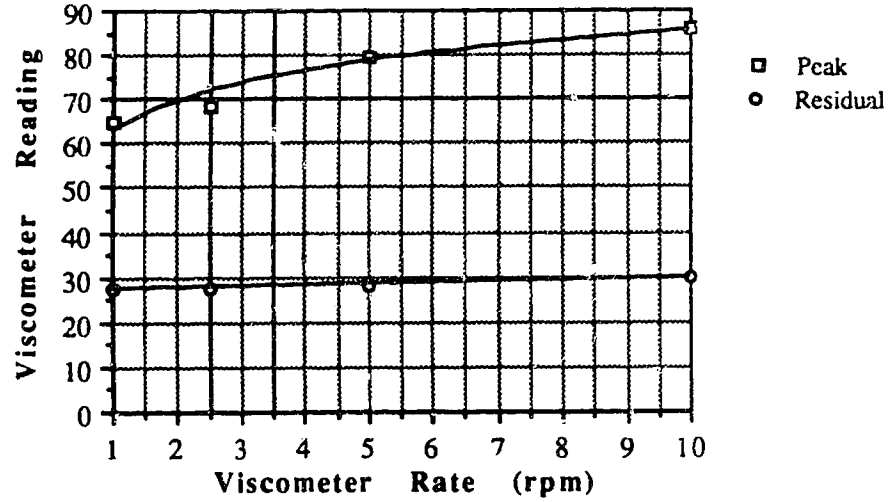

Figure A.95 Viscosity Test V15030D

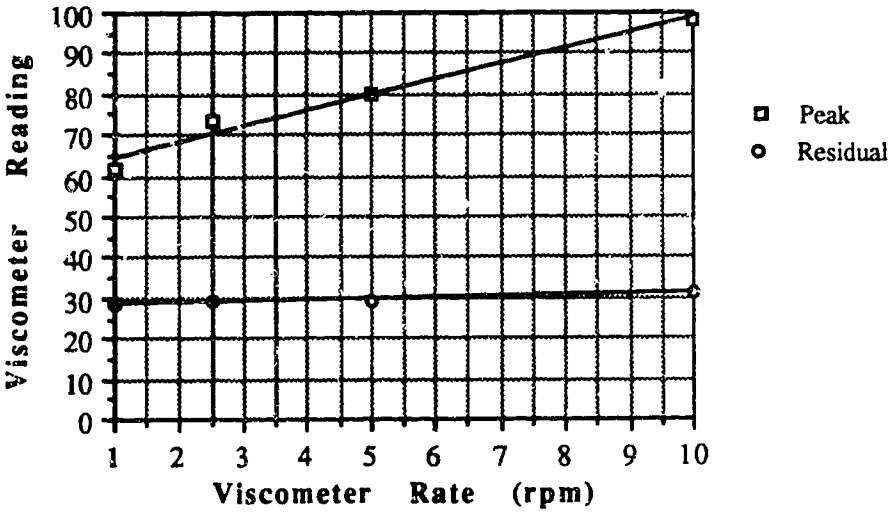

Figure A.96 Viscosity Test V15040D

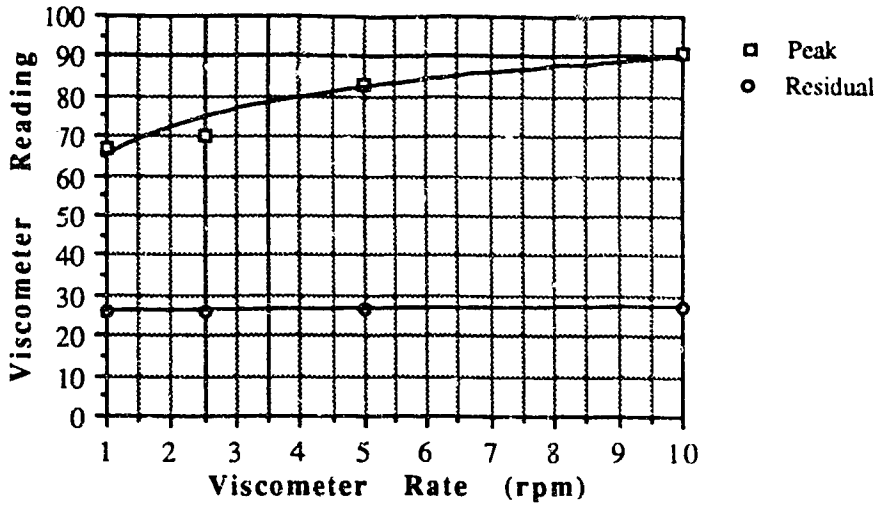

Figure A.97 Viscosity Test V15051D

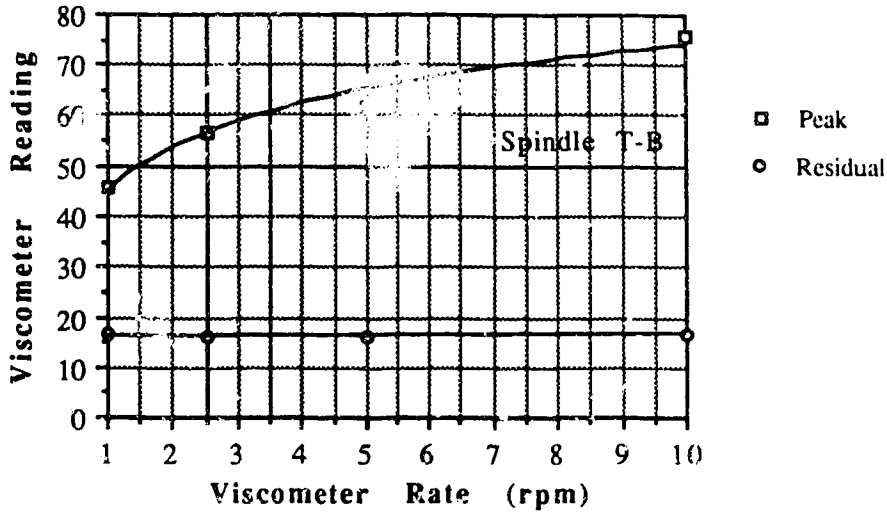

Figure A.98 Viscosity Test V15092D

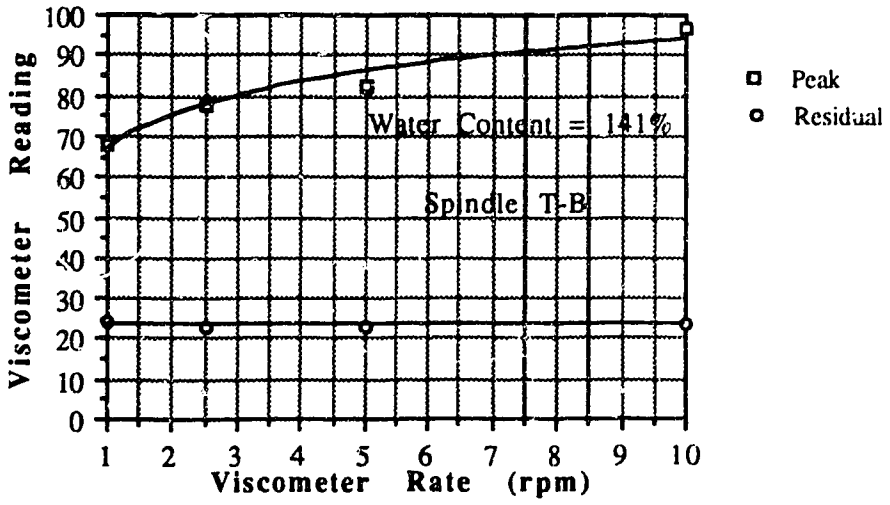

Figure A.99 Viscosity Test V15470D

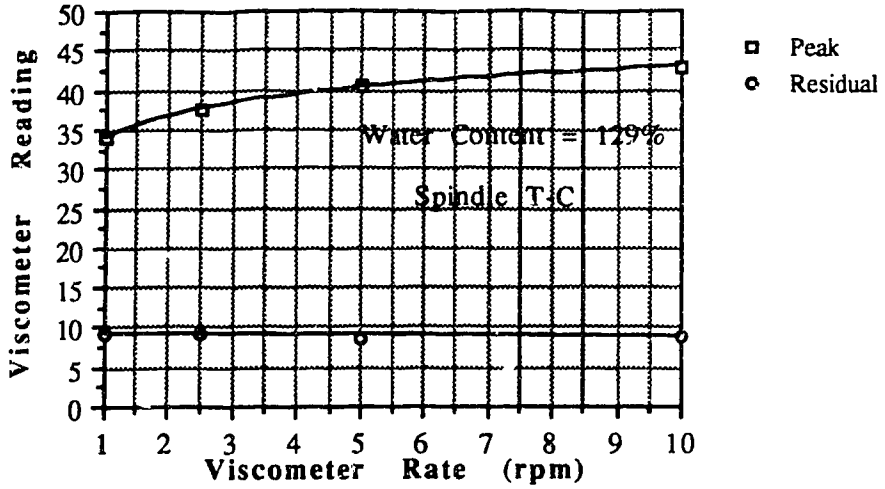

Figure A.100 Viscosity Test V15680D

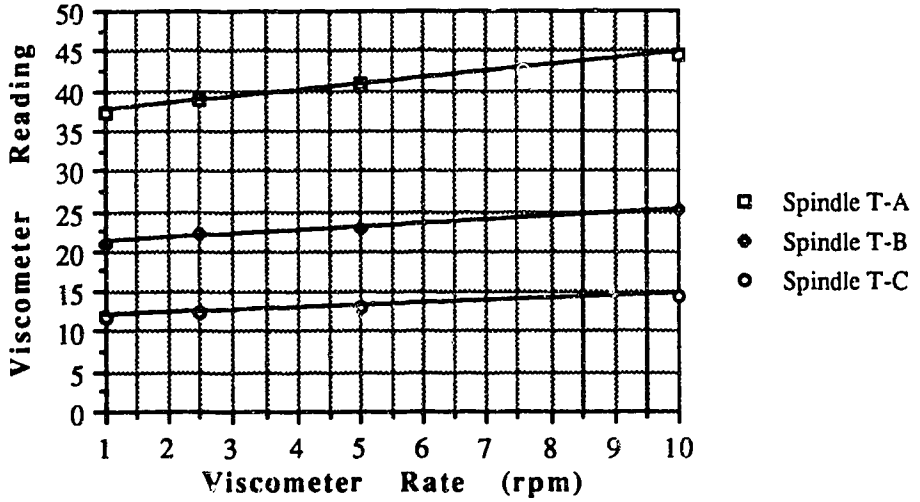

Figure A.101 Viscosity Test V10000M

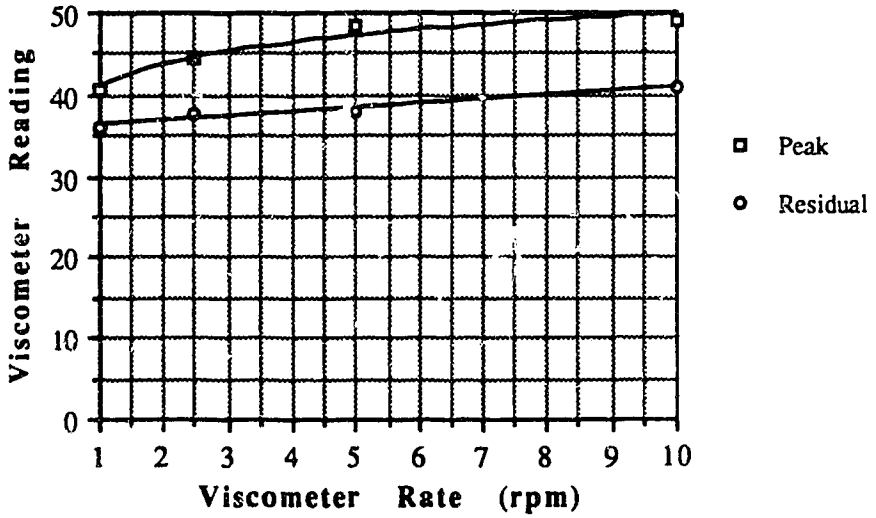

Figure A.102 Viscosity Test V10005M

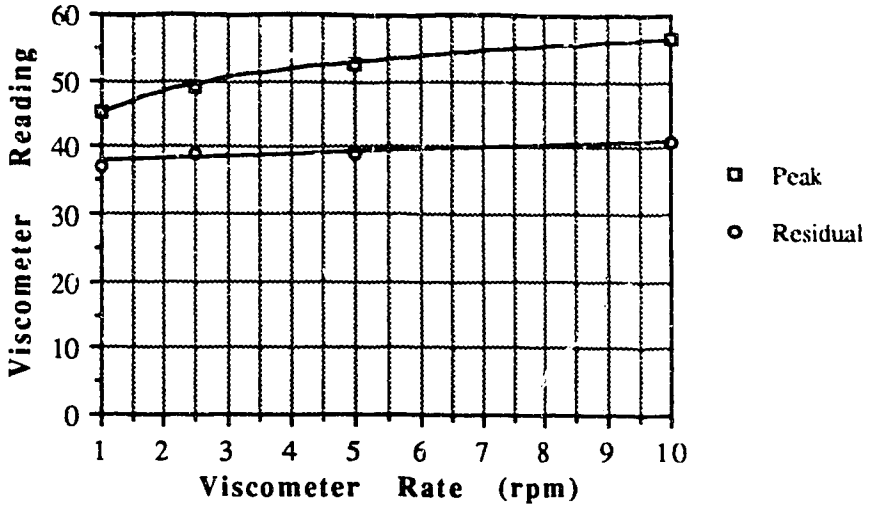

Figure A.103 Viscosity Test V10010M

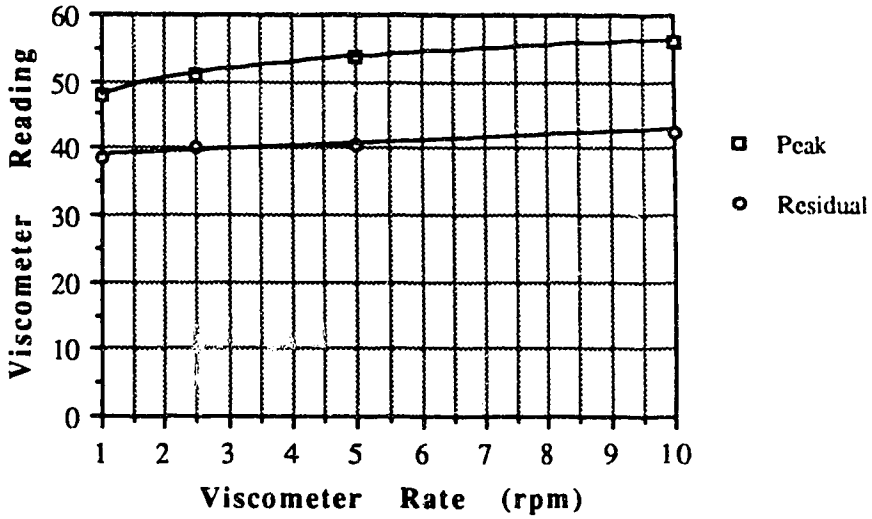

Figure A.104 Viscosity Test V10020M

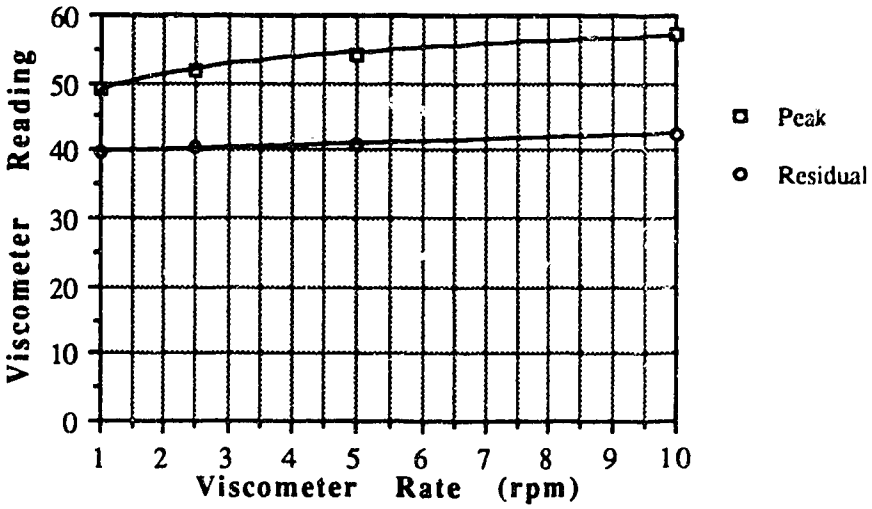

Figure A.105 Viscosity Test V10030M

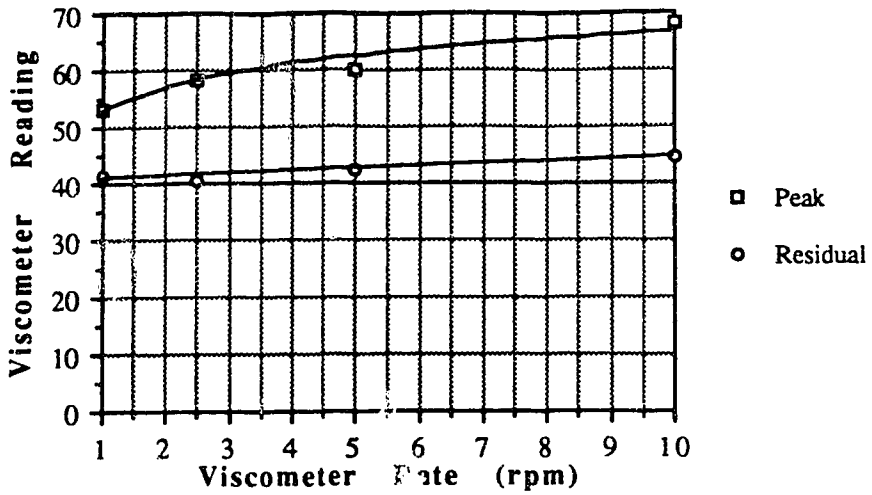

Figure A.106 Viscosity Test V10001H

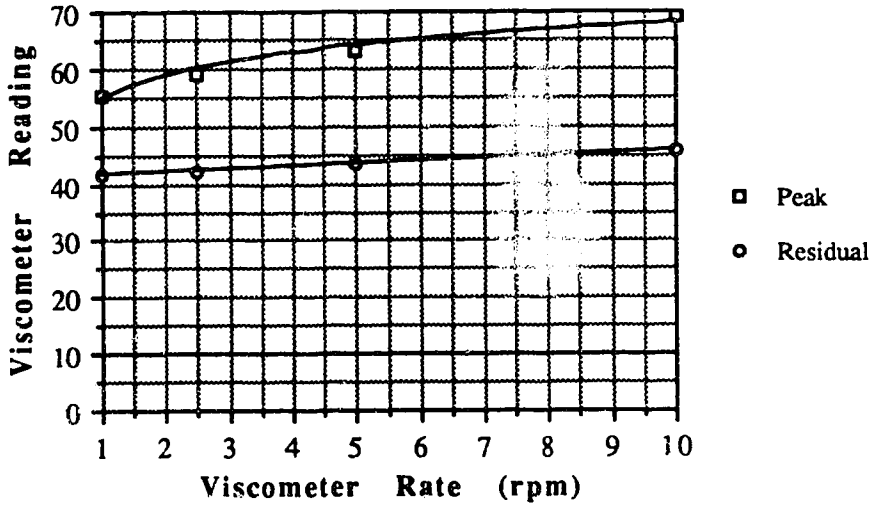

Figure A.107 Viscosity Test V10002H

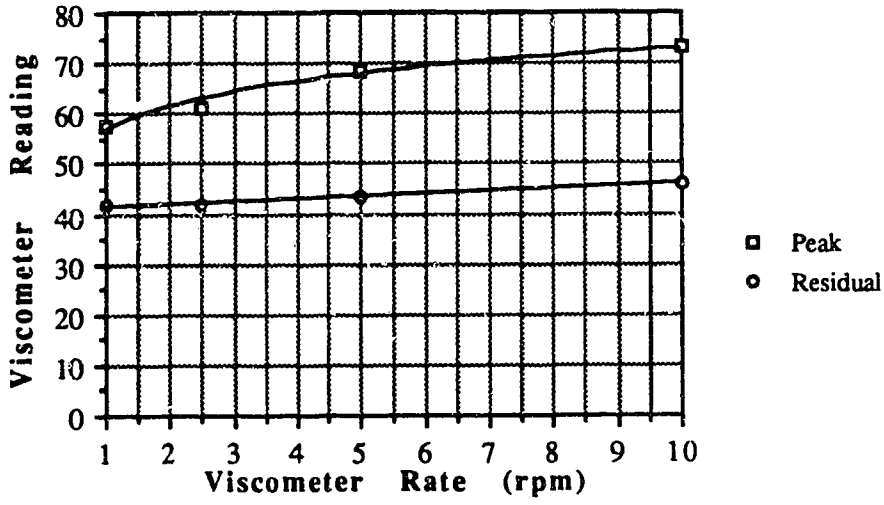

Figure A.108 Viscosity Test V10003H

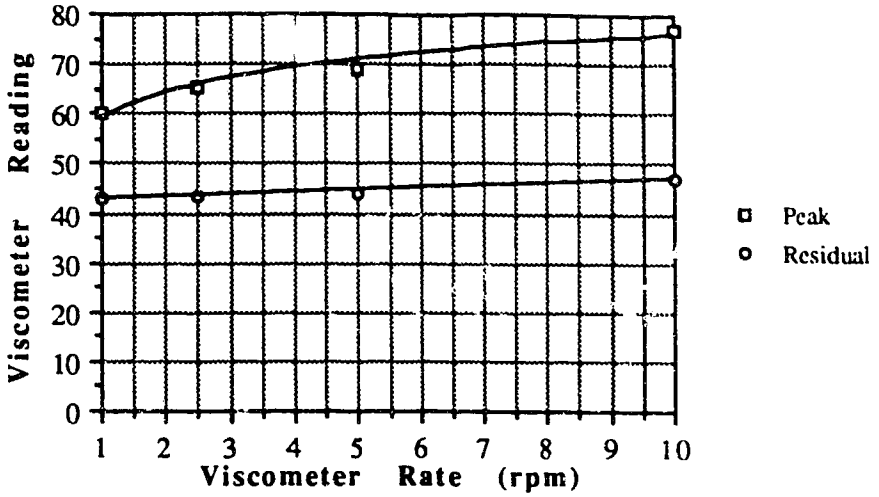

Figure A.109 Viscosity Test V10004H

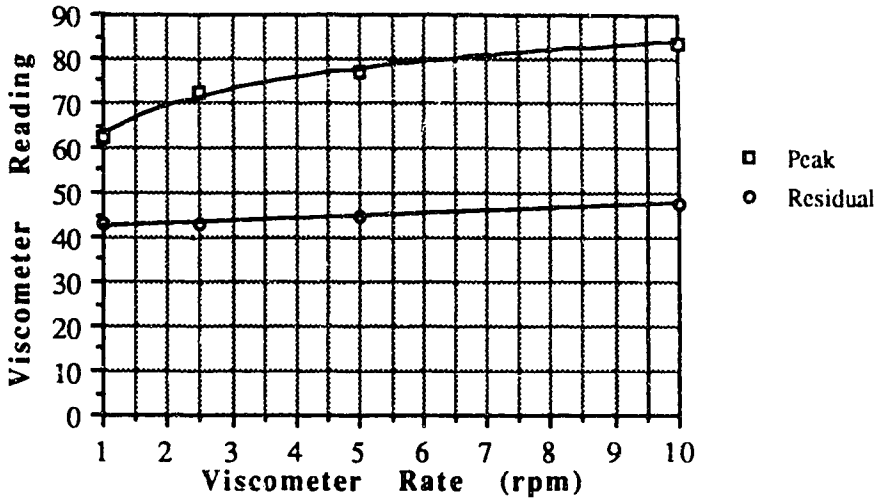

Figure A.110 Viscosity Test V10008H

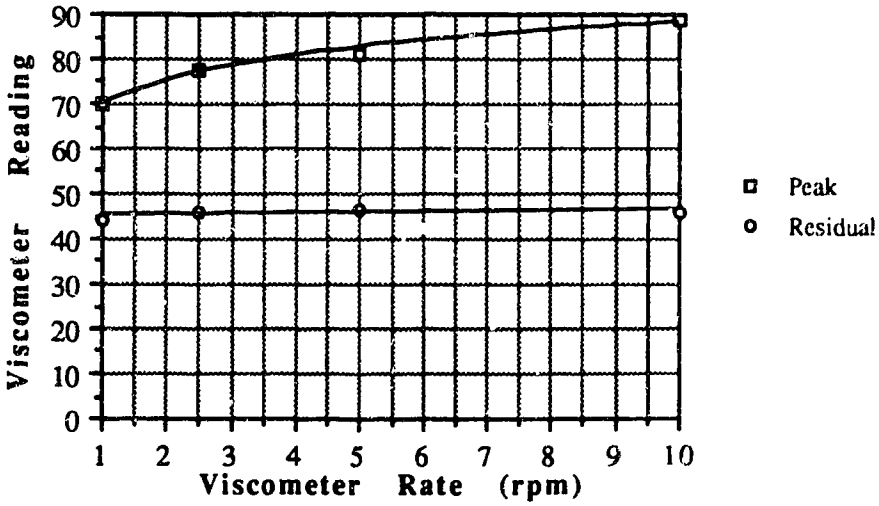

Figure A.111 Viscosity Test V10012H

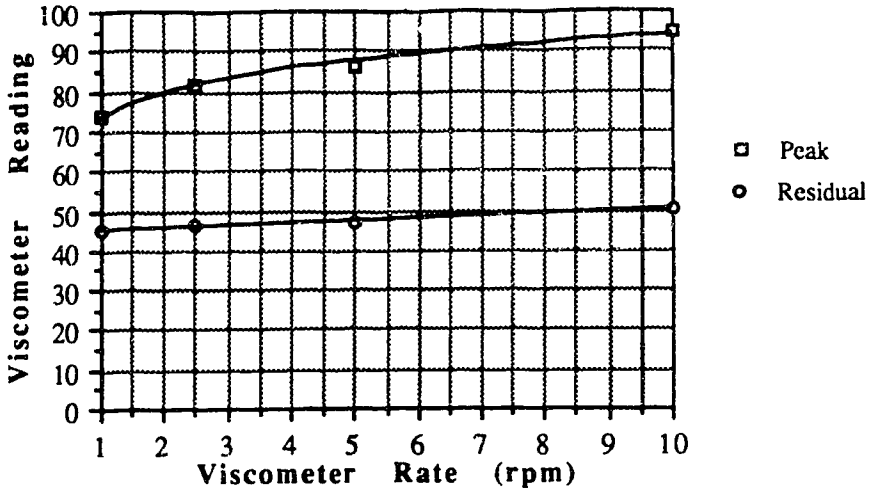

Figure A.112 Viscosity Test V10018H

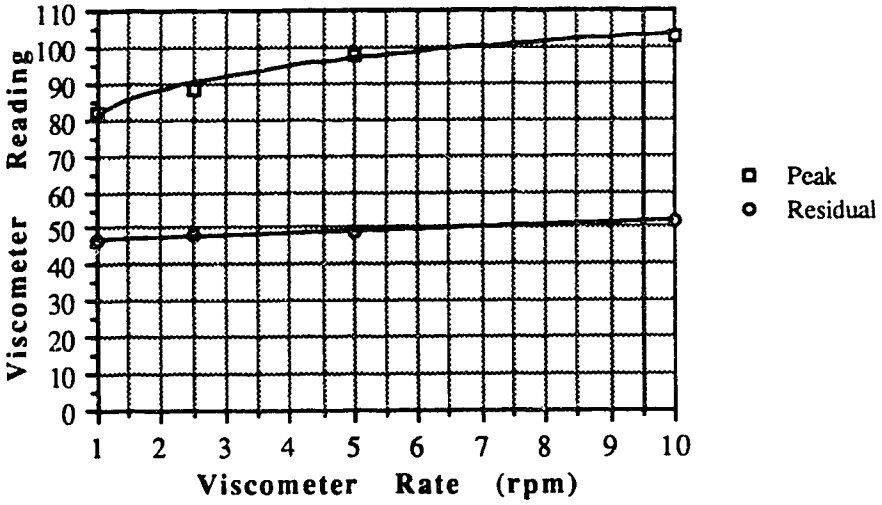

Figure A.113 Viscosity Test V10001D

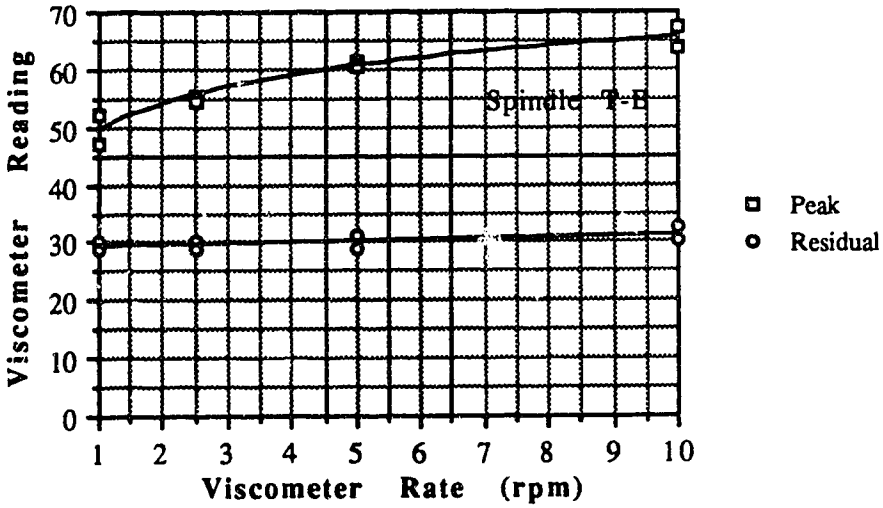

Figure A.114 Viscosity Test V10002D

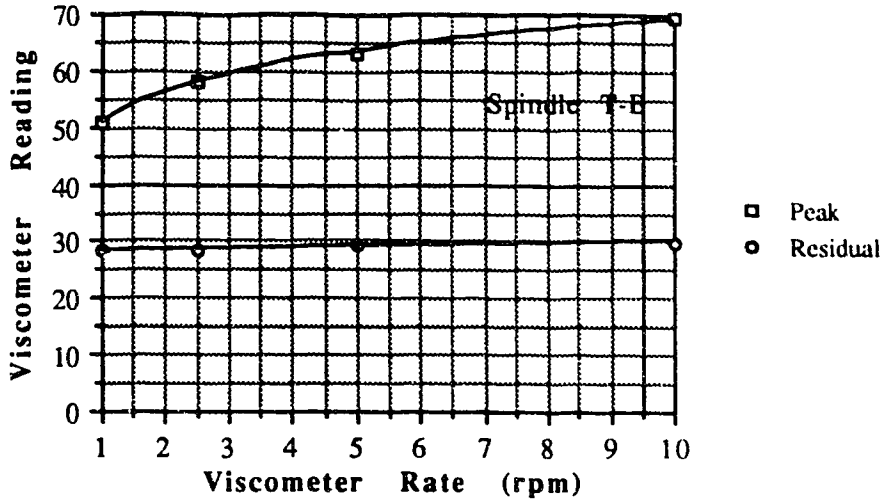

Figure A.115 Viscosity Test V10003D

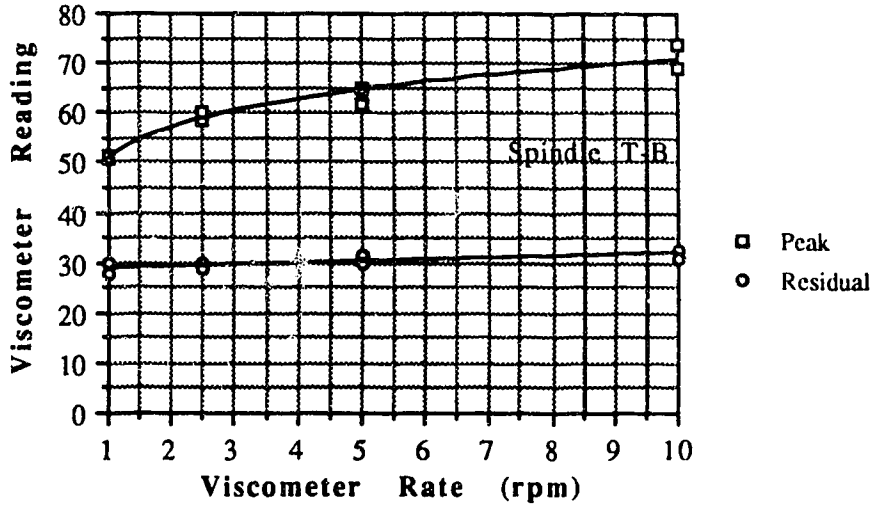

Figure A.116 Viscosity Test V10004D

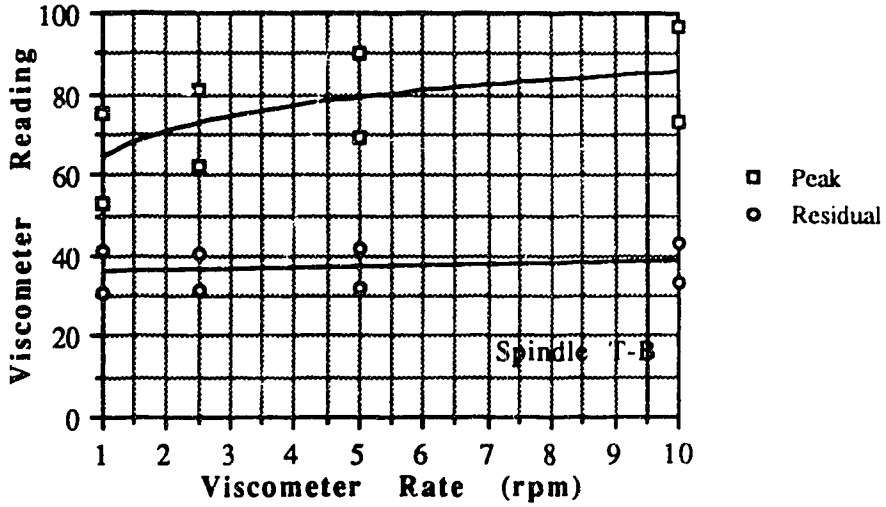

Figure A.117 Viscosity Test V10005D

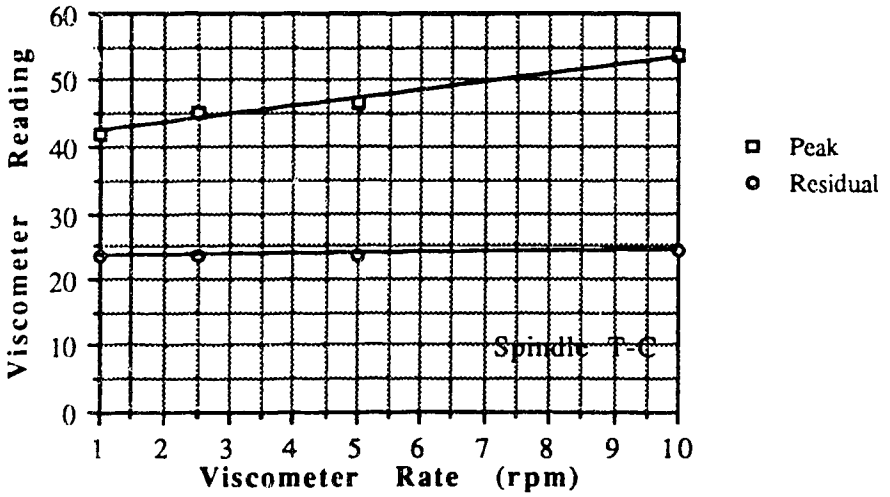

Figure A.118 Viscosity Test V10006D

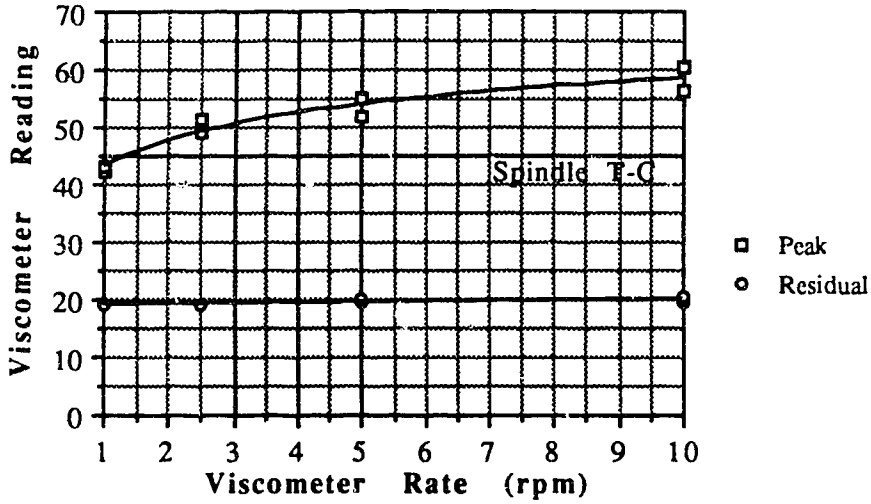

Figure A.119 Viscosity Test V10010D

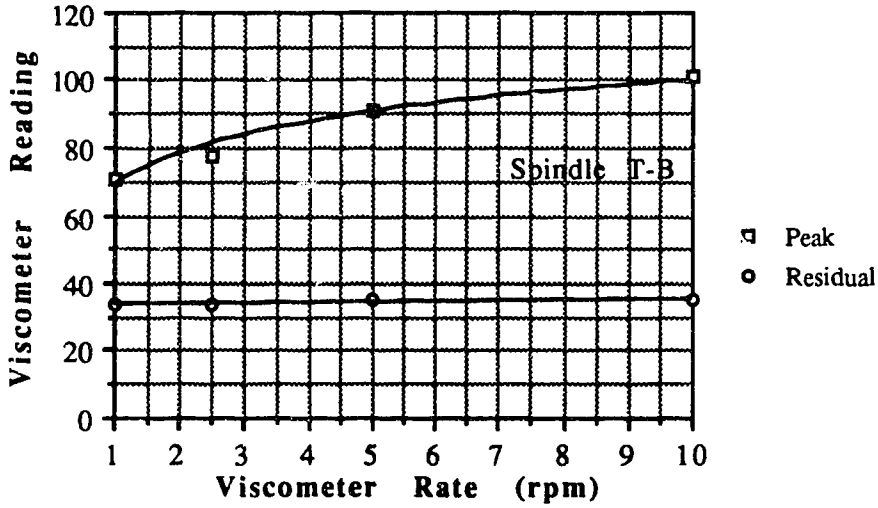

Figure A.120 Viscosity Test V10020D

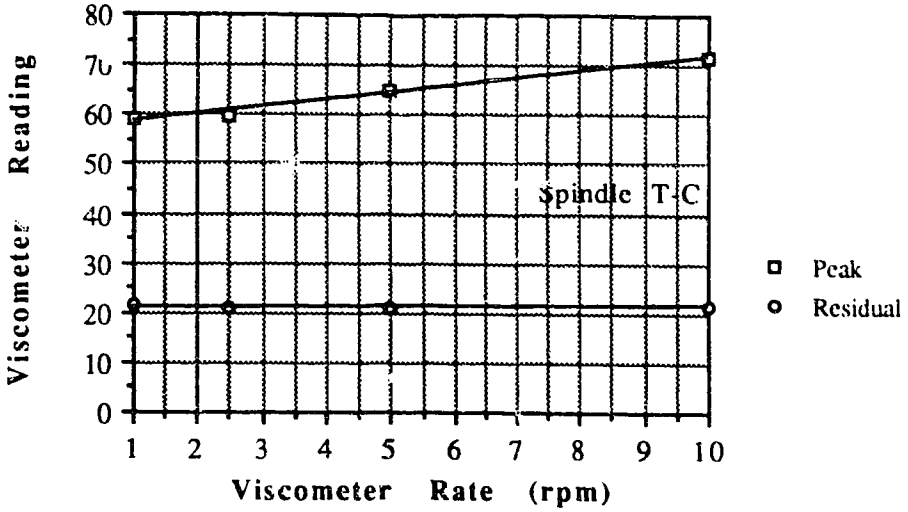

Figure A.121 Viscosity Test V10021D

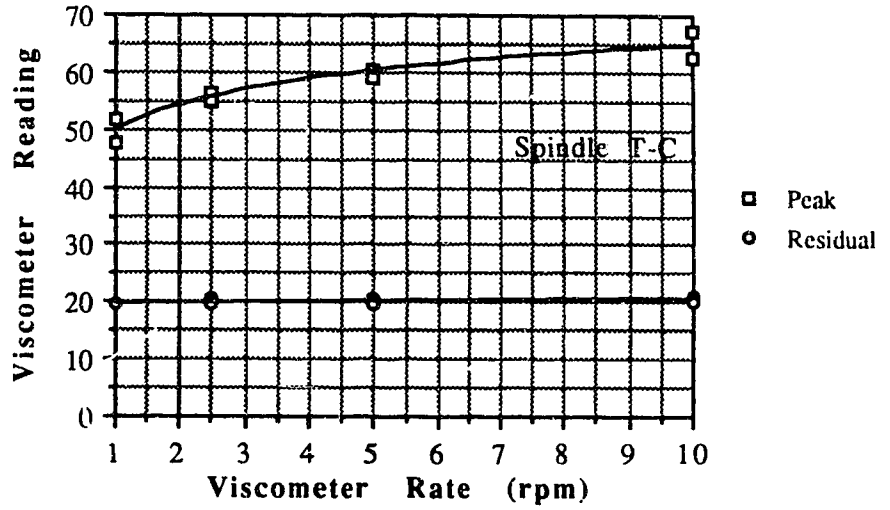

Figure A.122 Viscosity Test V10040D

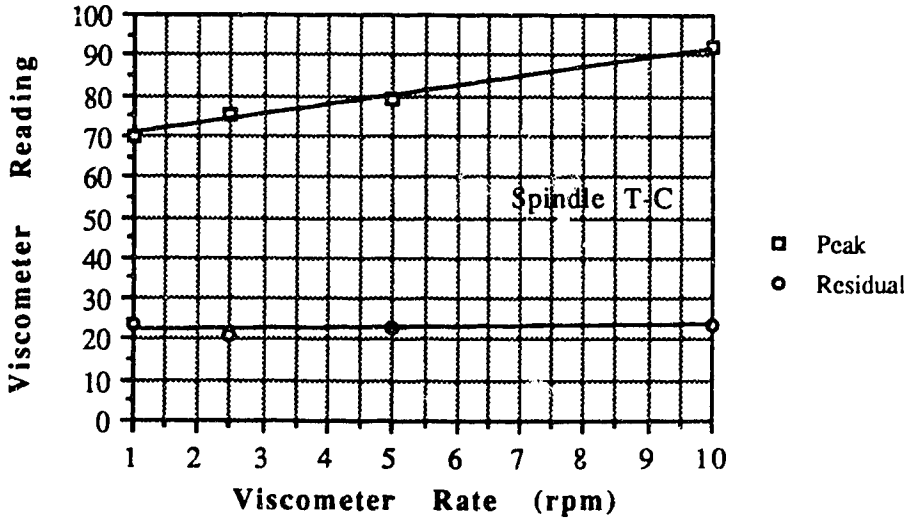

Figure A.123 Viscosity Test V10095D

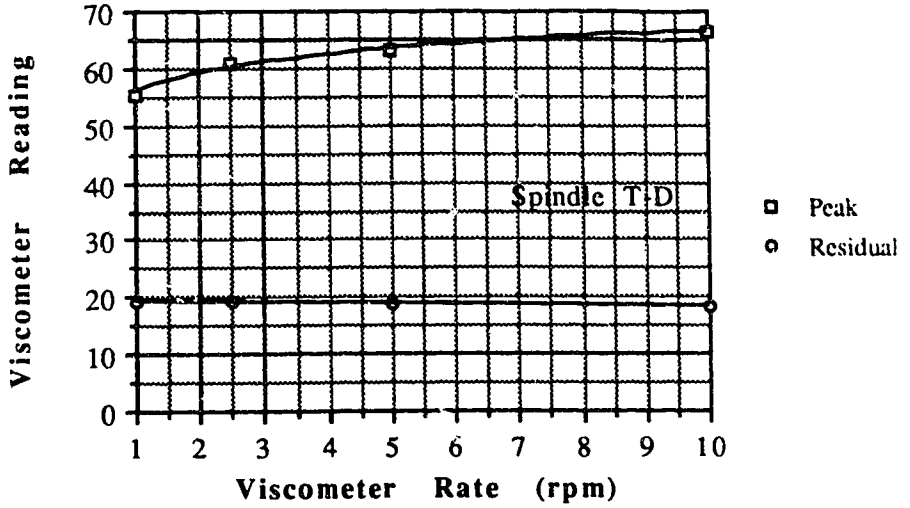

Figure A.124 Viscosity Test V10473D

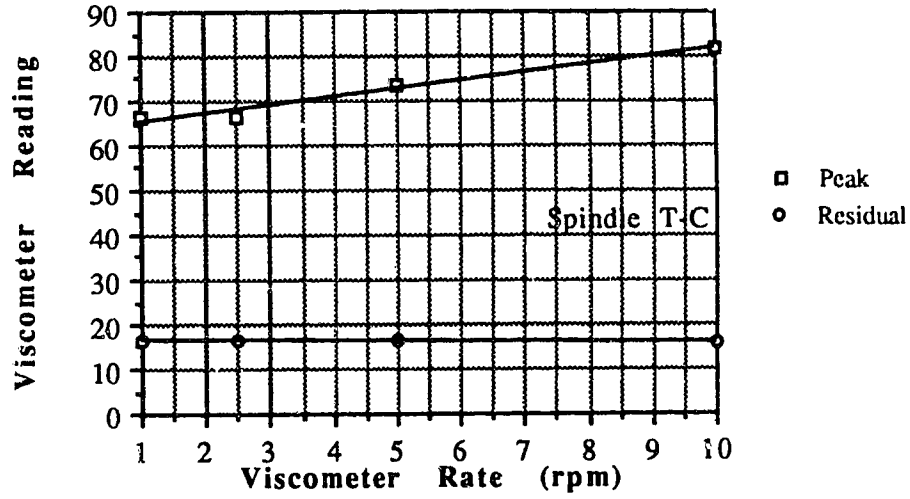

Figure A.125 Viscosity Test V10680D

APPENDIX B. Apparent Viscosity Plots

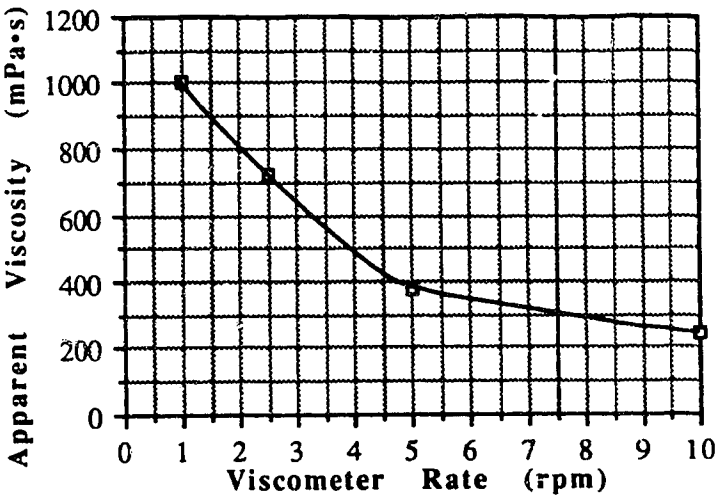

Figure B.1 Apparent Viscosity V4000M

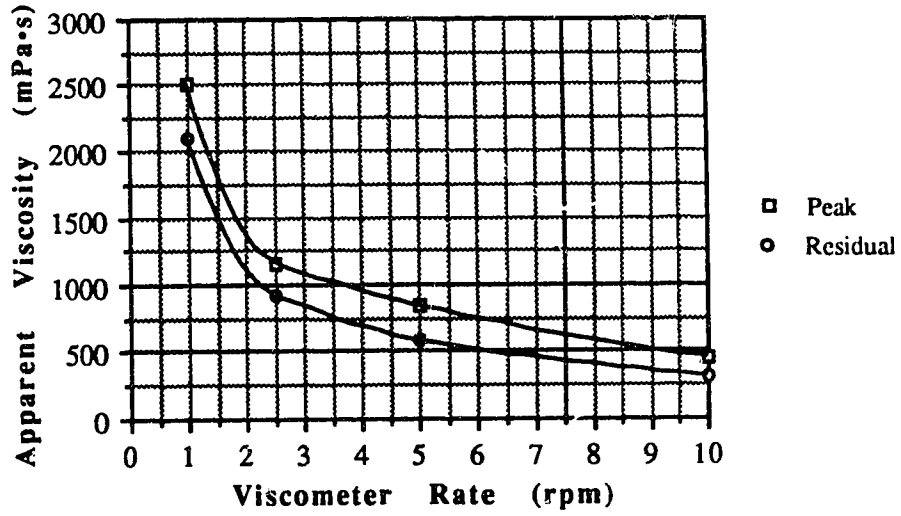

Figure B.2 Apparent Viscosity V40005M

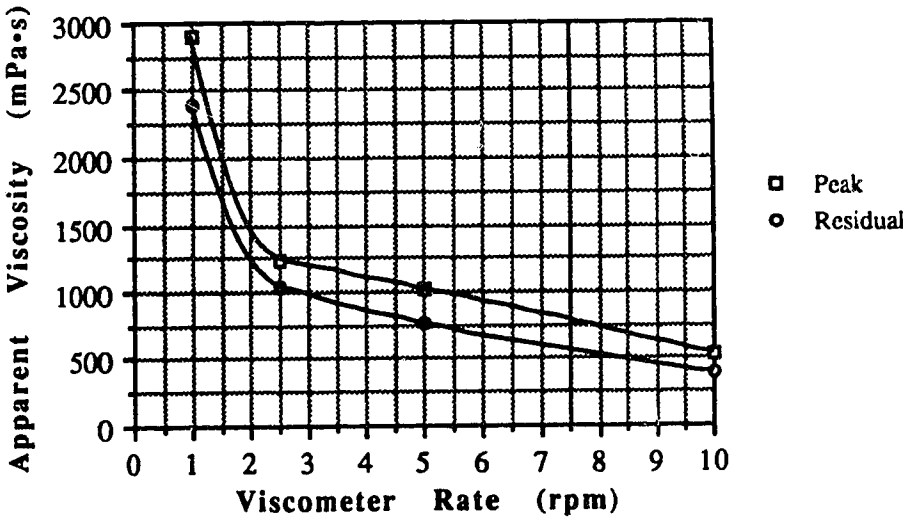

Figure B.3 Apparent Viscosity V40010M

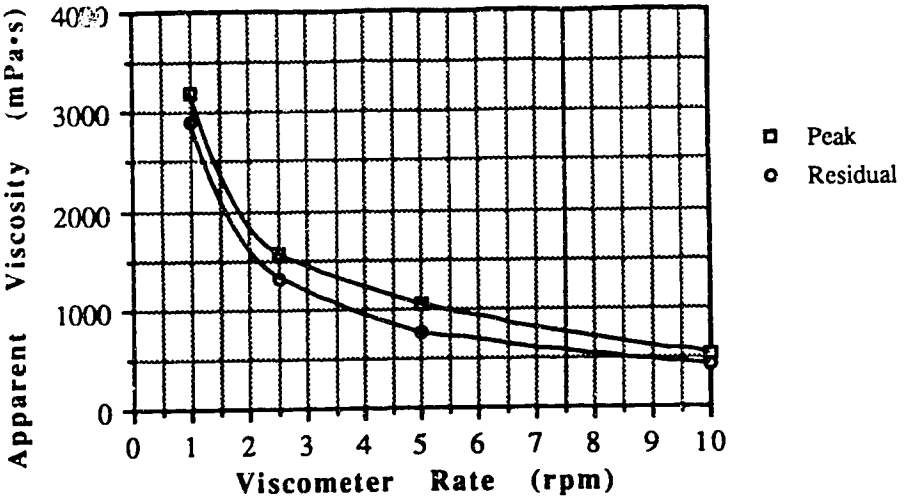

Figure B.4 Apparent Viscosity V40020M

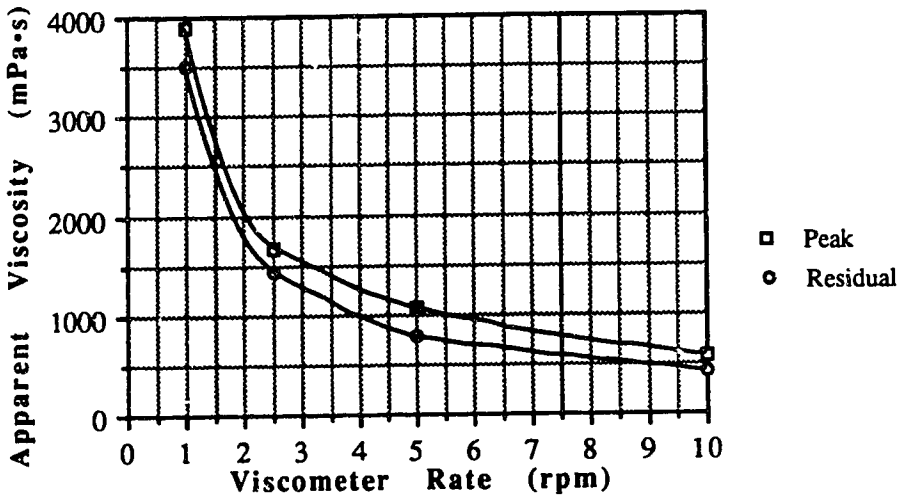

Figure B.5 Apparent Viscosity V40030M

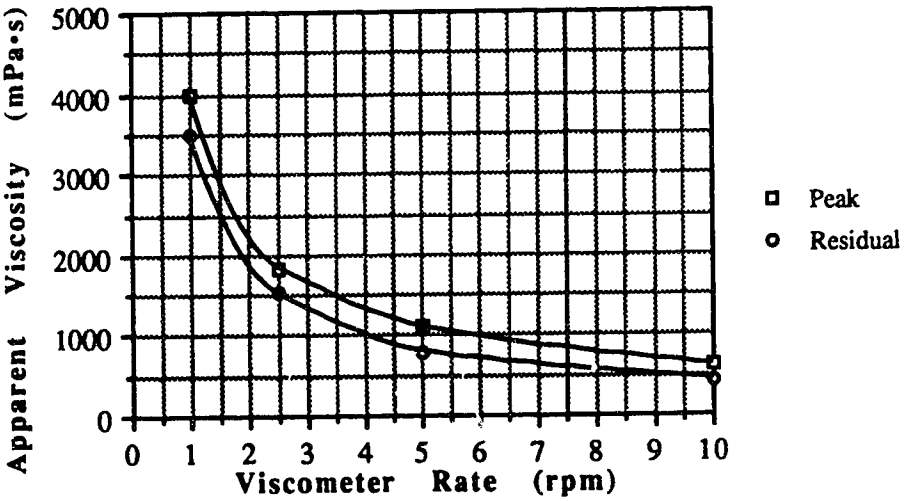

Figure B.6 Apparent Viscosity V40001H

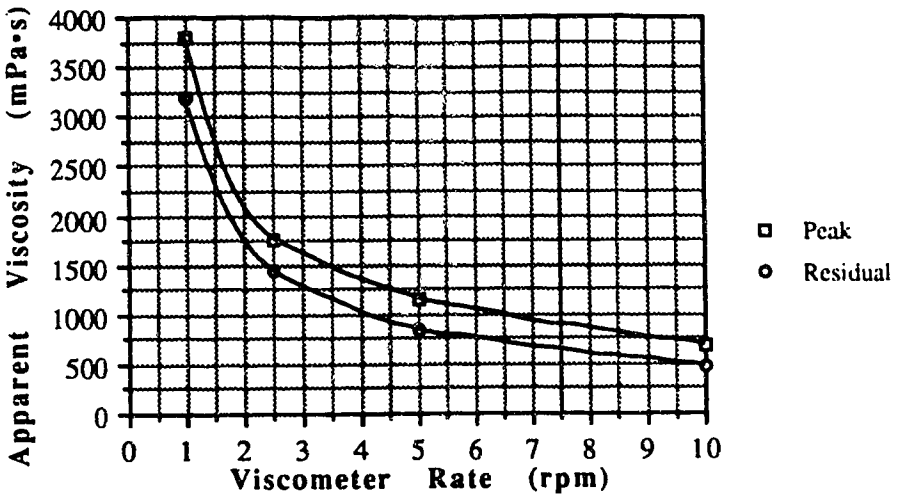

Figure B.7 Apparent Viscosity V40002H

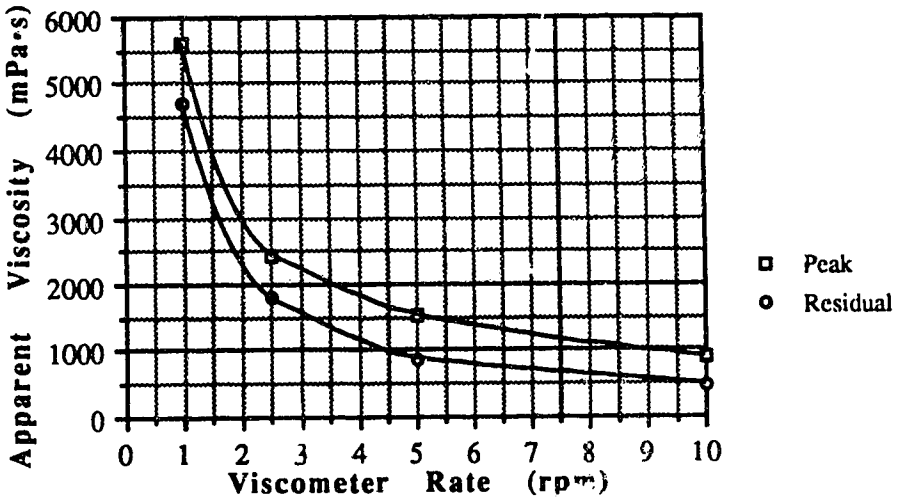

Figure B.8 Apparent Viscosity V40003H

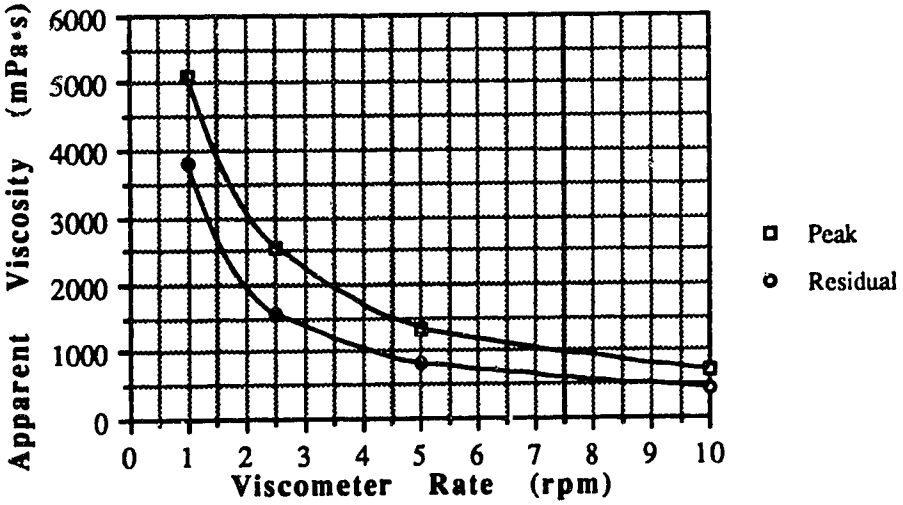

Figure B.9 Apparent Viscosity V40004H

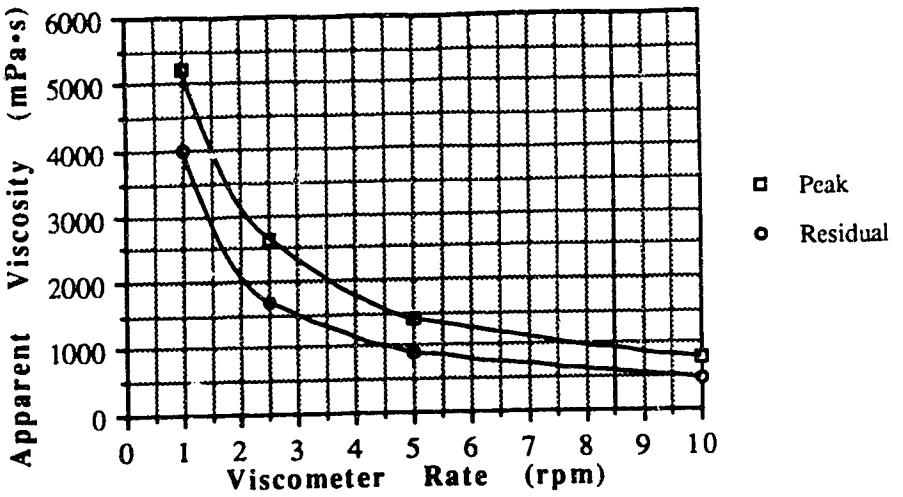

Figure B.10 Apparent Viscosity V40008H

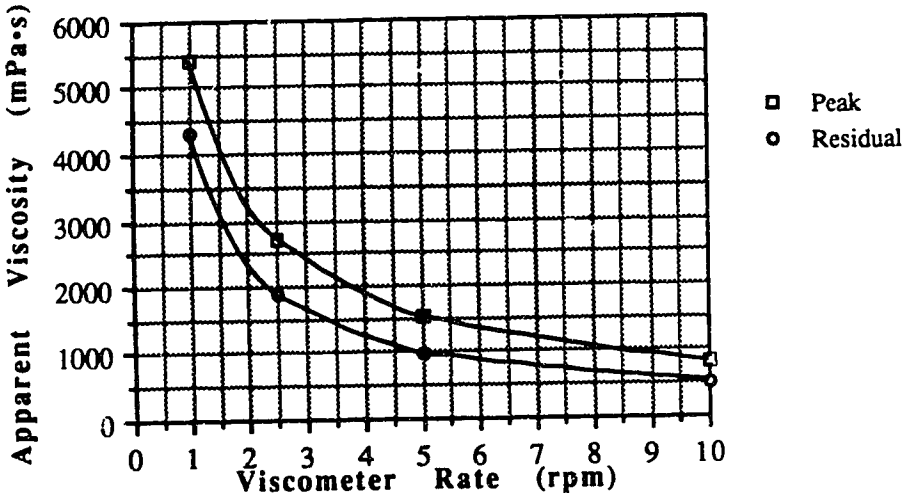

Figure B.11 Apparent Viscosity V40012H

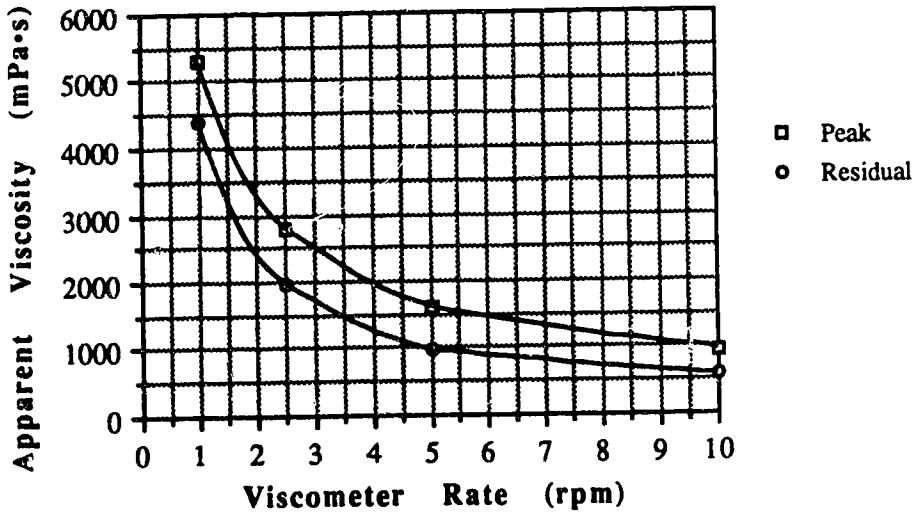

Figure B.12 Apparent Viscosity V40018H

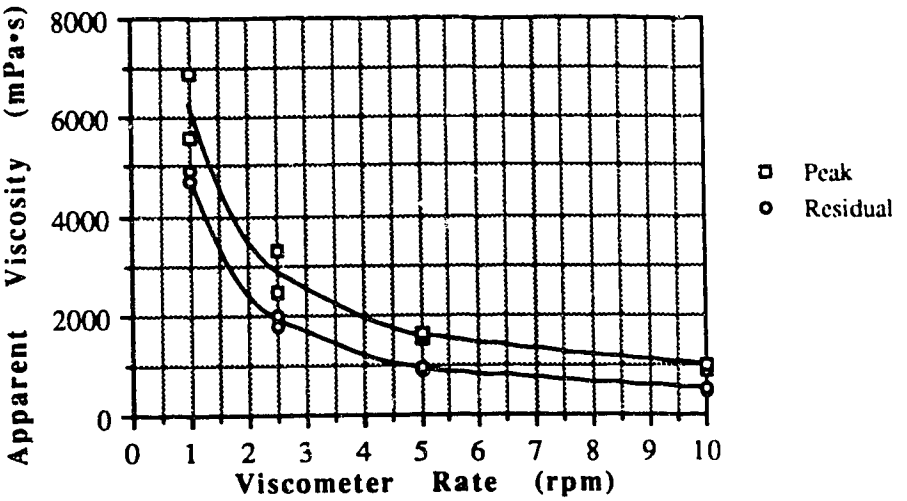

Figure B.13 Apparent Viscosity V40001D

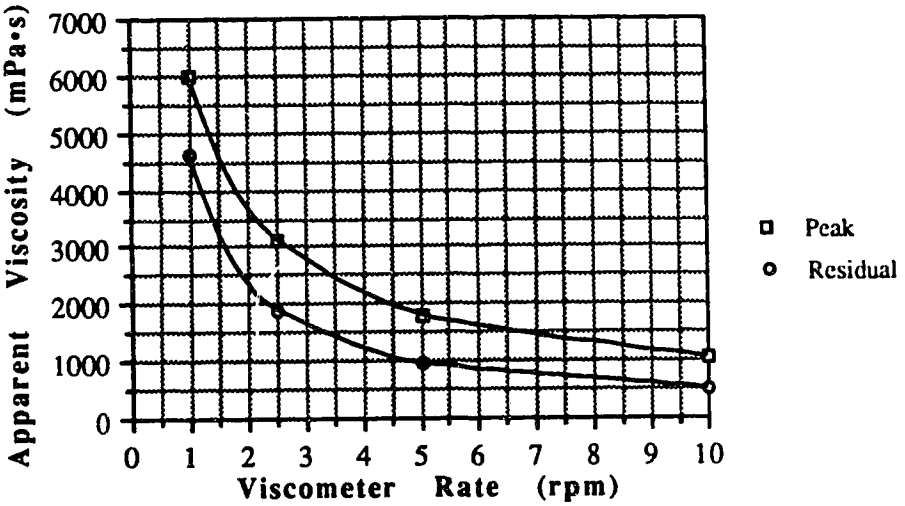

Figure B.14 Apparent Viscosity V40002D

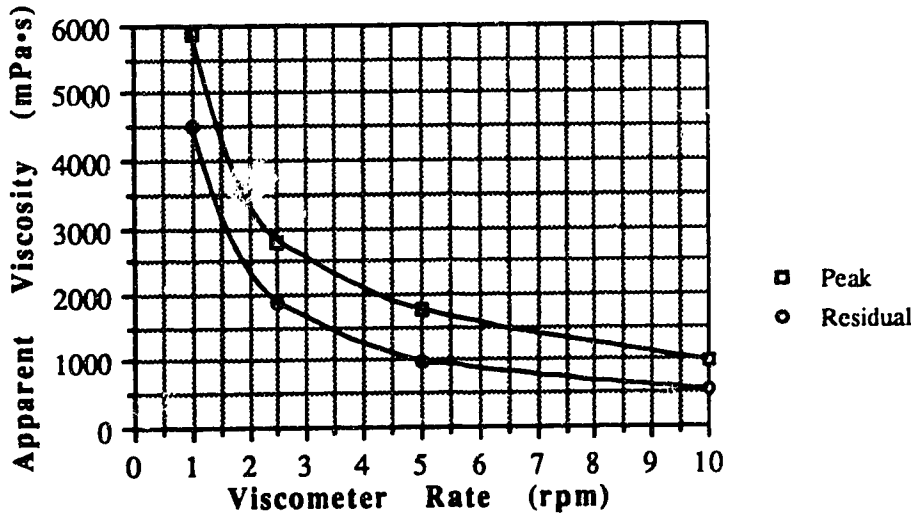

Figure B.15 Apparent Viscosity V40003D

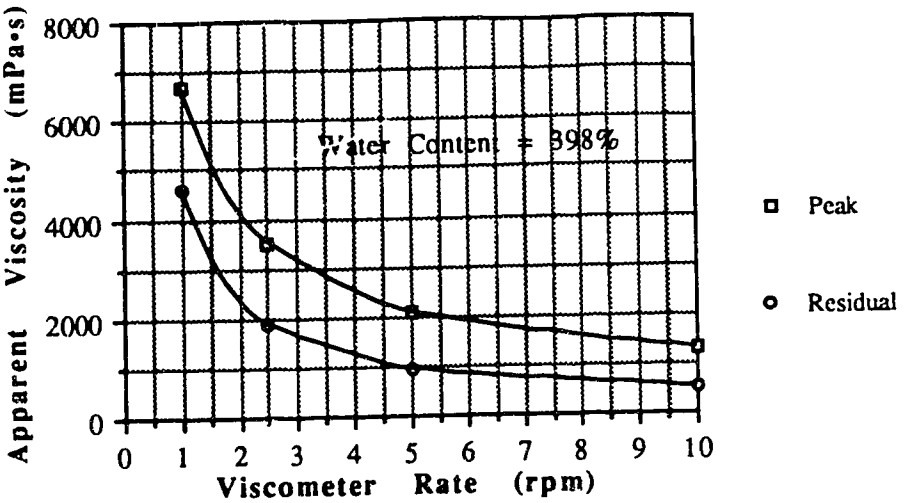

Figure B.16 Apparent Viscosity V40004D

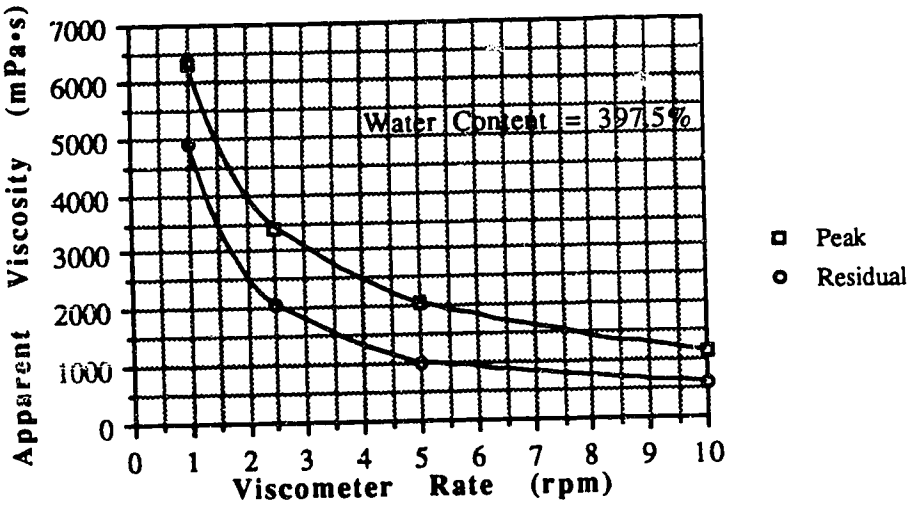

Figure B.17 Apparent Viscosity V40005D

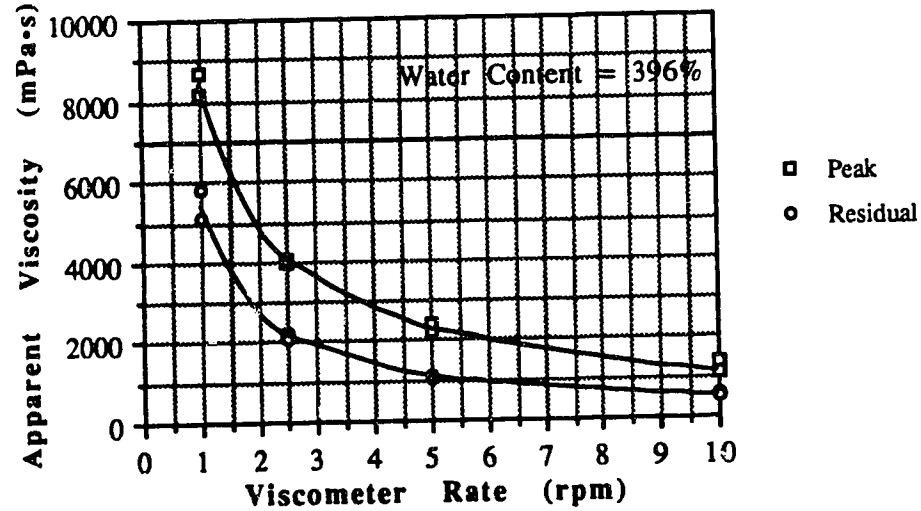

Figure B.18 Apparent Viscosity V40010D

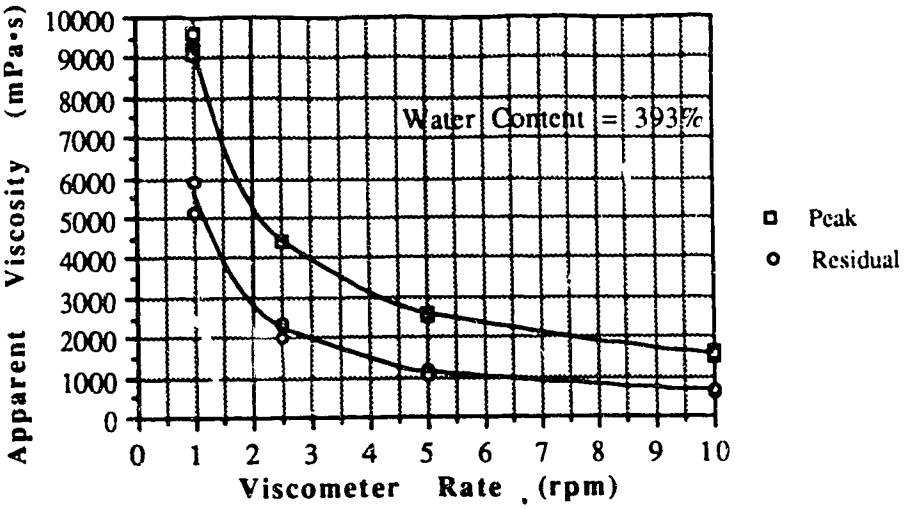

Figure B.19 Apparent Viscosity V40020D

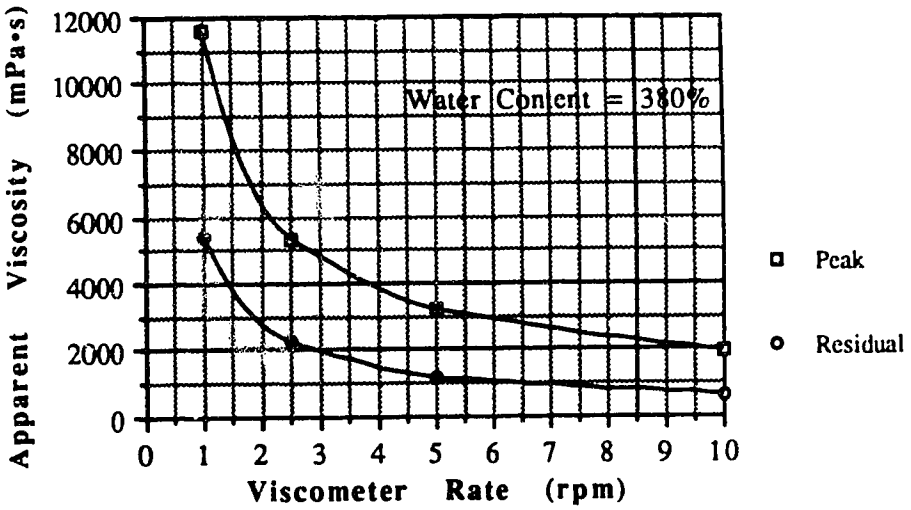

Figure B.20 Apparent Viscosity V40033D

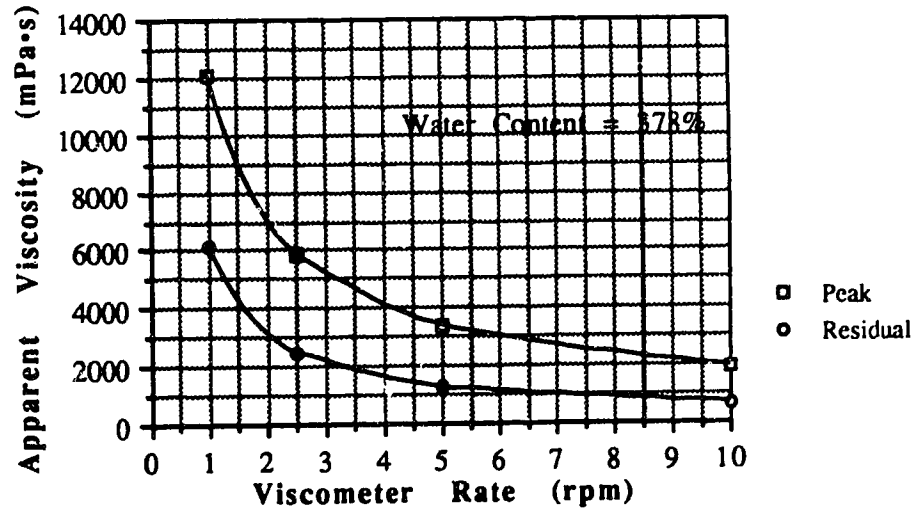

Figure B.21 Apparent Viscosity V40040D

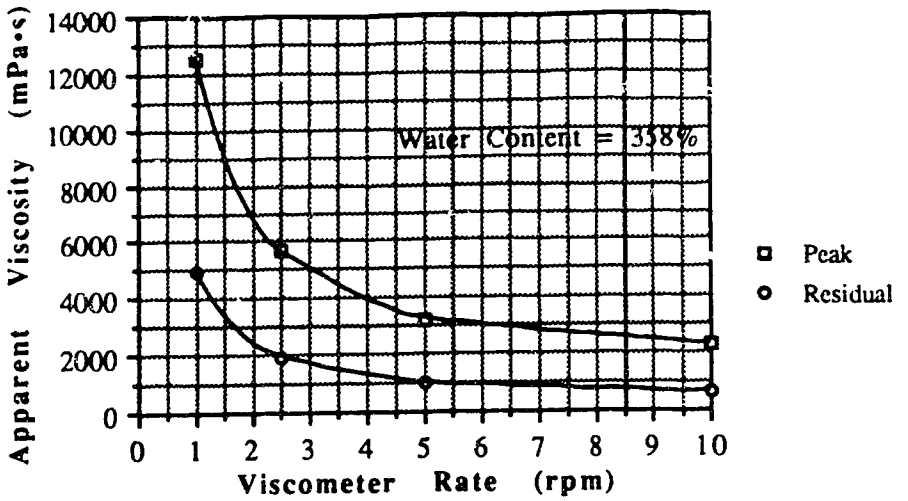

Figure B.22 Apparent Viscosity V40064D

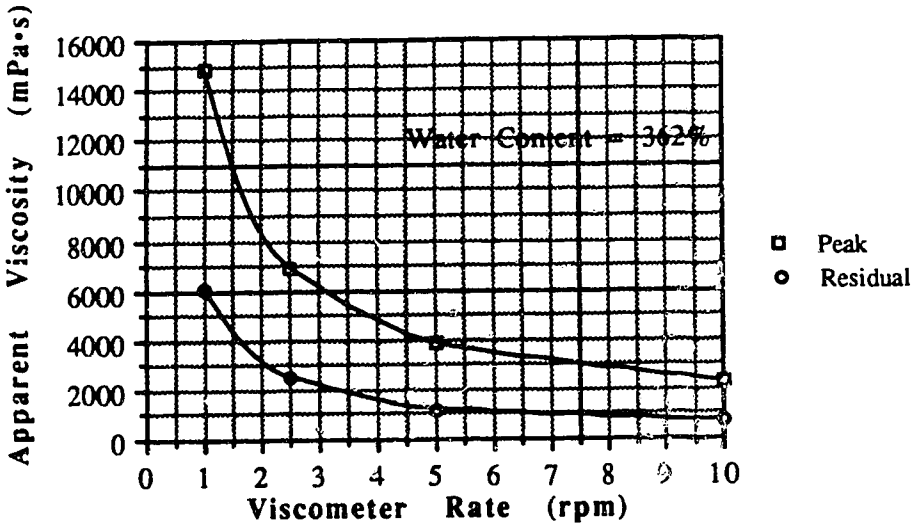

Figure B.23 Apparent Viscosity V40070D

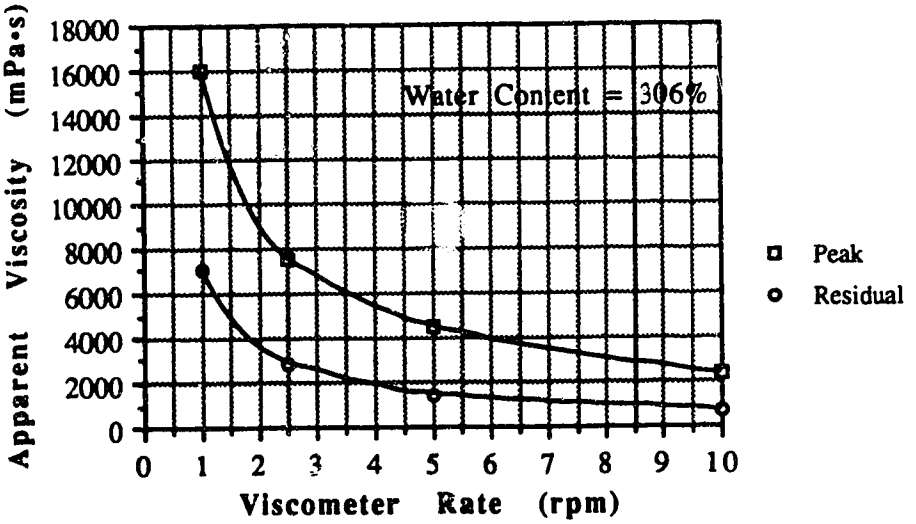

Figure B.24 Apparent Viscosity V40160D

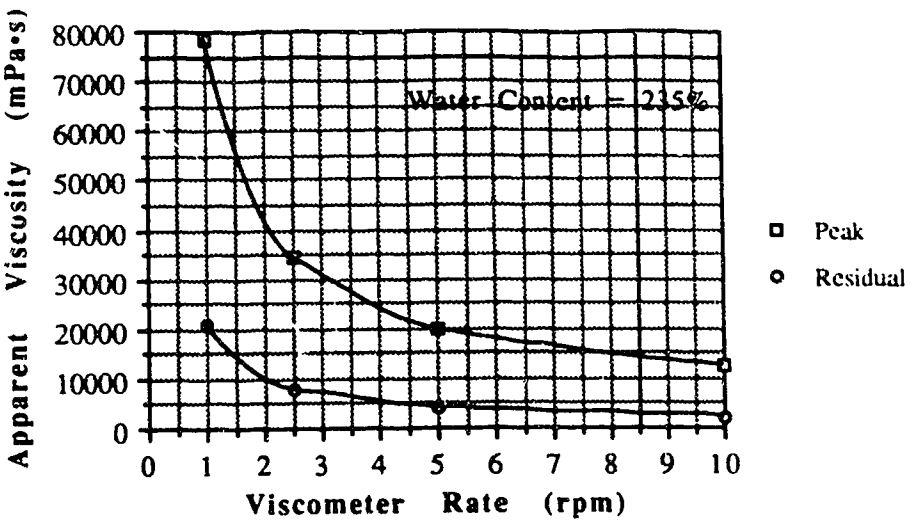

Figure B.25 Apparent Viscosity V40470D

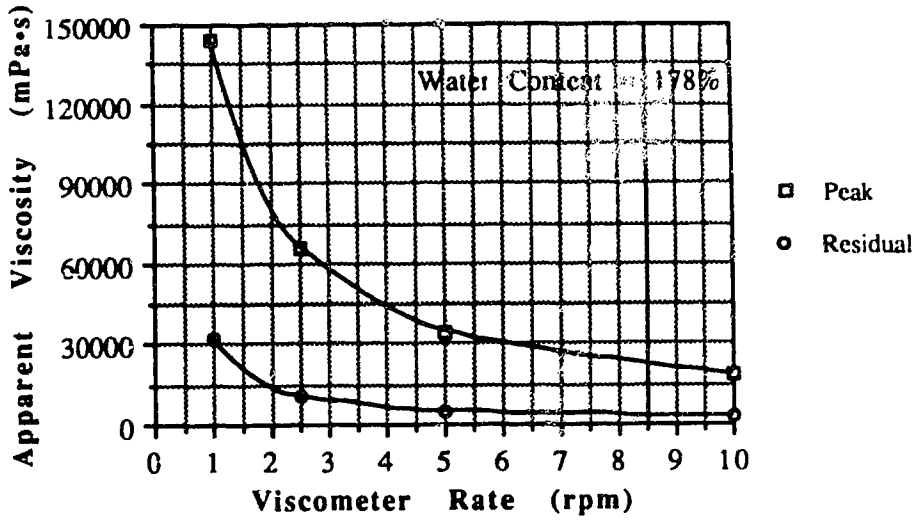

Figure B.26 Apparent Viscosity V40680D

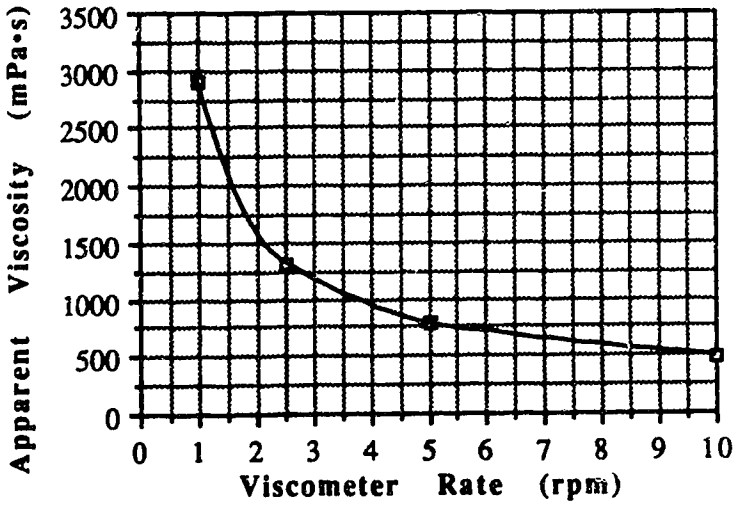

Figure B.27 Apparent Viscosity V30000M

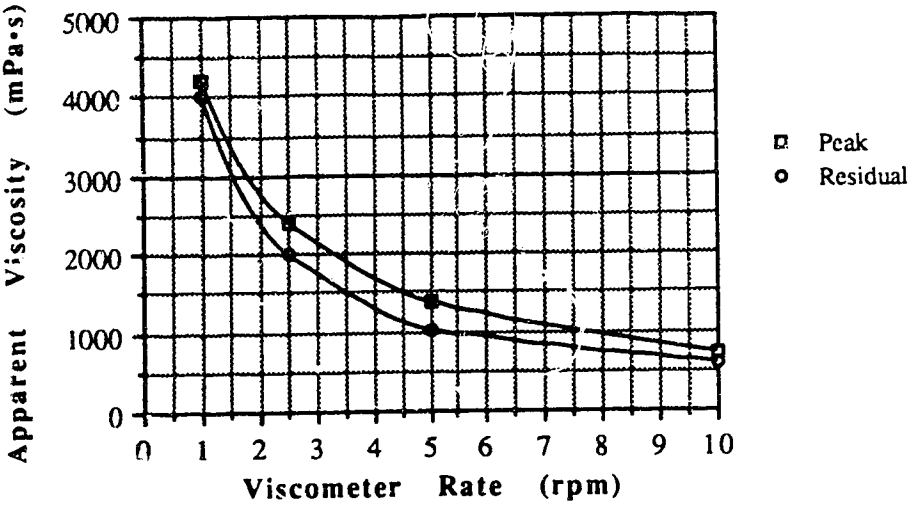

Figure B.28 Apparent Viscosity V30005M

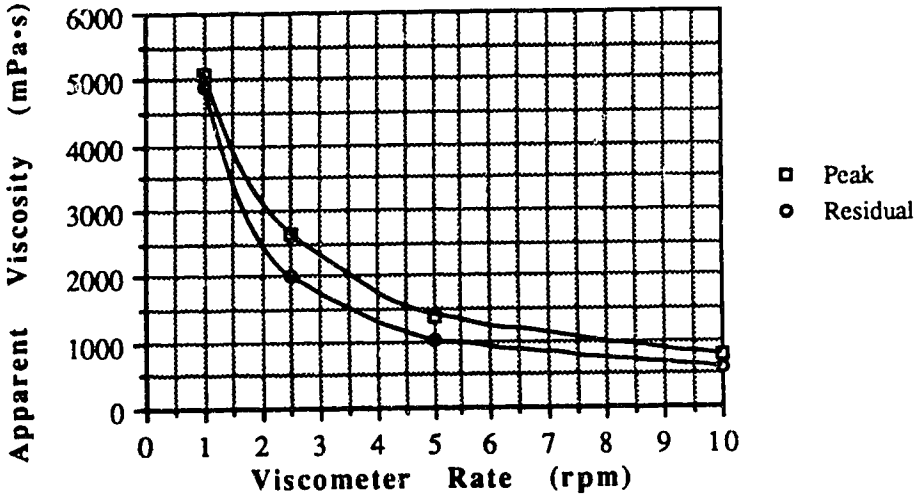

Figure B.29 Apparent Viscosity V30010M

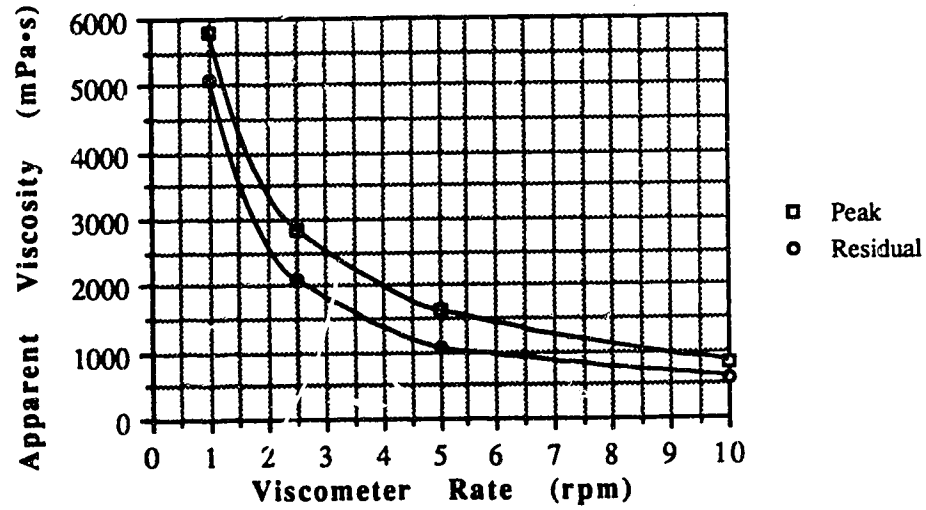

Figure B.30 Apparent Viscosity V30020M

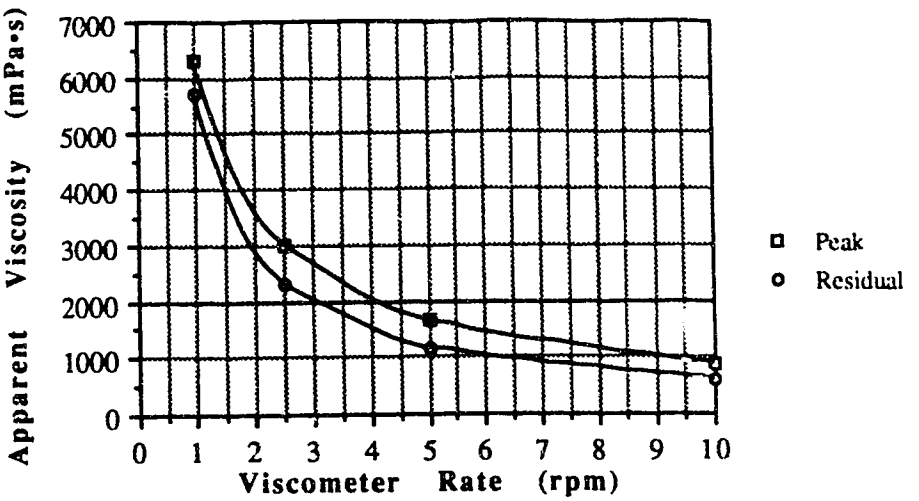

Figure B.31 Apparent Viscosity V30030M

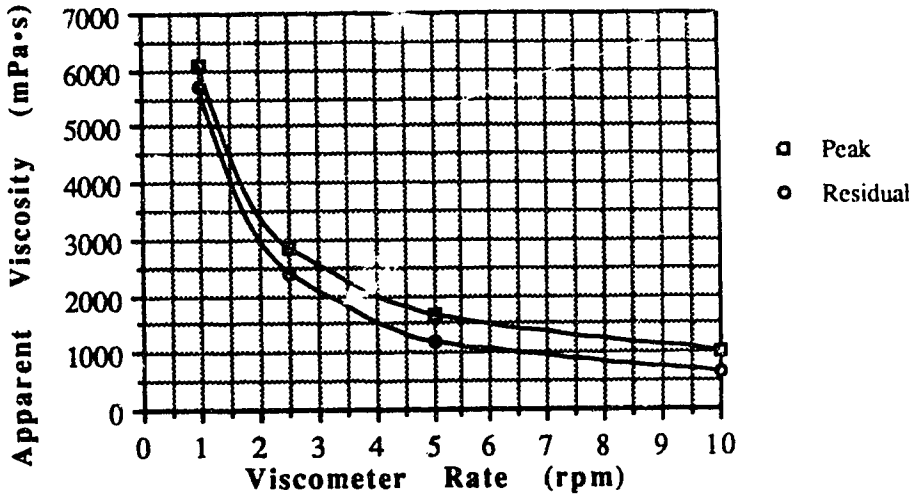

Figure B.32 Apparent Viscosity V30001H

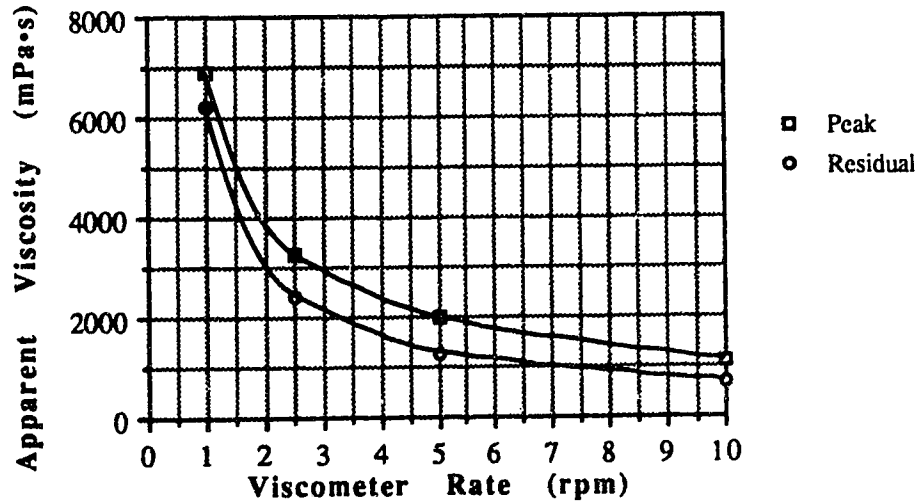

Figure B.33 Apparent Viscosity V30002H

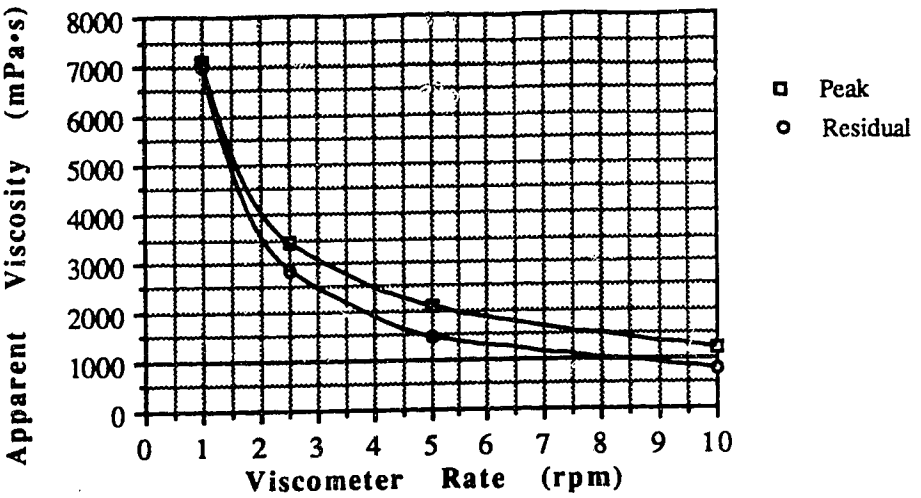

Figure B.34 Apparent Viscosity V30003H

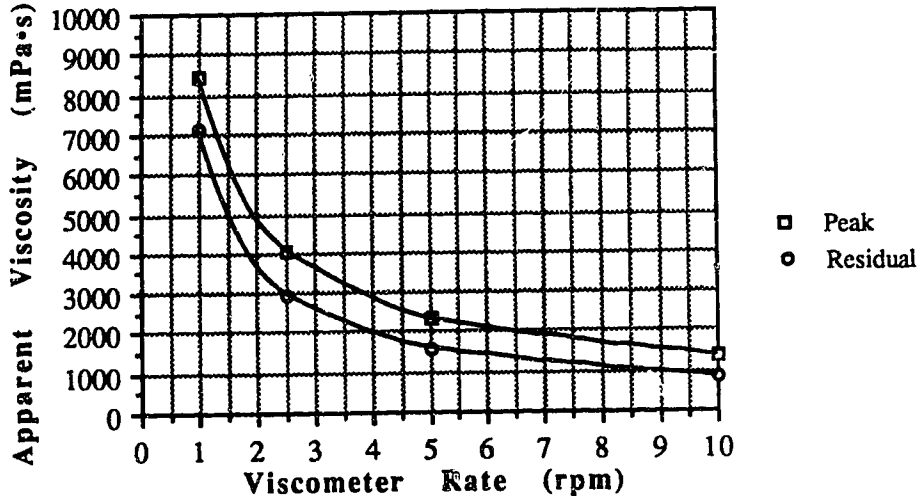

Figure B.35 Apparent Viscosity V30004H

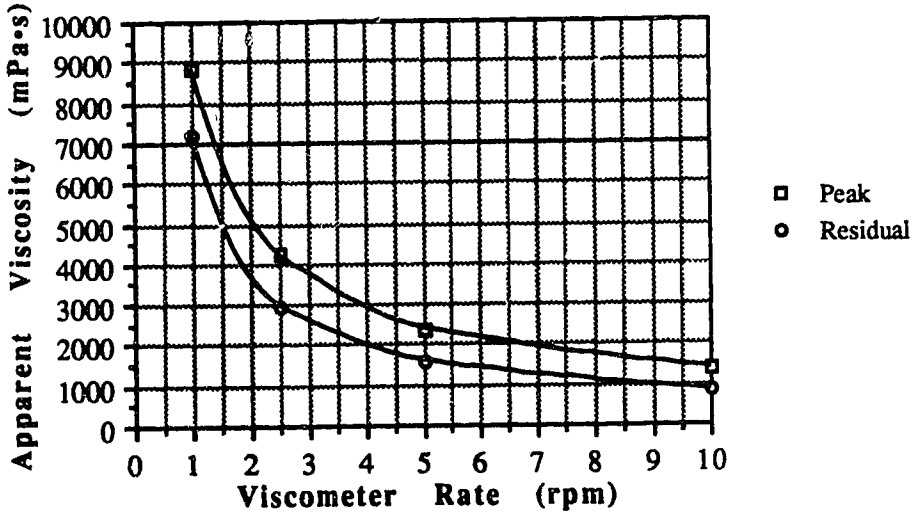

Figure B.36 Apparent Viscosity V30008H

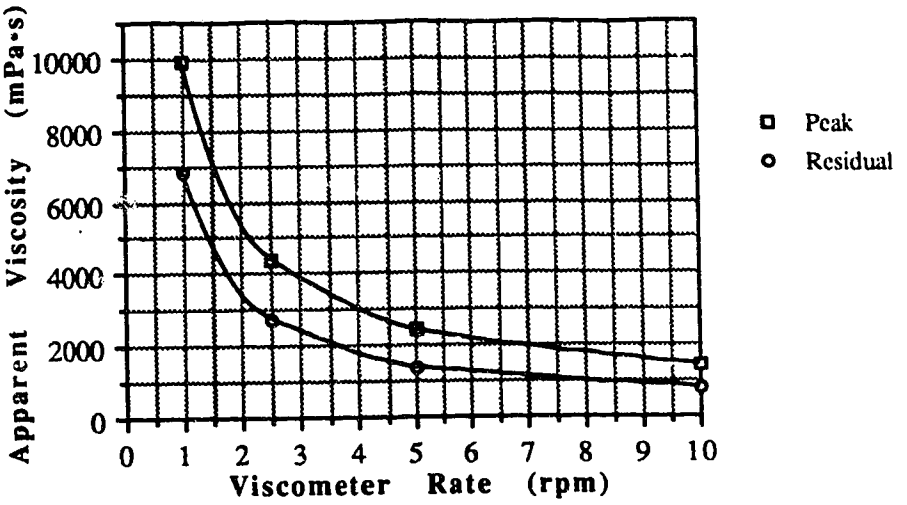

Figure B.37 Apparent Viscosity V30012H

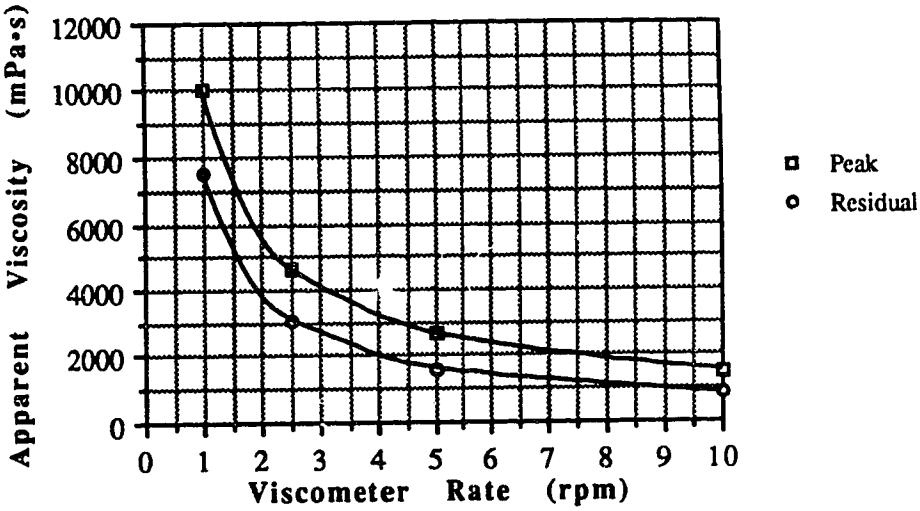

Figure B.38 Apparent Viscosity V30018H

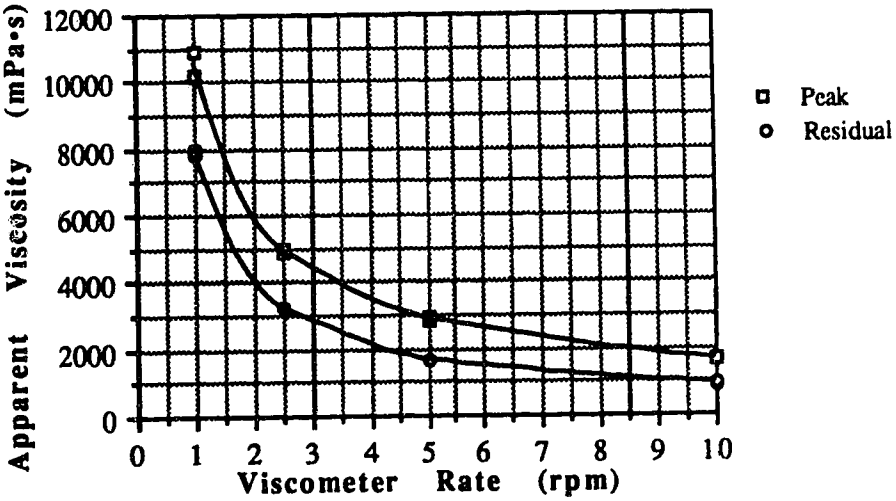

Figure B.39 Apparent Viscosity V30001D

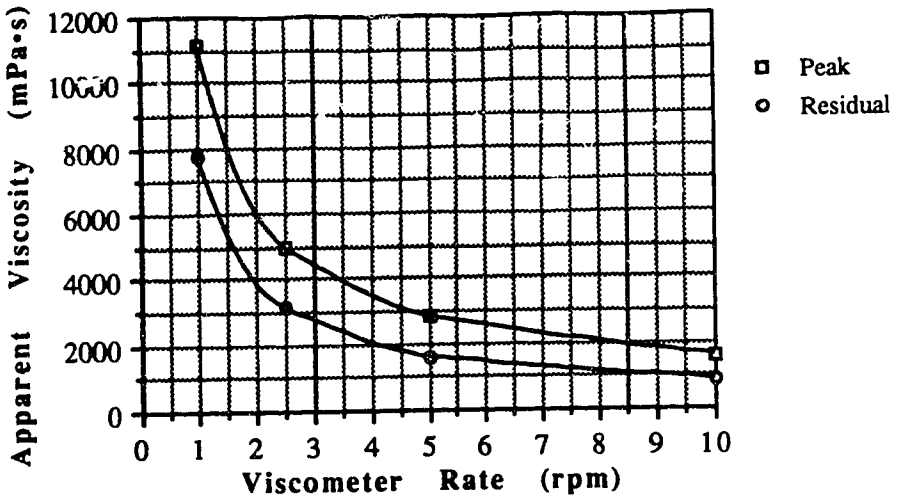

Figure B.40 Apparent Viscosity V30002D

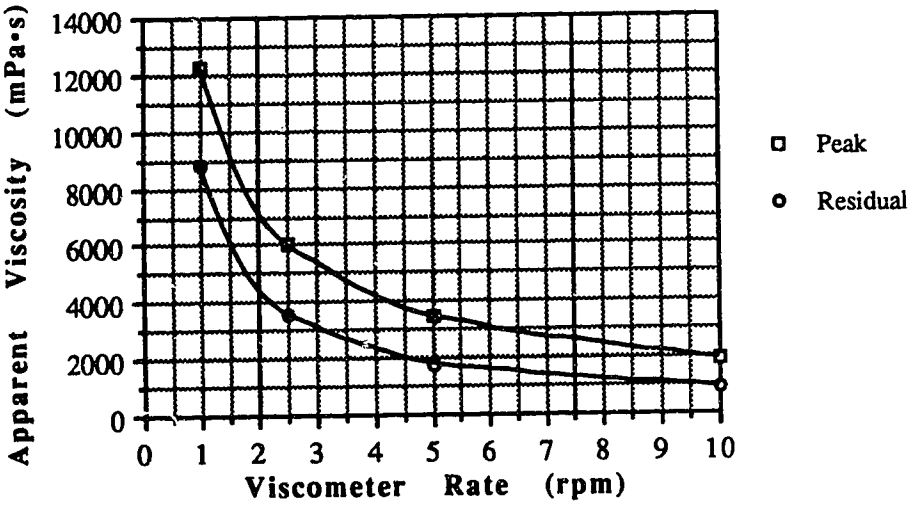

Figure B.41 Apparent Viscosity V30003D

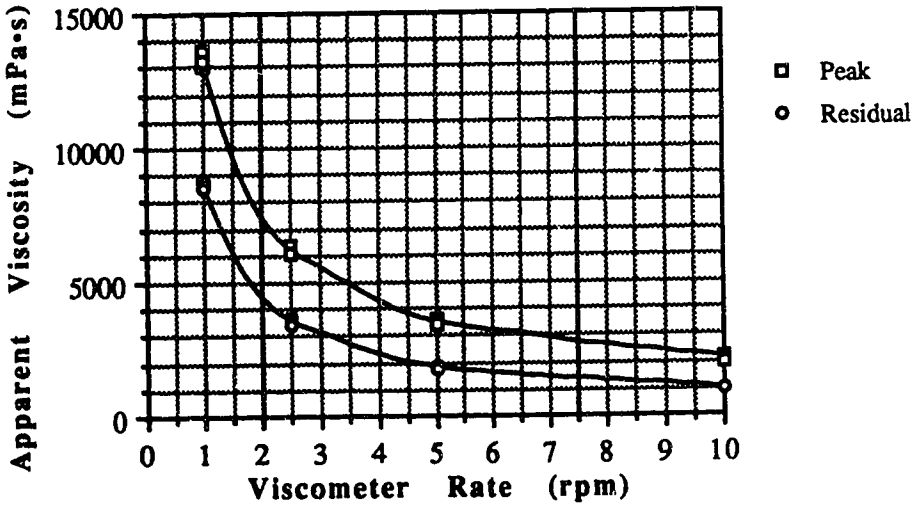

Figure B.42 Apparent Viscosity V30004D

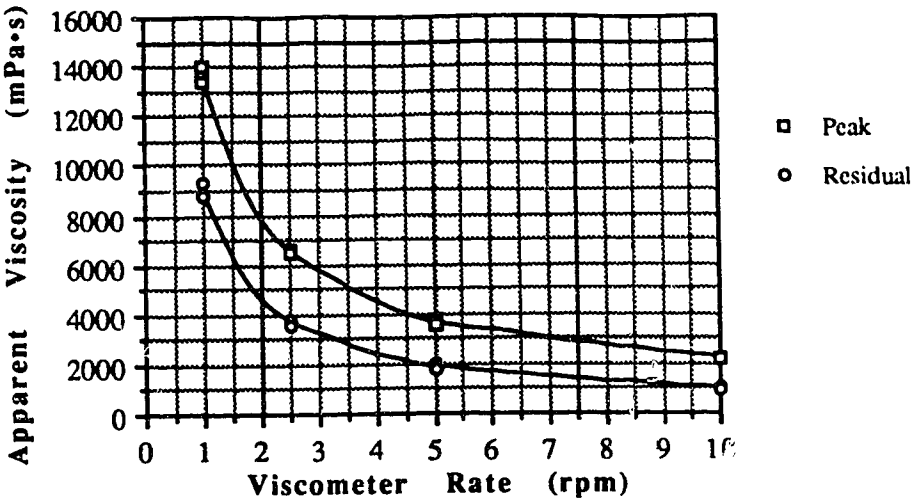

Figure B.43 Apparent Viscosity V30005D

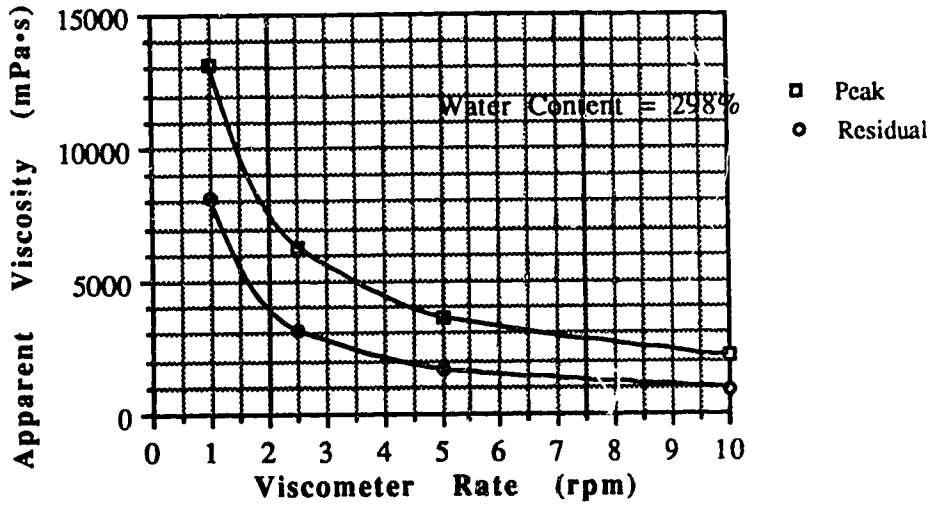

Figure B.44 Apparent Viscosity V30006D

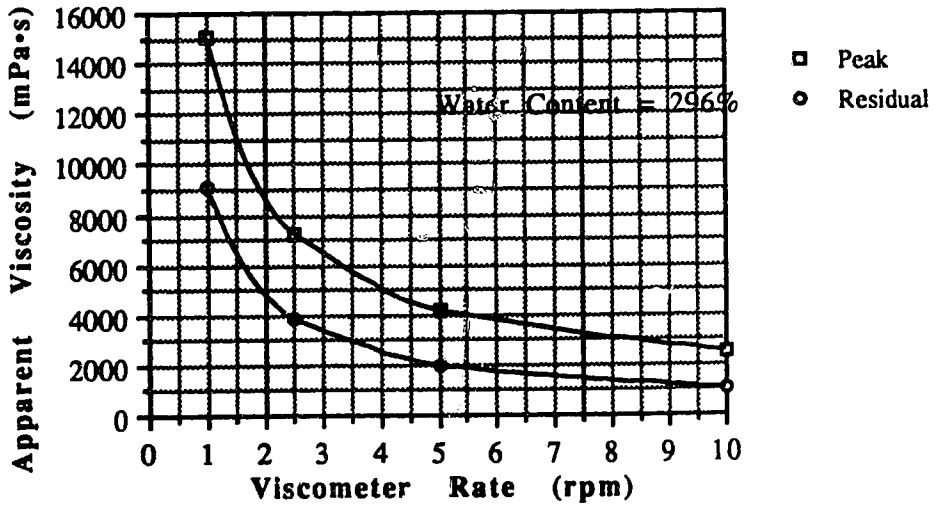

Figure B.45 Apparent Viscosity V30010D

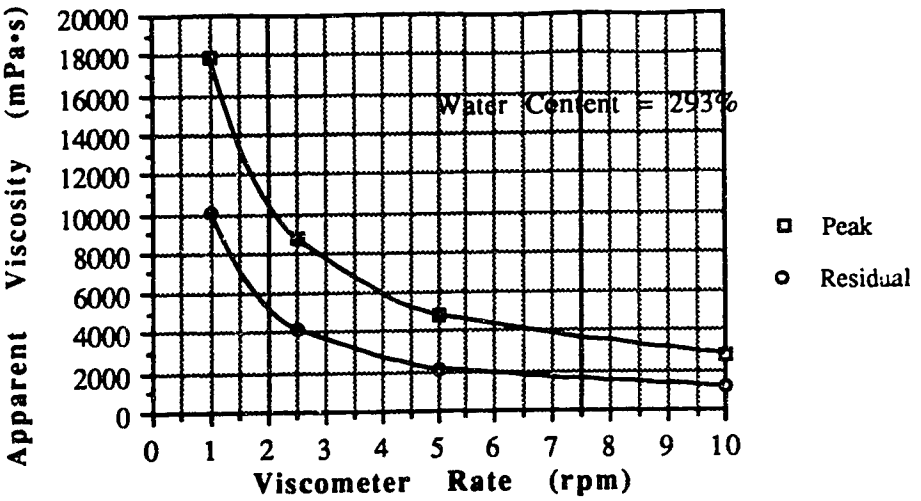

Figure B.46 Apparent Viscosity V30020D

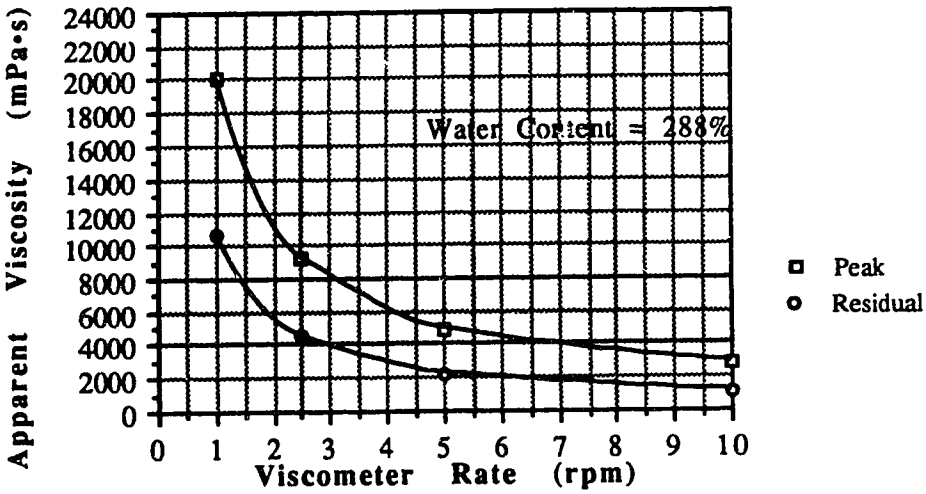

Figure B.47 Apparent Viscosity V30040D

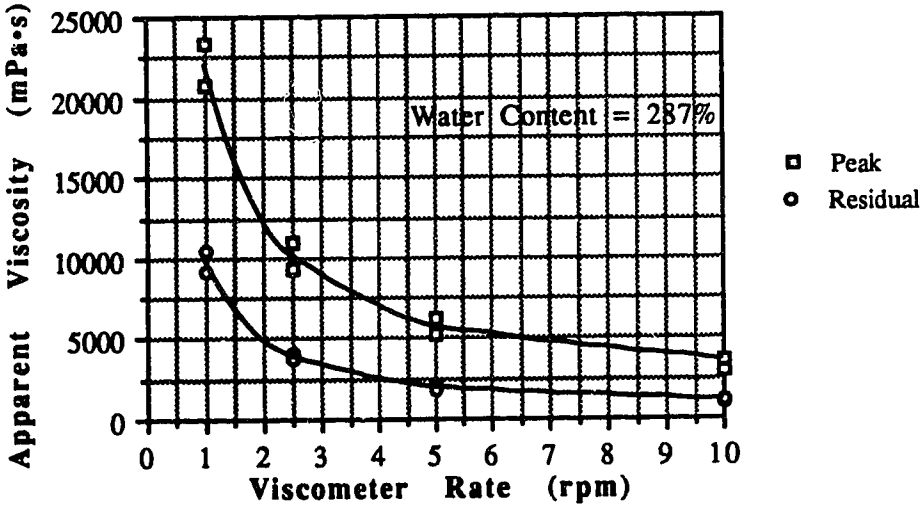

Figure B.48 Apparent Viscosity V30050D

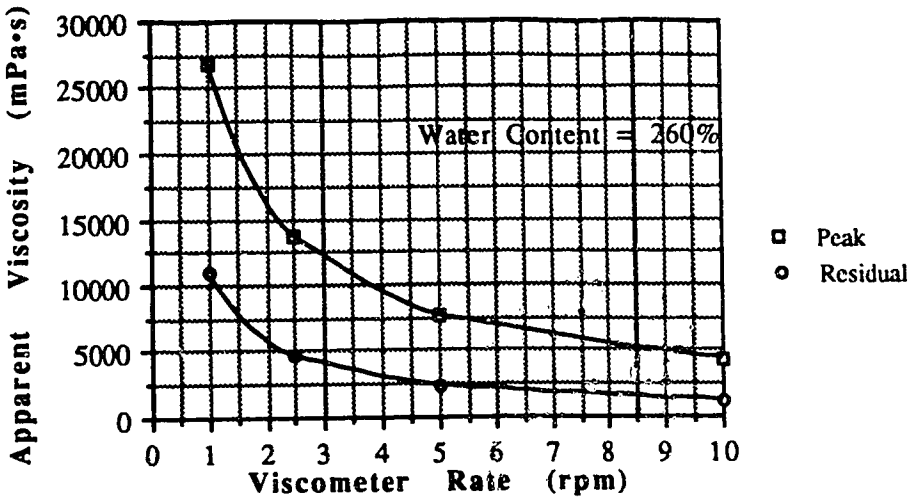

Figure B.49 Apparent Viscosity V30160D

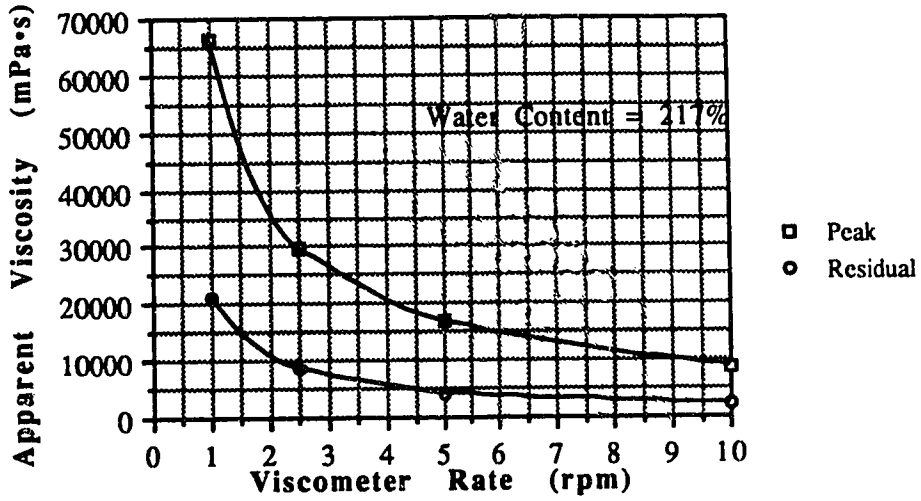

Figure B.50 Apparent Viscosity V30470D

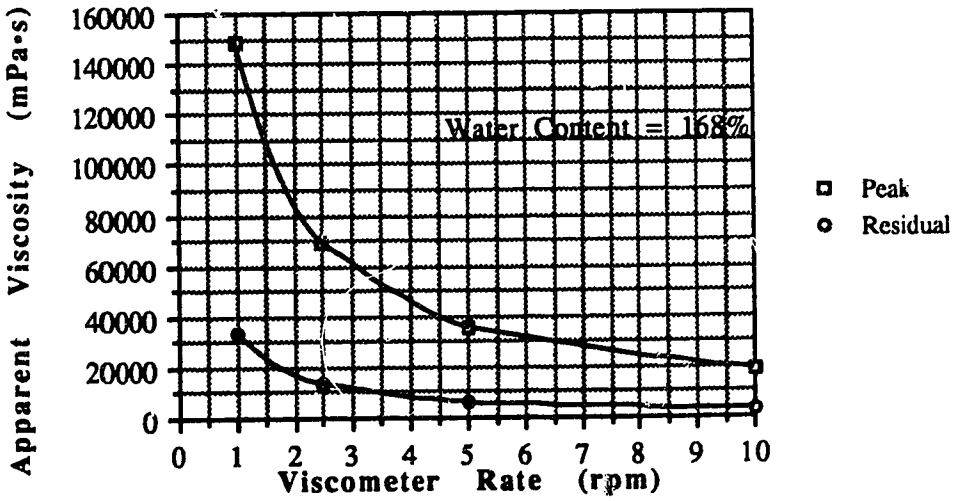

Figure B.51 Apparent Viscosity V30660D

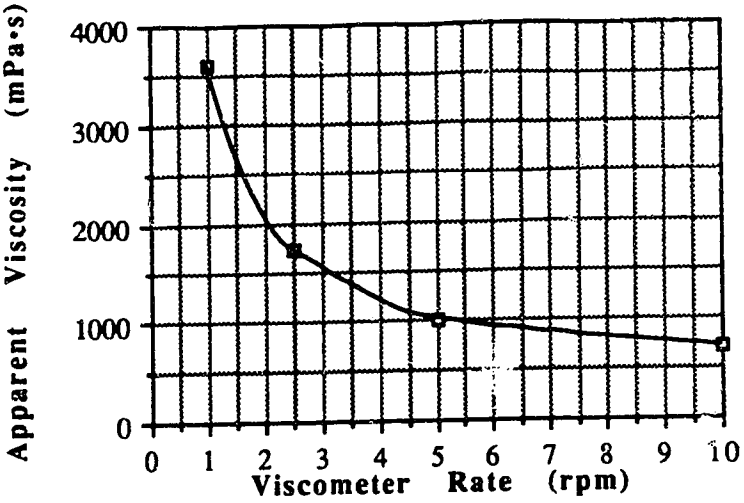

Figure B.52 Apparent Viscosity V23000M

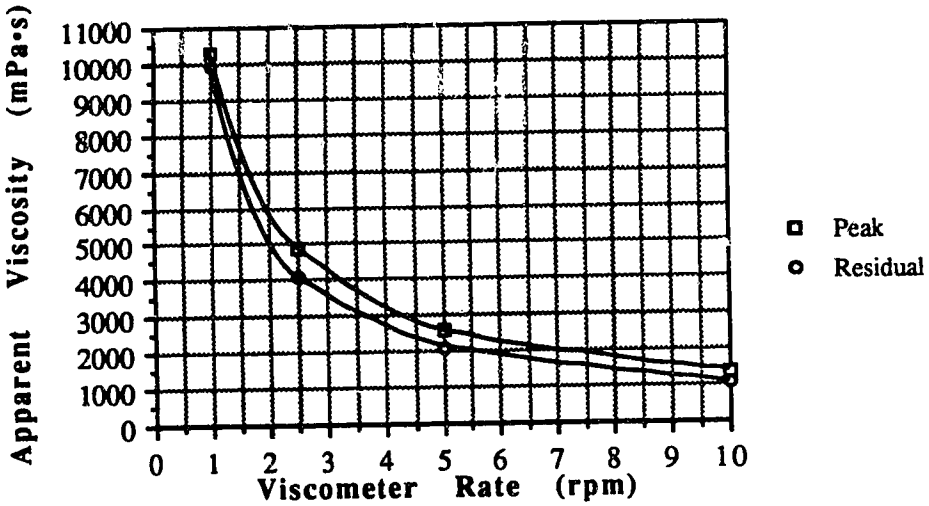

Figure B.53 Apparent Viscosity V23005M

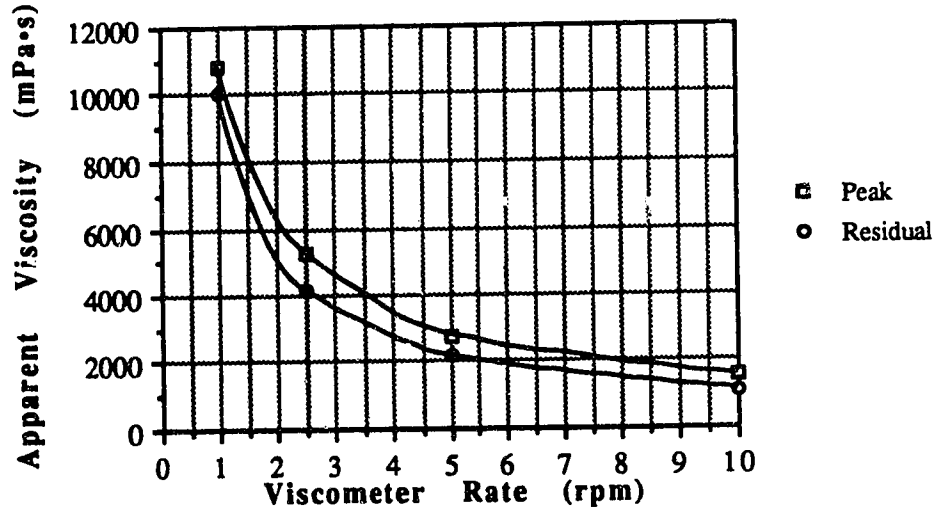

Figure B.54 Apparent Viscosity V23010M

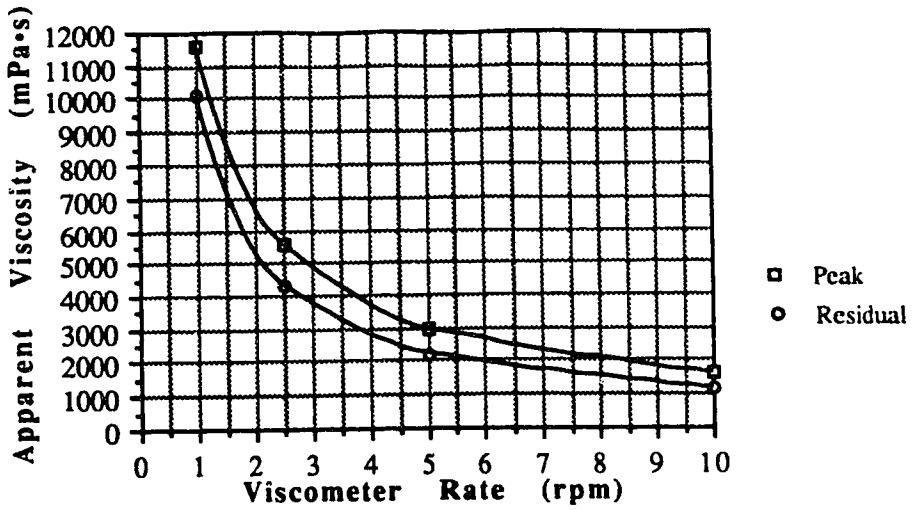

Figure B.55 Apparent Viscosity V23020M

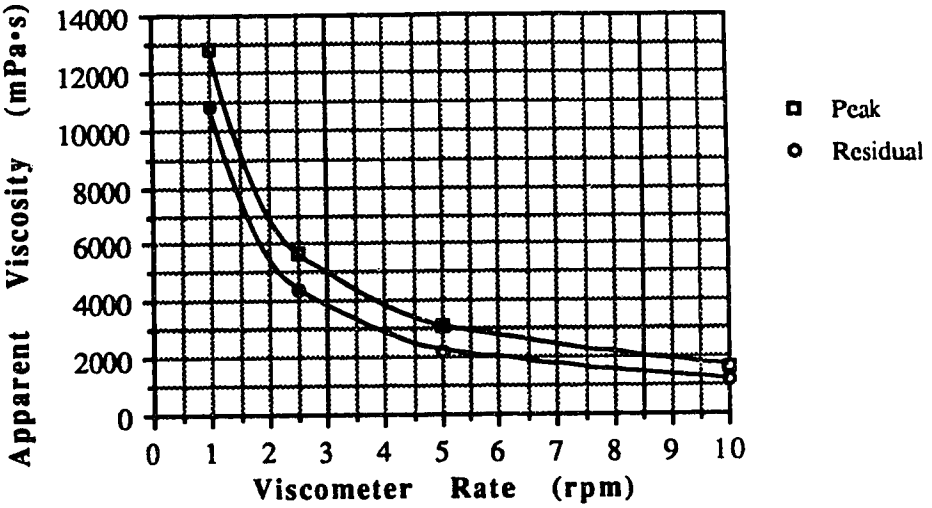

Figure B.56 Apparent Viscosity V23030M

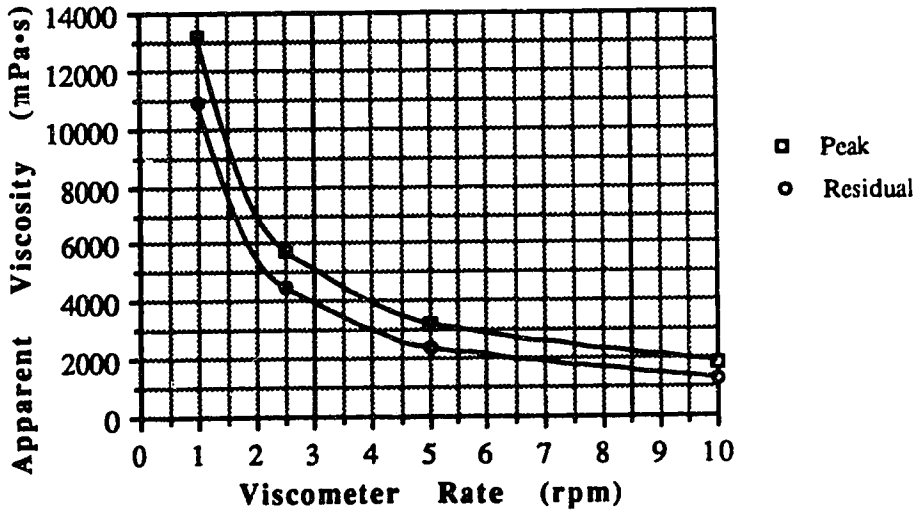

Figure B.57 Apparent Viscosity V23001H

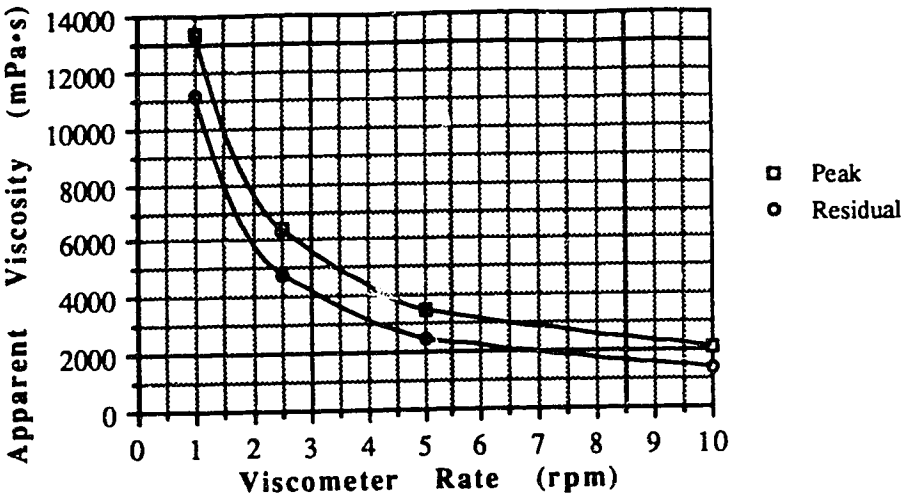

Figure B.58 Apparent Viscosity V23002H

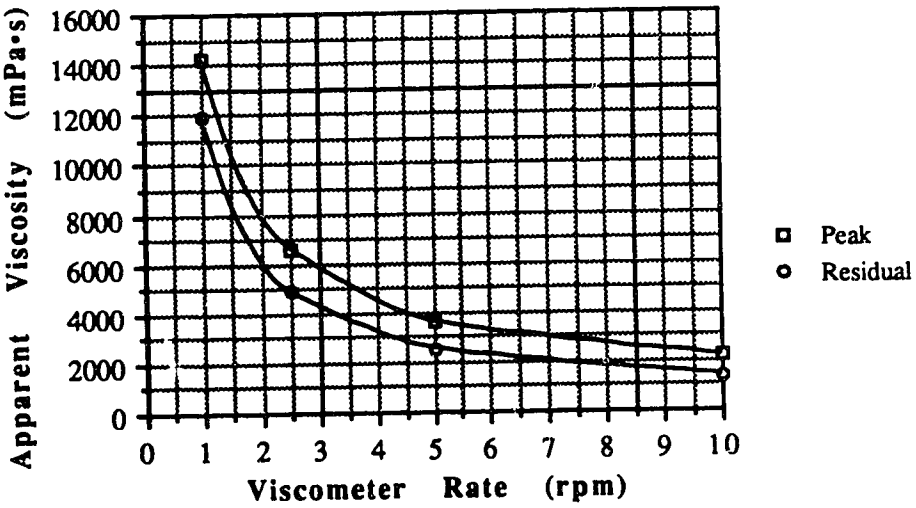

Figure B.59 Apparent Viscosity V23003H

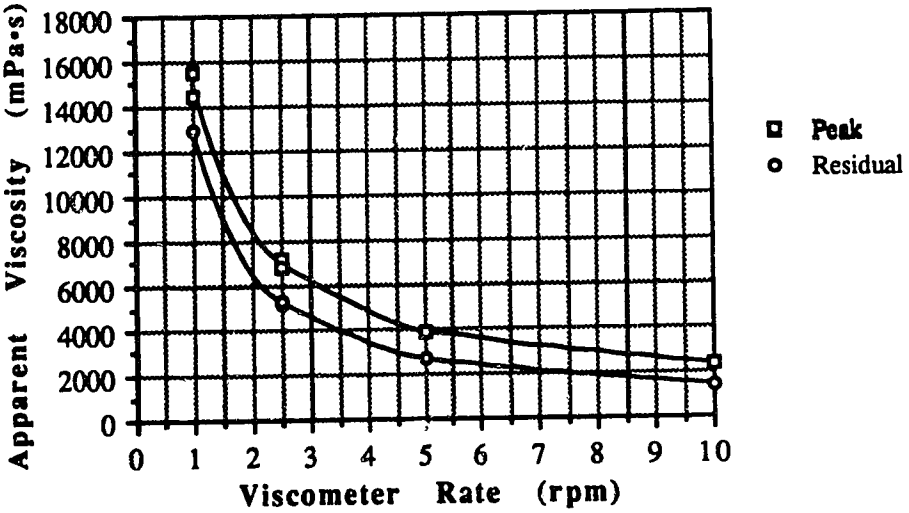

Figure B.60 Apparent Viscosity V23004H

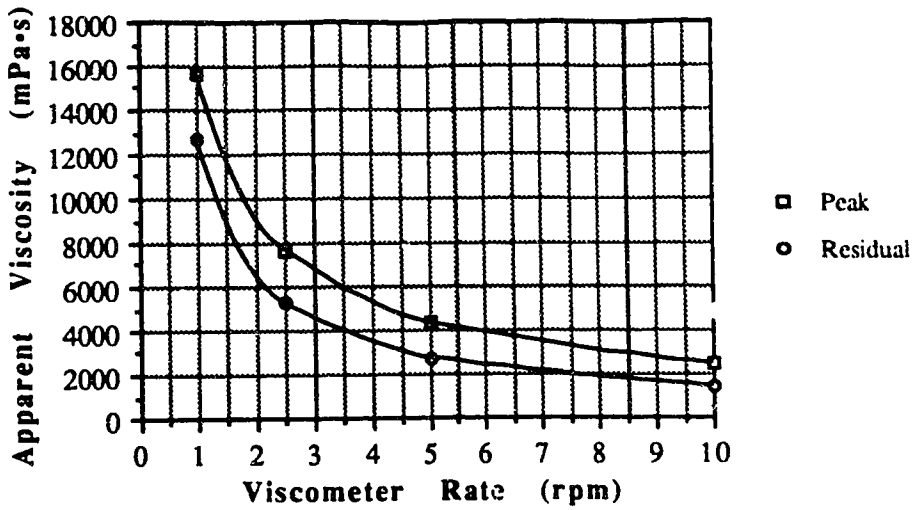

Figure B.61 Apparent Viscosity V23008H

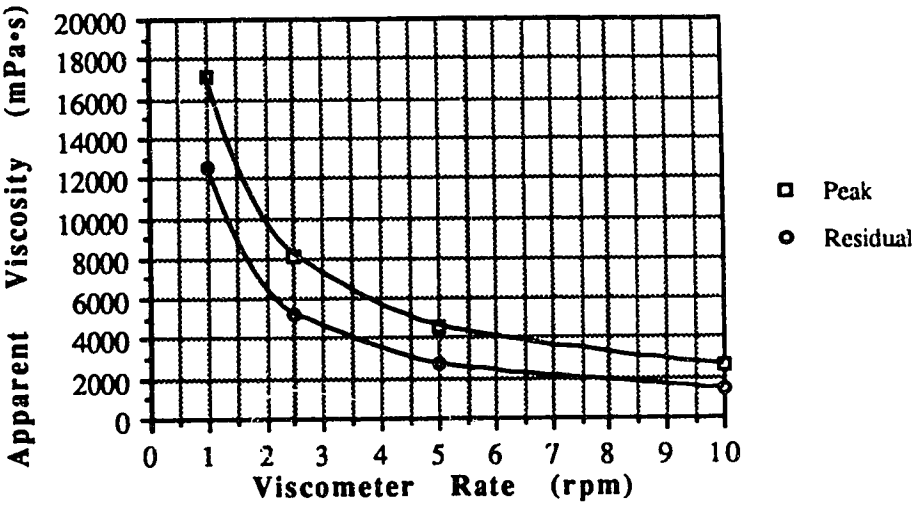

Figure B.62 Apparent Viscosity V23012H

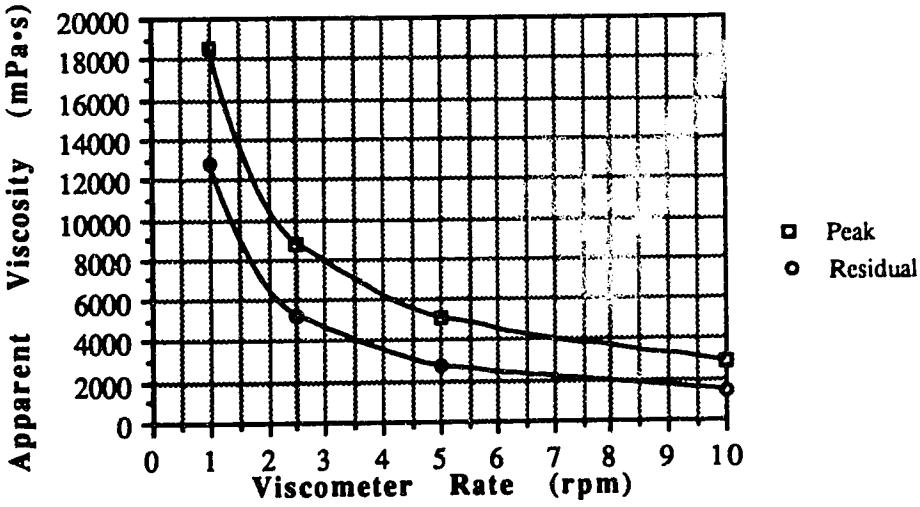

Figure B.63 Apparent Viscosity V23018H

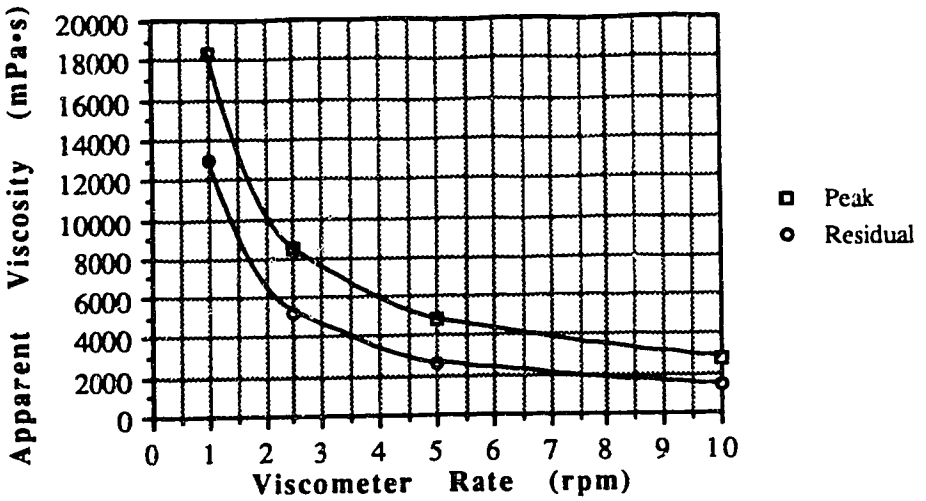

Figure B.64 Apparent Viscosity V23001D

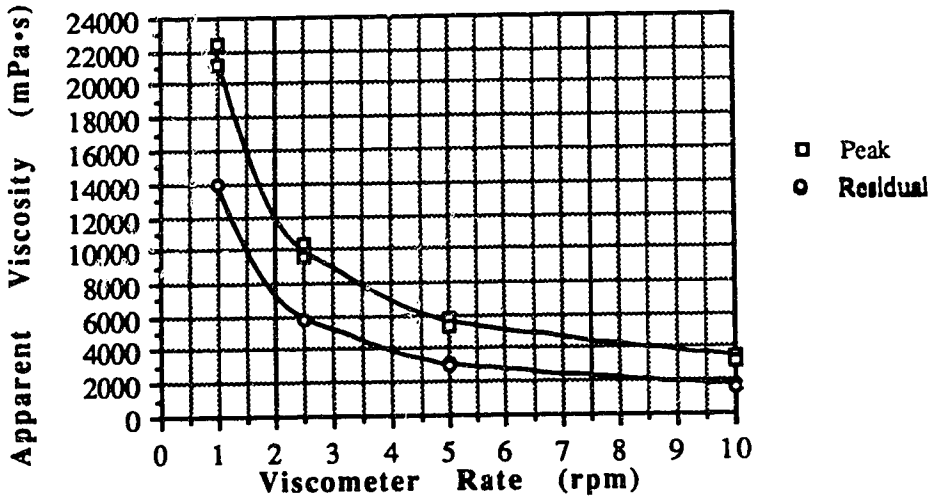

Figure B.65 Apparent Viscosity V23002D

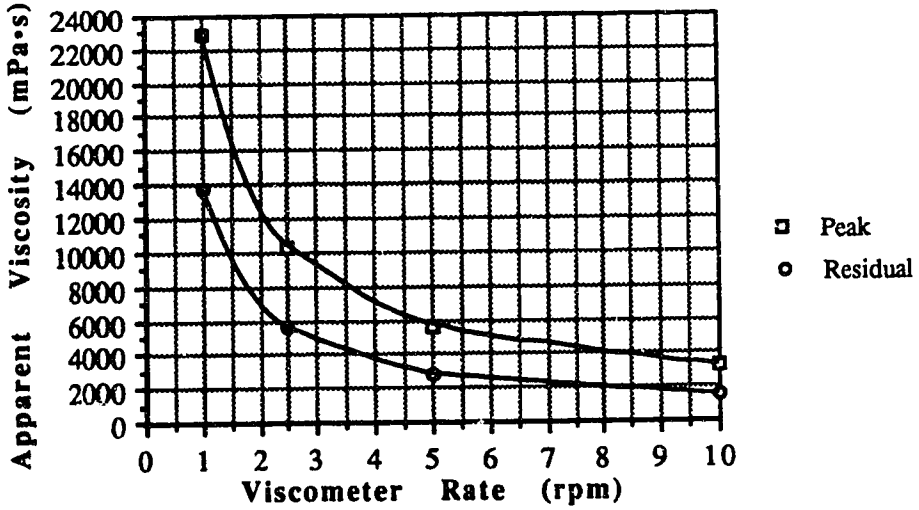

Figure B.66 Apparent Viscosity V23003D

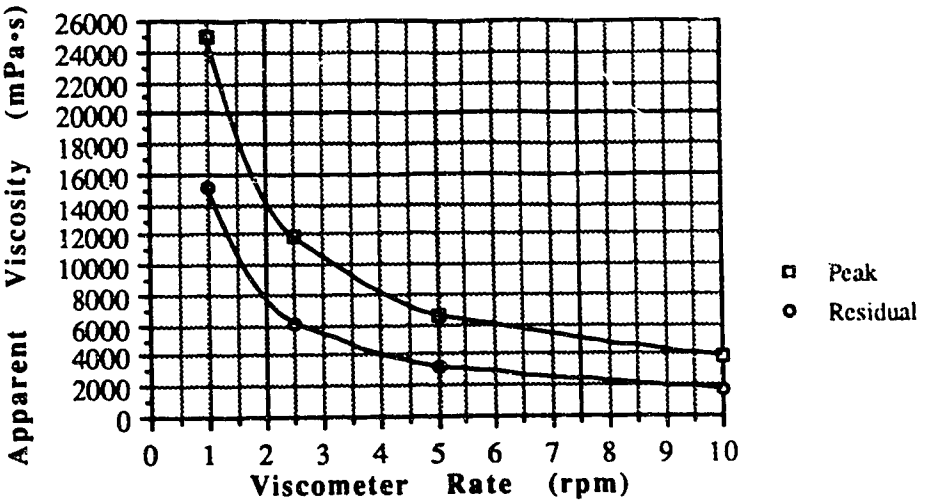

Figure B.67 Apparent Viscosity V23004D

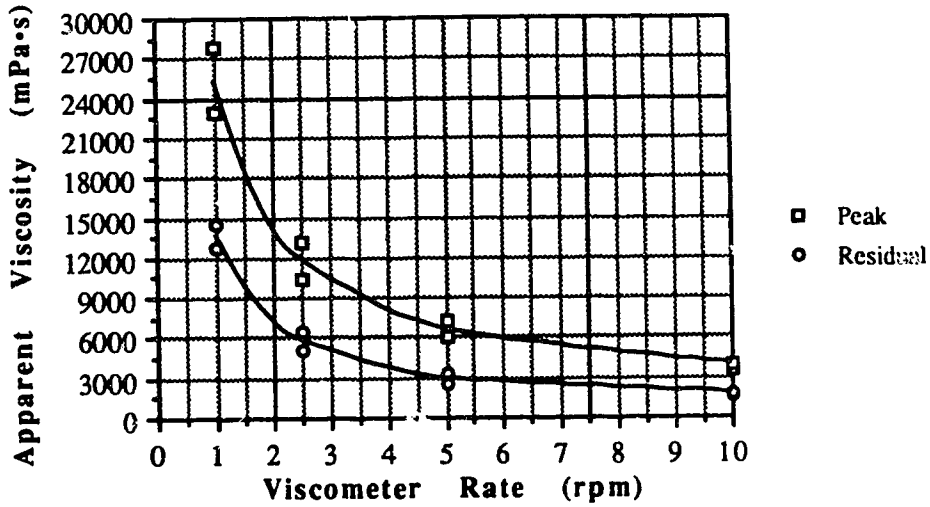

Figure B.68 Apparent Viscosity V23005D

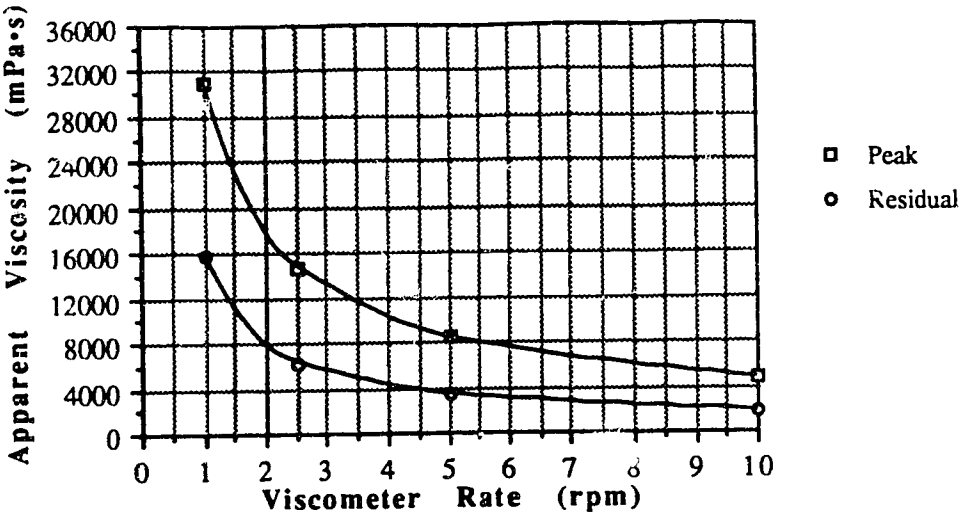

Figure B.69 Apparent Viscosity V23010D

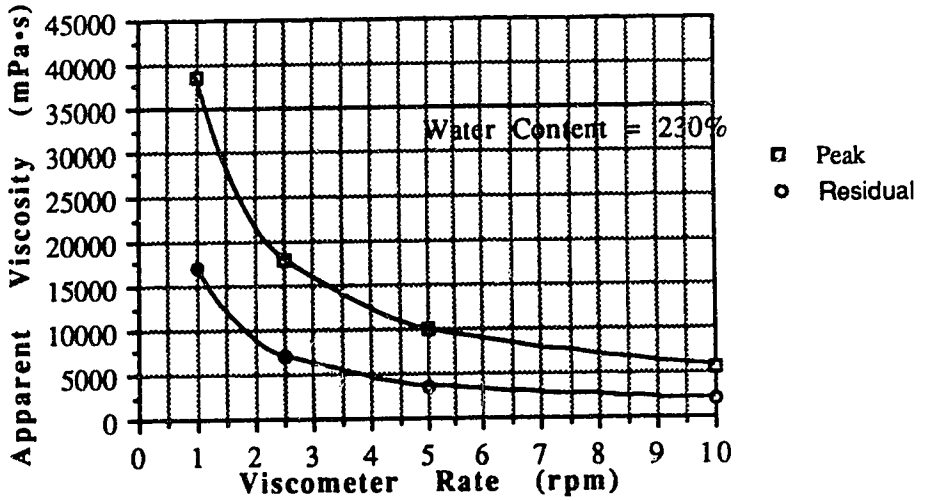

Figure B.70 Apparent Viscosity V23020D

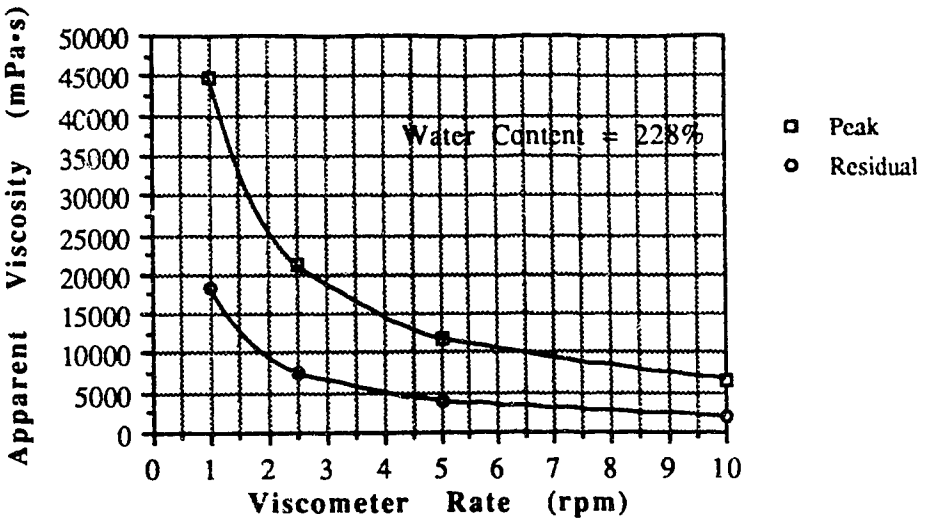

Figure B.71 Apparent Viscosity V23040D

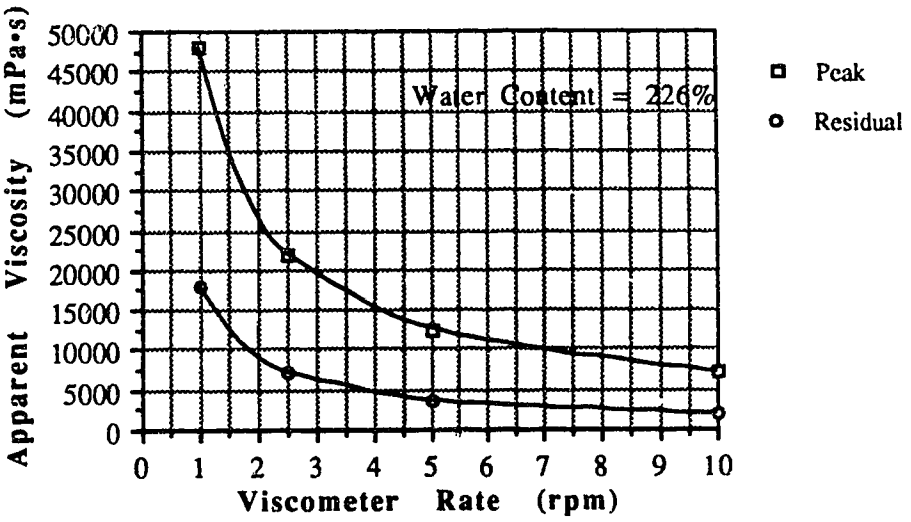

Figure B.72 Apparent Viscosity V23075D

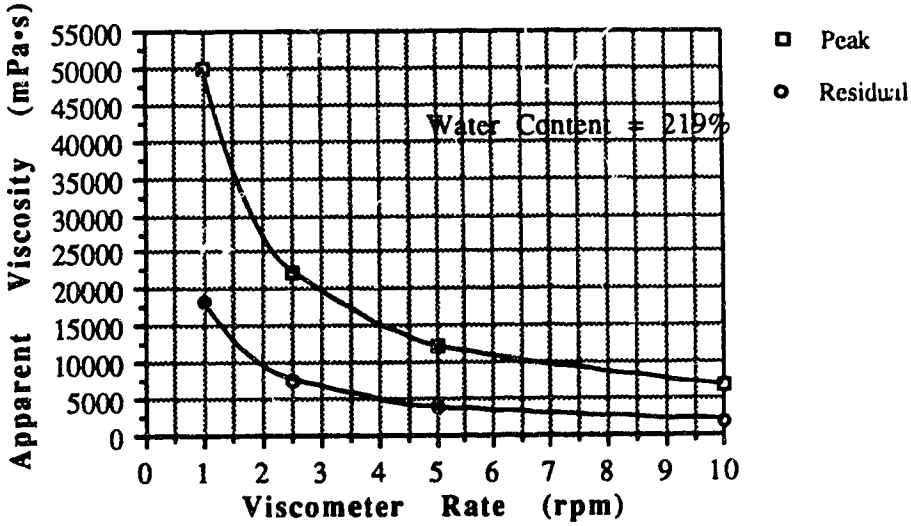

Figure B.73 Apparent Viscosity V23090D

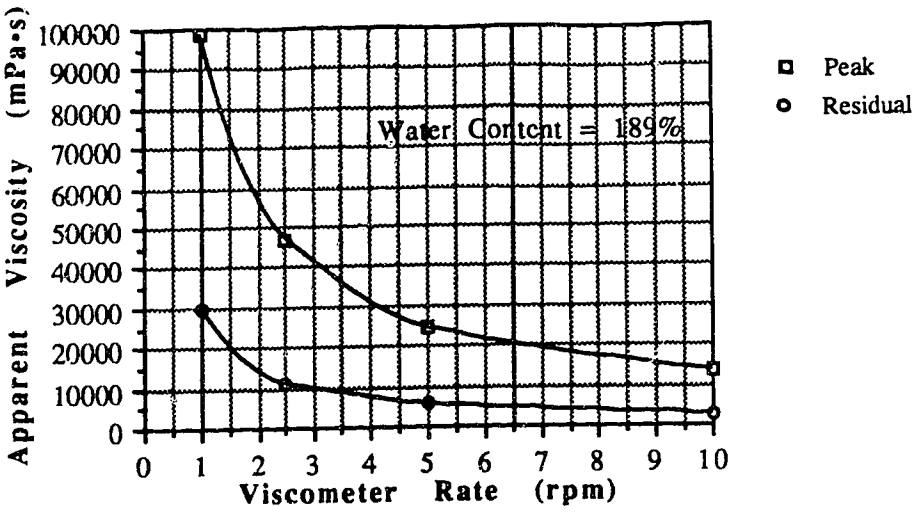

Figure B.74 Apparent Viscosity V23494D

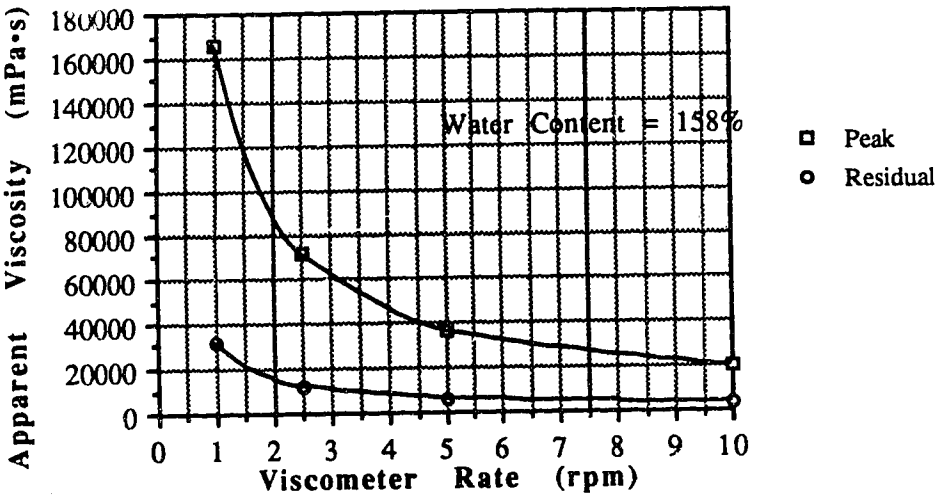

Figure B.75 Apparent Viscosity V23682D

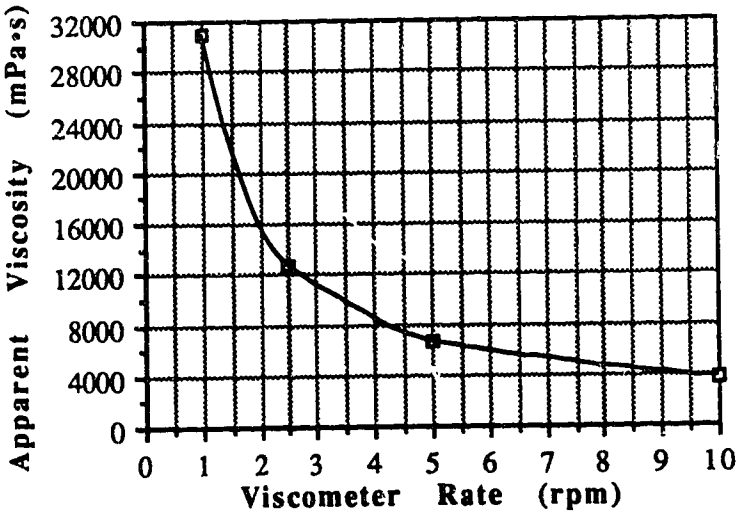

Figure B.76 Apparent Viscosity V15000M

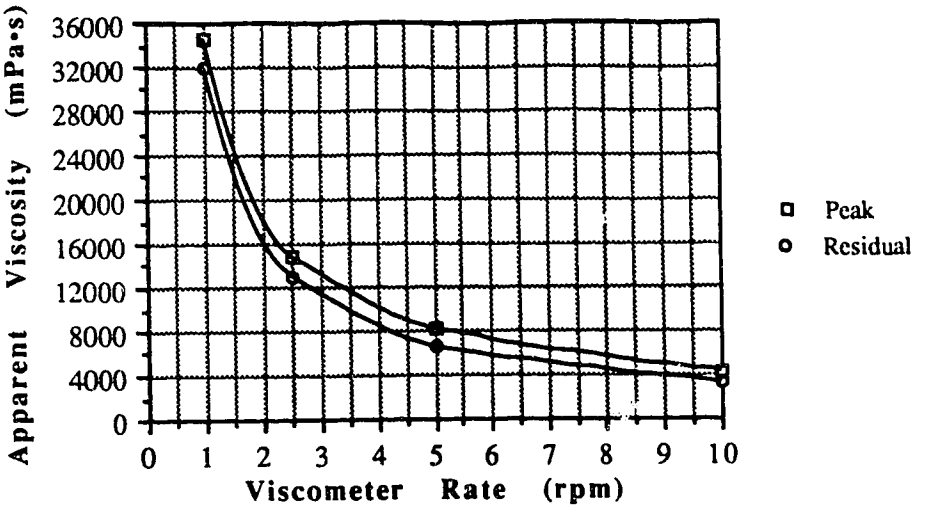

Figure B.77 Apparent Viscosity V15005M

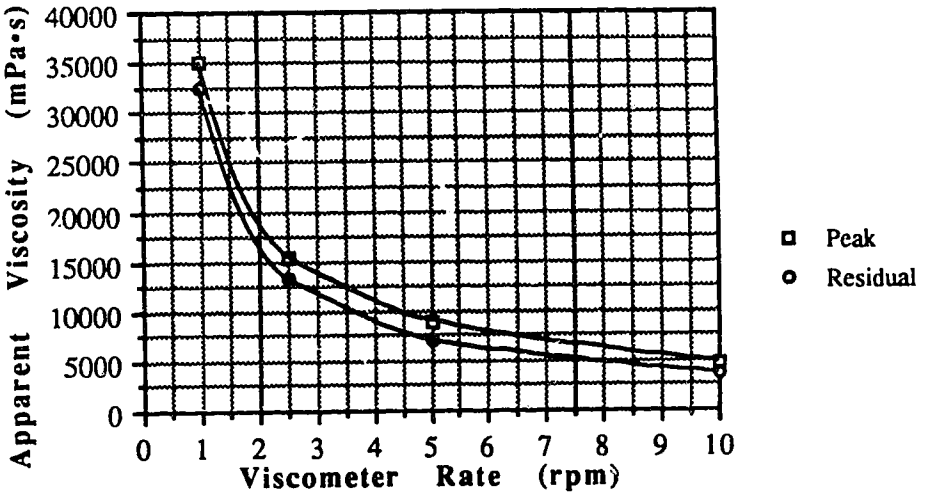

Figure B.78 Apparent Viscosity V15010M

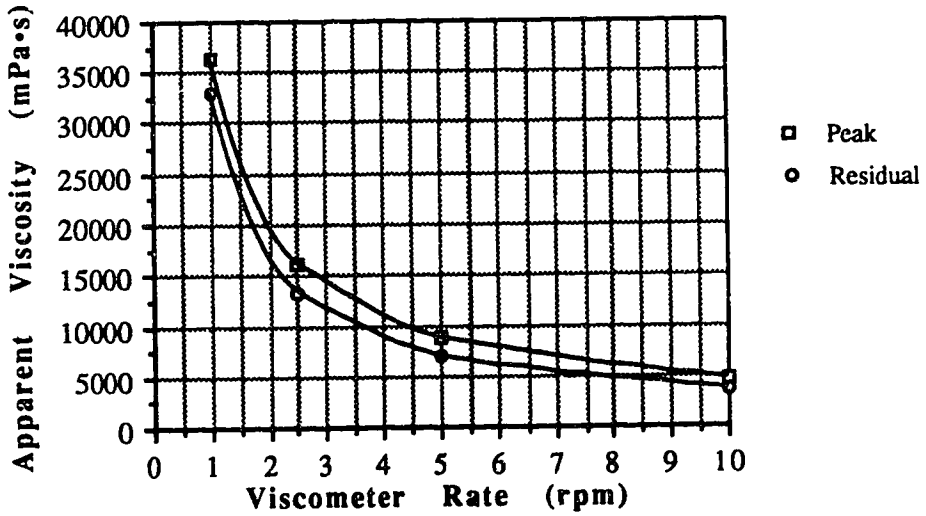

Figure B.79 Apparent Viscosity V15020M

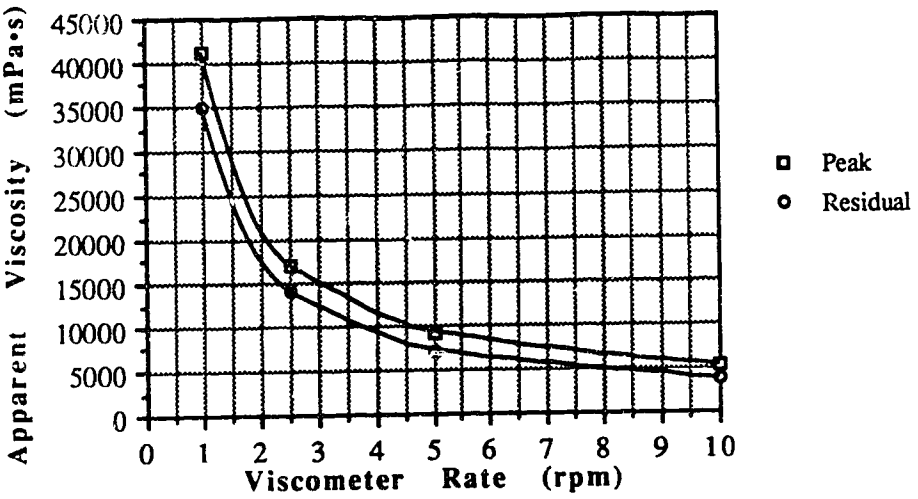

Figure B.80 Apparent Viscosity V15030M

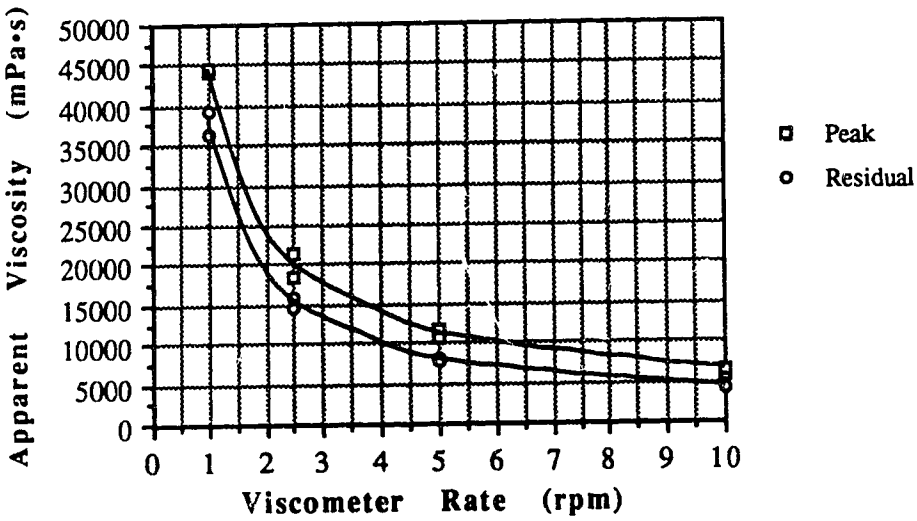

Figure B.81 Apparent Viscosity V15001H

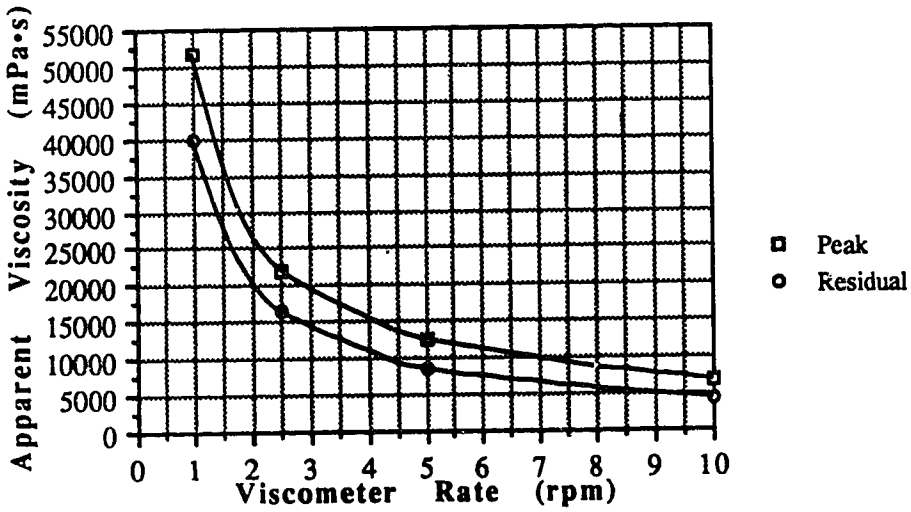

Figure B.82 Apparent Viscosity V15002H

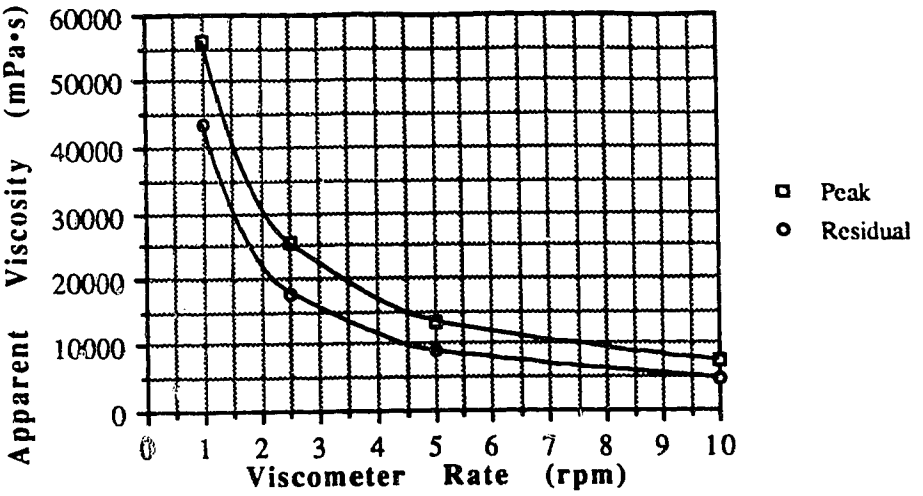

Figure B.83 Apparent Viscosity V15003H

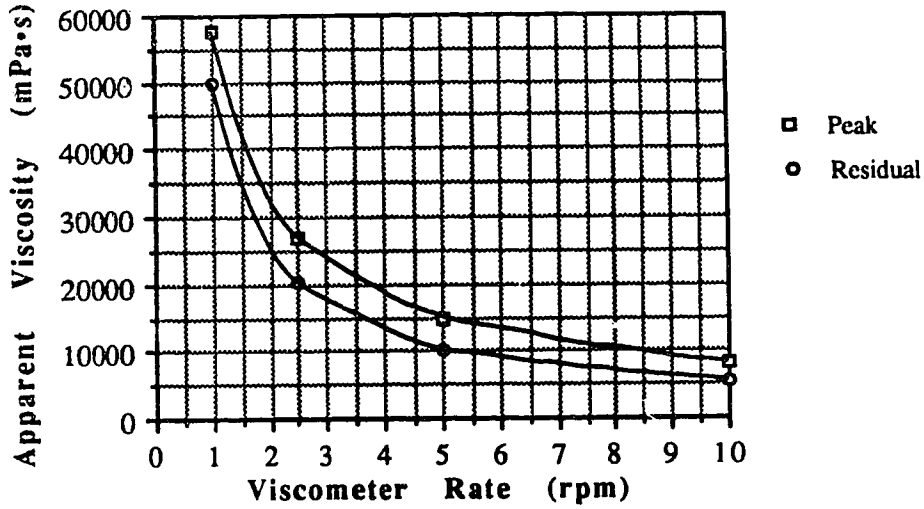

Figure B.84 Apparent Viscosity V15004H

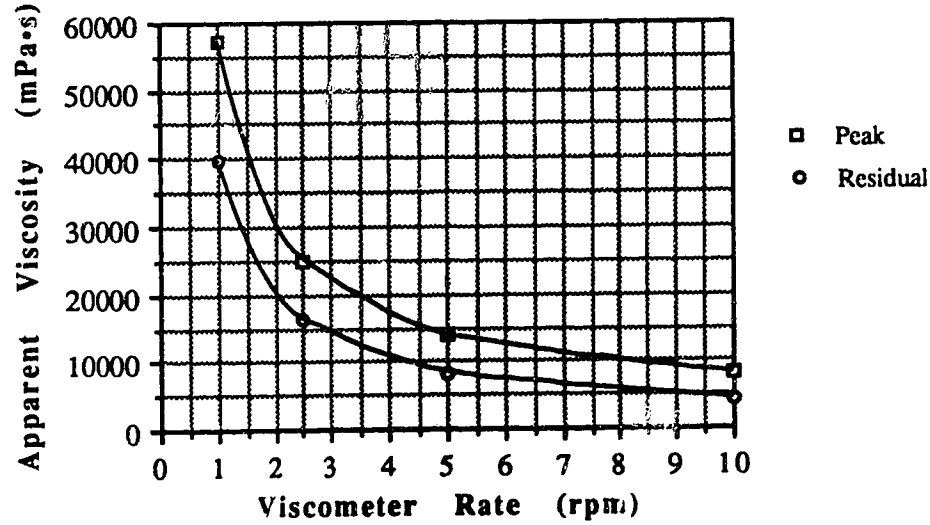

Figure B.85 Apparent Viscosity V15008H

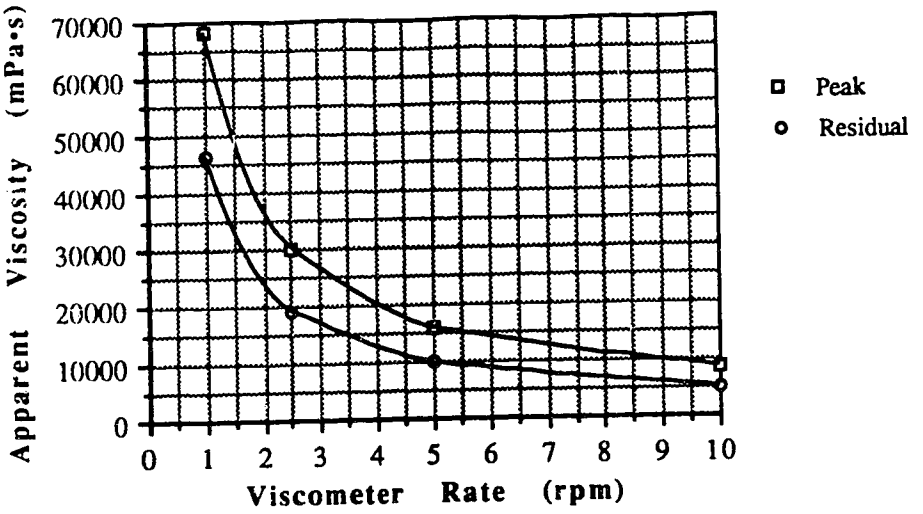

Figure B.86 Apparent Viscosity V15012H

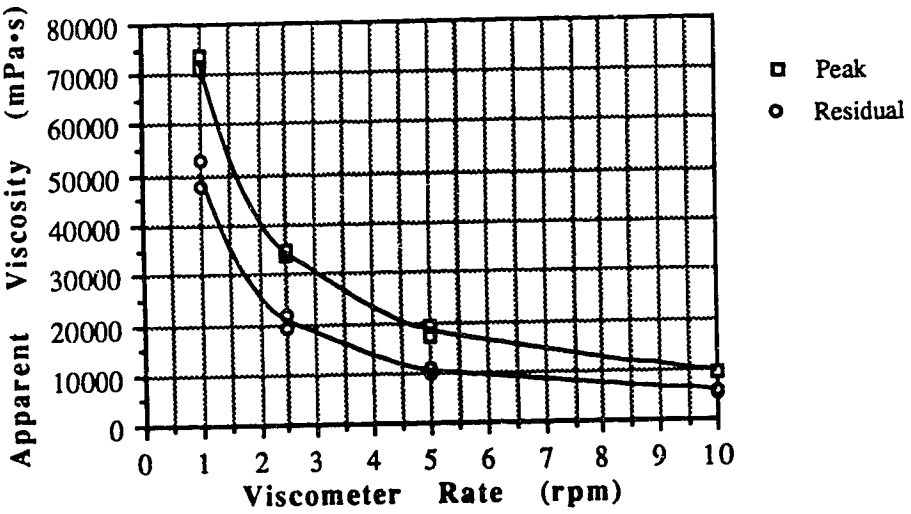

Figure B.87 Apparent Viscosity V15018H

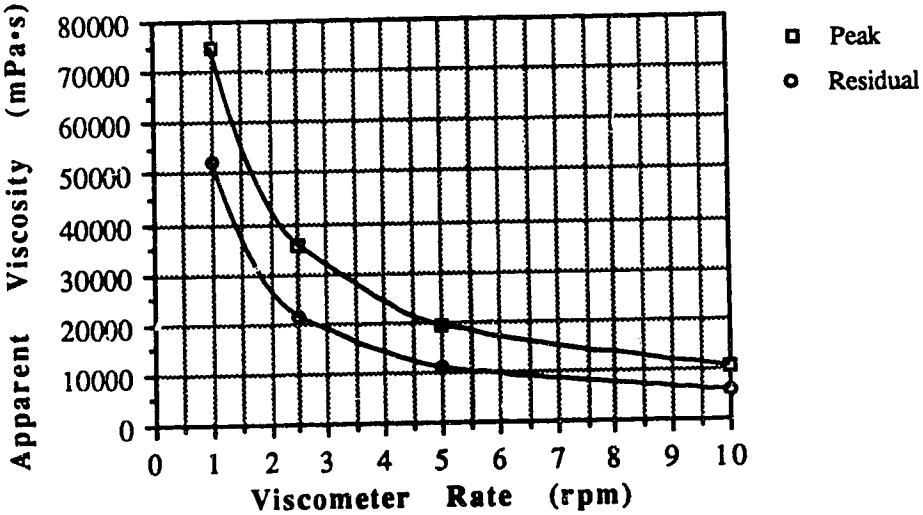

Figure B.88 Apparent Viscosity V15001D

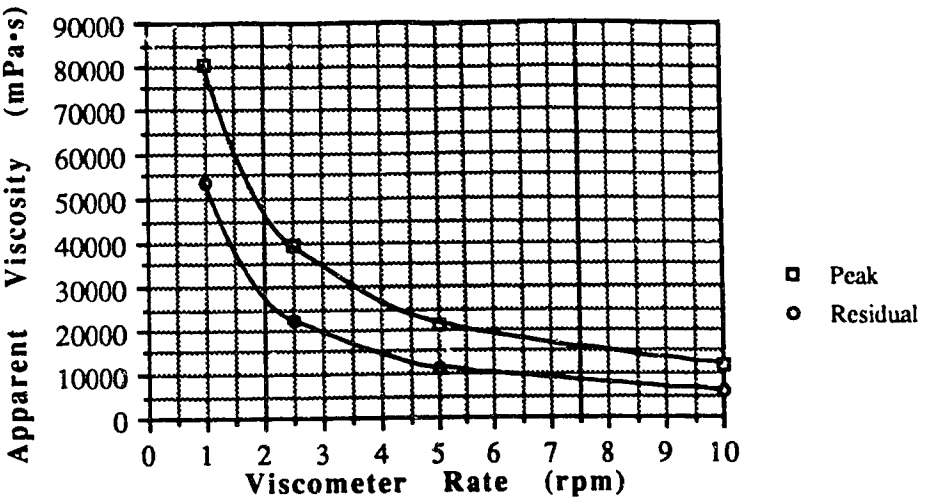

Figure B.89 Apparent Viscosity V15002D

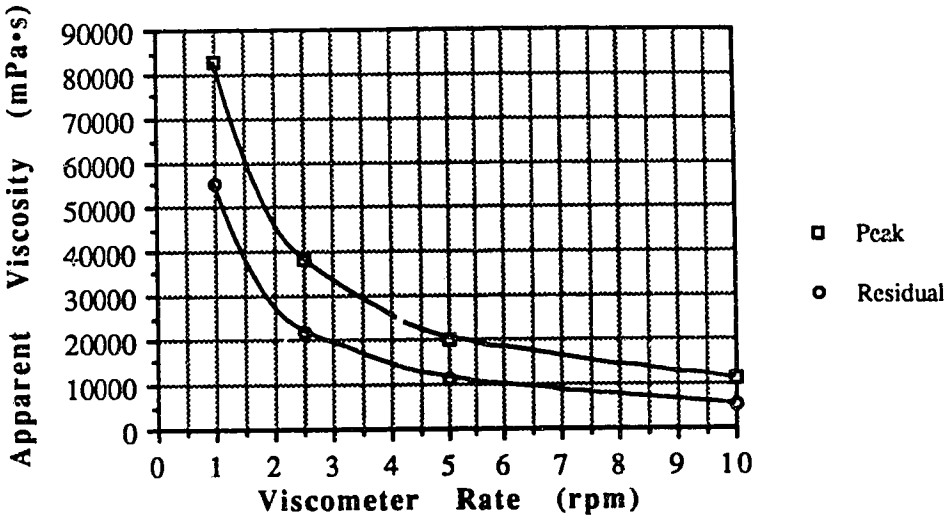

Figure B.90 Apparent Viscosity V15003D

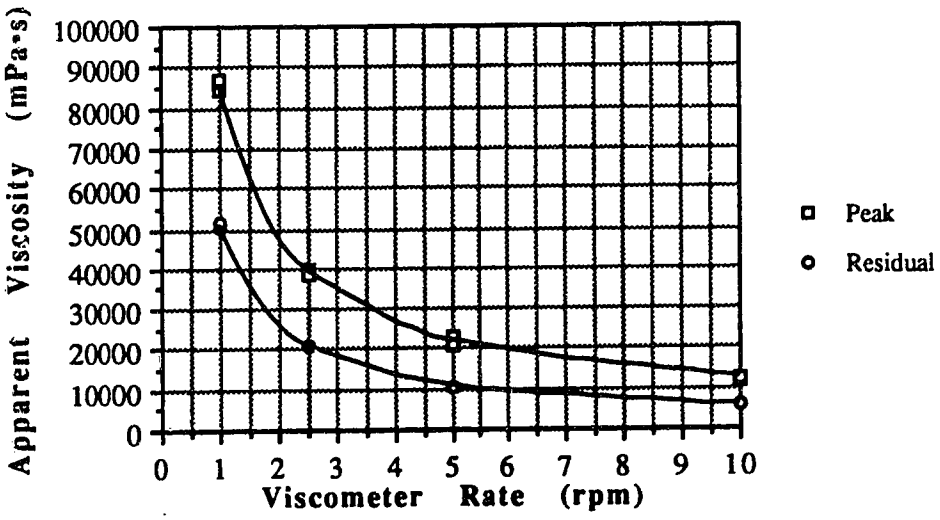

Figure B.91 Apparent Viscosity V15004D

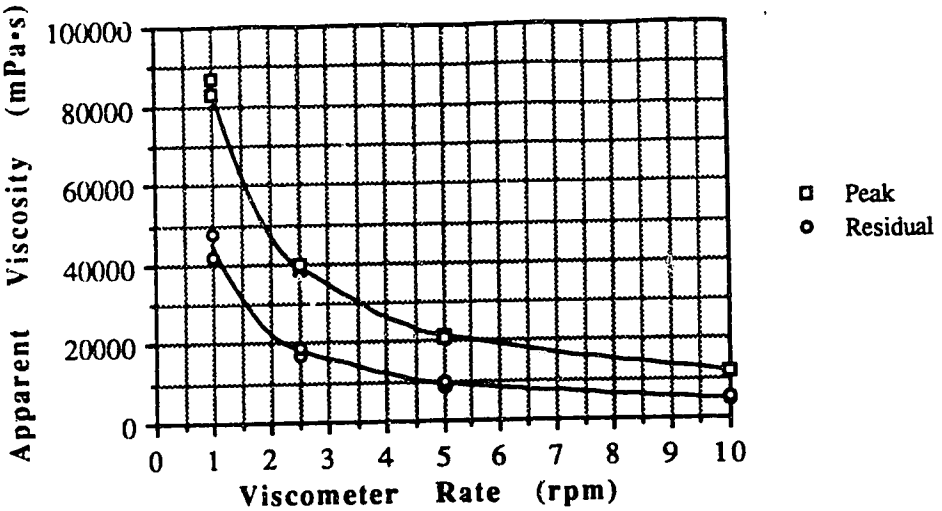

Figure B.92 Apparent Viscosity V15005D

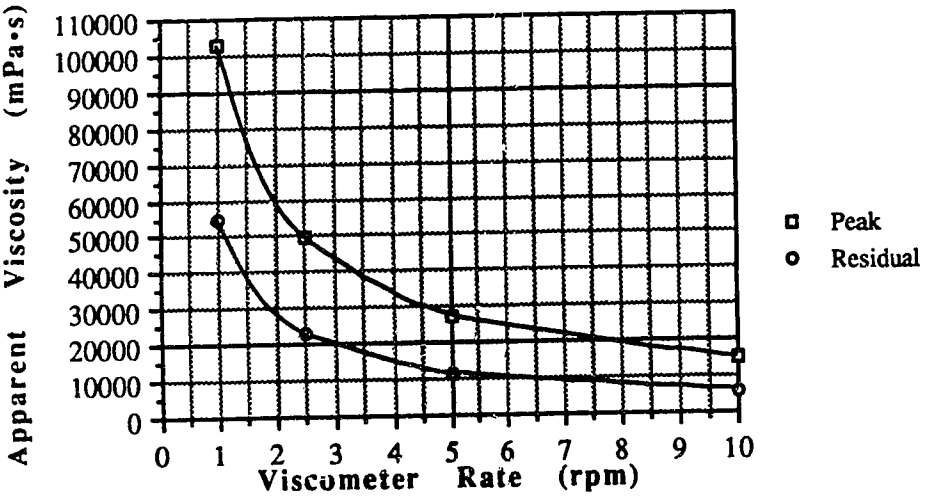

Figure B.93 Apparent Viscosity V15010D

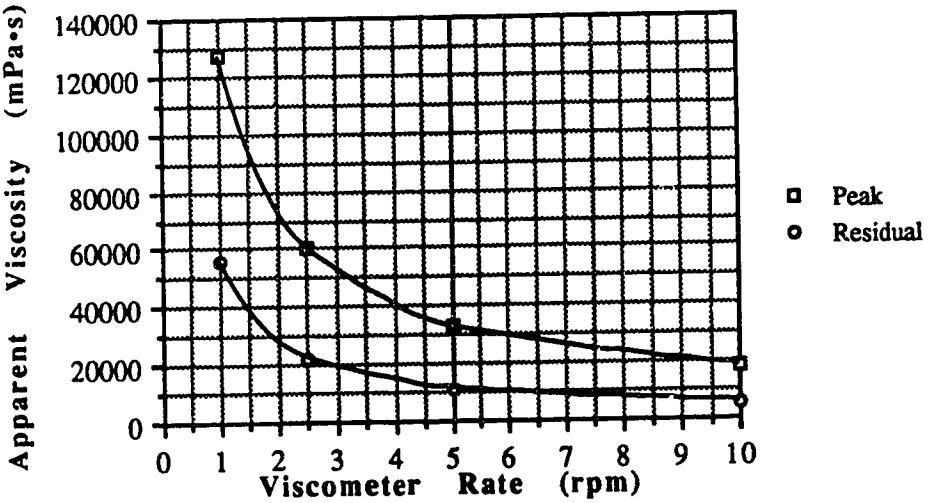

Figure B.94 Apparent Viscosity V15020D

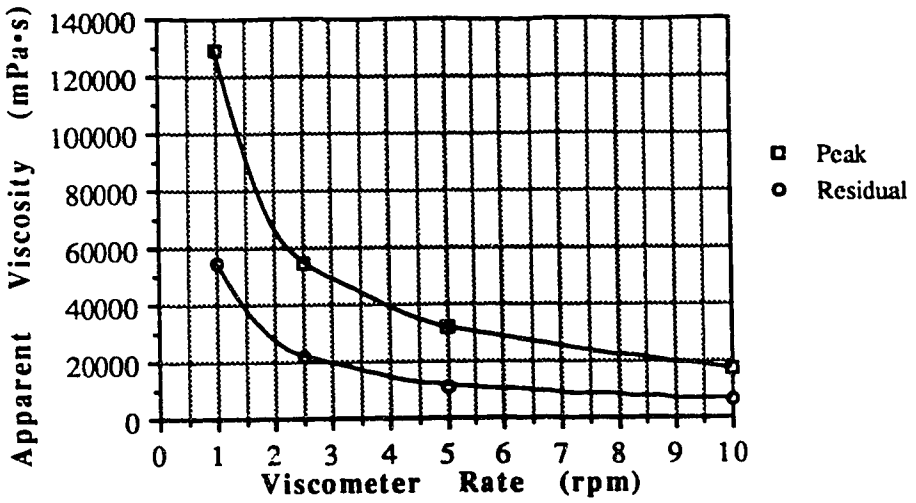

Figure B.95 Apparent Viscosity V15030D

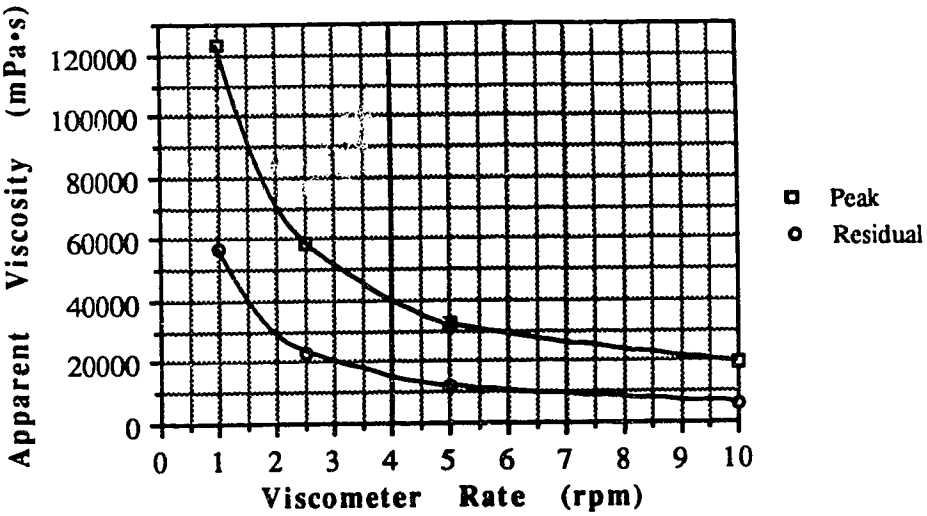

Figure B.96 Apparent Viscosity V15040D

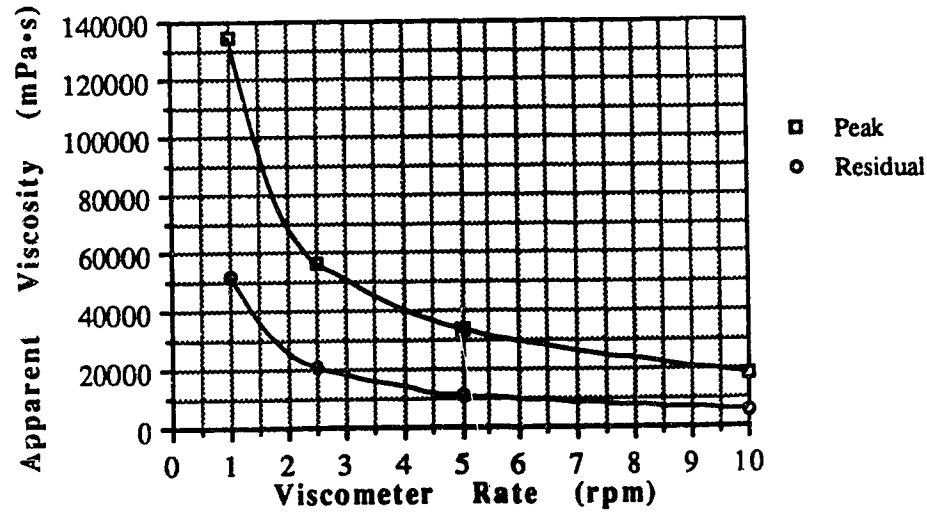

Figure B.97 Apparent Viscosity V15051D

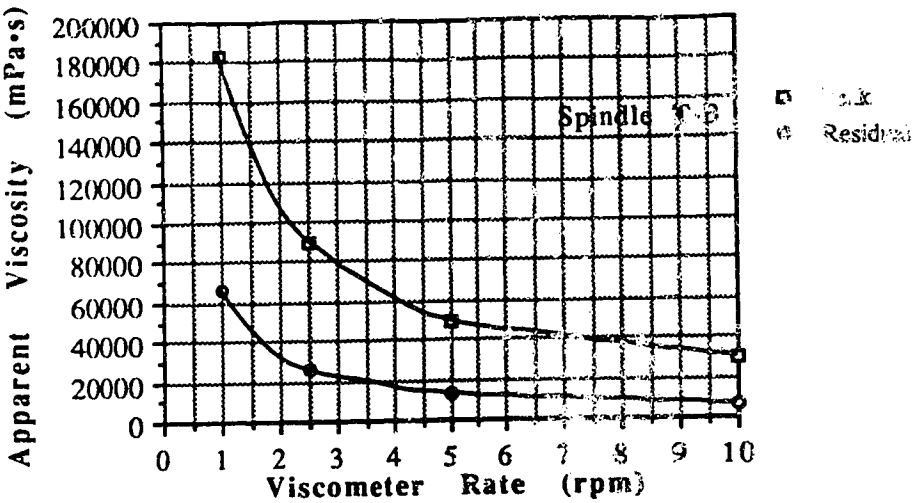

Figure B.98 Apparent Viscosity V15092D

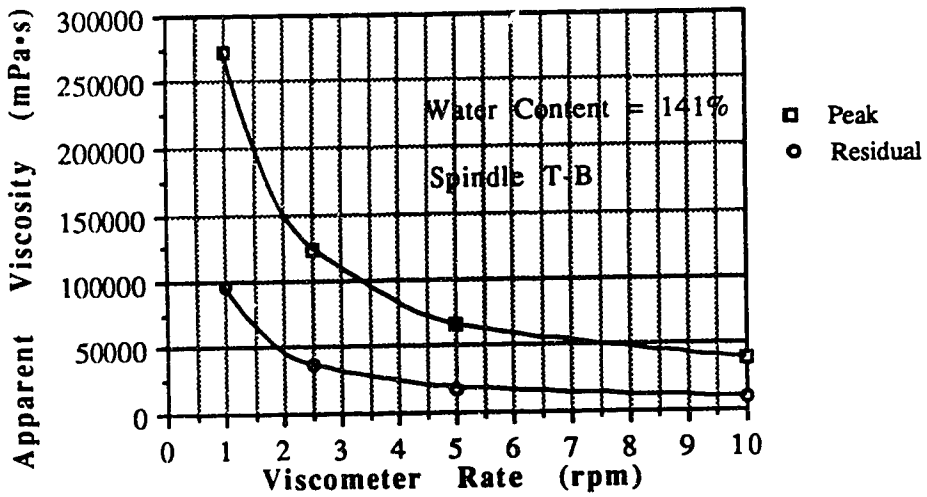

Figure B.99 Apparent Viscosity V15470D

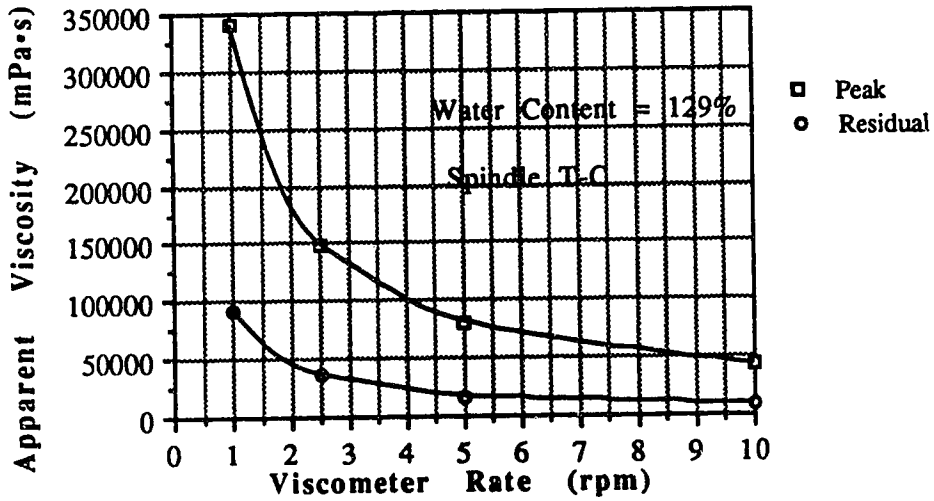

Figure B.100 Apparent Viscosity V15680D

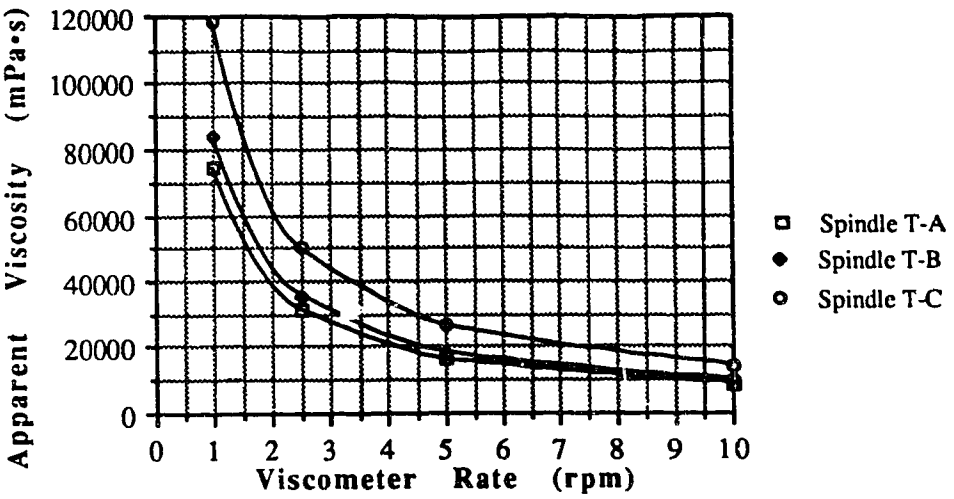

Figure B.101 Apparent Viscosity V10000M

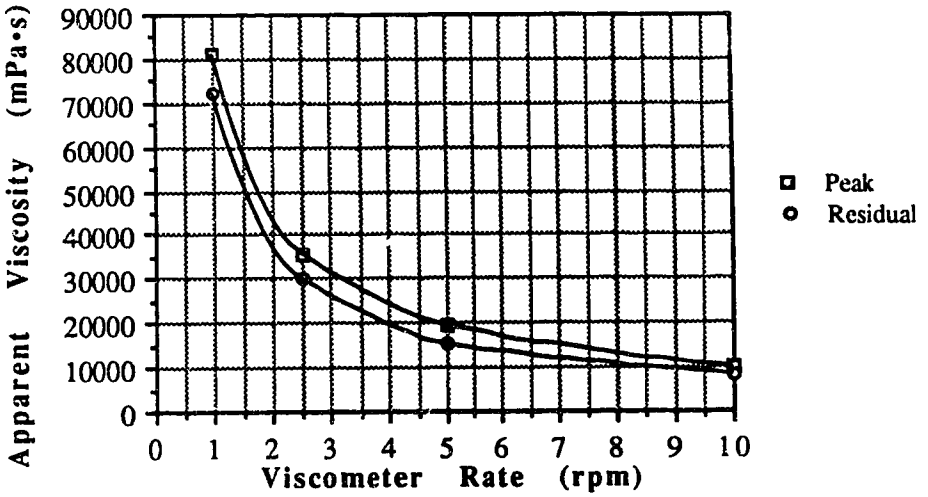

Figure B.102 Apparent Viscosity V10005M

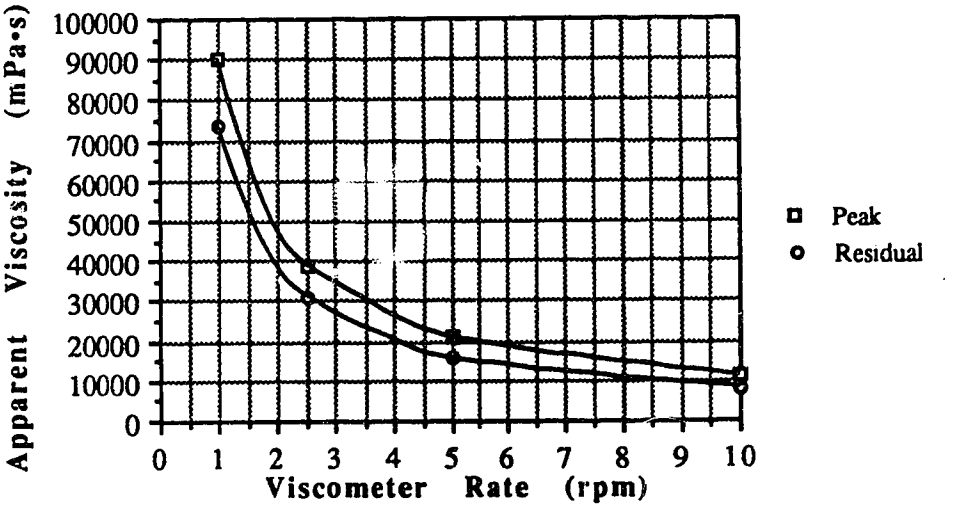

Figure B.103 Apparent Viscosity V10010M

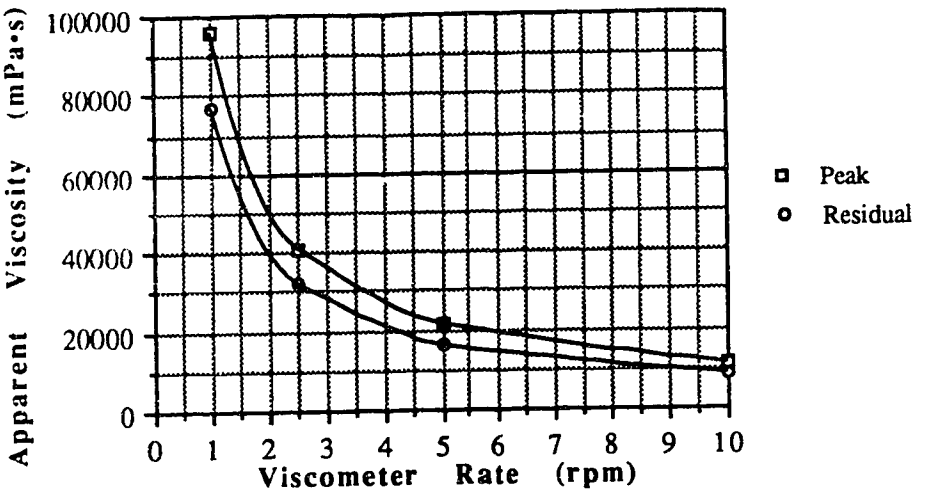

Figure B.104 Apparent Viscosity V10020M

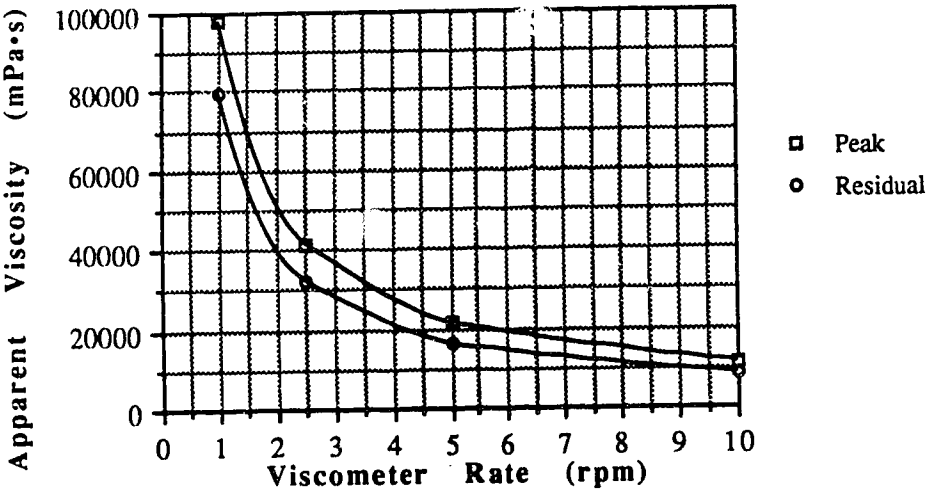

Figure B.105 Apparent Viscosity V10030M

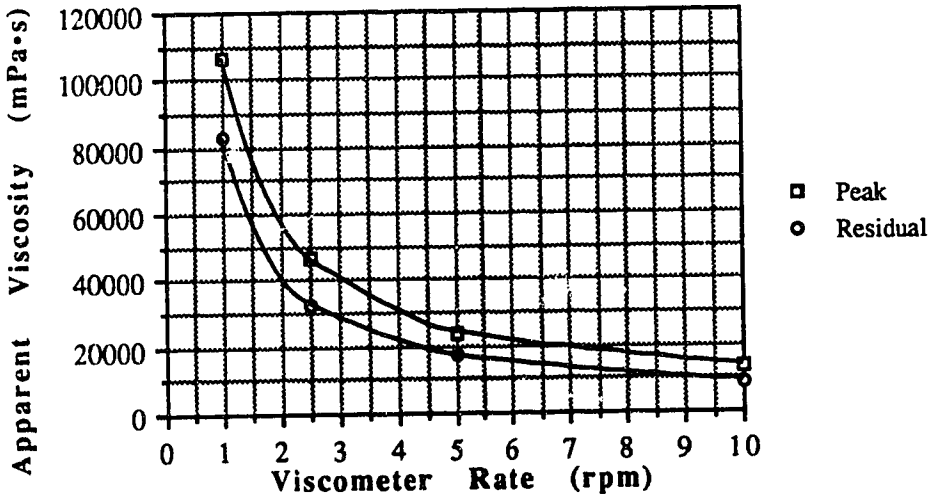

Figure B.106 Apparent Viscosity V10001H

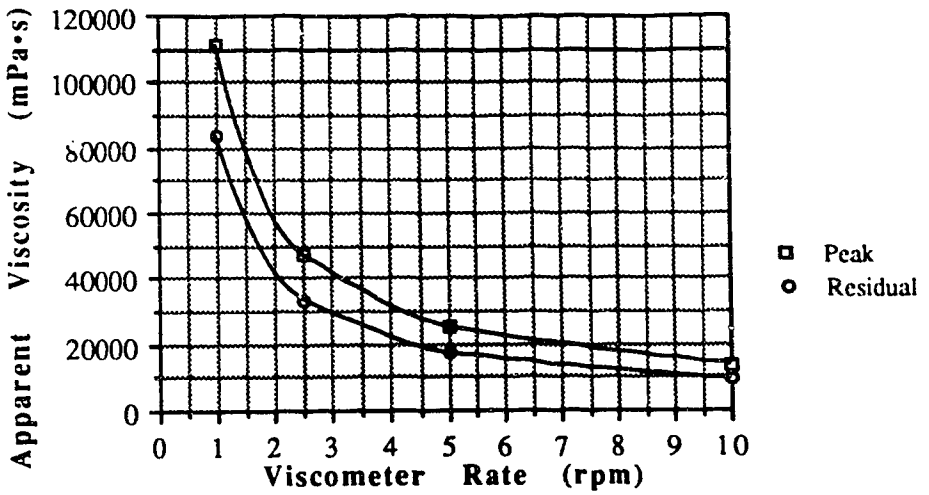

Figure B.107 Apparent Viscosity V10002H

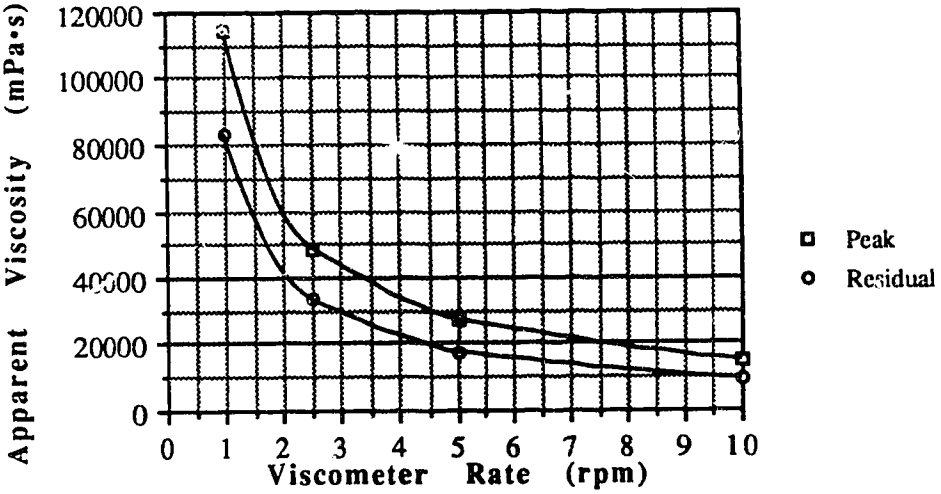

Figure B.108 Apparent Viscosity V10003H

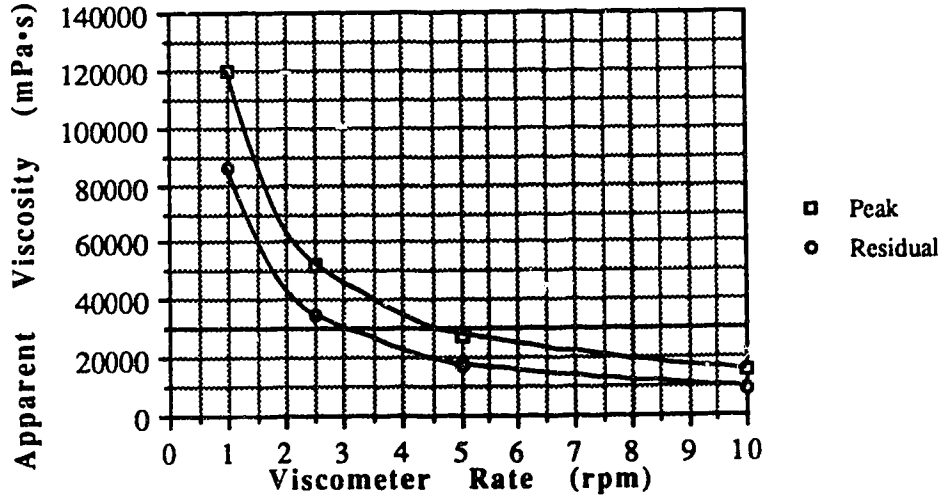

Figure B.109 Apparent Viscosity V10004H

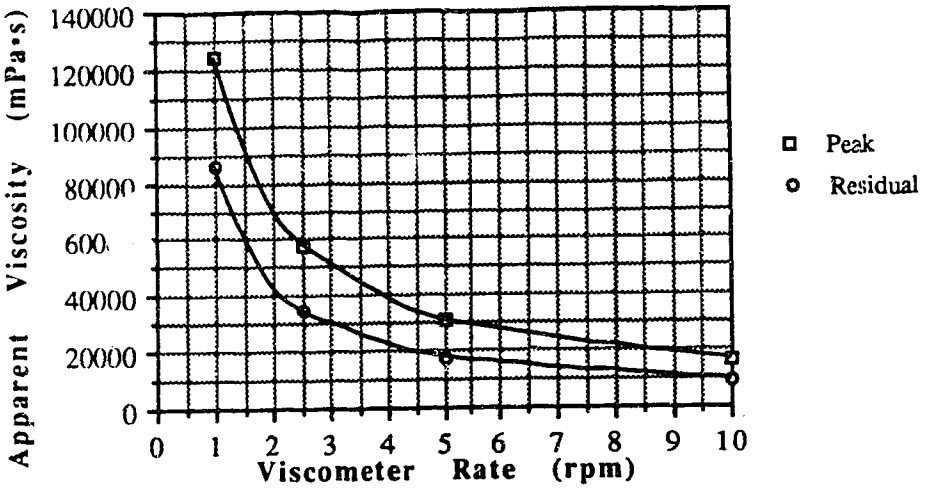

Figure B.110 Apparent Viscosity V1008H

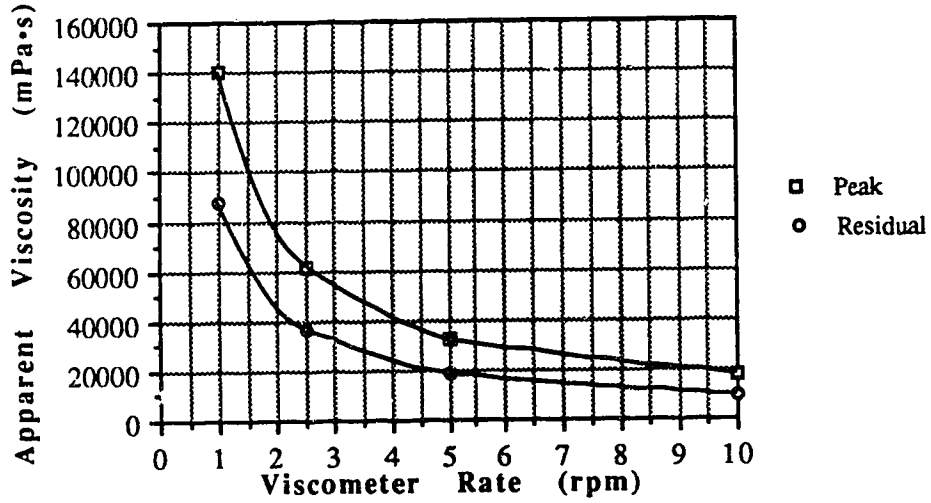

Figure B.111 Apparent Viscosity V10012H

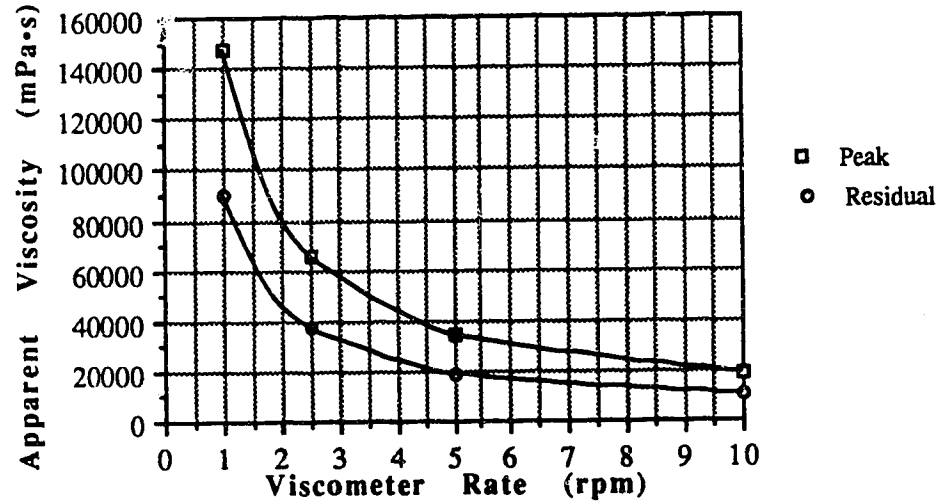

Figure B.112 Apparent Viscosity V10018H

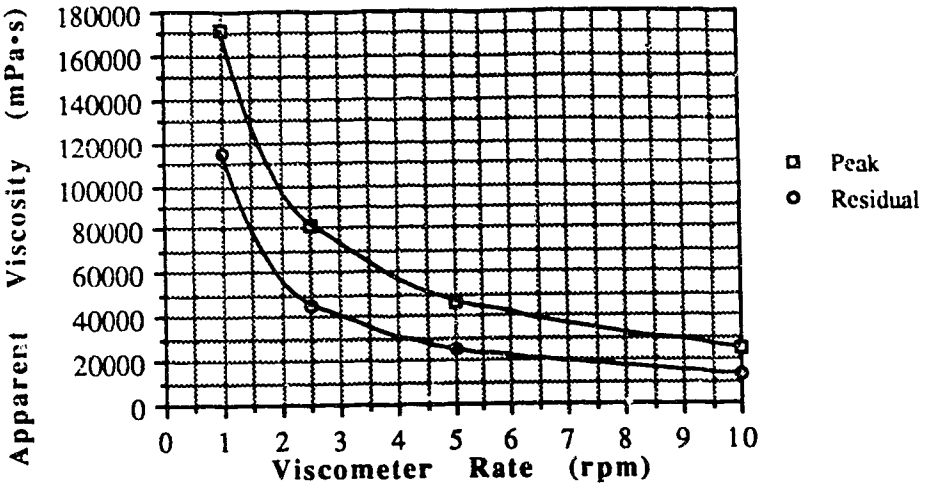

Figure B.113 Apparent Viscosity V10001D

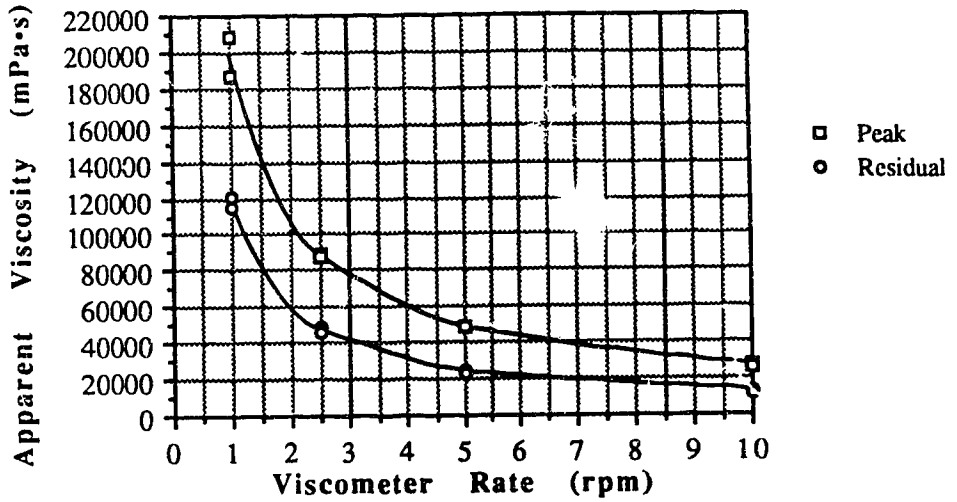

Figure B.114 Apparent Viscosity V10002D

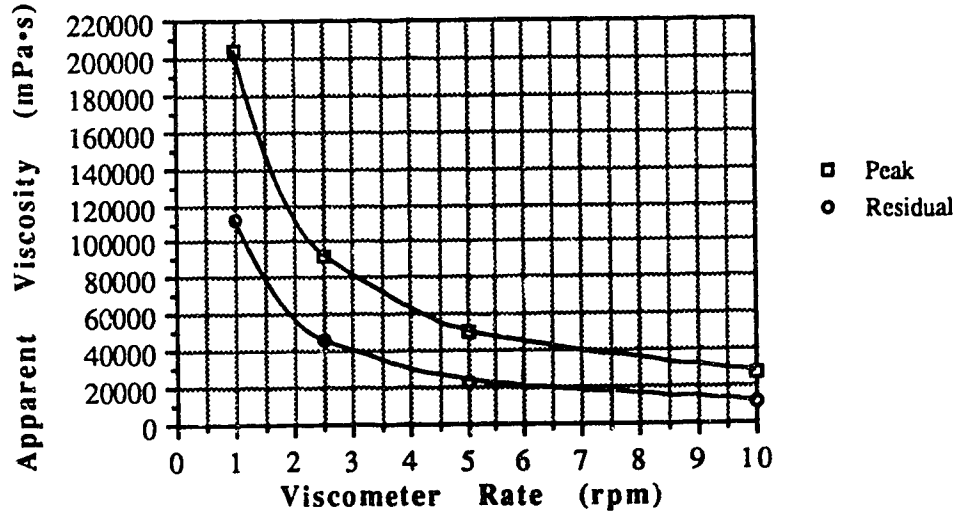

Figure B.115 Apparent Viscosity V10003D

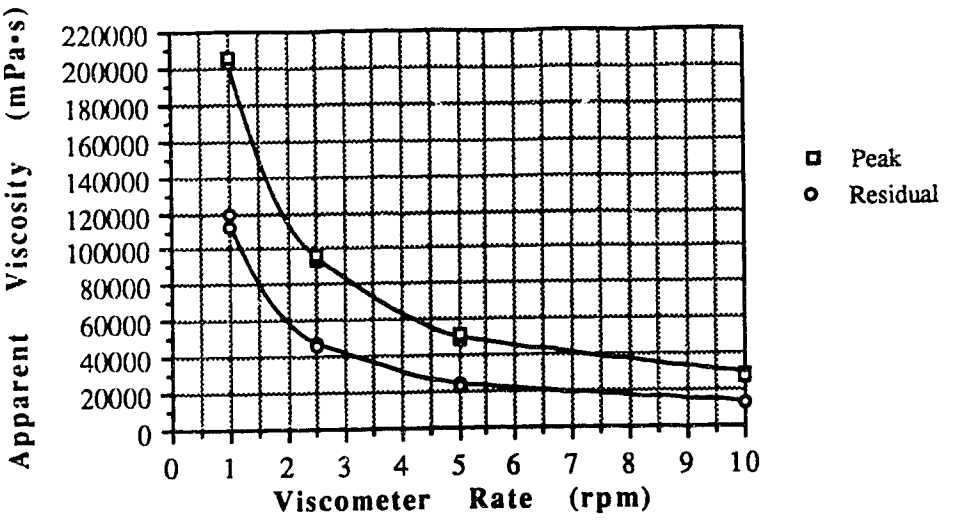

Figure B.116 Apparent Viscosity V10004D

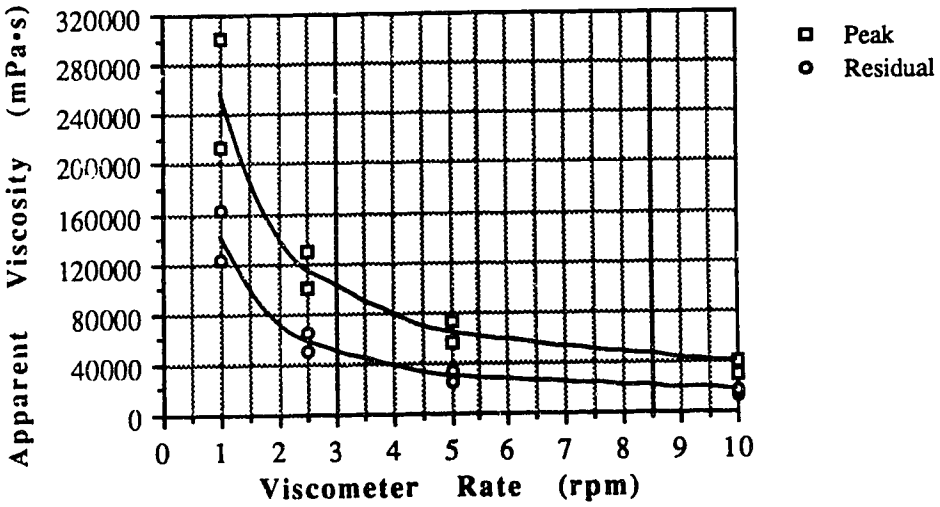

Figure B.117 Apparent Viscosity V10005D

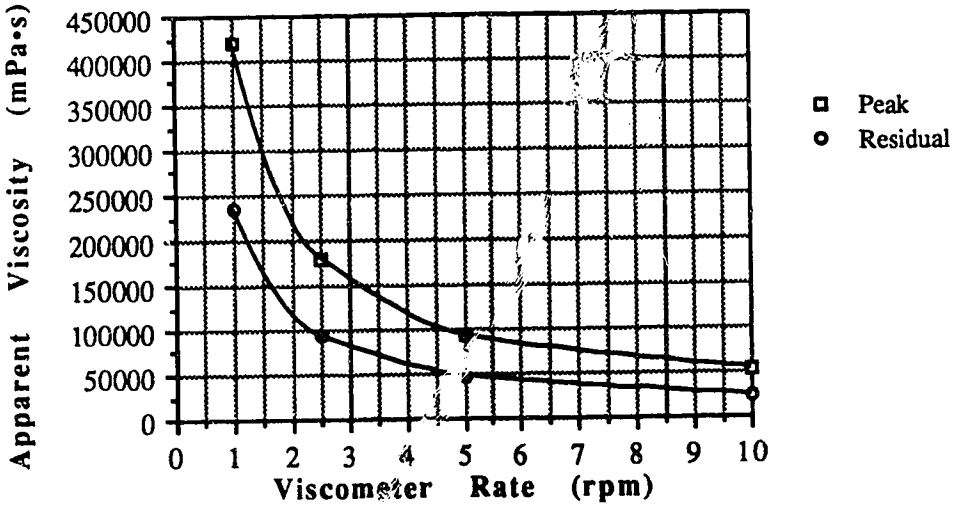

Figure B.118 Apparent Viscosity V10006D

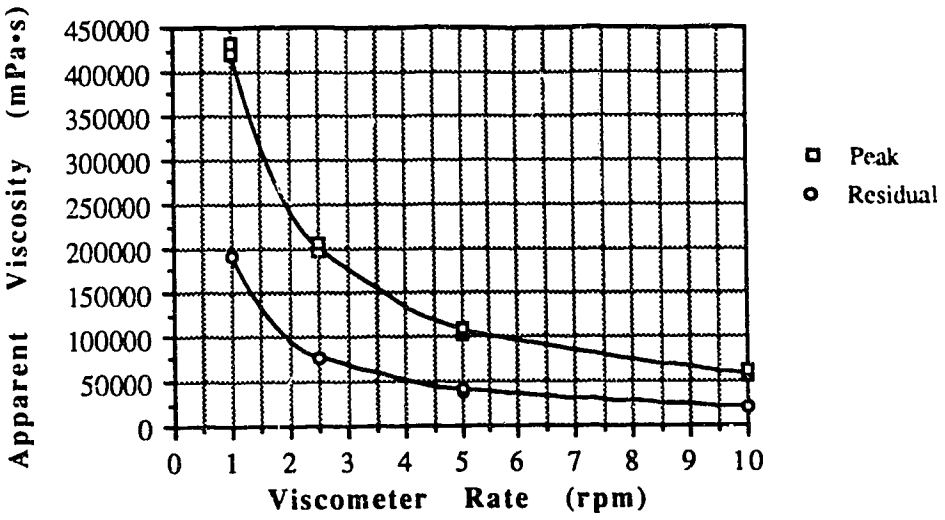

Figure B.119 Apparent Viscosity V10010D

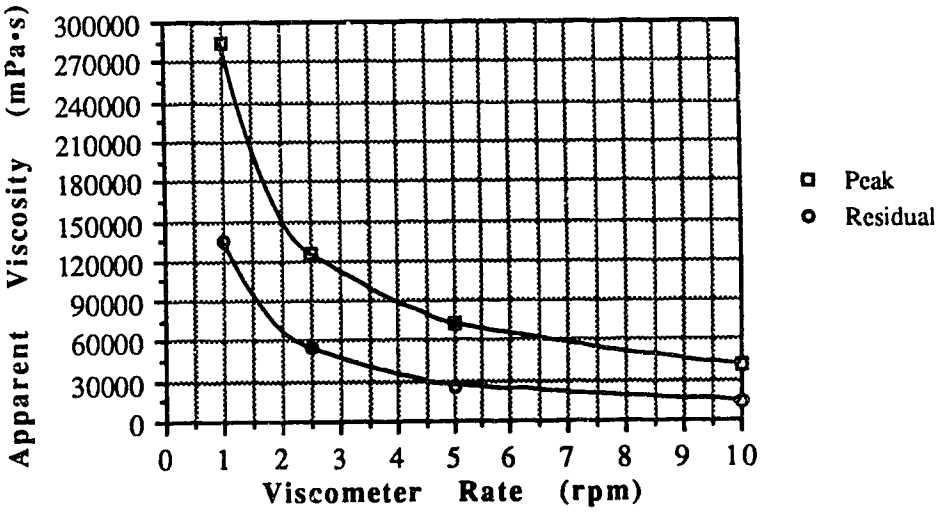

Figure B.120 Apparent Viscosity V10020D

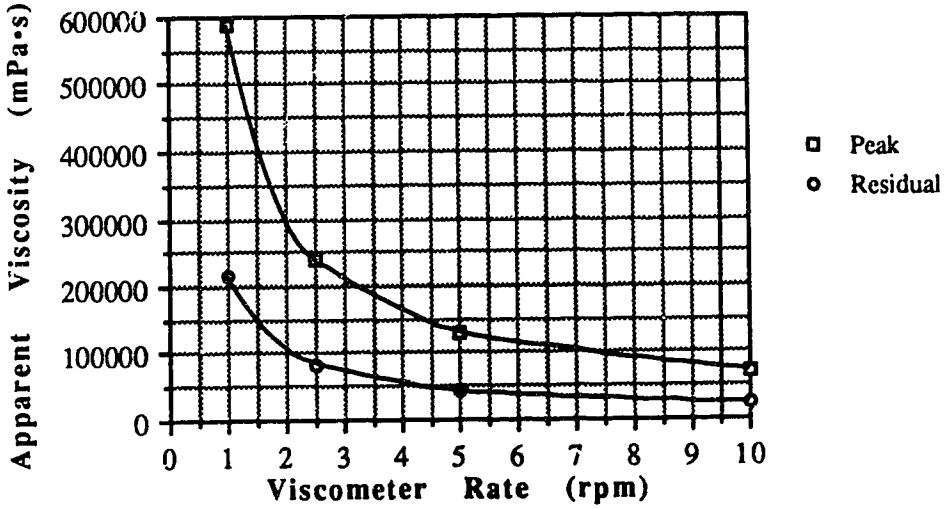

Figure B.121 Apparent Viscosity V10021D

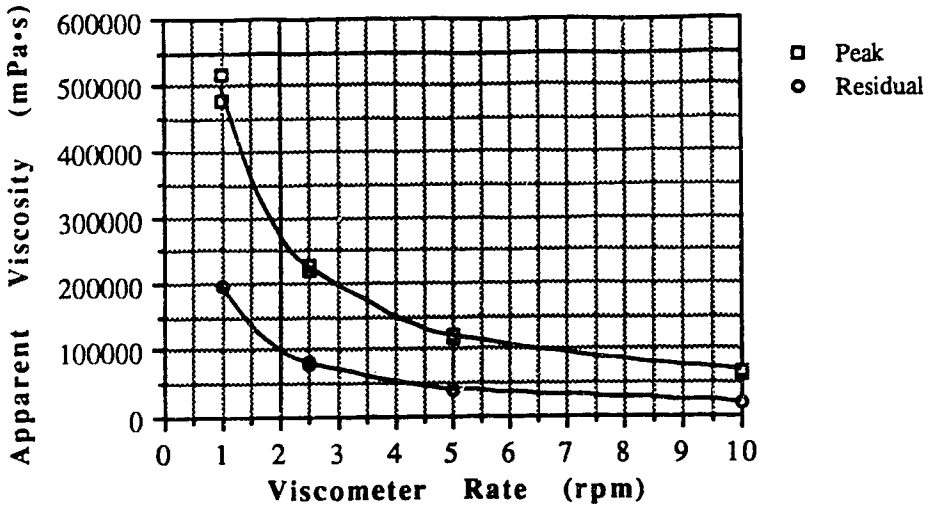

Figure B.122 Apparent Viscosity V10040D

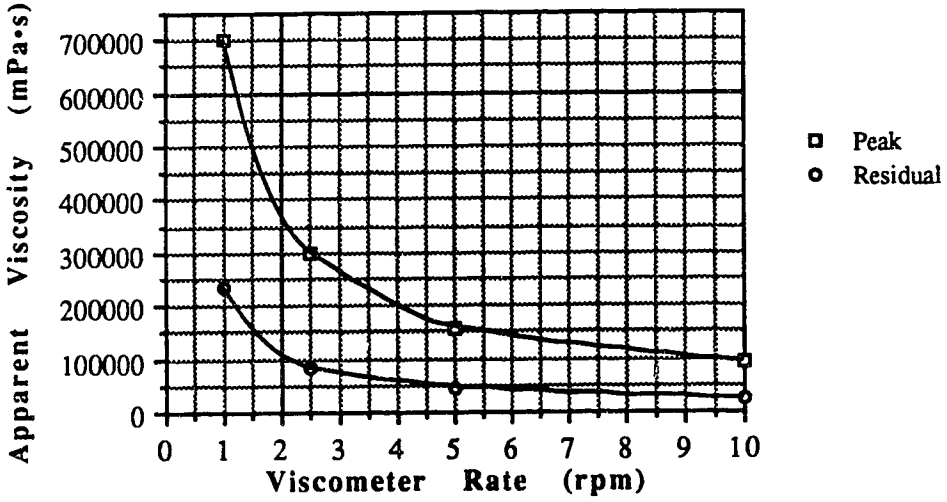

Figure B.123 Apparent Viscosity V10095D

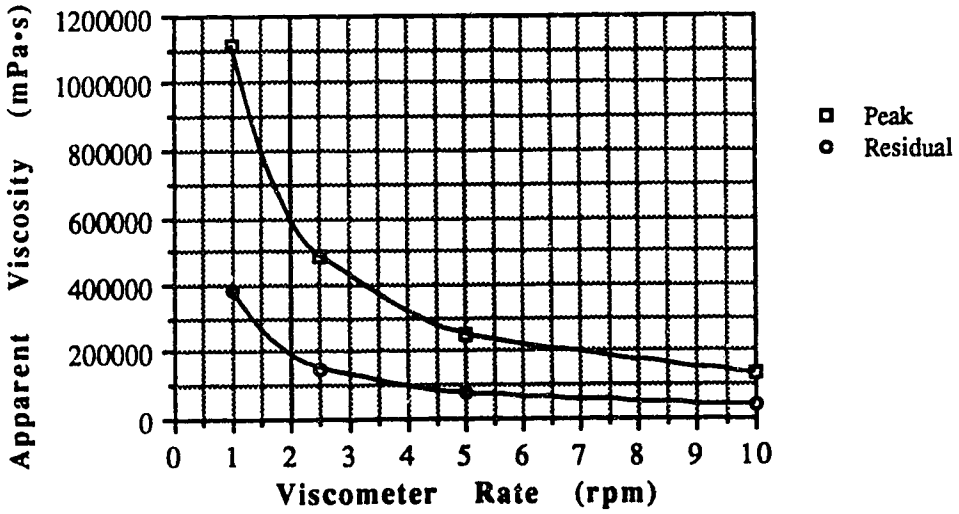

Figure B.124 Apparent Viscosity V10473D

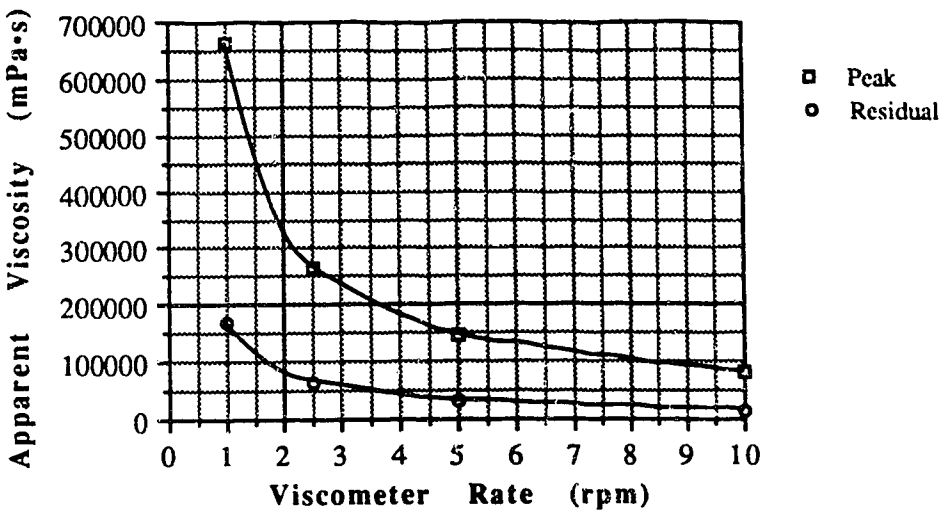

Figure B.125 Apparent Viscosity V10680D

APPENDIX C. Shear Vane Test Plots

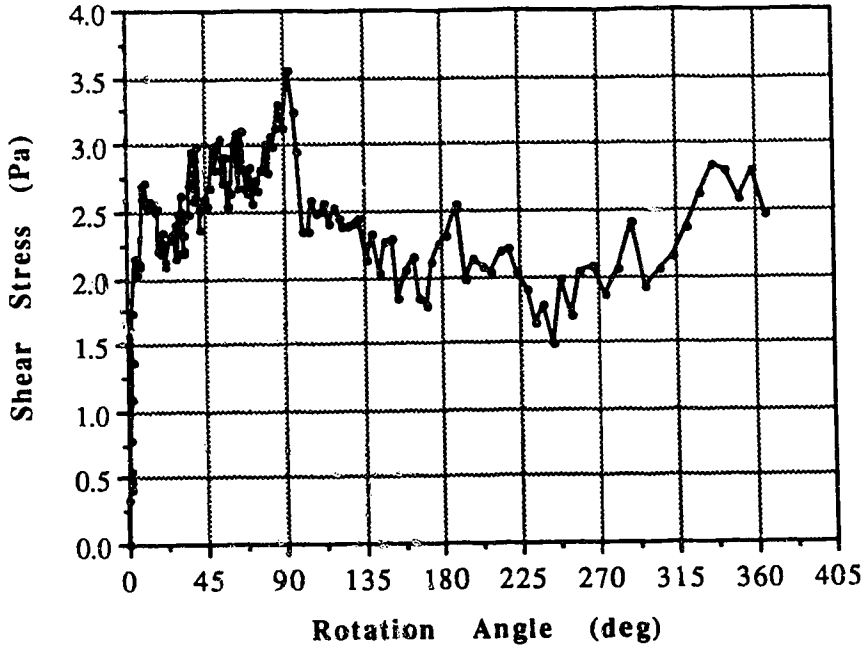

Figure C.1 Vane Shear Test S40000M

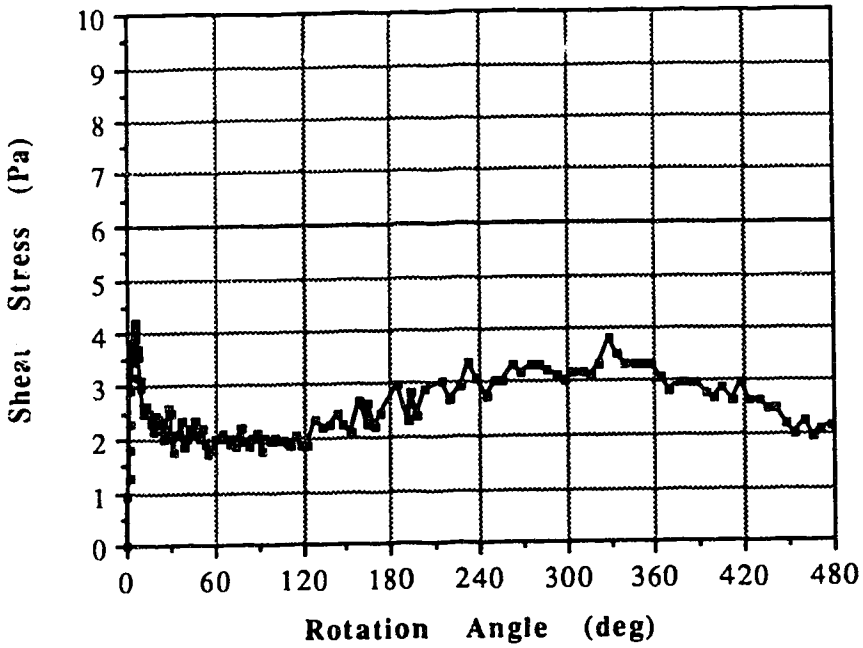

Figure C.2 Vane Shear Test S40002HR

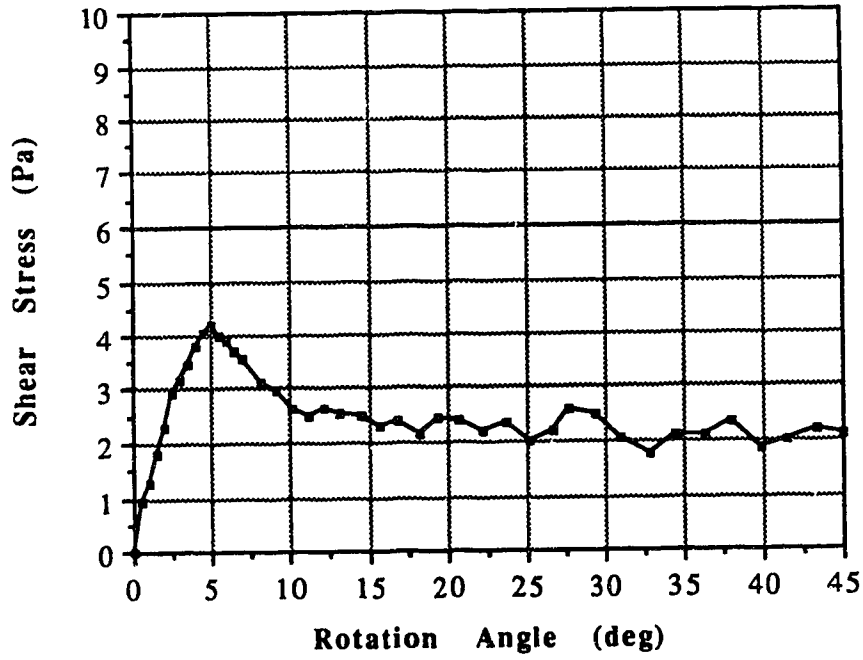

Figure C.3 Vane Shear Test S40002HP

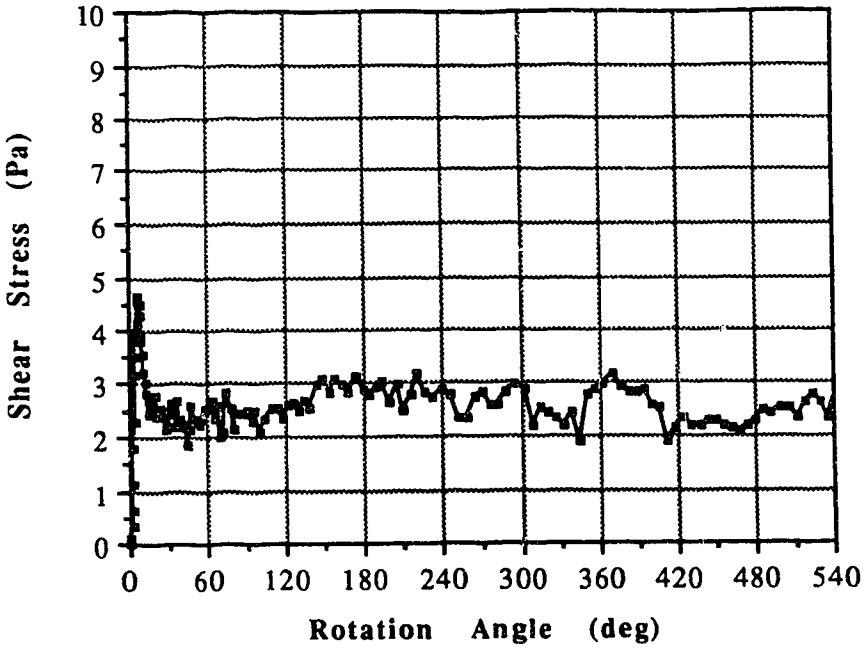

Figure C.4 Vane Shear Test S40008HR

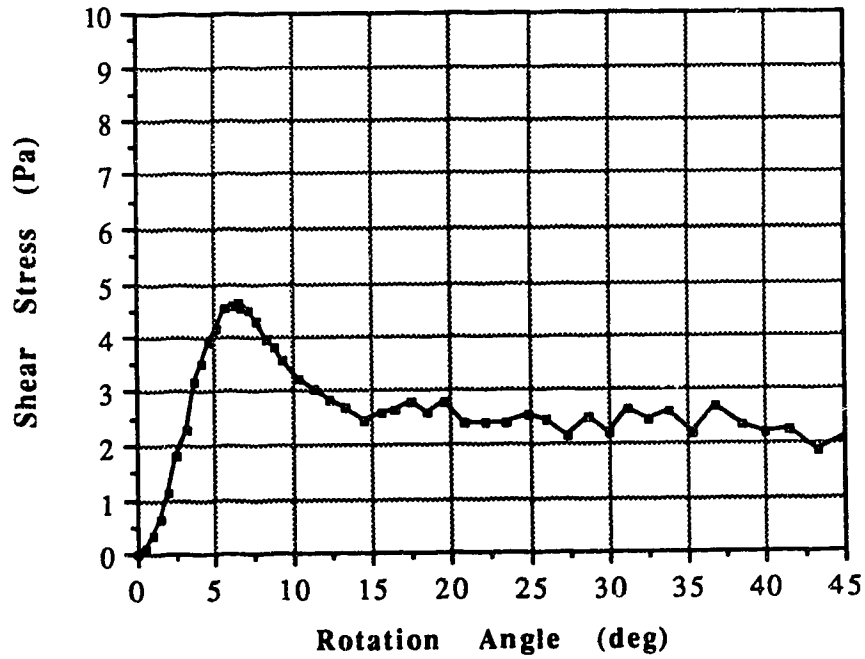

Figure C.5 Vane Shear Test S40008HP

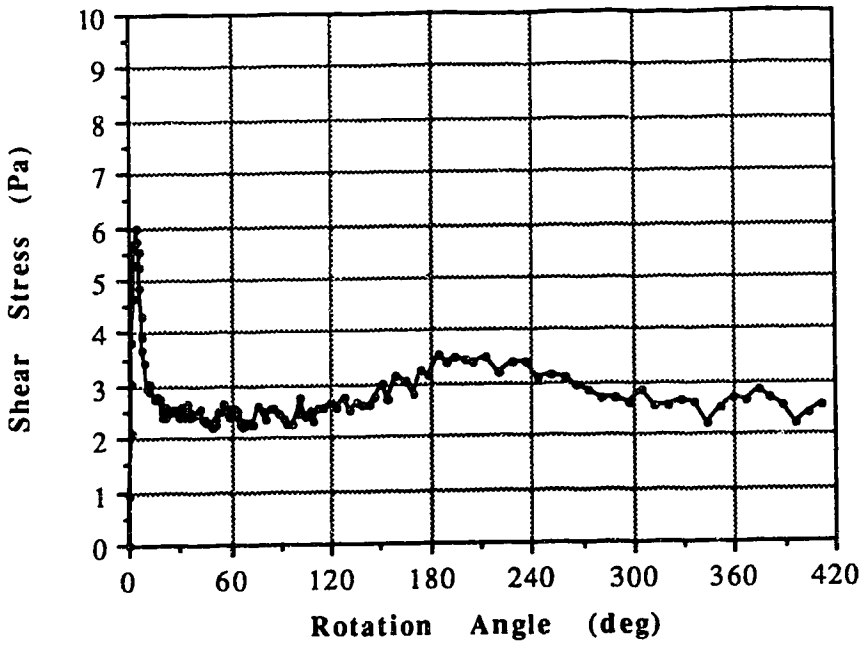

Figure C.6 Vane Shear Test S40001DR

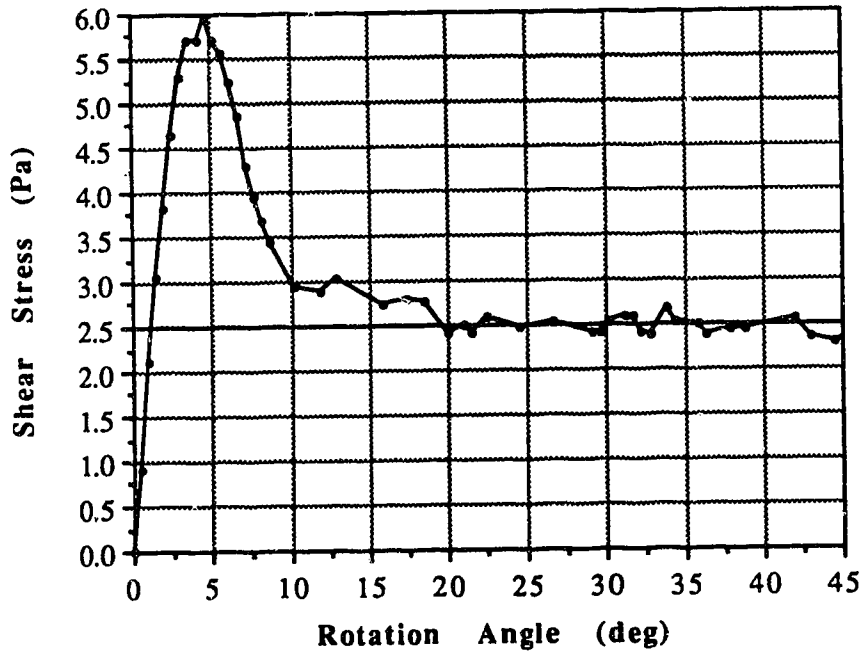

Figure C.7 Vane Shear Test S40001DP

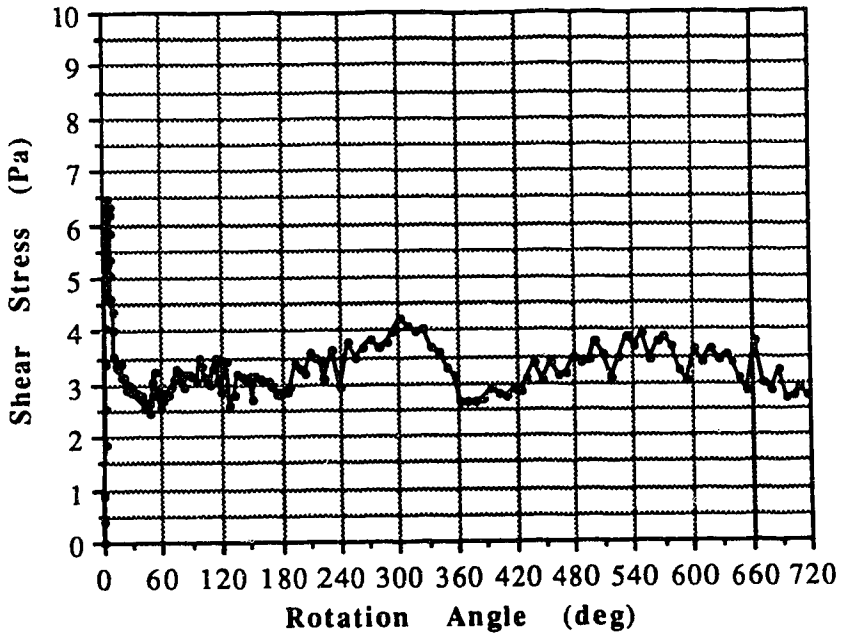

Figure C.8 Vane Shear Test S40002DR

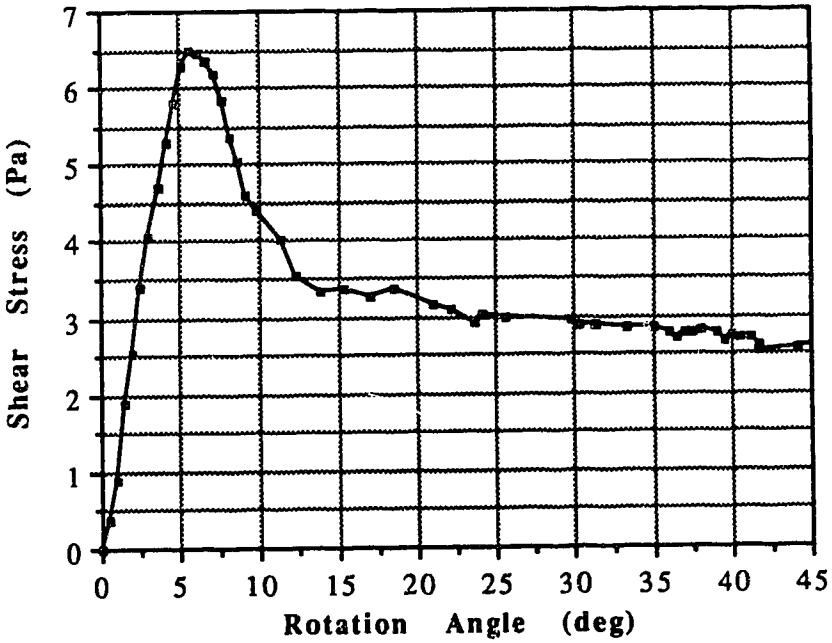

Figure C.9 Vane Shear Test S40002DP

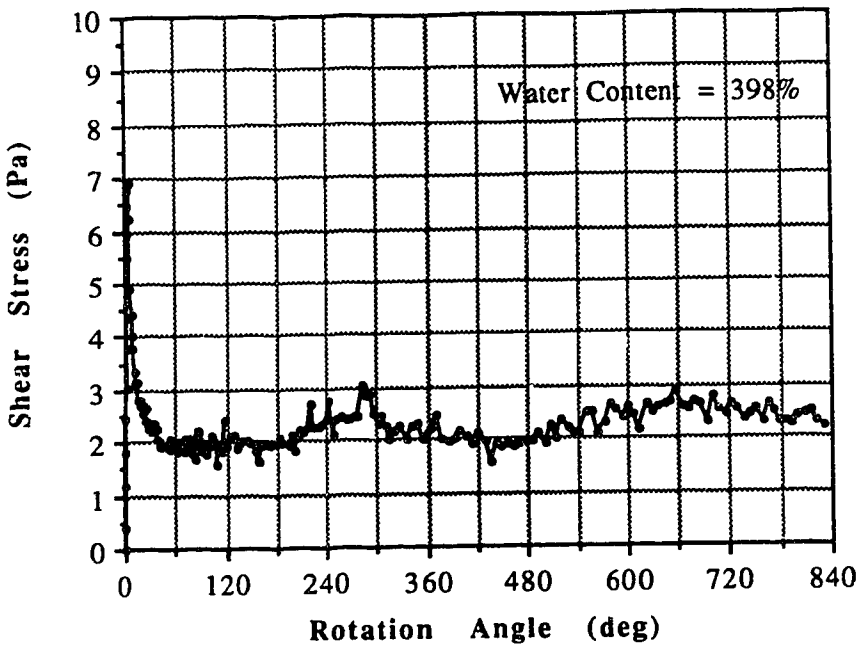

Figure C.10 Vane Shear Test S40005DR

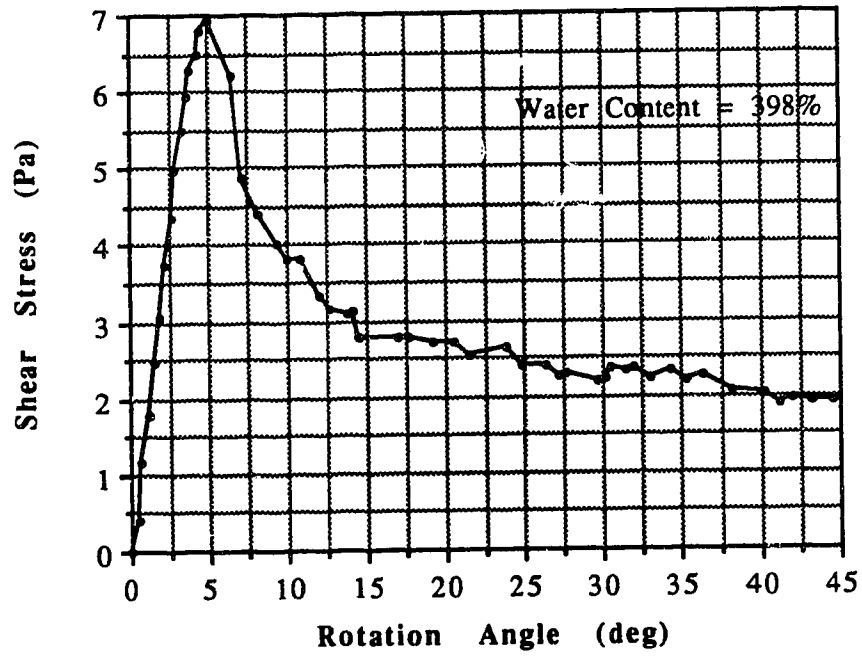

Figure C.11 Vane Shear Test S40005DP

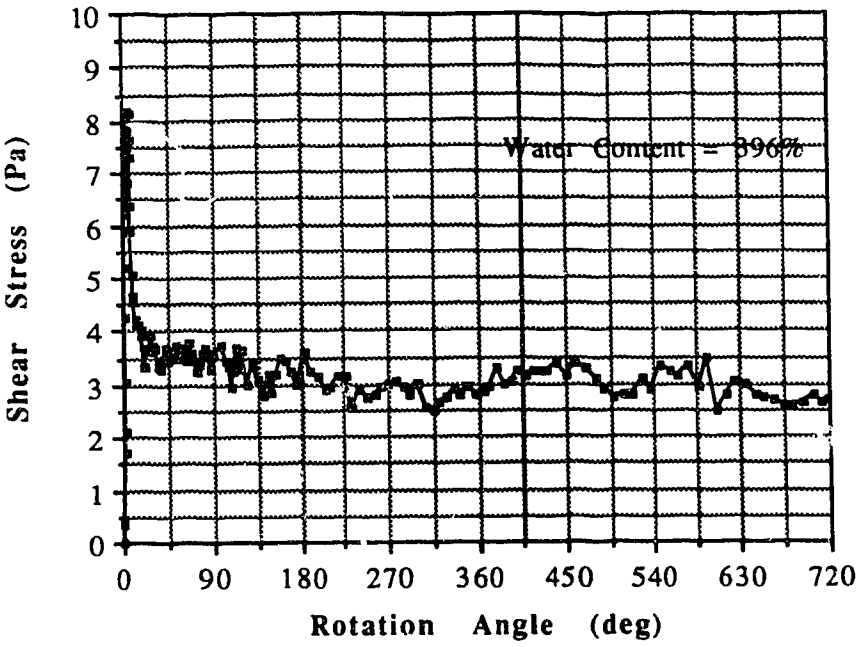

Figure C.12 Vane Shear Test S40010DR

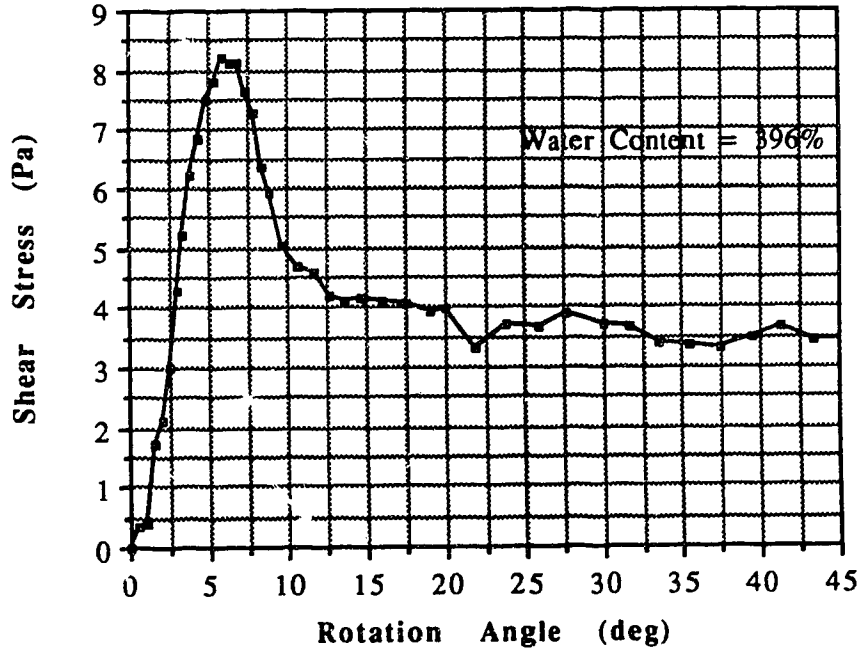

Figure C.13 Vane Shear Test S40010DP

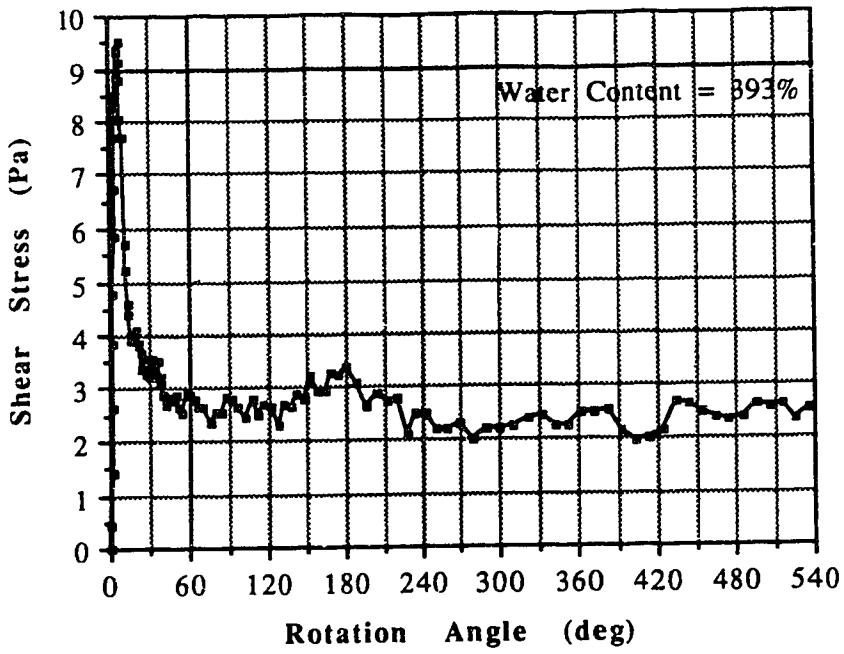

Figure C.14 Vane Shear Test S40020DR

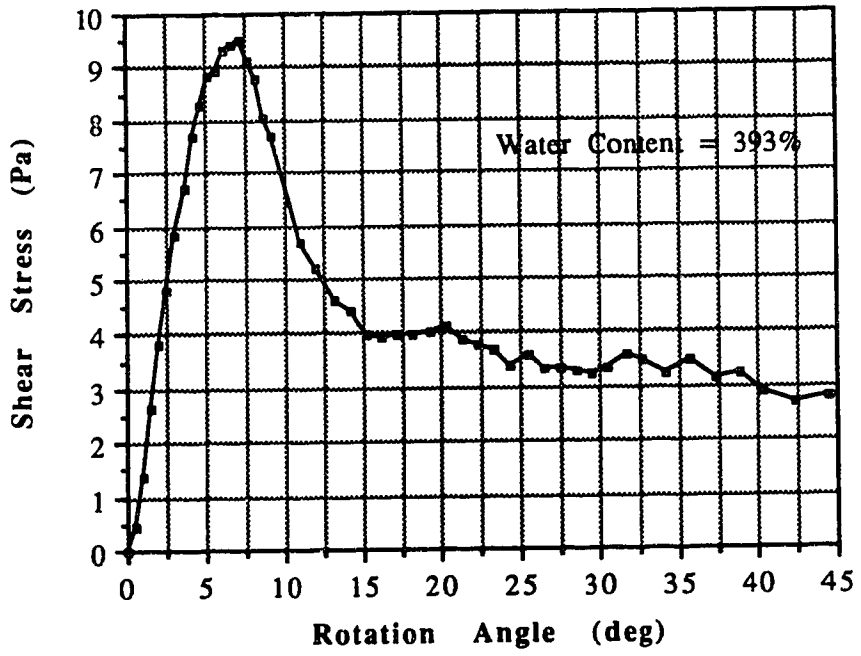

Figure C.15 Vane Shear Test S40020DP

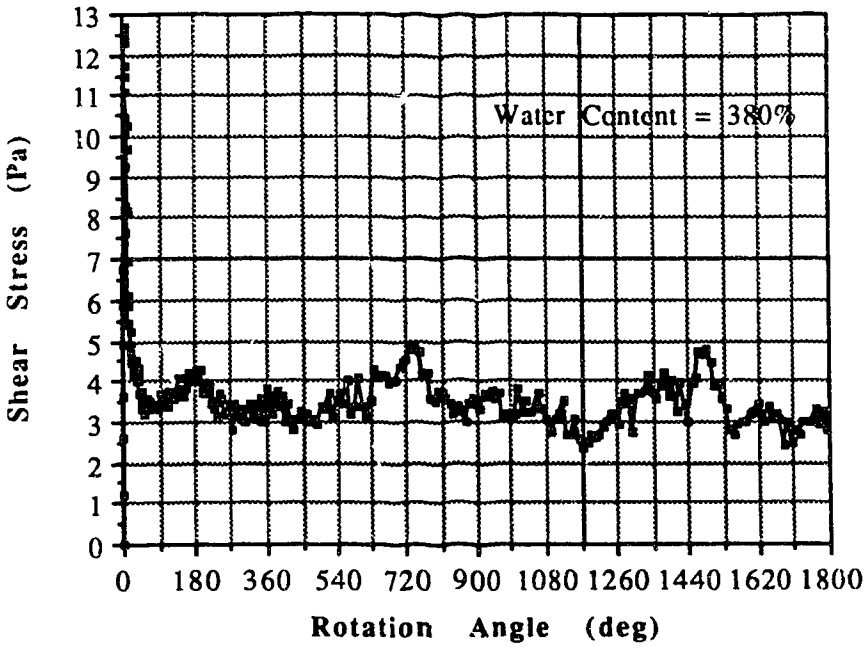

Figure C.16 Vane Shear Test S40033DR

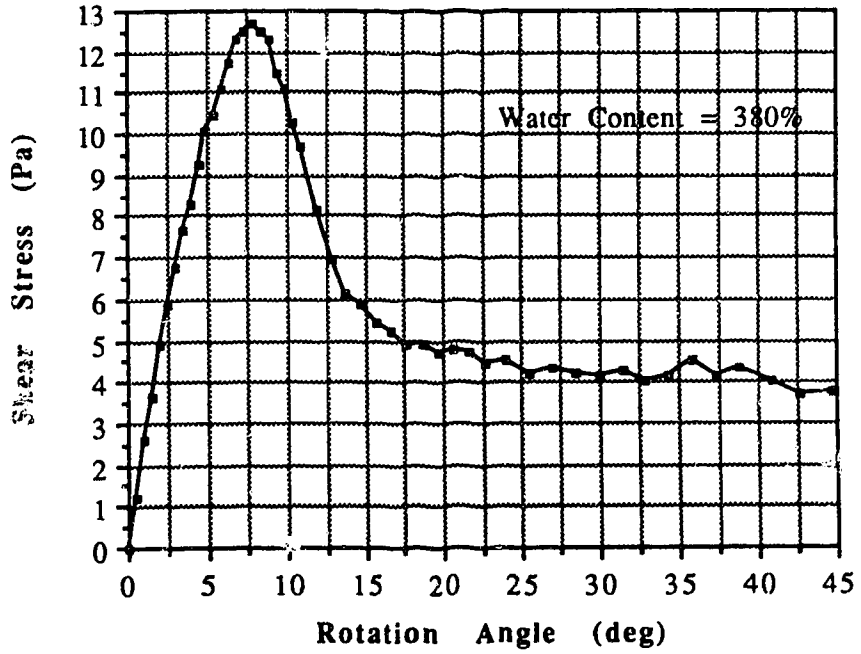

Figure C.17 Vane Shear Test S40033DP

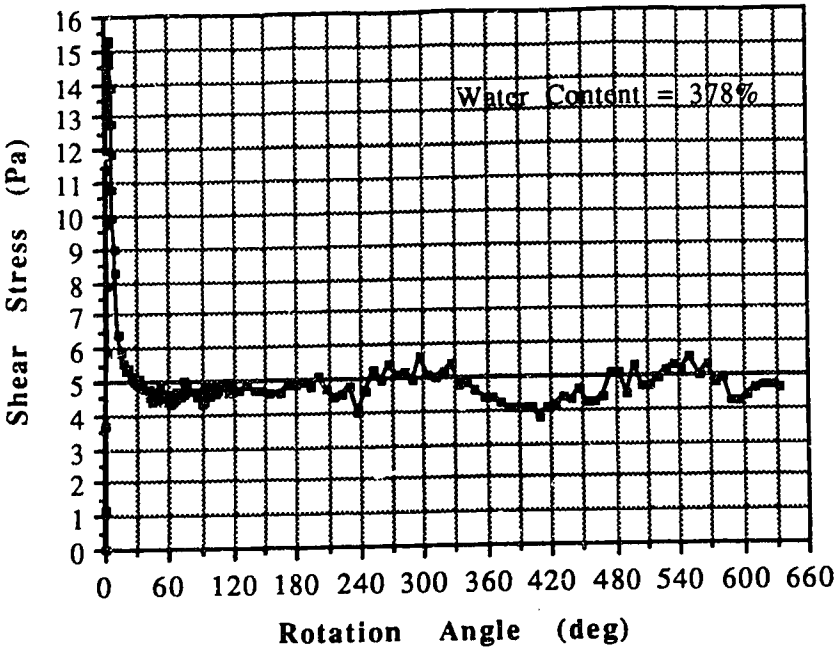

Figure C.18 Vane Shear Test S40040DR

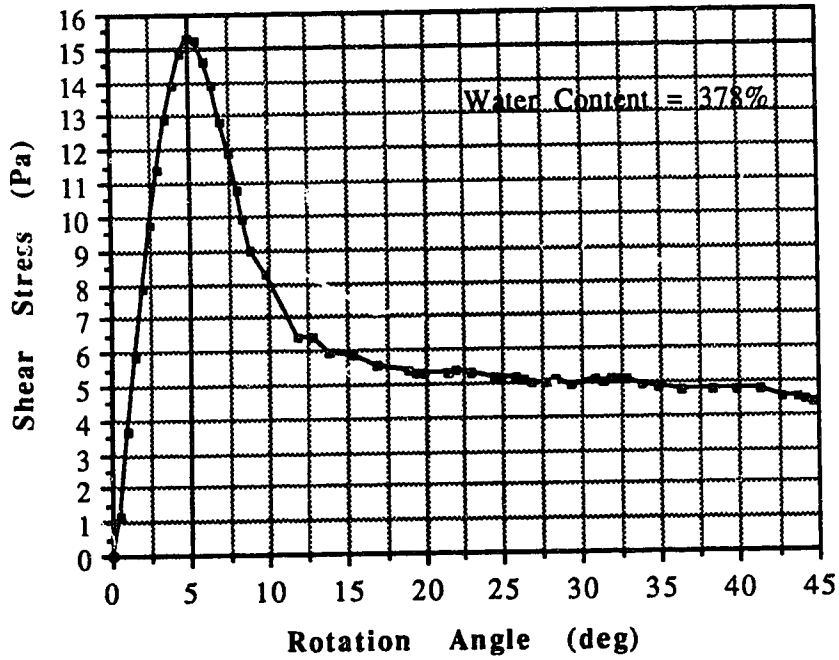

Figure C.19 Vane Shear Test S40040DP

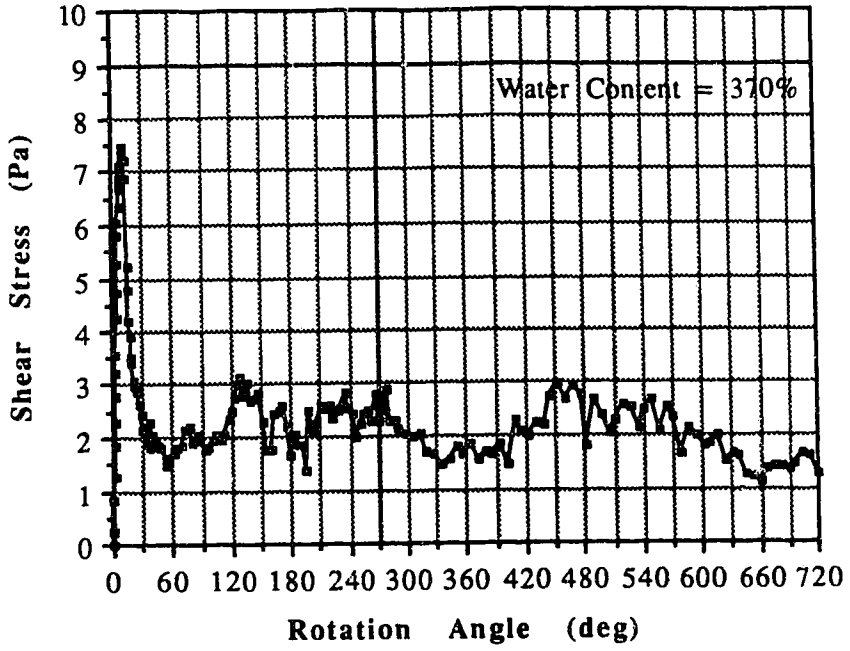

Figure C.20 Vane Shear Test S40050DR

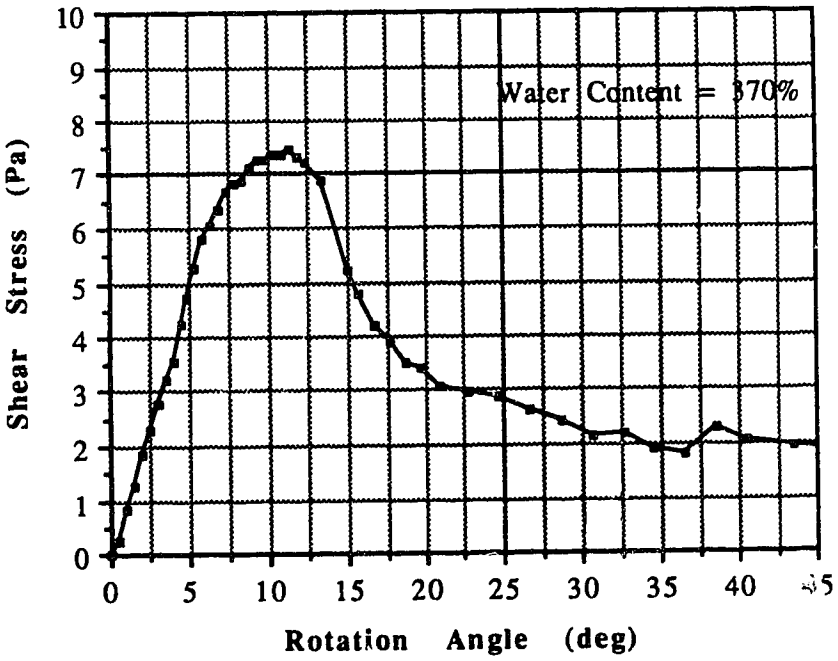

Figure C.21 Vane Shear Test S40050DP

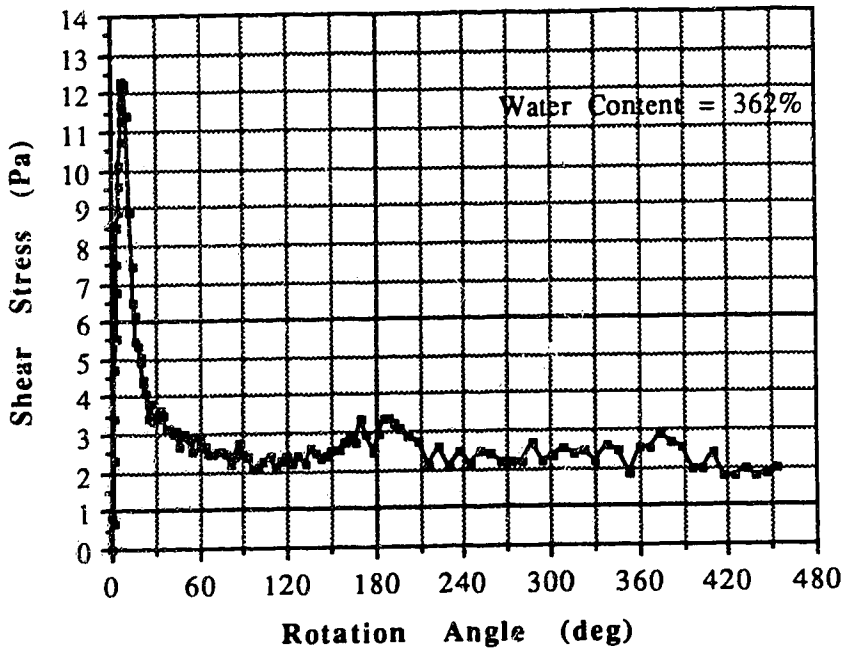

Figure C.22 Vane Shear Test S40060DR

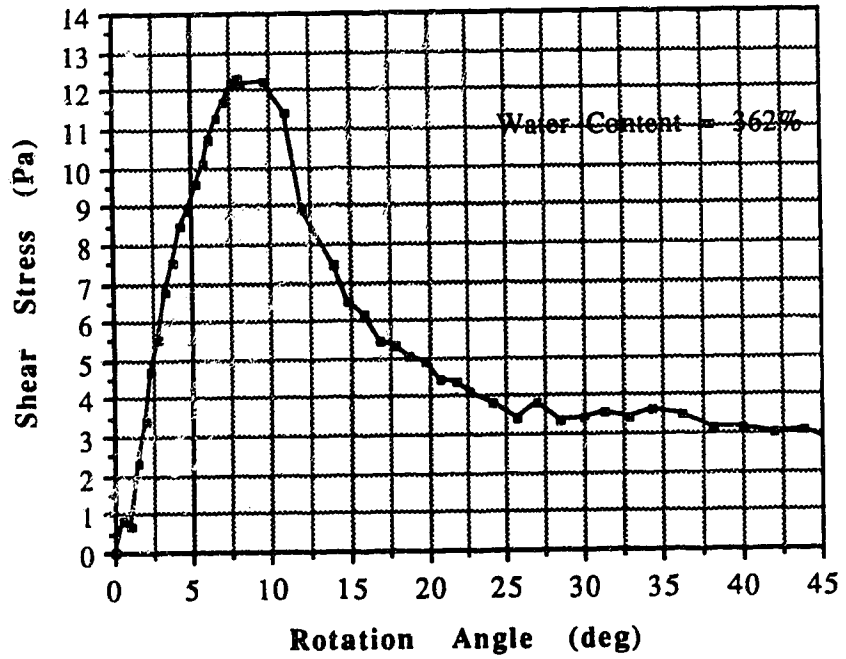

Figure C.23 Vane Shear Test S40060DP

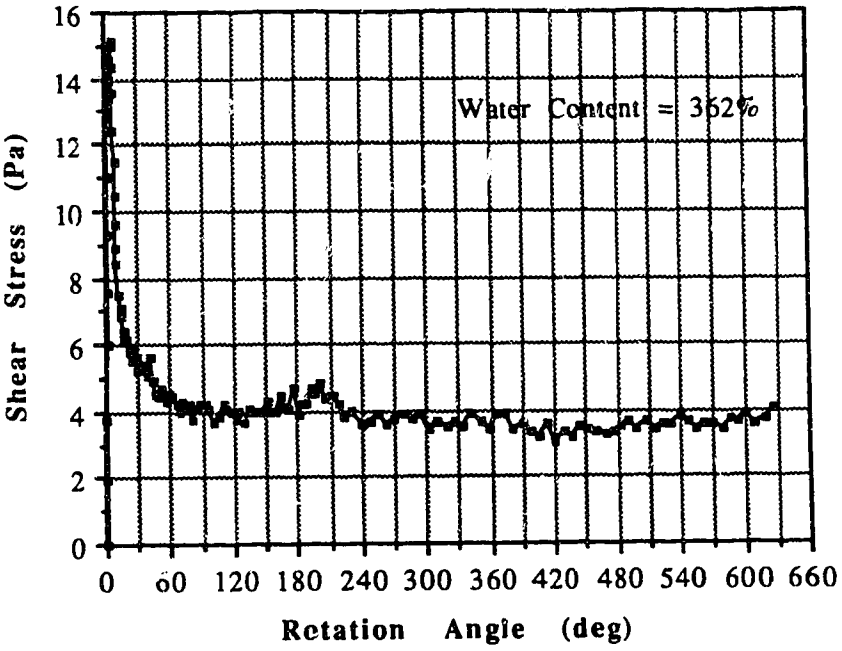

Figure C.24 Vane Shear Test S40070DR

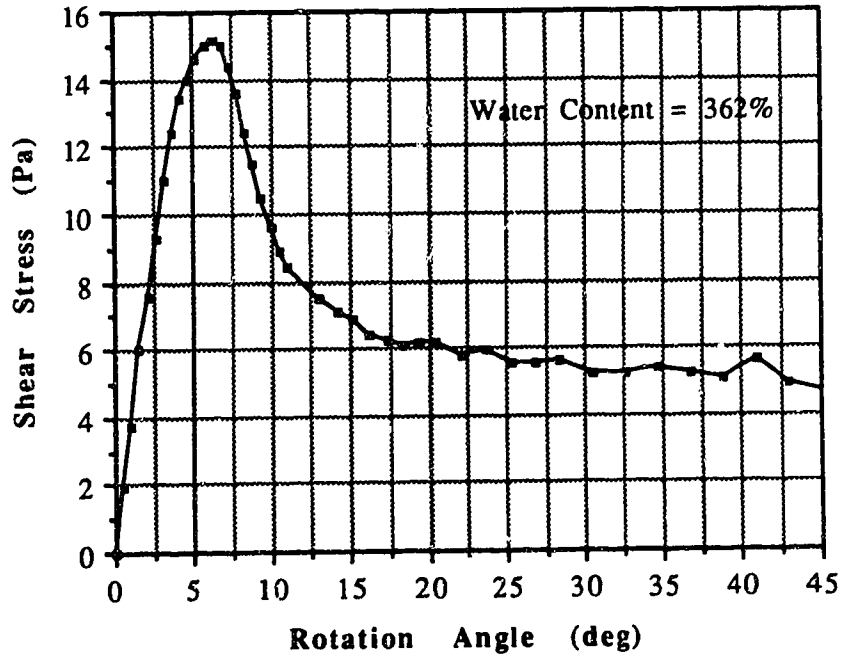

Figure C.25 Vane Shear Test S40070DP

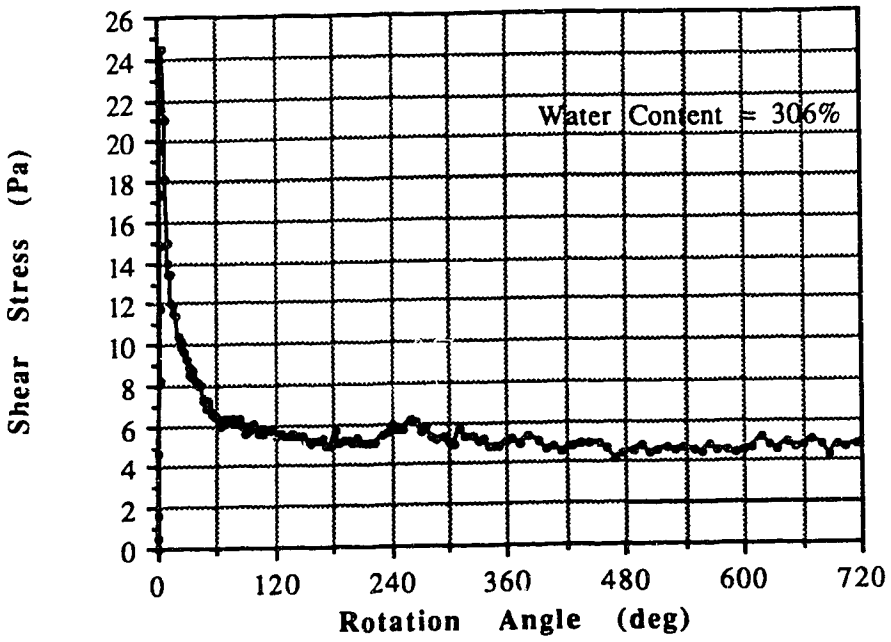

Figure C.26 Vane Shear Test S40160DR

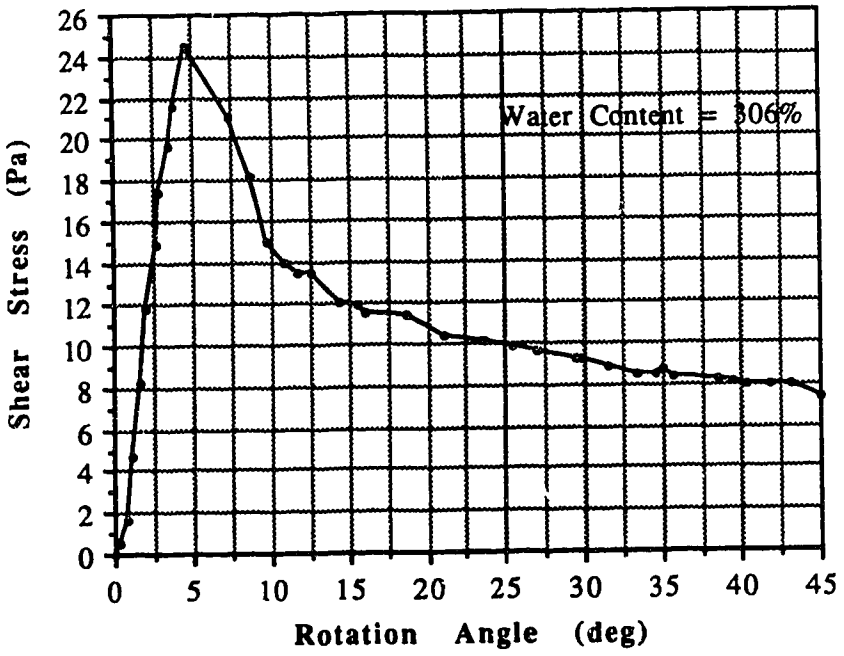

Figure C.27 Vane Shear Test S40160DP

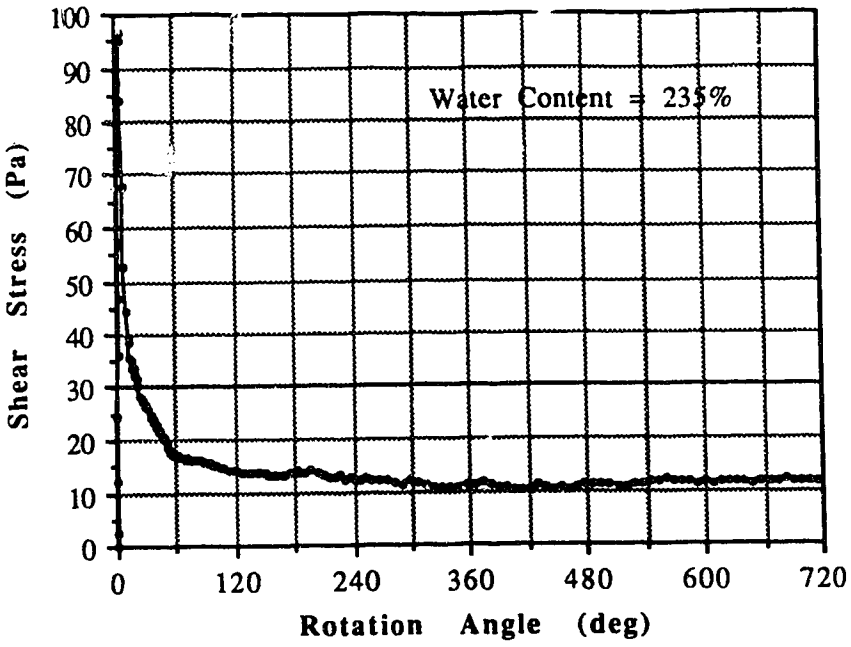

Figure C.28 Vane Shear Test S40470DR

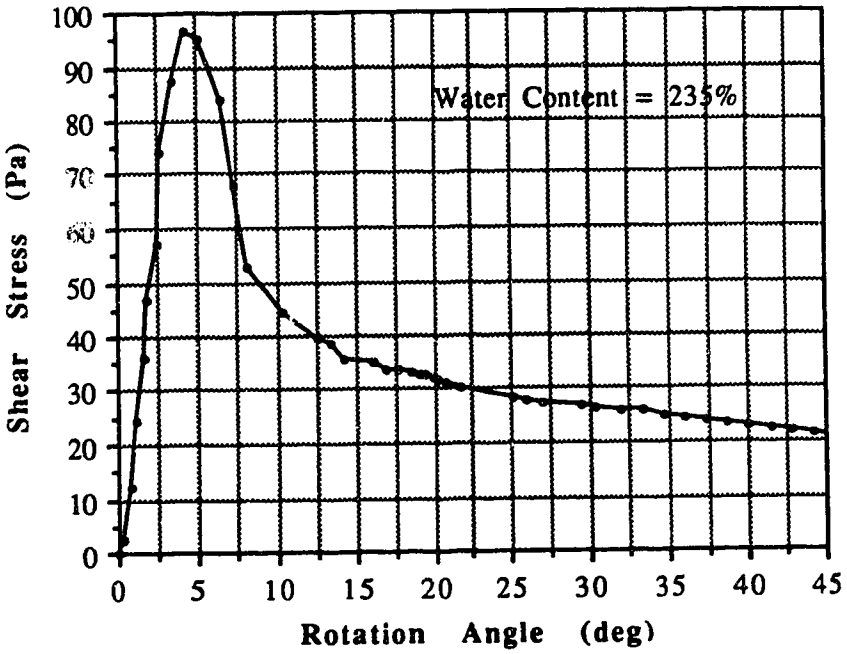

Figure C.29 Vane Shear Test S40470DP

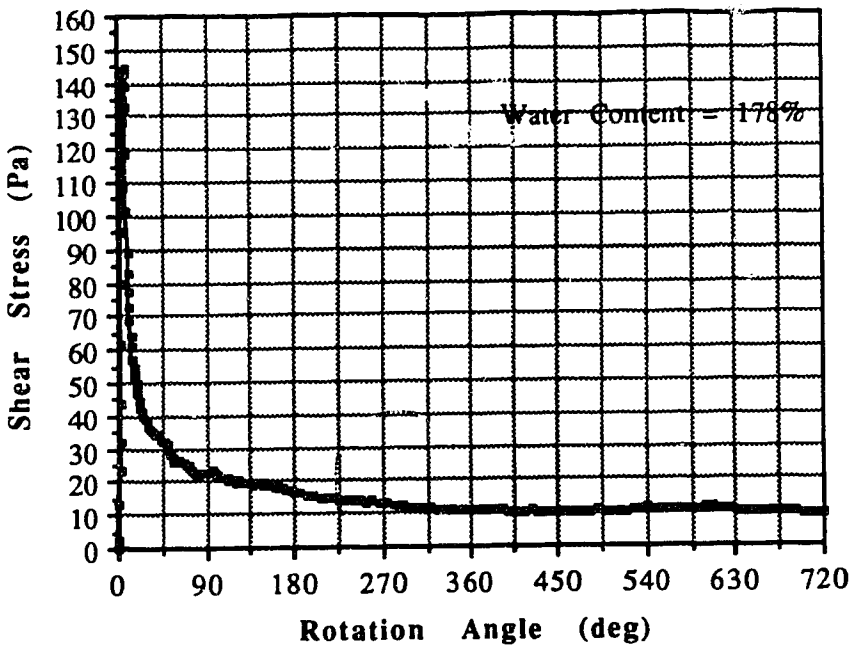

Figure C.30 Vane Shear Test S40680DR

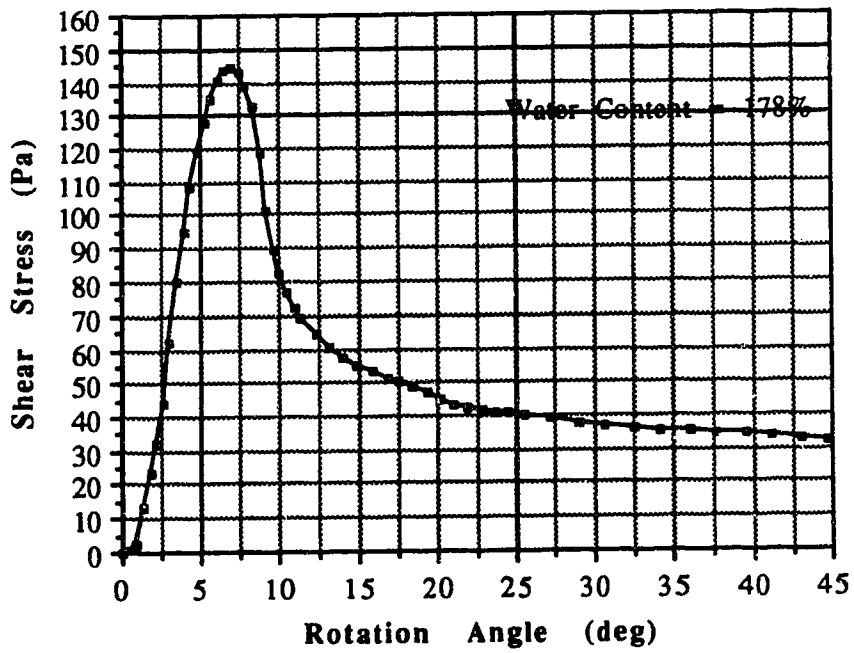

Figure C.31 Vane Shear Test S40680DP

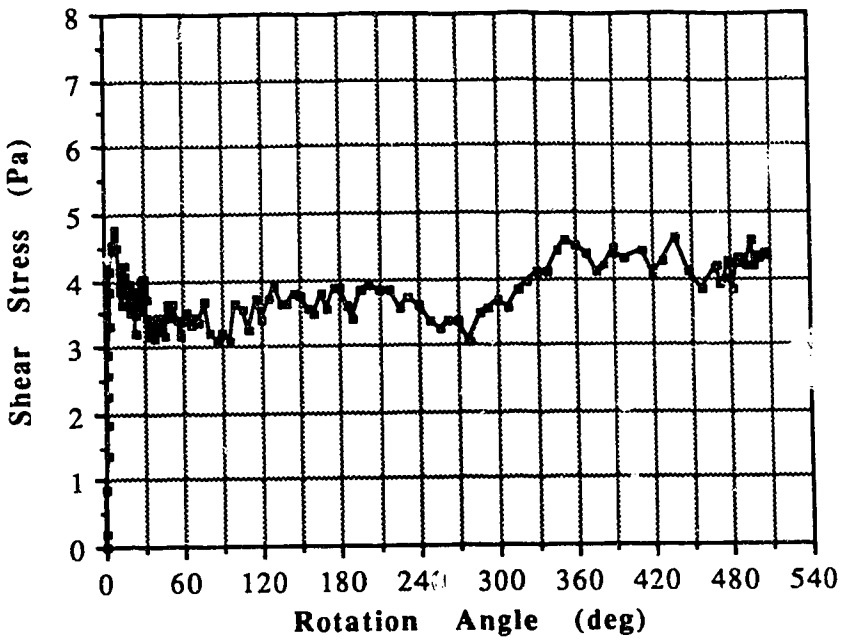

Figure C.32 Vane Shear Test S30000M

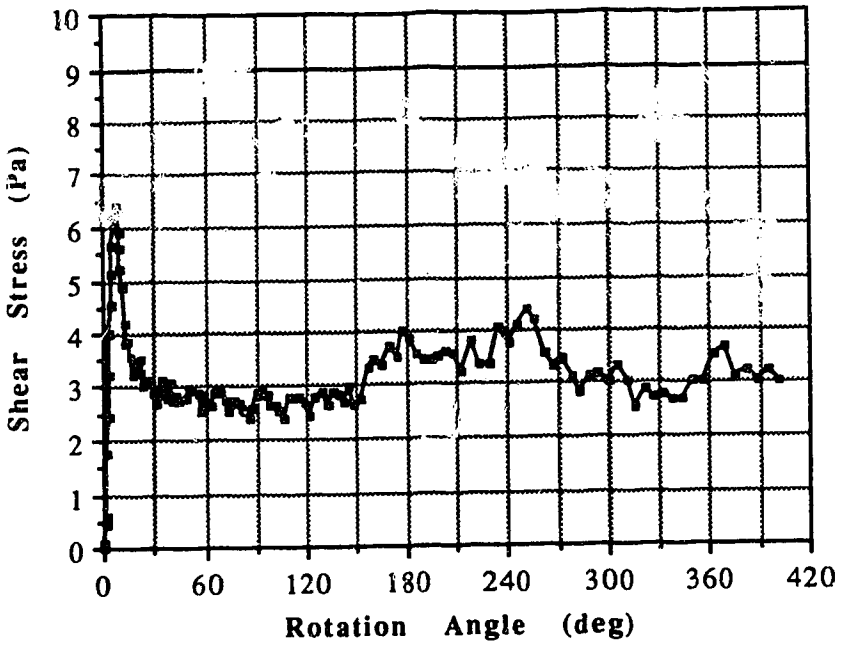

Figure C.33 Vane Shear Test S30002HR

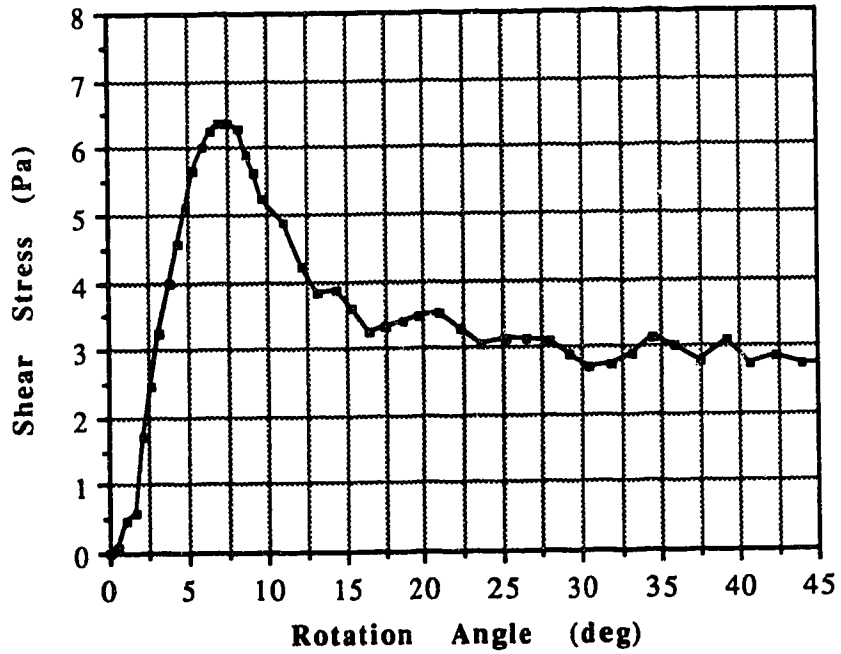

Figure C.34 Vane Shear Test S30002HP

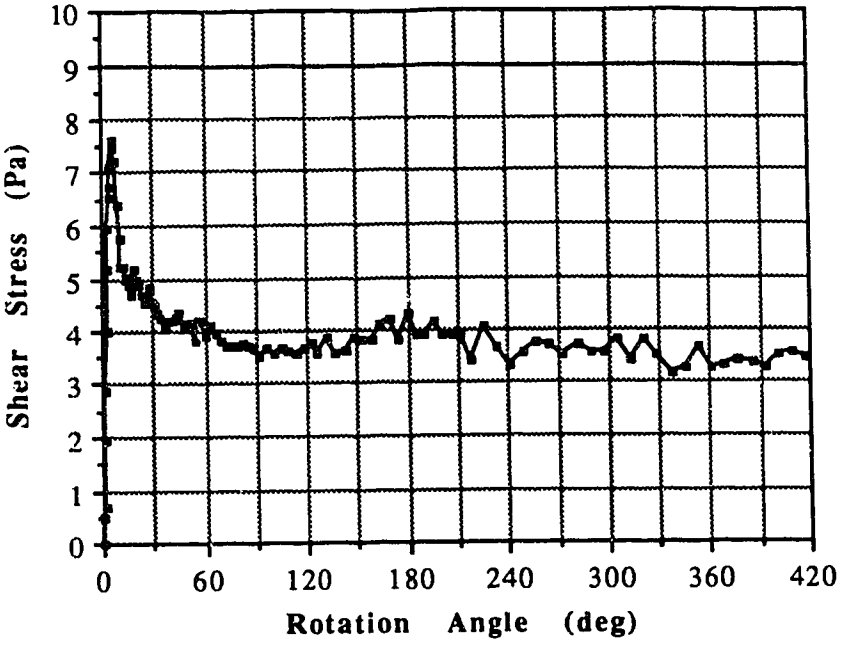

Figure C.35 Vane Shear Test S30008HR

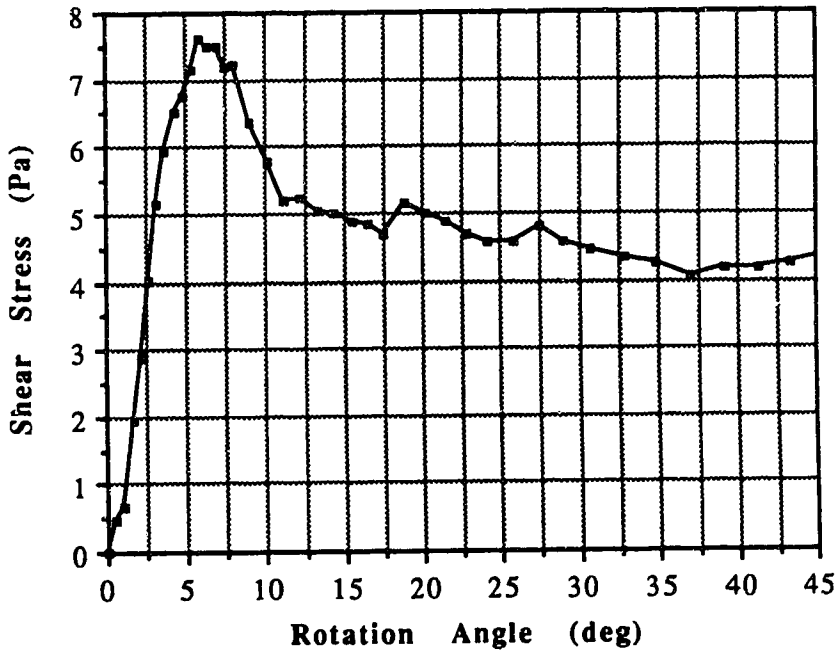

Figure C.36 Vane Shear Test S30008HP

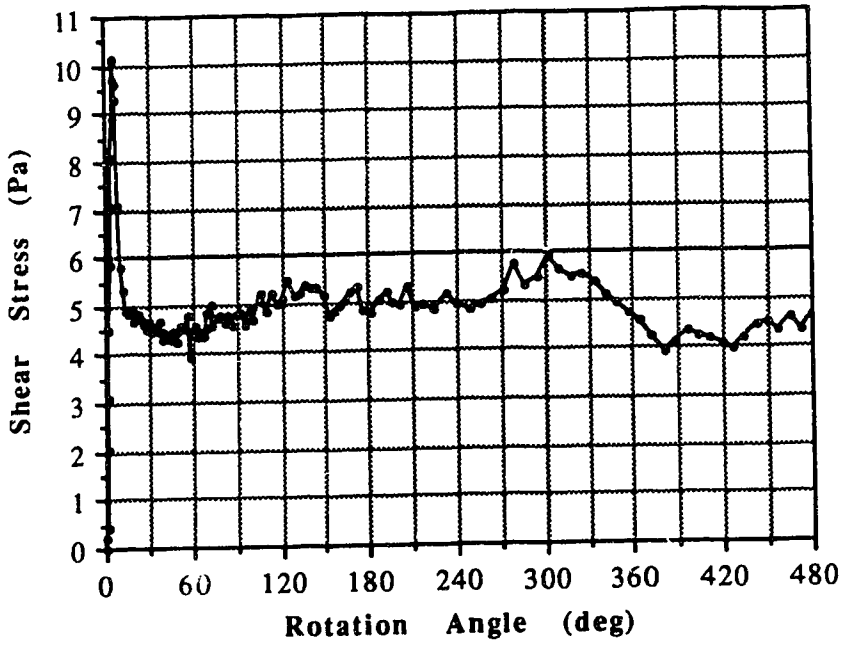

Figure C.37 Vane Shear Test S30001DR

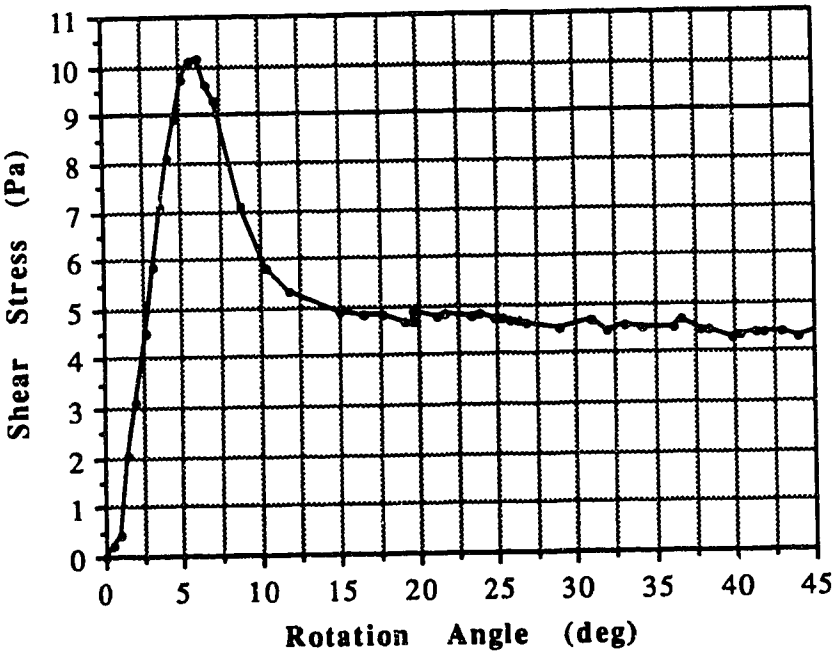

Figure C.38 Vane Shear Test S30001DP

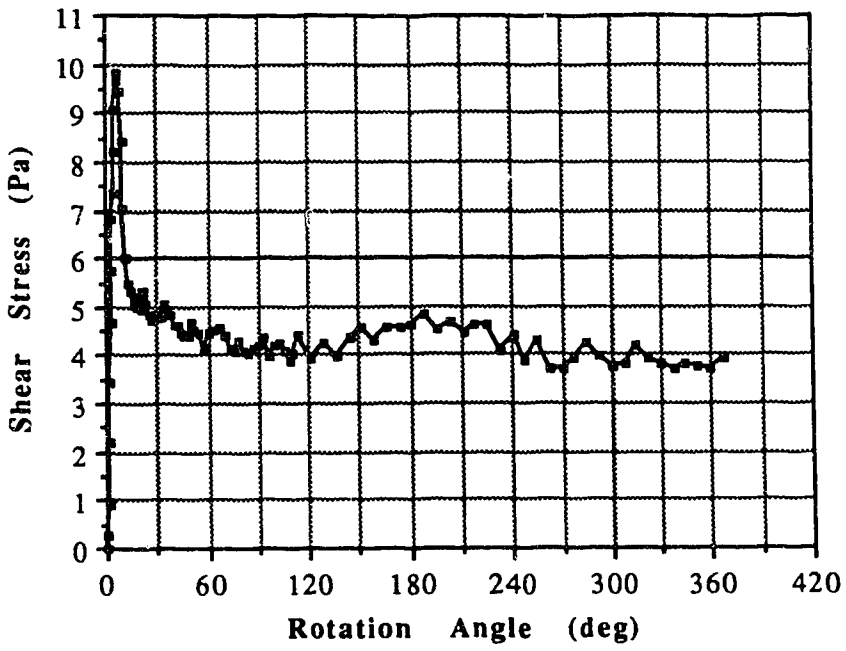

Figure C.39 Vane Shear Test S30002DR

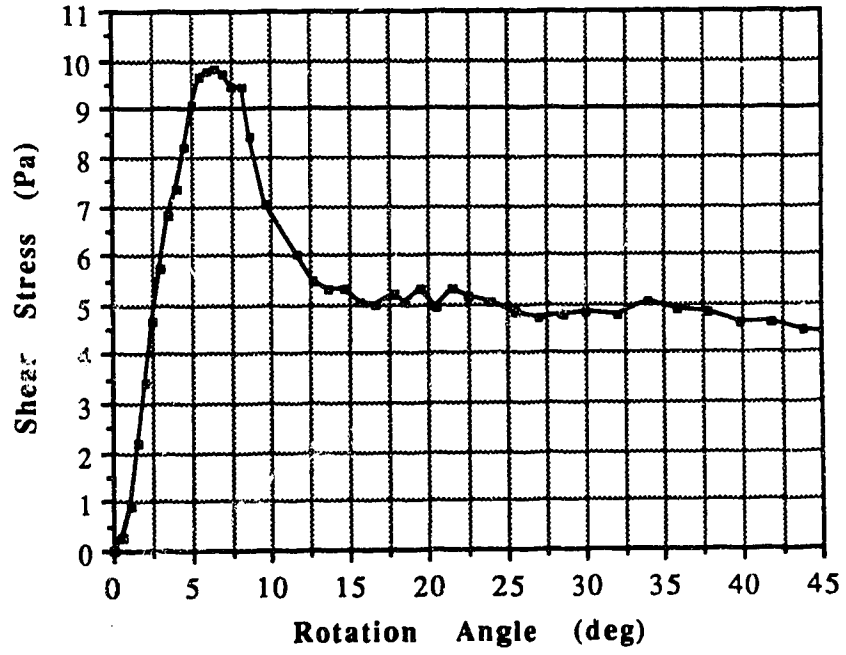

Figure C.40 Vane Shear Test S30002DP

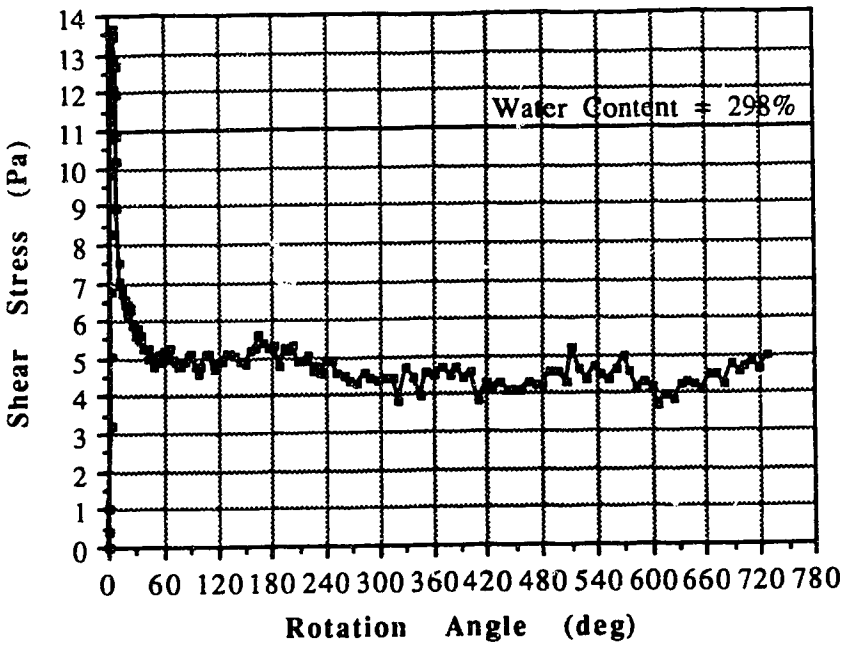

Figure C.41 Vane Shear Test S30006DR

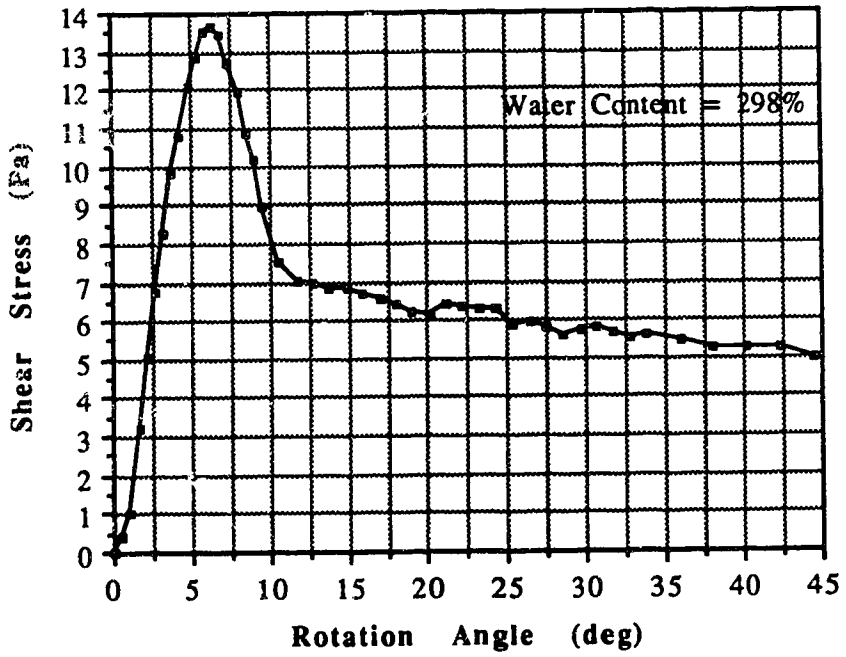

Figure C.42 Vane Shear Test S30006DP

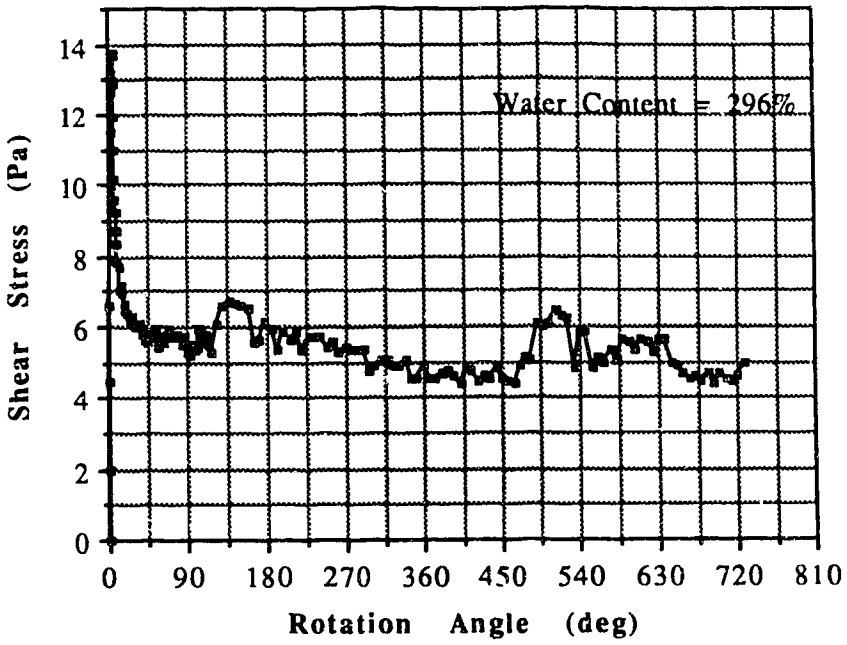

Figure C.43 Vane Shear Test S30010DR

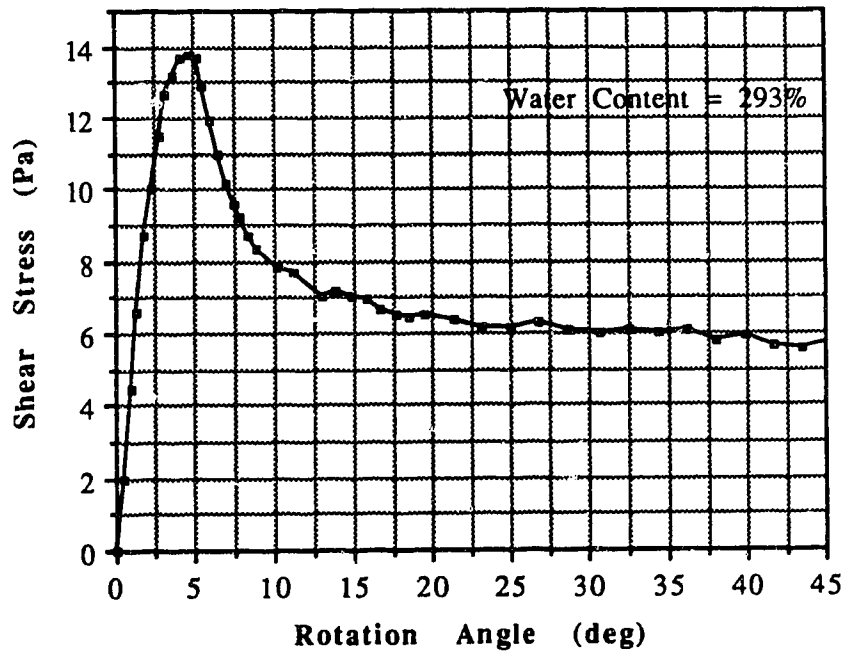

Figure C.44 Vane Shear Test S30010DP

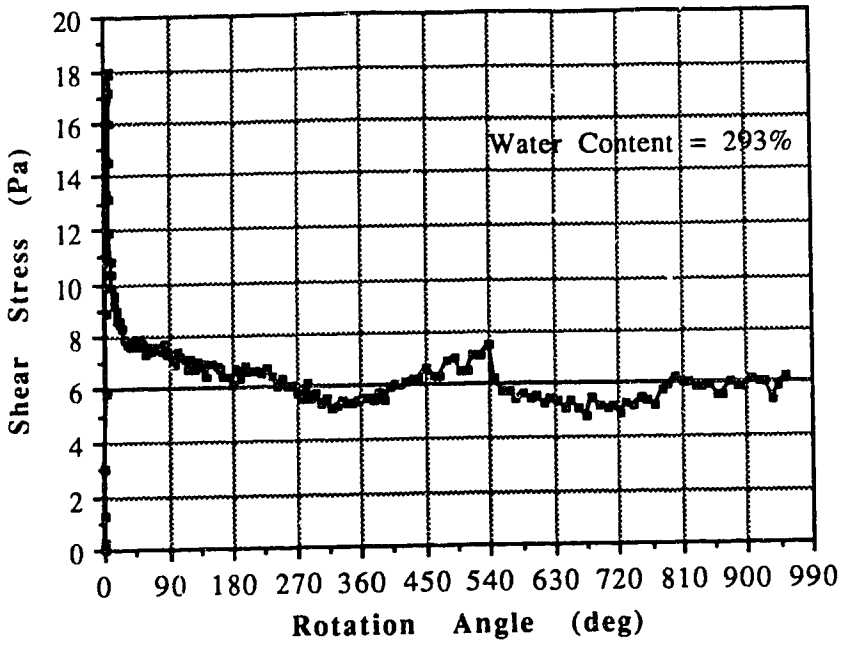

Figure C.45 Vane Shear Test S30020DR

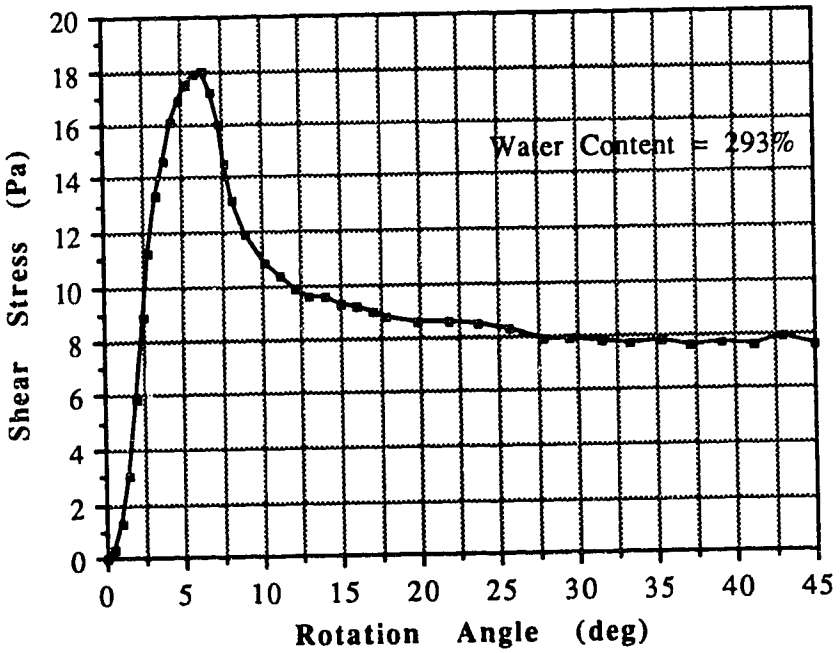

Figure C.46 Vane Shear Test S30020DP

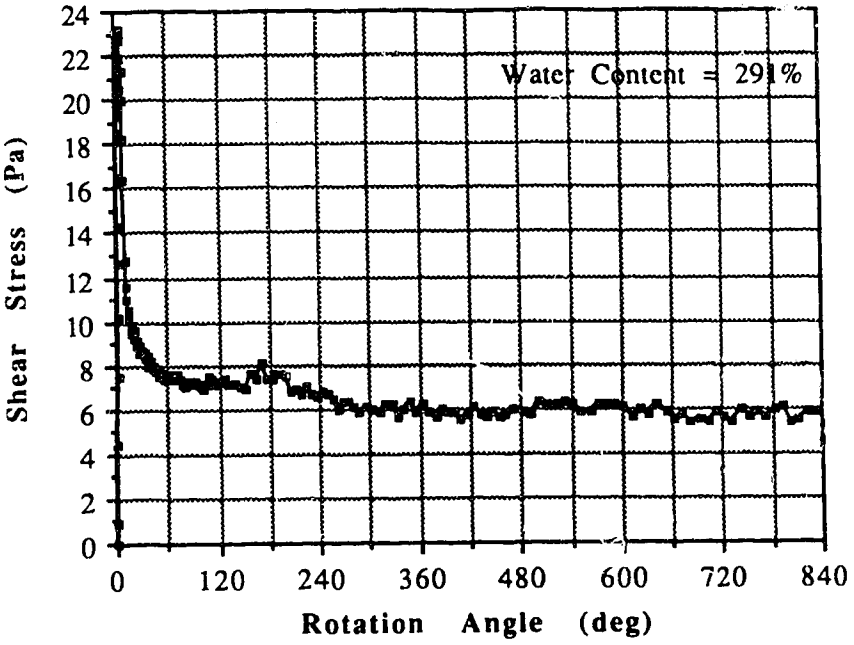

Figure C.47 Vane Shear Test S30030DR

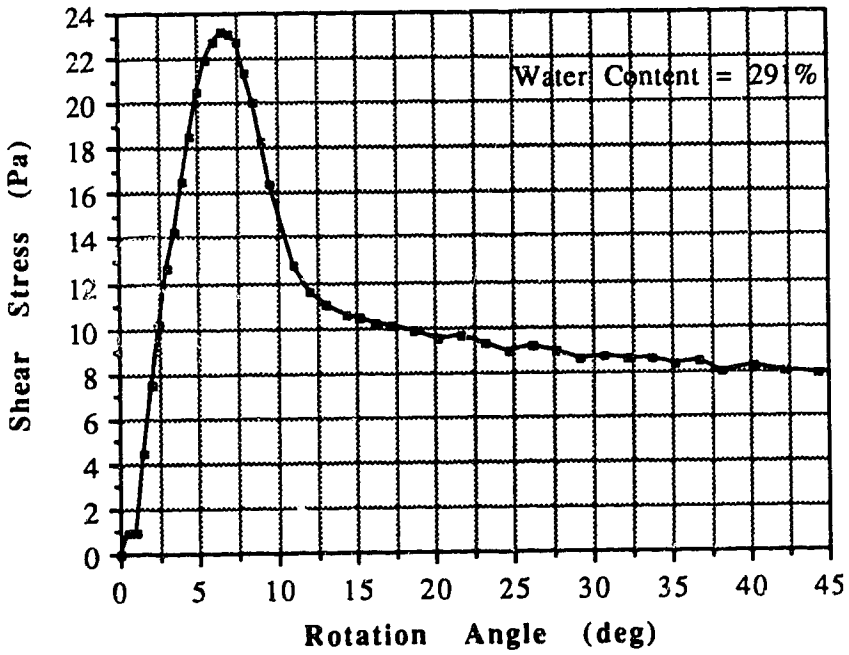

Figure C.48 Vane Shear Test S30030DP

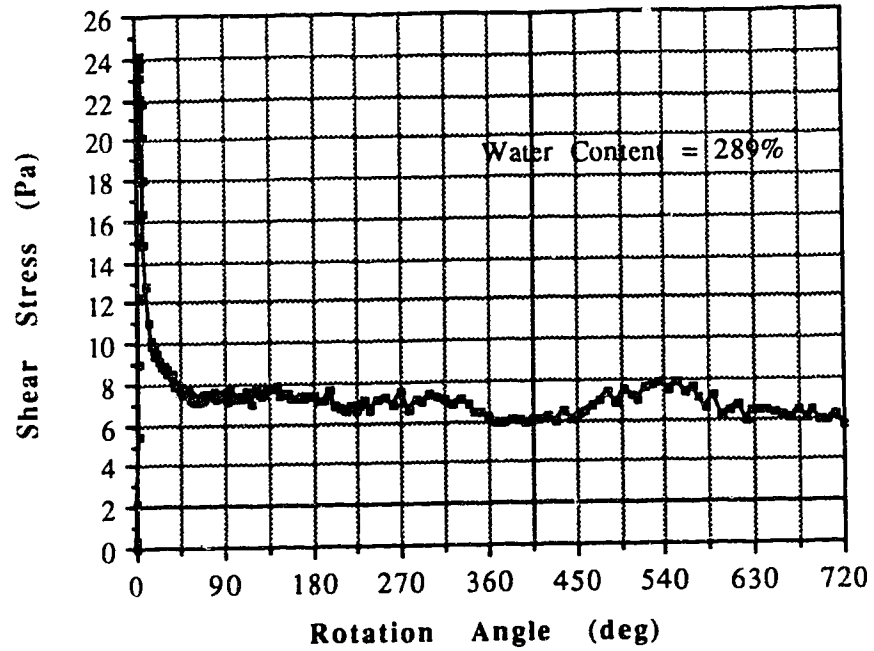

Figure C.49 Vane Shear Test S30041DR

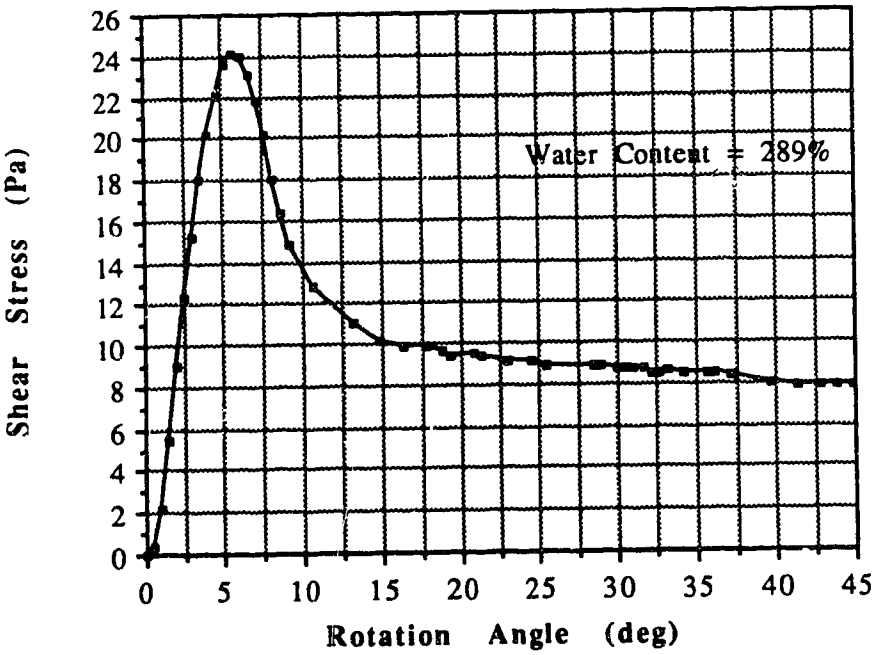

Figure C.50 Vane Shear Test S30041DP

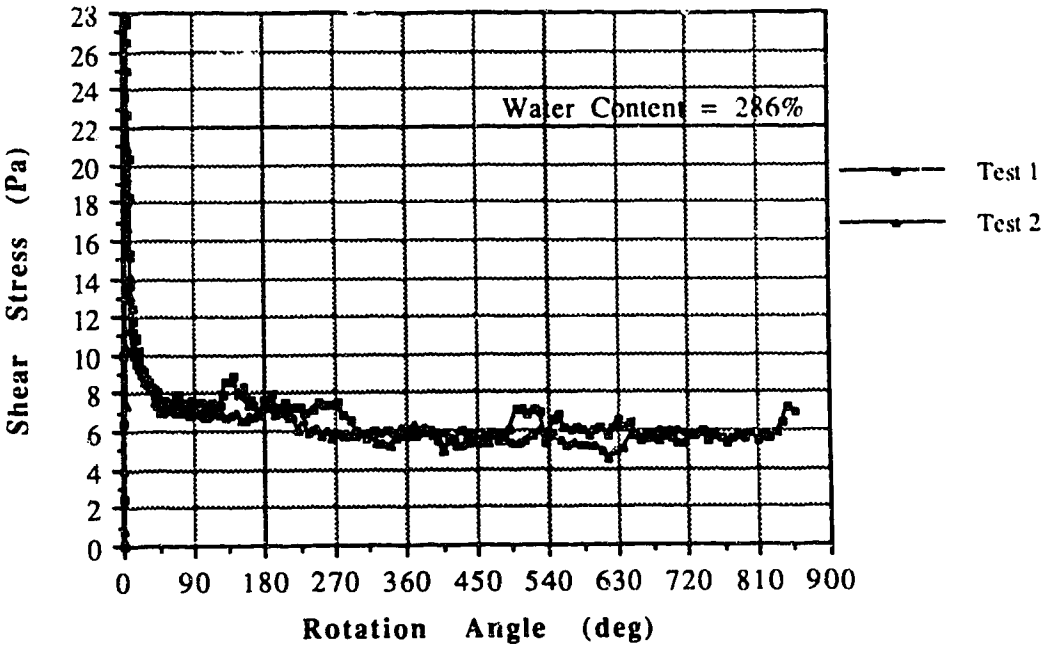

Figure C.51 Vane Shear Test S30050DR

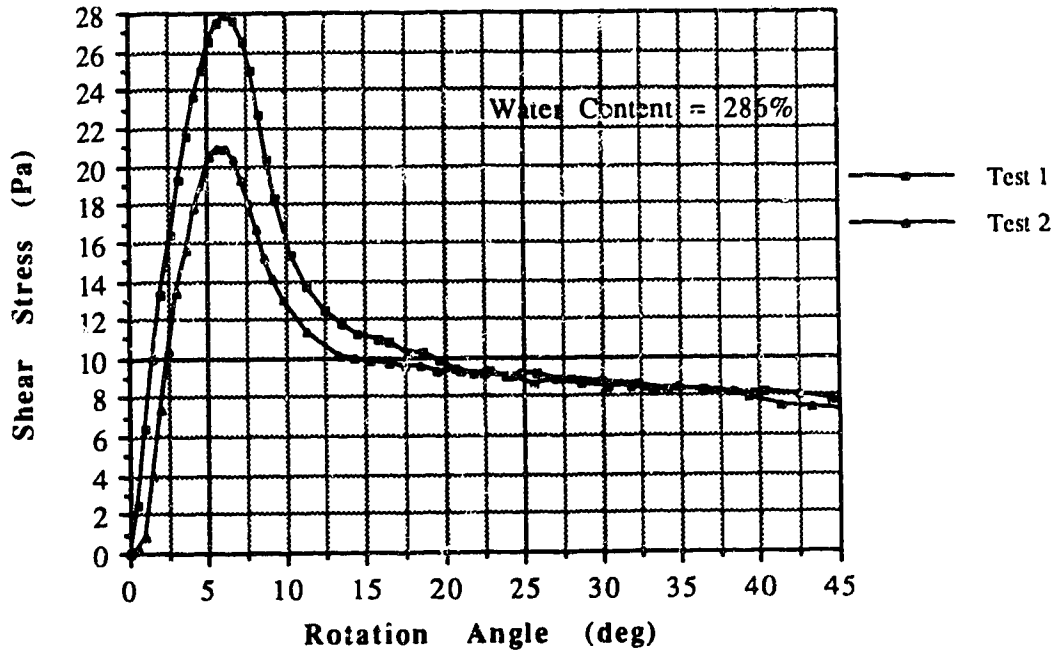

Figure C.52 Vane Shear Test S30050DP

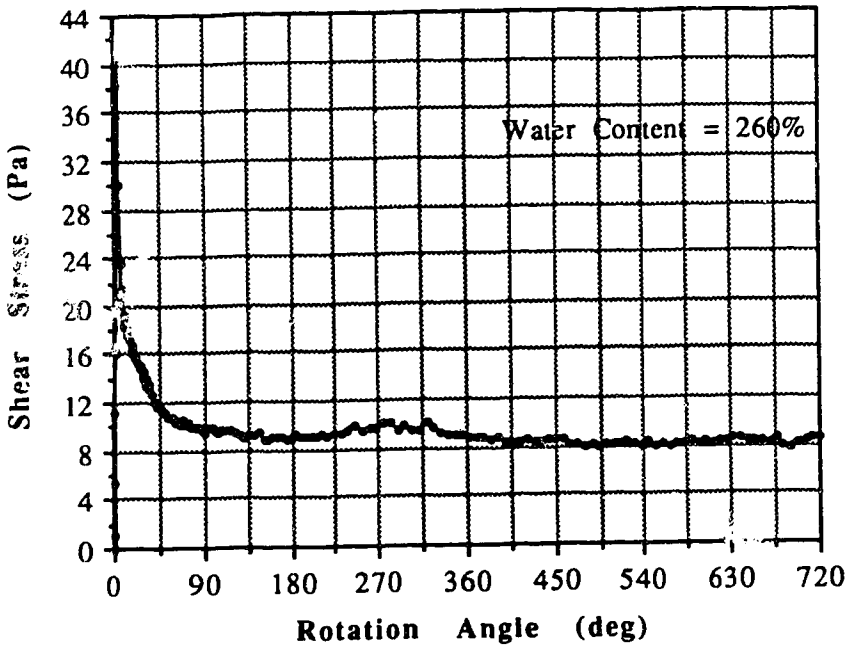

Figure C.53 Vane Shear Test S30160DR

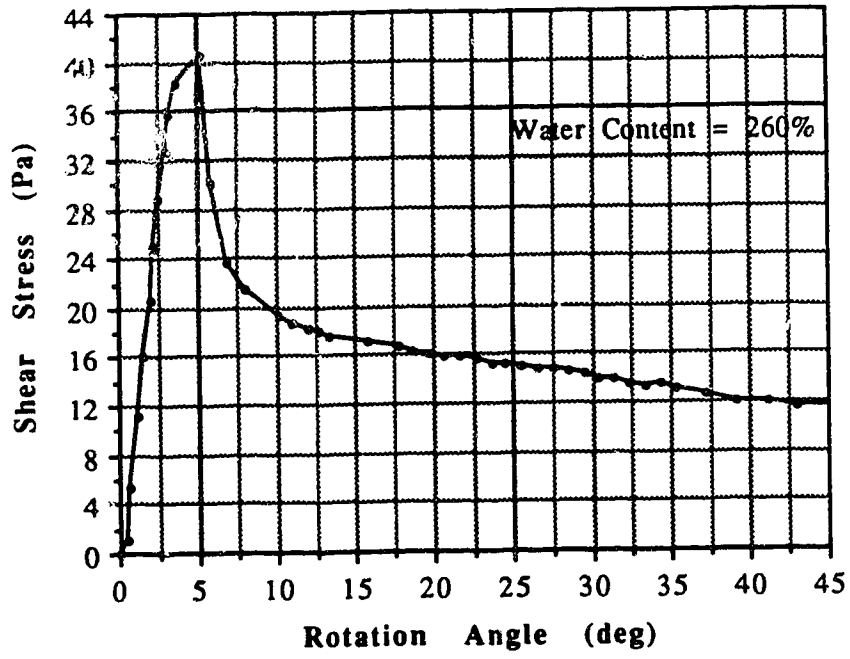

Figure C.54 Vane Shear Test S30160DP

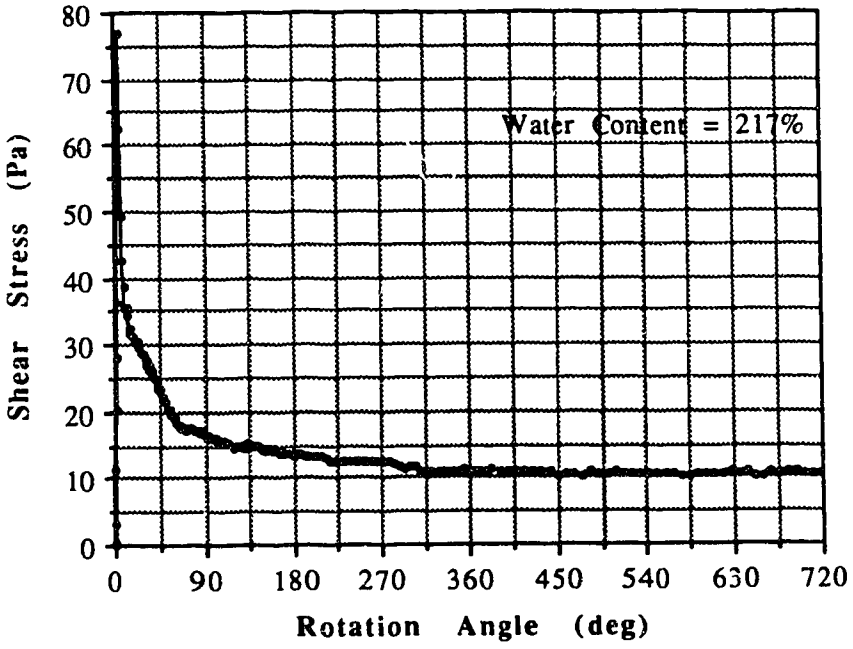

Figure C.55 Vane Shear Test S30470DR

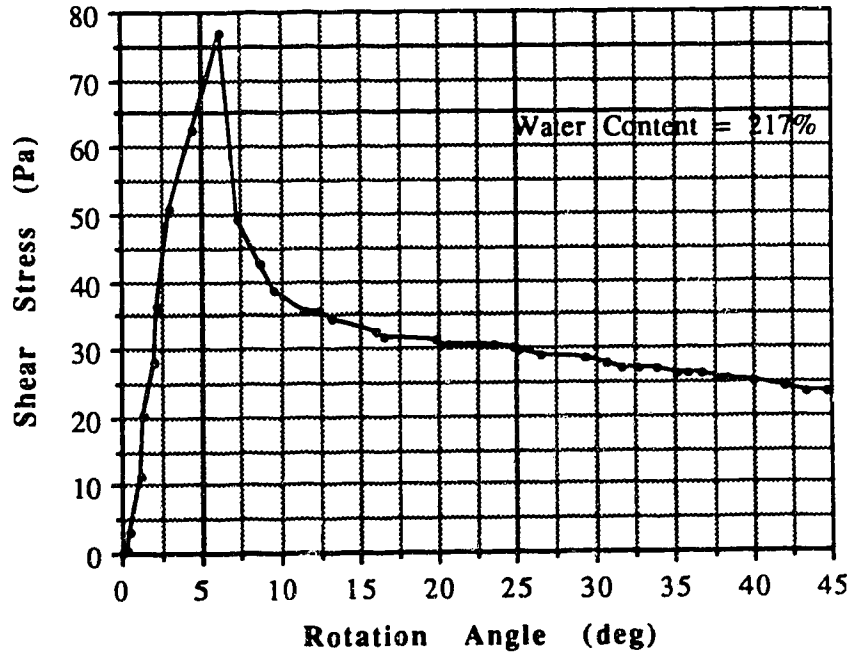

Figure C.56 Vane Shear Test S30470DP

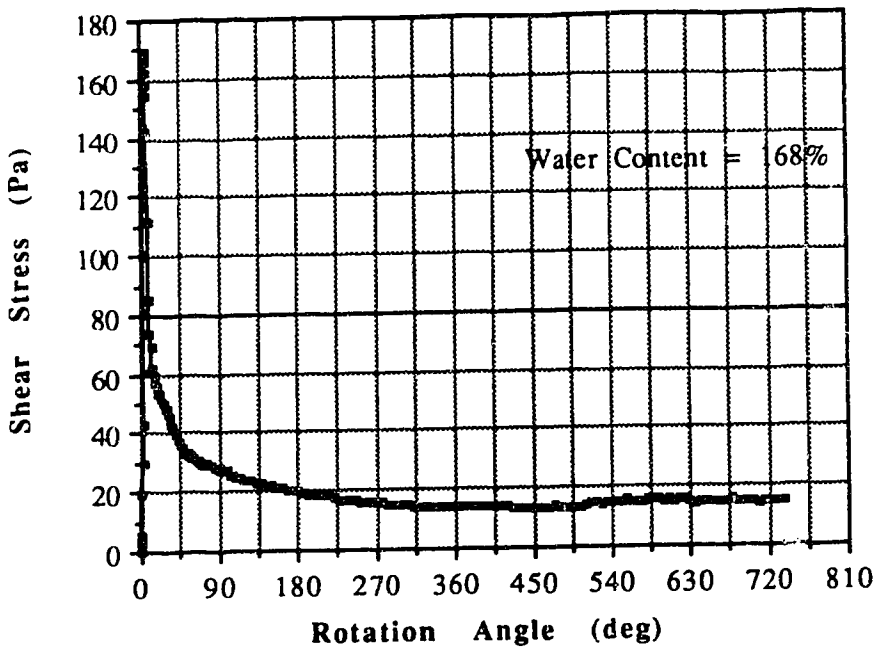

Figure C.57 Vane Shear Test S30680DR

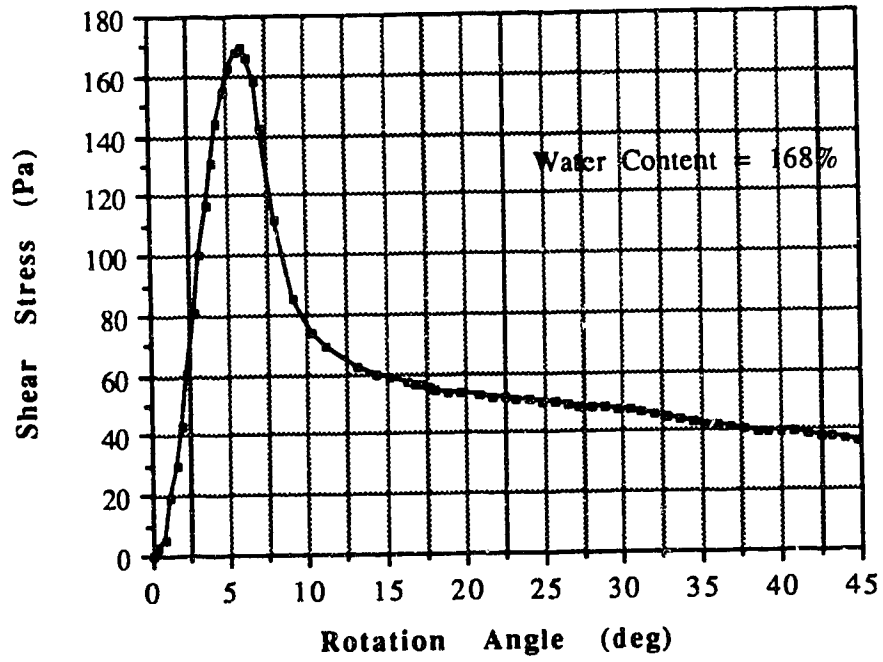

Figure C.58 Vane Shear Test S30680DP

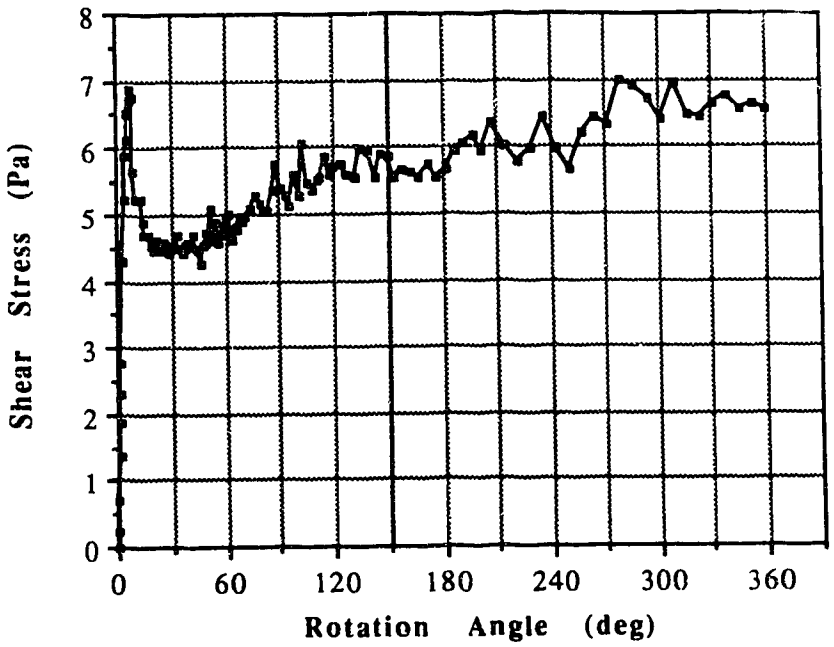

Figure C.59 Vane Shear Test S23000M

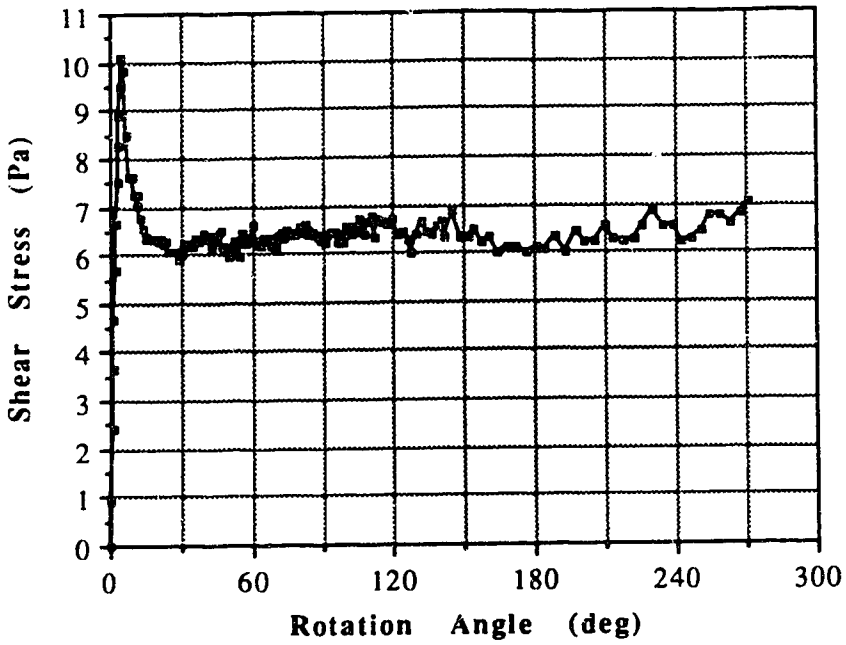

Figure C.60 Vane Shear Test S23002HR

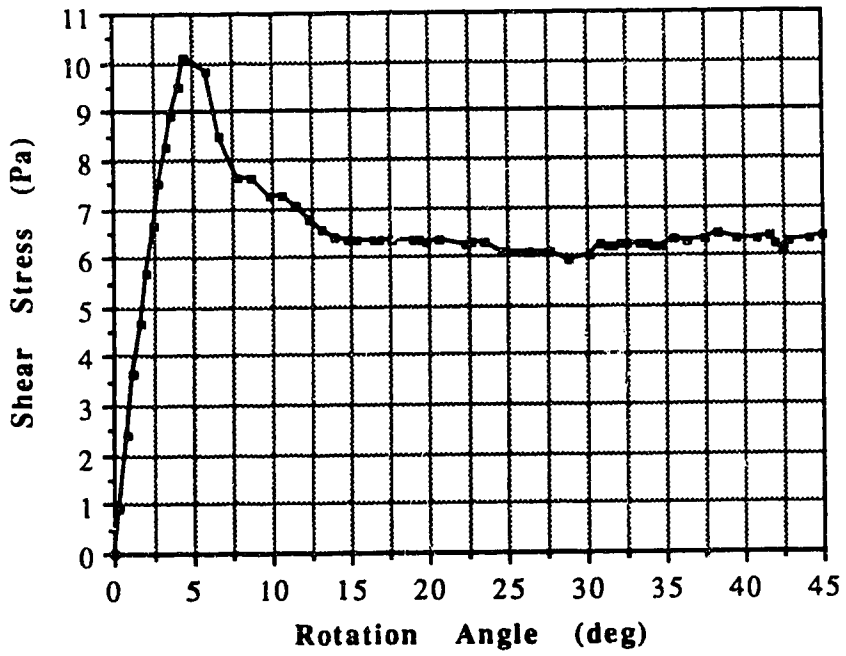

Figure C.61 Vane Shear Test S23002HP

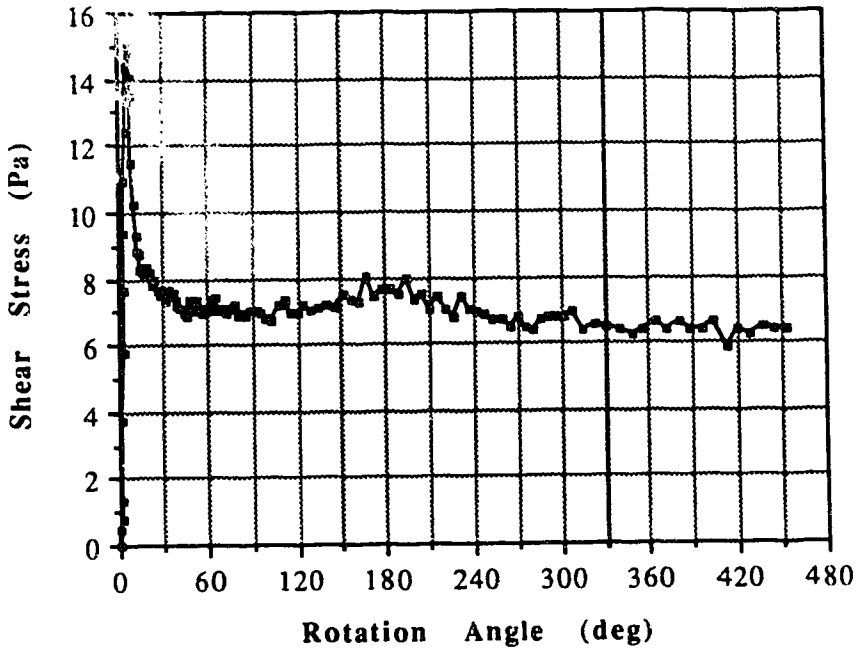

Figure C.60 Vane Shear Test S23008HR

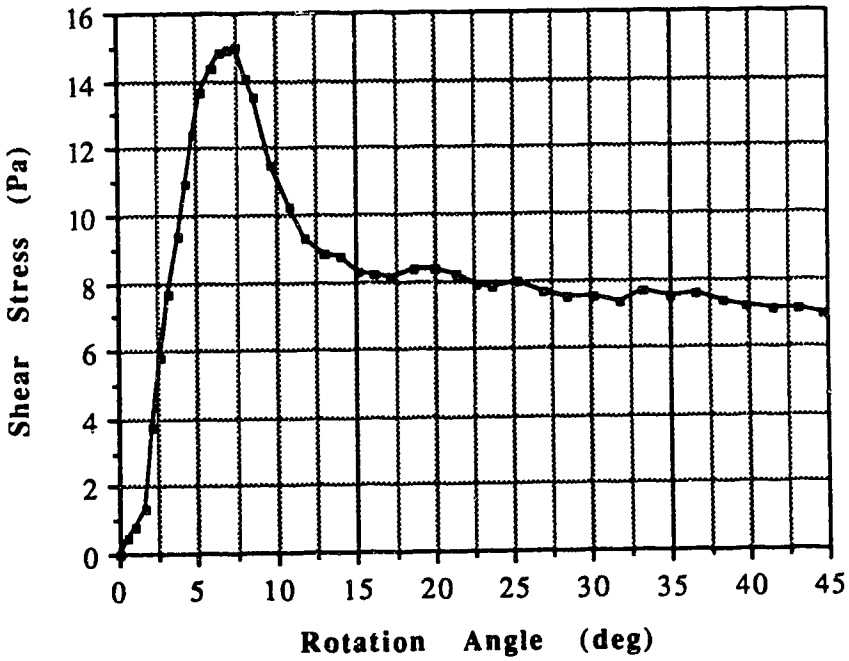

Figure C.61 Vane Shear Test S23008HP

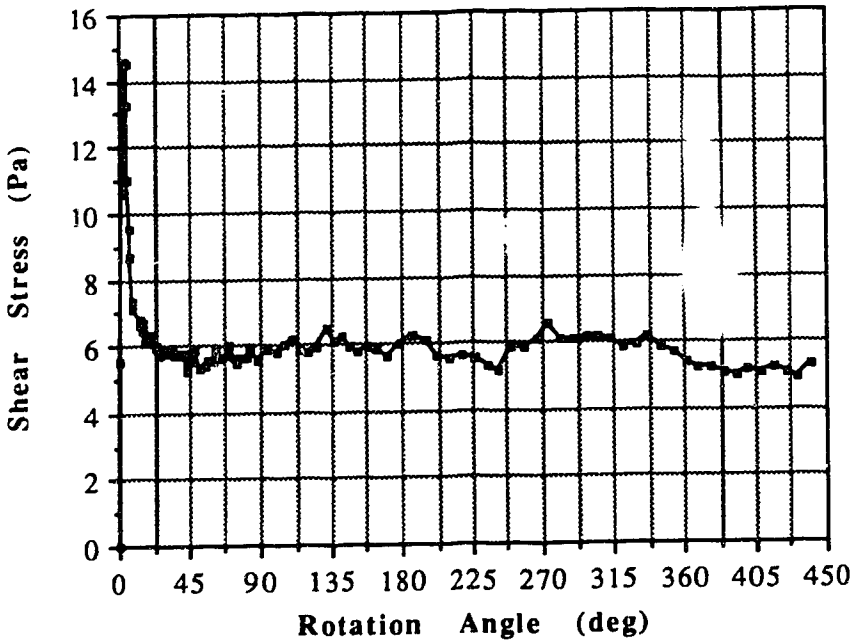

Figure C.64 Vane Shear Test S23001DR

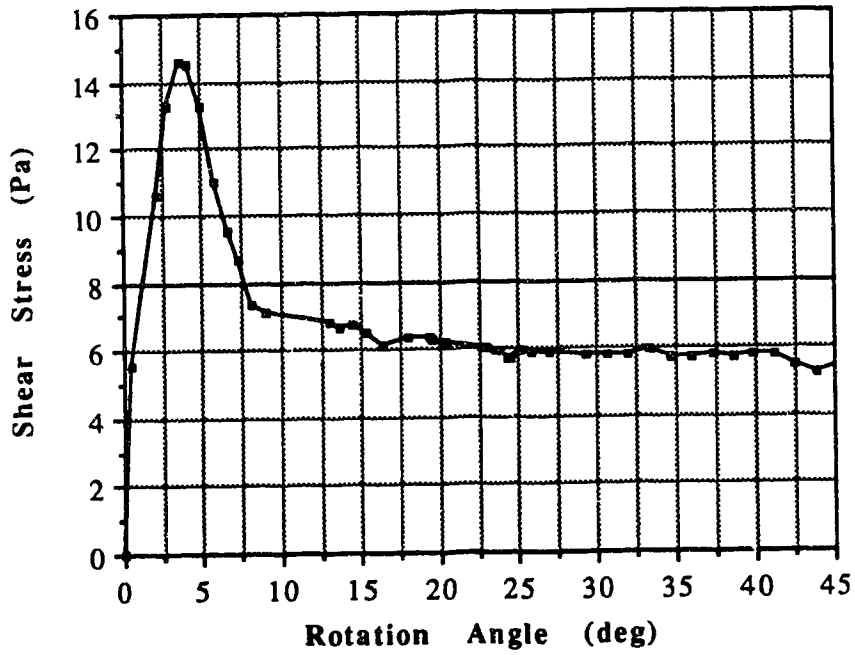

Figure C.65 Vane Shear Test S23001DP

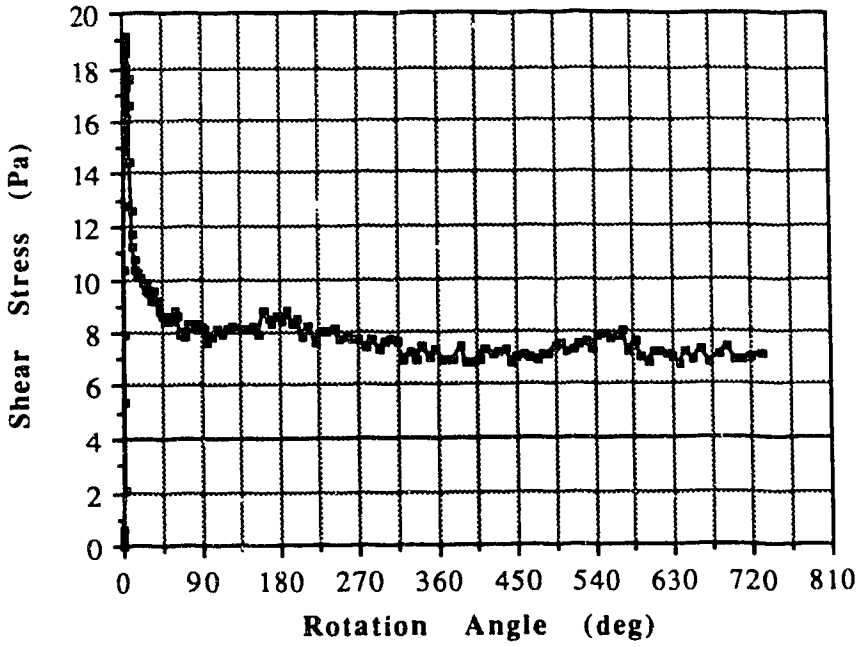

Figure C.66 Vane Shear Test S23002DR

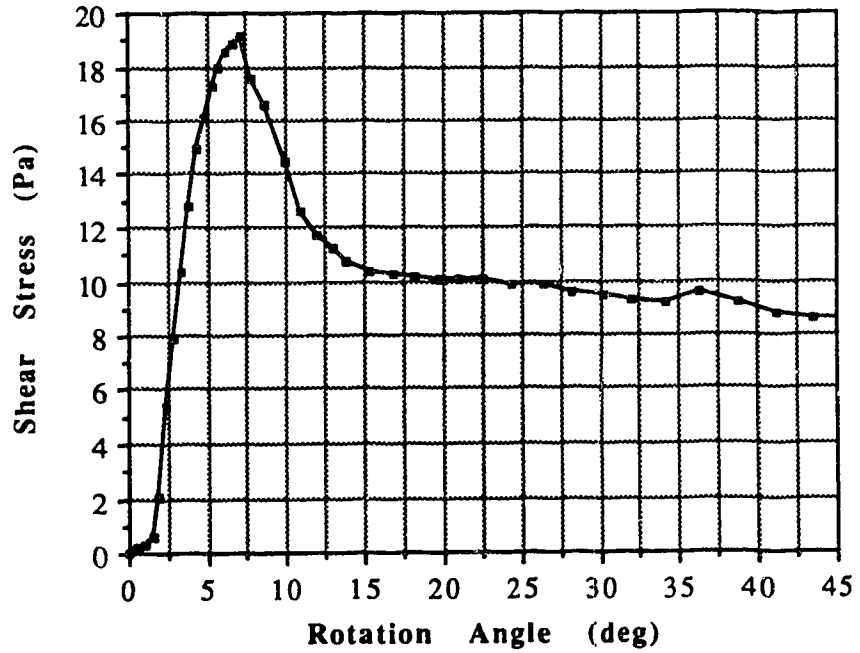

Figure C.67 Vane Shear Test S23002DP

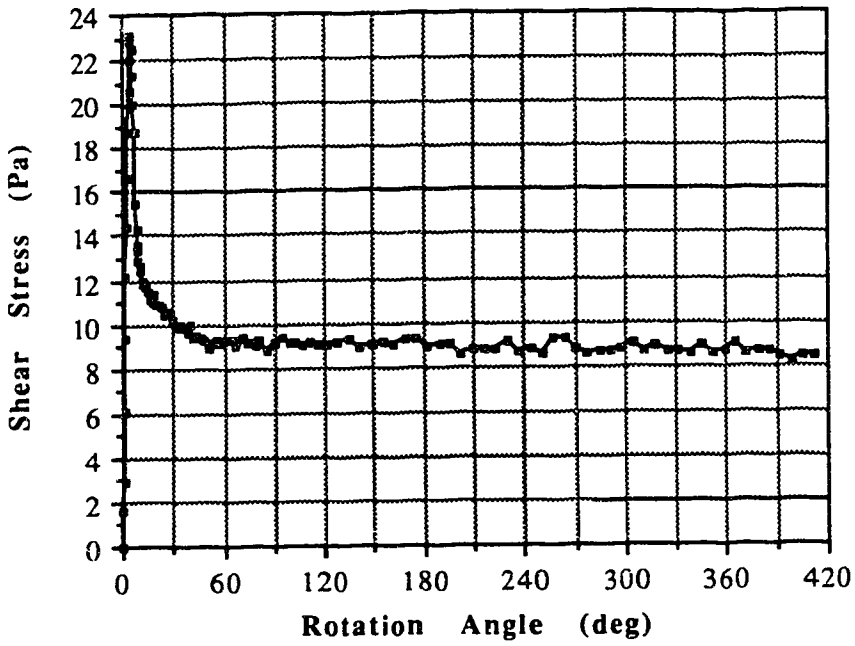

Figure C.68 Vane Shear Test S23005DR

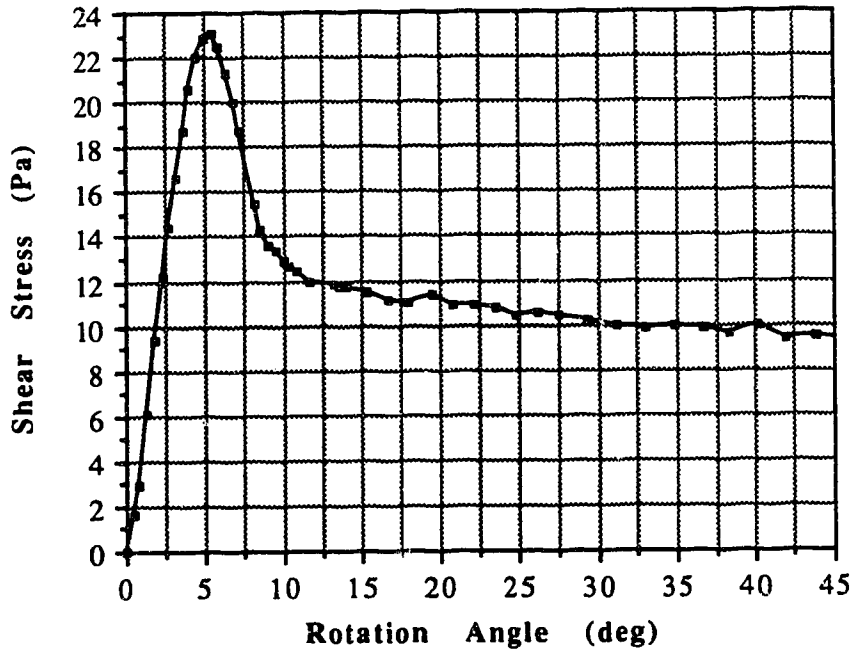

Figure C.69 Vane Shear Test S23005DP

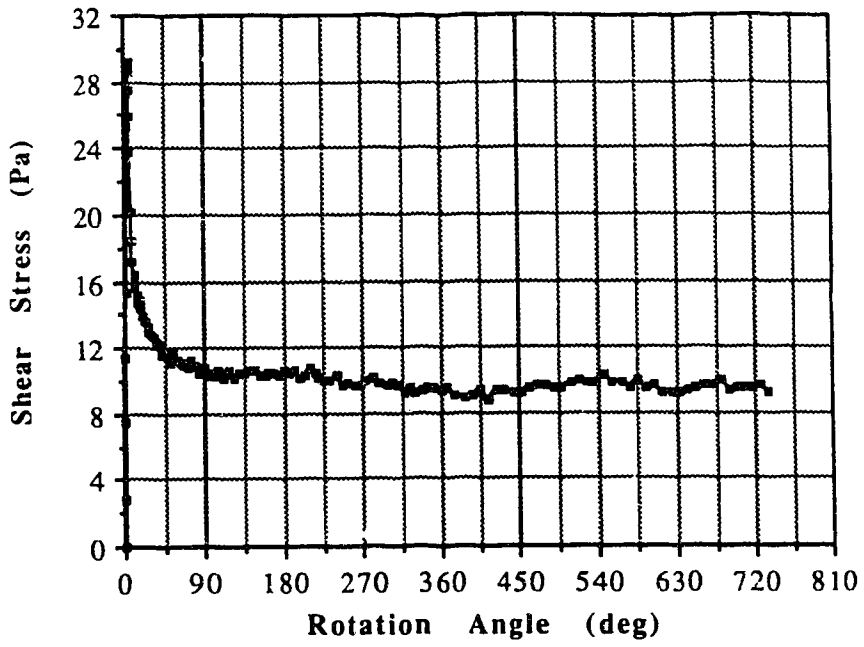

Figure C.70 Vane Shear Test S23010DR

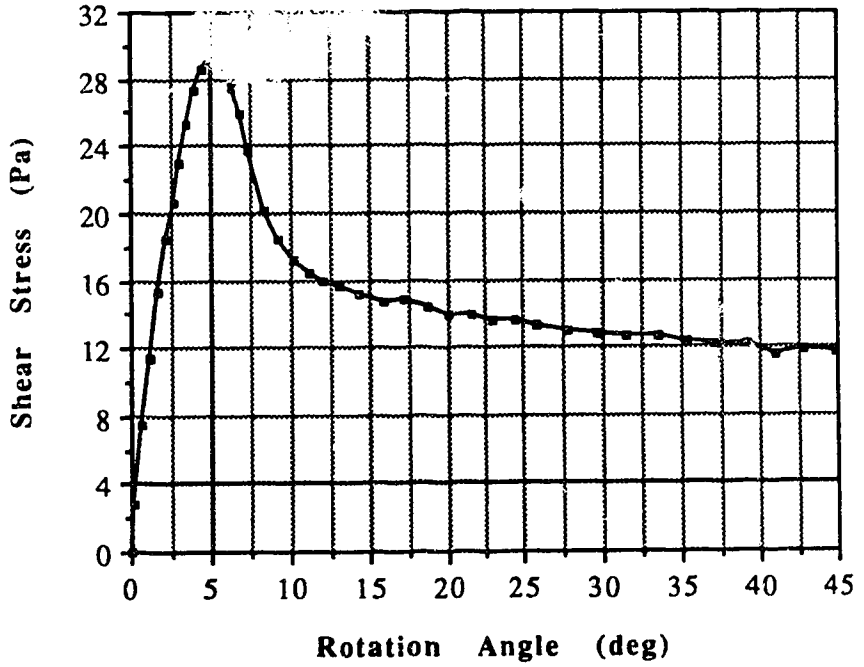

Figure C.71 Vane Shear Test S23010DP

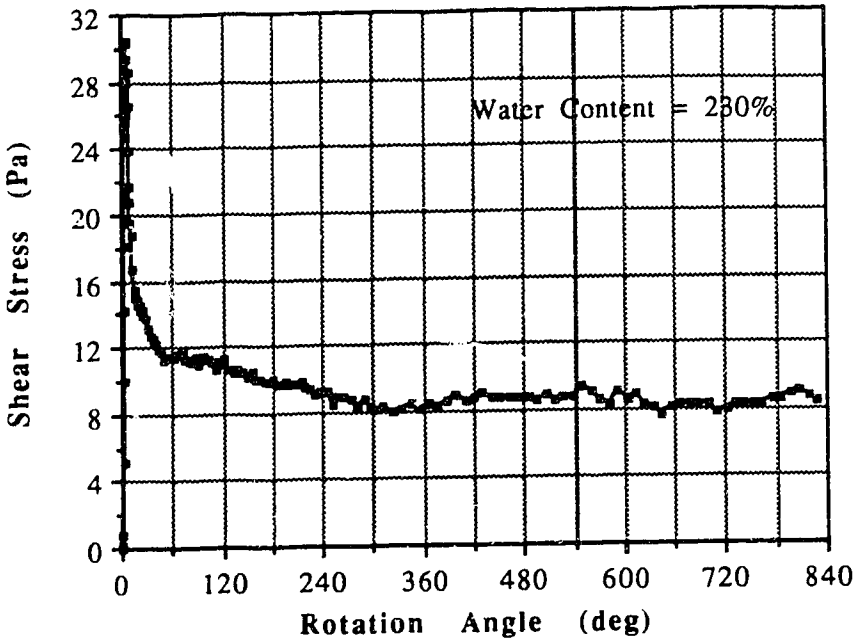

Figure C.72 Vane Shear Test S23020DR

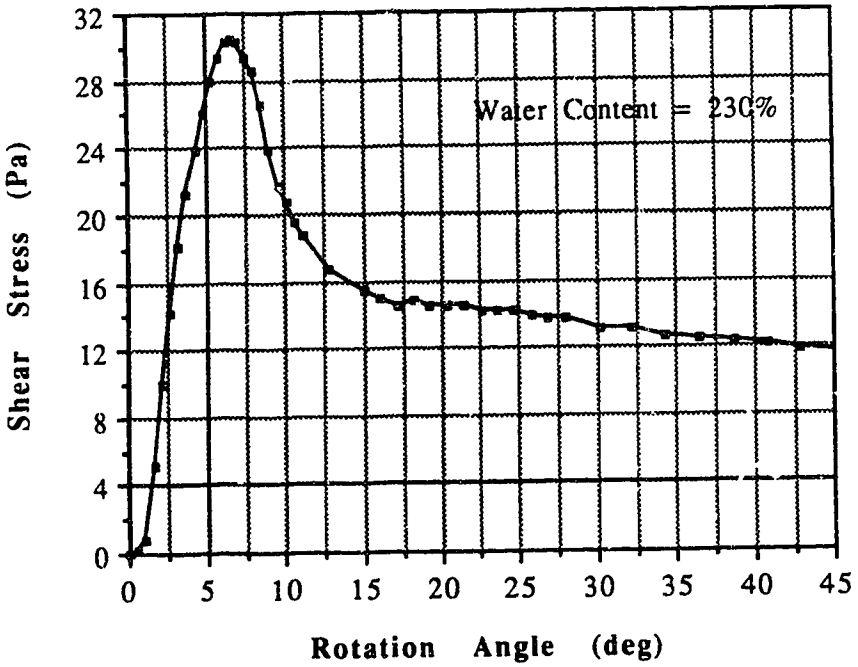

Figure C.73 Vane Shear Test S23020DP

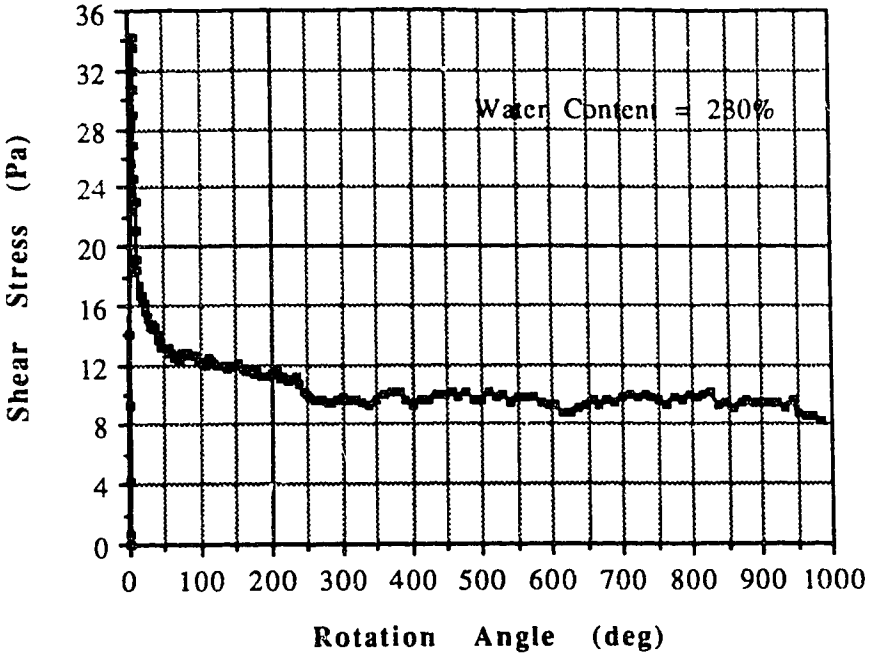

Figure C.74 Vane Shear Test S23030DR

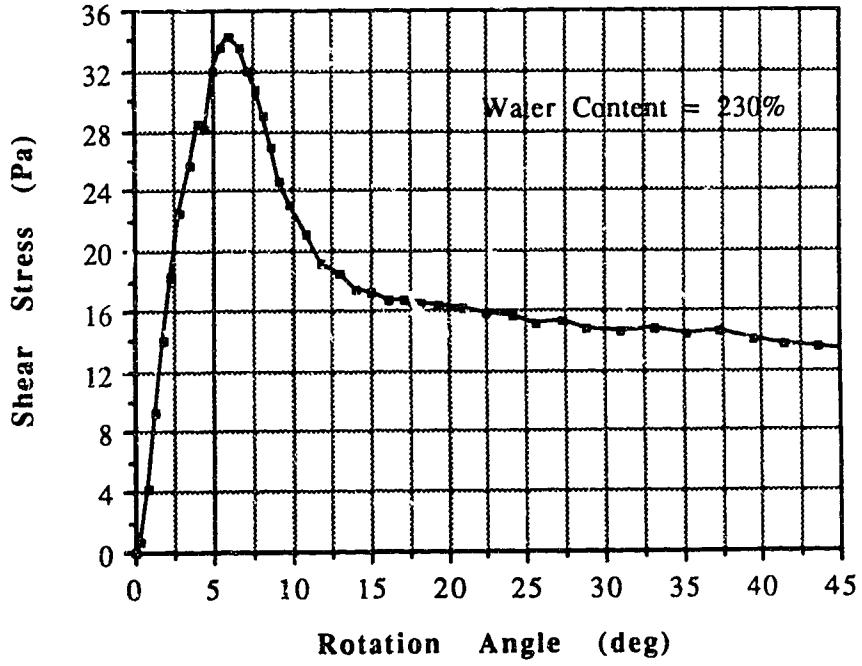

Figure C.75 Vane Shear Test S23030DP

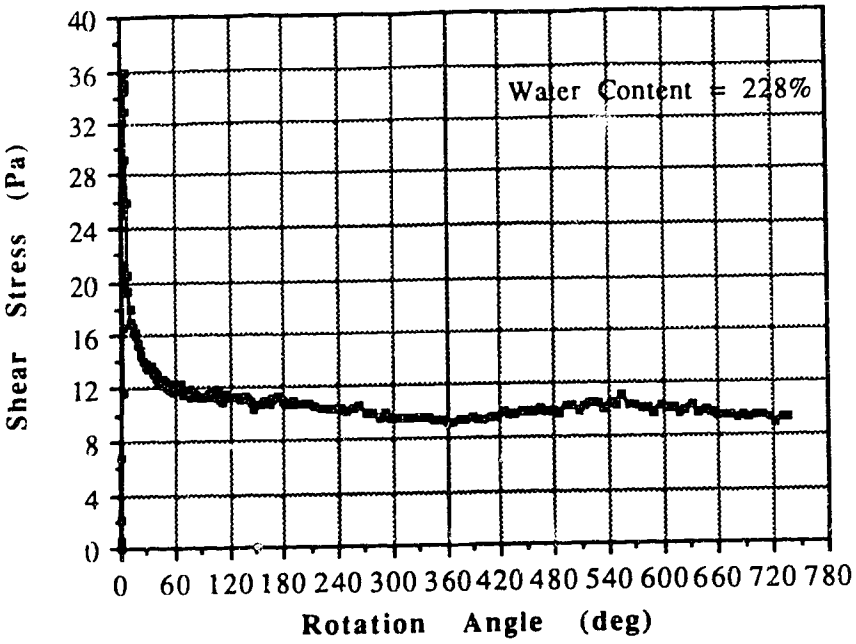

Figure C.76 Vane Shear Test S23041DR

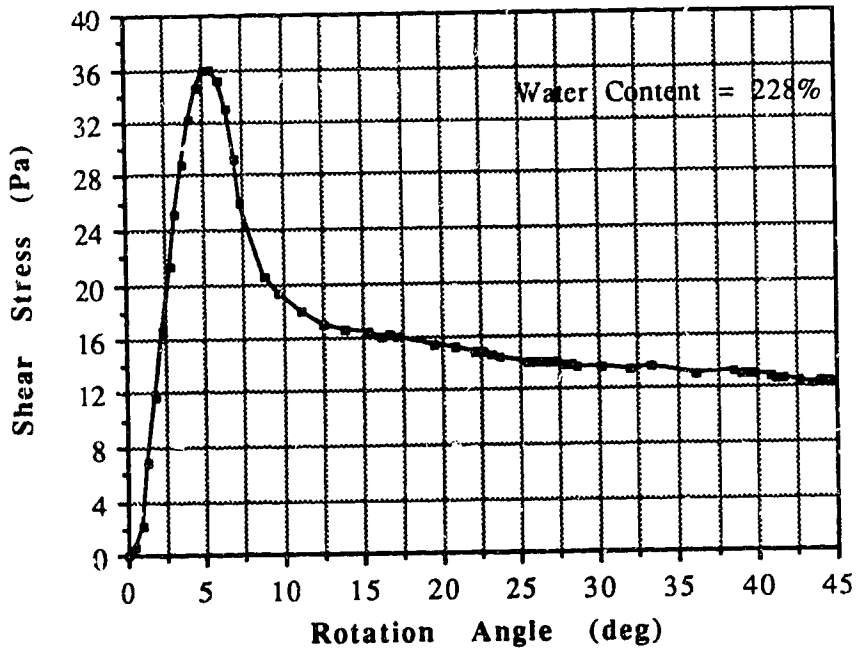

Figure C.77 Vane Shear Test S23041DP

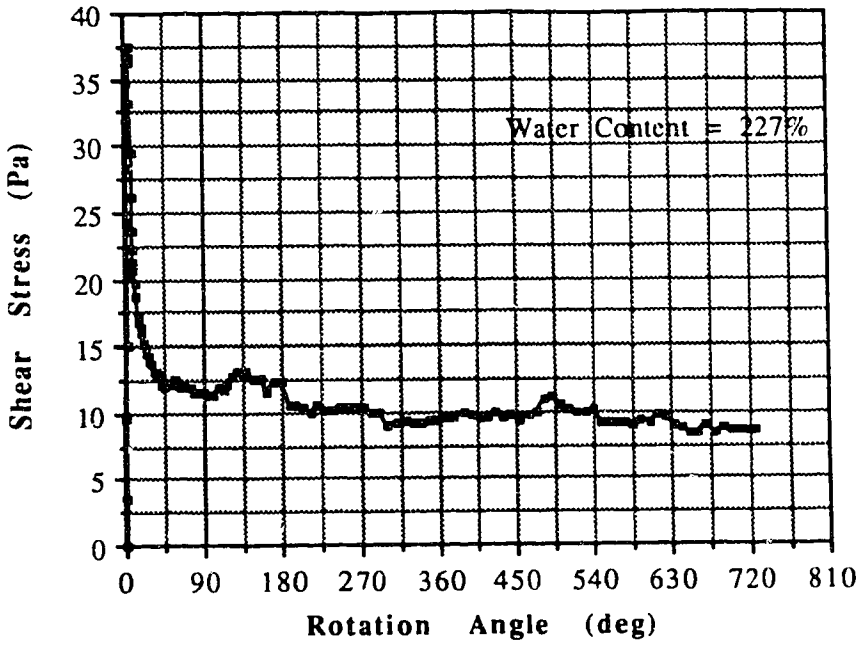

Figure C.78 Vane Shear Test S23050DR

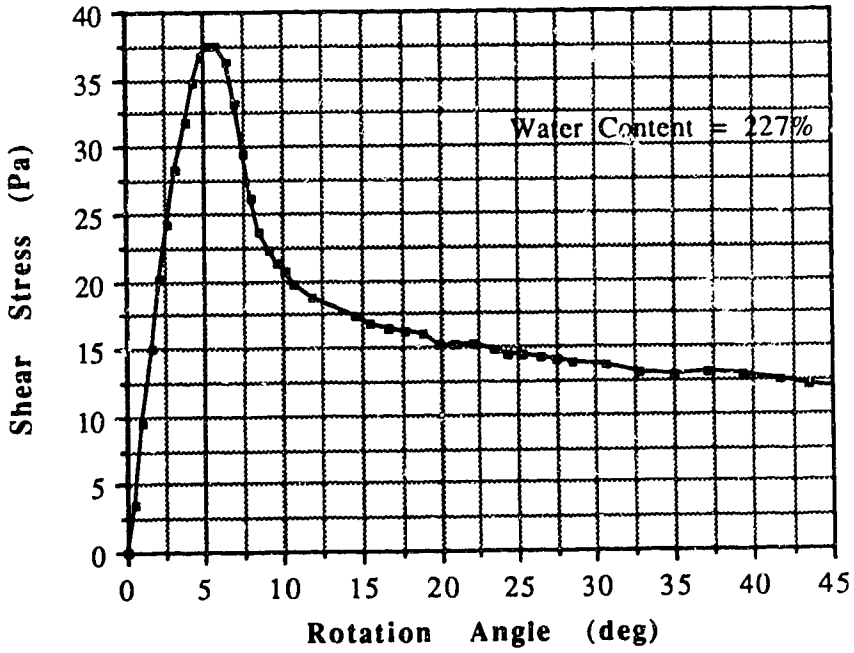

Figure C.79 Vane Shear Test S23050DP

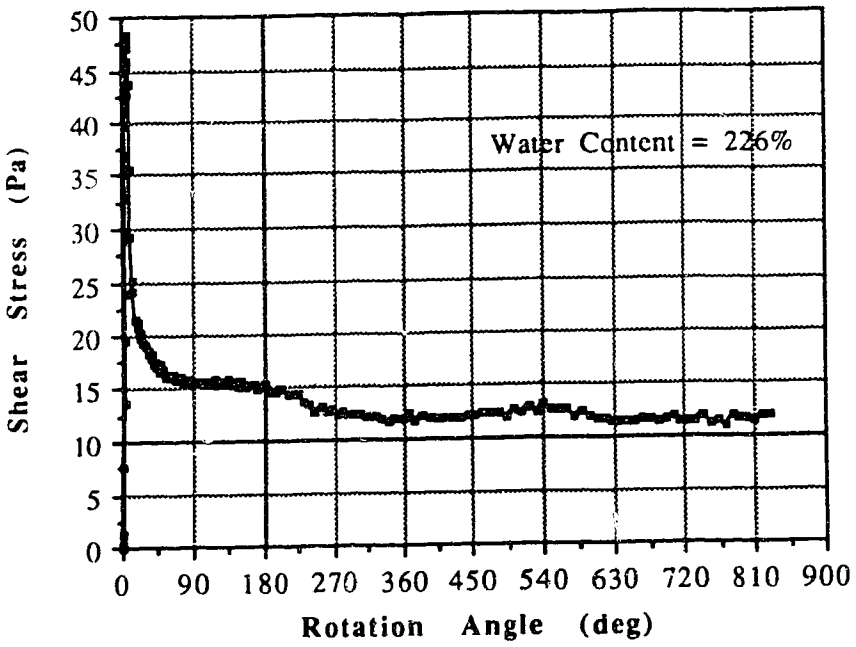

Figure C.80 Vane Shear Test S23072DR

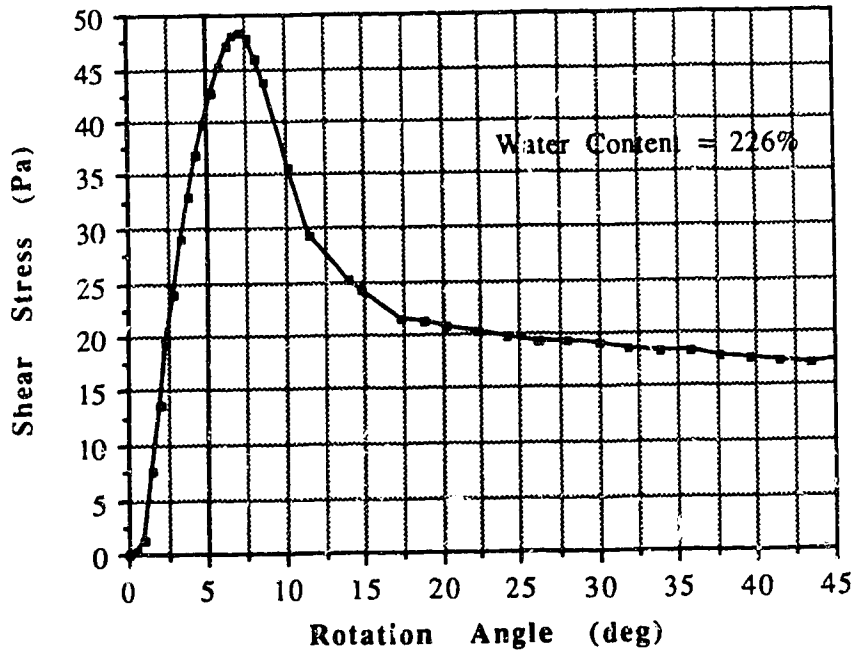

Figure C.81 Vane Shear Test S23072DP

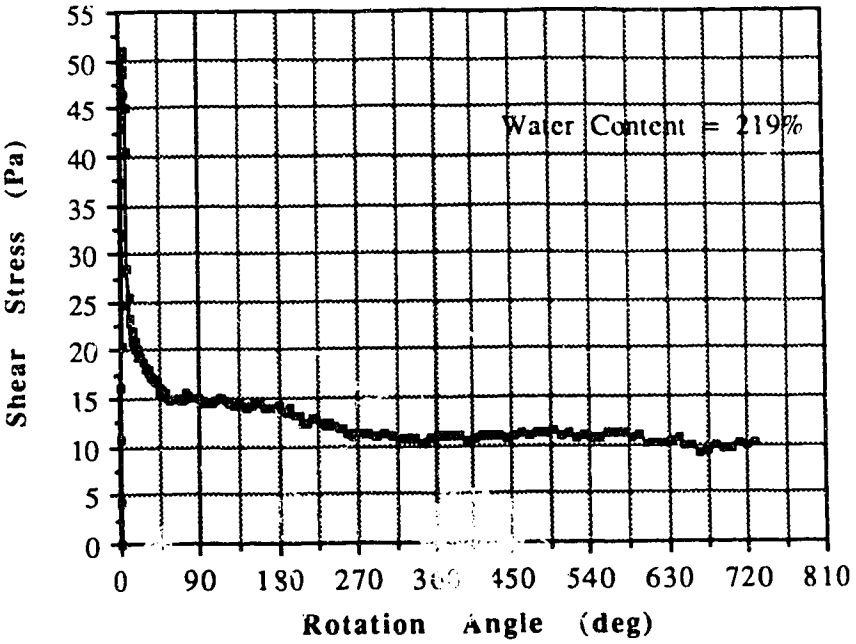

Figure C.82 Vane Shear Test S23090DR

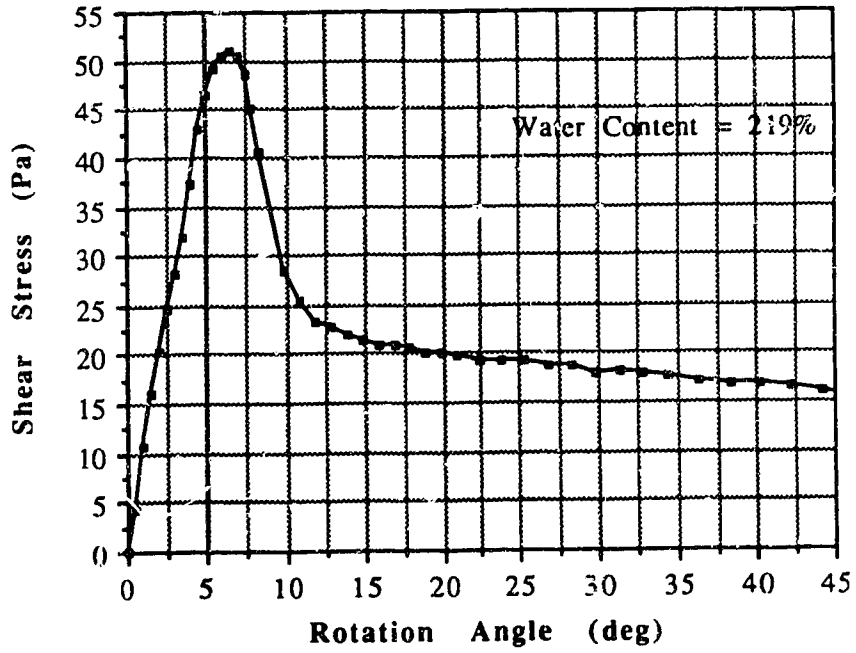

Figure C.83 Vane Shear Test S23090DP

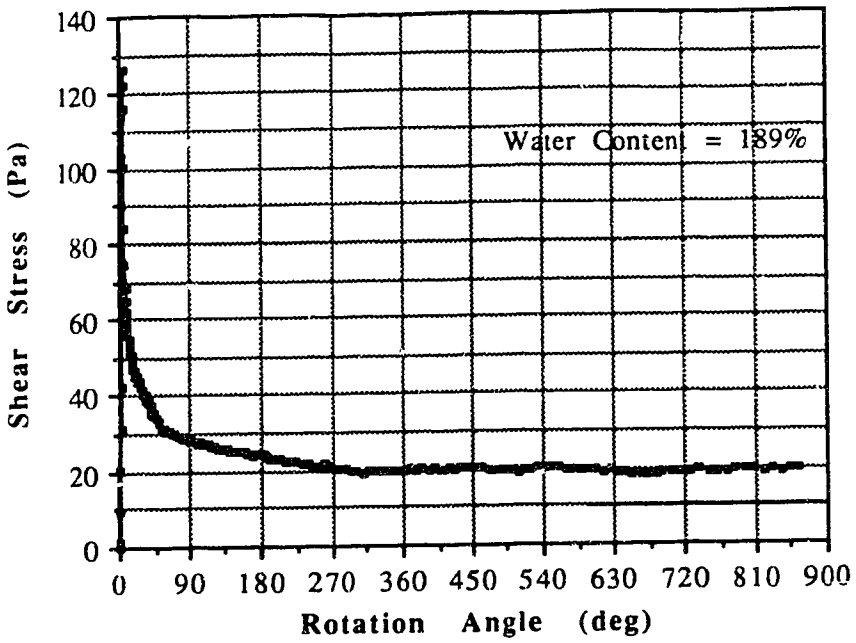

Figure C.84 Vane Shear Test S23490DR

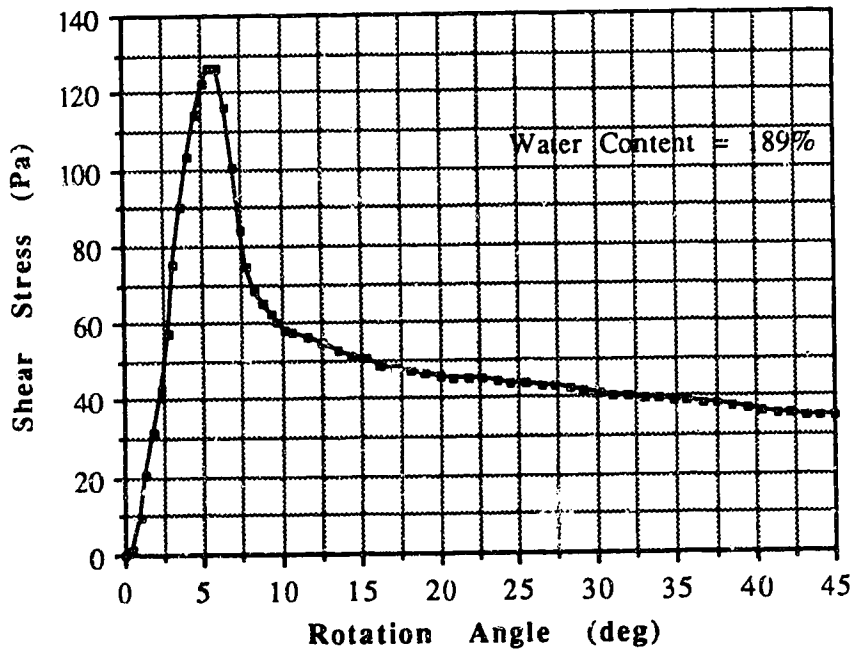

Figure C.85 Vane Shear Test S23490DP

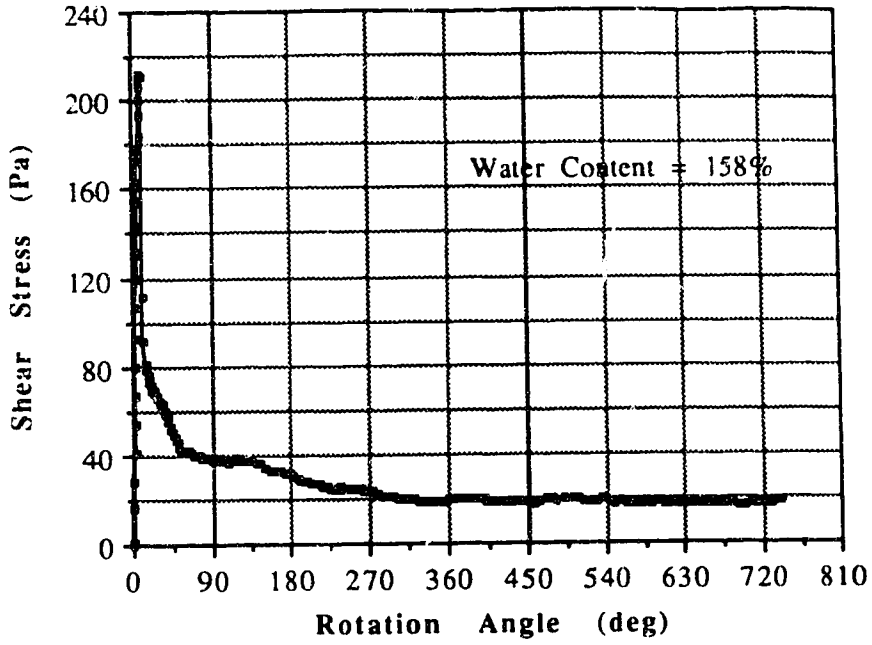

Figure C.86 Vane Shear Test S23680DR

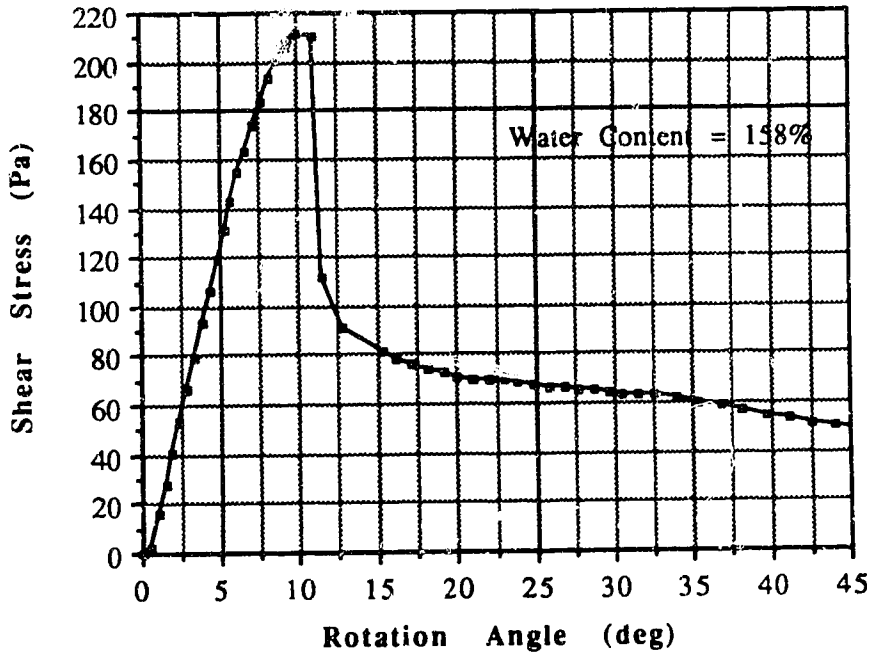

Figure C.87 Vane Shear Test S23680DP

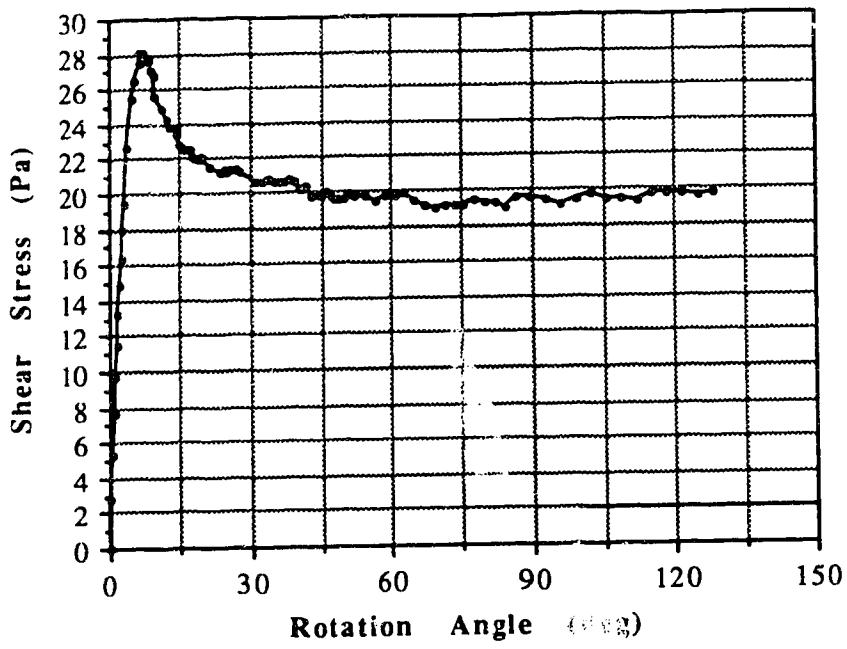

Figure C.88 Vane Shear Test S15000M

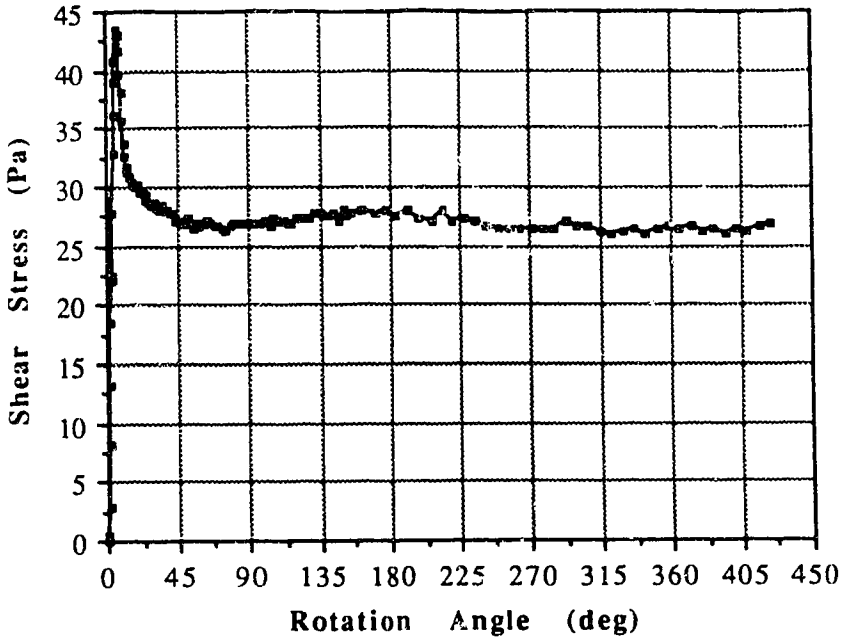

Figure C.89 Vane Shear Test S15002HR

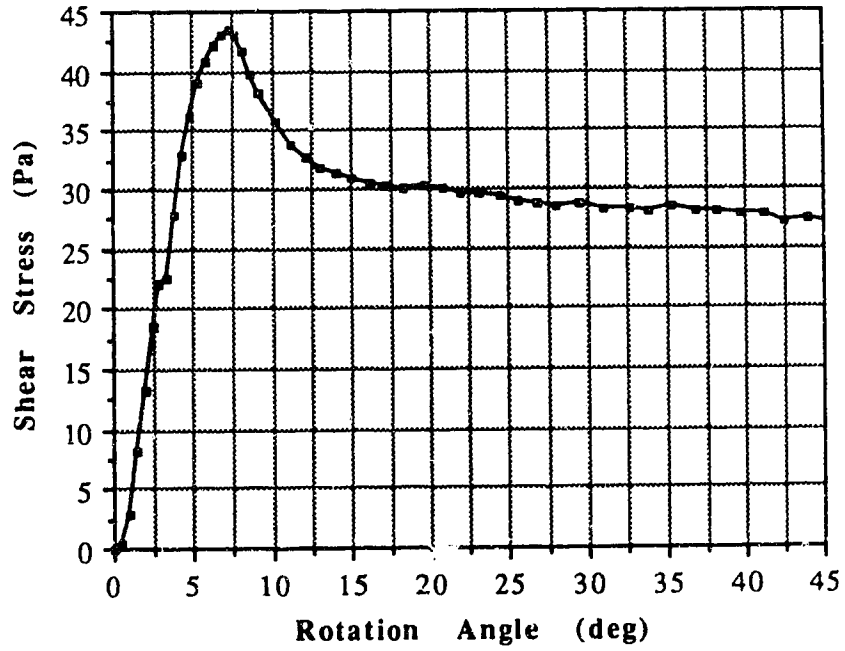

Figure C.90 Vane Shear Test S15002HP

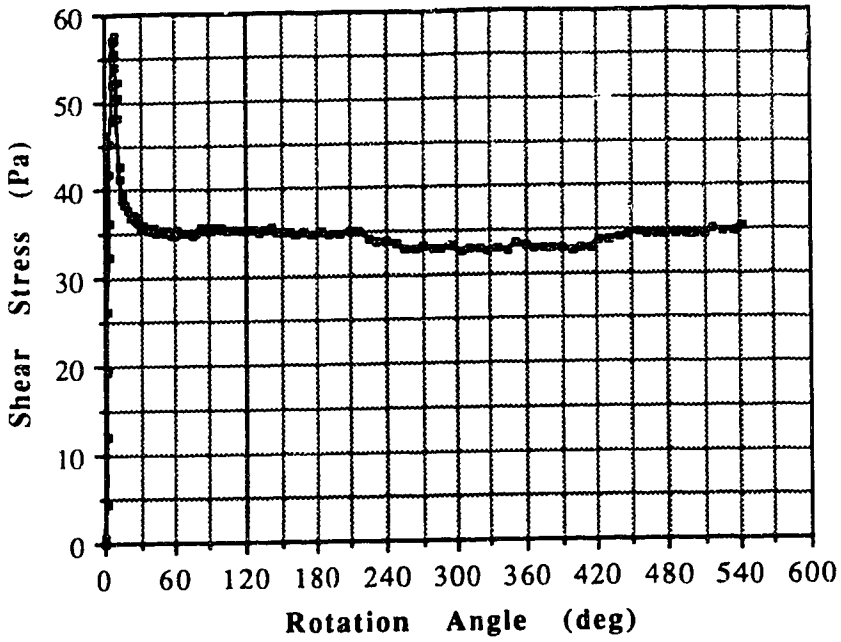

Figure C.91 Vane Shear Test S15008HR

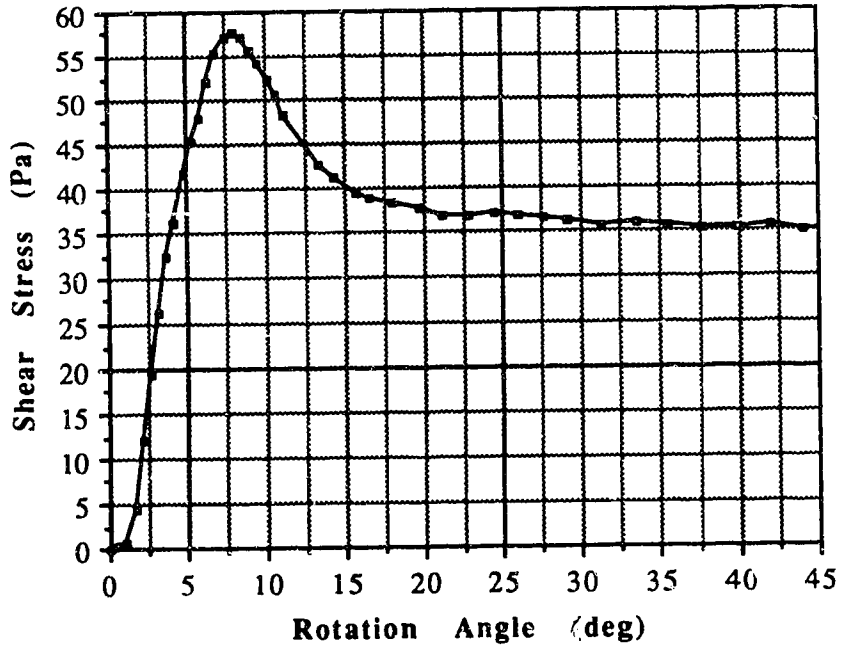

Figure C.92 Vane Shear Test S15008HP

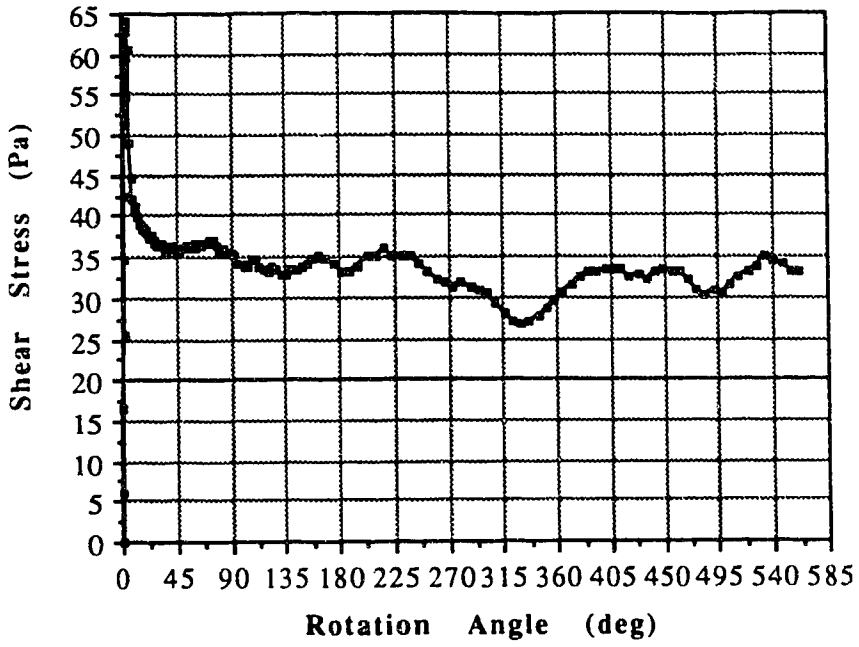

Figure C.93 Vane Shear Test S15020HR

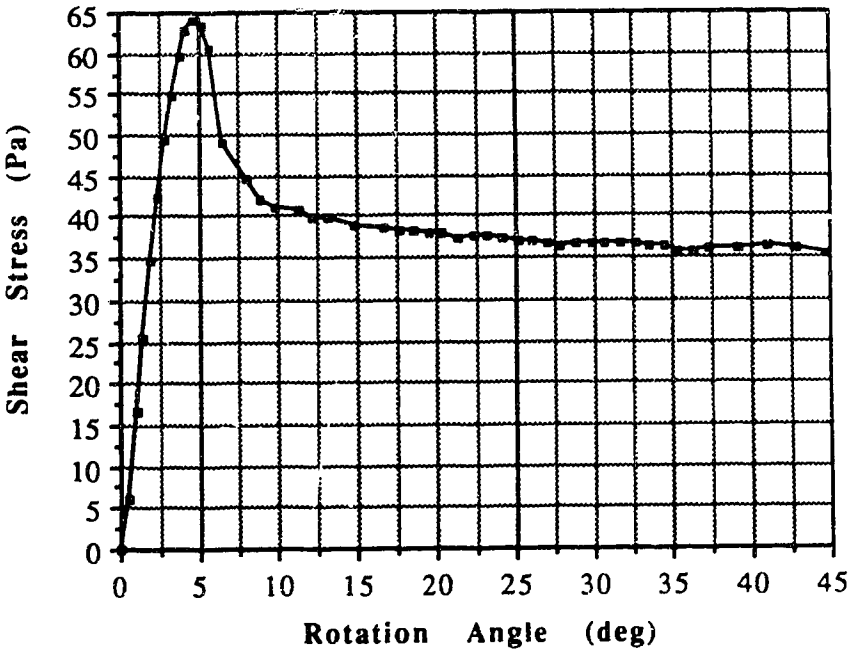

Figure C.94 Vane Shear Test S15020HP

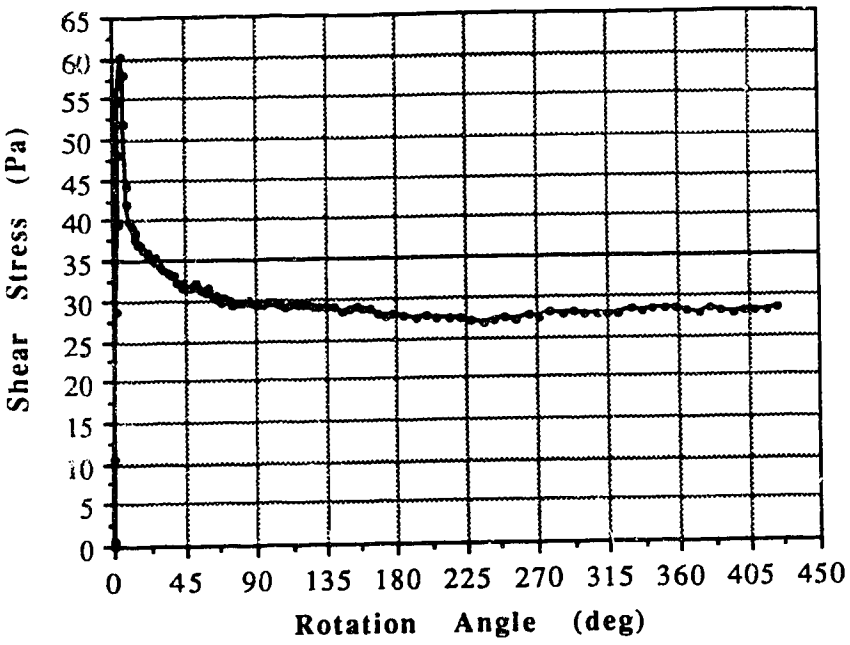

Figure C.95 Vane Shear Test S15001DR

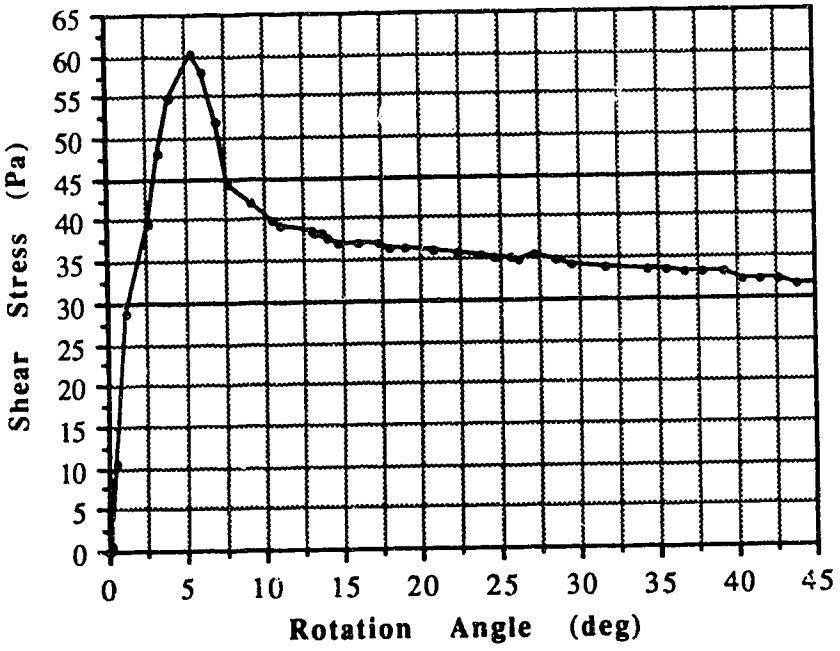

Figure C.96 Vane Shear Test S15001DP

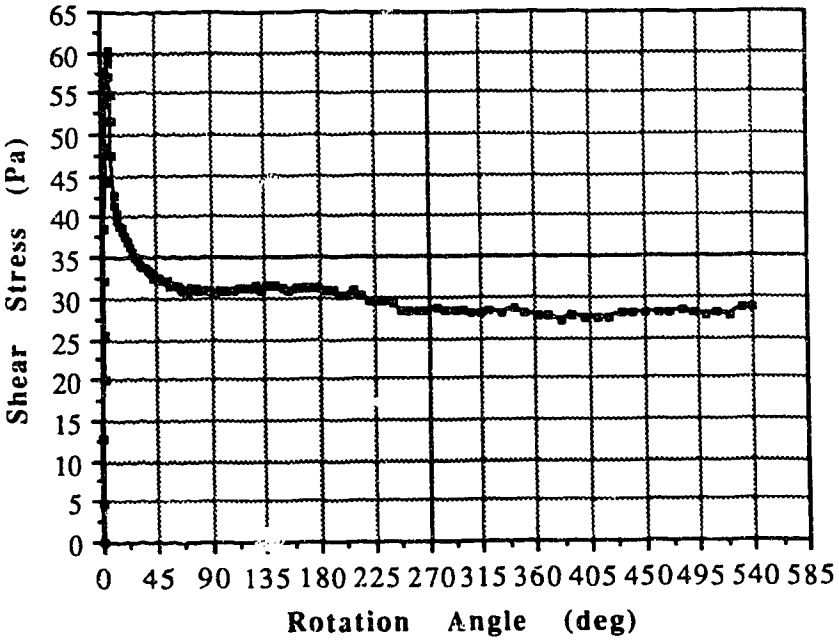

Figure C.97 Vane Shear Test S15002DR

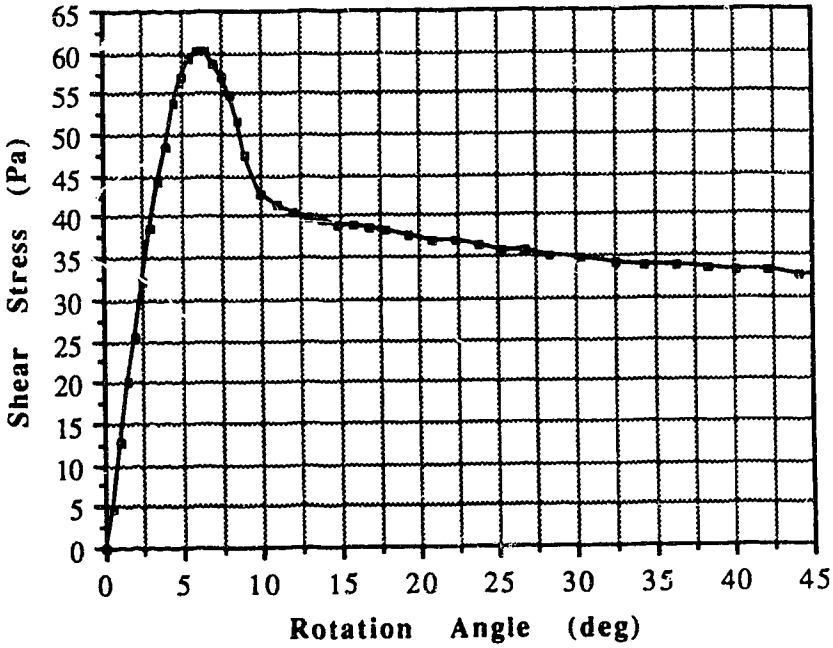

Figure C.98 Vane Shear Test S15002DP

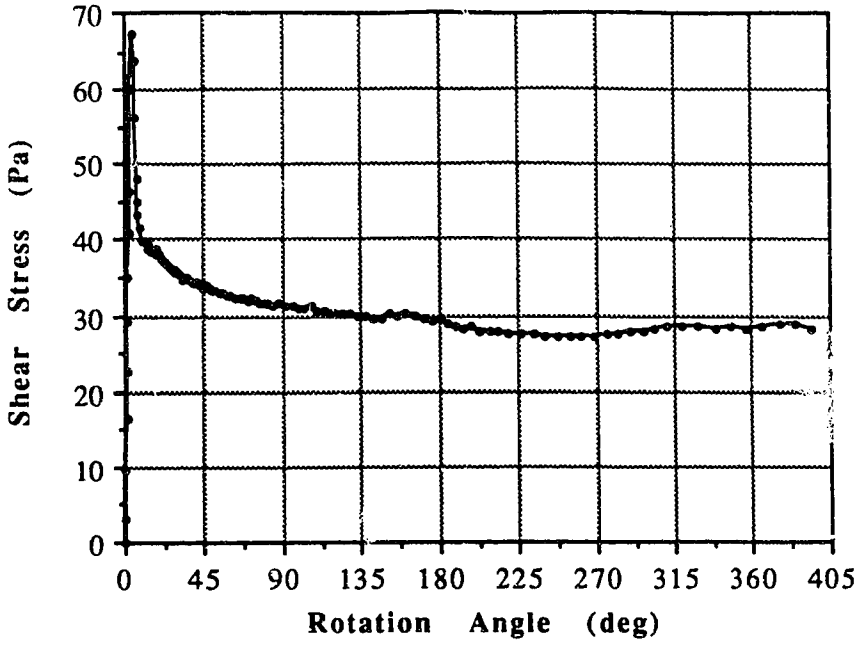

Figure C.99 Vane Shear Test S15003DR

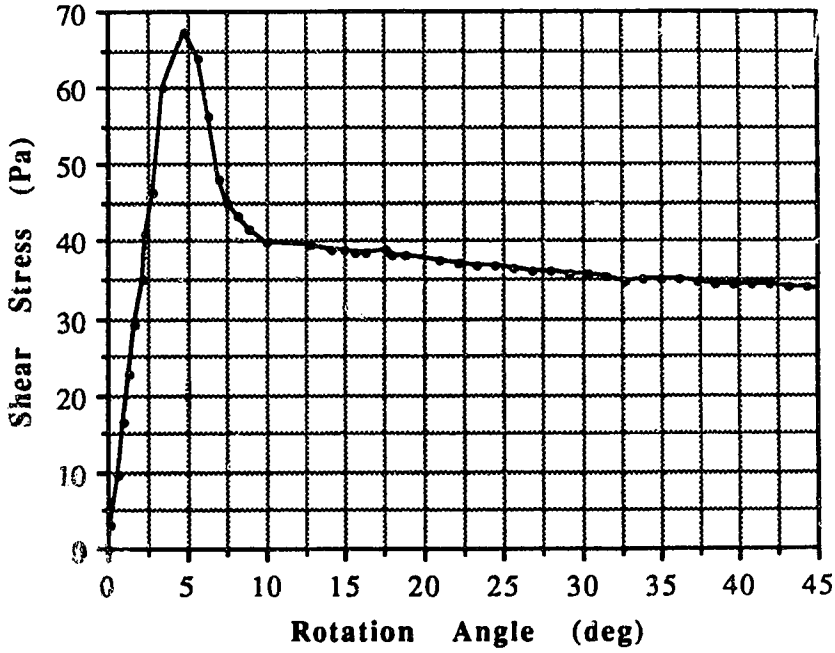

Figure C.100 Vane Shear Test S15003DP

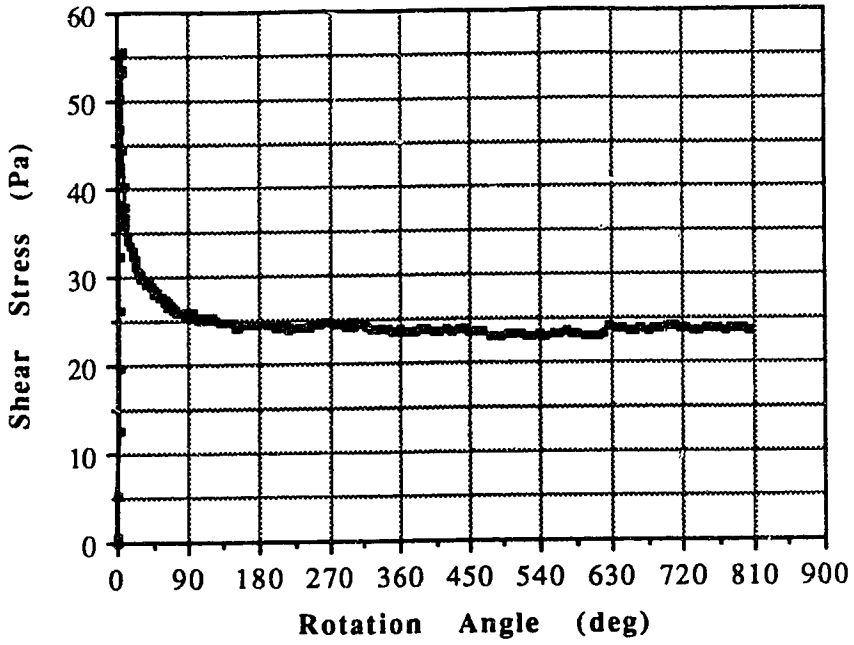

Figure C.101 Vane Shear Test S15005DR

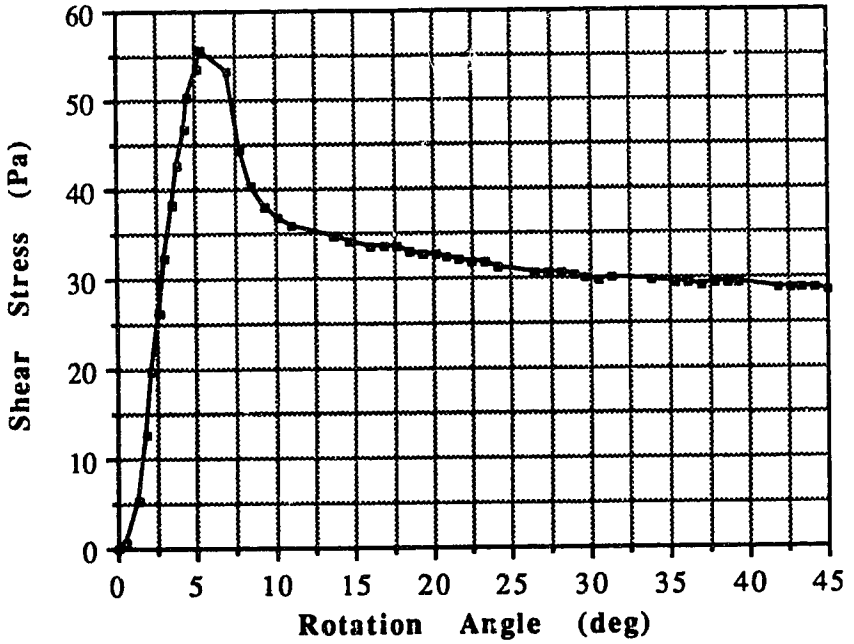

Figure C.102 Vane Shear Test S15005DP

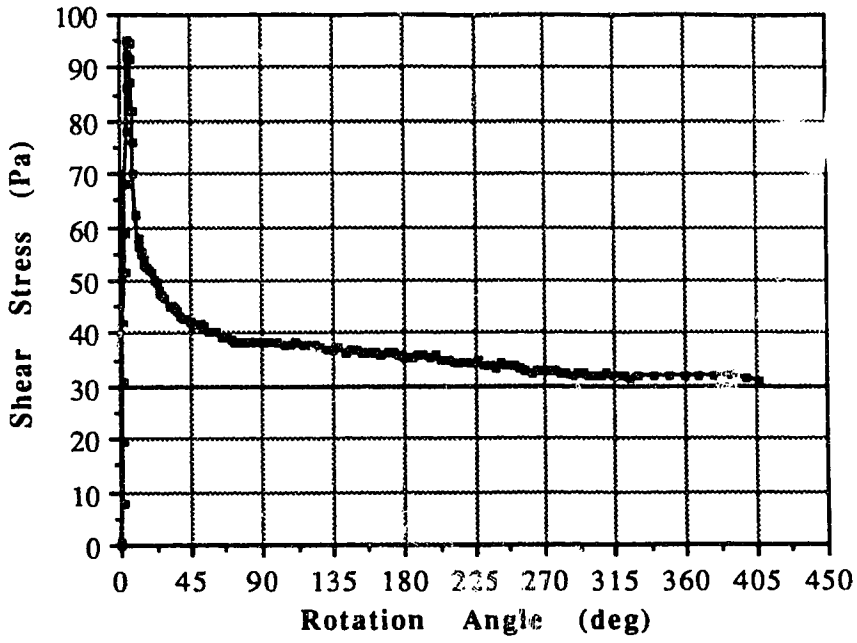

Figure C.103 Vane Shear Test S15010DR

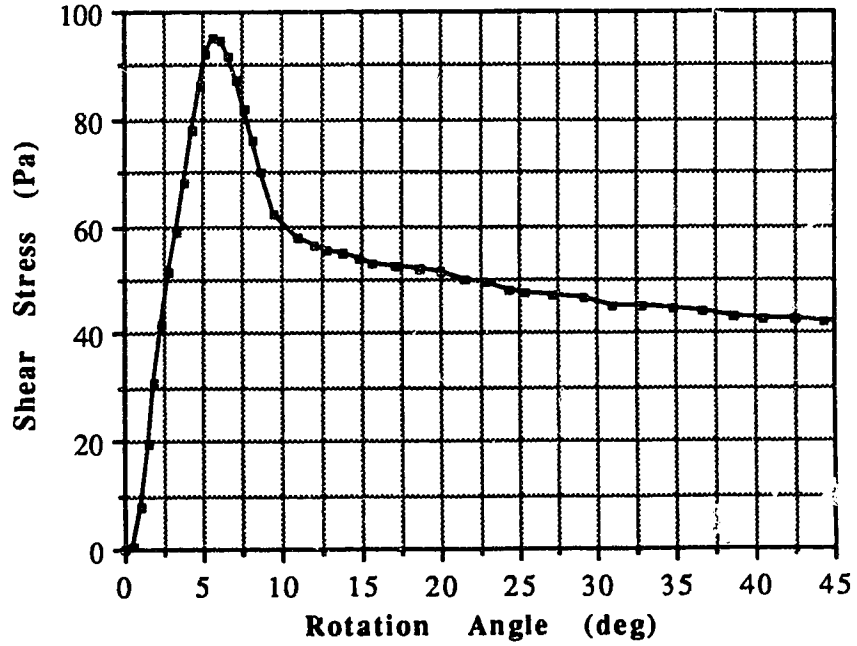

Figure C.104 Vane Shear Test S15010DP

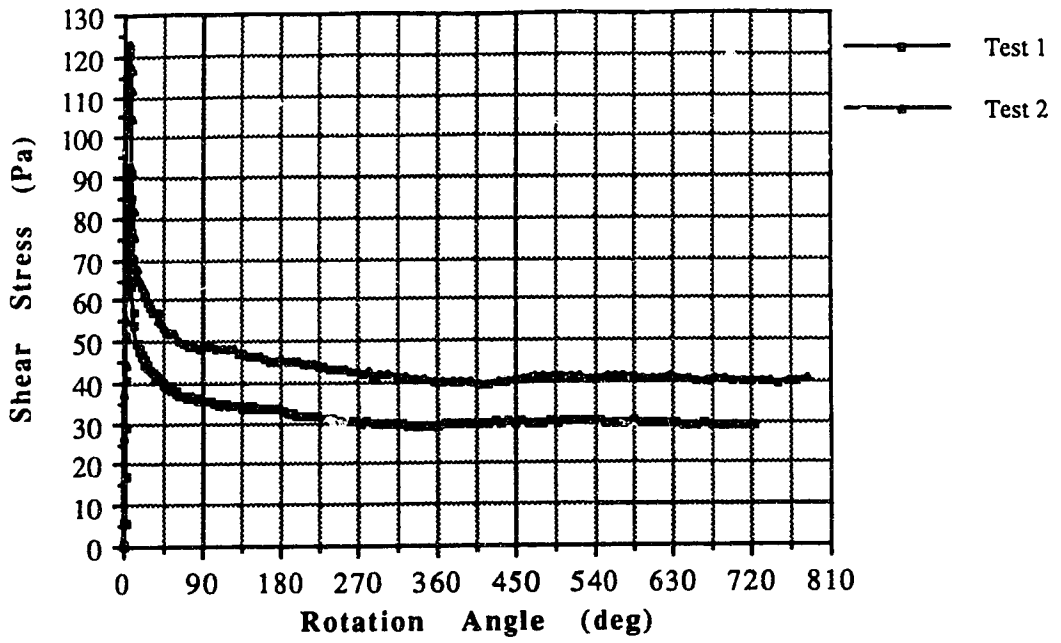

Figure C.105 Vane Shear Test S15020DR

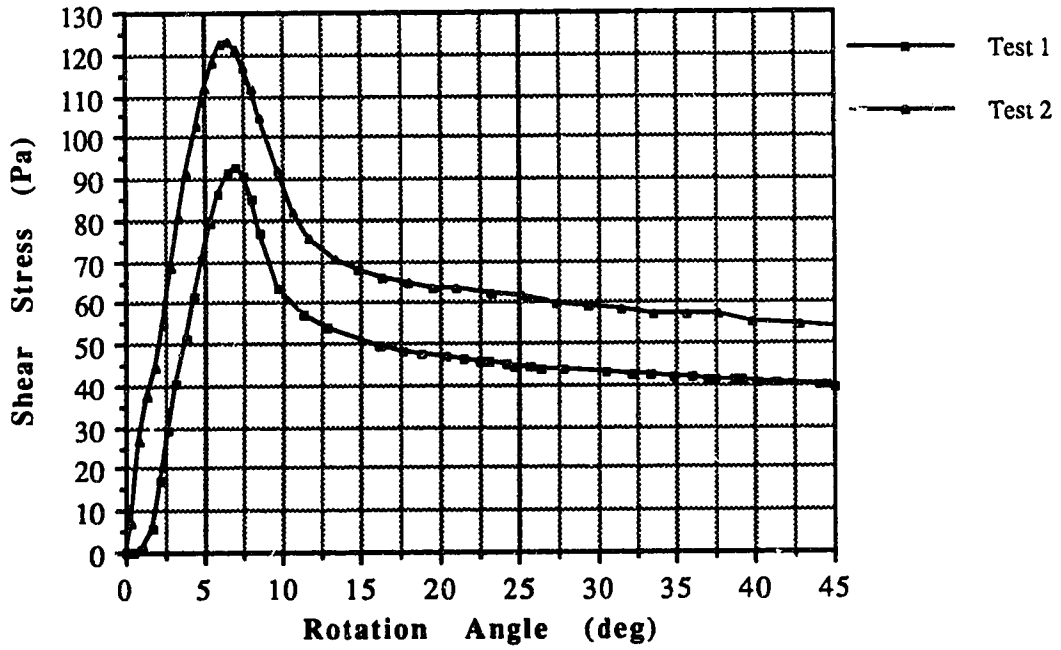

Figure C.106 Vane Shear Test S15020DP

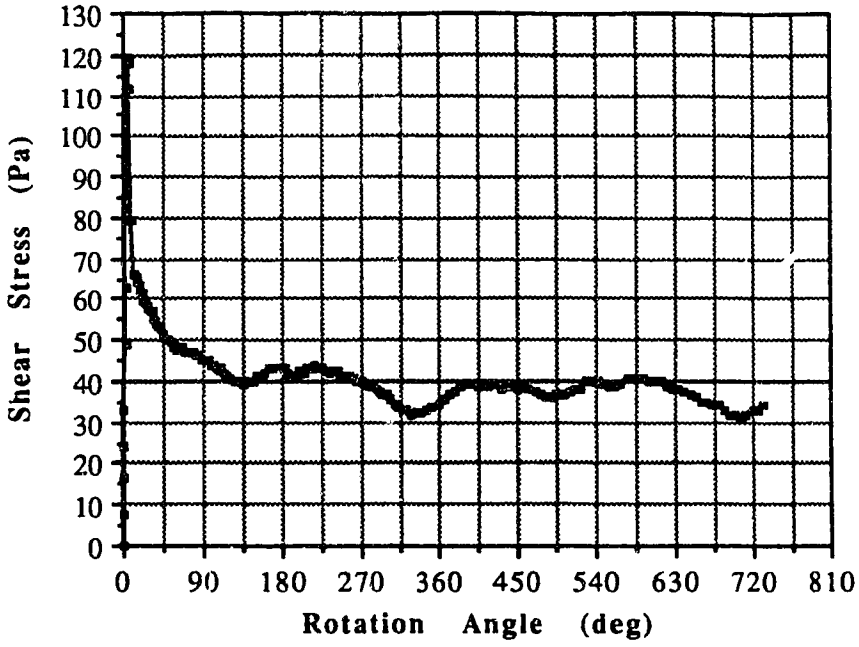

Figure C.107 Vane Shear Test S15040DR

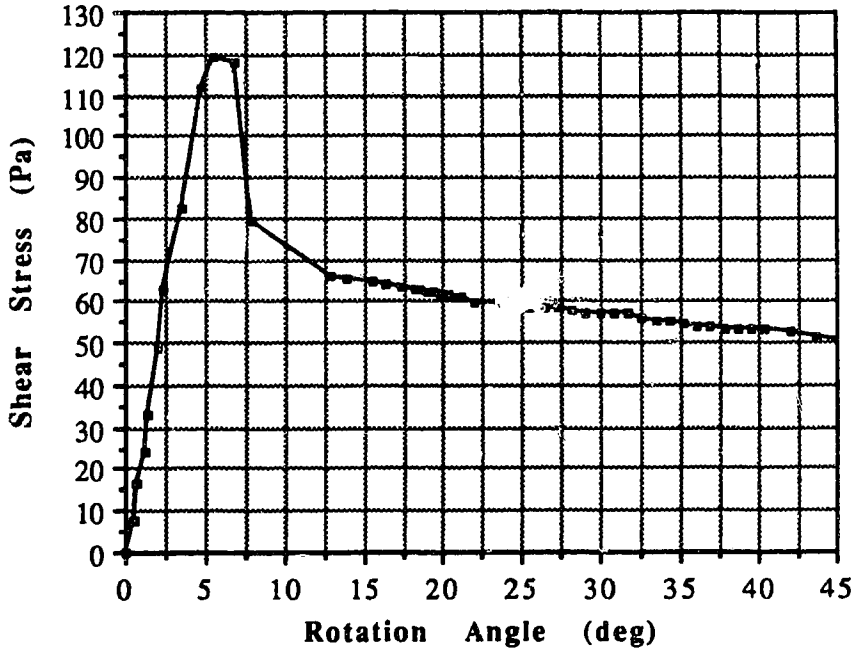

Figure C.108 Vane Shear Test S15040DP

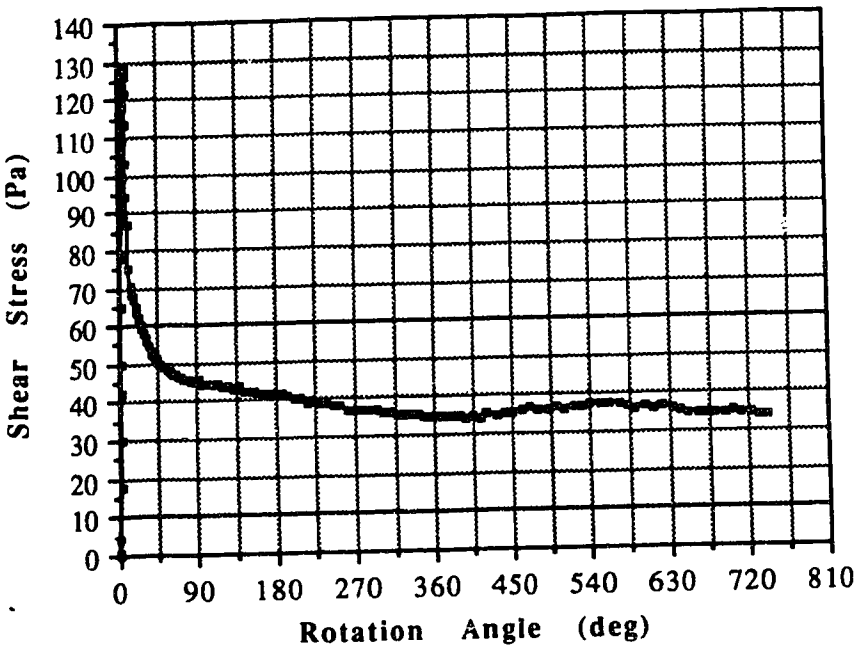

Figure C.109 Vane Shear Test S15045DR

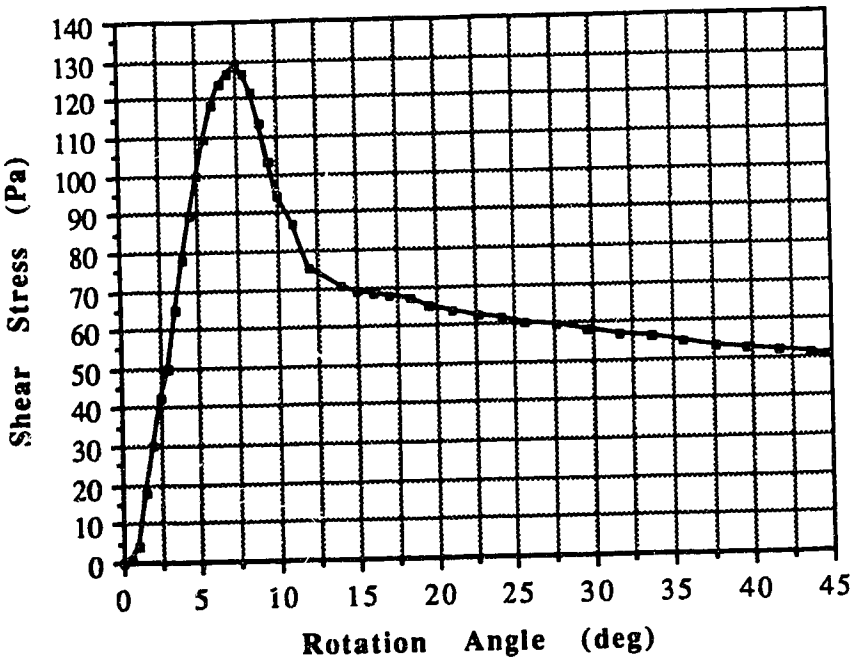

Figure C.110 Vane Shear Test S15045DP

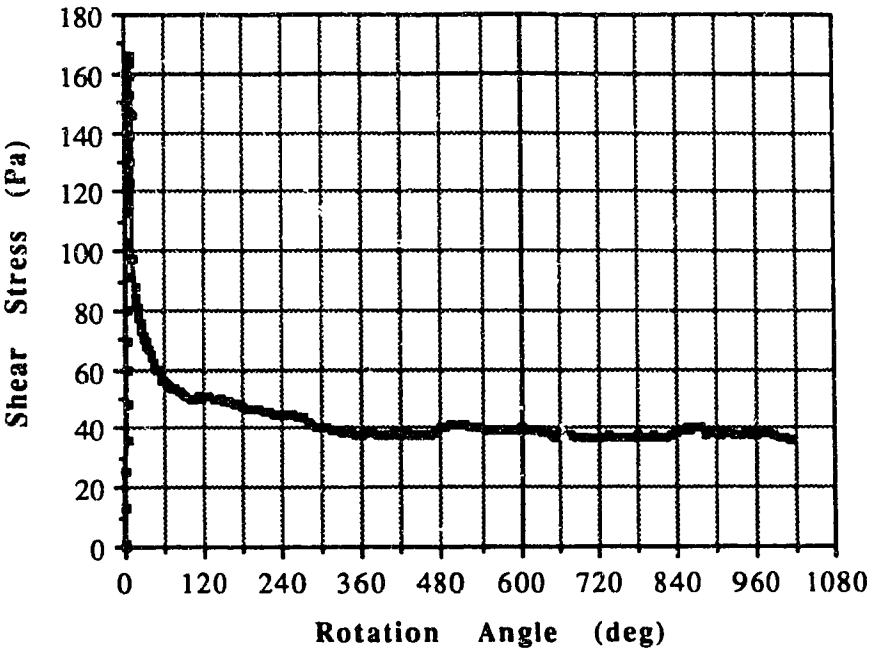

Figure C.111 Vane Shear Test S15090DR

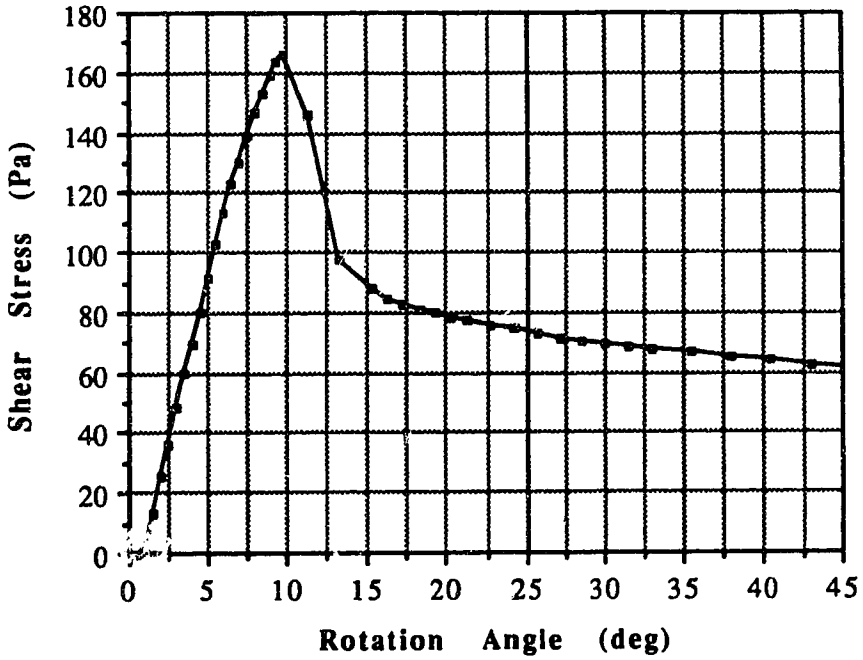

Figure C.112 Vane Shear Test S15090DP

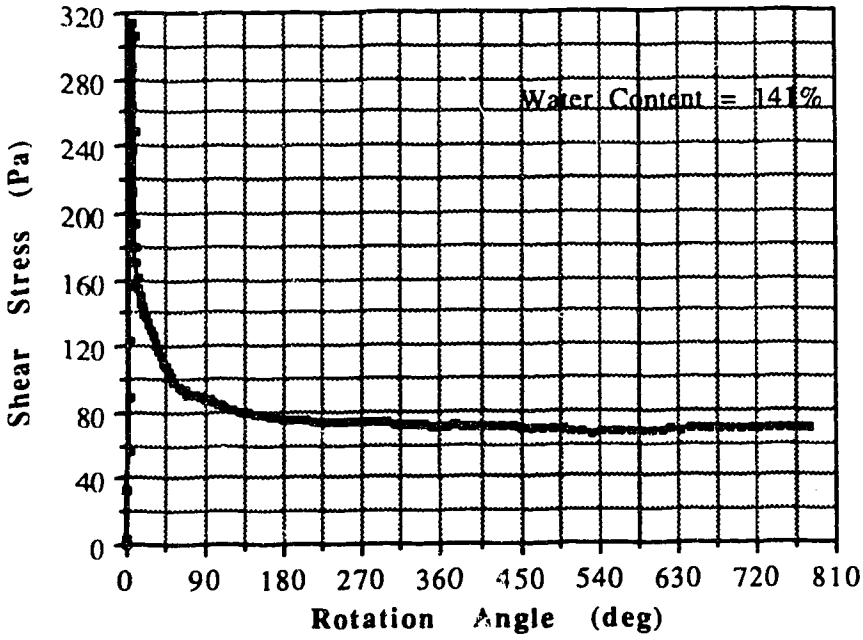

Figure C.113 Vane Shear Test S15470DR

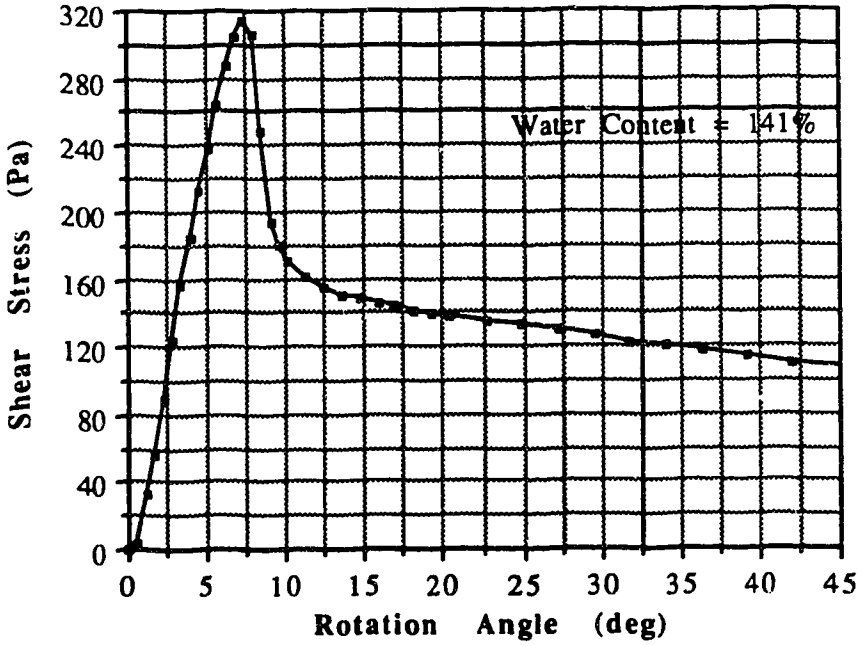

Figure C.114 Vane Shear Test S15470DP

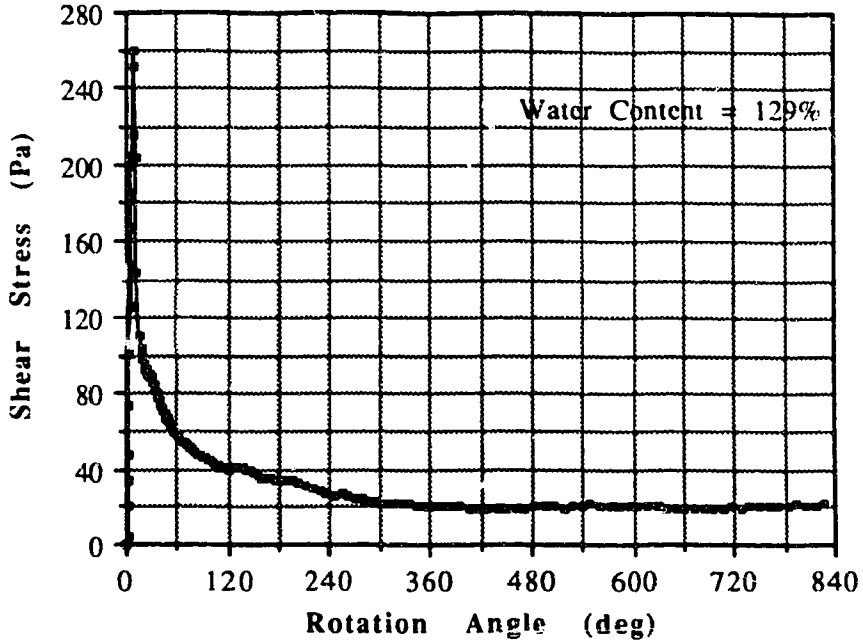

Figure C.115 Vane Shear Test S15680DR

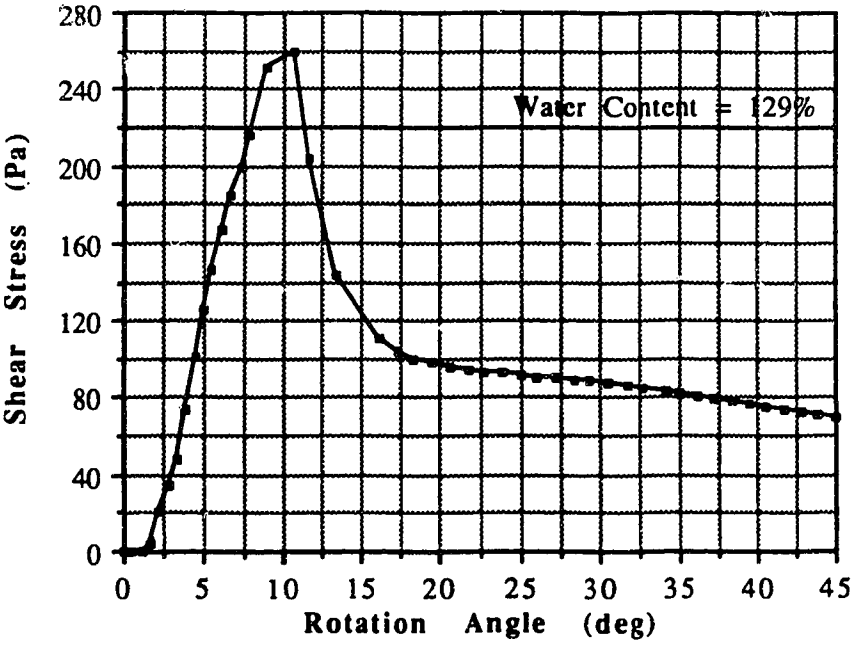

Figure C.116 Vane Shear Test S15680DP

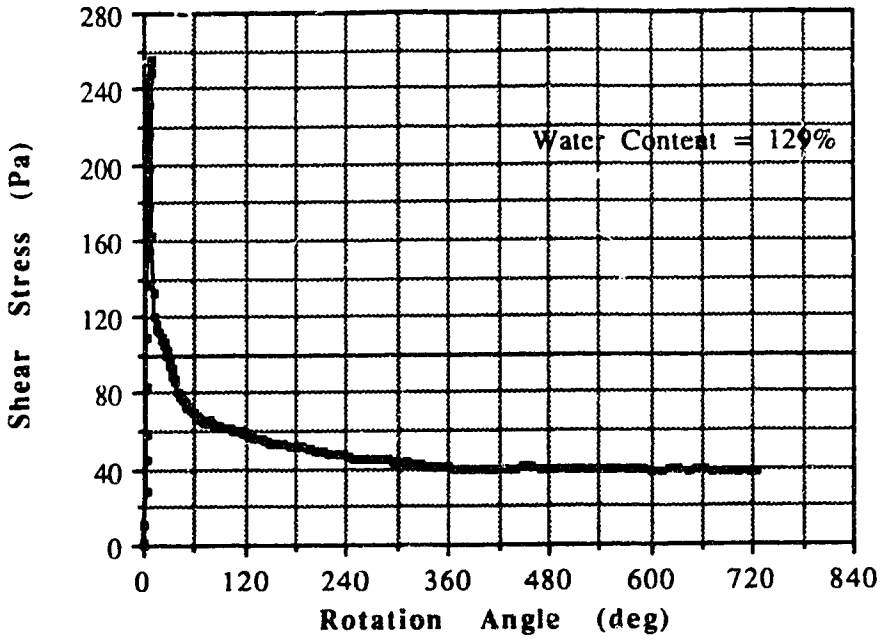

Figure C.117 Vane Shear Test S15684DR

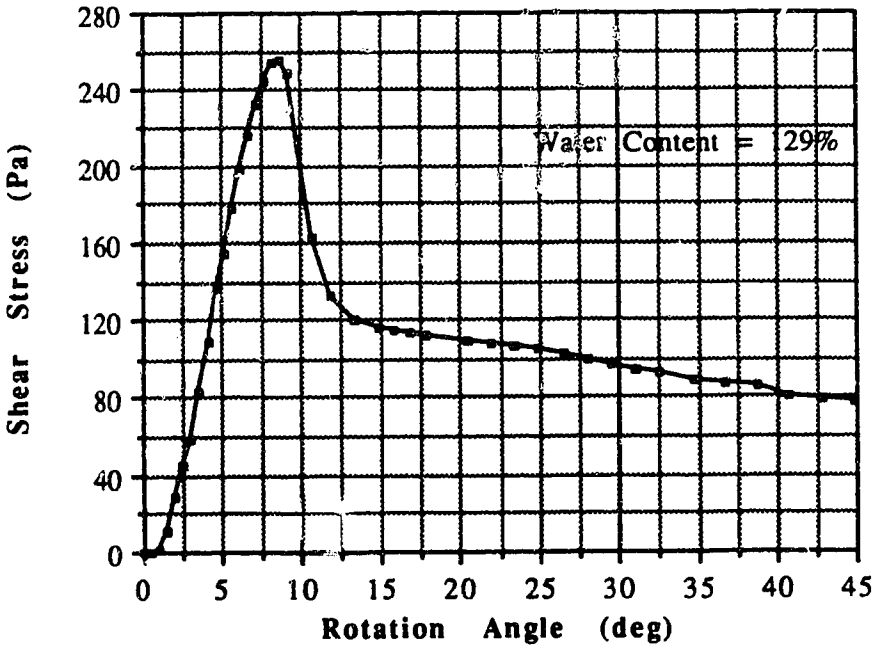

Figure C.118 Vane Shear Test S15684DP

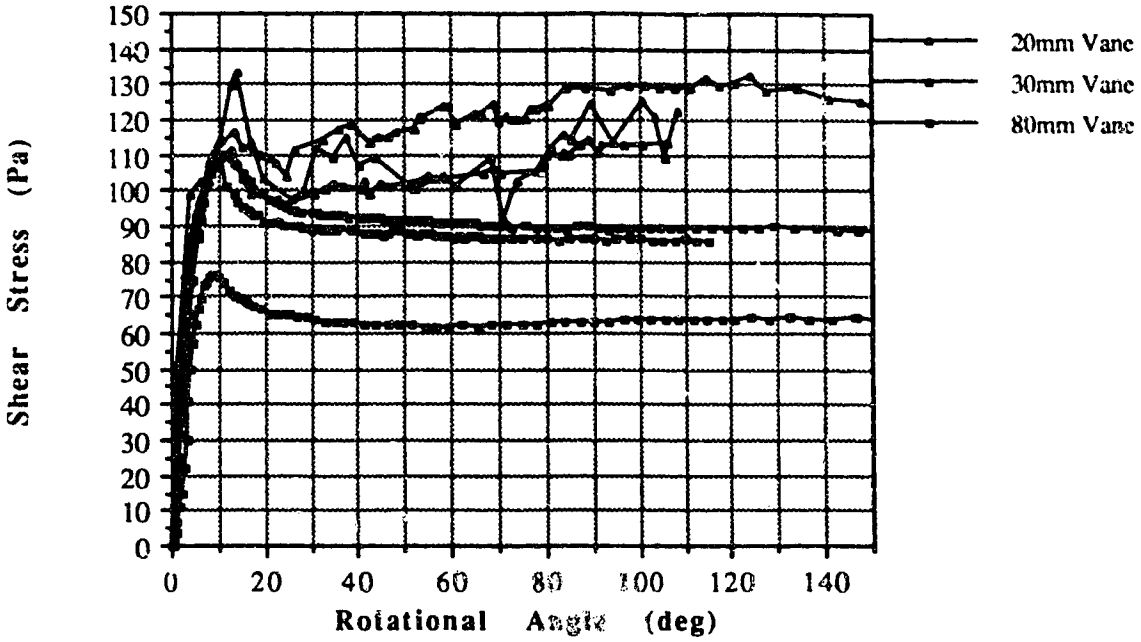

Figure C.119 Vane Shear Test S10000M

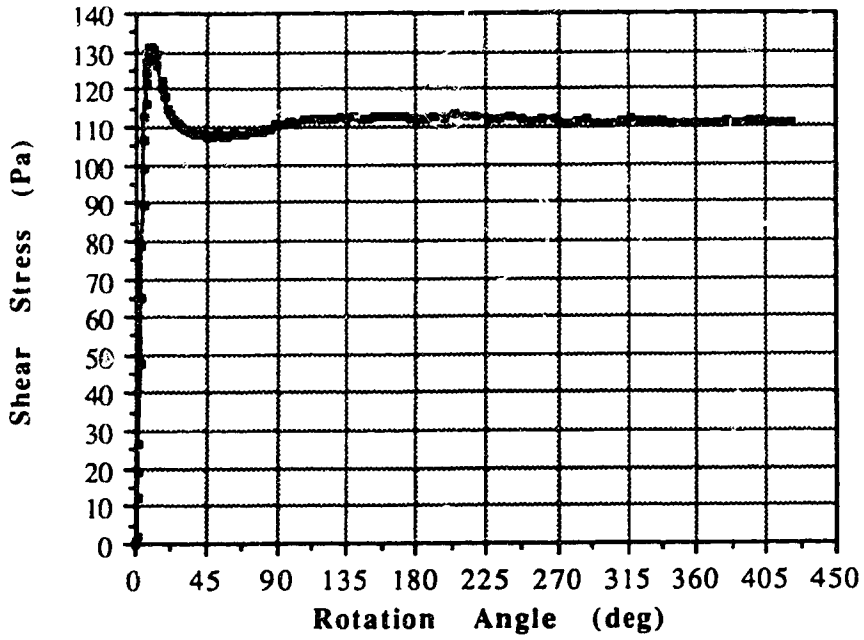

Figure C.120 Vane Shear Test S10002HR

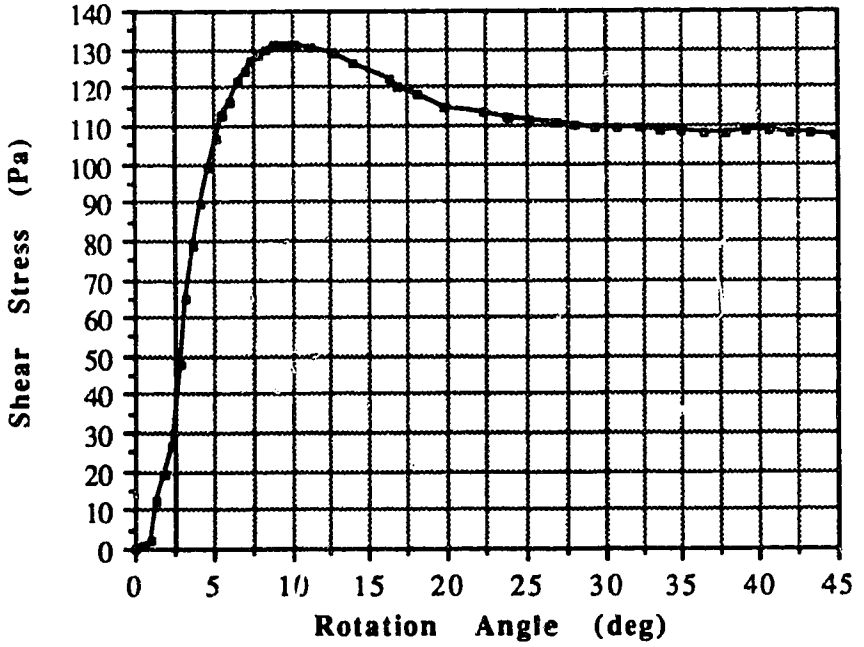

Figure C.121 Vane Shear Test S10002HP

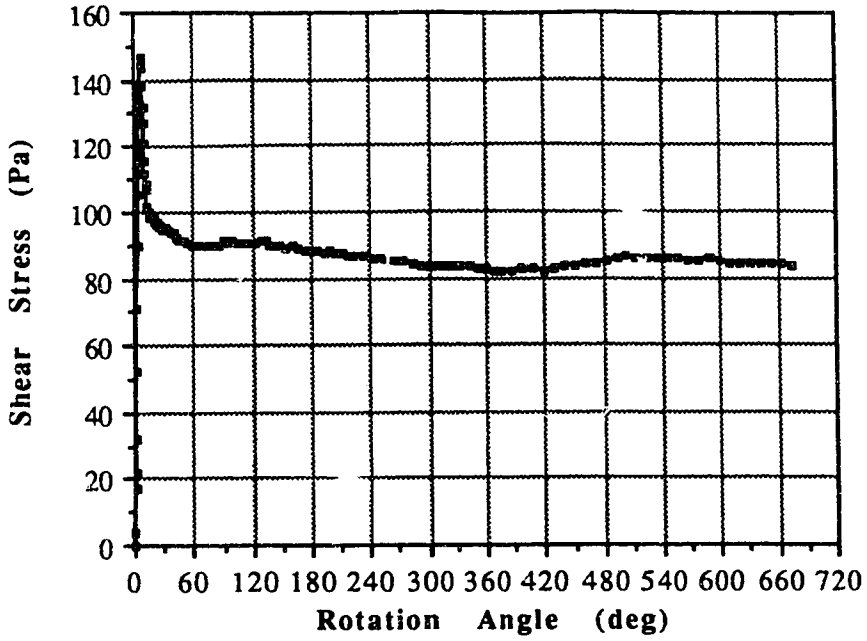

Figure C.122 Vane Shear Test S10008HR

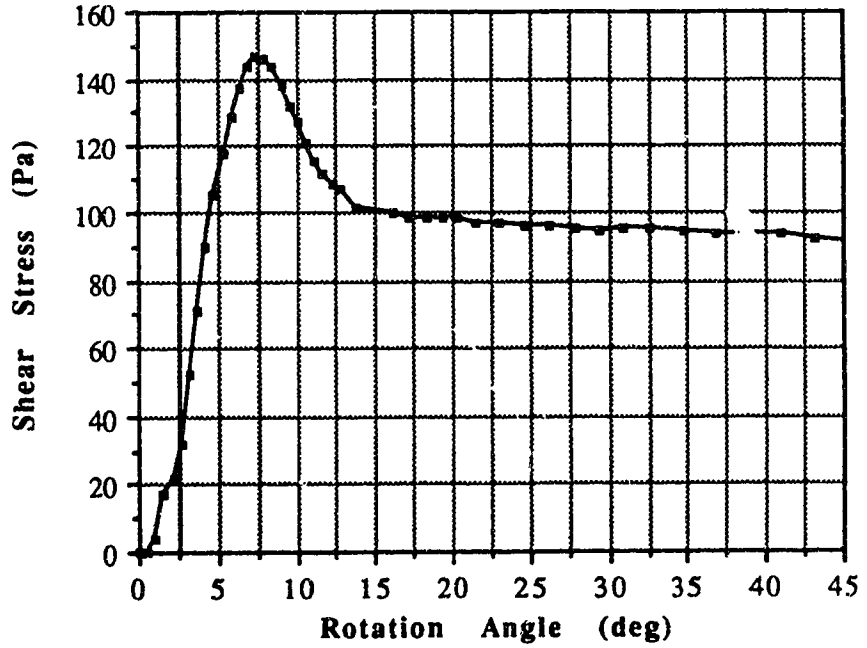

Figure C.123 Vane Shear Test S10008HP

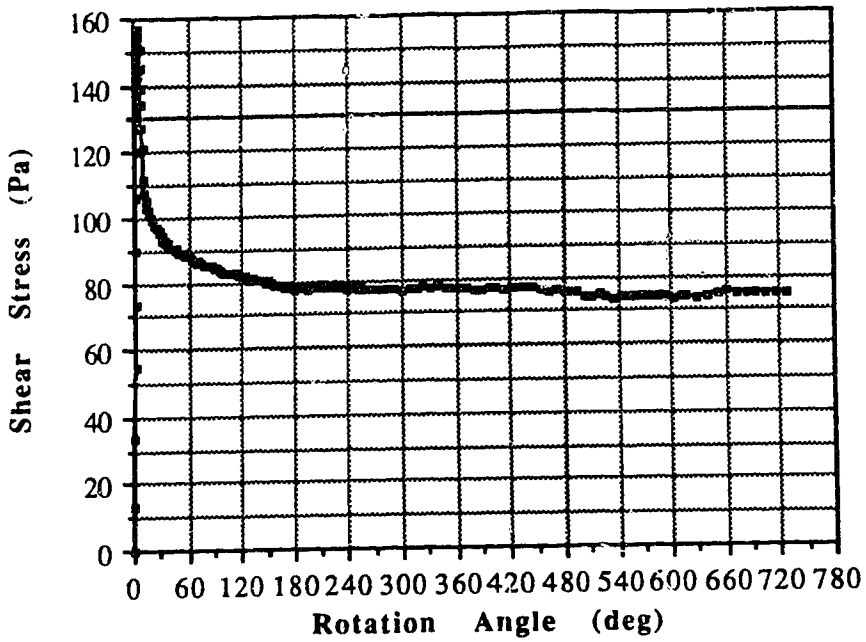

Figure C.124 Vane Shear Test S10001DR

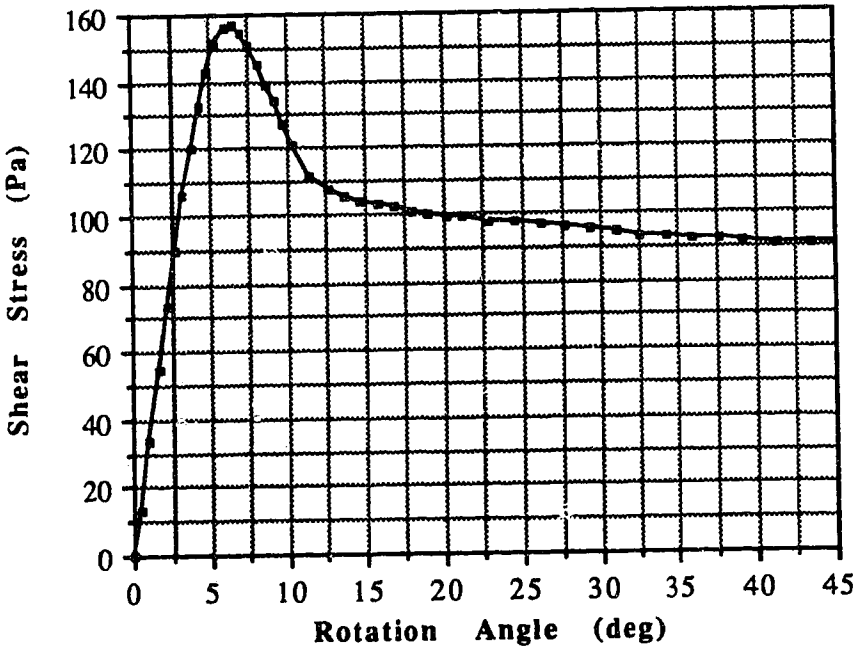

Figure C.125 Vane Shear Test S10001DP

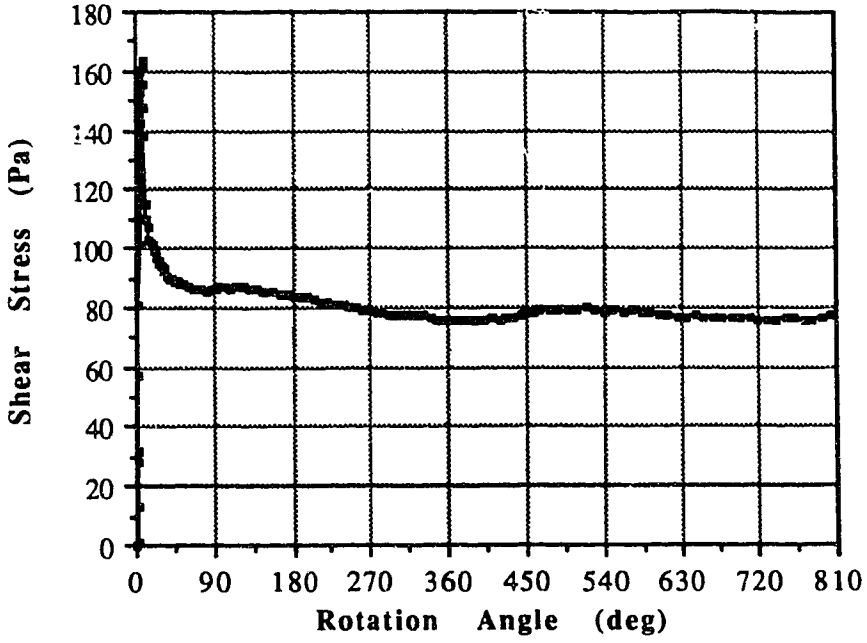

Figure C.126 Vane Shear Test S10002DR

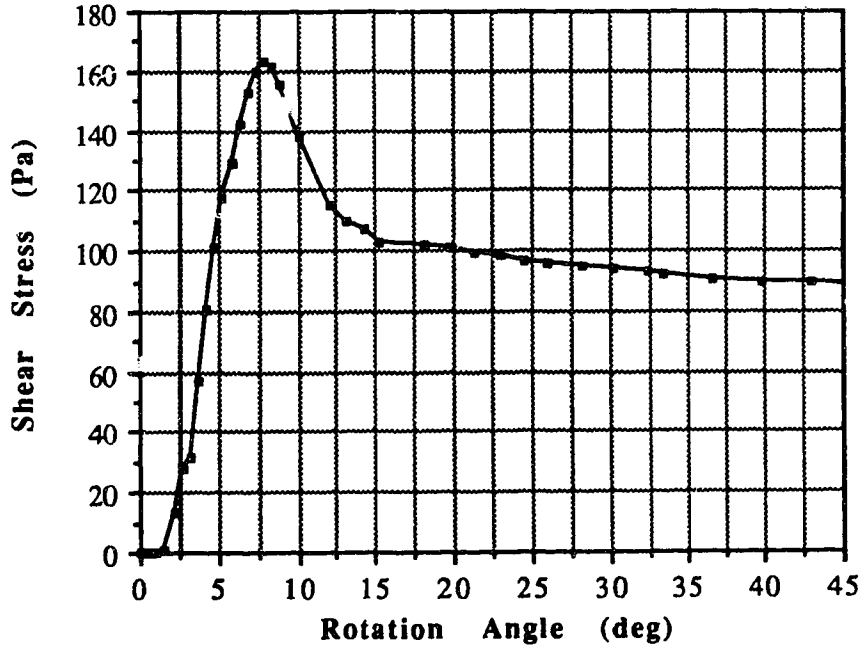

Figure C.127 Vane Shear Test S10002DP

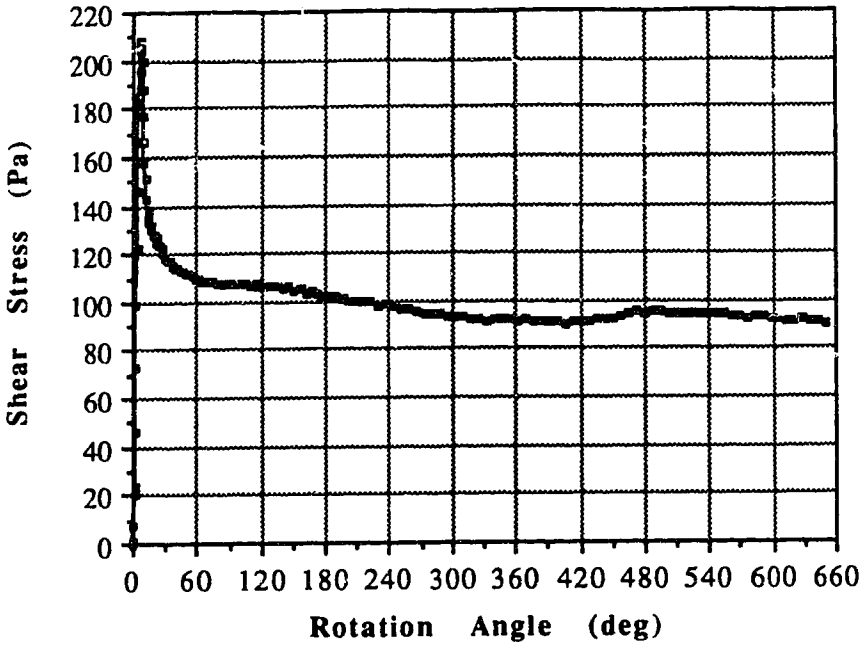

Figure C.128 Vane Shear Test S10005DR

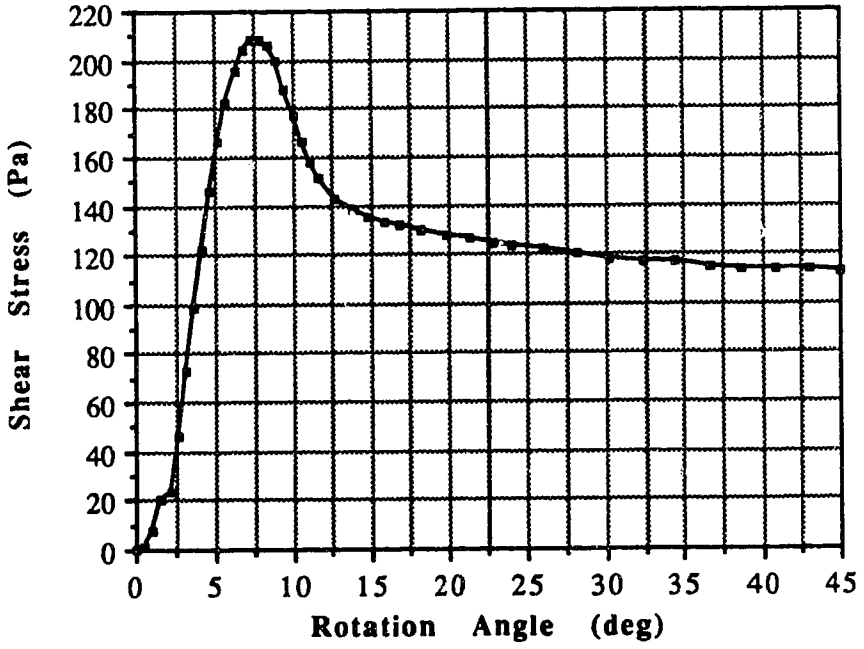

Figure C.129 Vane Shear Test S10005DP

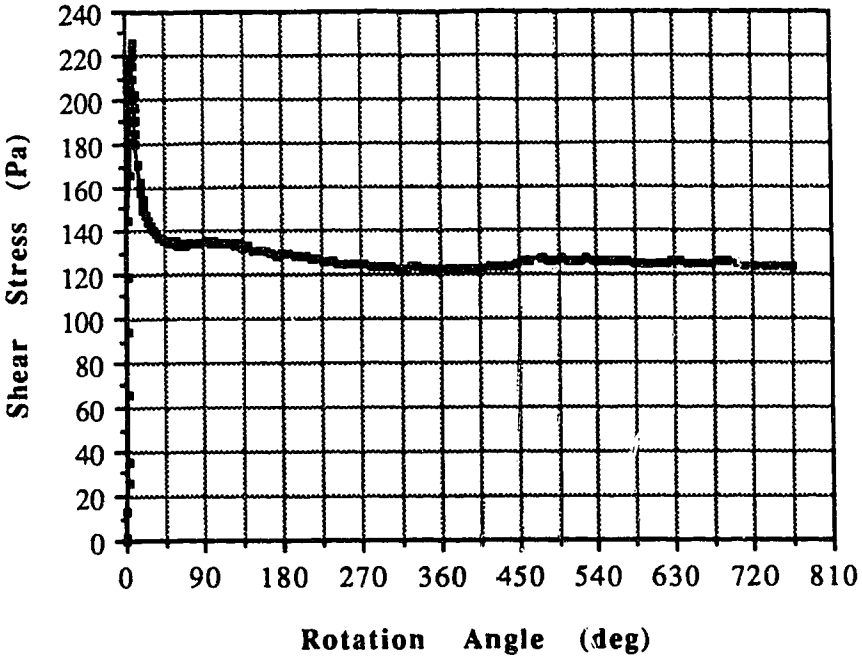

Figure C.130 Vane Shear Test S10006DR

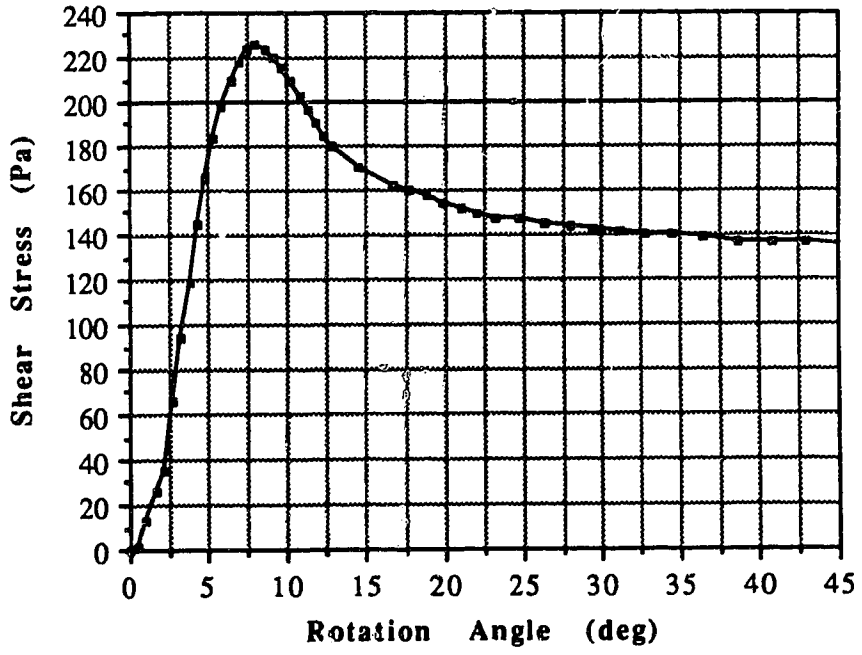

Figure C.131 Vane Shear Test S10006DP

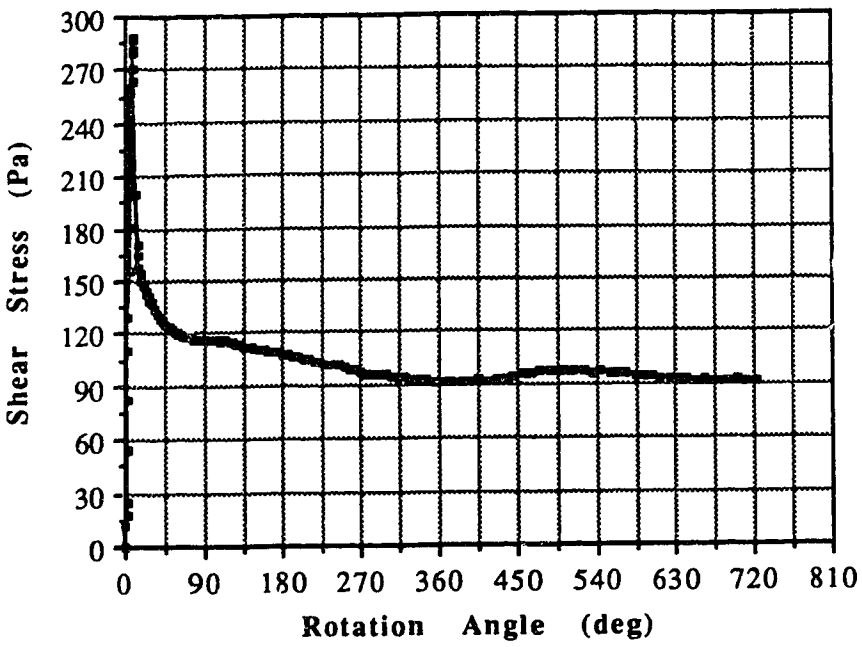

Figure C.132 Vane Shear Test S10010DR

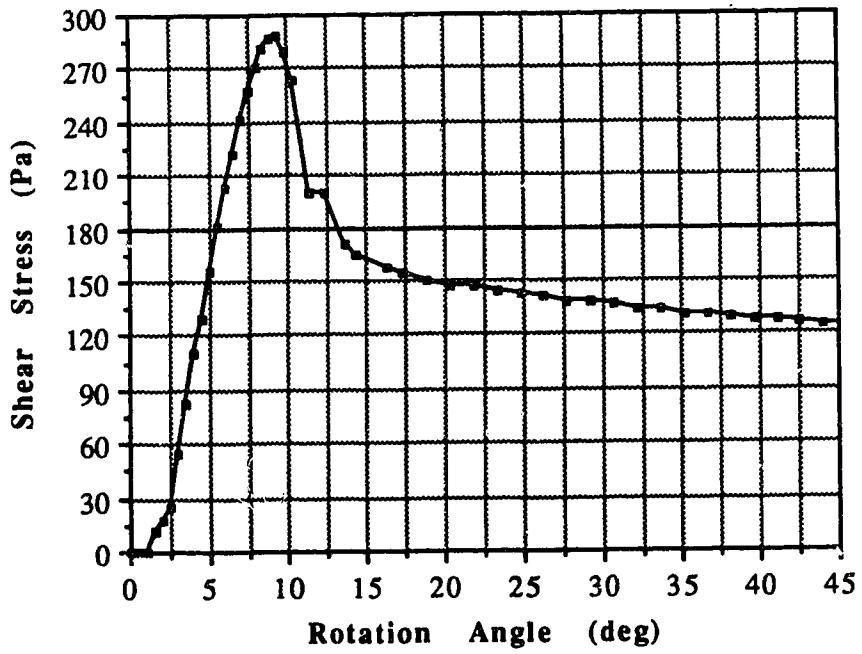

Figure C.133 Vane Shear Test S10010DP

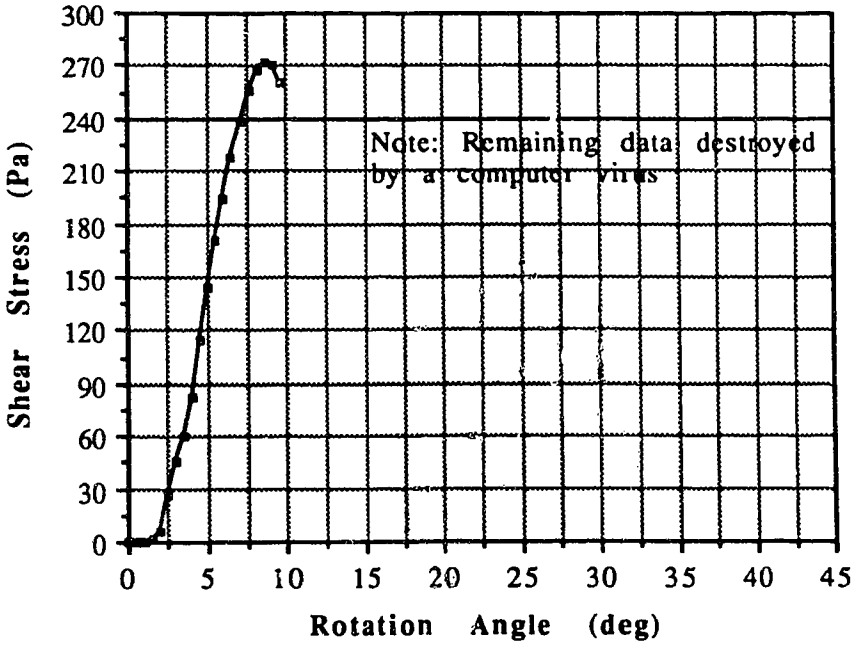

Figure C.134 Vane Shear Test S10015DP

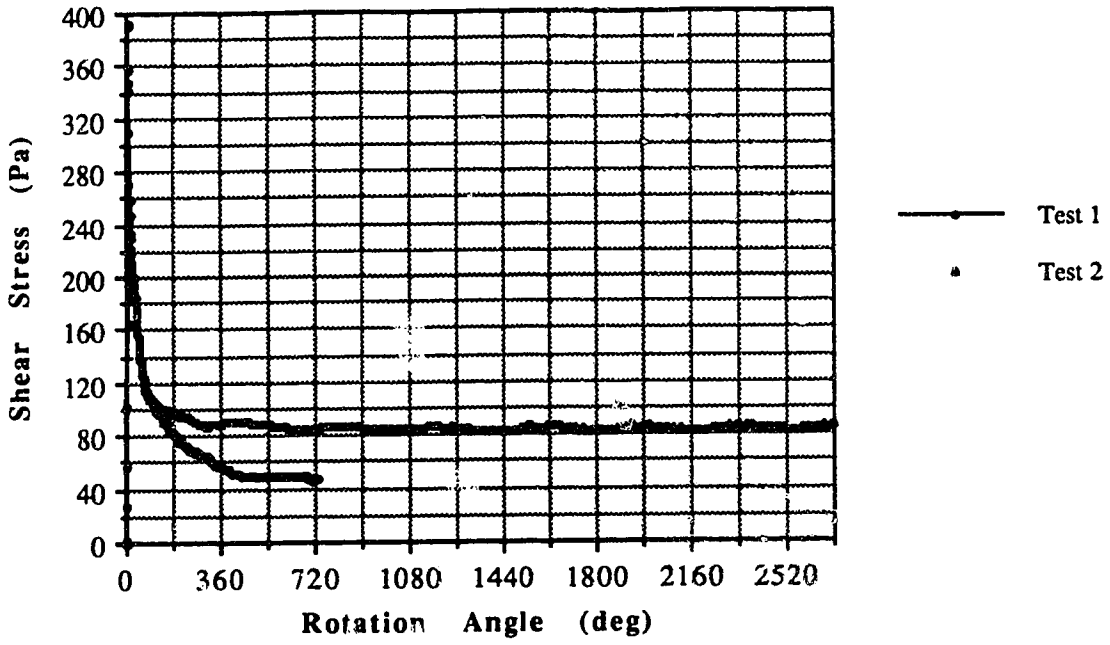

Figure C.135 Vane Shear Test S10020DR

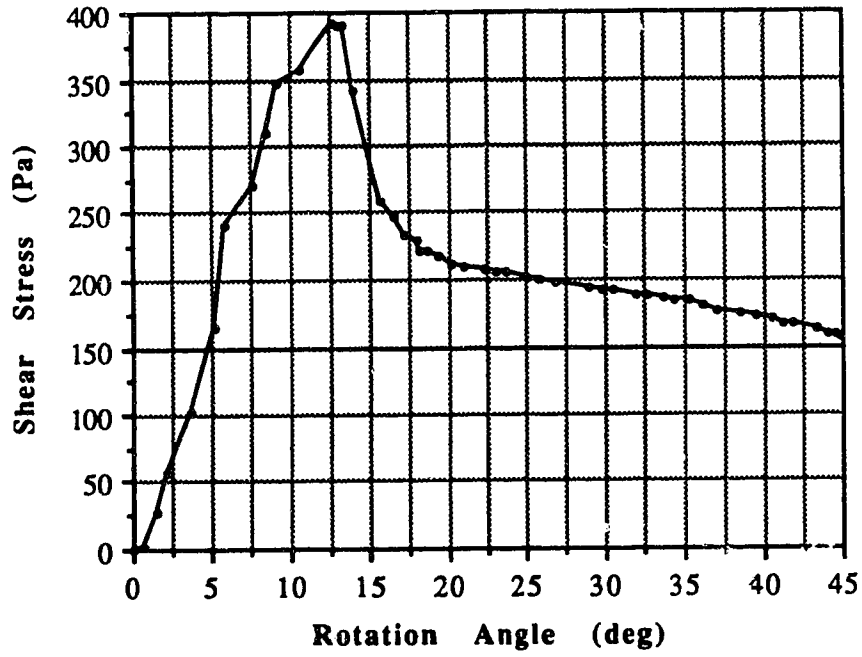

Figure C.136 Vane Shear Test S10020DP

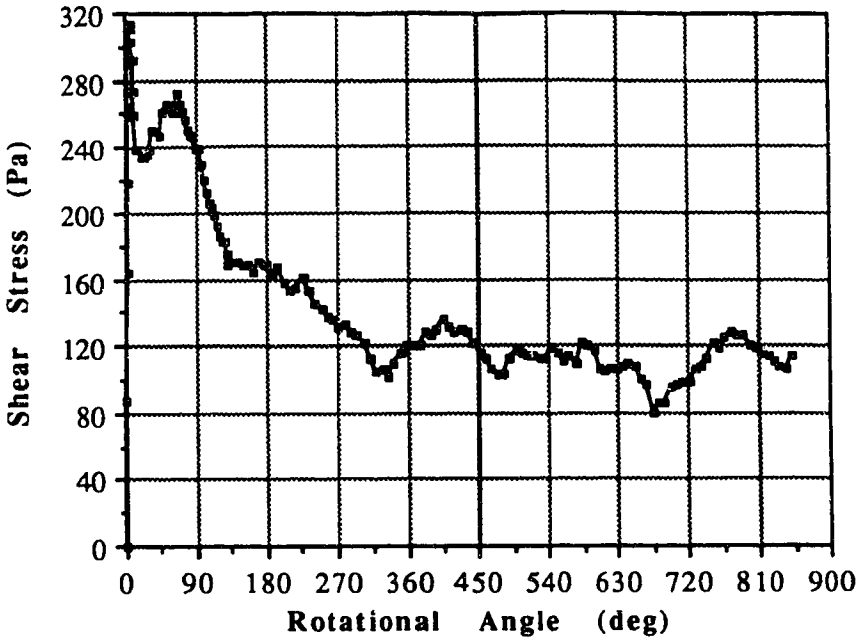

Figure C.137 Vane Shear Test S10040DR

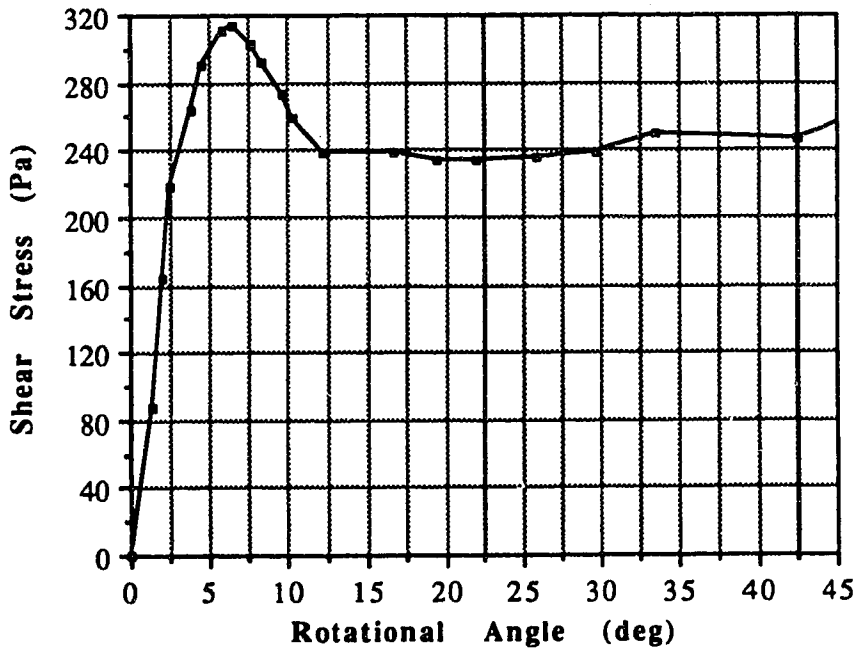

Figure C.138 Vane Shear Test S10040DP

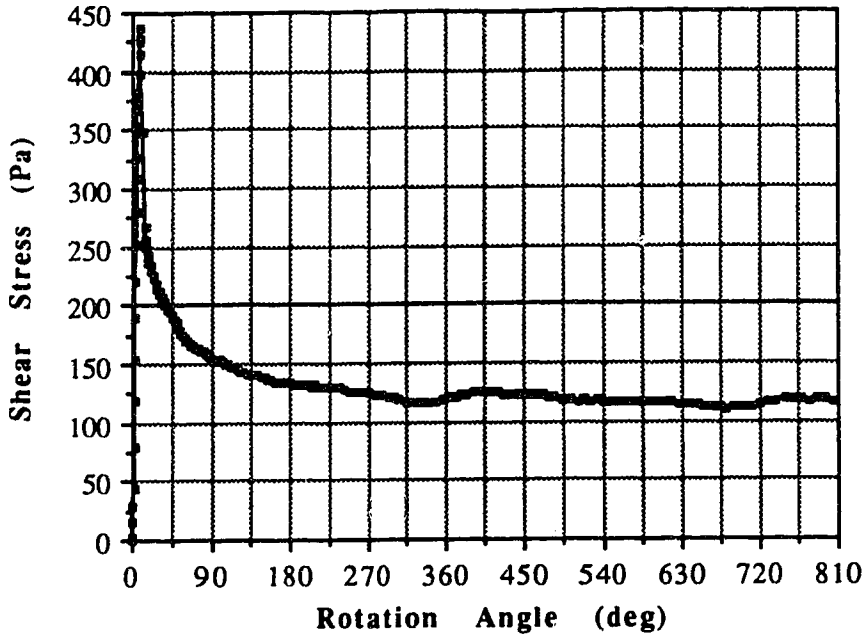

Figure C.139 Vane Shear Test S10090DR

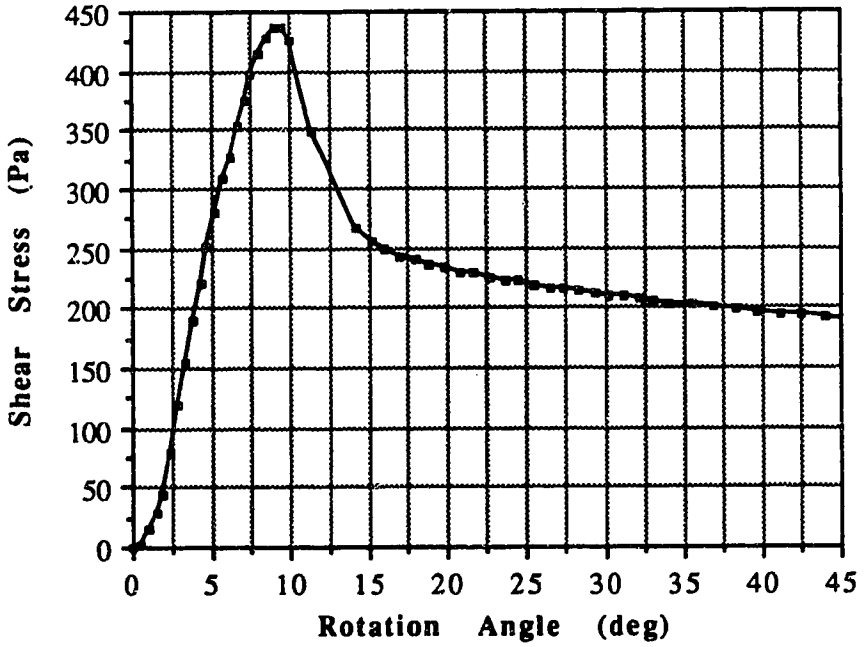

Figure C.140 Vane Shear Test S10090DP

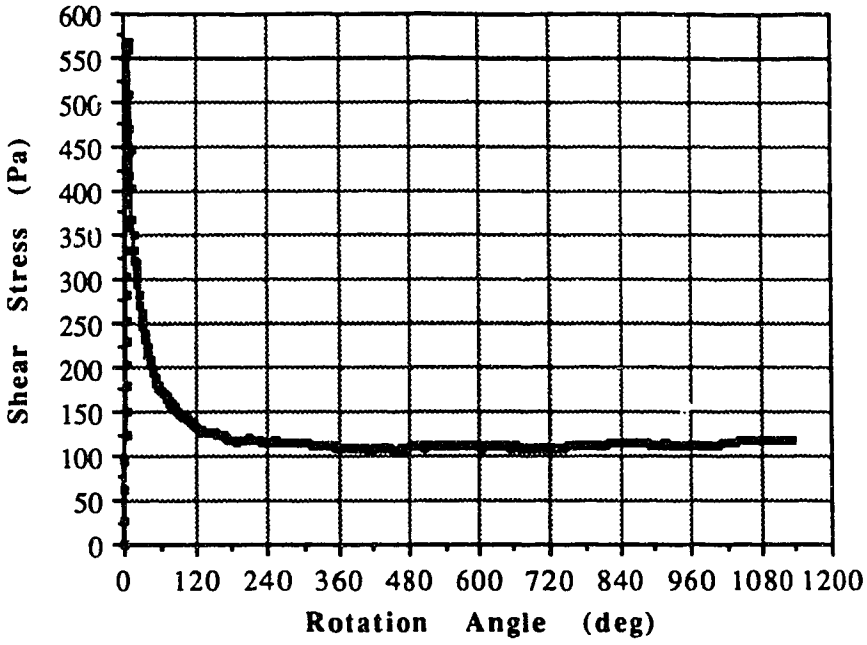

Figure C.141 Vane Shear Test S10470DR

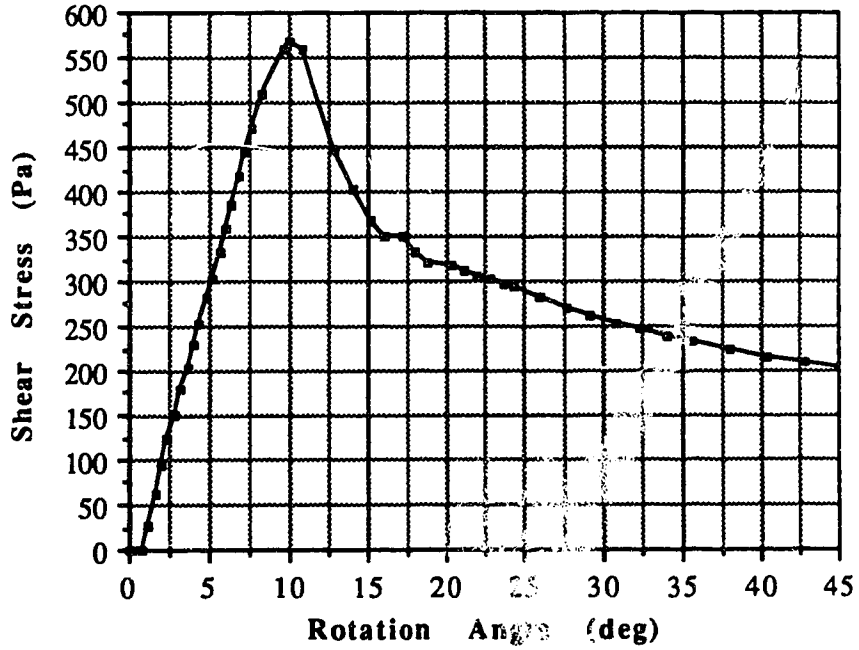

Figure C.142 Vane Shear Test S10470DP

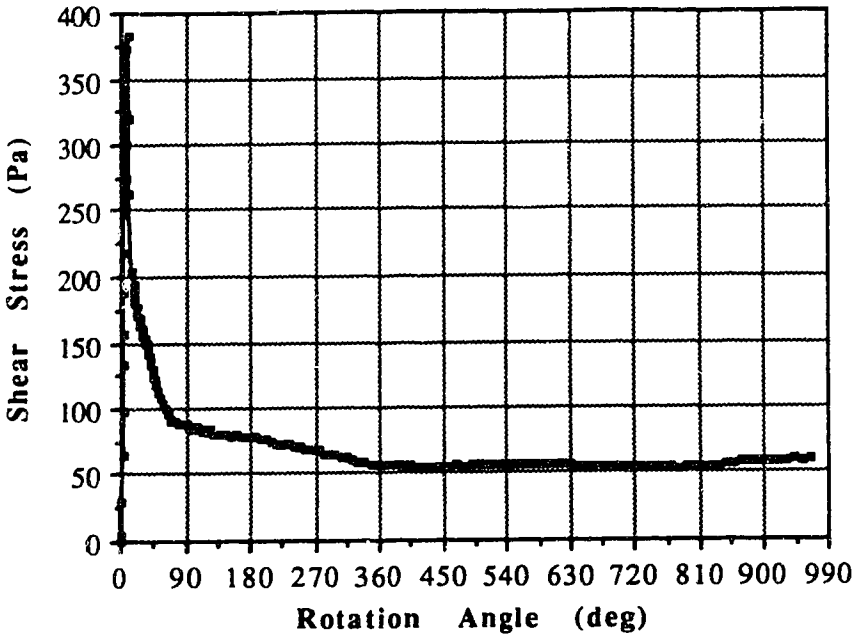

Figure C.143 Vane Shear Test S10680DR

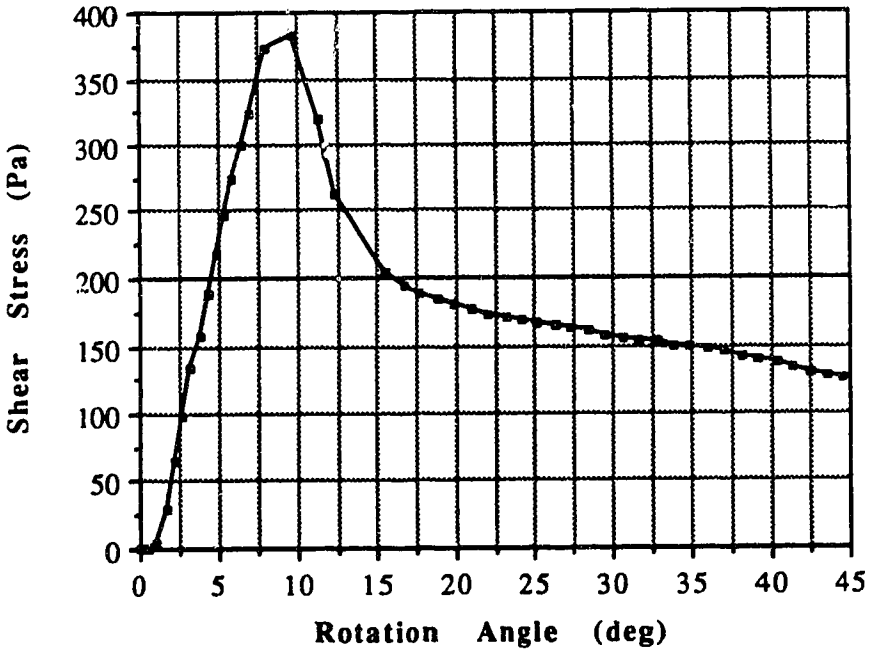

Figure C.144 Vane Shear Test S10680DP

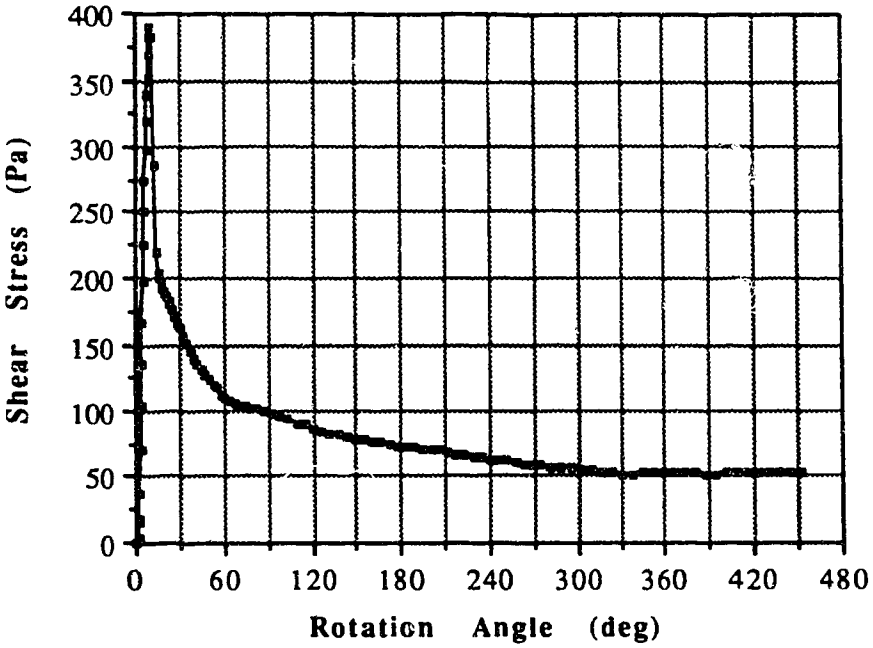

Figure C.145 Vane Shear Test S10701DR

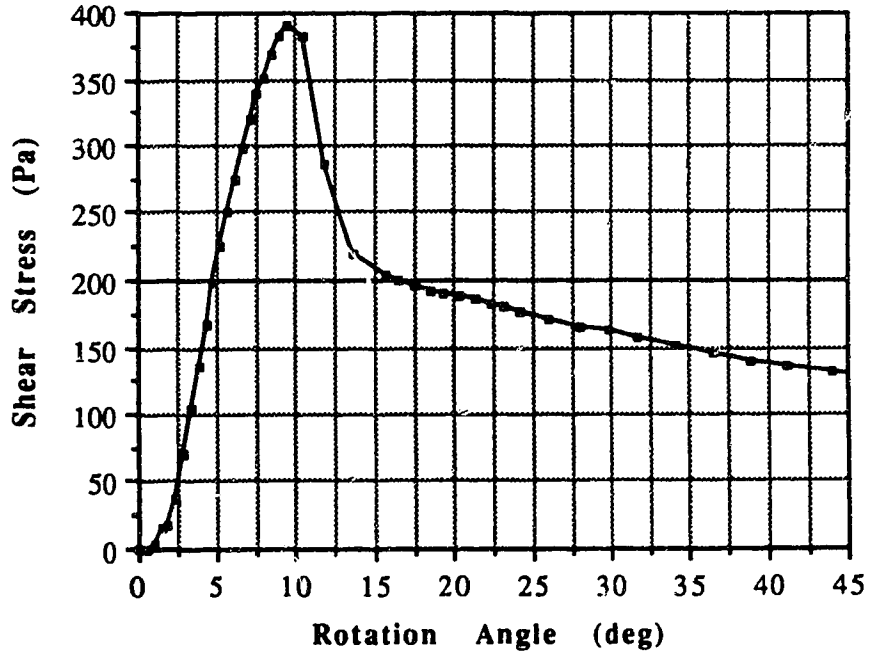

Figure C.146 Vane Shear Test S10701DP

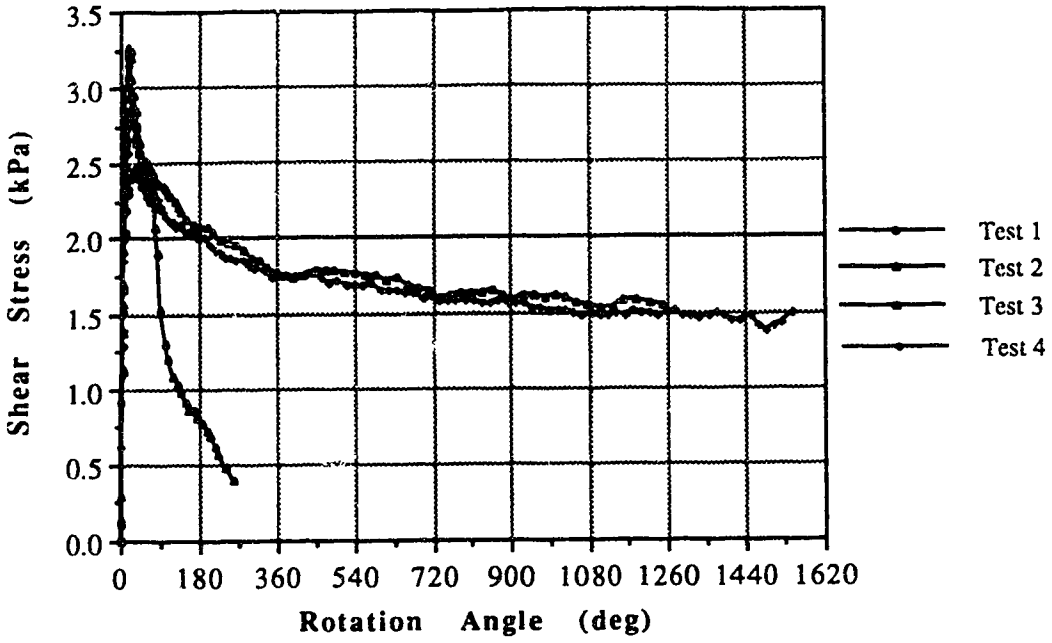

Figure C.147 Vane Shear Test S47000M

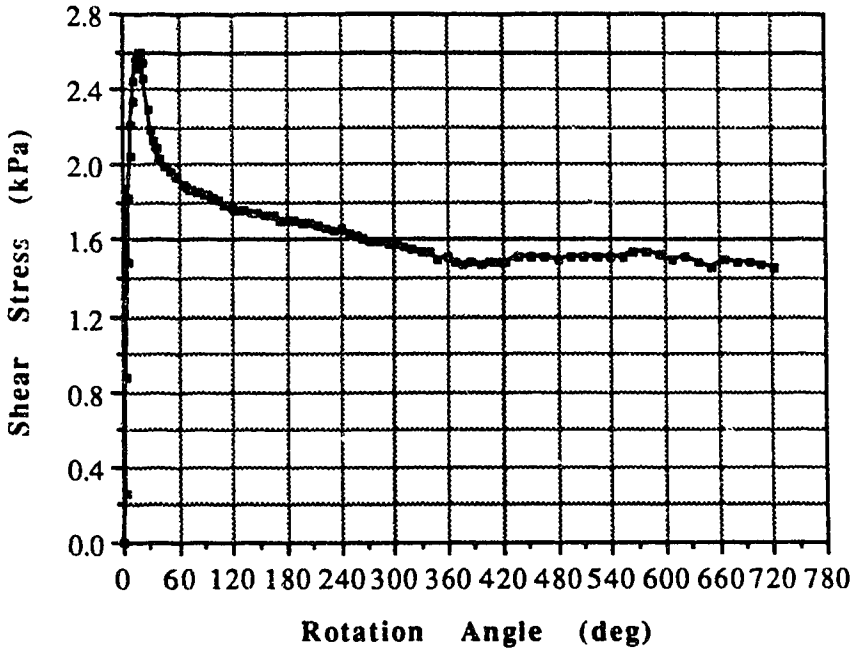

Figure C.148 Vane Shear Test S47002HR

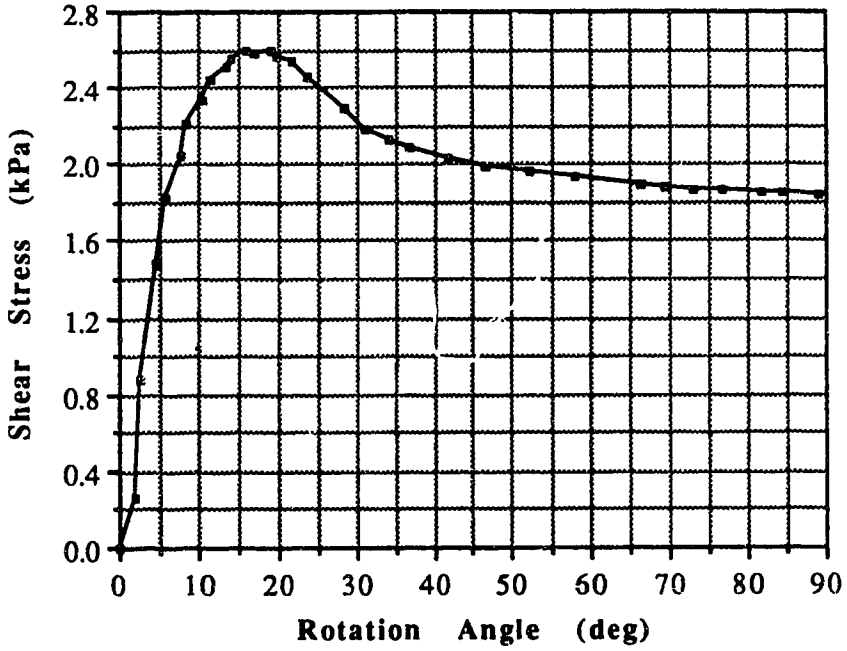

Figure C.149 Vane Shear Test S47002HP

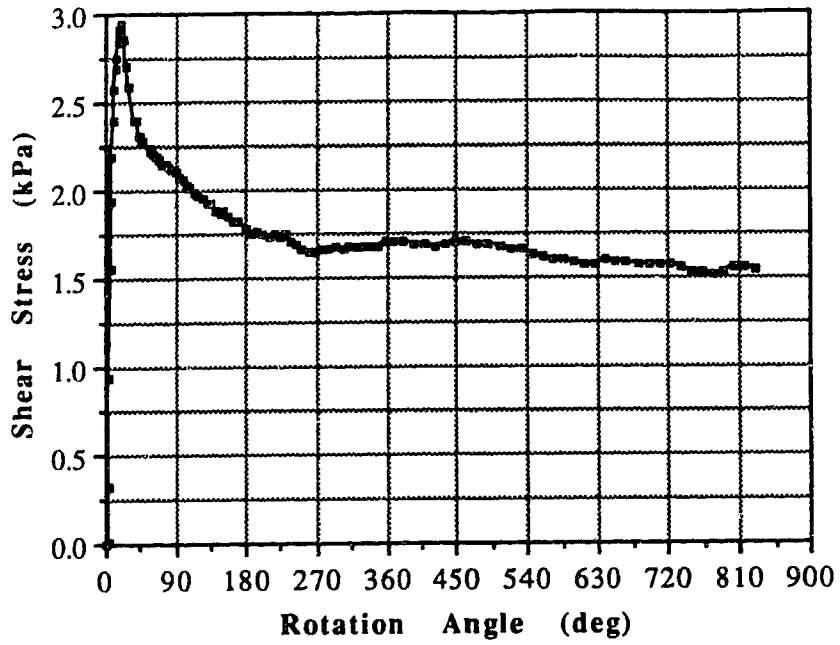

Figure C.150 Vane Shear Test S47008HR

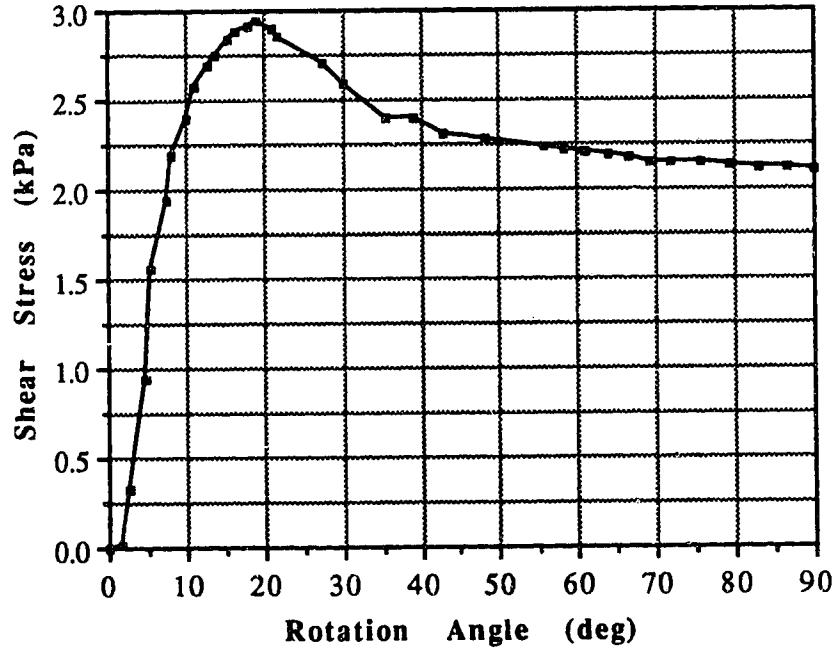

Figure C.151 Vane Shear Test S47008HP

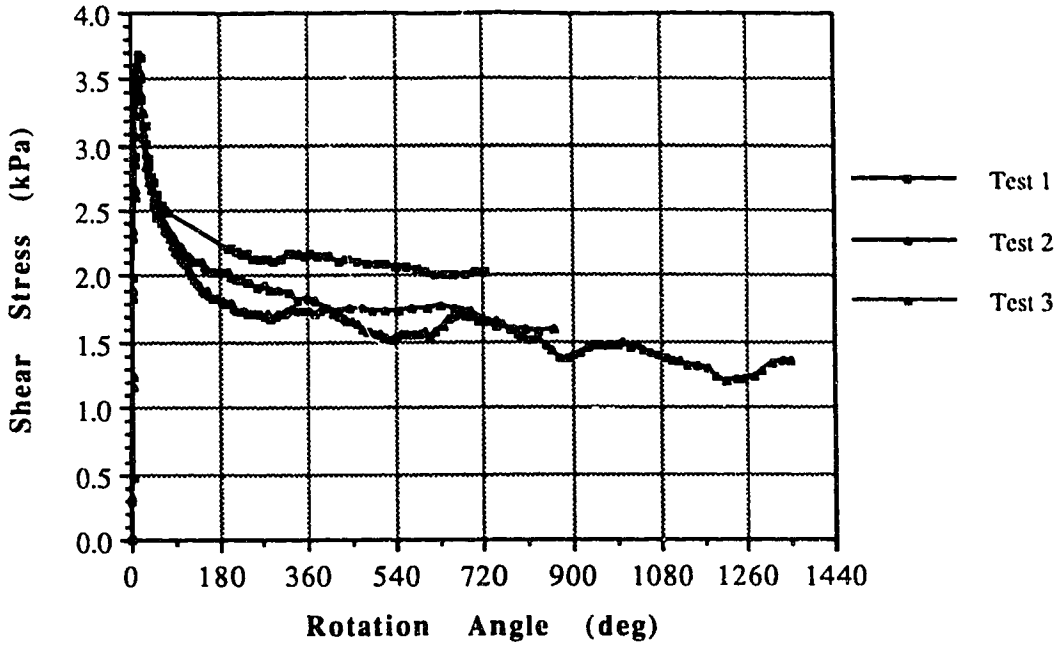

Figure C.152 Vane Shear Test S47001DR

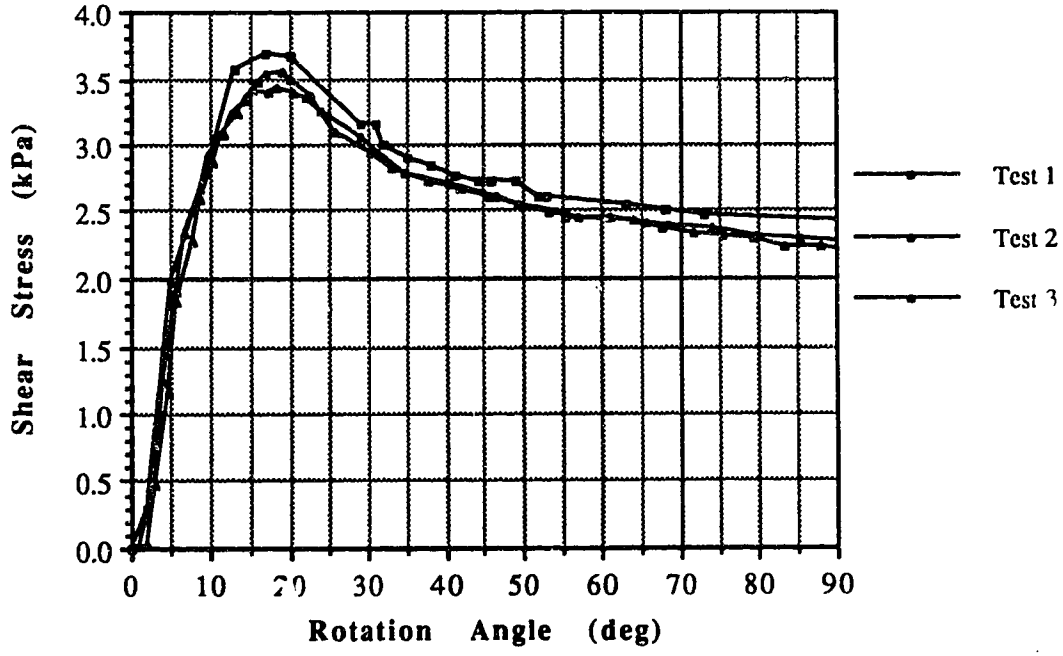

Figure C.153 Vane Shear Test S47001DP

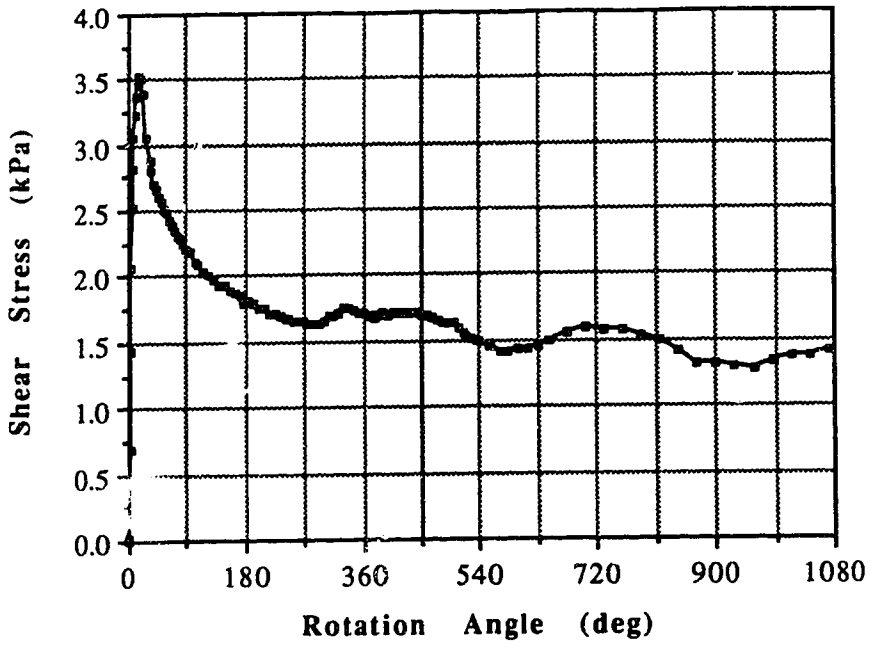

Figure C.154 Vane Shear Test S47002DR

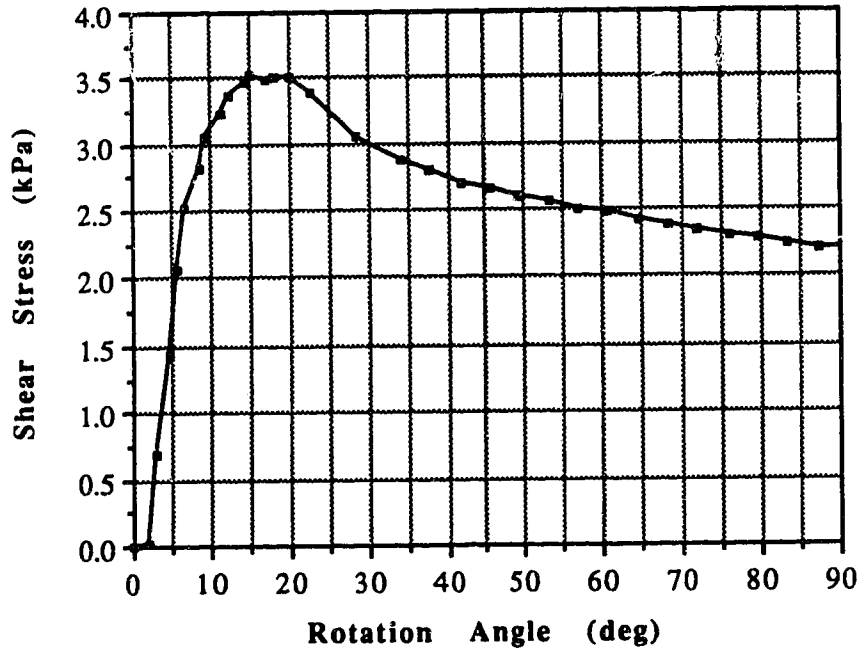

Figure C.155 Vane Shear Test S47002DP

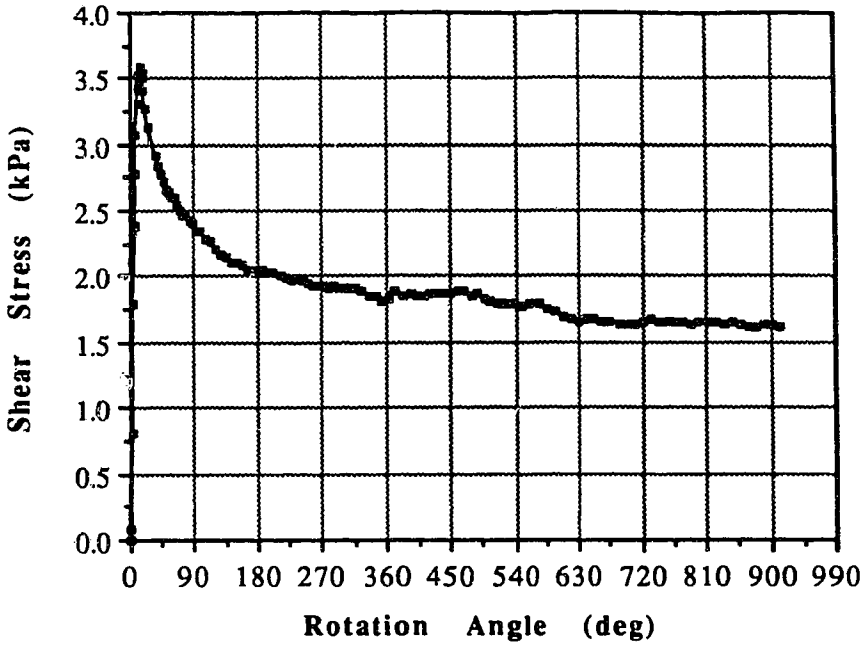

Figure C.156 Vane Shear Test S47005DR

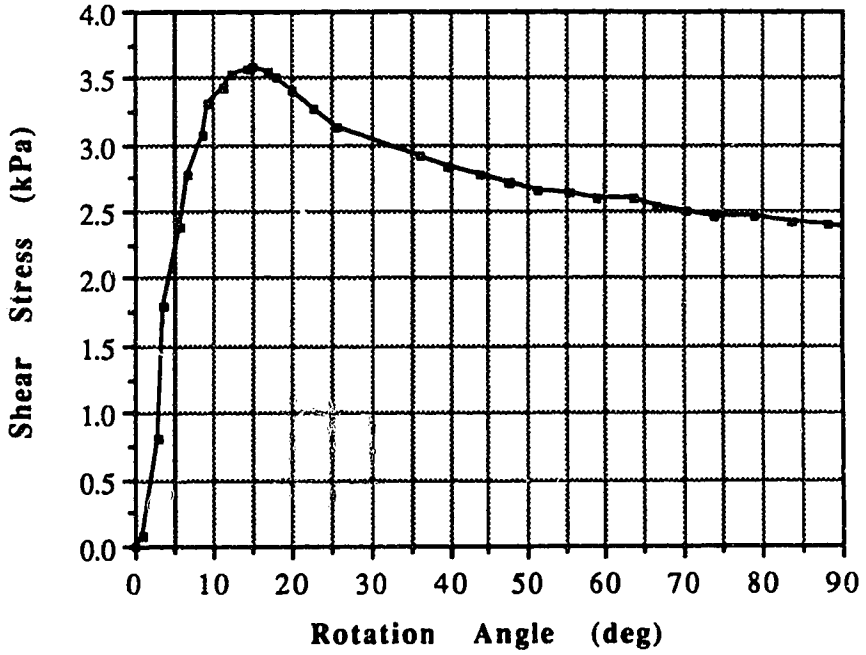

Figure C.157 Vane Shear Test S47005DP

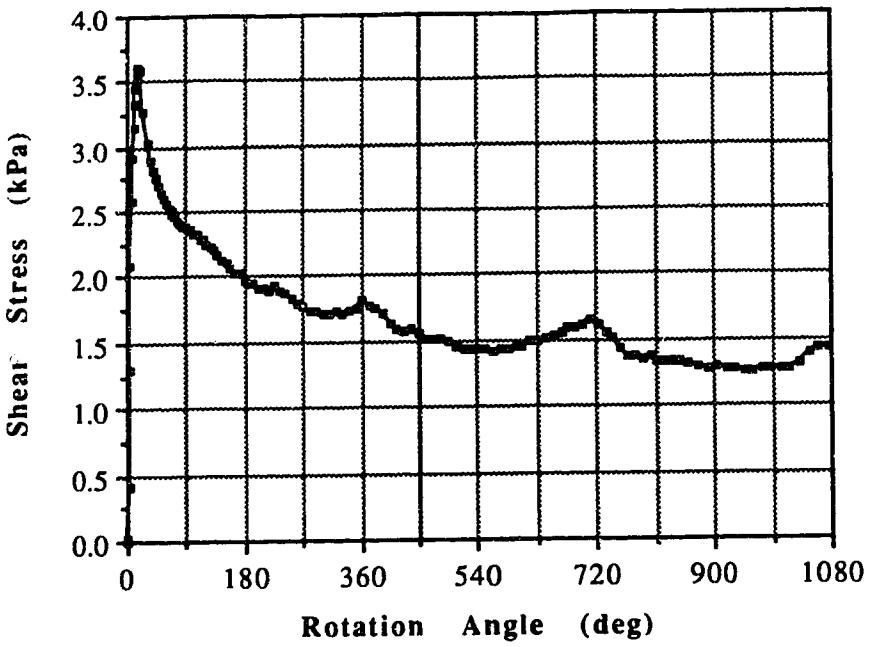

Figure C.158 Vane Shear Test S47007DR

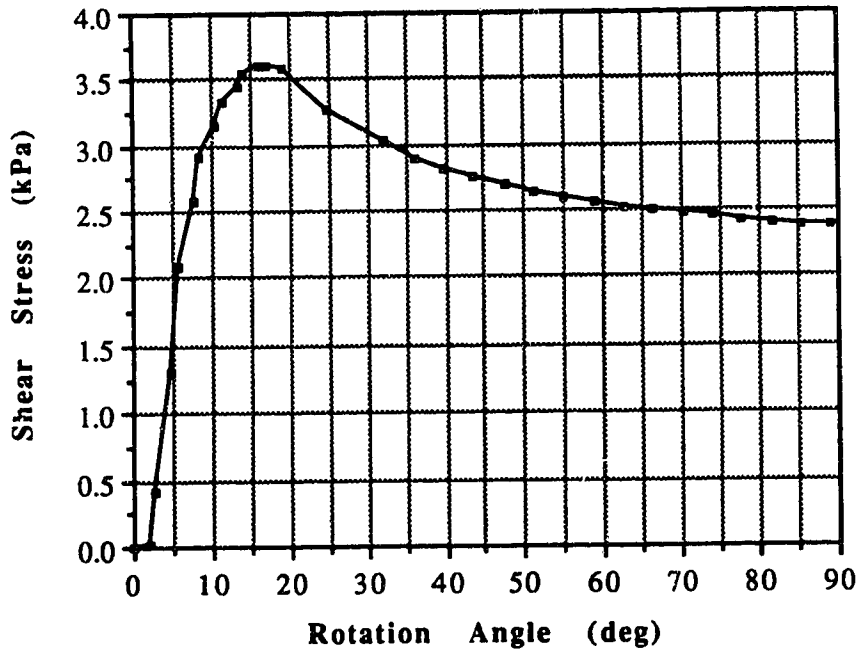

Figure C.159 Vane Shear Test S47007DP

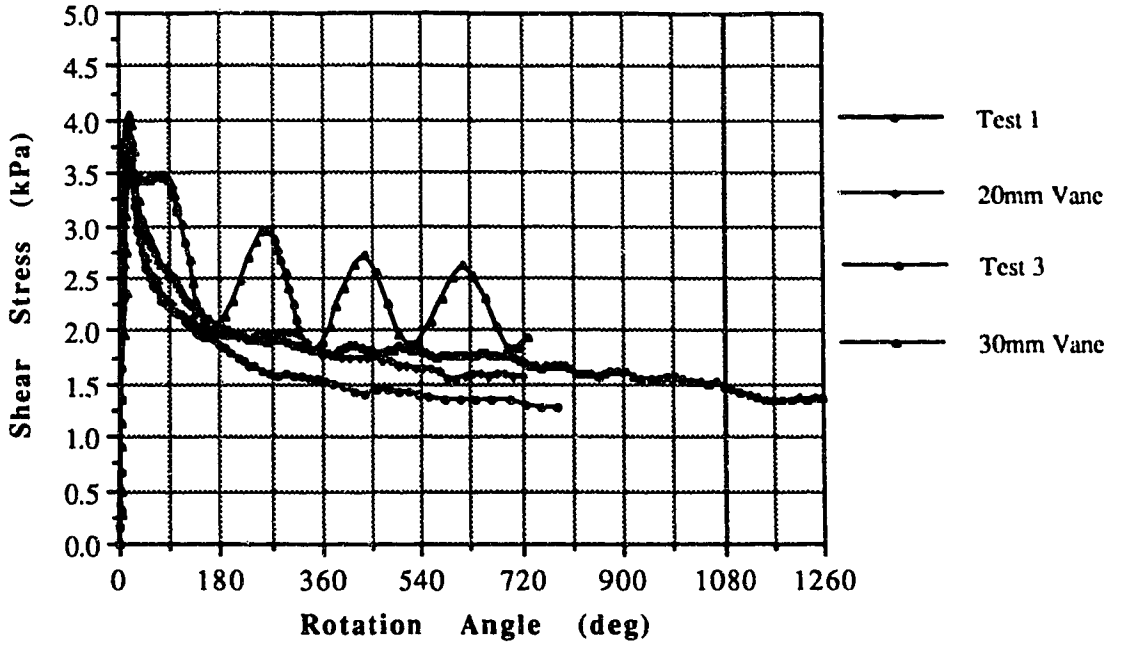

Figure C.160 Vane Shear Test S47010DR

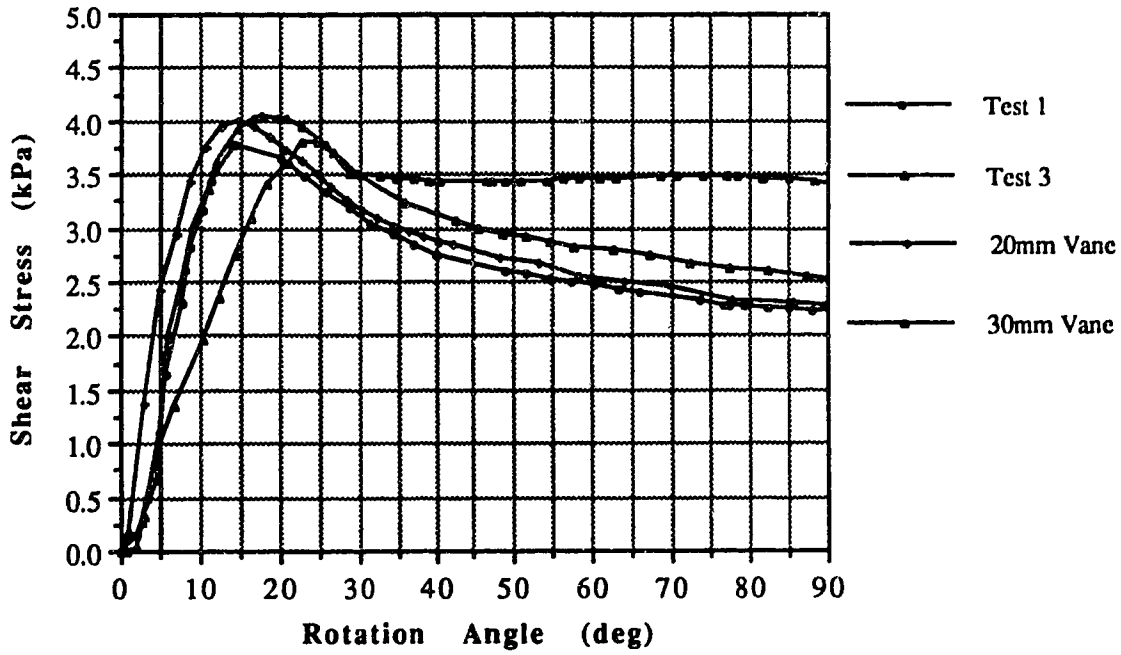

Figure C.161 Vane Shear Test S47010DP

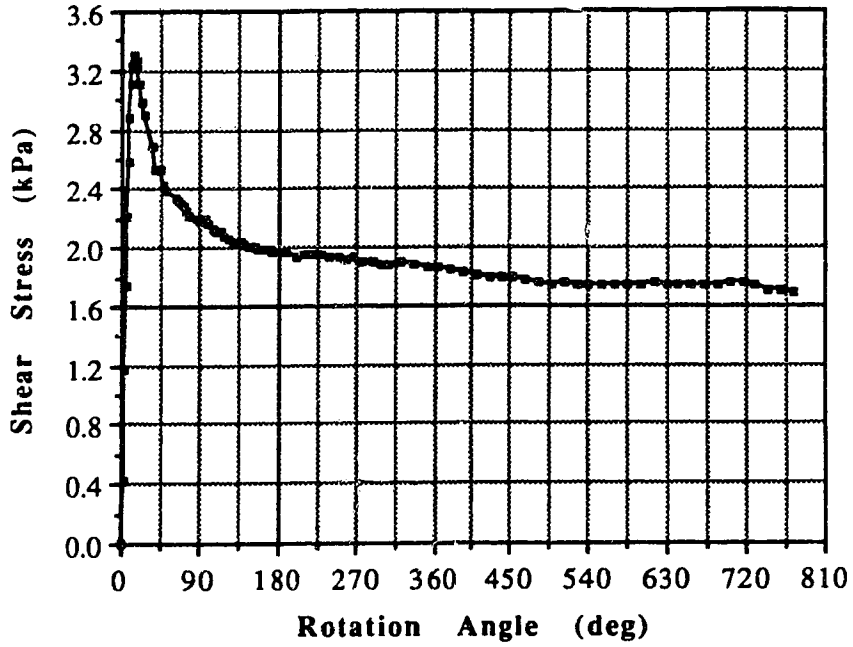

Figure C.162 Vane Shear Test S47021DR

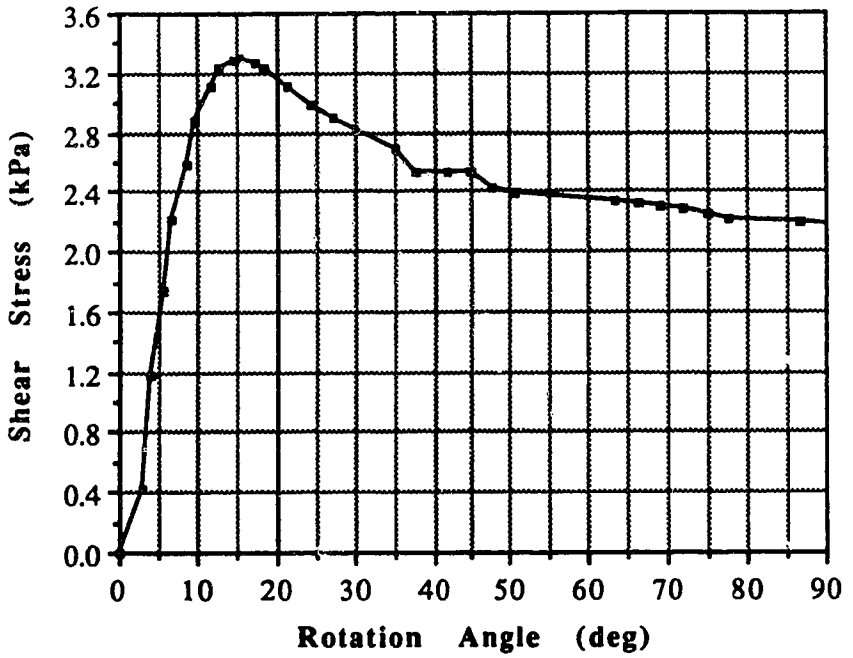

Figure C.163 Vane Shear Test S47021DP

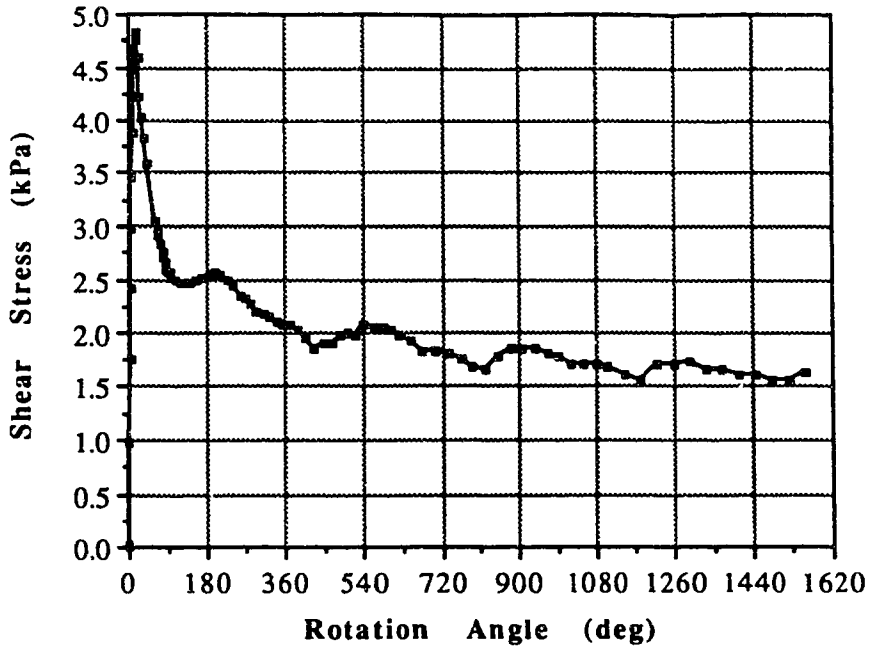

Figure C.164 Vane Shear Test S47060DR

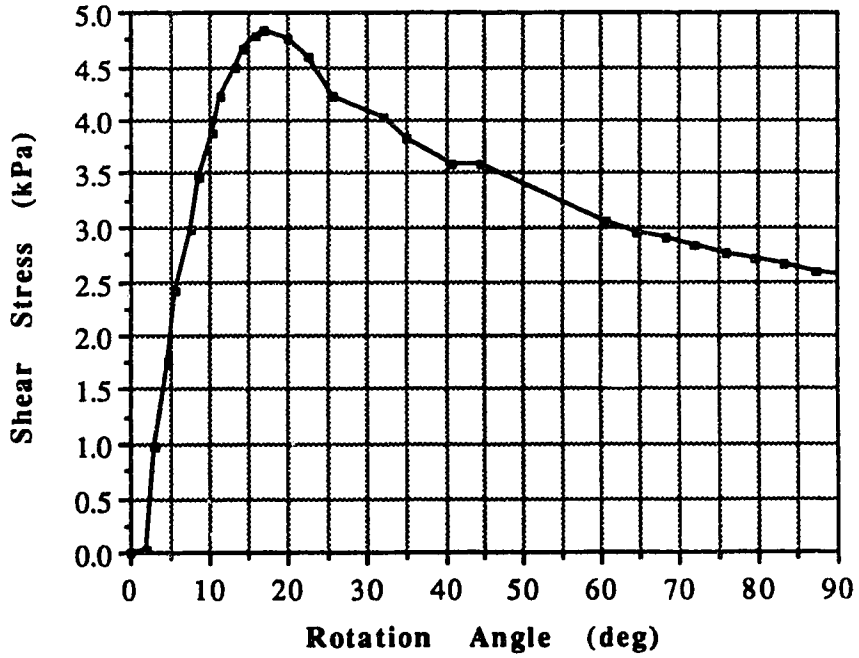

Figure C.165 Vane Shear Test S47060DP

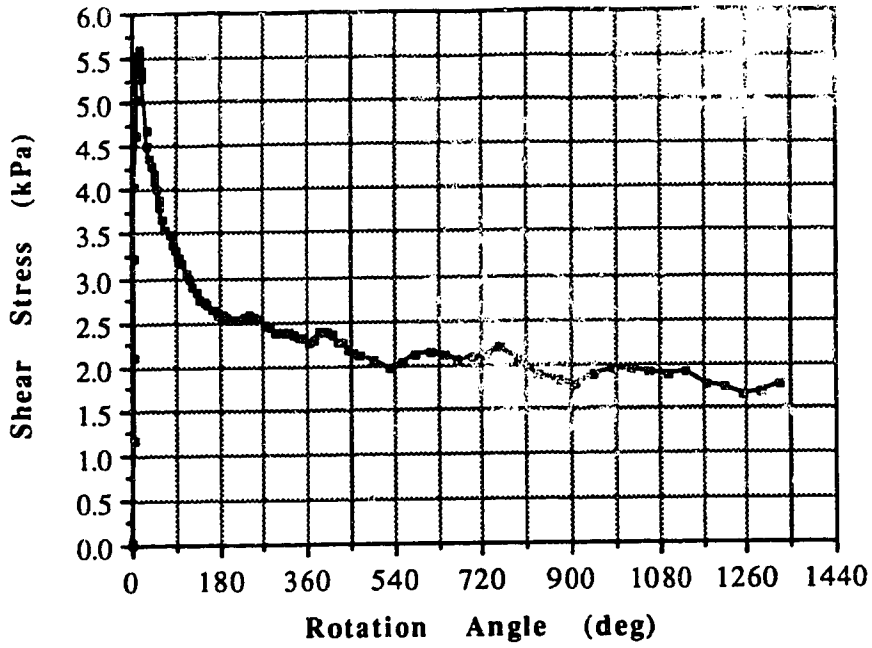

Figure C.166 Vane Shear Test S47087DR

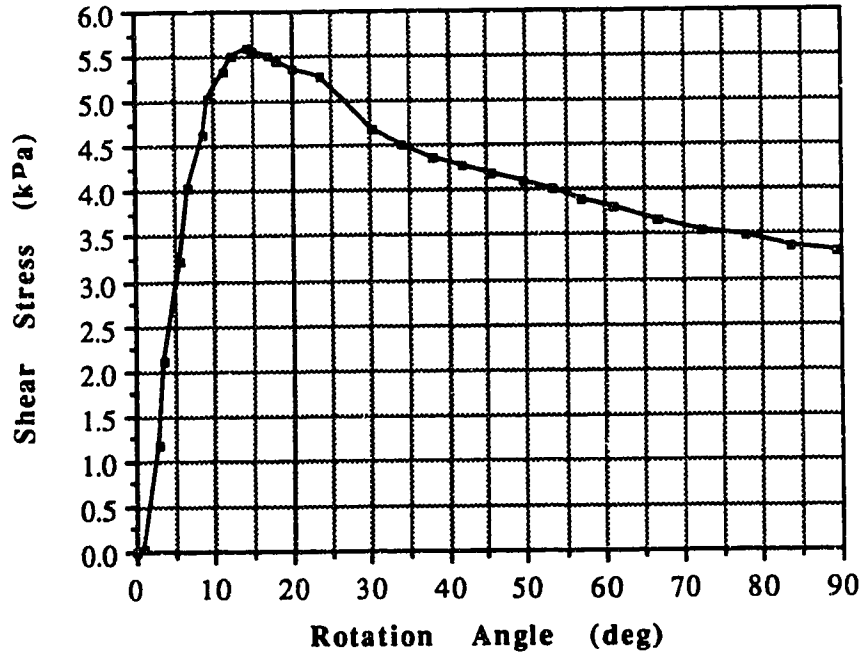

Figure C.167 Vane Shear Test S47087DP

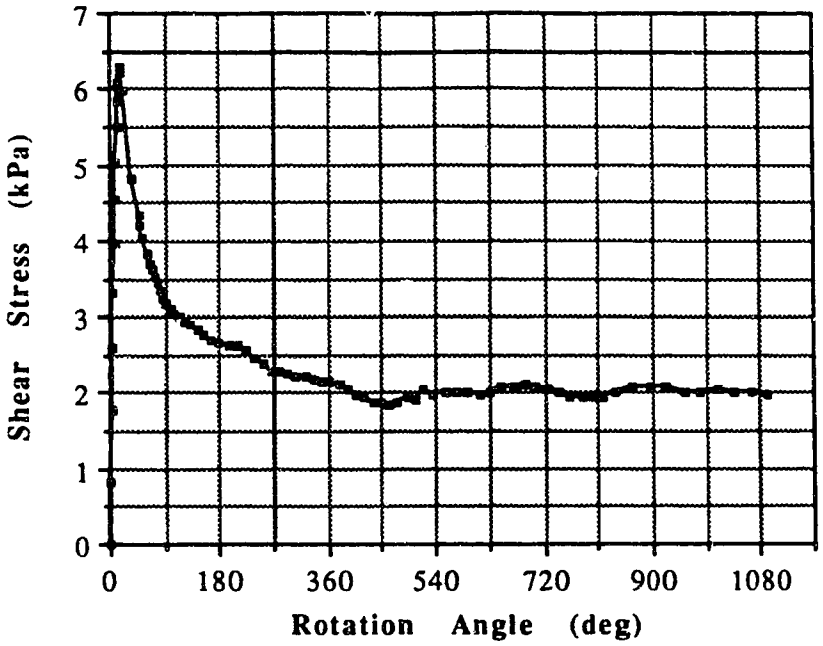

Figure C.168 Vane Shear Test S47160DR

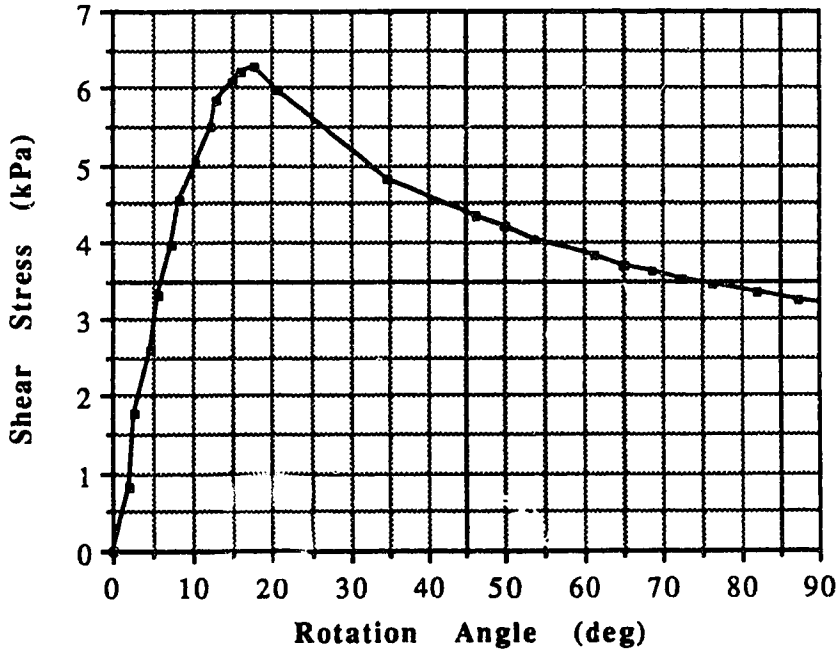

Figure C.169 Vane Shear Test S47160DP

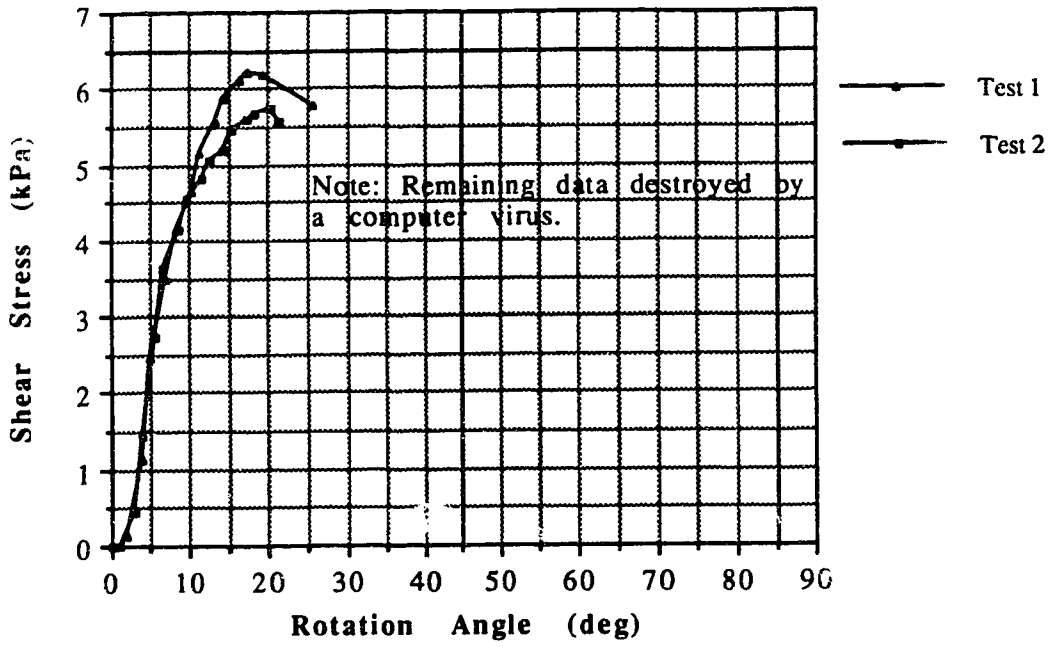

Figure C 170 Vane Shear Test S47181DP

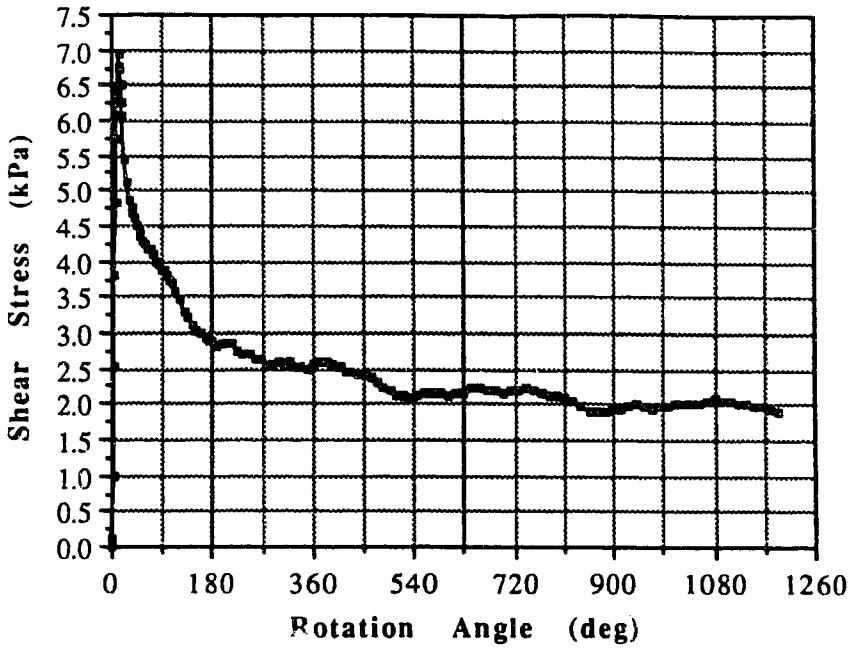

Figure C.171 Vane Shear Test S47194DR

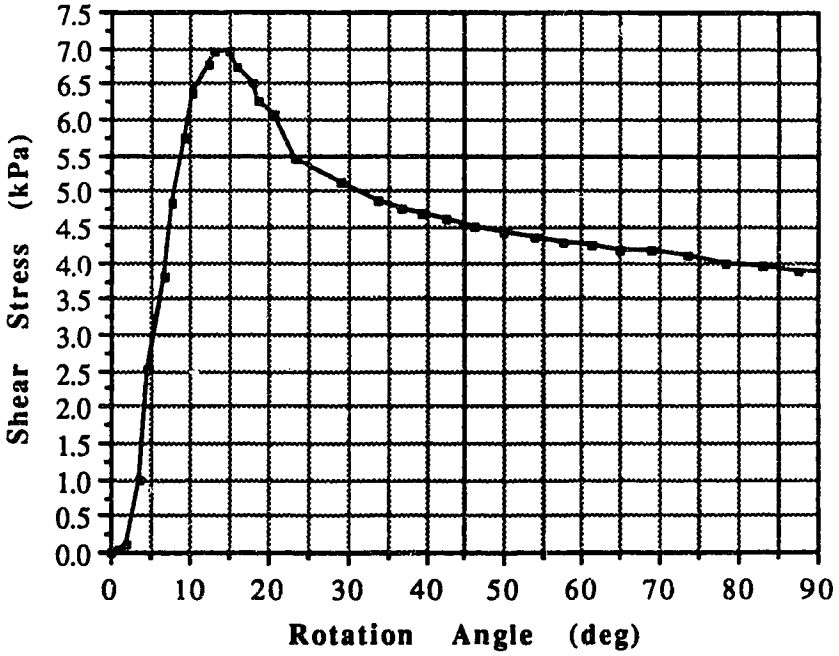

Figure C.172 Vane Shear Test S47194DP

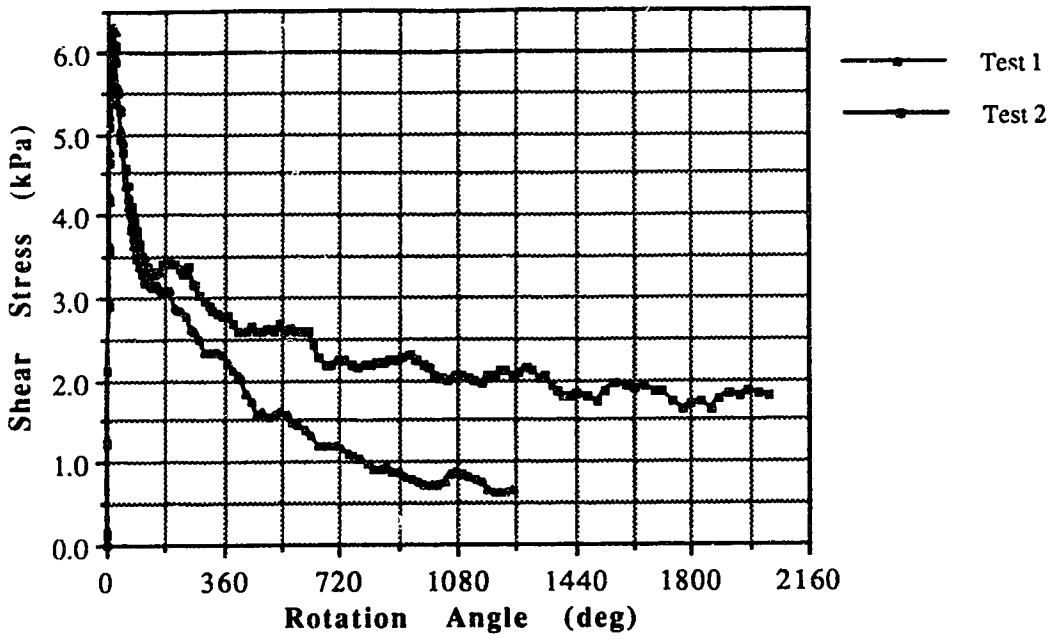

Figure C.173 Vane Shear Test S47410DR

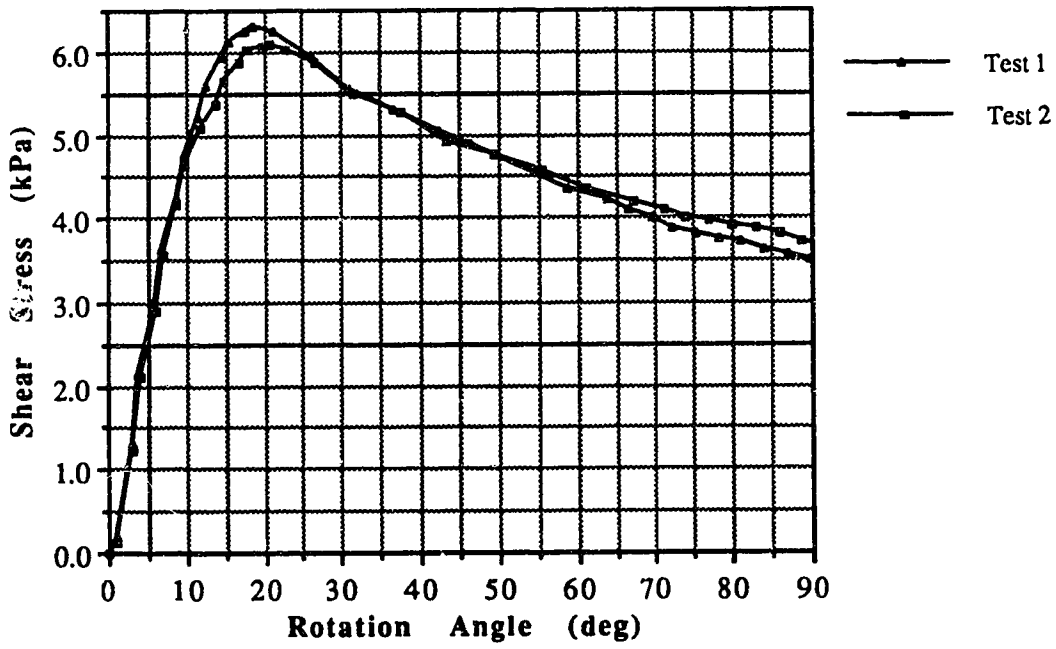

Figure C.174 Vane Shear Test S47410DP

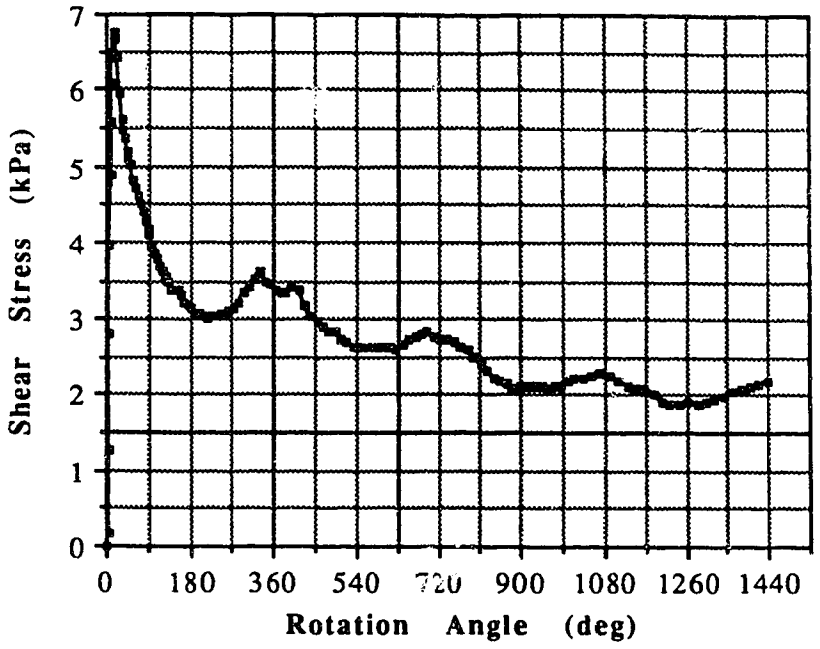

Figure C.175 Vane Shear Test S47460DR

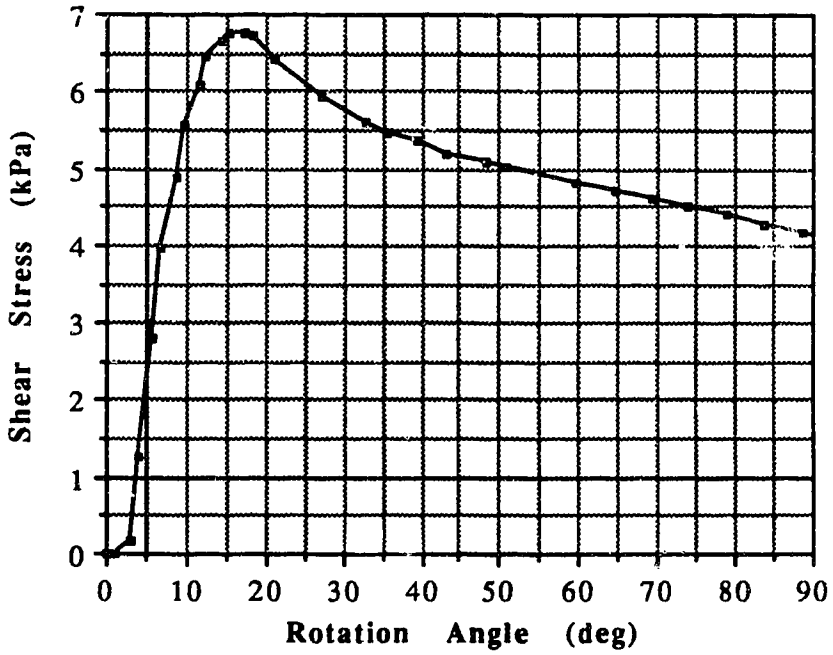

Figure C.176 Vane Shear Test S47460DP

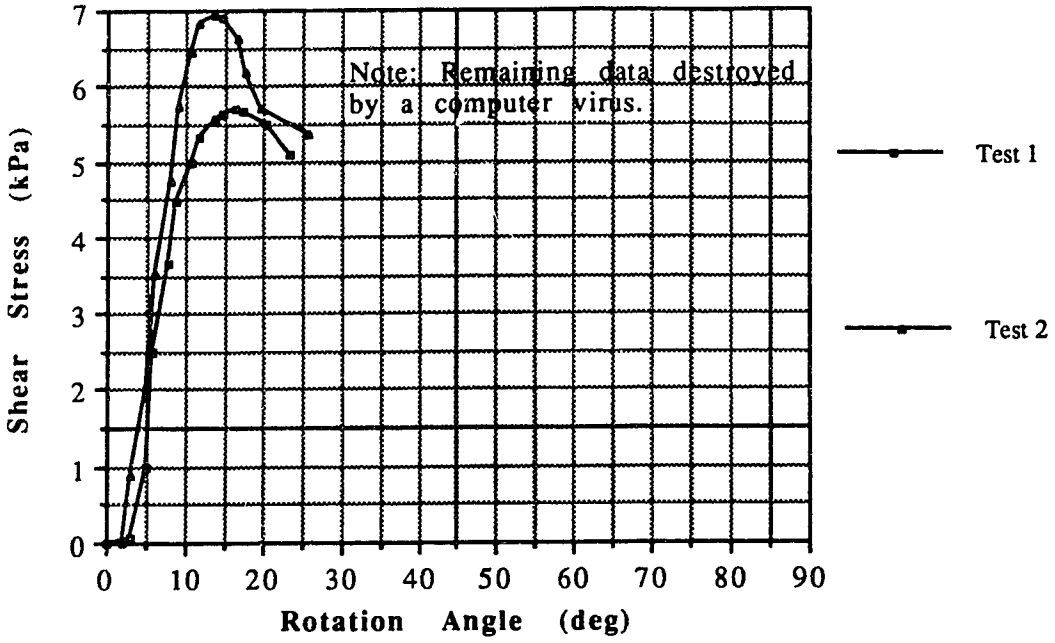

Figure C.177 Vane Shear Test S47510DP

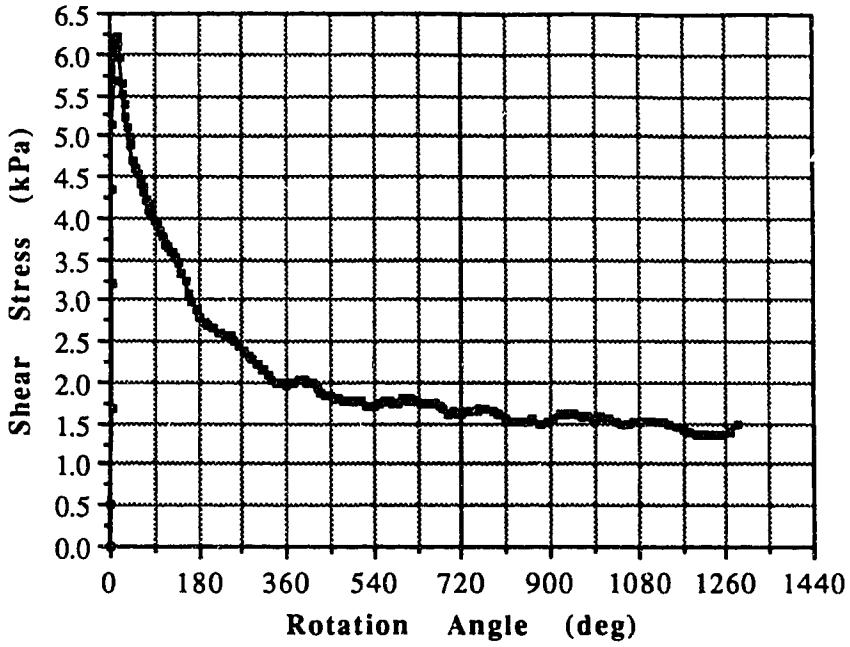

Figure C.178 Vane Shear Test S47523DR

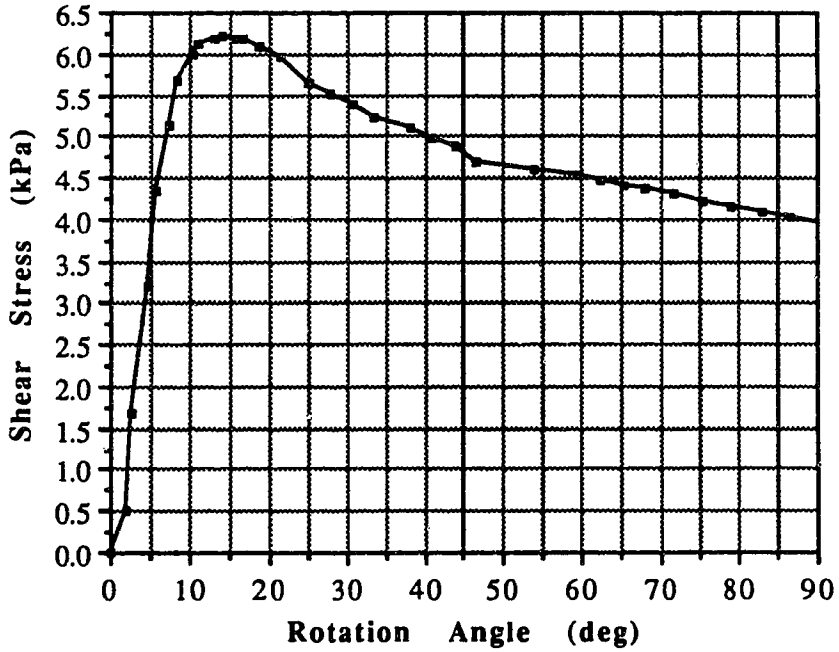

Figure C.179 Vane Shear Test S47523DP